



NEO Lithium Corp

Feasibility Study (FS) - 3Q Project

NI 43-101 Technical Report

Catamarca, Argentina

Mark King, PhD, P.Geo.

Marek Dworzanowski, BSc Metallurgical Eng.

Date: November 25th 2021

Table of contents

1.	Summary	16
1.1	Introduction	16
1.2	Reliance on Other Experts.....	16
1.3	Property Description and Location.....	16
1.4	Accessibility, Climate, Local Resources, Infrastructure, and Physiography.....	17
1.5	History	18
1.6	Geological Setting and Mineralization	18
1.7	Deposit Types	19
1.8	Exploration	19
1.9	Drilling	20
1.10	Sample Preparation, Analysis, and Security.....	20
1.11	Data Verification.....	21
1.12	Mineral Processing and Metallurgical Testing	21
1.13	Mineral Resource Estimate.....	22
1.14	Mineral Reserve Estimates	23
1.15	Mining Methods – Wellfield	25
1.16	Process Recovery Methods	25
1.17	Project Infrastructure.....	25
1.18	Market Studies and Contracts	26
1.19	Sustainability Program. Environmental, Social Responsibility, and Governance.....	27
1.20	Capital and Operating Costs.....	28
1.21	Economic Evaluation	30
1.22	Adjacent Properties.....	33
1.23	Other Relevant Data and Information	33
1.24	Interpretation and Conclusions	33
1.25	Recommendations	35
2.	Introduction.....	37
2.1	Authorization and Purpose	37
2.2	Report Responsibility Matrix	37
2.3	Sources of Information.....	38
2.4	Special Considerations for Brine Resources	40
2.5	Details on Property Inspection by QPs	42
2.6	Statement of Independence.....	43
2.7	Units of Currency	44
2.8	Use of Report.....	44

3.	Reliance on Other Experts	45
4.	Property Description and Location	46
4.1	Location	46
4.2	Description	46
4.3	Type of Mineral Tenure	50
4.4	Mining Rights Opinion	53
5.	Accessibility, Climate, Local Resources, Infrastructure, and Physiography	57
5.1	Accessibility	57
5.2	Climate	57
5.3	Local Resources	62
5.4	Infrastructure	62
5.5	Physiography	62
6.	History	64
7.	Geological Setting and Mineralization	65
7.1	Regional Geology	65
7.2	Salar Basin Geology	66
7.3	Salar In-Fill Geology	74
7.4	Structures	79
7.5	Mineralization	80
7.6	Surface Water	81
7.7	Groundwater Piezometry	85
7.8	Water Balance	88
7.9	Surface and Shallow Brine Hydrochemistry	88
7.10	Subsurface Brine Hydrochemistry	92
8.	Deposit Types	95
9.	Exploration	97
9.1	Overview	97
9.2	Vertical Electric Sounding (“VES”) Surveys	98
9.3	Seismic Survey (2017/18 Program)	100
9.4	Surface Brine Sampling Program	102
9.5	Ongoing Monitoring Programs	102
9.6	Pumping Test Program	105
9.7	Data Processing	106
10.	Drilling	110
10.1	Overview	110
10.2	Diamond Drilling	111
10.3	Rotary Drilling	114

11.	Sample Preparation, Analyses, and Security.....	116
11.1	Overview	116
11.2	Sample Collection	116
11.3	Sample Preparation	121
11.4	Brine Analysis	121
11.5	Field QA/QC Program.....	122
11.6	Laboratory Duplicate Analysis	130
11.7	Sample Security.....	132
12.	Data Verification	133
12.1	Project Review and Interaction	133
12.2	Independent Duplicate Sampling.....	134
13.	Mineral Processing and Metallurgical Testing	137
13.1	Introduction	137
13.2	Modelling of the 3Q Process.....	137
13.3	Modeling of the Solar Evaporation Pond System	138
13.4	Experimental Work at 3Q Salar	139
13.5	Lithium Carbonate Process at the Fiambalá Site	142
13.6	Next Steps	151
14.	Mineral Resource Estimates	152
14.1	Method Overview	152
14.2	Resource Model Development	152
14.3	Mineral Resource Zones.....	157
14.4	Brine Characterization within the Resource Model.....	158
14.5	Mineral Resource Estimate.....	164
15.	Mineral Reserve Estimates	166
15.1	Overview	166
15.2	3D Groundwater Flow Model Construction.....	166
15.3	3D Model Calibration	179
15.4	3D Model Configuration for Evaluating Laguna Drawdown and Water Balance Changes.....	183
15.5	3D Model Configuration for Evaluating Reserves.....	183
15.6	Constraints for the Reserve Estimation Pumping Scenario.....	185
15.7	Reserve Estimate Results	188
15.8	2D Model of Freshwater / Brine Interaction	195
15.9	Closing	198
16.	Mining Methods - Wellfield	200
17.	Recovery Methods	204
17.1	Overview	204

17.2	Salar Site	206
17.3	Fiambalá Site	213
18.	Project Infrastructure	221
18.1	Area and Facilities	221
19.	Market Studies and Contracts	237
19.1	Benchmark Mineral Intelligence Market Study	237
19.2	Pricing For Economic Analysis	239
19.3	Contracts	239
20.	Environmental Studies, Permitting, and Social or Community Impact	240
20.1	Sustainability Program	240
20.2	Environmental	240
20.3	Environmental Baseline Studies	241
20.4	Social Responsibility Plan	246
20.5	Governance	247
21.	Capital and Operating Costs	250
21.1	Capital Cost Estimate	250
21.2	Operating Cost Estimate	254
22.	Economic Analysis	258
22.1	Overview	258
22.2	Evaluation Criteria	258
22.3	Income Tax and Royalties	258
22.4	Capital Expenditures	260
22.5	Production Ramp Up and Schedule	260
22.6	Operating Costs	261
22.7	Lithium Carbonate Prices	261
22.8	Production Revenues	261
22.9	Investment and Depreciation	262
22.10	Cash Flow Projection	262
22.11	Economic Evaluation Results	265
23.	Adjacent Properties	268
24.	Other Relevant Data and Information	269
25.	Interpretation and Conclusions	270
25.1	Brine Resources and Reserves	270
25.2	Infrastructure and Process Design	271
25.3	Economic Analysis	272
25.4	Project Risks	272
25.5	Conclusions	273

26.	Recommendations	274
26.1	Brine Resources and Reserves	274
26.2	Engineering	274
27.	List of Abbreviations	276
28.	Date, Signature, and Certificate	280
29.	References	284

Table index

Table 1-1: Summary of the Mineral Resource Estimate at lithium grade cut-off values of 800 and 400 mg/L (Effective Date: October 26, 2021).	23
Table 1-2: Summary of the lithium Reserve Estimate – 3Q Project.	24
Table 1-3: Capital expenditures, estimates for the 3Q Project.	29
Table 1-4: Operating expenditure, estimated for the 3Q Project.	30
Table 1-5: Economic indicators.	30
Table 1-6: Cash flow projection table.	32
Table 2-1: 3Q FS Responsibility Matrix.	38
Table 4-1: Status of mineral claims in the 3Q Project.	51
Table 7-1: Volume and average composition of the Mineral Resource Estimate defined for the 3Q Project (for 800 mg/L lithium cut-off).	81
Table 7-2: Comparison of selected brine chemistry for the Mineral Resource Estimate defined at the 3Q Project (for the 800 mg/L cut-off), with other lithium brine deposits.	81
Table 7-3: Annual water balance for the 3Q Salar, based on flow modelling (Section 15).	88
Table 9-1: Summary of the exploration work reported previously - 3Q Project.	97
Table 9-2: Summary of the 2018-21 exploration work – 3Q Project.	98
Table 9-3: Aquifer hydraulic parameters determined from pumping tests, using FEFLOW.	108
Table 10-1: Summary of diamond drilling contractors and well installation – 3Q Project.	112
Table 10-2: Summary of RBRC results from the diamond cores.	113
Table 10-3: Summary of rotary drilling contractors; monitoring, logging, and downhole geophysical services; and well installation – 3Q Project.	114
Table 14-1: Volume changes in updated geological model relative to the PFS.	156
Table 14-2: Summary of primary geological units in the Resource Model.	156
Table 14-3: Mineral Resource categorization for the 3Q Project, based on borehole spacing and variography. Resource Zones are shown on Figure 14-4.	158
Table 14-4: Summary of the Mineral Resource Estimate at lithium grade cut-off values of 800 and 400 mg/L (Effective Date: October 26, 2021).	165
Table 15-1: Precipitation statistics for 2017 to 2021.	172
Table 15-2: Summary of free water evaporation rates (E_0), calculated with data from the 3Q Vaisala weather station (2017 to 2020).	173
Table 15-3: Calibrated evaporation factors by zone.	173
Table 15-4: Sub-basin outflows estimated with HEC-HMS, and final calibrated outflows used in the numerical model.	177
Table 15-5: Hydrogeological material properties applied in the Groundwater Flow Model.	179

Table 15-6: Calibration statistics for simulated water level residuals.....	180
Table 15-7: Summary of the lithium Reserve Estimate – 3Q Project.....	189
Table 15-8: Concentration trends for additional components in the recovered brine over the 50- year Project life.	191
Table 15-9: Sensitivity of Reserve Estimation and drawdown to hydrogeological characterization.	195
Table 16-1: Construction specifications for the production wells, as simulated for the Reserve Estimate.	200
Table 16-2: Pumping rate schedule for the production wells, as simulated for the Reserve Estimate.	201
Table 17-1: Main Mass Balance Results for the Pre-concentration and Concentration ponds	213
Table 19-1: Price forecast for battery grade lithium chemicals, 2020 real terms (USD/MT).	239
Table 20-1: Taxa of cyanophytes, diatoms, chlorophytes, and indicator invertebrates in sites nearby the 3Q salar.	244
Table 20-2: Actions by NLC which support the UN Sustainable Development Goals.	249
Table 21-1: Total capital expenditures for the 3Q Project.....	250
Table 21-2: Brine production wellfields and pipeline delivery system cost estimate.	251
Table 21-3: Evaporation ponds cost estimate.	251
Table 21-4: Crystallization plant cost estimate.....	252
Table 21-5: Lithium carbonate plant cost estimate.	252
Table 21-6: General services cost estimate.	252
Table 21-7: Infrastructure cost estimate.	253
Table 21-8: Total operational expenditures for the 3Q Project.	254
Table 21-9: Ponds and plants reagents costs.....	255
Table 21-10: Salt harvesting and transportation costs.....	255
Table 21-11: Energy costs.	256
Table 21-12: Manpower costs.	256
Table 21-13: Catering and camp services costs.	257
Table 21-14: Product transportation costs.	257
Table 21-15: Indirect costs.	257
Table 22-1: Capex schedule for the 3Q Project.	260
Table 22-2: Production ramp up and schedule.	261
Table 22-3: Projected lithium carbonate prices.....	262
Table 22-4: Production revenues, constant 2020, USD 000.....	262
Table 22-5: Investment and depreciation schedule - USD 000.	263
Table 22-6: Project summary cash flow projection - USD 000.	264

Table 22-7: Before and after taxes, economic results.	265
Table 22-8: Project After Taxes, NPV (8%) sensitivity.....	265
Table 22-9: Project After IRR Taxes sensitivity.....	266
Table E-1: Summary of drilling specifications – diamond and rotary methods (vertical holes).	310

Figure index

Figure 2-1: Evaluation framework considered applicable to lithium brine prospects.	41
Figure 4-1: Property Location Map – 3Q Project.....	47
Figure 4-2: Catchment area of the 3Q Salar.	48
Figure 4-3: Claims held in the 3Q Project.	52
Figure 5-1: Topography and roads in the 3Q Project catchment.	58
Figure 5-2: Daily solar radiation (calculated on a monthly basis) recorded by the Vaisala weather station – 3Q Project.	59
Figure 5-3: Monthly average air temperature recorded by the Vaisala weather station - 3Q Project.	59
Figure 5-4: Daily total precipitation recorded by the Vaisala weather station – 3Q Project.	60
Figure 5-5: Monthly average relative humidity recorded by the Vaisala weather station - 3Q Project.	61
Figure 5-6: Daily wind speed (calculated on a monthly basis) recorded by the Vaisala weather station – 3Q Project.	61
Figure 5-7: Daily average evaporation (calculated on a monthly basis) recorded by the Vaisala weather station - 3Q Project.	62
Figure 7-1: Geological map of the 3Q Project area (see Figure 7-2, for lithology legend).	67
Figure 7-2: Lithostratigraphic legend for the 3Q Project geological map shown on Figure 7-1.....	68
Figure 7-3: Conceptual cross-section showing structural systems in the vicinity of 3Q Salar.	80
Figure 7-4: Surface stream gauging points in the 3Q Salar watershed.	82
Figure 7-5: Average annual flow rate monitoring data for the main surface streams and laguna levels in the 3Q Salar watershed.	83
Figure 7-6: Bathymetry of Laguna 3Q and Laguna Verde.	84
Figure 7-7: Example of wind fetch effect observed in Laguna 3Q (decreased level) and well PP1-D-4 (increased level), when sustained wind speed is >60 km/h from WNW to NNW. Well PP1-D-8 is shown as an example of a well that is responsive to precipitation but not wind fetch.....	85
Figure 7-8: Salar and laguna piezometric levels collected by data logger and manual methods; rainfall from the Vaisala weather station.....	86
Figure 7-9: General brine flow gradients, based on the salar and lake level monitoring network.	87
Figure 7-10: Surface brine concentration distributions for lithium, potassium, barium, and boron.....	89
Figure 7-11: Surface brine concentration distributions for chloride, sodium, calcium, and sulfate.....	90
Figure 7-12: North-South transect of surface brine concentrations for boron, strontium, barium, calcium, magnesium, potassium, and lithium.	91

Figure 7-13: Simulated evaporation of a water sample from Rio Salado (top). Water and brine samples collected during the first four 3Q Project sampling campaigns, superimposed on simulation results (bottom).	92
Figure 7-14: North-south distribution of lithium, sulfate, strontium, and potassium in subsurface brine samples from the 2017-2021 drilling campaigns.	93
Figure 7-15: Vertical distribution of lithium, sulfate, strontium, potassium, and density in subsurface brine samples from the 2017-2021 drilling campaigns.	94
Figure 9-1: Surface geophysics (VES and Seismic) conducted to date - 3Q Project.	99
Figure 9-2: Chronology of surface brine sampling and monitoring locations in the 3Q Salar.	103
Figure 9-3: Interpolation of the magnesium-lithium ratio in surface brine samples collected in 2015 through 2018.	104
Figure 9-4: Chronology of pumping tests conducted at the 3Q salar.	107
Figure 9-5: Simulated and measured drawdown for 72-hr pumping tests at PB1-R-18 and PB2-R-23.	109
Figure 10-1: Drill platform and borehole locations and chronology – 3Q Project.	111
Figure 11-1: Lithium results for the 2015/16 Program reference samples. Statistics calculated from sample results.	123
Figure 11-2: Potassium results for the 2015/16 Program reference samples. Statistics calculated from sample results.	123
Figure 11-3: Lithium results for mid-range reference samples, compared with Round Robin Mean and Standard Deviation.	125
Figure 11-4: Lithium results for high-range reference samples, compared with Round Robin Mean.	125
Figure 11-5: Potassium results for mid-range reference samples, compared with Round Robin Mean.	126
Figure 11-6: Potassium results for high-range reference samples, compared with Round Robin Mean.	126
Figure 11-7: Field duplicates versus original sample results for lithium (mg/L).	127
Figure 11-8: Field duplicates versus original sample results for potassium (mg/L).	127
Figure 11-9: Field duplicates versus original sample results for magnesium (mg/L).	128
Figure 11-10: Blank sample results for lithium.	129
Figure 11-11: Blank sample results for potassium.	129
Figure 11-12: ASL internal laboratory duplicate results for lithium.	130
Figure 11-13: ASL internal laboratory duplicate results for potassium.	131
Figure 11-14: ASL internal laboratory duplicate results for calcium.	131
Figure 11-15: ASL internal laboratory duplicate results for magnesium.	132
Figure 12-1: Original samples versus QP duplicate lithium samples.	134

Figure 12-2: Original samples versus QP duplicate potassium samples.....	135
Figure 12-3: Original samples versus QP duplicate magnesium samples.	135
Figure 12-4: Original samples versus QP duplicate calcium samples.	136
Figure 13-1: Work window for Pre-Concentration Ponds model fore the 3Q Project.	138
Figure 13-2: Work window for CaCl ₂ process model (ponds and CaCl ₂ Crystallization Plant) at the 3Q Project.	139
Figure 13-3: Work window for the Fiambalá process model.	143
Figure 13-4: SX-B flowsheet.	145
Figure 14-1: Plan of sections used for geological model update (left) and model volume changes relative to the PFS (right).	154
Figure 14-2: Example sections, geological model updates.	155
Figure 14-3: 3D configuration of primary geological units in the Resource Model	157
Figure 14-4: Configuration of Resource classification zones defined for the 3Q Project.....	158
Figure 14-5: Distribution of lithium in the top layer and along the centreline of the Resource Model.	160
Figure 14-6: Distribution of potassium in the top layer and along the centreline of the Resource Model.	161
Figure 14-7: Lithium cut-off grade curves for average concentration and mass.	162
Figure 14-8: Lithium distribution within the Resource, at a range of cut-off grades.	163
Figure 15-1: Conceptual inflow and outflow features of the 3Q Salar. Lateral inputs from sub- basins and vertical input from precipitation are shown in A (plan and section). B, C, and D show three different scenarios for evaporation outputs.	168
Figure 15-2: Footprint of the Reserve Model and topographic surface elevation.	170
Figure 15-3: 3D fence diagrams showing layering of the Resource and Reserve Models.	171
Figure 15-4: Monthly average precipitation and calculated evaporation, from the 3Q Vaisala weather station.	172
Figure 15-5: Spatial distribution of evaporation factors for salar crust and lakes.	174
Figure 15-6: Depth-Dependent Factor (f_{ev}), for salar crust and lakes.	175
Figure 15-7: Locations of specified lateral inflow into the 3Q Salar and lagunas from surrounding sub-basins.	176
Figure 15-8: Measured and simulated inflow from the Rio Salado, based on 2017 monitoring data.	178
Figure 15-9: 3D view of horizontal hydraulic conductivity (top) and geological units (bottom).	179
Figure 15-10: Comparison of simulated and measured water levels.	182
Figure 15-11: Initial lithium grade distribution in plan view (A) and three-dimensional full and cut- away views (B). Resource zones (C).	185
Figure 15-12: Locations of the existing and future production wells.	187

Figure 15-13: Simulated wellhead LEC production over the 50-year Project life.	189
Figure 15-14: Simulated Reserves over the 50-year Project life.	190
Figure 15-15: Simulated average lithium grade trends in pumped brine over the 50-year Project life.....	190
Figure 15-16: Temporal evolution of simulated drawdown in the production wells.	192
Figure 15-17: Temporal progression of simulated average annual drawdown in Lagunas 3Q and Verde.	192
Figure 15-18: Temporal progression of simulated drawdown at ground surface.....	193
Figure 15-19: Progression of the simulated water budget.	194
Figure 15-20: Location of 2D density dependent flow and transport models.....	196
Figure 15-21: Freshwater and mixing zones at the margins of the 3Q Salar, as simulated in the 2D variable density model under natural conditions.	197
Figure 15-22: Depth-dependent drawdown applied beneath Laguna 3Q for the Rio Salado 2D model.	198
Figure 15-23: Simulated change in the freshwater / brine interface due to pumping – 2D Rio Salado model.	198
Figure 16-1: Wellfield and distribution of pumping rates, as simulated for the Reserve Estimate.....	203
Figure 17-1: Block diagram of the process.	206
Figure 17-2: Brine extraction well and pre-concentration ponds.....	208
Figure 17-3: Concentration Ponds and Crystallization Plant.	212
Figure 17-4: Reception Ponds and SX.....	214
Figure 17-5: Stage 0 – Ca and Mg Removal.....	215
Figure 17-6: Stage 1 – Ca(OH) ₂ Precipitation.....	216
Figure 17-7: Stage 2 – CaCO ₃ Precipitation.	217
Figure 17-8: Stage 3 – Li ₂ CO ₃ Precipitation.....	218
Figure 17-9 Drying and Packing.....	218
Figure 18-1: Main installations for the salar site.....	222
Figure 18-2: Salar site – main installations.	226
Figure 18-3: Salar site – workers camp.	227
Figure 18-4: Salar site – contractor’s camp.	227
Figure 18-5: Fiambalá site – general installations.....	230
Figure 18-6: Fiambalá site – plant installations.....	231
Figure 18-7: Fiambalá site – control room for the Lithium Carbonate Plant.	234
Figure 18-8: Fiambalá site – plant access.	235
Figure 18-9: Fiambalá site – offices.	235

Figure 18-10: Fiambalá site – laboratory building.	236
Figure 19-1: Price forecast for battery-grade lithium carbonate and lithium hydroxide, 2020 real terms (USD/MT).	239
Figure 22-1: Projected lithium carbonate prices.	261
Figure 22-2: Project after taxes, NPV (8%) sensitivity.	266
Figure 22-3: Project After Taxes IRR sensitivity.	267
Figure A-1: Selley log locations and correlation line.	290
Figure A-2 Correlation of two outcrop Selley Logs, on the eastern margin of 3Q Salar.	291
Figure B-1: Isopach map for the Fanglomerate unit.	292
Figure B-2: Isopach map for the Lower Sediments unit.	293
Figure B-3: Isopach map for the Massive Halite unit.	294
Figure B-4: Isopach map for the Porous Halite unit.	295
Figure B-5: Isopach map for the Upper Sediments unit.	296
Figure B-6: Isopach map for the Hyper-Porous Halite unit.	297
Figure C-1: Isopach map for the Hyper-Porous Halite unit.	298
Figure C-2: VES section 3.	299
Figure C-3: VES section 4.	300
Figure C-4: VES section 5.	301
Figure D-1: Section interpretation of seismic line 1.	302
Figure D-2: Section interpretation of seismic line 2.	303
Figure D-3: Section interpretation of seismic line 3.	304
Figure D-4: Section interpretation of seismic line 5.	305
Figure D-5: Section interpretation of seismic line 7.	306
Figure D-6: Section interpretation of seismic line 9.	307
Figure D-7: Section interpretation of seismic line 11.	308
Figure D-8: Section interpretation of a composite of seismic lines 10, 11, and 12.	309
Figure G-1: Well capture (particle tracks) at five and 10 years after start of production. The 3D particle tracks are projected onto the 2D surface image.	314
Figure G-2: Well capture (particle tracks) at 20 and 30 years after start of production. The 3D particle tracks are projected onto the 2D surface image.	315
Figure G-3: Well capture (particle tracks) at 40 and 50 years after start of production. The 3D particle tracks are projected onto the 2D surface image.	316

Photo index

Photo 4-1: Seasonal flooding in northern 3Q Salar.....	49
Photo 4-2: Southward view from the north end of Laguna 3Q.....	49
Photo 4-3: View of the 3Q Project Camp.....	50
Photo 5-1: Drilling Platform on 3Q Salar.....	63
Photo 5-2: Pit excavation for shallow brine sampling, on the rough surface of 3Q Salar.....	63
Photo 7-1: (top) Outcrops of andesitic-dacitic rocks of the El Cuerno Formation, in the northwest of the mapped area. (bottom) Brecciated rock in contact with intermediate volcanics	66
Photo 7-2: Outcrops of the El Cuerno Formation, in the southwest of the mapped area, west of Laguna Verde. Outcrops are partially covered by modern deposits (alluvial fans).....	69
Photo 7-3: Los Aparejos Formation. Outcrops assignable to this formation have only been identified in the northern end of the mapped area, immediately north of Laguna 3Q, and could possibly form the deep aquifer (Fanglomerate) observed in salar drilling	70
Photo 7-4: Outcrop of the Tres Quebradas Porphyry, in the north zone of the Project.....	70
Photo 7-5: Interbedded sediments corresponding to Laguna Verde Strata in sandy-silty outcrop (left) and conglomerate facies (right).....	71
Photo 7-6: Reddish sandstone facies assignable to Laguna Verde Strata, east of 3Q Salar.....	71
Photo 7-7: Basaltic volcanic mantles of Pissis in the south sector (Rio Valle Ancho valley).....	72
Photo 7-8: Volcaniclastic deposits corresponding to "Cerro Nacimientos Lavas".....	73
Photo 7-9: Core from the hydrogeological basement, with a dip varying from 5 to 40 degrees.....	73
Photo 7-10: Reddish-grey Fanglomerate in core from PP1-D-22, at a depth of approximately 587 m.....	75
Photo 7-11: Transition between Lower Sediments (reddish-brown) and white Massive Halite, at 461.5 m.....	76
Photo 7-12: Porous Halite shown in core from borehole PP1-D-22, at 78 m depth.....	77
Photo 7-13: The boundary between Upper Sediments and Hyper-Porous Halite.....	78
Photo 7-14: Alluvial fan deposits and filling materials in inactive fluvial channels, on the northwest margin of Laguna Verde.....	79
Photo 9-1: VES equipment.....	100
Photo 9-2: Vibroseis Sercell with seismometers set up at 20 m spacing (left). Interior controls for the seismic equipment (right).....	101
Photo 10-1: Aerial view of diamond drilling platform.....	113
Photo 10-2: Reviewing diamond core, at a storage warehouse in Fiambalá.....	114
Photo 10-3: Rotary drill setup on 3Q Salar.....	115
Photo 11-1: Collecting brine samples from shallow hand-excavated pits.....	116

Photo 11-2: Collecting samples and performing soundings in Laguna 3Q, with hip waders.	117
Photo 11-3: Collecting samples from Laguna 3Q, from a boat.	117
Photo 11-4: Measuring streamflow in 3Q River.	118
Photo 11-5: Measuring field parameters in streamflow.	118
Photo 11-6: Packer assembly being placed in PP1-D-17.	120
Photo 11-7: Progressive clearing of the tracer from the packed interval, as purging proceeds.	120
Photo 11-8: Pumping test setup at well PB2-R-3.	121
Photo 13-1: Views of Pilot Ponds - 3Q Project.	140
Photo 13-2: Work in CaCl ₂ Pilot Ponds - 3Q Project.	140
Photo 13-3: Equipment used in studies by CIMS JRI.	142
Photo 13-4: Analytical laboratory in the Fiambalá Pilot Plant.	144
Photo 13-5: SX-scrubbing and stripping tests.	146
Photo 13-6: Facilities for testing the difference stages of Li ₂ CO ₃ production in the Li ₂ CO ₃ Pilot Plant.	147
Photo 13-7: Pilot settler test and pilot press filter filtration tests.	148
Photo 13-8: Equipment used in stage tests.	148
Photo 13-9: Equipment used for Stage 2 tests.	149
Photo 13-10: Equipment used for pilot tests of Stage 3, counter-clockwise from top: carbonation pilot reactors, lithium carbonate filter, and dryer.	150

Appendices

Appendix A – SELLEY LOG - LOG AND CORRELATION LINE LOCATIONS
Appendix B – ISOPACH MAPS FOR THE SIX SALAR UNITS
Appendix C – VES SECTIONS FROM THE 2017/18 PROGRAM
Appendix D – INTERPRETED SEISMIC SECTIONS
Appendix E – SUMMARY OF ALL DRILLING SPECIFICATIONS
Appendix F – ROUND ROBIN REPORTS FOR MID-RANGE AND HIGH-RANGE REFERENCE SAMPLES
Appendix G – PARTICLE TRACKS FROM FEFLOW, SHOWING PRODUCTION WELL CAPTURE ZONES
Appendix H – LITHIUM MARKET REPORT FOR NLC

1. Summary

1.1 Introduction

The following Technical Report was prepared by Groundwater Insight Inc. (“GWI”) and Worley (“WOR”) at the request of Neo Lithium Corporation (“NLC”). The Report documents a Feasibility Study (“FS”) for the Tres Quebradas (“3Q”) Project, in Catamarca Province, Argentina, and it complies with the requirements of National Instrument (“NI”) 43-101. It builds upon previous Resource and Reserve Estimates and a Preliminary Feasibility Study for the Project (King, 2017; King, 2018; King and Zandonai, 2021). The mineral deposits discussed herein are related to lithium in brine contained within salar deposits and two brine lakes, at the 3Q Salar.

This Report provides a comprehensive assessment of geological, technical, engineering, operational, and commercial aspects (economic analysis) of the 3Q Project. GWI and WOR were commissioned to evaluate the technical merits of the 3Q Project and to determine the conditions under which the 3Q Project should advance to the construction stage.

Preparation of the updated Resource and Reserve Estimates, and supporting documentation, was supervised by Mark King, Ph.D., P.Geol., F.G.C., a “Qualified Person” (“QP”) who is “independent” of NLC, as such terms are defined by NI 43-101. Dr. King supervised preparation of Sections 4 to 12, 14, 15, 20, and 23, as well as associated information in Sections 1, 2, 3, 16, 25, and 26.

Marek Dworzanowski acted as QP for the preparation of engineering materials for this report. Mr. Dworzanowski is an independent metallurgical engineer. He has no relationship with NLC as defined by NI 43-101. Mr. Dworzanowski supervised preparations of Sections 13, 17 to 19, 21, 22, and 24, as well as associated information in Sections 1, 2, 3, 16, 25, and 26.

In addition, the authors relied extensively on NLC and its independent consultants, as cited in the study text and references, for information on costs, prices, legislation, and tax in Argentina, as well as for general project data and information.

1.2 Reliance on Other Experts

The authors have relied upon, and, to the extent permitted under Item 3 of Form 43-101F1, disclaim responsibility for the following expert reports or opinions concerning legal and environmental matters:

- The law firm of Martin and Miguens provided an ownership and claim Title Opinion (February 2021) and an updated claim holdings memo (October 2021), which are summarized in this Report. The Title Opinion states that agreements with third parties are no longer applicable. Sections 4.3 and 4.4 of this Report rely on the Title Opinion and memo. The QPs have not researched title or mineral rights of the Project and express no opinion as to the ownership status of the 3Q Project properties.
- An extensive range of environmental, land use, and climate studies have been conducted for the 3Q Project, with primary contributions by GT Ingeniería SA and Servicios Integrales Mineros Catamarca SRL, as consultant to NLC. These studies are summarized in Section 20.

1.3 Property Description and Location

The 3Q Project is located in the southwestern zone of Catamarca Province, Argentina. The closest paved road to the Project is Ruta Nacional 60 (“RN60”), which connects San Fernando

del Valle de Catamarca (population 212,000), the capital city of Catamarca Province, to the border with Chile, via Paso de San Francisco.

The 3Q Project includes a designated Mining Group covering 26,679.66 ha (the core of which will encompass mining activity) and a further 8682.4 ha, for a total of 35,362.06 ha of tenements in a salar/lake system. The NLC properties are oriented northwest-southeast and extend for 40 km along the bottom of the basin, which includes salar surfaces and brine lakes.

All information regarding the legal status of the 3Q Project tenements (the “Properties”) was provided by the law firm of Martin and Miguens, Argentinean legal counsel for NLC, and includes:

- legal status of the Mining Group, Magdalena Claim, and Lodomar XI Claim (February 2021); and
- acquisition and legal status of the Bautista Claim (October 2021).

This information has not been independently verified by the QP.

NLC, through a wholly owned subsidiary, LIEX, has good and marketable title to 12 Mining Claims and one Exploration Claim that make up the 3Q Project tenements. It is the opinion of NLC legal counsel that:

- LIEX has good and marketable title to each of the claims comprising the 3Q Project Properties as of the date hereof, free and clear of any liens or other encumbrances registered on title with the Mining Authority;
- each of the claims comprising the Properties is in good standing under the applicable laws; and
- there are no competing claims by third parties with respect to the Properties.

NLC legal counsel advises that, up to February 9, 2021, they are not aware of any litigation or undisclosed liabilities involving LIEX. Several specific legal counsel opinions are stated in the subsections below.

The 3Q Project is located in a “Ramsar” site, which is defined as an area with special interest for conservation of freshwater wetlands, particularly with regards to bird nesting sites. Under Argentinean environmental legislation, Mining is permitted in a Ramsar site, provided that it complies with all environmental law requirements.

NLC complies with the environmental regulations of the province of Catamarca, Argentina and international regulations. The baseline study and the Environmental Impact Report for the Project and access areas demonstrate that significant negative environmental impacts can be minimized, and positive impacts may be enhanced with mining activities. There are no aboriginal communities (or inhabitants) in the 3Q Project.

Access to the 3Q Project can be maintained during winter conditions, with appropriate management. Industrial water sources to the 3Q Project camp have remained unfrozen since they were established in October 2016.

There are no other known significant risk factors, besides those noted in this Report, which may affect access, title, or otherwise the right or ability to perform work on the 3Q Project property.

1.4 Accessibility, Climate, Local Resources, Infrastructure, and Physiography

The 3Q Project can be accessed from RN60 via a gravel road at F2 Gauss Kruger coordinates 2,582,627E and 6,943,080N. RN60 is a paved year-round highway that joins the capital city of Catamarca Province (San Fernando del Valle de Catamarca) with the border of Chile, via Paso de San Francisco.

NLC has been collecting meteorological data at the 3Q Project since October 2016, with an automatic “Vaisala” weather station. These data have been compiled and analyzed to support pond engineering and other objectives.

The closest population centre to the 3Q Project is the town of Fiambalá, Argentina (population 5,000). It is located 170 km east of the Project and can be reached from the Project in a driving time of approximately three hours. Tinogasta (population 20,000) is located 210 km from the Project and can be reached in 3.5 hours. The capital city of Catamarca Province (San Fernando del Valle de Catamarca, population 210,000) is 560 km from the Project.

A detailed review of Project infrastructure considerations is provided in Section 18, for the Salar site and for the Fiambalá site.

The catchment area of the 3Q Salar is demarcated by some of the highest volcanoes on earth, including Pissis, Tres Cruces, Nacimiento, and Ojos del Salado (Section 7). These volcanoes are surrounded by extensive lava and pyroclastic flows. The 3Q Salar occupies the centre of a north-south oriented ovoid catchment area approximately 80 km long and 45 km wide. The brine lakes of the 3Q Project are the lowest points in the catchment.

1.5 History

The claims where the 3Q Project is located were staked by a third-party private owner who previously staked six lithium and potassium mining claims in the vicinity of Laguna Verde. On January 11, 2016, this owner assigned the mining rights underlying the six lithium and potassium mining claims to Messrs. Waldo Pérez, Pedro Gonzalez, and Gabriel Pindar.

On April 5, 2016, Messrs. Pérez, González, and Pindar assigned all their rights in these properties to LIEX S.A. in consideration of a nominal aggregate payment of 10,000 Argentinean pesos (approx. \$CDN 890 in the aggregate) and an aggregate 1.5% gross revenue royalty over the claims.

Messrs. Pérez and Pindar, both directors of NLC. LIEX S.A., staked four additional lithium and potassium mining claims in the same area, in January 2016. Two additional claims were also staked by LIEX S.A. in January 2016. LIEX S.A. acquired the final claim (of the current package of 13) through an Assignment of Mining Rights dated October 1, 2021.

The catchment area of the 3Q Salar has a limited history of mining interest. The only known previous exploration campaigns were for gold and copper.

1.6 Geological Setting and Mineralization

Geological mapping of the 3Q Project area was conducted by the Argentinean company Hidroar, on behalf of NLC, during the 2016/17 Field Program. A subsequent geology review and update was led by Santiago Grosso during the 2017/18 Field Program. The work by Mr. Grosso involved a review of previous and new drilling results, borehole geophysical logs, seismic interpretation, VES interpretation, and Tertiary outcrop mapping.

Following the 2018-21 Field Program, a follow-up geology update was undertaken by GWI. This update incorporated new drilling results and borehole geophysical logs into the previous interpretations.

The area within and just outside the 3Q Project catchment is characterized by volcanic cones reaching heights of 6,000 m asl or greater. Successive tectonic episodes and reactivation of hydrogeomorphological dynamics in an extremely arid environment have formed low level drainage networks. This has resulted in conformation of inter-mountain basin areas, such as the 3Q Salar, and positive relief in the area.

Salar in-fill units were differentiated in 3Q Salar and are the target of the current exploration. These salar in-fill units, or geological units, from deepest to shallowest are:

- **Fanglomerate** - overlies the hydrogeologic basement and is composed of fanglomerates, medium-coarse sandstones, and sedimentary breccias;
- **Lower Sediments** - composed of sandstones and siltstones with minor gypsum laminae;
- **Massive Halite** - composed of fine to very coarse-grained halite;
- **Porous Halite** - composed of medium to coarse-grained halite, with granular intervals of loose crystals;
- **Upper Sediments** - composed of reddish sandstones, silty sandstones, gravel, and plastic clays, mixed with halite crystals; and
- **Hyper-Porous Halite** - composed of medium to coarse-grained halite with high inter-crystalline porosity.

The salar units have been mapped through an integrated interpretation of borehole cores, borehole cuttings, seismic surveys, VES surveys, and downhole geophysics.

Overall, the information at the 3Q Project indicates that the lithium and potassium grades and the levels of impurities compare favourably against other brine deposits.

A monitoring network was installed to better understand groundwater behaviour in the 3Q Salar. Groundwater has been monitored in the shallow and deep aquifer units since October 2017.

1.7 Deposit Types

The 3Q Salar has aspects of both evaporite-dominant and clastic-dominant salar types. Within the salar, there is a substantial occurrence of evaporite sequences in excess of 200 m. However, there are also three laterally extensive clastic units (Upper Sediments, Lower Sediments, and Fanglomerate) that show evidence of extended periods of clastic-dominant deposition. Furthermore, there are frequent thin clastic layers, ranging from a few to several cm, within the evaporite units. These clastic layers tend to increase in frequency and/or thickness, with proximity to the formal clastic units, often forming a gradual transition zone from the evaporite units to the clastic units.

1.8 Exploration

An initial reconnaissance and four full field exploration programs have been conducted to date at the 3Q Project to evaluate the lithium development potential of the deposit:

1. Reconnaissance (“Recon”) – 2015 (first reported by King, 2016);
2. Program 1 - 2015/16 (first reported by King, 2016);
3. Program 2 - 2016/17 (first reported by King, 2017);
4. Program 3 - 2017/18 (first reported by King, 2018); and
5. Program 4 – 2018-21 (first reported herein).

Exploration components conducted during the first four exploration programs, previously documented as listed above, include:

- 636 surface brine and water samples collected from the salar surface, lakes, and rivers (including 116 QA/QC samples);
- 55 VES stations along 13 sections throughout and surrounding the salar;
- Seismic survey with 11 lines (total of 49.34 km) within 3Q Salar and the surrounding area;

- 6,145.7 m of diamond drilling in 23 boreholes and construction of 20 wells;
- 310 core samples for analysis of RBRC;
- 3,114.3 m of rotary drilling in 26 boreholes and construction of 27 wells;
- 284 subsurface brine samples (including 66 QA/QC samples) collected from packers and wells; and
- 15 72-hour pumping tests, one three-hour step test, and two six-hour pumping test in pumping trenches.

The 2018-21 Program, first reported herein, consisted of:

- 1,296.0 m of rotary drilling in six boreholes and construction of five wells;
- 70 subsurface brine samples (including 12 QA/QC samples) collected from wells;
- One 19-day pumping test and three 72-hour pumping tests;
- 316 flow rates recorded from 17 river monitoring stations, as part of an ongoing monitoring program that was initiated in December 2016; and
- 441 surface brine and water samples (including 108 QA/QC samples) collected from lakes and rivers as part of an ongoing surface monitoring program.

Results from these exploration programs were used to support the modelling, Resource Estimate, and Reserve Estimate presented in this Report.

1.9 Drilling

Three rounds of drilling have been conducted:

- The first round was done during the 2016/17 Field Program, from January to April 2017;
- The second round was done during the 2017/18 Field Program, from October 2017 to April 2018; and
- The third round was done during the 2018-21 Field Program from February to May 2019 and March to June 2021.

The drilling objectives were as follows:

- To obtain samples for characterizing subsurface brine chemistry;
- To characterize salar geology with continuous cores, downhole geophysics, and other drilling information;
- To install pumping and observation wells for hydrogeological characterization.

Boreholes were planned and grouped in “platforms” where, if feasible, a diamond borehole was installed first on each platform, and used to guide the subsequent installation of rotary boreholes and wells.

1.10 Sample Preparation, Analysis, and Security

All sample collection, QA/QC, and secure transport was performed under the supervision of Waldo Perez, Ph.D., P.Geo. Based on results from the QA/QC Program, the QP considers the 3Q Project dataset to be acceptable for the evaluation of the brine Resources and Reserves at the 3Q Project.

1.11 Data Verification

Dr. Mark King (QP) provided review and input to the design and execution of all rounds of field exploration at the 3Q Project. The QP visited the 3Q Project on five occasions:

- 2015/16 Program: March 2016 for three days to conduct an independent QA/QC program (King, 2016);
- 2016/17 Program: January 2017 for three days during the first drilling campaign (King, 2017);
- 2017/18 Program: October 21-23, 2017 and April 10-14, 2018, during the second drilling campaign (King, 2018); and
- 2018-21 Program: December 12-16, 2018, during the monthly surface water monitoring and sampling program (King and Zandonai, 2021).

Independent sampling was conducted during the first three Programs, and during the monthly monitoring program in December 2018, with previous results first documented in earlier reports (King, 2016, 2017, and 2018; King and Zandonai, 2021). The QP did not visit the 3Q Project to observe the third round of drilling (2018-21 Program) due to COVID-19 travel restrictions. No additional independent sampling was conducted after the December 2018 monthly surface water monitoring and sampling program. However, Dr. King was in frequent communication with NLC and the field team to discuss field methods and monitor results related to drilling, brine sampling, pumping tests, and other exploration activities.

Based on these activities, it is the opinion of the QP that an acceptably rigorous set of field and data interpretation methods were used in preparing the Mineral Resource and Reserve Estimates for the 3Q Project.

1.12 Mineral Processing and Metallurgical Testing

NLC has conducted extensive processing and metallurgical studies as well as pilot test work, to identify the preferred process for its 3Q Project. It was concluded that simple evaporation and precipitation of salts with minimal reagents combined with the industry standard carbonation process can obtain Lithium Carbonate Battery Grade (“BG”) from the brine at the 3Q Project.

Process studies and metallurgical test work suggest that it is convenient to split production units at two processing sites: 3Q Salar and Fiambalá based on the relative advantages of each site.

At the 3Q Salar Site, brine will be extracted from wells, evaporated, and subjected to crystallization of calcium chloride to reach a 3.3% lithium content. This concentrated brine will be trucked to the Fiambalá Site where mainly boron, calcium, magnesium, and sodium are removed from the concentrated brine before reaching carbonation, drying, and packaging where the process finished by producing lithium carbonate ready for export.

The unique environmental conditions at 3Q Salar make it possible to concentrate the brine in evaporation ponds. Space is available to build the ponds in a suitable location, from a geotechnical perspective. The location can accommodate expansion if necessary. In addition, there is enough space for stockpiling waste salts that are a natural by-product of the solar evaporation process.

The tests and modelling performed to date, provide significant information for validation and base line design of the processing flow for the Project. The results provide robust support for the design of the process.

The main studies for each site, their objectives and conclusions are as follows:

- 3Q Salar Site: Sodium chloride, potassium chloride, boric acid, and calcium chloride are removed from the brine to attain a 3.3% lithium concentration.

- The tests conducted in the salar include modelling of the Evaporation Ponds System and operation of 1:600 scale Pilot Evaporation Ponds.
- Crystal properties, sedimentation coefficients, porosity, particle distribution and other physical parameters were obtained.
- Environmental conditions were measured.
- **Fiambalá:** Boron and remaining impurities are removed from the concentrated brine; lithium carbonate is obtained through the designed process.
 - Simulation models have been developed to establish the base line of the process at the Fiambalá Plant. These models enable simulation of the SX-B process and removal of other impurities.
 - The Pilot SX-Boron and Pilot Plan Processing of Stages 0, 1, 2, and 3 are currently in operation and support the process design basis of this study.
 - Simulation models have been developed to establish the base line for operation of the Lithium Carbonate Plant and to consider different routes to produce Battery Grade Lithium Carbonate.

1.13 Mineral Resource Estimate

An updated Mineral Resource Estimate was developed for the 3Q Project using the three-dimensional (“3D”) model FEFLOW (DHI-WASY, 2021). The software was operated by Aqua Insight Inc., specialists in FEFLOW applications. As a check of the Resource calculations, the resource was re-interpolated in Leapfrog software. The QP provided technical oversight of the modelling and considers the results to be valid and appropriate for a Measured, Indicated, and Inferred Mineral Resource Estimate, as defined by the CIM and referenced by NI 43-101.

The Mineral Resource Estimate is summarized in Table 1-1, for two cut-off grades: 400 and 800 mg/L. The Mineral Resource defined by the 400 mg/L cut-off extends for the full extent of the Mineral Resource Zone, from Laguna 3Q in the north to Laguna Verde in the south. Meanwhile, the Mineral Resource within the 800 mg/L cut-off is limited to approximately the northern third of the Mineral Resource Zone.

The presentation of Mineral Resources in this Report conforms with NI 43-101 and CIM Standards. As defined under these standards, Mineral Resources that are not Mineral Reserves do not have demonstrated economic viability.

Table 1-1: Summary of the Mineral Resource Estimate at lithium grade cut-off values of 800 and 400 mg/L (Effective Date: October 26, 2021).

	Lithium Grade Cut-Off 800 mg/L				Lithium Grade Cut-Off 400 mg/L			
	Measured	Indicated	M&I	Inferred	Measured	Indicated	M&I	Inferred
	Volume [m³]				Volume [m³]			
	2.01E+08	1.55E+08	3.57E+08	3.34E+07	4.50E+08	1.13E+09	1.58E+09	7.57E+08
	Average Concentration [mg/L]				Average Concentration [mg/L]			
Lithium	923	922	923	918	792	576	637	561
Boron	1,352	1,343	1,348	1,308	1,140	787	887	744
Potassium	8,366	8,335	8,353	8,210	7,382	5,616	6,119	5,475
Magnesium	1,532	1,529	1,531	1,535	1,402	2,371	2,095	2,301
Calcium	40,560	40,679	40,611	40,772	35,162	31,026	32,202	30,020
Strontium	730	732	731	735	654	571	595	564
Sodium	78,980	78,405	78,730	77,670	82,702	86,413	85,358	88,494
Sulfate	462	442	453	372	377	308	327	290
	Tonnage¹				Tonnage¹			
Lithium	186,000	143,000	328,000	31,000	356,000	652,000	1,009,000	425,000
Lithium Carbonate	988,000	759,000	1,747,000	163,000	1,897,000	3,472,000	5,369,000	2,261,000
Boron	272,000	208,000	479,000	44,000	513,000	891,000	1,404,000	563,000
Boric Acid	1,555,000	1,187,000	2,741,000	250,000	2,934,000	5,098,000	8,032,000	3,218,000
Potassium	1,682,000	1,288,000	2,970,000	275,000	3,322,000	6,360,000	9,682,000	4,142,000
Potash	3,213,000	2,461,000	5,674,000	525,000	6,346,000	12,147,000	18,492,000	7,911,000
Magnesium	308,000	236,000	544,000	51,000	631,000	2,685,000	3,316,000	1,741,000
Calcium	8,155,500	6,287,000	14,443,000	1,364,000	15,824,000	35,131,000	50,956,000	22,713,000
Calcium Chloride	21,590,000	17,416,000	40,006,000	3,777,000	43,834,000	97,313,000	141,147,000	62,916,000
Sulfate	93,000	68,000	161,000	12,000	170,000	348,000	518,000	219,000
	Ratios				Ratios			
Mg/Li	1.66	1.66	1.66	1.67	1.77	4.12	2.27	4.10
K/Li	9.06	9.04	9.06	8.95	9.32	9.75	6.63	9.75
SO₄/Li	0.50	0.48	0.49	0.41	0.48	0.53	0.35	0.52
Ca/Li	43.94	44.10	44.03	44.42	44.39	53.86	34.91	53.48

Note: ¹ Tonnage values are rounded

1.14 Mineral Reserve Estimates

The Mineral Reserve Estimate for the 3Q Project (effective date October 26, 2021) was supported by a numerical groundwater flow and transport model constructed with the finite-element code FEFLOW (DHI-WASY, 2021). The modelling tools were developed and applied by Paul Martin, M.Sc. and Martinus Brouwers, M.A.Sc. with technical direction of the QP. The model incorporated geological, hydrological, hydrogeological, brine chemistry, and geophysical data from 3Q field programs.

To estimate Reserves, the calibrated FEFLOW model was run according to constraints that were identified through discussions with NLC and are related to target grades, flows, and duration. The constraints specified by NLC as targets for the lithium Reserve Estimate include the following:

- The target duration of production is 50 years.
- Production will commence with an initial pond-filling period consisting of:
 - nine months of pumping at 196 L/s at a target blended lithium grade of 647 mg/L;
 - followed by eight months of pumping at 305 L/s at a target blended lithium grade of 647 mg/L;
 - followed by four months of pumping at 305 L/s at a target blended lithium grade of 940 mg/L.
- After initial pond-filling, the target for pumping is to maintain an average rate of 260 L/s.
- After initial pond-filling, the target wellhead production rate is approximately 420,000 tonnes/year of lithium carbonate equivalent (“LCE”). This is achieved with the target pumping rate (260 L/s) and a target blended lithium grade of 940 mg/L, with a tolerance of between 893 and 960 mg/L. The blended grade of recovered brine should be maintained in this range for as long as possible.
- Existing wells should be used to the maximum extent possible with new wells added as required, to meet LCE targets.

Reserve Estimate results (Table 1-2) are summarized as follows:

- Total Reserves (Proven and Probable) are estimated at 1,670,000 tonnes of LCE, over a 50-year life of Project;
- Proven and Probable Reserves for lithium equate to 31% of the Measured and Indicated Resources (5,369,000 tonnes LCE @ 400 mg/L cut-off (Section 14); and
- The average lithium grade predicted for the entire production period is 786 mg/L; it ranges from > 900 mg/L in early years to 585 mg/L at year 50.

The Reserve Estimate was prepared in accordance with the guidelines of National Instrument 43-101 and uses the best practice methods specific to brine Resources and Reserves.

Table 1-2: Summary of the lithium Reserve Estimate – 3Q Project.

Year	Brine Volume ¹ [Mm ³]	Average Lithium Grade ¹ [mg/L]	Lithium Metal [tonnes]		LCE [=5.32xLi] [tonnes]		Resource Recovered ² [%]
			Proven	Probable	Proven	Probable	
1	4.7	655	1,689	1,377	8,993	7,331	0.3
2	9.6	747	3,977	3,181	21,171	16,931	0.7
3-10	65.6	942	38,549	22,111	205,187	117,694	6.0
11-20	82.0	922	48,853	24,850	260,034	132,273	7.3
21-30	82.0	775	41,647	20,454	221,677	108,873	6.2
31-40	82.0	708	37,415	19,535	199,150	103,979	5.6
41-50	82.0	626	31,570	18,695	168,040	99,507	5.0
20 Years	161.9	912	93,068	51,520	495,384	274,229	14.3
Total 50 Years (Reserve Estimate)³	408	786	203,700	110,200	1,084,300	587,600	31

1. Brine produced from outside the Measured + Indicated Resource is included here but excluded from Reserves.

2. Based on Measured + Indicated Resources of 5,369,000 tonnes LCE (400 mg/L cut-off) as presented in Section 14.

3. Reserve Estimate numbers have been rounded.

1.15 Mining Methods – Wellfield

Implementation of the FEFLOW model for Reserve Estimation provided conceptual design characteristics for the simulated brine production wellfield with a total of 15 wells over the 50-year Project life.

1.16 Process Recovery Methods

The 3Q Project production installations are split between two sites, the first one being located on the Tres Quebradas Salar, and the second one is in the vicinity of the Fiambalá town. Salar Site is the location of the Brine Wells, the Evaporation Ponds, as well as the CaCl₂ Crystallization Plant, while the Fiambalá Site will be the location of the Lithium Carbonate Plant.

Concentrated brine will be trucked from the salar site to the Fiambalá site. NLC has determined that there are CAPEX and OPEX savings associated with reducing the project's footprint on the salar, in addition to lower environmental impact, as well as better personnel welfare. This, considering that the salar site is at an average altitude of 4,100 metres above sea level (m asl), and accordingly, it has a harsh mountain climate, and it is very scarcely inhabited, while the Fiambalá site is at an altitude of 1,500 m asl, thus it enjoys a moderate climate, and improved conditions for personnel.

The Fiambalá Li₂CO₃ Plant includes, as a first step, the removal of boron contained in the brine through a solvent extraction (SX) process. From there, the boron free brine will be pumped to precipitation Stage 0, where calcium (Ca) and magnesium (Mg) will be removed through the addition of reagents, followed by solid-liquid separation. Given the high Ca content of the concentrated brine, after Stage 0, another stage is considered, in order to precipitate more of the Ca contained in the brine and re-use it within the process. This is carried out in Stage 1, through the addition of sodium hydroxide (NaOH), followed by solid-liquid separation. While the solids from Stage 1 are re-used in Stage 0, Ca reduced brine is pumped to the next stage (Stage 2), to remove all remaining Ca present in the brine. This is done through the addition of a soda ash solution, followed by solid-liquid separation. Finally, when all the contaminants are removed, the brine will feed a lithium carbonate precipitation stage, where Li₂CO₃ solids will precipitate through the addition of a soda ash solution. Precipitated solid lithium carbonate will then undergo solid-liquid separation, to remove excess liquid, as well as for washing the final product. Dewatered solids will feed the Li₂CO₃ drying stage.

After the drying stage, solid battery grade lithium carbonate will be packed and stored in the final product warehouse. From Fiambalá it can be exported through the ports in Argentina or in Chile.

1.17 Project Infrastructure

The Project Infrastructure to be built at the Salar site is as follows:

- Process installations:
 - Pre-concentration ponds
 - Concentration ponds
 - Crystallization plant (which include all defined equipment: crystallizers, polishing filters, centrifuges, chiller)
 - Dispatch ponds and truck loading area
- Process Ancillary Services:
 - Compressed air generation, storage, and distribution
 - Industrial water treatment plant for production of soft treated water

- Hydrochloric acid storage and distribution
- Electrical generation and distribution (thermal and solar)
- General Ancillary Services
 - Truck and lightweight vehicles workshop
 - Access control station
 - Truck scales
 - Truck parking area
 - Wastewater treatment plant
 - Workers camp installations
 - Canteen/kitchens
 - Laundry rooms
 - Dining rooms
 - Common rooms (recreational activities)
 - Emergency fire stations, plant fire system
 - Polyclinic (first aid area)
 - Fuel storage and distribution stations
 - Non-hazardous and domestic industrial waste management areas
 - Hazardous waste area
- Temporary installations
 - Contractors camp installations

1.18 Market Studies and Contracts

In August 2021, the Company engaged Benchmark Mineral Intelligence (BMI) to complete a comprehensive analysis of the lithium market including current and future demand, current and future supply, and related lithium pricing forecasts. In September 2021 BMI provided an updated report reflecting rapidly changing markets for lithium carbonate.

1.18.1 Lithium Demand

Lithium-ion batteries have become the dominant battery technology for use in Electric Vehicles (EVs), as well as consumer electronics and stationary grid storage. This dominance is likely to continue given the level of investment in lithium-ion battery cell capacity being undertaken at present versus other battery technologies.

The outlook for 2022–2030 has lithium demand growth forecast to significantly outpace increases in supply. The market weakness in 2020 is projected to have added to the probability of delays in the development of projects in the possible and probable categories. Lithium prices will rise due to market deficits and the need to stimulate investment

1.18.2 Lithium Supply

The supply demand balance for mined lithium indicates a significant short to medium term deficit of lithium supply in the market.

This is forecast to change in coming years as a raft of new brine and hard-rock deposits progress from development stage through to production.

1.18.3 Lithium Pricing

Benchmark's price forecast methodology considers three temporal horizons: short-term, medium-term, and long-term.

- Short-term methodology: The short-term outlook on price developments is guided by primary price research conducted by Benchmark's analysts to ascertain the current direction of market pricing.
- Medium-term methodology: Medium- and long-term pricing in commodity markets is often determined by the level at which the highest-cost producer needed to supply the market can continue to operate; for lithium this would be at a cash cost level of around USD 9,000/t LCE (2020 real terms) in 2025. This point informs medium-term price forecast, but due to the ongoing need to incentivise new projects market prices are likely to be well above this level successively each year. Prices are likely to rise well above marginal production costs.
- Long-term methodology (2030–2040): The projects in the pipeline will begin to come through over the coming decade to meet rising demand. Ultimately prices will settle close to a long-term average of USD 12,110/t for lithium carbonate and USD 12,910/t for lithium hydroxide (both in real 2021 terms). At these price levels IRRs provide sufficient incentive for investment over the forecast period.

1.18.4 Pricing For Economic Analysis

The Economic Analysis for the 3Q Project utilized the Benchmark Mineral's Battery Grade Lithium Carbonate pricing scenario up to 2030 (see chapter 19 for more details) and extended the base price of USD 12,110/t lithium carbonate to the end of the mine life.

1.18.5 Contracts

As of the date of this study, the Company had not signed any sales contracts for its future production of lithium carbonate.

1.19 Sustainability Program. Environmental, Social Responsibility, and Governance

The NLC sustainability program emphasizes three main pillars: Environmental, Social and Governance ("ESG"). Following the international commitments of United Nations on Climate Change, NLC has embraced Sustainability Development Goals ("SDGs") as a guide, seeking to create a high standard sustainable industry. NLC ESG program, based on the SDGs has the following values: transparency and open communication with the community, equal opportunities, respect, and commitment.

Environmental

NLC hired two consulting companies to conduct environmental studies: GT Ingeniería SA ("GT") and Servicios Integrales Mineros Catamarca SRL ("Seimcat"). GT developed the following documents:

- The Environmental Baseline Study, completed in 2018;
- The Environmental Impact Report ("EIR") for the exploration stage, completed in 2019; and
- The first version of the Environmental Impact Assessment ("EIA") for the exploitation stage of the 3Q Project, completed in 2019.

Seimcat completed the following documents:

- Updated Environmental Impact Report ("EIR") for the exploration stage in 2021; and

- The updated Environmental Impact Assessment (“EIA”) for the exploitation stage, completed in 2021.

Authorities have granted in due course all the authorizations and permits required for the exploration and test work carried out by NLC at the 3Q Project. The 2021 EIA has been approved and promoted to public audience to be held on December 17, 2021 in Fiambalá, prior to the final approval for construction.

Social responsibility

NLC has developed a Social Responsibility Plan (“SRP”), designed as a tool for managing community affairs, and strengthening the relationship between the Company and the communities in Tinogasta department. The purpose of the SRP is to facilitate communication with the local population, and to strengthen the communication and connection with institutions and public agencies of Fiambalá and Tinogasta municipalities, which are present in the area of influence of the Project. This SRP is led by the community relations team located in Fiambalá and directed by Lic. Matias Berardini.

Governance

In addition to strict compliance with current legal obligations, the company also considers socio-environmental responsibilities required to provide a satisfactory response to the expectations of the stakeholders regarding the Project.

During the 5 years working period NLC had the following consultants:

- In 2016, NLC has contracted Roberto Lencina, member Working Group for the Incorporation of Social Responsibility in the Professional Profile of Engineers and Geologists-Environmental and Social Responsibility Society of the Canadian Institute of Mining, who continues accompanying the team in all Sustainability matters.
- Dr. Jan Boon and Mr. Pablo Lumerman in 2018 to facilitate certification by developing and implementing an auditable set of procedures and protocols that address all dimensions of the CSR
- In March 2021, NLC contracted Golder, an international company and leader in ESG, to conduct an external Due Diligence of the social responsibility program of the company.
- In April 2021, NLC signed a commitment with the Argentine Chamber of Mining Entrepreneurs to adopt the protocols of the HMS program.
- In April 2021, NLC signs a contract with Universidad Nacional de San Martin (“UNSAM”) in order to guide the process of the development of the Sustainability program.

The Company is committed to developing and implementing strategies to promote sustainable development and to protect the environment and the welfare of the people who may be affected by the operations of the Project. These strategies will align the Company’s management system with the principles of Toward Sustainable Mining, program adopted by Argentinian Mining Chamber and certify the Sustainability program of the Company under international standards for the mining sector.

1.20 Capital and Operating Costs

Capital and Operational Expenditures (“CAPEX” and “OPEX”) were estimated by Worley with an accuracy of $\pm 15\%$. CAPEX estimates are shown in Table 1-3 including direct and indirect costs for the implementation of the entire 3Q Project, including:

- Brine production wellfields and pipeline delivery system;
- Evaporation ponds;

- Platforms, earthworks, and earth movements;
- Crystallization Plant;
- Lithium Carbonate Plant;
- General Services;
- Infrastructure; and
- Indirect and Owner's Costs.

The capital expenditure for the 3Q Project, including equipment, materials, indirect costs, and contingencies during the construction period has been estimated at USD 370,550,823. This value excludes interest expenses, sunk costs, legal costs, Mineral licenses costs, escalation and any other start up cost not specifically mentioned in the corresponding detail.

This value includes the following estimations:

- Direct Project Costs are USD 286,928,462;
- Indirect Project Costs are USD 43,920,488; and
- Project Contingencies are USD 39,701,874.

Table 1-3: Capital expenditures, estimates for the 3Q Project.

Area	Description	Capex Schedule			
		2022 (USD 000's)	2023 (USD 000's)	2024 (USD 000's)	Total (USD 000's)
1000	Brine Extraction Wells	16,171			16,171
2000	Evaporation Ponds	37,352	80,930	6,225	124,508
5000	Brine Treatment Plant		18,292	18,292	36,584
4000	Lithium Carbonate Plant		42,600	42,600	85,200
5000	General Services				-
6000	Infrastructure	14,680	9,786		24,466
	Subtotal	68,203	151,608	67,117	286,928
	Indirect Cost	10,440	23,207	10,274	43,920
	Contingencies	4,719	10,489	24,494	39,702
	Total	83,362	185,304	101,885	370,551

Operating Expenses ("OPEX") are presented in Table 1-4. A \pm 15% OPEX estimate for the 20,000 TPY Lithium Carbonate facility has been prepared with a cost of USD 2,953 per tonne produced. This estimate is based on vendor quotes for main costs such as reagents, fuel (diesel and natural gas), electricity and transportation, as well as catering and camp services.

Table 1-4: Operating expenditure, estimated for the 3Q Project.

Operation Costs	USD / Tonne Li ₂ CO ₃	Total USD / Year
DIRECT COSTS		
Chemical Reagents	1,580	31,599,353
Salt Removal and Transport	372	7,434,633
Energy	315	6,295,434
Manpower	264	5,271,845
Reagents & Other Items Transport	329	6,576,850
DIRECT COSTS SUBTOTAL	2,859	57,178,115
INDIRECT COSTS		
General & Administration - Local	32	633,789
Catering & Camp Services	63	1,255,600
INDIRECT COSTS SUBTOTAL	95	1,889,389
TOTAL PRODUCTION COSTS	2,953	59,067,504

Brine processing costs and outputs are based on process definition by computer simulation and test work. Reagent consumption rates were determined by mass balance calculations and validated in our pilot plant operations.

Transportation cost of reagents and final product were obtained from a Logistic Study developed for this purpose.

Energy consumption has been determined on an equipment-by-equipment basis and design utilization rate.

Manpower levels are based on Worley's experience as well as local information provided directly by NLC.

1.21 Economic Evaluation

Complementing the Feasibility Study, an economic analysis of the Project was conducted to determine its financial viability. CAPEX, OPEX, and pricing assumptions described in the different sections of this report were used to produce the results of this model. Table 1-6 shows the Project cash flow projection.

The economic indicators are summarized in Table 1-5.

Table 1-5: Economic indicators.

Disc. Rate	8 %	Pre-Tax NPV, MUSD
NPV	1,129 MUSD	1,630
IRR	39.5 %	Pre-Tax IRR, %
Payback	2.3 years	46.7%

The economics of the 3Q Project are robust and consider all the previous analysis and proper inputs defined by NLC for 50 years of production. The items considered include:

- CAPEX: the capital investment to build the 20,000 TPY lithium carbonate 3Q Project is USD 370.5 million with an accuracy of +/- 15%. This cost covers ponds, facilities, equipment,

infrastructure, direct and indirect costs and includes USD 39.7 million in contingency allowance.

- OPEX: the operating cost of the project has been estimated at USD 2,953 with an accuracy of (+/- 15%) for the 20,000 TPY lithium carbonate production. This cost puts the 3Q project in the lowest quartile cost of production of all lithium projects.
- CAPEX and OPEX estimates for the Project yield approximately USD 1,129 million of NPV, 39.5% of IRR and a Payback period of approximately 2 years and 3 months after taxes, evaluated in real terms for year 2021. Further, the timing for the Project is favorable, given the forecasted demand for lithium over the next 50 years.
- Sensitivity Analysis: shows the project is very resilient under economic pressure. Its low cost structure makes it an attractive investment even under low price scenarios that are typical in the mining industry. Lithium carbonate price has the highest impact on NPV and IRR; while CAPEX and OPEX have a lesser effects on the total results.

Table 1-6: Cash flow projection table.

NLC 3Q PROJECTED CASH FLOW SCHEDULE														
Year	2022	2023	2024	2025	2026	2027	2028	2029	2033	2043	2053	2063	2073	Total
Period			1	2	3	4	5	6	10	20	30	40	50	
Revenues	-	-	194,450	312,722	290,146	272,596	259,021	251,838	243,582	208,219	197,135	197,135	197,135	10,425,070
Li2CO3 Battery grade	-	-	102,342	312,722	290,146	272,596	259,021	251,838	243,582	208,219	197,135	174,703	102,003	10,332,962
Li2CO3 Technical grade	-	-	92,108	-	-	-	-	-	-	-	-	-	-	92,108
Cash Expenditures	-	-	(50,007)	(75,568)	(70,014)	(63,942)	(67,109)	(70,326)	(68,595)	(58,728)	(55,636)	(50,386)	(56,454)	(2,935,060)
OPEX Li2CO3	-	-	(42,517)	(63,382)	(58,703)	(53,258)	(57,153)	(60,802)	(59,401)	(50,869)	(48,195)	(42,783)	(22,112)	(2,484,742)
Provincial Royalty	-	-	(4,558)	(7,480)	(6,943)	(6,580)	(6,056)	(5,731)	(5,525)	(4,720)	(4,468)	(4,631)	(5,251)	(257,444)
Founder's Royalty	-	-	(2,917)	(4,691)	(4,352)	(4,089)	(3,885)	(3,778)	(3,654)	(3,123)	(2,957)	(2,957)	(2,957)	(165,993)
Mining Licenses	-	-	(15)	(15)	(15)	(15)	(15)	(15)	(15)	(15)	(15)	(15)	(15)	(762)
Remediation	-	-	-	-	-	-	-	-	-	-	-	-	(26,119)	(26,119)
Operating Cash Flow	-	-	144,442	237,154	220,132	208,654	191,912	181,513	174,987	149,491	141,500	146,749	140,681	8,131,156
Operating Margin %	-	-	74%	76%	76%	77%	74%	72%	72%	72%	72%	74%	71%	
Non Cash Expenditures	-	-	(226,856)	(79,870)	(80,115)	(6,402)	(7,170)	(5,336)	(2,869)	(2,869)	(2,869)	(2,869)	-	(535,205)
Depreciation	-	-	(222,330)	(74,301)	(74,780)	(1,339)	(1,913)	(2,295)	(2,869)	(2,869)	(2,869)	(2,869)	-	(497,086)
Amortization	-	-	(2,400)	(2,400)	(2,400)	(2,400)	(2,400)	-	-	-	-	-	-	(12,000)
Remediation Allowance	-	-	(2,126)	(3,169)	(2,935)	(2,663)	(2,858)	(3,040)	-	-	-	-	-	(26,119)
Profit Before Taxes	-	-	(82,414)	157,283	140,017	202,252	184,741	176,177	172,117	146,621	138,630	143,880	140,681	7,595,951
Income Taxes	-	-	-	(22,461)	(42,005)	(60,676)	(55,422)	(52,853)	(51,635)	(43,986)	(41,589)	(43,164)	(42,204)	(2,278,785)
Profit After Taxes	-	-	(82,414)	134,823	98,012	141,576	129,319	123,324	120,482	102,635	97,041	100,716	98,477	5,317,166
Depreciation, Amortization & Allowance	-	-	226,856	79,870	80,115	6,402	7,170	5,336	2,869	2,869	2,869	2,869	-	535,205
Operating After Tax Cash Flow	-	-	144,442	214,693	178,127	147,978	136,490	128,660	123,351	105,504	99,910	103,585	98,477	5,852,371
Non Operating Cash Flow	(92,115)	(204,761)	(103,830)	1,387	11,349	419	(4,086)	(4,263)	(2,670)	(533)	(2,670)	(2,641)	11,427	(472,485)
Total Investment	(83,362)	(185,304)	(101,885)	-	-	-	-	-	-	-	-	-	-	(370,551)
VAT on CAPEX	(8,753)	(19,457)	(10,698)	-	-	-	-	-	-	-	-	-	-	(38,908)
Refund VAT on CAPEX	-	-	8,753	19,457	10,698	-	-	-	-	-	-	-	-	38,908
Sustaining Capital	-	-	-	(574)	(1,435)	(2,008)	(2,295)	(2,582)	(2,869)	(2,869)	(2,869)	(2,869)	-	(126,535)
A - Working Capital	-	-	(10,629)	-	-	-	-	-	-	-	-	-	-	(10,629)
Working Capital Δ	-	-	-	(5,216)	1,170	1,361	(974)	(912)	111	1,305	111	127	9,214	10,629
VAT on OPEX	-	-	-	(12,280)	(11,364)	(10,298)	(11,116)	(11,884)	(11,608)	(9,922)	(9,394)	(8,325)	(4,203)	(475,727)
Refund VAT on OPEX	-	-	-	-	12,280	11,364	10,298	11,116	11,696	10,954	9,482	8,426	6,416	471,524
Cash Flow Before Interest and Tax	(92,115)	(204,761)	40,612	238,541	231,480	209,073	187,825	177,250	172,317	148,958	138,830	144,108	152,108	7,630,548
Accumulated Cash Flow (Before Interest and Tax)	(92,115)	(296,876)	(256,263)	(17,723)	213,758	422,830	610,656	787,905	1,484,041	3,180,965	4,603,990	6,082,100	7,630,548	
Income Taxes (30%)	-	-	-	(22,461)	(42,005)	(60,676)	(55,422)	(52,853)	(51,635)	(43,986)	(41,589)	(43,164)	(42,204)	(1,422,228)
After Tax Cash Flow	(92,115)	(204,761)	40,612	216,080	189,475	148,397	132,403	124,396	120,682	104,972	97,241	100,944	109,904	5,351,762
Accumulated After Tax Cash Flow	(92,115)	(296,876)	(256,263)	(40,183)	149,292	297,689	430,092	554,488	1,044,655	2,233,389	3,226,882	4,262,285	5,351,762	
Cumulative Profit Before Taxes	-	-	(82,414)	74,869	214,886	417,138	601,879	778,057	1,464,620	3,158,585	4,590,362	6,066,049	7,595,951	
Cumulative Profit After Taxes	-	-	(82,414)	52,408	150,420	291,997	421,316	544,640	1,025,234	2,211,010	3,213,253	4,246,235	5,317,166	

1.22 Adjacent Properties

There are no known properties adjacent to the 3Q Project where lithium prospecting has been conducted. The only known previous exploration campaigns were for gold and copper, done by El Dorado, Rio Tinto, and Newcrest in the 90's and early 2000's, and by NGEx Minerals in 2019 through 2021.

The nearest lithium brine prospects, projects and mines are located in Argentina and Chile and include:

- Fenix Lithium Mine located 250 km NNE of the 3Q Project, in the salar del Hombre Muerto in the same Province in which the 3Q Project is located (Catamarca), operated by Livent Corp since 1998.
- Sal de Vida Project located in Hombre Muertos salar and operated by Galaxy corp.
- Sal de Oro Project located in Hombre Muerto salar and operated by Posco Corp.
- Blanco Project located 340 km NNW in the Maricunga Salar, Chile, owned by Minera Salar Blanco.
- Laguna Verde Project located 200 km NNE in Chile operated by Ultra Resources.

1.23 Other Relevant Data and Information

There is no other data or information relevant to this report.

1.24 Interpretation and Conclusions

1.24.1 Brine Resources and Reserves

Preparation of the updated Mineral Resource and Reserve Estimates documented in this report, with an effective date of October 26, 2021, was prepared by Mark King, Ph.D., P.Geo., F.G.C.. The mineral deposits that are the focus of these estimates are related to lithium in brine contained within salar deposits and two brine lakes in the 3Q Salar.

The Mineral Resource and Reserve Estimates conform with National Instrument 43-101 (NI 43-101) and the Canadian Institute of Mining, Metallurgy, and Petroleum Definition Standards for Resources and Reserves (CIM Standards). The following interpretations and conclusions are supported by the 3Q Project data collected to date:

- Conditions in the 3Q Salar have led to the accumulation of brine with economic grades of lithium.
- The data indicate that the highest grades occur in the north end of the Resource zone, just south of Laguna 3Q. An evaluation of evaporation pathways indicates that the lithium accumulation is due to evaporation of the inflowing rivers and geothermal springs, especially Rio Salado.
- A numerical flow and transport model was developed to support the updated Reserve Estimate for the Project. The model was developed with FEFLOW software, and it is considered to provide a reasonable representation of site conditions. The model allows prediction of brine recovery trends for the Reserve Estimate.
- Within the wellfield simulated in the model, brine recovery is focused on Measured and Indicated Resources, primarily in the upper three geological units (Hyper-Porous Halite, Upper Sediments, and Porous Halite). The lowest two salar units (Lower Sediments, and Fonglomerate) are known to have reasonable permeability and good lithium grades.

However, they are not currently targeted for brine recovery, because they are almost entirely classified as Inferred Resources.

- The northern area of elevated grade is a particularly useful location to conduct deeper sampling and hydraulic testing, aimed at converting Inferred Resources to Indicated or Measured.
- Numerical modelling results indicate that the 50-year production scenario would have minimal drawdown effects on the Laguna 3Q and Laguna Verde.
- The thickness of the deep Fonglomerate unit remains mostly unconfirmed. It was intercepted by six boreholes but only two reached the bottom of the unit.
- A trend of decreasing magnesium to lithium ratio is indicated towards the north of the Resource zone.

1.24.2 Project Process and Infrastructure

Infrastructure

- Salar Site:
 - The Pre-Concentration Ponds and Concentration ponds will be constructed in the centre of the salar with aggregate sourced nearby. The walls of the ponds and general orientation of the ponds are designed to allow harvesting, and to maximize evaporation.
 - The NaCl salts removed from the Pre-Concentration Ponds will be stockpiled in the south sector of the Salar and will be used as a platform to support future ponds. Potassium salts will be disposed of in a separate stockpile, outside the Salar, for possible future use.
 - For salts removed from the Calcium Removal Ponds System a Salt Storage Facility (SSF) will be built on the southeast side of the Salar. The SSF will include two storage areas with capacities of 8 Mm³ and 42 Mm³ ensuring capacity to the end of life of mine.
 - Power generation is projected to be produced by means of a Photovoltaic - Gas Hybrid System, which reduces power costs. This system can use gas (LNG) to supply additional energy when loads are high or to minimize fuel consumption when loads are low.
 - The industrial water requirements in the Salar will be supplied from regionally available and permitted water wells and from water recovered from the Calcium Chloride Deposit Area.
 - The existing access road to the site will be enhanced to allow the safe transit of trucks and lorries.
- Fiambalá:
 - The Processing Plant will be built in the Industrial Park of Fiambalá. This Plant will have a Boron Extraction System, Calcium and Magnesium removal circuits, Lithium carbonate precipitation, Drying, Packaging and Storage areas preparing for the export of lithium carbonate.
 - The liquid waste from the Solvent Extraction stage and solid waste from the Alkaline Process will be disposed of in storage ponds that include all the necessary infrastructure required by National Regulations.
 - Electricity provided to Fiambalá town comes from Tinogasta Transformer Station via a 33 kV Medium Voltage Line. At present, electricity transport capacity is saturated by Fiambalá local demand. Consequently, it is expected that a second 33 kV Medium Voltage Line capable of transporting the 8 MW required by the plant will be constructed.

- A Water Treatment Plant will be installed to supply drinking water and high purity water required for the process. The industrial water sources are permitted water wells located in the area within the industrial facilities.
- Maintenance facilities are also included in the design within the Fiambalá facilities.

Process and Design

- The 3Q brine Pre-Concentration process can be carried out in a conventional manner (classic dry-harvest operation) through solar evaporation ponds.
- The lithium concentration process for the pre-concentrated brine can be carried out with crystallizers to remove $\text{CaCl}_2 \cdot 6\text{H}_2\text{O}$ from the brine.
- The sequence of evaporation, saturation, supersaturation, and precipitation can be achieved by combining ponds (evaporation) and crystallizer plant (solids handling and solid-liquid separation).
- Boron at the salar is removed by adding a controlled amount of concentrated HCl to promote the formation of H_3BO_3 .
- SX-B process in Fiambalá is able to quantitatively remove boron without lithium co-extraction.
- The Alkaline Process developed by our technicians can produce battery grade lithium carbonate at a very competitive cost as well as reducing freshwater consumption.
- The Pilot Lithium Carbonate Plant in Fiambalá has validated the process design by producing the desired quality of lithium carbonate within the requested parameters of a potential customer.

1.24.3 Conclusions

NLC has de-risked the 3Q Project technically and financially. A systematic low-cost approach and innovative research was applied to overcome the complexity of the brine and site logistics. The recovery process shows a significantly positive NPV for the Project.

Technical work conducted to date is favorable for the economic outlook of the 3Q Project, including the following results.

- 3Q Project exploration has supported the estimation of Mineral Resources and Reserves. The project contains sufficient mineral Reserves to support the feasibility of a 20,000 TPY Lithium Carbonate production facility with a 50-year mine life
- Pumping tests and numerical modelling have confirmed the capacity of the aquifers at the site to produce the brine required by the mine plan
- The economics of the 3Q Project are robust and consider all the previous analysis and proper inputs defined by NLC for 50 years of production
- The market conditions look optimal due to a very high demand scenario that will continue to grow for the foreseeable future.
- In total, the project is attractive for investment and development.

1.25 Recommendations

1.25.1 Resources and Reserves Recommendations

The following exploration and analysis activities are proposed to potentially enhance Resources and Reserves:

Mineral Resources

- It is recommended to drill at least 3 wells down to at least 400 m below salar surface elevation (> 3686 m asl) in the northern high-grade zone to potentially deepen the Measured and Indicated Resources to 250 and 400 m depth, respectively.
- The lower permeable units (Lower Sediments and Fanglomerate) contain about 30% of the Resource, all in the Inferred category. It is recommended to drill six more deep boreholes (target depth 800 m) in the central and northern salar, to potentially deepen the Measured and Indicated Resource zones.
- It is also recommended to drill at least 3 boreholes down to 400 m below ground surface in the Blue Sky zone to the east and south of Laguna 3Q. This area is also east of the current Resource model, and the objective of this drilling is to potentially expand the model towards the east.

Mineral Reserves

- Five additional long term pumping tests should be conducted in association with the Resource drilling recommended above. The tests would target the Lower Sediments and Fanglomerate at depth under the high-grade northern zone, and the Blue Sky zone to the east of the current Resource model. The objective of the tests is to characterize the hydraulic properties of the drilled units.
- Monitoring should continue for the rivers (flow and chemistry), salar brine levels, lake levels and meteorology.
- Results from all the investigations recommended above (drilling, sampling, pumping tests) should be used to define additional Measured and Indicated Resources, as appropriate. The numerical FEFLOW model should then be revised and re-run, to update Reserves.
- The FEFLOW numerical model should be updated on an ongoing basis, as additional exploration, early production, and environmental monitoring data become available.

1.25.2 Engineering Recommendations

This DFS Report indicates favorable economics for the 3Q Project. It is recommended that NLC move forward to complete Detailed Design and commence Construction of critical infrastructure (Roads and Camps), subject to financing.

Recommendations for the 3Q Project

- Continuing immediately with the Detailed Engineering of the Calcium Chloride crystallizer plant.
- Pilot Plant: It is recommended that the pilot plant is changed to operate on a continuous basis to simulate potential problems, and to start training future operators
- It is recommended that subproducts are studied and developed as part of the strategy to minimize waste and further utilize potential project resources
- A cost - benefit analysis should be conducted to evaluate truck fleet ownership versus truck fleet contracting. This study should be preceded by a more detailed transportation evaluation to minimize distances and operational costs.
- Engineering Optimization should be conducted for plant layouts to minimize construction costs and to further define equipment selection criteria (cost, quality, reliability, etc.).

2. Introduction

2.1 Authorization and Purpose

The following Technical Report was prepared by Groundwater Insight Inc. (“GWI”) and Worley (“WOR”) at the request of Neo Lithium Corporation (“NLC”). The Report documents a Feasibility Study (“FS”) for the Tres Quebradas (“3Q”) Project, in Catamarca Province, Argentina, and it complies with the requirements of National Instrument (“NI”) 43-101. It builds upon previous Resource and Reserve Estimates and a Preliminary Feasibility Study for the Project (King, 2017; King, 2018; King and Zandonai, 2021). The mineral deposits discussed herein are related to lithium in brine contained within salar deposits and two brine lakes, at the 3Q Salar.

This Report provides a comprehensive assessment of geological, technical, engineering, operational, and commercial aspects (economic analysis) of the 3Q Project. GWI and WOR were commissioned to evaluate the technical merits of the 3Q Project and to determine the conditions under which the 3Q Project should advance to the construction stage.

Preparation of the updated Resource and Reserve Estimates, and supporting documentation, was supervised by Mark King, Ph.D., P.Geo., F.G.C., a “Qualified Person” (“QP”) who is “independent” of NLC, as such terms are defined by NI 43-101. Dr. King supervised preparation of Sections 4 to 12, 14, 15, 20, and 23, as well as associated information in Sections 1, 2, 3, 16, 25, and 26.

Marek Dworzanowski acted as QP for the preparation engineering materials for this report. Mr. Dworzanowski is an independent metallurgical engineer. He has no relationship with NLC as defined by NI 43-101. Mr. Dworzanowski supervised preparations of Sections 13, 17 to 19, 21, 22, and 24, as well as associated information in Sections 1, 2, 3, 16, 25, and 26.

The QPs relied extensively on NLC and its independent consultants, as cited within the text and references of this Report.

This FS Report is produced for Public Reporting under Canadian NI 43-101 (2014), and was prepared in accordance with the requirements of:

- Disclosure and reporting requirements of the TSV Venture Exchange (TSX);
- Canadian National Instrument 43-101, Standards of Disclosure for Mineral Projects, Form 43-101F1 and Companion Policy 43-101CP (NI 43-101, 2016);
- Canadian Institute of Mining, Metallurgy and Petroleum Definition Standards (CIM, 2014); and
- Canadian Institute of Mining, Metallurgy and Petroleum, Best Practice Guidelines for Resource and Reserve Estimation for Lithium Brines (Hains, 2012).

All figures in this Report were prepared for this Report, unless otherwise indicated.

The results presented in this FS Report are a guide to indicate the potential reward versus risk for the 3Q Project and should not be regarded as a final measure of value at this stage of study.

2.2 Report Responsibility Matrix

In preparing this report, GWI and WOR relied on information from NLC and their independent consultants. GWI and WOR have verified this information, making due inquiry of all material issues. QP responsibilities for the various sections of the report are shown in Table 2-1.

Table 2-1: 3Q FS Responsibility Matrix.

Item	Section	Lead Company	Responsible Qualified Person
1	Summary	All	Mark King / Marek Dworzanowski
2	Introduction	All	Mark King / Marek Dworzanowski
3	Reliance on Other Experts	All	Mark King / Marek Dworzanowski
4	Property Description and Location	GWI	Mark King
5	Accessibility, Climate, Local Resources, Infrastructure, & Physiography	GWI	Mark King
6	History	GWI	Mark King
7	Geological Setting and Mineralization	GWI	Mark King
8	Deposit Types	GWI	Mark King
9	Exploration	GWI	Mark King
10	Drilling	GWI	Mark King
11	Sample Preparation, Analyses, and Security	GWI	Mark King
12	Data Verification	GWI	Mark King
13	Mineral Processing and Brine Testing	NLC	Marek Dworzanowski
14	Mineral Resource Estimates	GWI	Mark King
15	Mineral Reserve Estimates	GWI	Mark King
16	Mining Methods - Wellfield	GWI	Mark King / Marek Dworzanowski
17	Recovery Methods	NLC/WOR	Marek Dworzanowski
18	Project Infrastructure	WOR	Marek Dworzanowski
19	Market Studies & Contracts	NLC	Marek Dworzanowski
20	Environmental Studies, Permitting & Social/Community Impacts	NLC/GWI	Mark King
21	Capital & Operating Costs	WOR	Marek Dworzanowski
22	Economic Analysis	NLC	Marek Dworzanowski
23	Adjacent Properties	GWI	Mark King
24	Other Relevant Data and information	All	Marek Dworzanowski
25	Interpretation and Conclusions	All	Mark King / Marek Dworzanowski
26	Recommendations	All	Mark King / Marek Dworzanowski

2.3 Sources of Information

Mark King, Ph.D., P.Geo., F.G.C. has 33 years of experience as a consulting hydrogeologist. He has served as Technical Manager on major groundwater projects in Canada, the United States, and South America. His expertise is an appropriate foundation for a lithium brine QP, based on the following:

- He has worked, in various levels of detail, on more than 18 salars in Chile, Argentina, and Nevada.
- From 2009 to 2012, Dr. King served as the QP for three rounds of NI 43-101 Reports for Lithium Americas, culminating in a lithium brine Reserve Estimate.
- Over a three-year period, concluding in 2016, he directed SEAWAT modelling efforts related to an Albemarle permit application at Salar Atacama.
- In 2011, Dr. King served as the independent QP for work conducted by Talison Lithium, at the Salares Seven Lithium Brine Project in Chile.

- From 2013 to present, he conducted Due Diligence Studies of seven different salars in Argentina and Chile, for four different clients.
- From 2016 to present, Dr. King supervised preparation of four previous Technical Reports for the 3Q Project (King, 2016, 2017 and 2018; King and Zandonai, 2021); and contributed certain sections of a third Technical Report for the Project (Pitts, 2017).
- From 2016 to 2018, he directed the development of conceptual and numerical models for the Albemarle Silver Peak lithium brine deposit in Clayton Valley, Nevada.
- In 2017, he directed a Resource Estimate for Albemarle at Salar de Antofalla in Argentina.
- In 2019, Dr. King served as one of two QPs for the NI 43-101 compliant Technical Report on Resource and Reserve Estimates for the Albemarle Salar Atacama Project, which was prepared for submission to the Chilean Nuclear Energy Commission (CCHEN).

In many of the subject areas covered in this Report, Dr. King has relied on other experts, including the following:

- Initial geological mapping of the site was conducted by the Argentinean company Hidroar. Hidroar also conducted an independent check comparison of the cores and logs.
- Seismic interpretation and a second round of geological mapping and was provided by Mr. Santiago Grosso. Mr. Grosso added to the geological interpretation provided in Section 7; he also led the cross-sectional interpretation that formed the basis of the previous solids model discretized into Vulcan.
- Initial Vulcan Resource block modelling for the previous Resource Estimate (King 2018; Zandonai and King, 2021) was done by Argentinean Geologist Mr. Daniel Quiroga, a specialist in that software.
- FEFLOW Resource modelling for the current Resource Estimate was done by Paul Martin, P.Eng. and Martinus Brouwers, M.A.Sc., of Aqua Insight Inc., specialists in that software.
- The Mineral Reserve Estimate for the 3Q Project was supported by a numerical groundwater flow and transport model constructed with the finite-element code FEFLOW (DHI-WASY, 2021). The model was developed and applied by Paul Martin, P.Eng., and Martinus Brouwers, M.A.Sc., of Aqua Insight Inc., with technical direction of the QP.
- Details of the 3Q Project field programs were discussed in detail with Waldo Perez, Ph.D., P. Geo. (EGBC, Canada), in advance of the field work. Dr. Perez is CEO and President of NLC. He is a geologist with a technical background in mineral exploration, including lithium brines.

Marek Dworzanowski is an independent consulting metallurgical engineer with 40 years experience in the global mining industry. He holds a BSc(Hons) in Mineral Processing from the University of Leeds. He is an honorary Fellow of the Southern African Institute of Mining and Metallurgy (FSAIMM), membership number 19594. He is a Fellow of the Institute of Materials, Minerals and Mining (FIMMM), membership number 485805. He is registered as a Chartered Engineer with the Engineering Council of the United Kingdom, registration number 485805.

His expertise is an appropriate foundation for a lithium brine QP, based on the following:

- QP for the Minera Salar Blanco PEA for Proyecto Blanco in Chile in 2017;
- QP for Millennial Lithium PEA for the Pastos Grandes Project in Argentina in 2018;
- QP for Advantage Lithium PEA for the Cauchari Project in Argentina in 2018;
- QP for the Minera Salar Blanco FS for Proyecto Blanco in Chile in 2018;
- QP for Millennial Lithium FS for the Pastos Grandes Project in Argentina in 2019;

- QP for Advantage Lithium PFS for the Cauchari Project in Argentina in 2019;
- QP for Standard Lithium PEA for the Lanxess Smackover Project in the USA in 2019; and
- QP for Centaur Resources PEA for Proyecto Pacha in Argentina in 2019.

In many of the subject areas covered in this Report, Mr. Dworzanowski has relied on NLC and Worley.

Site studies by qualified contractors and consultants, exploration data from past work by the Company, and claim information documentation supplied by legal counsel used in this Report were made available to the QPs by NLC.

WOR's cost estimation and design work has relied on information and criteria from its project database. For major capital equipment items and raw materials, WOR has requested budgetary quotations from third parties.

2.4 Special Considerations for Brine Resources

2.4.1 Overview of Evaluation Framework

NI 43-101 applies to all disclosures of scientific or technical information for mineral properties owned by, or explored by, companies which report these results on stock exchanges within Canada. NI 43-101 defines the term "mineral project" as "any exploration, development or production activity **in respect of** a natural solid inorganic material, including industrial minerals."

The exploration activity on the 3Q Project is **in respect of** lithium, a natural solid inorganic material, which is an industrial mineral. The natural occurrence of the lithium within a liquid, i.e., brine, does not preclude the application of the NI 43-101 reporting framework, although certain evaluation approaches are required that will be different to those used for solid phase mineralization.

NI 43-101 provides a rigorous reporting framework for mineral projects hosted in brine while also providing the necessary flexibility to accommodate the characteristics and analytical parameters specific to brine. Furthermore, reporting on mineral projects hosted in a brine pursuant to NI 43-101 provides the necessary level of protection expected by investors.

The approach used herein to evaluate the Resources and Reserves of the 3Q Project is based on the framework in the CIM Standards, with some enhancements to accommodate the special considerations for brine.

The CIM Standards define a Mineral Resource as:

"a concentration or occurrence of solid material of economic interest in or on the Earth's crust in such form, grade or quality and quantity that there are reasonable prospects for eventual economic extraction."

And a Mineral Reserve as:

"the economically mineable part of a Measured and/or Indicated Mineral Resource. It includes diluting materials and allowances for losses, which may occur when the material is mined or extracted and is defined by studies at Pre-Feasibility or Feasibility level as appropriate that include application of Modifying Factors. Such studies demonstrate that, at the time of reporting, extraction could reasonably be justified."

The evaluation framework used for this Project is shown on Figure 2-1. The figure identifies the primary enhancements to conventional, solid phase, mineral evaluation, namely: 1) characterization of host formation porosity (for Resources), and 2) characterization of host formation permeability and boundary conditions (for Reserves). Certain components of this

framework are enhancements of, or otherwise in addition to, those already contained in the CIM Standards as provided by CIM (2014) and in OSC, APGO, and TSX (2008).

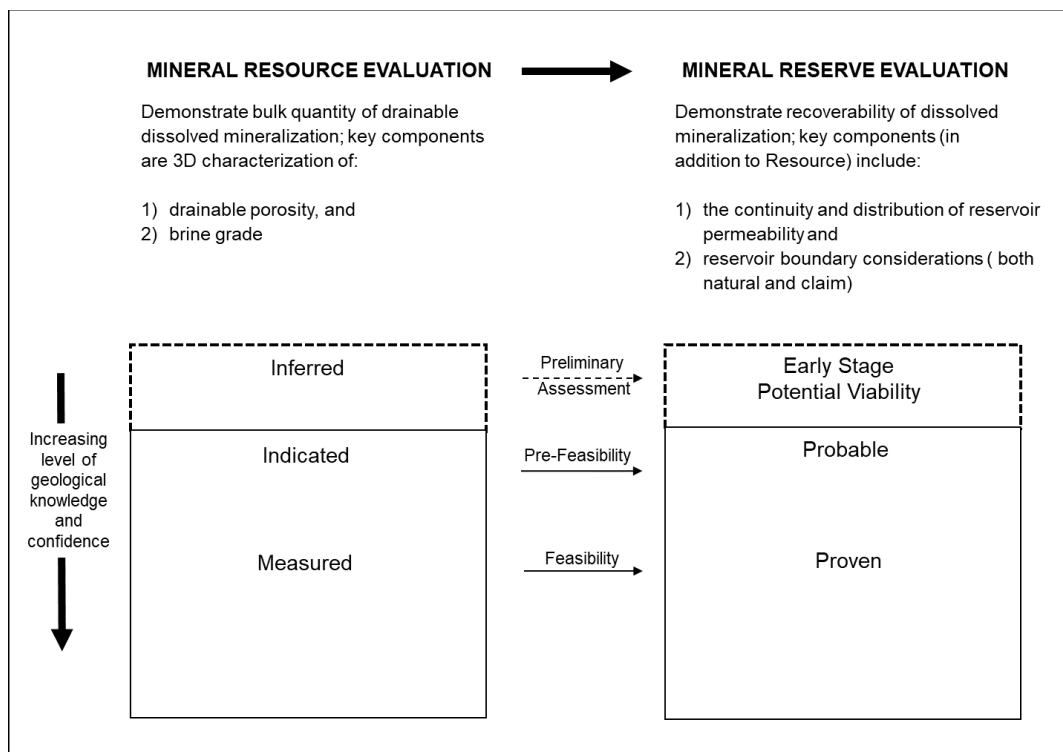


Figure 2-1: Evaluation framework considered applicable to lithium brine prospects.

2.4.2 Brine Resource Estimation – Porosity

Evaluation of the Resource potential of a brine deposit includes estimation of two key components:

- the continuity and distribution of brine grade; and
- the portion of host material that contains drainable brine (i.e., the drainable porosity).

The first of these is analogous to solid deposits. Brine grade is determined through detailed sampling and an understanding of site geology, conceptually similar to solid deposit exploration. The second component (drainable porosity) does not have a direct analogy to solid deposits. The term “porosity” denotes the ratio of the volume of void spaces in a rock or sediment to the total volume of the rock or sediment (e.g., Fetter, 1994). It is relevant to brine deposits because brine occurs in the pore spaces of a rock or sediment. However, not all the brine present in the pore space constitutes a Resource. A portion of the brine will not be recoverable due to:

- partial retention of brine by capillary tension within the pore spaces; and
- dead-end pores that are not hydraulically connected to the broader pore network.

For a brine Resource Estimate, a porosity-related parameter known as Specific Yield (“Sy”) has come into common use to estimate the drainable portion of host material. Sy is defined as the ratio of the volume of water a rock or soil will yield by gravity drainage to the bulk volume of the rock or soil (e.g., Fetter, 1994). Meanwhile, Total Porosity (“P”) is defined as ratio of the total pore space of a rock or soil to the bulk volume of the rock or soil. Consequently, the difference between P and Sy is that portion of the pore space that will not drain under gravitational forces.

Brine Resource Estimates are supported by the development of a geological model which, at the Resource Estimate stage, is primarily used to characterize the distribution of Sy throughout the zone of estimation.

2.4.3 Brine Reserve Estimation – Permeability and Boundary Conditions

A more sophisticated model is required for brine Reserve Estimation, as described in Section 15 of this report. In addition to the full range of modifying factors, this advanced level of estimation evaluates the volume of brine that can be recovered from the basin, taking technical considerations into account. These technical considerations are both site- and deposit-specific, regardless of whether a mineral deposit is solid or brine. However, the two following considerations are unique to brine deposits and are incorporated into the numerical flow model developed for the Reserve Estimate:

- the continuity and distribution of permeability (a measure of the ease with which brine can be pumped from the brine reservoir); and
- brine reservoir boundary conditions (applicable for brine flow and grade).

Permeability is evaluated through testing to define values for two primary hydraulic properties of the host material:

- hydraulic conductivity—a coefficient of proportionality describing the rate at which water can move through permeable media (e.g., Freeze and Cherry, 1979); and
- specific storage—the volume of water that a unit volume of aquifer releases from storage in response to a unit decline in hydraulic head (e.g., Freeze and Cherry, 1979).

These properties were evaluated with aquifer pumping tests and numerical modelling (Section 9.66 and Chapter 15 respectively).

Setting the reservoir boundary conditions involves specification of fluid flow and grade at the boundaries around the brine reservoir. These specified conditions affect the predicted response of the brine deposit to production pumping. They are required for the Reserve Estimate because they determine the predicted duration and rate at which the brine can be pumped before unacceptable effects occur, which may include (depending on the site):

1. Recovery of non-economic grades (due to brine dilution),
2. Excessive drawdown at production wells,
3. Environmental effects on nearby surface water bodies, or
4. Effects to third party property holders.

For this Project, boundary conditions were evaluated with pumping tests, numerical modelling results, hydrogeological interpretations, targeted boundary investigation programs, and assessment of brine grade distributions.

2.5 Details on Property Inspection by QPs

Mark King (QP for Resource and Reserve Estimation) conducted the following 3Q Project field and office activities that are relevant to the current Report:

- He supervised preparation of four previous Technical Reports for the 3Q Project (King, 2016, 2017, and 2018; King and Zandonai, 2021).
- He contributed certain sections of a fifth Technical Report for the 3Q Project (Pitts, 2017).
- In advance of all four Field Programs (including the most recent 2018-21 Program) Dr. King engaged in frequent discussions with NLC, to ensure acceptability of the dataset.

- He visited the 3Q Project during the 2015/16, 2016/17, and 2017/18 Field Programs, and once during a monthly monitoring and sampling program in December 2018 (2018-21 Program). He conducted independent sampling during these three Programs and during the monthly monitoring program.
- During the October 2017 and April 2018 visits to the site, Dr. King met with the expert team assembled by NLC to assist in designing the Field Program and interpreting the results. This team included: a seismic specialist (Santiago Grosso), a geochemist and numerical modeller (Dr. Sergio Bea); a stratigraphy specialist (Dr. Sergio Georgieff), and a structural geology specialist (Dr. Jose Sosa Gomez).
- Also, during the October 2017 and April 2018 field visits, Dr. King reviewed core and cuttings available up to that time, with the 3Q expert team.
- From July 10-12, 2018, Dr. King worked out of the Mendoza office of NLC with Daniel Quiroga. Mr. Quiroga is a geologist with expertise in Vulcan, the software used to quantify the previous Mineral Resource Estimate documented in King (2018) and King and Zandonai (2021).
- Dr. King did not visit the 3Q Project during the drilling and exploration components of the 2018-21 Program due to COVID-19 travel restrictions. However, Dr. King was in frequent communication with NLC and the field team to discuss field methods and monitor results related to drilling, brine sampling, pumping tests, and other exploration activities.
- Throughout all Field Programs, Dr. King was in frequent communication with NLC and the field team, to discuss field methods, performance, and ongoing results.
- Dr. King worked closely with Paul Martin, M.Sc., P.Eng., and Martinus Brouwers, M.A.Sc., on development of the FEFLOW hydrogeological model and numerical model that support the Resource and Reserve Estimates presented in this report.

Dr. King (QP) is of the opinion that the geological and hydrogeological work conducted for the 3Q Project meets or exceeds international and CIM standards.

Mr. Marek Dworzanowski, QP for the Engineering in this report, spent seven nights in quarantine in Mendoza, Argentina, from February 4-10, 2021, due to COVID-19 regulations. Then three nights were spent in Fiambalá in Catamarca Province, from February 11-13, 2021. During this time the following activities were conducted to gain familiarity with the 3Q Project:

- Friday February 12: Mr. Dworzanowski visited the LIEEX offices, Pilot Plant, and LIEEX's analytical laboratories in Fiambalá. The site of the future lithium carbonate plant in Fiambalá was also visited.
- Saturday February 13: Mr. Dworzanowski visited the 3Q Salar. During this time, Mr. Dworzanowski saw the original pilot evaporation ponds; the current pilot evaporation ponds in operation; the northern part of the salar, which constitutes the current reserves and resources; a number of production wells; the site for the future production evaporation ponds; camp facilities; the analytical laboratory; and the 70 km mine road from Route 60 to the camp.

2.6 Statement of Independence

About Groundwater Insight Inc. (GWI) and Dr. Mark King

GWI is an independent consulting company, and Dr. Mark King is President of the company. GWI was contracted by NLC to develop this FS report. Neither GWI, nor Dr. King, have, or have had previously, any material interest in NLC or mineral properties in which NLC has any interest. The relationship of GWI (and Dr. King) with NLC is solely one of professional association between client and independent consultant.

About WOR

WOR is an independent consulting company contracted by NLC to develop this FS report. Neither WOR, nor the authors of this report, have or have had previously, any material interest in NLC or the mineral properties in which NLC has any interest. WOR's relationship with NLC is solely one of professional association between client and independent consultant.

This report is prepared in return for professional fees based upon agreed commercial rates and the payment of these fees is not contingent on the results of this report. No member or employee of WOR is, or is intended to be, a director, officer, or other direct employee of NLC.

About Marek Dworzanowski

Marek Dworzanowski is an independent consulting metallurgical engineer. He has not had any material interest in NLC, and he is an independent consultant for NLC and for WOR. The relationship of Marek Dworzanowski with NLC is solely one of professional association between client and independent consultant.

2.7 Units of Currency

Unless otherwise stated, all units used in this report are metric. The concentration of dissolved brine constituents, including lithium, is reported in mg/L, unless otherwise noted. All currency values in the report are expressed in US dollars ("USD"), and sometimes million US dollars ("MMUSD").

2.8 Use of Report

WOR and GWI prepared this report with data and information provided by NLC and third parties, in accordance with National Instrument 43-101 and NI 43-101 F1 pursuant to the agreed contractual terms of the present engagement. WOR and GWI represent that reasonable care was exercised in preparing of this report, that the report complies with published industry standards for such works, and that it is subject to the terms and conditions of engagement between GWI and NLC and WOR and NLC.

The recommendations and opinions contained in this report assume that unknown, unforeseeable, or unavoidable events will not occur. Such events may adversely affect the cost, progress, scheduling, or ultimate success of the Project. Any discussion of legal issues contained in this report merely reflects technical analysis on the part of GWI and WOR and does not constitute legal opinions or the advice of legal counsel.

GWI and WOR have relied extensively on reports, opinions, and statements of various third-party experts and on the Company on matters relating to legal, political, environmental, tax, and pricing of commodities for which pricing is not publicly available. While GWI and WOR believe that such information is true and accurate, GWI and WOR disclaim any and all responsibility and liability in relation thereto. In this regard, legal information concerning title to the 3Q Project may be found in Section 4 for the Project site. Project environmental considerations are found in Section 20. Lithium Carbonate BG commodity pricing is found in Section 19.

Expected accuracy of the estimates contained in this report is $\pm 15\%$.

This report is considered current as of October 26, 2021.

3. Reliance on Other Experts

The authors have relied upon, and, to the extent permitted under Item 3 of Form 43-101F1, disclaim responsibility for, the following expert reports or opinions concerning legal and environmental matters:

- The law firm of Martin and Miguens provided an ownership and claim Title Opinion (February 2021) and an updated claim holdings memo (October 2021), which are summarized in this Report. The Title Opinion states that agreements with third parties are no longer applicable. Sections 4.3 and 4.4 of this Report rely on the Title Opinion and memo. The QPs have not researched title or mineral rights of the Project and express no opinion as to the ownership status of the 3Q Project properties.
- An extensive range of environmental, land use, and climate studies have been conducted for the 3Q Project, with primary contributions by GT Ingeniería SA and Servicios Integrales Mineros Catamarca SRL, as consultant to NLC. These studies are summarized in Section 20.

4. Property Description and Location

4.1 Location

The 3Q Project is located in the southwestern zone of Catamarca Province, Argentina (Figure 4-1). The closest paved road to the Project is Ruta Nacional 60 (“RN60”), which connects San Fernando del Valle de Catamarca (population 212,000), the capital city of Catamarca Province, to the border with Chile, via Paso de San Francisco.

The closest population centre to the 3Q Project is the town of Fiambalá, Argentina (population 5,000). It is located 170 km east of the Project and can be reached from the 3Q Project in a driving time of approximately three hours. The capital city of Catamarca Province (San Fernando del Valle de Catamarca) is 560 km southeast of the 3Q Project.

4.2 Description

The 3Q Project includes a designated Mining Group covering 26,679.66 ha (the core of which will encompass mining activity) and a further 8,682.40 ha, for a total of 35,362.06 ha of tenements in a salar/lake system, as shown on Figure 4-2, and Photo 4-1, 4-2, and 4-3. The NLC properties are oriented northwest-southeast and extend for 40 km along the bottom of the basin, which includes salar surfaces and brine lakes. The surface elevations and areas of the brine lakes are somewhat variable, depending on antecedent weather conditions. The lakes are described in more detail in Section 7.6.2.

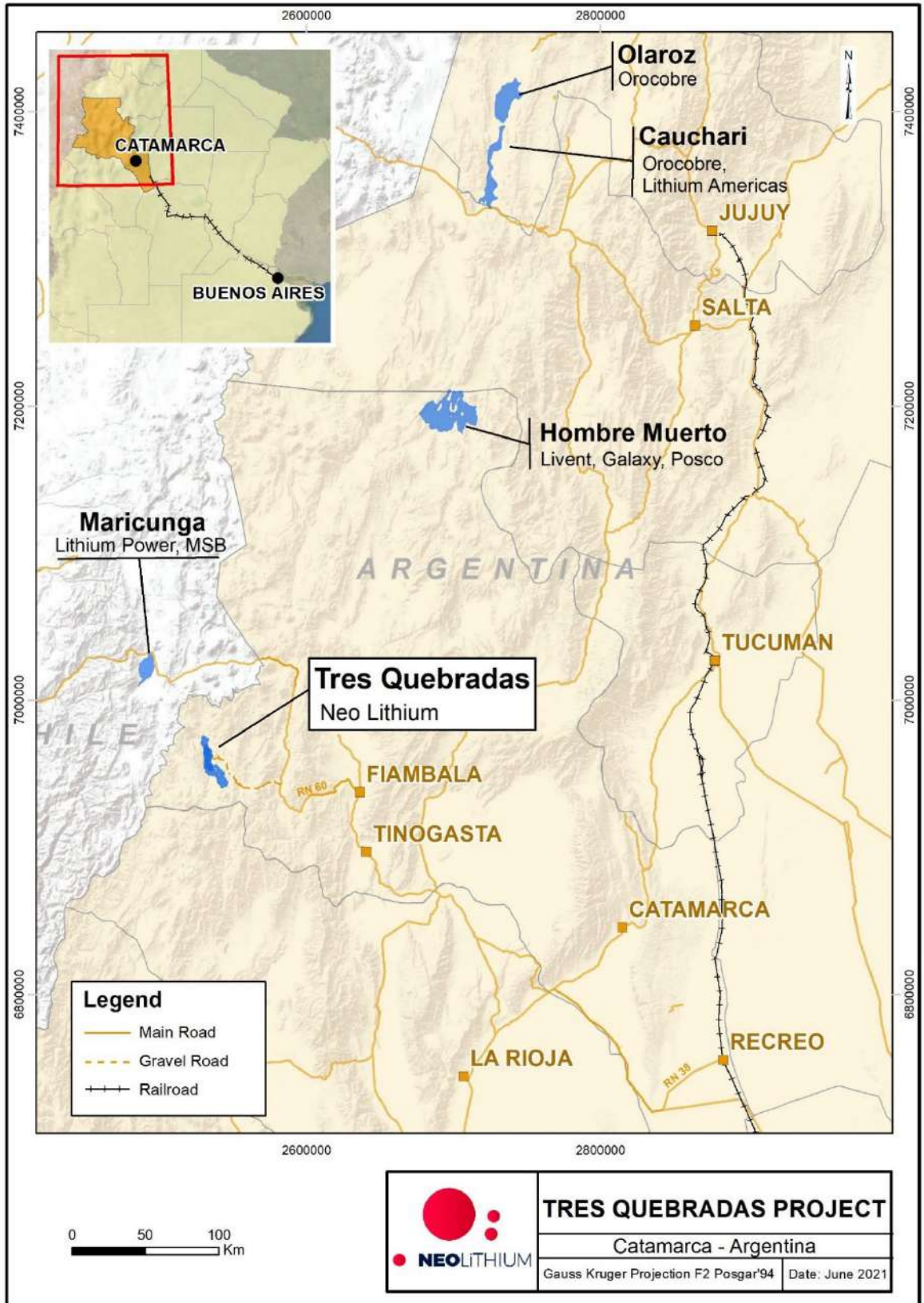


Figure 4-1: Property Location Map – 3Q Project.

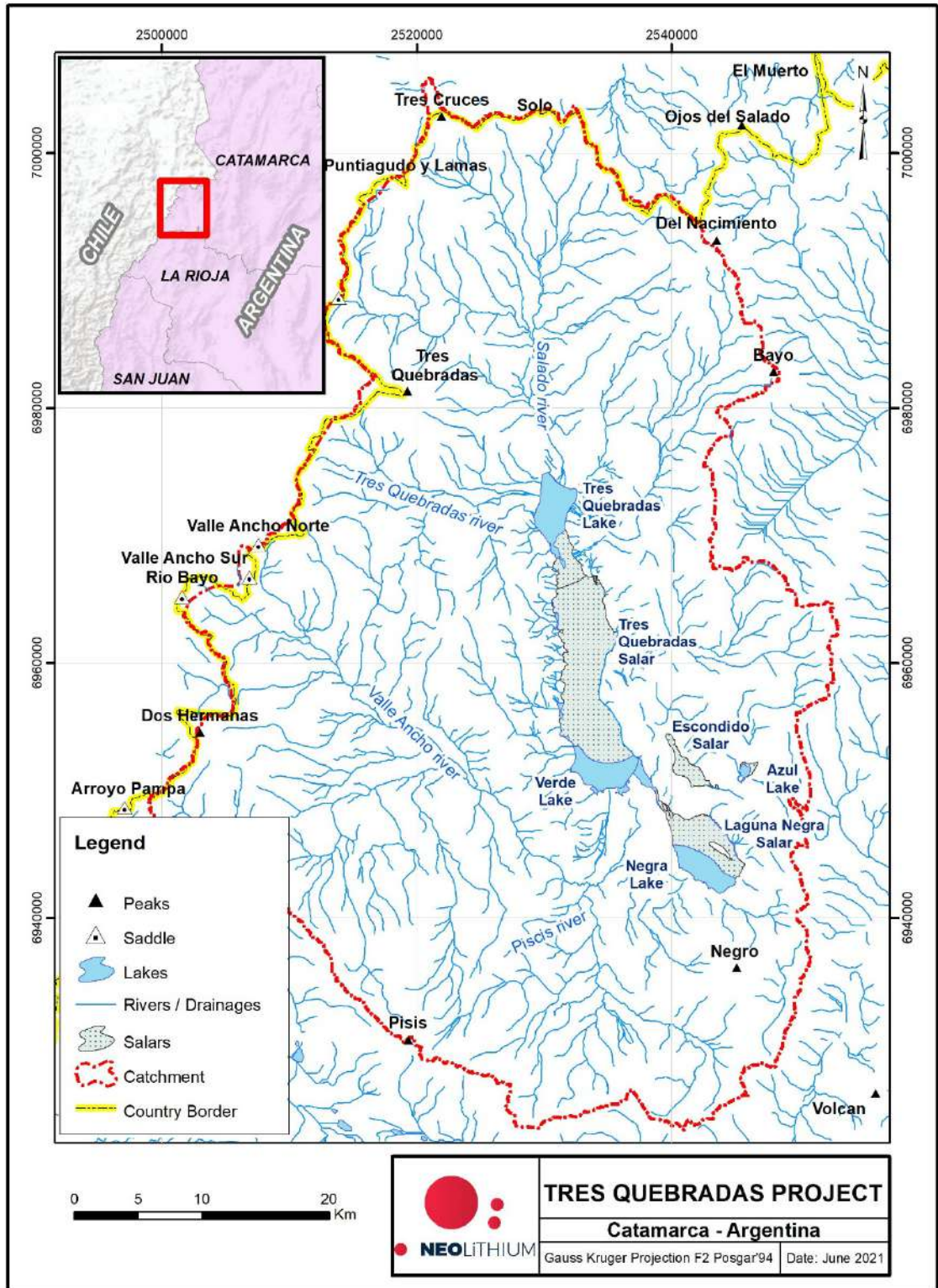


Figure 4-2: Catchment area of the 3Q Salar.



Photo 4-1: Seasonal flooding in northern 3Q Salar.



Photo 4-2: Southward view from the north end of Laguna 3Q.



Photo 4-3: View of the 3Q Project Camp.

4.3 Type of Mineral Tenure

All information regarding the legal status of the 3Q Project tenements (the “Properties”) was provided by the law firm of Martin and Miguens, Argentinean legal counsel for NLC, and includes:

- legal status of the Mining Group, Magdalena Claim, and Lodomar XI Claim (February 2021); and
- acquisition and legal status of the Bautista Claim (October 2021).

This information has not been independently verified by the QP.

Current 3Q Properties are listed in Table 4-1 and shown on Figure 4-3. NLC, through a wholly owned subsidiary (“LIEX S.A.” or “LIEX”) has good and marketable title to all the claims of the 3Q Project, which include one Exploration Claim and 12 Mining Claims. The Claims are registered with the mining authority of Catamarca and are free and clear of any liens or other encumbrances. There are no additional tenements included in the 3Q Project.

Under Argentinean law, Exploration Claims allow for the exploration of a mineral property and Mining Claims allow for mineral exploitation. Mining Claims are unlimited in duration and remain the holder’s property as long as the holder meets obligations under the Argentinean National Mining Code, as amended, including annual canon payments and minimum investment commitments. Exploration Claims are limited in duration.

Further, Argentinean Law allows the assembly of selected Mining Claims into a “Mining Group”. A company may then process all documentation and environmental permits in one single file for the group rather than individual files for each claim. The central group of 10 3Q Project properties has been placed in a Mining Group (Figure 4-3 and Table 4-1). The recently acquired Bautista Claim has not yet been incorporated into the Mining Group. The Lodomar XI and Magdalena claims are also outside of the Mining Group, and no mining activity is currently planned for these latter two properties.

Table 4-1: Status of mineral claims in the 3Q Project.

Claim Name	Permit ID	Title Holder	Claim Type	Area (ha)	Status	Included in Mining Group
Lodomar I	23M2010	LIEX	Mining Claim	1,980.87	Registration of LIEX as the owner completed	Yes
Lodomar II	24M2010	LIEX	Mining Claim	1,974.54	Registration of LIEX as the owner completed	Yes
Lodomar III	25M2010	LIEX	Mining Claim	1,750.62	Registration of LIEX as the owner completed	Yes
Lodomar IV	26M2010	LIEX	Mining Claim	1,538.03	Registration of LIEX as the owner completed	Yes
Lodomar V	27M2010	LIEX	Mining Claim	1,920.47	Registration of LIEX as the owner completed	Yes
Lodomar VI	28M2010	LIEX	Mining Claim	1,091.28	Registration of LIEX as the owner completed	Yes
Lodomar VII	3L2016	LIEX	Mining Claim	3,982.13	Granted Property	Yes
Lodomar VIII	2L2016	LIEX	Mining Claim	6,421.22	Granted Property	Yes
Lodomar IX	68L2016	LIEX	Mining Claim	1,235.80	Granted Property	Yes
Lodomar X	1L2016	LIEX	Mining Claim	4,784.70	Granted Property	Yes
Lodomar XI	4L2016	LIEX	Mining Claim	3,411.12	Granted Property	No
Magdalena	118L2018	LIEX	Exploration Claim	4,913.94	Granted Property	No
Bautista	95L2018	LIEX	Mining Claim	357.34	Granted Property	No
Total Area (ha)				35,362.06		

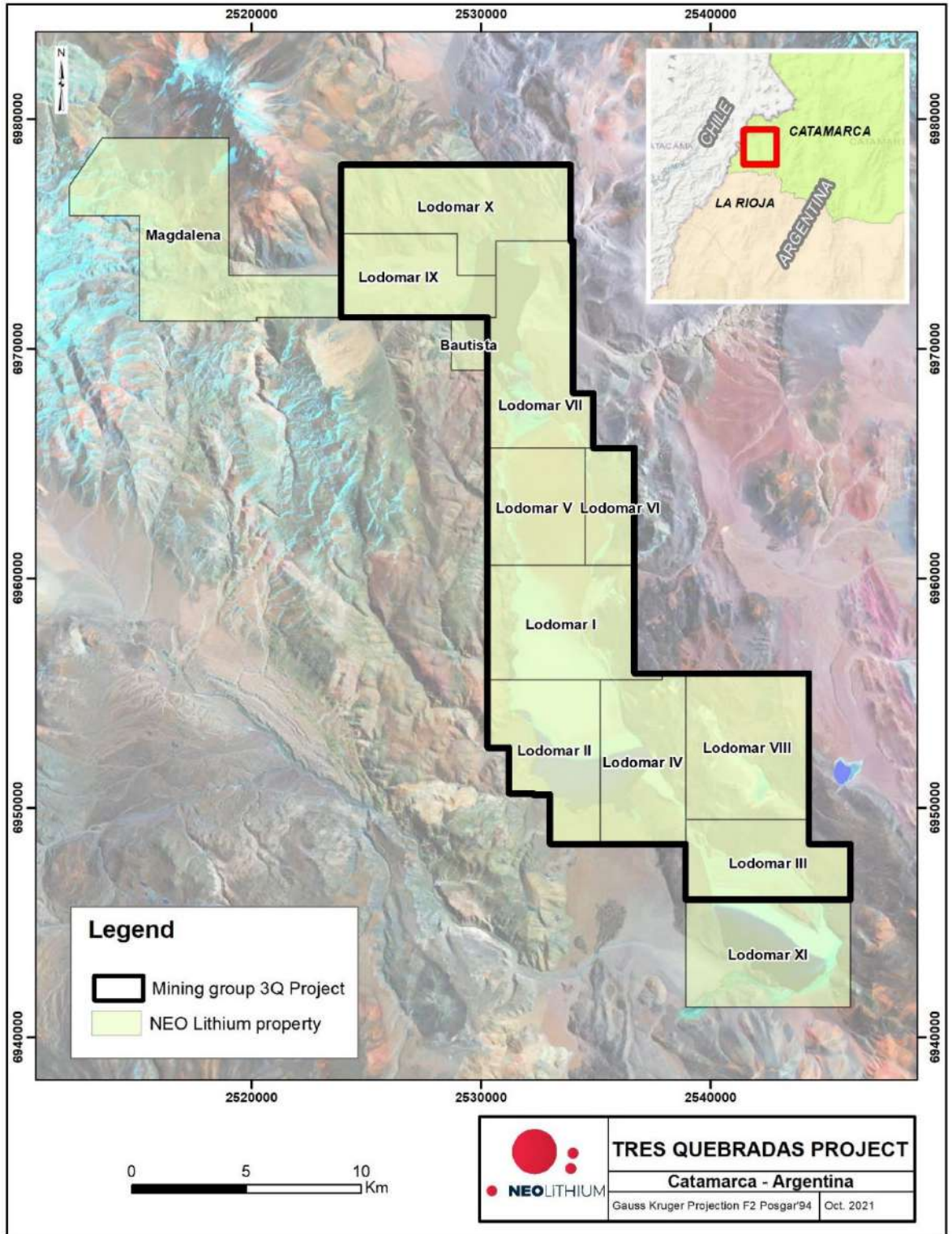


Figure 4-3: Claims held in the 3Q Project.

4.4 Mining Rights Opinion

4.4.1 Overview

It is the opinion of NLC legal counsel that:

- LIEX has good and marketable title to each of the claims comprising the 3Q Project Properties as of the date hereof, free and clear of any liens or other encumbrances registered on title with the Mining Authority;
- each of the claims comprising the Properties is in good standing under the applicable laws; and
- there are no competing claims by third parties with respect to the Properties.

NLC legal counsel advises that, up to February 9, 2021, they are not aware of any litigation or undisclosed liabilities involving LIEX. Several specific legal counsel opinions are stated in the subsections below.

4.4.2 Protected Areas

The 3Q Project is located in a “Ramsar” site, which is defined as an area with special interest for conservation of freshwater wetlands, particularly with regards to bird nesting sites. Under Argentinean environmental legislation, Mining is permitted in a Ramsar site, provided that it complies with all environmental law requirements.

LIEX has obtained all required environmental approvals, as described below and in Section 20.

4.4.3 Surface Access

The 3Q project is build in two sites 3Q salar and Fiambalá. In 3Q salar the company obtained a lien file #204/2016 titled "LIEX SOCIEDAD ANONIMA s / SERVIDUMBRE DE TRANSITO Y COMUNICACION PARA MINAS LODOMAR I, II, III, and others" through the Mining authority on August 31, 2017, which ensures full access (entrance and exit) to the Project Area and the use of the entire surface of the mineral property to build the mine and operate the project for the life of mine.

The lithium carbonate plant is built in the periphery of the city of Fiambalá on public land cadastral # 15-26-87-4024 from which the company obtained access to a total of 345 hectares of an industrial park that will encompass a total of 700 hectares that is being commissioned by the local municipality to build the 3Q lithium carbonate plant and other industries including mining and agroindustry. The agreement with the municipality to locate the 3Q project was signed on June 2019 and on September 2021 the municipality board inked the resolution # 712/2021 that set the land for exclusive use of mining and industry and LIEX SA use.

4.4.4 Water Rights

Water and Groundwater Rights in Catamarca Province are legislated under the Waters Provincial Law #2577, and the use of common or private waters is under the control of the Provincial Body for Hydraulic Resources. On May 22, 2020, under record Number 27/2020, titled “LIEX Soc. Anómia s/ SERVIDUMBRE DE USO Y CONDUCCION DE AGUA – DPTO. TINOGASTA”, LIEX requested from the Mining Authority the granting of legal easement for water use and transportation. The Mining Authority granted LIEX the requested easement on December 23, 2020.

4.4.5 Mining Group

On November 27, 2017, LIEX requested the constitution of a Mining Group covering 26,679.66 ha across 10 claims encompassing Properties Lodomar I to X, (Figure 4-3). This is recorded under Number 159/2017, titled "LIEX S.A. s/ GRUPO MINERO TRES QUEBRADAS, MINAS LODOMAR I, II,... ETC EN TINOGASTA". On March 3, 2020, through resolution number 56, the Mining Authority approved the constitution of this Mining Group.

4.4.6 Royalties

Article 6 of Provincial Law #4757 establishes a general mining royalty of 3% over the mineral value at mine mouth (Boca Mina). LIEX is required to pay this 3% royalty to the provincial government of Catamarca. The royalty base is calculated as the total mineral value at the time of production, less deductible costs such as mineral processing, transportation and related administration and overhead costs.

An Assignment of Rights Agreement dated April 5, 2016, between the Transferors and LIEX, established a royalty of 1.5%. Pursuant to this agreement, the Transferors sold and assigned to LIEX S.A., all of their respective rights, title and interest in and to the 3Q Properties (including, without limitation, Lodomar I to Lodomar VI, and all surface rights in respect thereof). In this agreement it was fixed, as a portion of the consideration, a royalty of 0.5% over gross revenues from production from the 3Q Properties for each Transferor, totaling an aggregate royalty of 1.5% over gross revenues from production from the 3Q Properties.

On July 7, 2018, Mr. Pedro José Alfonso González and Mr. Rubén Gabriel Pindar (two of the Transferors) sold, transferred, and assigned to Lithium Royalty Company LP I, all of their respective right, title and interest in, and to their Royalties (0.5% each) over gross revenues from production from the 3Q Properties.

In 2019 Mr. Waldo Alejandro Pérez (one of the Transferors) sold, transferred, and assigned to Mr. Rubén Gabriel Pindar, 50% of his respective right, title, and interest in, and to his Royalties (0.25%) over gross revenues from production from the Properties.

At the time of this Report, the aggregate royalty of 1.5% is structured as follows: 0.25% in the name of Mr. Waldo Alejandro Pérez; 0.25% in the name of Mr. Rubén Gabriel Pindar, and 1% in the name of Lithium Royalty Company LP I.

4.4.7 Glaciers

Decree 207/2011 regulated by Law 26639 specifies the Minimum Standards for the Protection of Glaciers and of the Peri-glacial Environment. The law establishes the implementation of an inventory and the time involved in the process of completion. There are no glaciers on, or near, the Properties (Section 20.1.3).

4.4.8 Environmental Liabilities

A detailed review of environmental studies conducted for the 3Q Project is provided in Section 20. NLC and LIEX comply with the environmental regulations of Argentina, Catamarca Province, and international regulations. The baseline studies and the Environmental Impact Report ("EIR") for the Project demonstrate that responsible mining activities will minimize any significant negative environmental impacts while also enhancing positive impacts to the area.

Most of the Project mining area is located on the hyper-arid salt flat, with scarce or no vegetation. As a result, the potential for environmental impacts to local flora is low.

The largest wetland (also with the highest biodiversity, mainly wetland birds) is located outside the Mining Group area, south of Laguna Negra, in an area where mining will not occur. The meadow in this wetland forms a functionally significant ecosystem where the native grassland

has a diversity of flora species, with permanent moisture. A second, much smaller meadow is located inside the Mining Group area, west of Laguna 3Q. A small meadow area also occurs east of this lagoon. A baseline study has been completed for the Mining Group area and no significant challenges were identified that cannot be managed with proper mining practices.

Potential environmental impacts to local fauna are predominantly related to earth moving and removal of scarce vegetation cover, for road construction and area leveling. Traffic will also increase. Fauna most affected by these activities are reptiles and micromammals (that are very scarce) with limited mobility.

The environmental liabilities related to flora and fauna will be minimized through implementation of an Environmental Management Plan. Specific steps that this plan described to mitigate impact include:

- training staff and contractors in flora and fauna care;
- monitoring and adjusting soil movement to minimize disturbances of vegetated areas;
- speed control of vehicles;
- continuous monitoring and control of flora and fauna (trend evaluation); and
- minimize access to wetland areas.

4.4.9 Permits

A detailed summary and review of permitting activities is provided in Section 20.1.2.

4.4.10 National Mining Investments Law

LIEX initiated the registration process with the National Registry of Mining Investments on August 30, 2016 (under record # S01-0403795/2016), as required by Law # 24196. The Registry duly registered LIEX on May 12, 2017, as Number 719 through resolution 2017-51-APN-SECM#MEM.

4.4.11 Fiscal Stability

Every Argentinean corporation is subject to the general tax regime of Argentina, which can be modified under certain circumstances. One such circumstance is described by the Fiscal Stability Regime of Argentina, which is a set of tax benefits that apply for a period of 30-years to mining projects owned by corporations that are duly registered in the Argentinean Registry of Mining Investments. A proponent registers by filing an Economic Study that demonstrates project compliance with certain requirements. The tax regime is maintained by the Argentinean Enforcement Authority.

LIEX is a beneficiary of the Fiscal Stability Regime. Through the filing of a 3Q Project Economic Study on February 26, 2018., the Enforcement Authority issued resolution #2019-120 on December 5, 2019, which granted LIEX the Fiscal Stability Regime for a 30-year period, beginning on the filing date (February 26, 2018).

During the 30-year term, the total LIEX tax burden may not be increased from amounts applicable as of February 26, 2018. This stability applies to all National, Provincial, and Municipal taxes, including direct taxes, fees, duties, and tariffs.

4.4.12 Aboriginal Communities

There are no inhabitants in the 3Q salar nor in the entire basin where the project is located. The closest communities are Fiambalá and Tinogasta, located 160 km and 210 km from the Project, respectively. There are no aboriginal communities in those cities that are recognized by the "Instituto Nacional de Asuntos Indígenas" (INAI), the entity in Argentina that monitors and foster

aboriginal communities. There are no self-proclaimed aboriginal groups or individuals according to the census carried out by the Company in the area.

4.4.13 Site Access Risk Factors

Experience from the past four winters has shown that access to the 3Q Project can be maintained during winter conditions, with appropriate management. During the winter months, the access road and camp were operated continuously. Fresh and Industrial water sources to the camp have remained unfrozen since they were established in October 2016. During the winter months, access occasionally requires heavy equipment to remove snow from certain creeks along the road, where it accumulates mostly due to wind. In the worst winter weather some exploration activities (for example, drilling) were temporarily curtailed.

4.4.14 Other Risk Factors

In 2019, the Argentinean Government re-introduced restrictions on the acquisition and transfer of foreign currency. These controls limit the ability for companies working in Argentina to make payments abroad. In this setting, future measures could be adopted by the Central Bank and the government to maintain or introduce further currency controls or restrictions, which may affect the future international competitiveness of the 3Q Project.

4.4.15 Closing

There are no other known significant risks to the 3Q Project, besides those noted in this Report, which may affect access, title, or otherwise the right or ability to perform work on the property.

5. Accessibility, Climate, Local Resources, Infrastructure, and Physiography

5.1 Accessibility

The 3Q Project can be accessed from RN60 (Figure 4-1 and Figure 5-1) via a gravel road, with a junction at F2 Gauss Kruger coordinates 2,582,627E and 6,943,080N. RN60 is a paved year-round highway that joins the capital city of Catamarca Province (San Fernando del Valle de Catamarca) with the border of Chile, via Paso de San Francisco.

As mentioned in Section 4.4, the access road and camp were operated continuously through the winters of 2017, 2018, 2019, and 2020. This experience indicates that with appropriate management, site access can be maintained during winter conditions.

5.2 Climate

NLC has been collecting meteorological data at the 3Q Project since October 2016, with an automatic Vaisala weather station. These data have been compiled and analysed to support pond engineering and other objectives. They are summarized in the following figures:

- Figure 5-2 – daily solar radiation;
- Figure 5-3 – monthly average air temperature;
- Figure 5-4 – daily total precipitation;
- Figure 5-5 – monthly average relative humidity;
- Figure 5-6 – daily average wind speed; and
- Figure 5-7 – daily average evaporation.

Evaporation and precipitation rates were previously evaluated by Instituto de Hidrogeología de Llanuras in Tandil, Argentina (IHLLA, 2019). The Vaisala weather station data and the IHLLA evaluation were used to support the selection of representative annual values for long term numerical modelling, as described in Section 15.2.

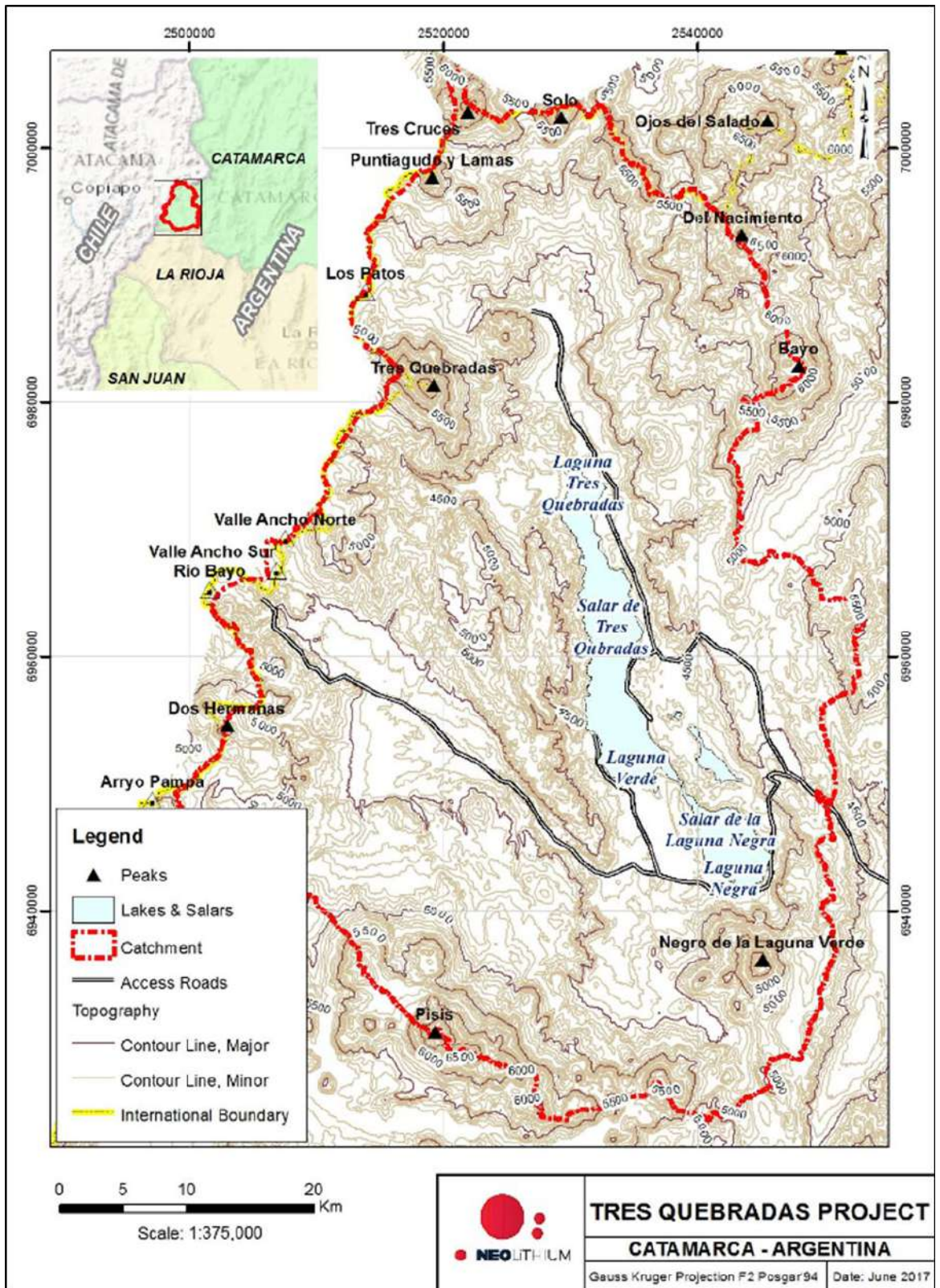


Figure 5-1: Topography and roads in the 3Q Project catchment.

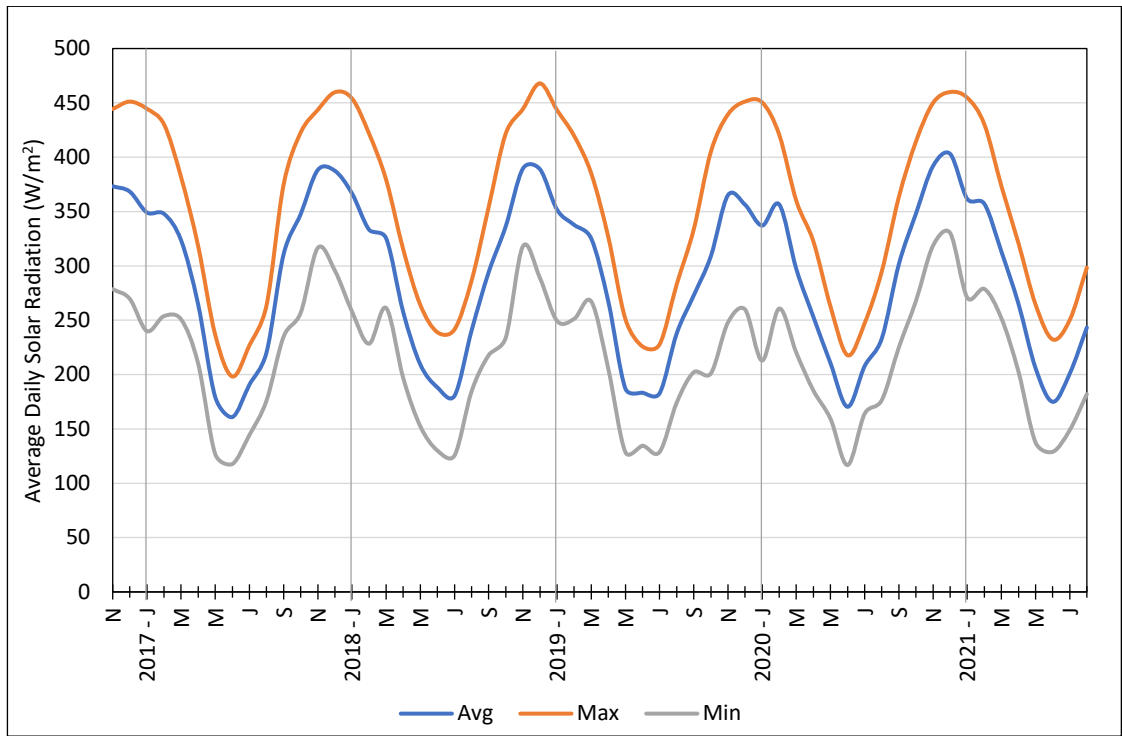


Figure 5-2: Daily solar radiation (calculated on a monthly basis) recorded by the Vaisala weather station – 3Q Project.

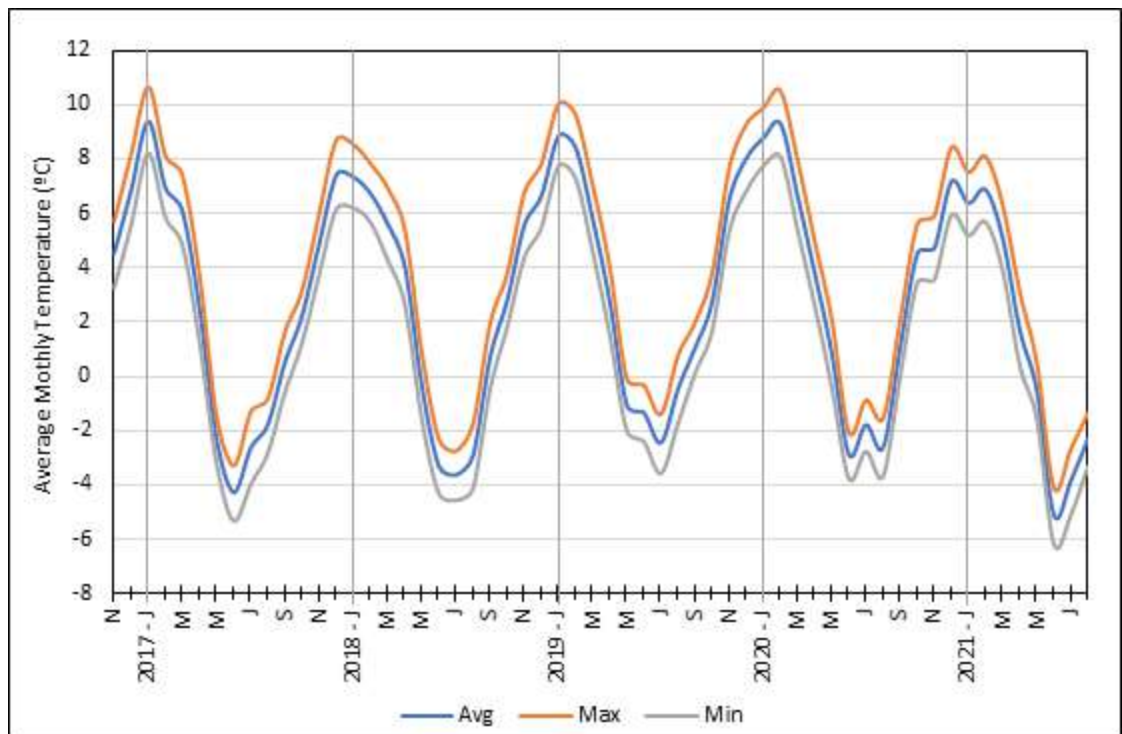


Figure 5-3: Monthly average air temperature recorded by the Vaisala weather station - 3Q Project.

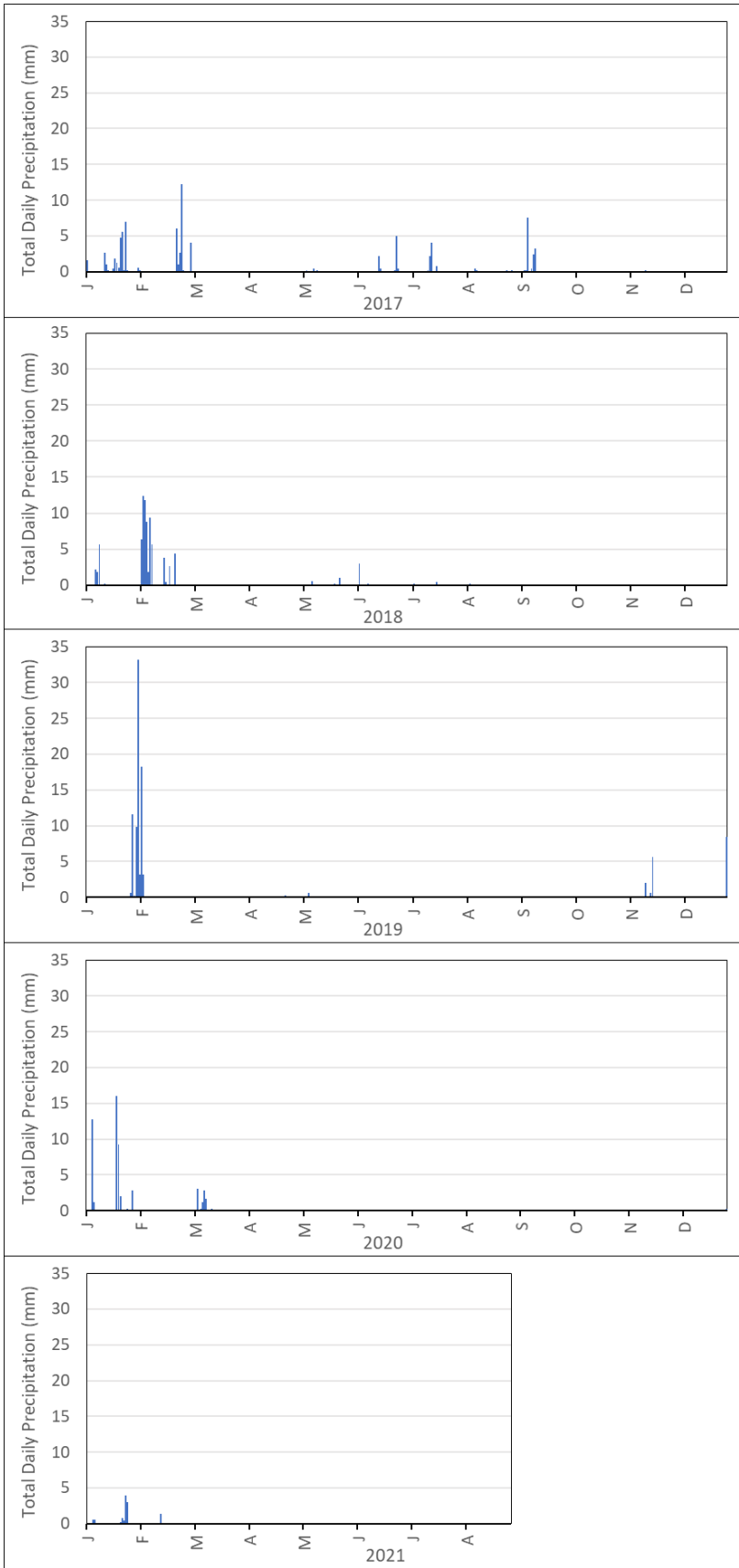


Figure 5-4: Daily total precipitation recorded by the Vaisala weather station – 3Q Project.

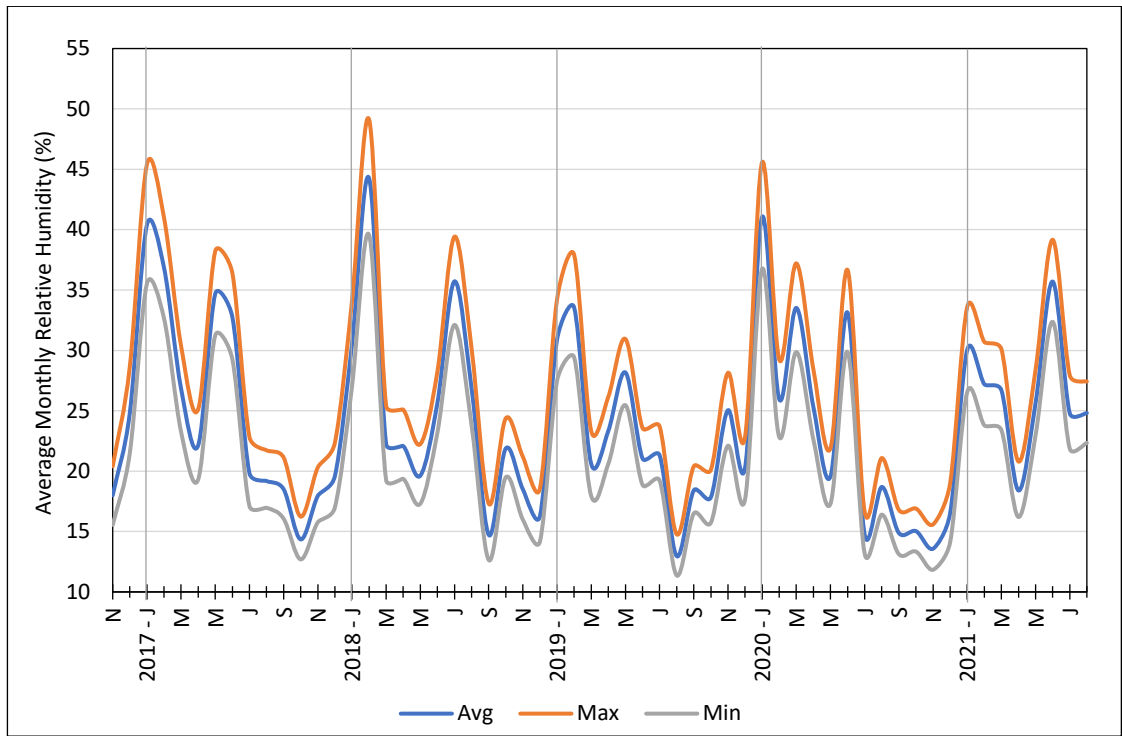


Figure 5-5: Monthly average relative humidity recorded by the Vaisala weather station - 3Q Project.

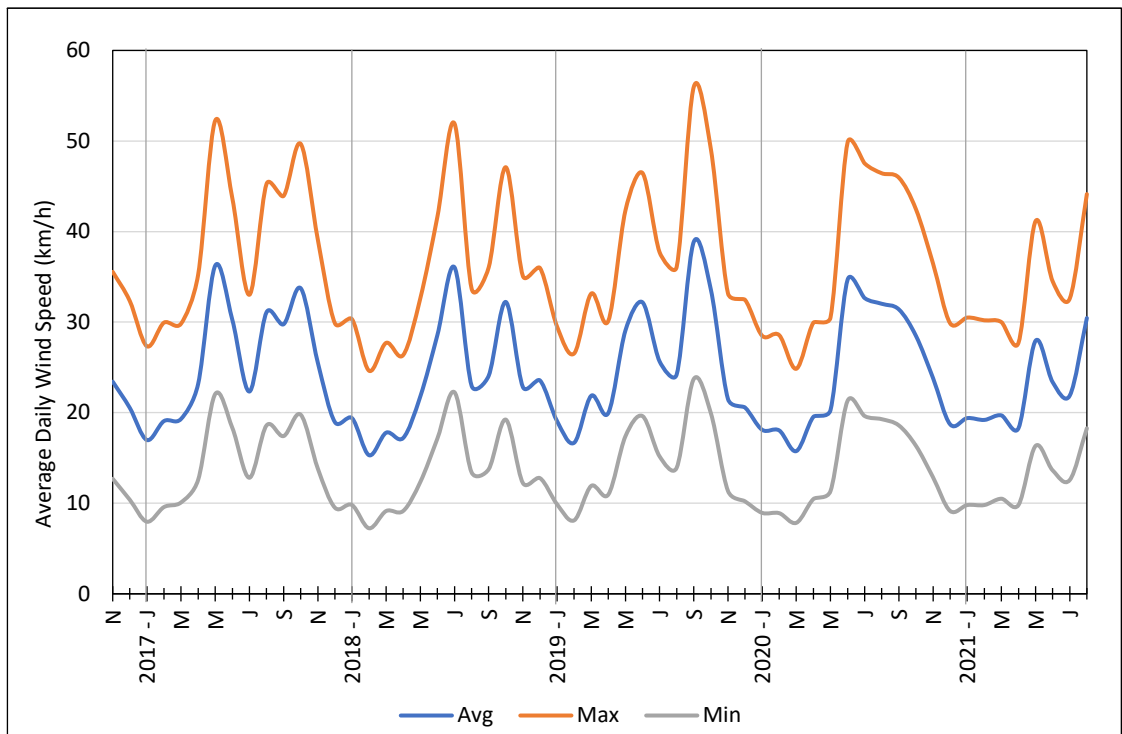


Figure 5-6: Daily wind speed (calculated on a monthly basis) recorded by the Vaisala weather station - 3Q Project.

Areas where the topographic contours show relatively gentle upward slopes from the lakes and salar are indicative of alluvial fans encroaching into the lakes and flat-lying salar surfaces. The salar deposits extend outward under these fans to varying degrees. Steeper slopes are indicative of bedrock surfaces that plunge under the edges of the salars and lakes, giving relatively sharp boundaries to the salar deposits. A full description of 3Q Project geology is provided in Section 7.



Photo 5-1: Drilling Platform on 3Q Salar.



Photo 5-2: Pit excavation for shallow brine sampling, on the rough surface of 3Q Salar.

6. History

A third-party private owner previously staked six lithium and potassium mining claims in the vicinity of Laguna Verde, in what is now known as the 3Q Salar. On January 11, 2016, this owner assigned the mining rights for the claims to Messrs. Waldo Pérez, Pedro González, and Gabriel Pindar.

On April 5, 2016, Messrs. Pérez, González, and Pindar assigned all their rights in these properties to LIEX S.A. in consideration of a nominal aggregate payment of 10,000 Argentinean pesos (approx. \$CDN 890 in the aggregate) and an aggregate 1.5% gross revenue royalty over the claims.

Messrs. Pérez and Pindar, both directors of NLC. LIEX S.A., staked four additional lithium and potassium mining claims in the same area, in January 2016. Two additional claims were also staked by LIEX S.A. in January 2016. LIEX S.A. acquired the final claim (of the current package of 13) through an Assignment of Mining Rights dated October 1, 2021.

Information regarding the legal status of the 3Q Project tenements was provided by the law firm of Martin and Miguens (Argentinean legal counsel for NLC) and is summarized in Section 4. This information has not been independently verified by the QP.

The catchment area of the 3Q Salar has a limited history of mining interest. The only known previous and current exploration campaigns were for gold and copper, and include the following:

- Work was conducted in 1995 to 1998 by El Dorado Gold Corporation, in the western area of the catchment (vicinity of Rio Valle Ancho) where they drilled, trenched, and conducted a large geophysical and exploration campaign in an area that spans both Catamarca and La Rioja Provinces. The access road to the 3Q Project area was constructed at that time.
- Rio Tinto PLC conducted exploration, trenching, and drilling in the vicinity of Rio Valle Ancho from 2004 to 2005.
- East of the salar basin, the company Newcrest conducted drilling, trenching and mineral exploration in a porphyry, in 1995 and 1996. Rugby Minerals conducted additional exploration in the same area in 2011.
- In 2019/21, NGEEx Minerals conducted sampling, geophysics, and geological mapping for copper and gold in the western area of the catchment (vicinity of Rio Valle Ancho). The project area covers approximately 1,000 km² and encompasses the area previously explored by El Dorado Gold Corporation, Rio Tinto, and Newcrest.

7. Geological Setting and Mineralization

7.1 Regional Geology

Geological mapping of the 3Q Project area was conducted by the Argentinean company Hidroar, on behalf of NLC, during the 2016/17 Field Program. A subsequent geology review and update was led by Santiago Grosso during the 2017/18 Field Program. The work by Mr. Grosso involved a review of previous and new drilling results, borehole geophysical logs, seismic interpretation, VES interpretation, and Tertiary outcrop mapping.

Following the 2018-21 Field Program, a follow-up geology update was undertaken by GWI. This update incorporated new drilling results and borehole geophysical logs into the previous interpretations.

The area within and just outside the 3Q Project catchment is characterized by volcanic cones reaching heights of 6,000 metres above sea level ("m asl") or greater (see Figure 5-1). Notable peaks near the Project area include:

- Mount Pissis (6,882 m asl) located to the southwest (and outside the Mining Property);
- Negro de la Laguna Verde (5,764 m asl);
- Nacimiento del Jagüe (5,824 m asl) to the southeast;
- Cazadero (6,433 m asl) to the northeast; and
- Ojos del Salado (6,893 m asl) also to the northeast.

Successive tectonic episodes and reactivation of hydrogeomorphological dynamics in an extremely arid environment have formed low level drainage networks. This has resulted in conformation of inter-mountain basin areas and positive relief in the area. The 3Q Project is located in an accumulation basin. The Cerro Negro de la Laguna Verde Volcano, located immediately to the south of Laguna Verde, occurred recently, possibly sealing a previous route of southward drainage.

7.2 Salar Basin Geology

The following geological summary for the 3Q Salar basin and surrounding areas is supported by the geological map provided on Figure 7-1.

El Cuerno Formation, Choiyoi Group (Permian)

This unit is exposed in a large area throughout the western zone between Laguna 3Q, Laguna Verde and the ravine of the Rio Valle Ancho. It was encountered in wells D-2, D-7, D-10, D-16, D-21, and D-22. It forms thick sequences of acidic and meso-silicic volcanic rocks, which come into contact by tectonic activity with evaporitic deposits and brine lakes along the west side of the salar. These rocks are part of a larger outcrop, which is partially dislocated and covered by subsequent volcanic activity. Dacitic rocks were identified from north to south, occasionally associated with rhyolites. They have porphyritic texture, sometimes amygdaloidal, and are less commonly brecciated. The rocks are formed by phenocrysts of plagioclase, alkali feldspar, and quartz as primary minerals. Accessory minerals include oxidized amphibole.

Andesites and andesitic porphyry were also observed. Subordinate reddish breccias with porphyritic texture, including plagioclases and feldspars, comprise the outcrop mapped on both margins of the Rio 3Q fan (see Photo 7-1). The fracturing of these rocks is moderate to low, with a general direction that is almost meridional and a dip of about 40° to the west.

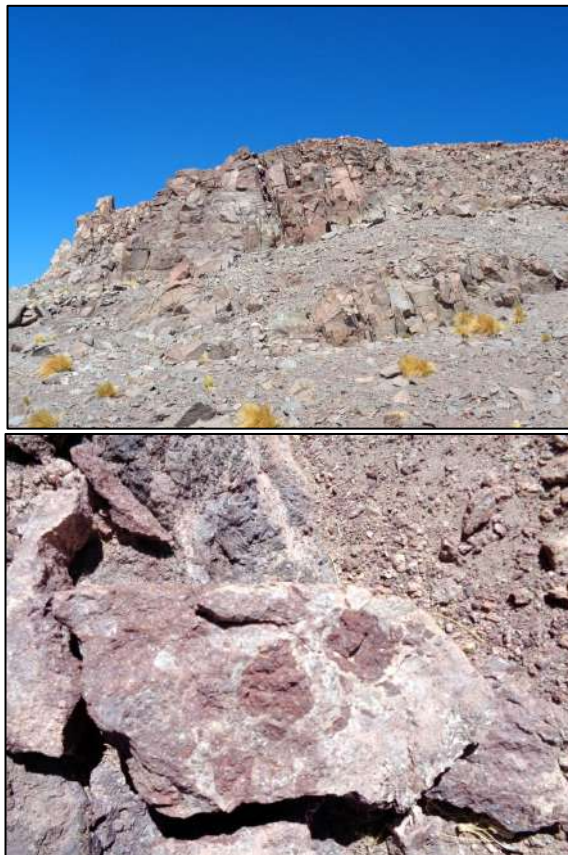


Photo 7-1: (top) Outcrops of andesitic-dacitic rocks of the El Cuerno Formation, in the northwest of the mapped area. (bottom) Brecciated rock in contact with intermediate volcanics

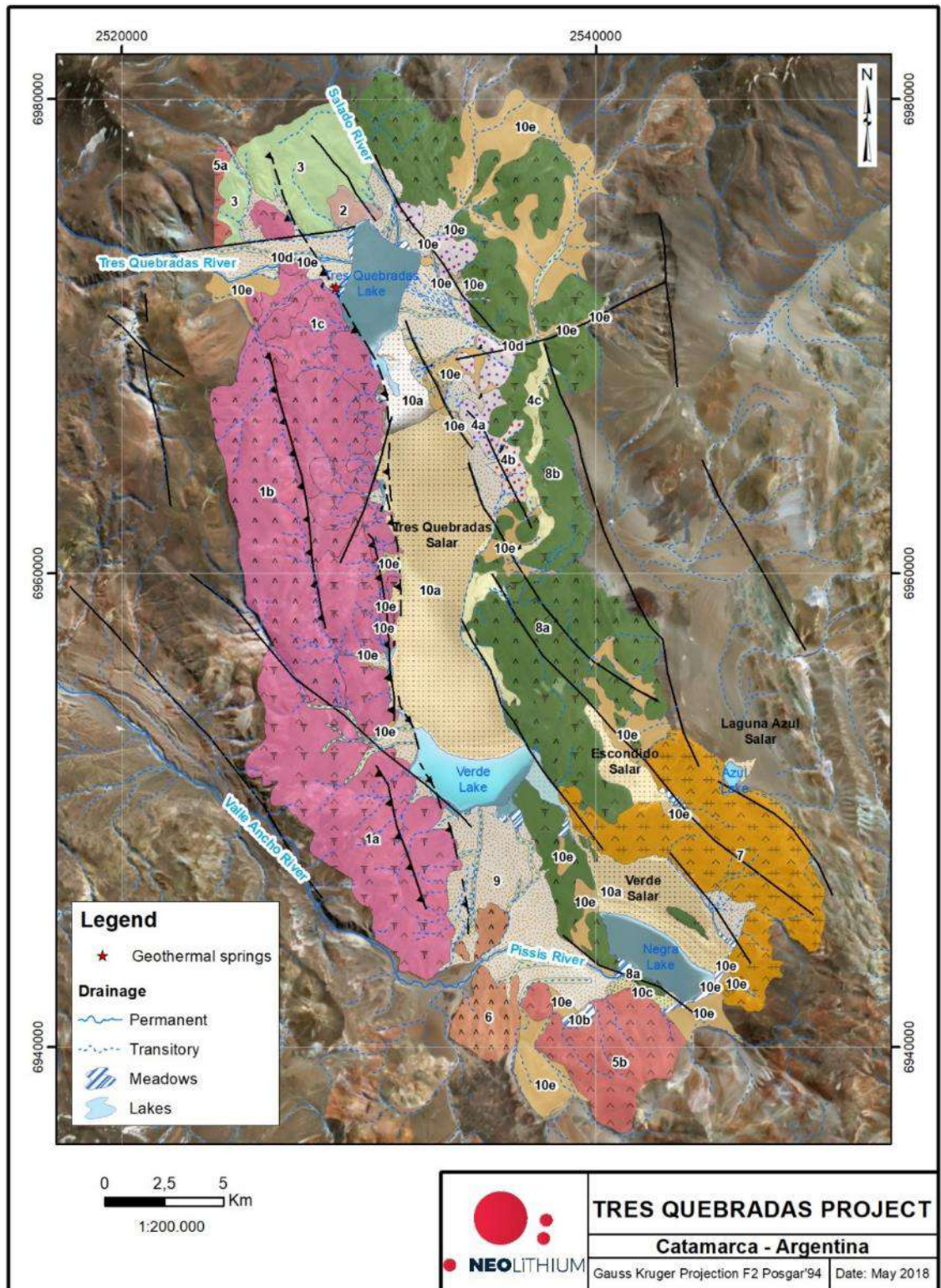




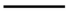


Figure 7-1: Geological map of the 3Q Project area (see Figure 7-2, for lithology legend).

LEGEND

Structures (Hidroar, April 2017)

-  Thrust fault
-  Fault wall
-  Inferred thrust fault
-  Strike / Dip
-  Structural lineament (Liex)

Geology (Hidroar, April 2017)

















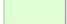




Quaternary		10e. Detritic cover
		10d. Channels fill
		10c. Coastal plain/salt
		10b. Flat deposit
		10a. Salt flat (transition zone)
		10a. Salt flat
		9. Aluvian fan
Plioceno		8b. Nacimientos's hill lavas (Andesites and rhyolites)
		8a. Nacimiento's hill lavas (Basalt)
		7. Campo Negro's dacites
Mioceno		6. Volcanic Complex of Pissis (Basalts)
		5b. Basal Complex of Pissis and Los Patos (Basalt)
		5a. Basal Complex of Pissis and Los Patos (Dacites and andesites)
Paleogeno Mioceno		4c. Lag.Verde Strata (Intercalated silts and sand with levels of gypsum)
		4b. Laguna Verde Strata (Red stratified sandstones)
		4a. Laguna Verde Strata (Violet stratified sandstone)
Mioceno		3. Tres Quebradas Porphyry
Paleogeno		2. Fm. Los Aparejos (Sandstones, siltstones and conglomerates)
Pérmico		1c. Fm. El Cuerno (Volcanic breccia)
		1b. Fm. El Cuerno (Basalt)
		1a. Fm. El Cuerno (Andesites and rhyolites)

Figure 7-2: Lithostratigraphic legend for the 3Q Project geological map shown on Figure 7-1.

Sequences of conglomerates, sandstones, dacites, and volcanic breccias of this formation were observed on the west side of Laguna Verde. Hydrothermal alteration was commonly apparent in the outcrops.

Further south, outcrops in the ravine of Rio Valle Ancho also exhibit hydrothermal alteration. Contrasting colours from dark grey to whitish, and a variety of associated ochre tones were observed. These are volcanic meso-silicic and acidic rocks, with characteristics of lava flows associated with dikes and breccias.

In some areas the rocks are partially covered by volcanics and/or modern scouring, forming large alluvial plains below outcrops. The alluvial fan of Rio 3Q to the northwest is an example, as are the alluvial fans that extend into Laguna Verde (see Photo 7-2).



Photo 7-2: Outcrops of the El Cuerno Formation, in the southwest of the mapped area, west of Laguna Verde. Outcrops are partially covered by modern deposits (alluvial fans).

Los Aparejos Formation– Paleogene (Eocene-Oligocene)

This formation consists of sedimentary deposits, including conglomerates with angular fragments of andesites in a sandy-pelitic matrix. Physical weathering can be observed, where the resulting material completely covers the outcrop (Photo 7-3). These rocks could be the Fanglomerates (Section 7.3) encountered as a deep aquifer in wells D-8, D-17, D-21, D-22, D-23, and R-25.



Photo 7-3: Los Aparejos Formation. Outcrops assignable to this formation have only been identified in the northern end of the mapped area, immediately north of Laguna 3Q, and could possibly form the deep aquifer (Fanglomerate) observed in salar drilling

Tres Quebradas Formation (Miocene)

This formation includes andesitic porphyry rocks, interrupted in areas by andesitic dikes with average thickness of 2.5 m (Photo 7-4).

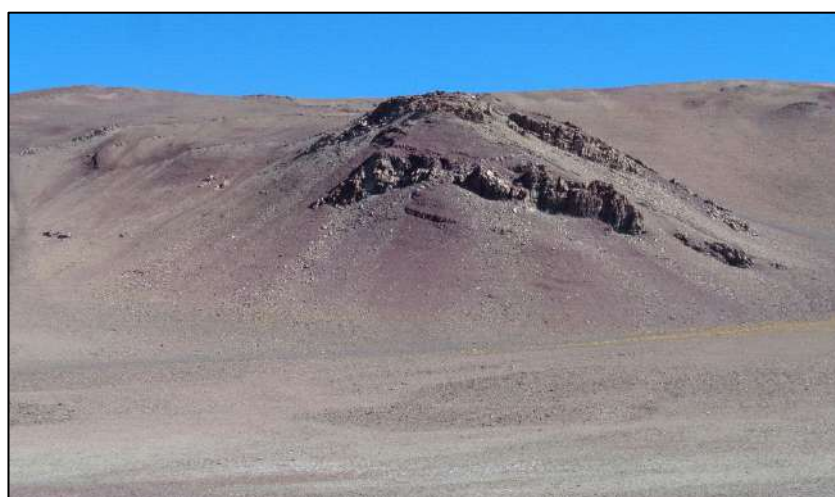


Photo 7-4: Outcrop of the Tres Quebradas Porphyry, in the north zone of the Project.

“Laguna Verde Strata” Member, Tamberías Formation (Calchaqueños Strata, Paleogene – Miocene)

These rocks are present as outcrops of predominantly sandy and silty epi-clastic sedimentary and subordinated tuffaceous material. They are often partially covered by modern alluvial materials. They outcrop around the eastern sector to Laguna 3Q and the salar, with general orientation NNW-SSE. They are in tectonic contact with evaporitic deposits to the west, and with volcanics corresponding to Cerro Nacimientos Lavas to the east.

The composition of these sedimentary rocks ranges from fine to coarse sand to very compact conglomeratic strata, with appreciable occurrence of gypsum at some locations. The colour of the deposits varies from greyish to purplish brown (Photo 7-5).

In some locations these rocks are massive, while in others they exhibit a tabular stratification or thin-bed laminations. Other clastic facies also assignable to this formation have been identified in

the eastern area, characterized by alternating sandstones with medium to thick red beds (Photo 7-6). At some locations it is possible to observe an "onyx" level of approximately 20 cm thick, overlying the sandstones.



Photo 7-5: Interbedded sediments corresponding to Laguna Verde Strata in sandy-silty outcrop (left) and conglomerate facies (right).

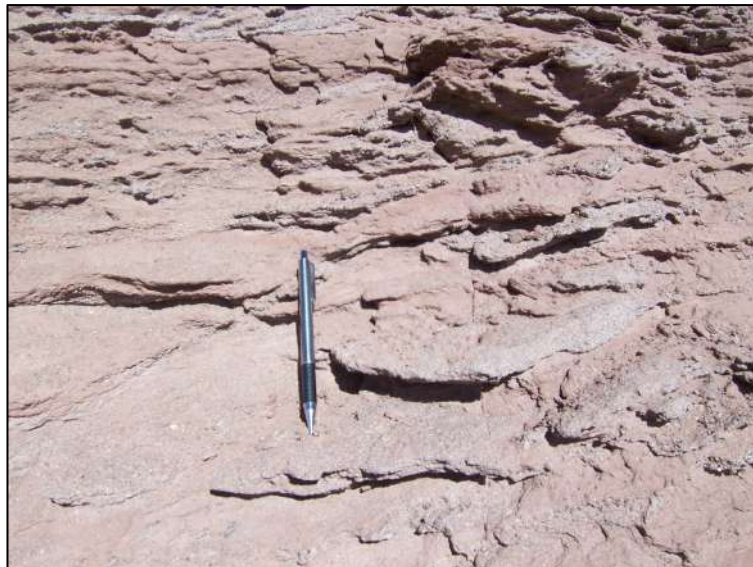


Photo 7-6: Reddish sandstone facies assignable to Laguna Verde Strata, east of 3Q Salar.

Selley Logs were surveyed at two different outcrops along the eastern margin of the salar and results are provided in Appendix A. One log is located 700 m east of the 3Q Project camp at the "Lomas Blancas", and the other is at borehole D-7. The two logs exhibit similar lithologies allowing stratigraphic correlation across the intervening distance of five kilometres. The lithology observed is a partial section of the Tertiary sediments where the base is not exposed, and the top is eroded. Seven packages of clay-silt-gypsum and sandstones sets are observable, with coarsening upward laminations. Silt sediments are predominant, but some sandstones are present near the top of the section. The sediments are interpreted to belong to the 4a member on Figure 7-1.

Diamond corehole D-21 is located approximately two kilometres east of the Selley Log correlation line midpoint, providing further insight into the stratigraphy between the two logs. In the lower sediments, at a depth of 557 to 564 m, red sandstones and siltstones interbedded with gypsum were encountered, which were similar to rocks observed in the outcrops.

Volcanic Complex of Pissis (Pliocene), Basal Complex of Pissis and Los Patos (Miocene) and Andean Basalts of Campo Negro (Miocene).

These Tertiary volcanic rocks are prominent in the southern end of the mapped area, southwest of Laguna Verde and Laguna Negra. They are readily apparent as lavas or volcanic mantles of basic-intermediate composition, with black to reddish colourations, often with vesicular structure and cooling fractures. Water may exfiltrate from the base of these units, so that vegetation develops at the foot of coladas (Photo 7-7).

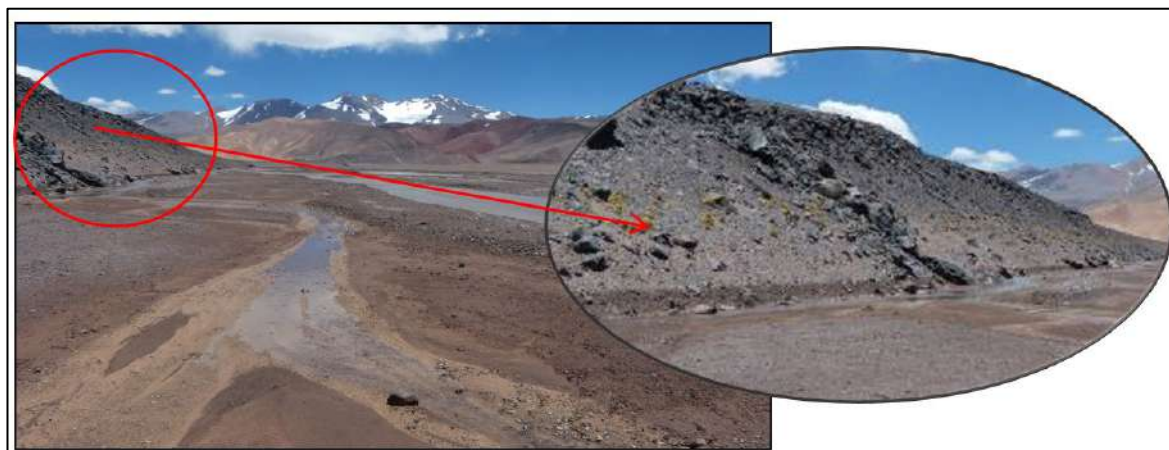


Photo 7-7: Basaltic volcanic mantles of Pissis in the south sector (Rio Valle Ancho valley).

These rocks correspond to the "Volcanic Complex of Pissis" (Pliocene), and volcanics of the "Basal Complex of Pissis and Los Patos" (Miocene). They are observed in the slopes of Cerro Tres Quebradas. Both complexes correspond to basaltic andesites. Rocks of rhyolitic composition are also occasionally present.

Also identified in the southeast sector are other volcanic mantles corresponding to the "Campo Negro" Andean Basalts unit, which in some sectors were observed as rhyolites. These rocks are of Miocene age.

Cerro Nacimientos Lavas (Pliocene - Quaternary)

The volcanic rocks observed in the eastern sector of the map area generally correspond to this stratigraphic unit of Pliocene - Quaternary age. In the vicinity of 3Q Salar these rocks directly overlie the clastic sequences of the "Laguna Verde Strata". Outcrops identified in the field correspond to rhyolites, andesites, and basalts with porphyritic texture. Tabular plagioclase phenocrysts and occasional volcanic glass fragments in a light aphanitic matrix (Photo 7-8) are observable. These volcanic rocks can be distinguished as lava mantles that generally cover the sedimentary rocks of the Laguna Verde Strata.



Photo 7-8: Volcaniclastic deposits corresponding to "Cerro Nacimientos Lavas".

Salar Basement

The hydrogeological basement of the salar is composed of Permian Volcanics (el Cuerno Formation, Choiyoi Group) in most of the salar area. Fractures can be abundant, but may be infilled with white quartz, reducing their permeability (Photo 7-9). These rocks outcrop on the western margin of the salar. Towards the eastern salar border, the basement is composed of Tertiary (Miocene) sandstones, siltstones, and gypsum from strata of the Laguna Verde and Tamberías Formations.



Photo 7-9: Core from the hydrogeological basement, with a dip varying from 5 to 40 degrees.

7.3 Salar In-Fill Geology

Salar in-fill units were differentiated in 3Q Salar and are the target of current exploration. From deepest to shallowest, these units are as follows:

- Fanglomerate (“FG”);
- Lower Sediments (“LS”);
- Massive Halite (“MH”);
- Porous Halite (“PH”);
- Upper Sediments (“US”); and
- Hyper-Porous Halite (“HPH”).

Through tectonic activity, these deposits are in contact with Paleozoic outcrops on the west salar margin. In the east they are also delineated by faults, where they make contact with clastic sequences of "Laguna Verde Strata", effusive Cenozoic volcanics, or modern alluvial-colluvial deposits. Discharges of thermal waters (or indirect evidence in temporarily inactive zones) are observed in the northern, southern, and western margins of the salar infill deposits.

These salar units were originally mapped through an integrated interpretation of borehole cores (Section 10.2), borehole cuttings (Section 10.3), seismic survey (Section 9.3), VES survey (Section 9.2), and downhole geophysics (Section 10). The resulting interpretations are summarized in six isopach maps, provided in Appendix B. These maps were used to prepare a series of salar sections that supported the geological modelling component of the Mineral Resource Estimate and Reserve Estimate previously reported in the PFS (King and Zandonai, 2021).

These geological interpretations have been updated for the northern salar based on 2018-21 drilling results (Section 10). Clastic sequences that correlate with the Fanglomerate and Lower Sediments were intersected by drilling beneath and east of the previous model domain. The northern extent of Porous Halite was also modified as this unit was not intersected with recent drilling. The resulting updates include:

- Fanglomerate: extended north and east from the previous extent (Appendix B, Figure B-1), filling the deepest portions of the northern salar;
- Lower Sediments: extended north and east from the previous extent into the northern salar (Appendix B, Figure B-2); and
- Porous Halite: truncated approximately 750 m south of the previous northern extent shown in Appendix B, Figure B-4.

These updates were used to support the geological modelling component of this FS (Section 14).

In terms of unit distributions, there is a trend of increasing thickness towards the eastern boundary of the salar in the Massive Halite, Lower Sediments, and Fanglomerate, suggesting a half graben disposition. The Porous Halite and Hyper-Porous Halite units are both thickest in the centre of the salar, while the Upper Sediments unit is thickest near the northeastern alluvial fans and thins to the south. A brief description of each unit is provided below.

Fanglomerate

The Fanglomerate unit overlies the hydrogeologic basement and is composed of fanglomerates, medium-coarse sandstones, and sedimentary breccias with 2-20 cm diameter clasts. The supporting matrix of the fanglomerates is composed of fine to coarse sandstone that is generally loose, with a high visual porosity. The sandstones are dark, reddish to black, containing quartz,

as well as lithic and biolitic clasts. This unit is present in the deepest parts of the basin and represents the early in-fill of the salar, in the form of ancient alluvial fans and fluvial sediments.

Photo 7-10 shows an example of Fanglomerate from the diamond core at borehole PP1-D-22, which included a 133 m thick occurrence of the unit. The core displays a coarsening upwards texture with elongated volcanic clasts ranging in diameter from 0.5-8 cm. The long axes of the clasts are generally vertical, suggesting a subaerial fan that experienced a buoyancy effect during mass wasting.



Photo 7-10: Reddish-grey Fanglomerate in core from PP1-D-22, at a depth of approximately 587 m.

Lower Sediments

This unit is composed of sandstones and siltstones, with minor gypsum laminae. It increases in thickness towards the eastern margins of the basin. Lower Sediments deposition occurred before evaporite accumulation in the basin. Generally, this unit exhibits folding, which may be due to synsedimentary tectonic subsidence. Photo 7-11 shows the boundary between the top of the Lower Sediments (reddish-brown) and the base of the Massive Halite, at a depth of 461.5 m.

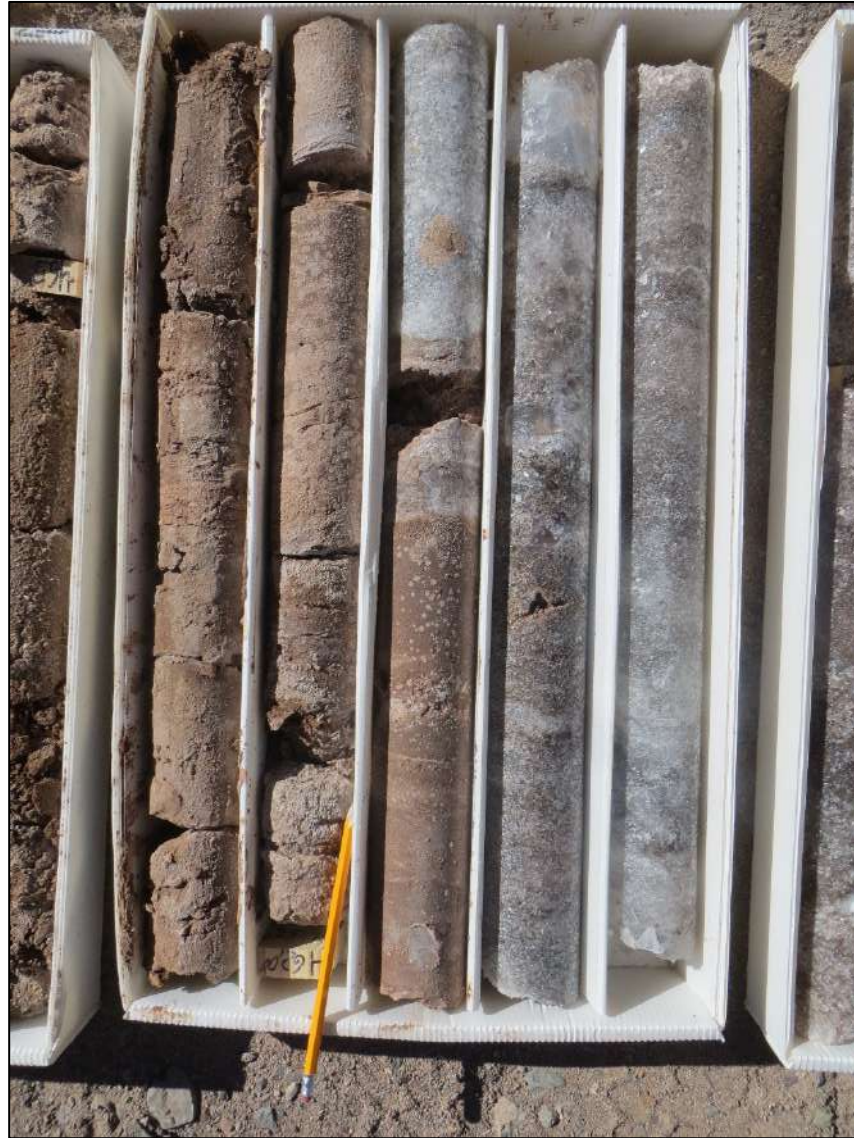


Photo 7-11: Transition between Lower Sediments (reddish-brown) and white Massive Halite, at 461.5 m.

Massive Halite

The Massive Halite unit consists of fine to coarse-grained halite. It was observed in a range of colours including white, grey, red, and black. The unit has a low visual porosity. In the upper extent, cubic crystals can be observed. At the base of the Massive Halite (Photo 7-11) individual crystals are not apparent, possibly due to dissolution and re-formation of smaller crystals. Minor intercalations of red clay are present, and also possible organic matter.

Porous Halite

The Porous Halite unit is composed of medium to coarse-grained halite, with granular intervals of loose, white to grey crystals (Photo 7-12). Visual porosity is moderate to high. The greatest thickness occurs in the centre of the salar basin. At well PP1-D-17, the transition between the Massive Halite and Porous Halite units was marked by a layer of aeolian sandstone.



Photo 7-12: Porous Halite shown in core from borehole PP1-D-22, at 78 m depth.

Upper Sediments

This unit is composed of reddish sandstones, silty sandstones, and plastic shales, mixed with halite crystals (Photo 7-13). Visual porosity is medium. The Upper Sediments unit forms a clastic wedge that is thickest in the northeastern sector of the salar and thins toward the south. Grain size displays a similar trend, becoming finer to the south. The primary source areas for these sediments are likely the catchments of Rio Salado and Rio 3Q, with additional input from smaller creeks. This unit was absent in some central salar locations, such as in boreholes PP1-D-10, D-16, and D-23.



Photo 7-13: The boundary between Upper Sediments and Hyper-Porous Halite.

Hyper-Porous Halite

The Hyper-Porous Halite unit is composed of medium to coarse-grained halite with high inter-crystalline porosity (Photo 7-13). Some voids were observed near the top of this unit. The unit is generally whitish, although some cycling of colours from white to red to black was observed. The maximum observed unit thickness was in the centre of the salar (89 m in core from borehole PP1-D-17). This unit effectively extends to the salar surface, which is typically composed of halite pinnacles with crests trending NNW-SSE. The pinnacles are highest in the north-central area of the salar.

Quaternary Alluvial Deposits

These materials occur mainly as fluvial deposits associated with surficial fans encroaching on the salar and into the lakes. They slope upward from the salar and lake surfaces to varying degrees and were not defined and mapped as a Resource unit. These detritic materials may overlie large sandy areas in some sectors around the salar and lakes. They consist mainly of unconsolidated alluvial to colluvial materials, with a range of compositions and granulometric heterogeneity, ranging from blocks of andesites and basalts to fine gravels and sands, and even finer alteration materials.

In terms of areal extent, the largest alluvial fans occur in the north and northwest of the 3Q Salar, associated with Rio 3Q and Rio Salado. There are also large fans to the southwest, between Laguna Verde and Laguna Negra (Photo 7-14).



Photo 7-14: Alluvial fan deposits and filling materials in inactive fluvial channels, on the northwest margin of Laguna Verde.

At the downgradient ends of these fan systems, zones of vegas and thermal springs may be present, with general diffuse drainage, wandering channels, vegetation growing in the margins, and development of saline efflorescence. Such is the case for the Rio Salado fan, whose headwaters are in the vicinity of Nevado Tres Cruces and Cordón de los Arrieros and are partially fed by hot spring systems.

7.4 Structures

Structural systems in the vicinity of 3Q Salar are shown in plan and section on Figure 7-1 and Figure 7-3, respectively.

Outside the western boundary of the salar, the presence of an inverse fault and two reverse faults is inferred, with approximate NNW-SSE orientation. In the mapped area, these faults generally involve andesitic, rhyolitic, and basaltic igneous rocks of the El Cuerno Formation. The sequences are shown in a succession of rhyolitic and andesitic rocks crowned by basaltic mantles. At other locations these structures contact the El Cuerno Formation with Tertiary or modern deposits, including a lineament that contacts 3Q Salar in-fill materials with these older rocks. There are also points of upwelling thermal waters at these locations.

On the eastern side of 3Q Salar, the most notable structure is a direct fault with a lower edge near the mid-point of the salar. This structure mainly affects sedimentary rocks of Laguna Verde Strata. It is indicated in the field by an escarpment observed in an alluvial fan. It is inferred from satellite images by the presence of outcrops in contact with the most modern evaporite deposits. As in the structures observed on the western side of the salar, the eastern structure also shows an approximate NNW-SSE orientation, aligning with the long axis of Salar 3Q.

Additional evidence of structural lineaments is indicated by the existence of E-W to WSW-ENE and NW-SE oriented streams. One of these is apparent on the north margin of the Rio 3Q valley and homonym brine lake, where an outcrop of the Los Aparejos Formation and the Tres Quebradas Porphyry underlies the El Cuerno Formation to the southwest.

Significant lineaments are also apparent to the northeast of 3Q Salar, in the ravine that is downstream of Cerro Campo Negro and in the southern sector of the mapped area, coinciding with the layout of Laguna Verde and Laguna Negra, and the alignment of Rio Valle Ancho.

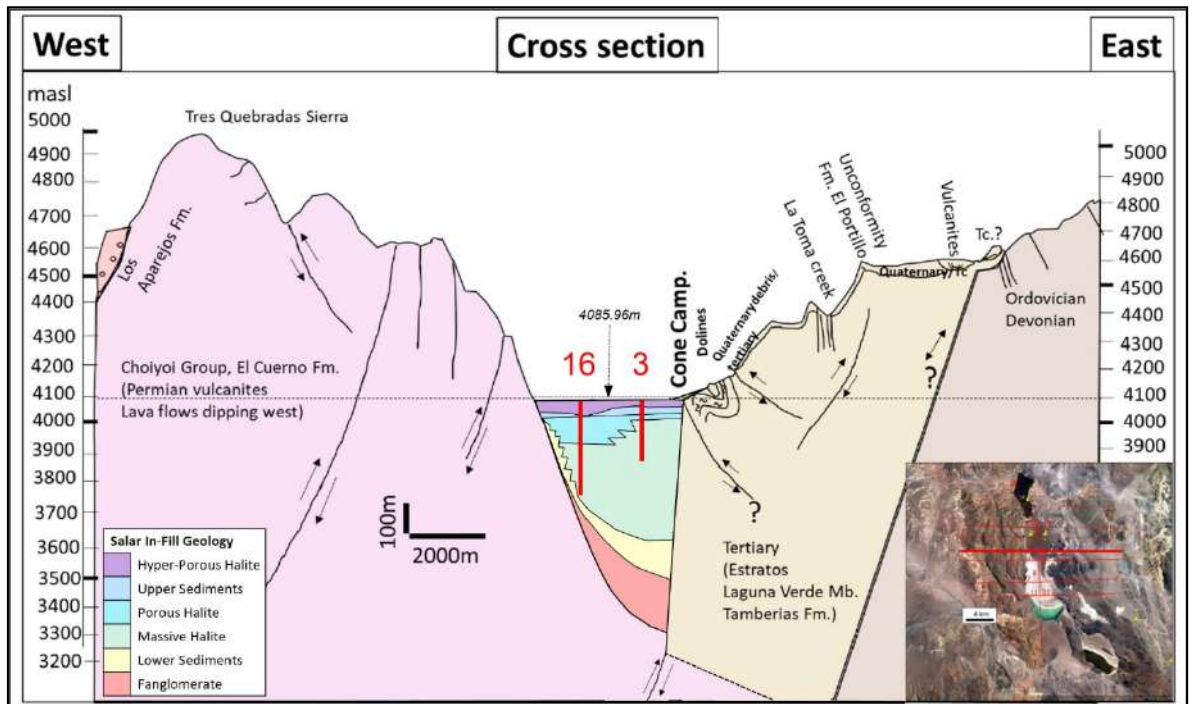


Figure 7-3: Conceptual cross-section showing structural systems in the vicinity of 3Q Salar.

7.5 Mineralization

Brine Resources in the 3Q Salar are defined relative to two cut-off values: 400 and 800 mg/L lithium (Section 13). The Resource within the 800 mg/L cut-off is limited to approximately the northern third of the salar, while the 400 mg/L cut-off extends from Laguna 3Q in the north to Laguna Verde in the south. Sampling methods and results are presented in Sections 10 and 11 and zone delineation criteria are described in Section 14.14.

A summary of the brine volume and chemistry in the Resource zone is provided in Table 7-1. Table 7-2 compares the chemistry from the 3Q Project with information from other lithium brine projects. As indicated in the table, 3Q Project lithium and potassium grades are favourable relative to other projects.

Two other important brine constituents summarized in Table 7-1 and Table 7-2 are sulfate and magnesium. These two parameters are considered brine impurities in that they affect the cost of brine processing. As indicated in the table, both magnesium and sulfate compare favourably with the other brines in the group, in that their ratios are at the low ends of both ranges.

Table 7-1: Volume and average composition of the Mineral Resource Estimate defined for the 3Q Project (for 800 mg/L lithium cut-off).

Parameter	Measured + Indicated	Inferred
Brine Volume (m ³)	3.57E+08	3.34E+07
Lithium (mg/L)	923	918
Mean Potassium (mg/L)	8,353	8,210
Magnesium (mg/L)	1,531	1,535
Mean Sulfate (mg/L)	453	372
Mean Boron (mg/L)	1,348	1,308
Mean Mg/Li Ratio	1.66	1.67
Mean SO ₄ /Li Ratio	0.49	0.41
Mean Density (g/ml)	1.22	1.22

Table 7-2: Comparison of selected brine chemistry for the Mineral Resource Estimate defined at the 3Q Project (for the 800 mg/L cut-off), with other lithium brine deposits.

Company	Location	mg/L					Density (g/cm ³)	Ratio (Mg/Li)	Ratio (SO ₄ /Li)
		Li	K	Mg	SO ₄	B			
SQM	Atacama, Chile [A]	1,835	22,626	11,741	20,180	783	1.22	6.40	11.00
Zhabuye Lithium	Zhabuye, China [B]	1,258	34,241	13	67,963	3,709	1.30	0.01	54.02
Lithium Power	Maricunga, Chile [C]	1,167	8,500	-	-	-	-	-	-
Western Mining Group	East Tajjinair, China [B]	808	86,654	17,404	178,475	1,061	1.26	21.53	22.80
Orocobre	Hombre Muerto, Argentina [D]	735	-	-	-	-	-	-	-
Livent	Hombre Muerto, Argentina [E]	747	7,435	1,025	10,279	422	1.21	1.37	13.76
Orocobre	Olaroz, Argentina [F]	690	5,730	2,270	-	1,050	1.21	2.4	-
Lithium Americas Corp.	Cauchari – Olaroz, Argentina [G]	592	4,801	1,403	16,866	1,094	1.22	2.37	28.49
LithiumX	Diablillos, Argentina [H]	501	5,512	-	-	556	-	-	-
Comibol	Uyuni, Bolivia [E]	424	8,719	7,872	10,294	242	1.21	18.57	24.29
Rincon Lithium	Rincon, Argentina [I]	403	8,003	3,697	12,383	488	1.22	9.18	30.76
CITIC Guoan	West Tajjinair, China [B]	257	101,219	8,447	183,581	380	1.23	32.81	713.05
Neo Lithium	Tres Quebrada [J]	923	8,353	1,531	453	1,348	1.22	1.66	0.49

Notes:

[A] SQM, 2009.

[B] Data from Dr. Haizhou Ma, Institute of Salt Lakes, China.

[C] Worley Parsons and Flo Solutions, 2019: Measured + Indicated Resource.

[D] Rosko *et al.*, 2021: results for Measured + Indicated Resource (500 mg/L cut-off).

[E] Data from Roskill, 2009.

[F] Houston and Gunn, 2011: results for Total Resource.

[G] Burga *et al.*, 2020: results for Updated Measured + Indicated Resource (300 mg/L cut-off). Density of 1.215 was assumed for converting B wt% to mg/L. K, Mg, and SO₄ calculated based on reported ratios.

[H] Reidel, 2017: results for Measured + Indicated Resource.

[I] Pavlovic and Fowler, 2004.

[J] Results documented in this Report; Measured + Indicated Resources (800 mg/L cut-off).

"-" = data not available

7.6 Surface Water

7.6.1 Rivers and Streams

Stream flow rates have been measured approximately monthly since December 2016, at the gauging points shown on Figure 7-4. Measured flow rates are shown on Figure 7-5. Most streams infiltrate to some degree into alluvial fans before discharging into the salar basin, which complicates water balance estimation. Further, most streams may partially freeze during the winter, with the exception of Rio Salado in the north.

In the northern area, Rio Salado and Rio 3Q discharge into Laguna 3Q (Figure 7-4) with average yearly flow rates of approximately 517 and 268 L/s, respectively (Figure 7-5). Maximum yearly

flow in Rio Salado occurred in August 2017 and 2019 and in September 2018. Conversely, the maximum yearly flow rates in Rio 3Q were recorded during the summer months (January and February) of 2017, 2018, and 2019. In 2020, the maximum flow rate for Rio Salado and Rio 3Q were recorded in May and September, respectively.

Flow rates recorded for Rio Pissis, located in the south of the salar watershed ranged from 0.8 to 2,369 L/s during the observation period. This river completely infiltrates into an alluvial fan before discharging as subsurface flow into the Lagunas Negra and Verde. The maximum flow rates for Rio Pissis were recorded in September or October of each observation year.

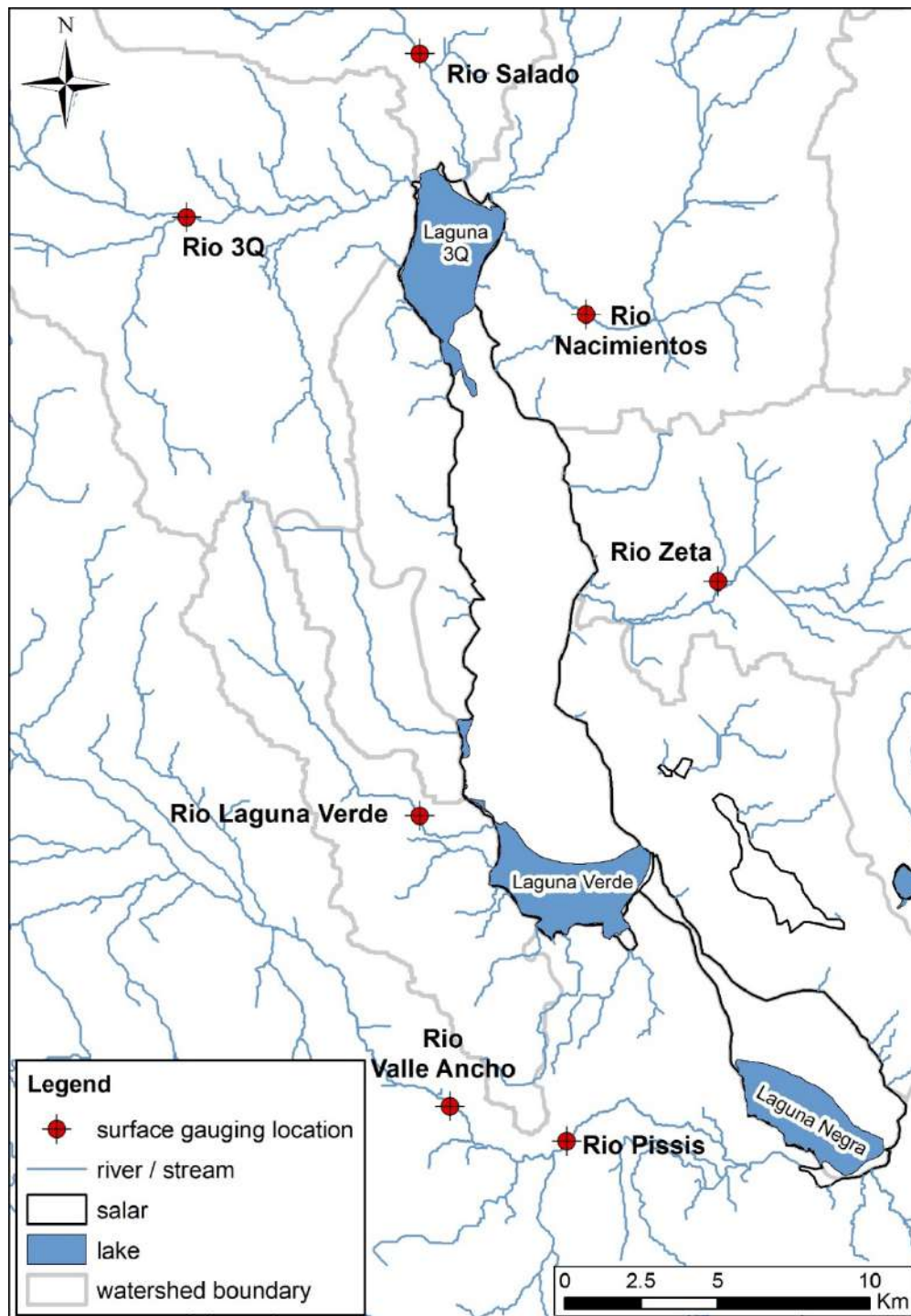


Figure 7-4: Surface stream gauging points in the 3Q Salar watershed.

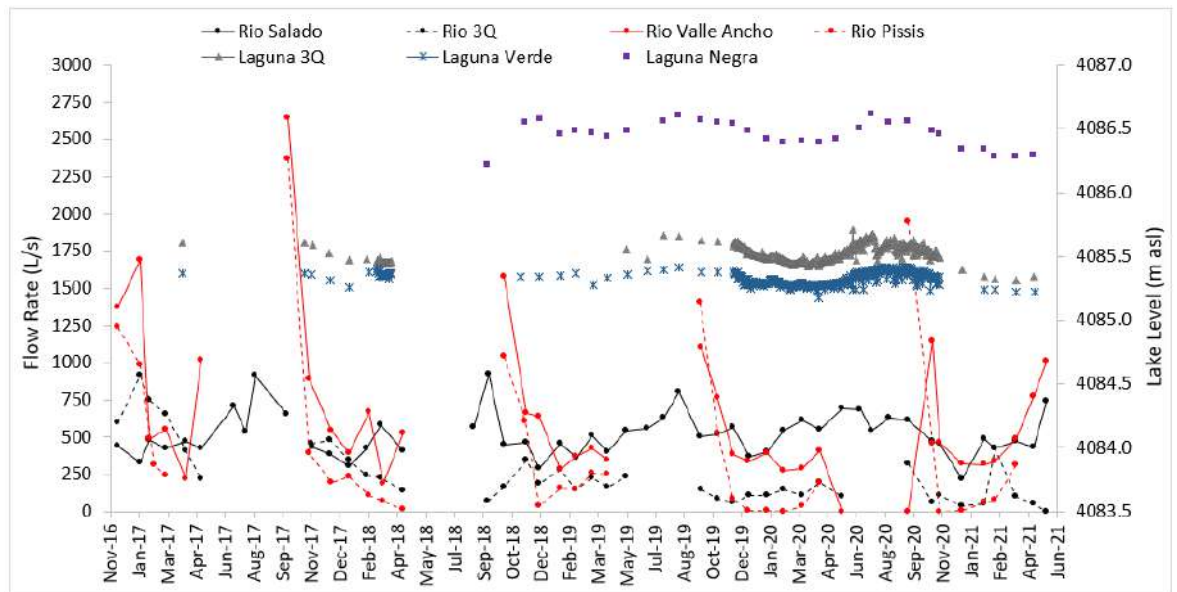


Figure 7-5: Average annual flow rate monitoring data for the main surface streams and laguna levels in the 3Q Salar watershed.

7.6.2 Permanent Surface Water Bodies

The 3Q Salar includes three permanent surface water (brine) bodies, all larger than 1,000 ha in area (Lagunas 3Q, Verde, and Negra; Figure 7-4). The bathymetry of Lagunas 3Q and Verde has been evaluated and shows that they have maximum depths of two metres and 1.5 metres, respectively (Figure 7-6). The shallowness, chemistry, and brine levels of these water bodies suggest a strong hydraulic connection with the shallow brine of the adjacent salar.

Lakes in the 3Q Salar are dynamic in terms of water level and surface area. Four topographic campaigns were carried out in the salar, to obtain accurate lake level measurements. Since February 2017, monthly lake level measurements have also been carried out. In March 2018 pressure sensors were installed in Lagunas 3Q and Verde. Hourly measurements were recorded in March 2018 and from November 2019 to November 2020 (Figure 7-5, Figure 7-7, and Figure 7-8). Relative measurements were converted to absolute values, using the results from the topographic campaigns.

As shown on Figure 7-5, Laguna Verde consistently exhibits the lowest surface elevation of the three permanent surface water bodies within the salar. The three lagunas showed lake level fluctuations of less than 0.5 m during the observation period. Laguna 3Q levels varied between 4,085.32 and 4,085.71 m asl. Laguna Verde had narrower level ranges, varying between 4,085.18 to 4,085.42 m asl. Levels at Laguna Negra varied between 4,086.22 to 4,086.61 m asl.

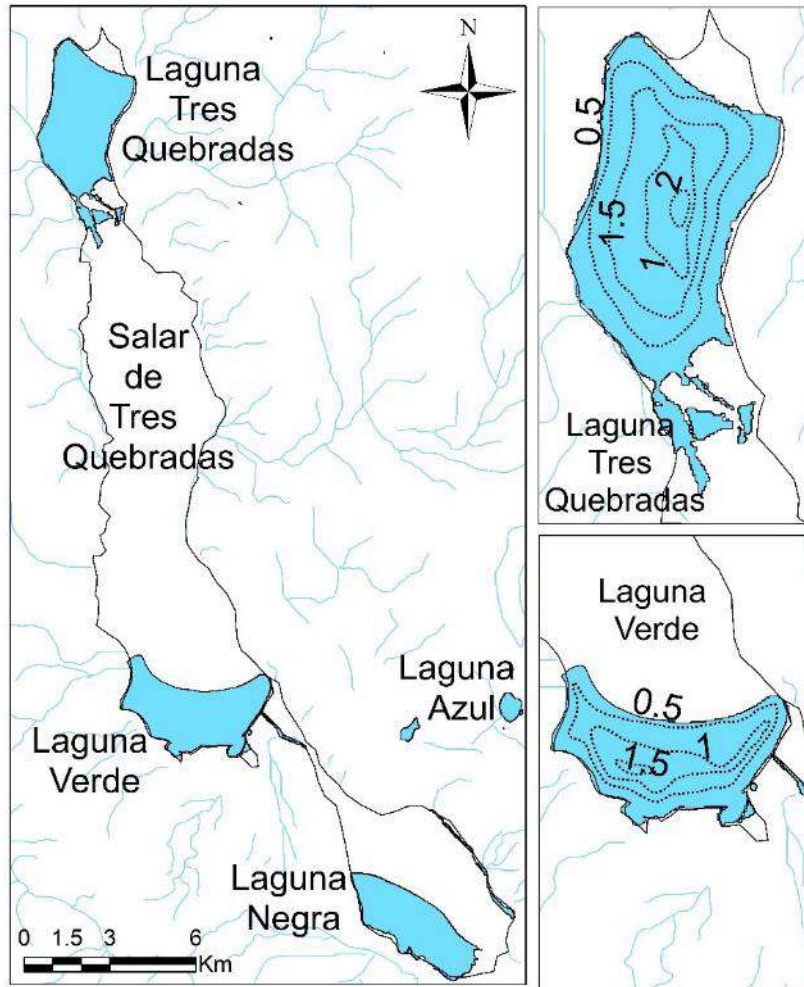


Figure 7-6: Bathymetry of Laguna 3Q and Laguna Verde.

Seasonal variation in observed in lake levels and surface areas of the lagunas are caused by seasonally varying inflows and evaporation. Additional shorter term (one to a few days) lake level variations, were observed in Laguna 3Q. A comparison of wind speed, wind direction, and lake levels demonstrates that these shorter-term variations are caused by wind fetch (Figure 7-7). Similarly, piezometric levels of wells located just south of Laguna 3Q within the narrow portion of the salar also show the affects of wind fetch (Section 7.6.3).

Figure 7-7 demonstrates the effect of wind fetch on Laguna 3Q and selected wells. During periods of sustained west-northwesterly to north-northwesterly winds of over 30 km/h, Laguna 3Q levels show a rapid decline, sometimes dropping up to 0.2 m. Conversely, piezometric levels in the wells close to the lake show rapid increases in piezometric levels, especially when the winds exceed 60 km/h.

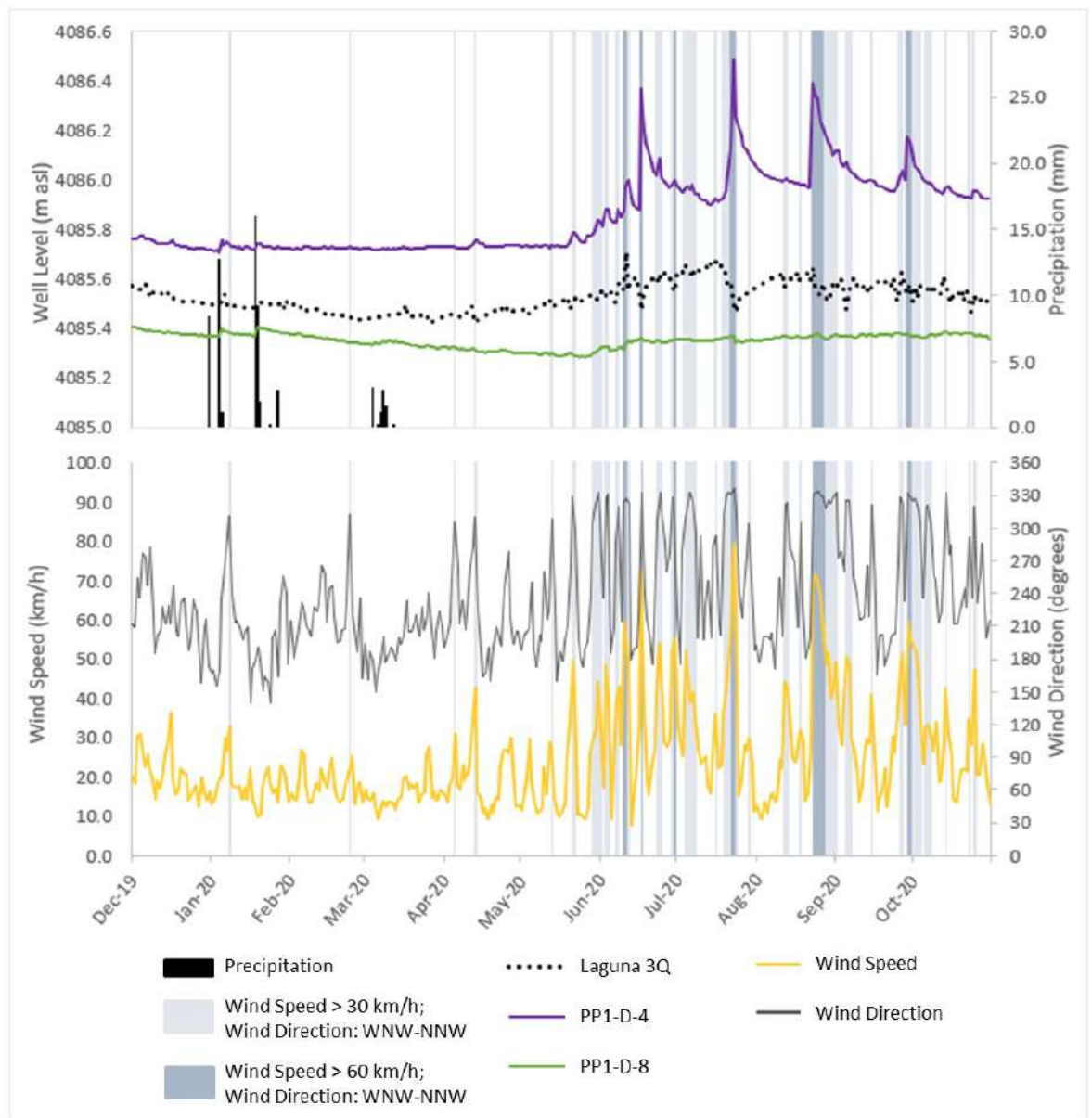


Figure 7-7: Example of wind fetch effect observed in Laguna 3Q (decreased level) and well PP1-D-4 (increased level), when sustained wind speed is >60 km/h from WNW to NNW. Well PP1-D-8 is shown as an example of a well that is responsive to precipitation but not wind fetch.

7.7 Groundwater Piezometry

An ongoing brine and groundwater monitoring program (shallow and deep) was initiated in October 2017, to better understand trends in and around the 3Q Salar. The temporal evolution of piezometric levels is shown on Figure 7-8, along with rainfall records, and lake levels. These data show a complex and variable range of piezometric trends and responses. During the observation period several wells became compromised due to salt precipitation. As a result, data impacted by salt precipitation were removed from the brine level data set used for numerical flow model calibration (Section 15.3).

Piezometric levels in Salar 3Q respond quickly to rainfall events, sometimes rising 0.2 m or more, and the effects tend to dissipate quickly. Meanwhile, the levels of Lagunas 3Q and Verde respond

more slowly, and they continue to rise over an extended period. These responses are consistent with direct precipitation input to the salar, versus a lagged and extended effect on the lakes, as they gradually receive the increased outflows from their respective watersheds. Laguna 3Q and wells located in the central, narrow portion of the salar also exhibit short-term rises in piezometric levels caused by wind fetch, as described in Section 7.6.2.

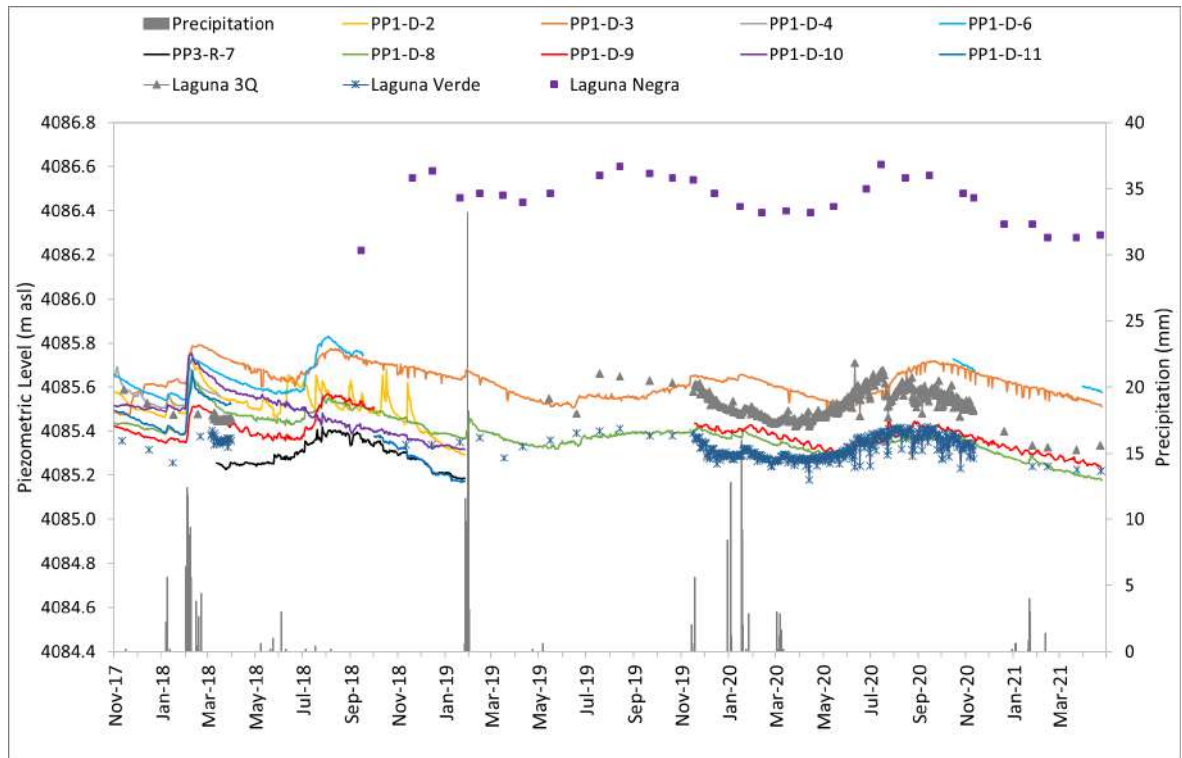


Figure 7-8: Salar and laguna piezometric levels collected by data logger and manual methods; rainfall from the Vaisala weather station.

General brine flow gradients within the salar were estimated based on piezometric levels. Observed trends are subtle due to the high permeability of the salar crust (typically Hyper-Porous Halite). However, there is a relatively consistent gentle outward hydraulic gradient trend from the east side of the central salar south towards Laguna Verde, north towards Laguna 3Q, and westward (Figure 7-9).

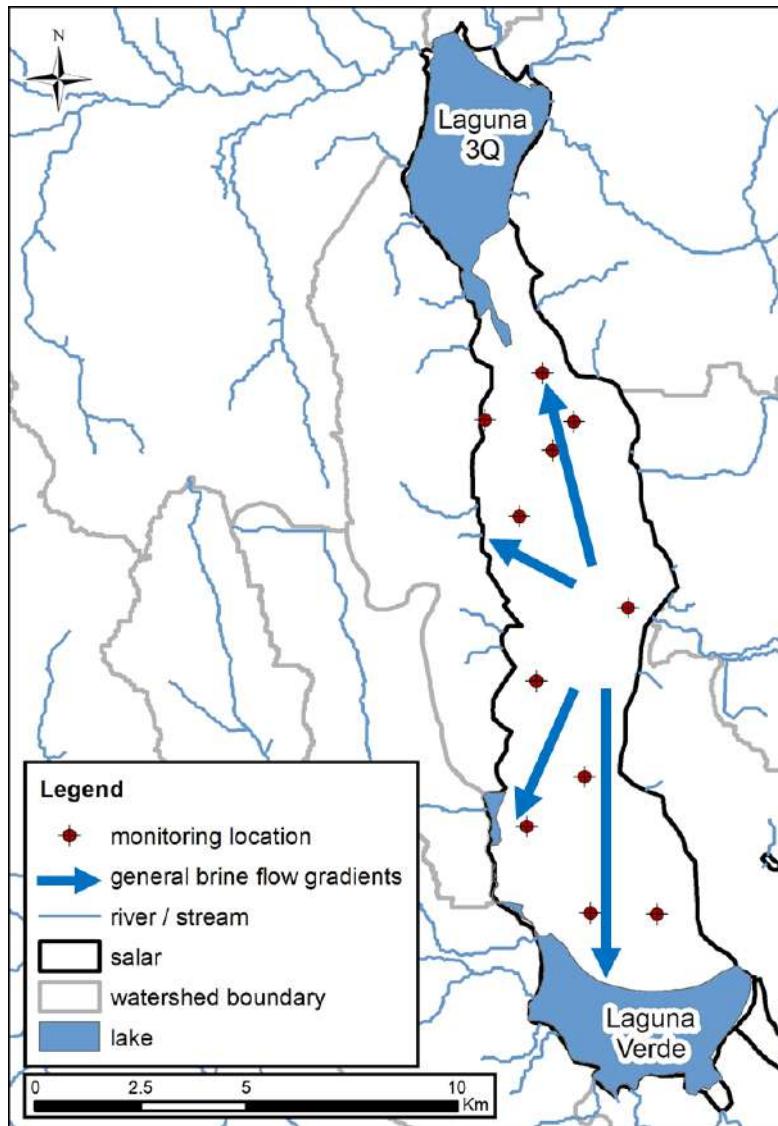


Figure 7-9: General brine flow gradients, based on the salar and lake level monitoring network.

7.8 Water Balance

An updated water balance for the 3Q Salar was performed as part of the development of the numerical Reserve Estimate model (Section 15). The updated annual water balance is based on FEFLOW modelling as described in Section 15.3, and results are provided in Table 7-3. Recharge to the salar occurs as lateral inflow from sub-watersheds, as surface stream flows, and as direct precipitation. Discharge from the salar is attributed to evaporation from the lakes, salar crust, and alluvial fans.

Table 7-3: Annual water balance for the 3Q Salar, based on flow modelling (Section 15).

Annual Water Balance	Salar de Tres Quebradas
Inflows	Average flow (L/s)
Recharge from precipitation	229
Sub-basin Inflow	1,389 ⁽¹⁾
Total inflows	1,618
Outflows	
Evaporation - lagunas	1,174
Evaporation - salar crust	214
Evaporation – alluvial fans	234
Pumping	0
Total outflows	1,622
Balance (Inflows-Outflows)	-4

(1) Initially based on Estimated HEC-HMS, calibrated through FEFLOW modelling.

7.9 Surface and Shallow Brine Hydrochemistry

Surface and shallow brine data from the 2015-2018 sampling campaigns were integrated and analyzed, including brine samples from:

- the salar crust;
- Lagunas 3Q and Verde; and
- the surface streams that discharge to the salar.

This analysis indicates that lithium, potassium, barium, boron, strontium and calcium follow similar spatial patterns, with the highest concentrations occurring in the northern part of the salar (Figure 7-10 and Figure 7-11). Lithium grades exceed 500 mg/L in Laguna 3Q, and also in the brine of the crust. Lithium locally increases to as high as 4,000 mg/L in the Laguna 3Q ponding zone. Sulfate, chloride, and sodium show distribution patterns that are affected by mineral equilibrium control with halite (“NaCl”) and gypsum (“CaSO₄·2H₂O”) (Figure 7-11).

These chemical trends in surface brine are shown in a N-S transect along the salar (Figure 7-12). The figure shows a general increasing trend from south to north for all the illustrated chemical components, with a peak occurring in the ponding zone of Laguna 3Q.

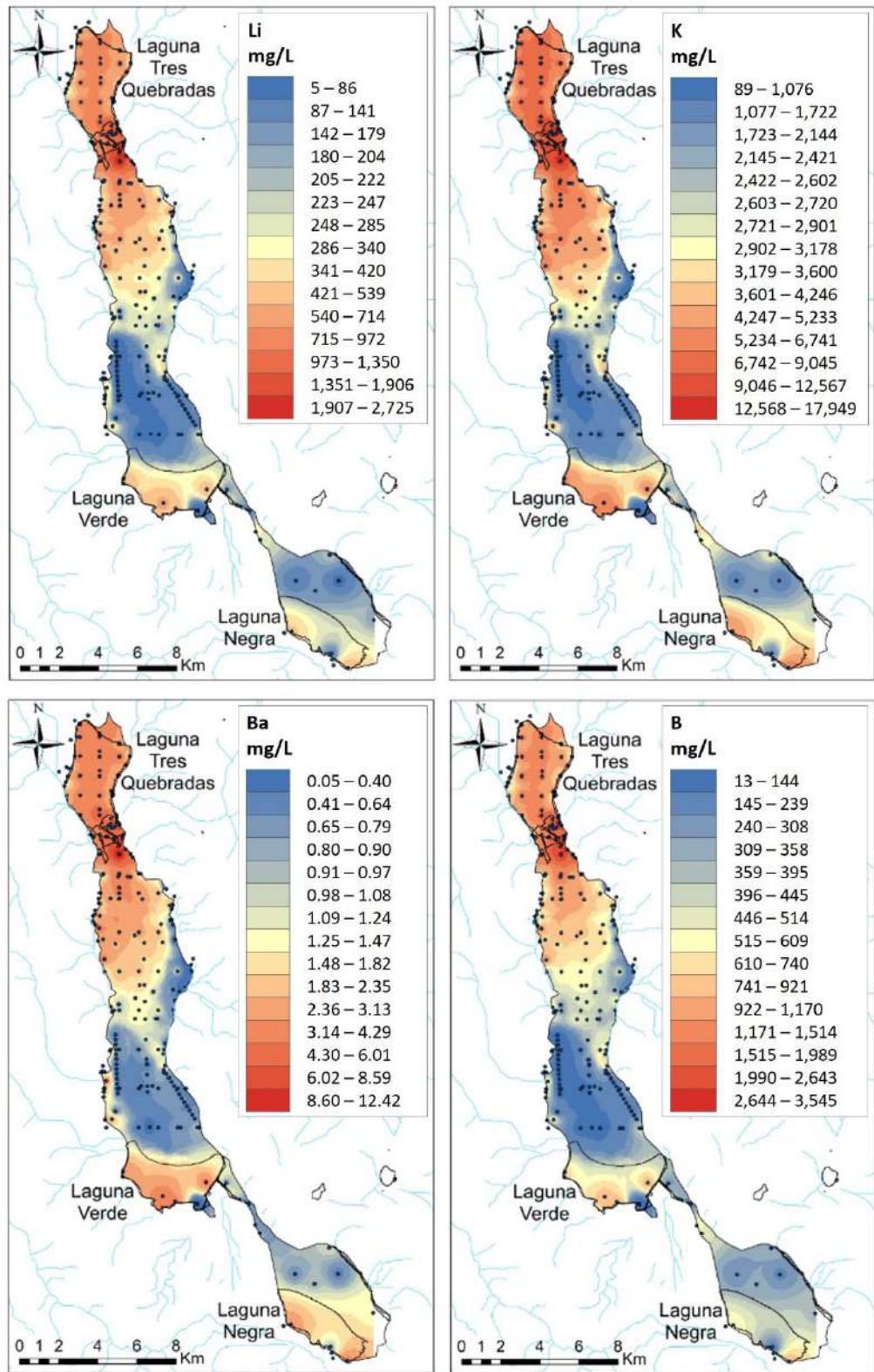


Figure 7-10: Surface brine concentration distributions for lithium, potassium, barium, and boron.

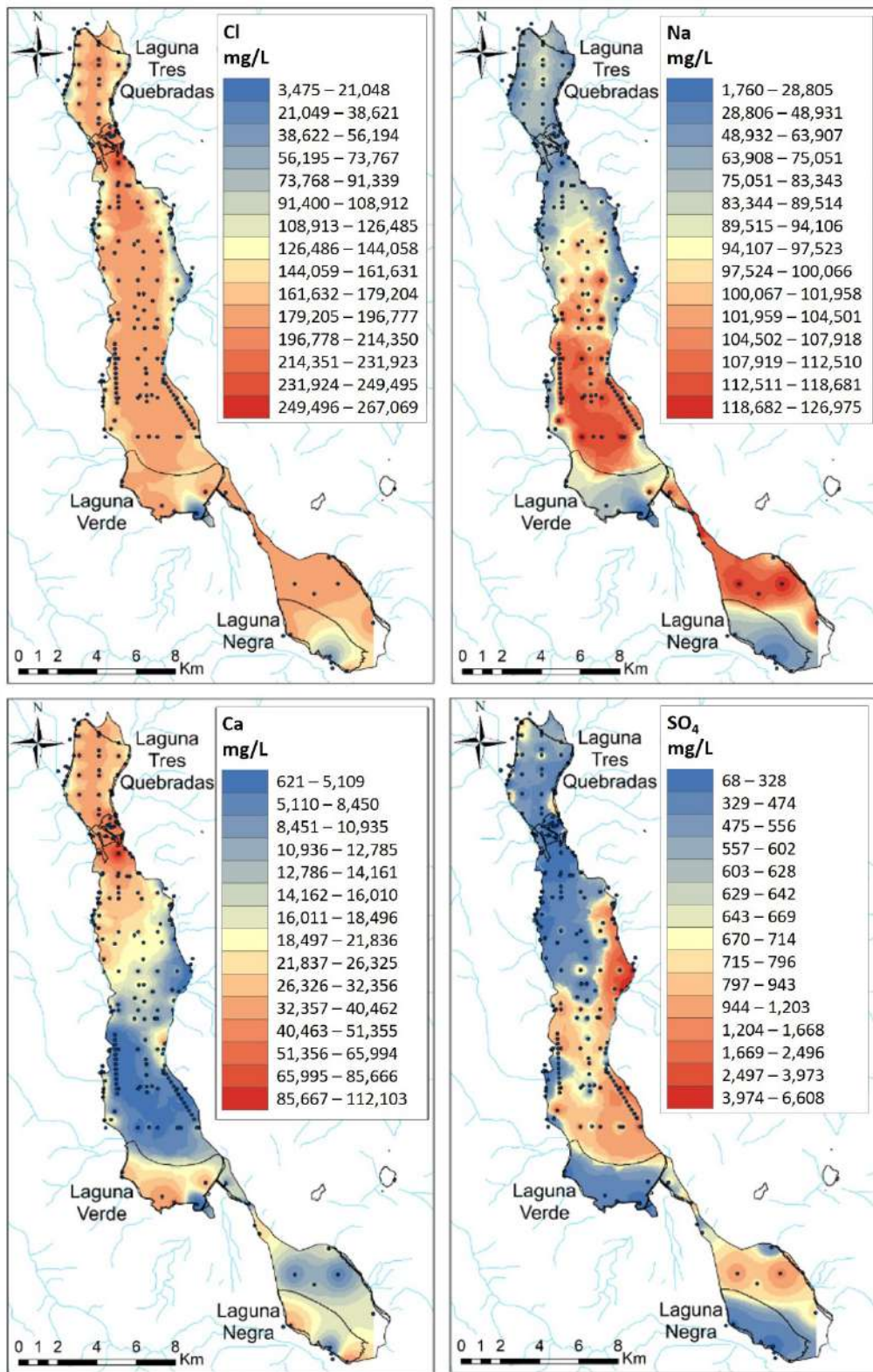


Figure 7-11: Surface brine concentration distributions for chloride, sodium, calcium, and sulfate.

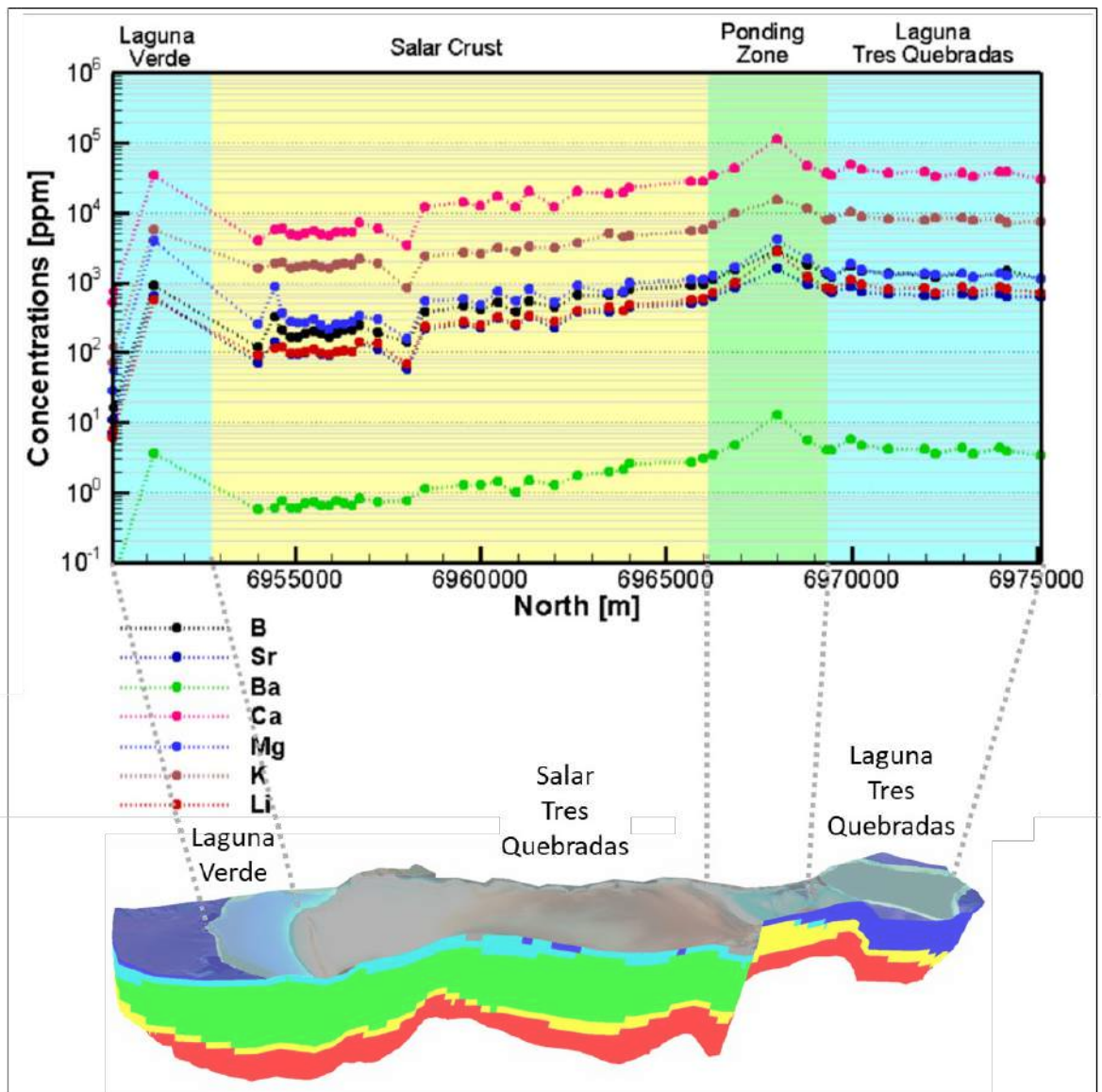


Figure 7-12: North-South transect of surface brine concentrations for boron, strontium, barium, calcium, magnesium, potassium, and lithium.

To better understand the genesis of the lithium-enriched brine, evaporation (by a factor of 100) was simulated for a water sample from Rio Salado, using a numerical thermodynamic model for concentrated brines ((1)PHREEQC). The starting lithium content of the sample was 35 mg/L. Results are shown on Figure 7-13. Simulated evaporation suggests that lithium-enriched brines in 3Q Salar could be explained through evaporation of Rio Salado water, by a factor of 20 to 40.

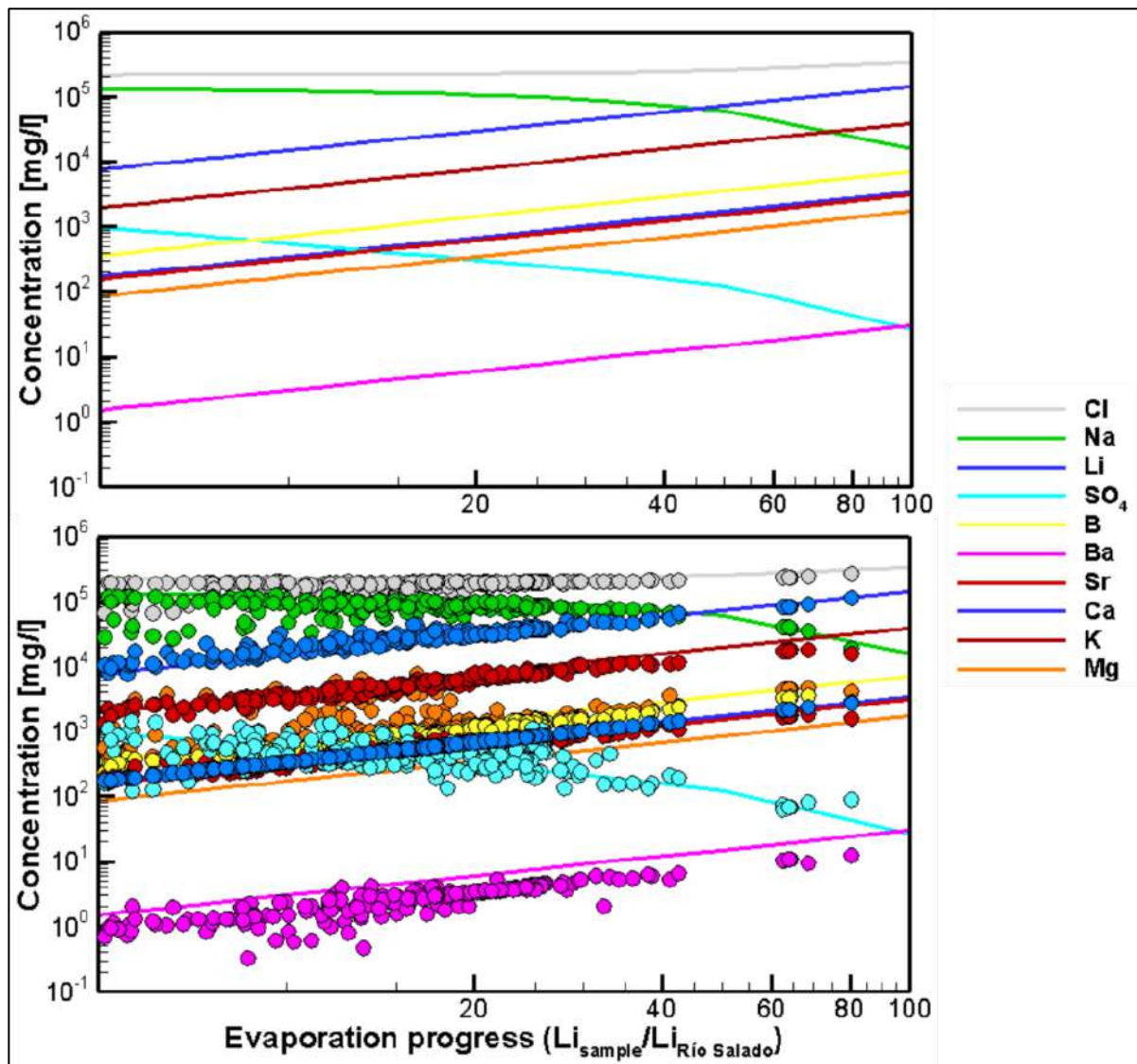


Figure 7-13: Simulated evaporation of a water sample from Rio Salado (top). Water and brine samples collected during the first four 3Q Project sampling campaigns, super-imposed on simulation results (bottom).

7.10 Subsurface Brine Hydrochemistry

Subsurface brine sampling conducted during the 2017-2021 drilling campaigns includes brines from all six primary geological units, including:

- Hyper-Porous Halite;
- Upper Sediments;
- Porous Halite;
- Massive Halite;
- Lower Sediments; and
- Fanglomerate.

Integration and analysis of data from these samples show similar horizontal hydrogeochemical trends to those observed in the surface and shallow brines (Section 7.9). For example, lithium, potassium, and strontium follow similar spatial trends of increasing concentration towards the

northern part of the salar (Figure 7-14). As observed in the surface and shallow brines, Sulfate decreases slightly towards the north. This distribution trend is considered a result of mineral equilibrium control with gypsum ($\text{CaSO}_4 \cdot 2\text{H}_2\text{O}$) precipitation (Figure 7-14).

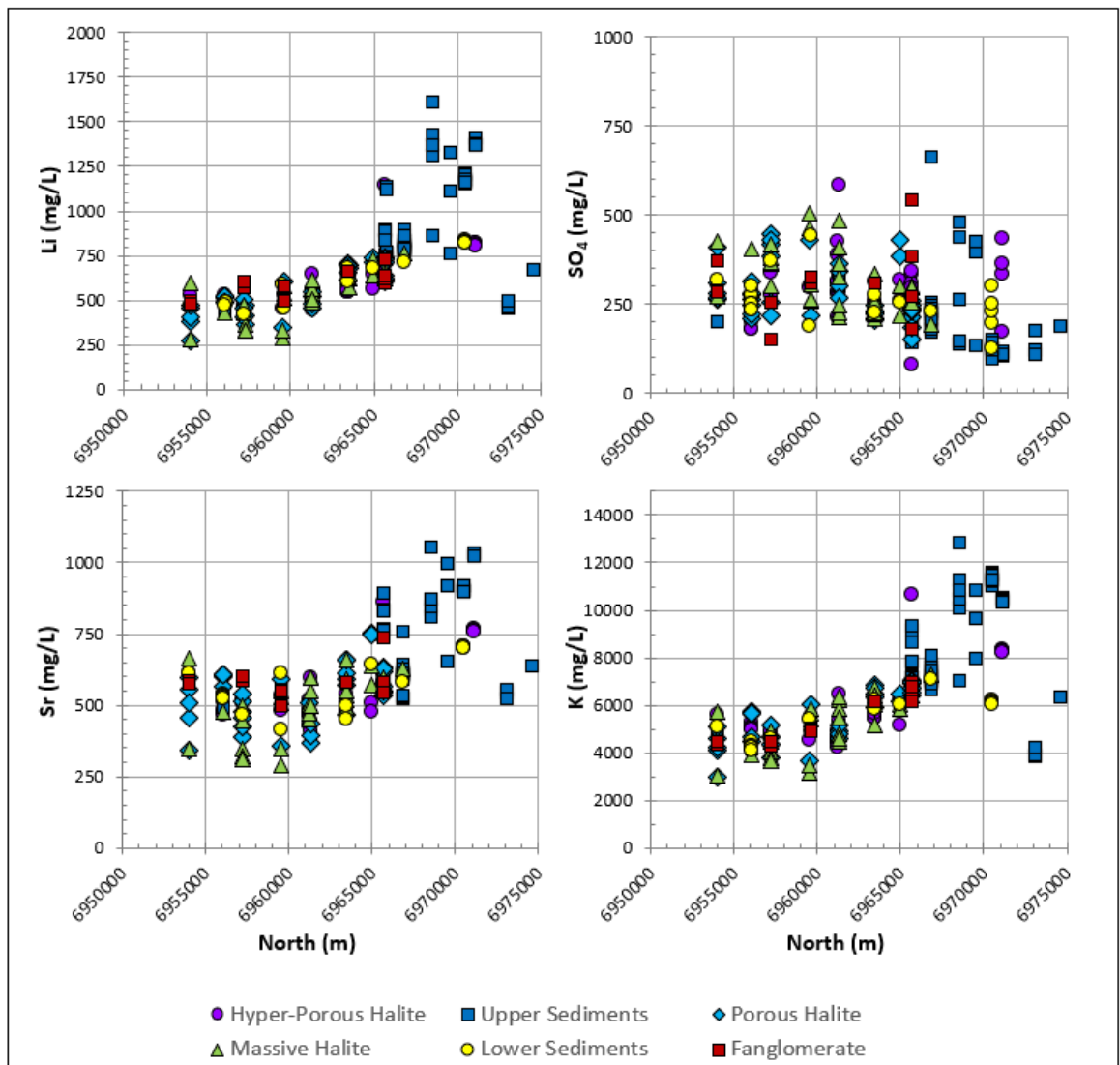


Figure 7-14: North-south distribution of lithium, sulfate, strontium, and potassium in subsurface brine samples from the 2017-2021 drilling campaigns.

Vertical trends in hydrogeochemistry indicate that subsurface brines are relatively homogenous with depth (Figure 7-15). The greatest variations in lithium, potassium, strontium, and sulfate concentrations occur in the upper Hyper-Porous Halite and Upper Sediments. Lithium grades exceed 500 mg/L throughout the geological column and grades in excess of 1,000 mg/L were detected in the two upper units, Hyper-Porous Halite and Upper Sediments.

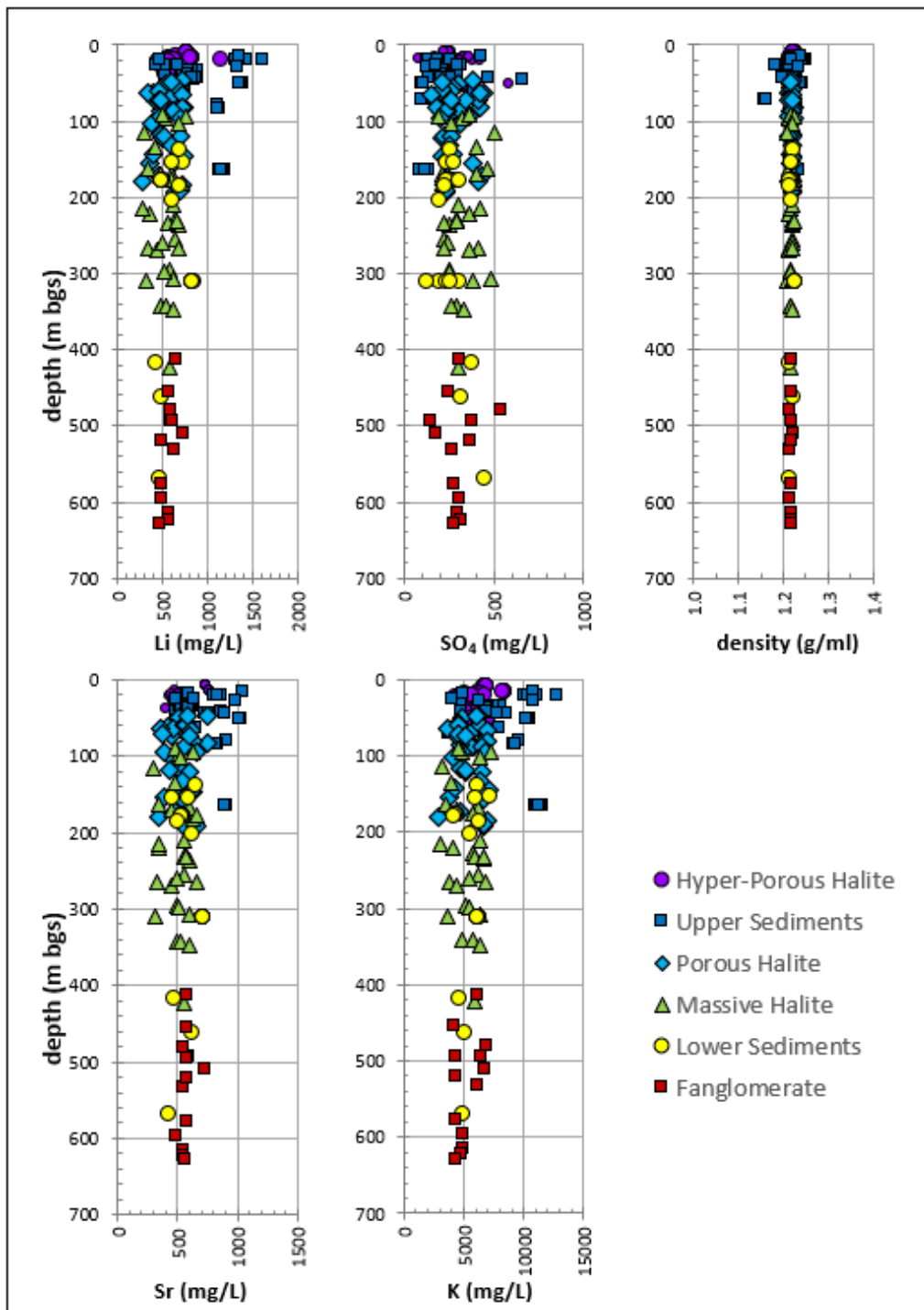


Figure 7-15: Vertical distribution of lithium, sulfate, strontium, potassium, and density in subsurface brine samples from the 2017-2021 drilling campaigns.

8. Deposit Types

Brine deposits containing economically important quantities of lithium can form in salars where the following favourable conditions are coincident:

- The salar catchment is “closed,” which means the outflow of water from the catchment (by processes other than evaporation) is negligible, in terms of the catchment water balance.
- A significant portion of the catchment area contains bedrock of suitable composition (i.e., containing lithium that can be leached).
- Geothermal waters have contacted the bedrock through fault systems and have become moderately concentrated in lithium (and other solutes).
- The moderately concentrated waters have accumulated in the low-lying area of the closed catchment.
- The prevailing climate is suitable to promote high rates of evaporation from the accumulated water (i.e., dry air, high winds, and minimal precipitation), leading to the formation of brine within the salar.
- Given the preponderance of lithium-bearing salars that are defined by fault-bounded dropped basins, this also appears to be an important condition. The process of basin lowering may provide a more prolonged period and a more focused zone for brine accumulation. The bounding faults may also be a direct source of lithium-enriched geothermal waters to the salar.

3Q Salar meets these conditions. The salar catchment is closed with no apparent outflows. Elevated levels of lithium have been detected in geothermal and cold waters flowing into the salar. There is clear evidence that evaporation has led to the accumulation of evaporites and lithium brines in the near-surface of the salar, in lakes, and at depth.

In terms of in-fill materials, salars that contain brine deposits are of two principal lithologic types: clastic-dominant and evaporite-dominant. The formation of one or the other lithology may depend on the energy of the system during deposition. Evaporite formation may be favoured during relatively dry periods of low inflow, and deposition of clastic materials during higher inflow periods. Similarly, deposition of clastic materials may be favoured around the margins of the salar basin, while the more quiescent central zone may be dominated by evaporites. Consequently, both types of deposits may occur at different levels and zones of a given salar, depending on the prevailing conditions of deposition.

Evaporite-dominant salars contain mostly halite deposits, which can reach hundreds of metres in thickness. Within approximately 50 m of the surface, the porosity and permeability of halite may be amenable to economic extraction of brines. However, deposit permeability may decrease rapidly with depth due to evaporite cementation and recrystallization. Classic examples of evaporite-dominant salars include Salar Hombre Muerto (Argentina) and Salar Atacama (Chile).

Clastic-dominant salars are characterized by predominantly clastic strata interbedded with minor evaporites, particularly halite. Porosity and permeability of the clastic layers are controlled by lithology, stratigraphy, and faults. Clastic-dominant salars are exemplified by the Silver Peak deposit in Nevada and Argentina's Cauchari and Olaroz Salars.

The 3Q Salar has aspects of both salar types. Within the salar, there is a substantial occurrence of evaporite sequences in excess of 200 m. However, there are also three laterally extensive clastic units (Upper Sediments, Lower Sediments, and Fanglomerate) that show evidence of extended periods of clastic-dominant deposition. Furthermore, there are frequent thin clastic layers, ranging from a few to several cm, within the evaporite units. These clastic layers tend to

increase in frequency and/or thickness, with proximity to the formal clastic units, often forming a gradual transition zone from the evaporite units to the clastic units.

9. Exploration

9.1 Overview

Five sets of field work have been conducted to date at the 3Q Project, to evaluate the lithium development potential of the deposit:

1. Reconnaissance (“Recon”) – 2015 (first reported by King, 2016);
2. Program 1 - 2015/16 (first reported by King, 2016);
3. Program 2 - 2016/17 (first reported by King, 2017);
4. Program 3 - 2017/18 (first reported by King, 2018); and
5. Program 4 – 2018-21 (first reported herein).

Exploration components conducted during the first four exploration programs are summarized in Table 9-1. Components of the 2018-21 program are summarized in Table 9-2.

Table 9-1: Summary of the exploration work reported previously - 3Q Project.

Exploration Component	Purpose	Description
Surface brine sampling in the Salar and Lakes (Recon, Programs 1, 2, and 3)	To map surface brine distributions; to evaluate lake dynamics	636 samples (including salar surface, lake, and river samples, and 116 QA/QC samples)
Vertical Electrical Sounding (“VES”) Surveys (Programs 2 and 3)	To map subsurface resistivity trends for use in siting boreholes; To evaluate strata and brine conditions near lakes and discharge zones	35 VES locations, along 8 sections throughout the salar 20 VES locations, along 5 sections surrounding the salar
Diamond Drilling (Programs 2 and 3)	To collect cores and brine samples; To monitor pumping tests	6,145.7 m of drilling in 23 boreholes Construction of 20 wells 310 core samples for RBRC
Rotary Drilling (Programs 2 and 3)	To conduct and to monitor pumping tests in shallow and deep aquifers	3,114.3 m of drilling in 26 boreholes Construction of 16 pumping wells and 11 observation wells
Brine sampling from packers and wells (Programs 2 and 3)	To map subsurface brine distributions	284 brine samples (including 66 QA/QC samples) from packers and wells
Pumping Trenches (Program 2)	To conduct pumping tests in the near-surface aquifer	Installation of 2 Pumping Trenches
Pumping Test Programs (Programs 2 and 3)	To determine aquifer characteristics and brine chemistry; To obtain hydraulic parameters for developing a numerical flow model	Pumping tests at 12 Pumping Wells (15-72 hr Constant Rate; 1-3 hr Step Test) 2-6 hr pumping tests in Pumping Trenches
2D Seismic Survey (Program 3)	To map the salar basement and in-fill deposits	11 seismic lines, along 49.34 km, inside and outside salar

Table 9-2: Summary of the 2018-21 exploration work – 3Q Project.

Exploration Component	Purpose	Description
Rotary Drilling	To conduct and to monitor pumping tests in shallow and deep aquifers; To test for aquifers outside of the previous (PFS) model domain	1,296.0 m of drilling in 6 boreholes; Construction of 3 pumping wells and 2 observations wells
Brine sampling from wells	To map subsurface brine distributions	70 brine samples (including 12 QA/QC samples) from wells
Pumping Test Program	To obtain hydraulic parameters for supporting updates to the numerical flow model	Pumping tests at 4 Pumping Wells (1-19 day Constant Rate; 3-72 hr Constant Rate)
Ongoing River Flow Rate Monitoring (since December 2016)	To monitor flow rates of streams and rivers that discharge into the salar basin, and to support numerical modelling lateral boundary inputs	316 flow rates recorded from 17 monitoring locations (Section 7-6)
Ongoing Lake and River Sampling	To monitor surface chemistry in lakes and rivers, and to support numerical modelling transport boundary conditions	441 samples (including 108 QA/QC samples) (collected since June 2018; earlier samples listed in Table 9-1)

9.2 Vertical Electric Sounding (“VES”) Surveys

VES lines conducted to date for the 3Q Project are shown on Figure 9-1. The initial set of eight lines (conducted in 2016 for the 2016/17 Field Program; A-A' through H-H' on Figure 9-1) were implemented to support the design of the initial drilling program. Results were first reported by King (2017). The first VES Survey identified the following geoelectric units and trends:

- A very highly conductive zone was identified which was interpreted as consisting mainly of evaporites and clastic sediments (Unit 1).
- A zone of medium conductivity was interpreted as porous or cavernous evaporitic sequences with possible clastic sequences (Unit 2).
- Units 1 and 2 have a combined thickness of over 90 m in the northern end of the salar.
- A lower conductivity unit was interpreted to consist of evaporites, extending to an average depth of 200 m (Unit 3).
- A lower conductivity zone was interpreted as Tertiary sediments (Unit 4).
- Units 1 and 2 were interpreted as having the best potential for containing brine.

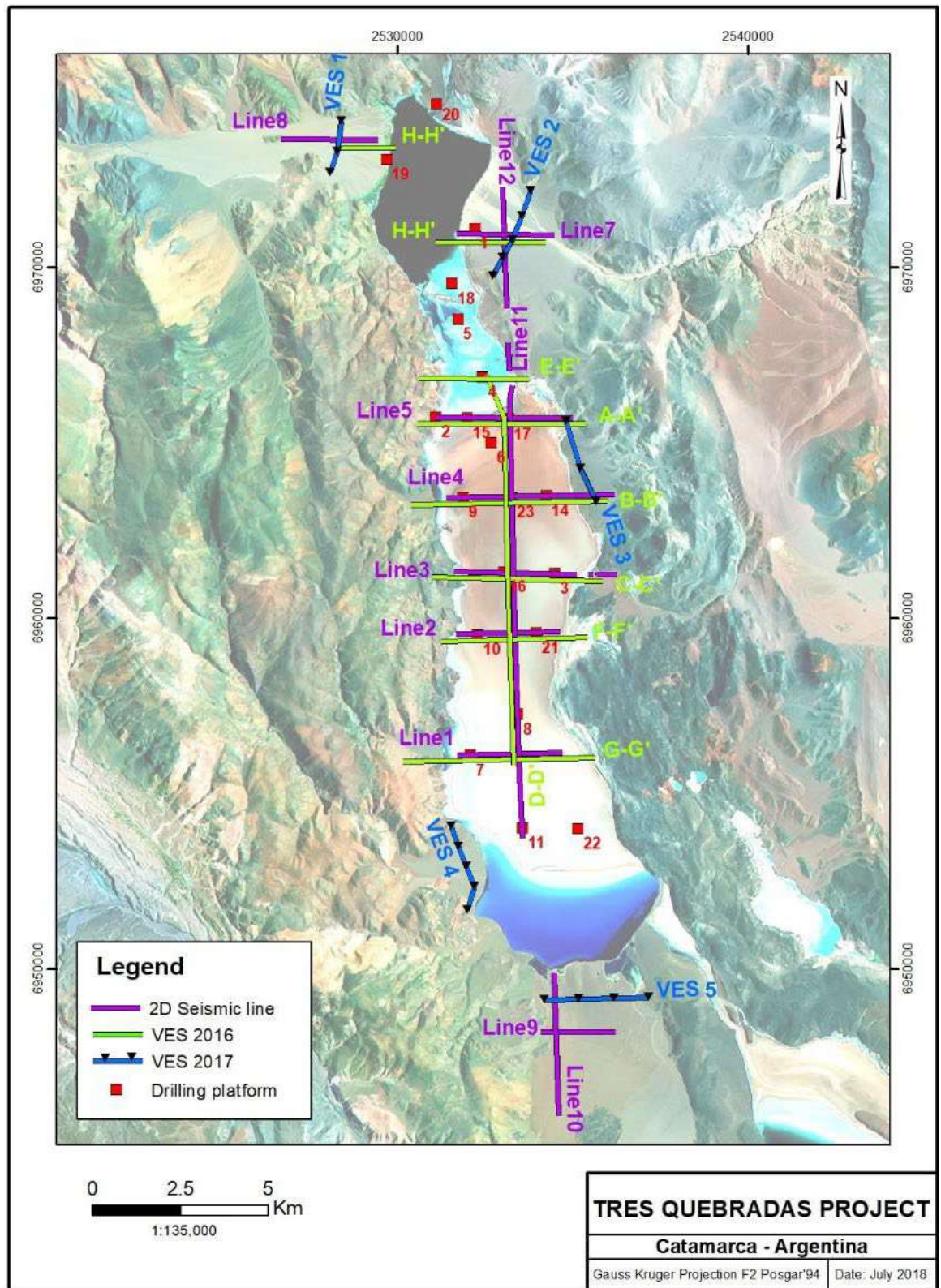


Figure 9-1: Surface geophysics (VES and Seismic) conducted to date - 3Q Project.

A second VES Survey was conducted in 2017, during the 2017/18 Field Program (see Photo 9-1 for equipment used). The objective of this second survey was to investigate stratigraphy and brine conditions adjacent to lakes, and to zones of potential groundwater discharge to the salar. The five new lines conducted for the second VES Survey are shown on Figure 9-1 and the new VES

sections are provided in Appendix C. Results were first reported by King (2018). The key findings from the 2017 VES Survey are as follows:

- At VES Line 1 the occurrence of basement was inferred, as a U-shaped valley in-filled with alluvial sediments. Salinity increases towards the bottom of the valley. The top of the basement is at a depth of approximately 175 m. Complimentary information indicates that it is composed of Permian Volcanics.
- At VES Line 3 it is inferred that the alluvial fan surface material extends to a depth of 75 m and is underlain by Miocene sediments up to 700 m deep. The Permian volcanic basement was not distinguishable.
- At VES Line 4 (in a southwest alluvial cone) it was inferred that clastic sediments extend to about 125 m and are underlain by Permian Volcanics (basement).
- VES line 5 shows a basement of Tertiary sediments at a depth of about 400 m, forming a valley filled with sand and gravels. Salinity increases downwards.



Photo 9-1: VES equipment.

9.3 Seismic Survey (2017/18 Program)

A two-dimensional (“2D”) Seismic Survey was conducted at the 3Q Project, along 49.3 km length of survey lines (Figure 9-1) and originally reported by King (2018). The objective was to investigate stratigraphy (basement and in-fill evaporites and sediments), especially at locations that were complementary to the VES Surveys (Section 9.2) and drilling (Section 10).

This Survey was performed by Union Geofisica Argentina S.A. (“UGA”) from October 24 to November 1, 2017. A Vibroseis Sercell (62,000 lbs) was used, with seismometer spacing of 20 m (Photo 9-2). Eleven seismic lines were acquired, with six located within the salar, and the remaining five outside. The eastern line tiles spanned from within the salar towards the outer limits, to analyze the structure of the border beneath the alluvial fans. The paths used to access the salar were initially constructed the year before, to perform the VES Survey, and were widened for the Seismic Survey.



Photo 9-2: Vibroseis Sercell with seismometers set up at 20 m spacing (left). Interior controls for the seismic equipment (right).

The processing was completed over a 40-day period, by Seiscenter S.A., located in Buenos Aires, Argentina. The following processing methodology was used:

1. Static (topographic) corrections were made for each geophone station with a geo-referenced survey prepared by UGA. Seismic tomography (seismic refraction method) was interpreted for each line.
2. Noise attenuation was used to eliminate ground roll noise and frequencies content.
3. Migration processing was incorporated using Pre-Stacking-Time-Migration methodology, where the seismic information signals are shifted, to improve the image of dipping reflectors.
4. A velocity was chosen every 50 Common Deep Points, and was estimated at a spacing of every 500 m. It was determined that the first strong (shallowest) signal reflector was due to the P-wave arrival.

Interpretation of the seismic sections is provided in Appendix D, with integration of VES and drilling results. These interpretations were developed by geophysicist Daniel Soubies and edited by geologist Santiago Grosso. The sections show that the salar is deeper in the centre than at the borders, with normal faults dipping towards the basin. The red horizon shown in the sections is interpreted as the “Seismic Basement”, which is a reflector beyond which the seismic signal was not able to effectively penetrate.

Line 11 (Appendix D) shows an extensive north-south image of the salar. It shows a reflector that clearly corresponds with the base of Massive Halite (“MH”) and another observable reflector that is the transition between the Porous Halite (“PH”) and MH. The strong reflection near the surface is noise from the arrival of the P-wave. At the south and north ends of Line 11, Lower Sediments (“LS”) and Fanglomerates (“FG”) are interpreted to thicken, and the MH thins. These trends were confirmed at wells D-17 and D-22.

Lines 1, 2, 3, and 5 cross the salar from east to west (Appendix D, Figures D-1, D-2, D-3, and D-4, respectively). They display a half-graben structure with the Permian volcanic (Choiyoi group) basement dipping approximately 14 degrees to the east. The LS and FG both thicken to the east. The eastern border of the salar shows a steep fault predominantly dipping west. Line 2 also shows numerous small faults dipping to the centre of the salar. The PH / MH boundary is interpreted to be at a depth of approximately 170 m below the surface. The deeper halite displays less interbedding in the centre of the salar, away from the influx of alluvial sediments.

Lines 7 and 12 cross the northeastern margin of the salar from east to west and north to south, respectively (Appendix D, Figures D-5 and D-6, respectively). These seismic sections were updated based on the lithology intersected in well R-25 as part of the 2018-21 Program. The units previously identified as Tertiary sediments (T1, T2, and T3) correlate with the Upper Sediments (“US”), LS, and FG. The updated sections show that the LS and FG extend into the northern salar

and fill a half graben structure within the Permian volcanic (Choiyoi group). The revised geology was confirmed at well R-26.

Appendix D shows a composite of seismic lines 10, 11, and 12 which reveal structures both within, and outside of the salar. Tectonic uplifting of the salar basement is evident, possibly the result of reverse basement thrusting.

9.4 Surface Brine Sampling Program

Surface brine sampling was conducted at the 3Q Project during all five field work sets, with the following activities and evolution of objectives:

- An initial Recon Program was conducted throughout the 3Q Salar basin during December of 2015, for a general indication of lithium presence at the site (reported by King, 2016).
- A systematic grid program of lake and salar surface sampling was implemented in 2015/16 Program, following favourable results from the Recon Program. The objective of this sampling was to determine the extent and trends of lithium in shallow brine (first reported by King, 2016).
- Additional surface brine samples were collected during the 2016/17 Program, to fill in gaps in the earlier work, and to test for changes due to weather (for example, precipitation inputs) (first reported by King, 2017).
- During the 2017/18 Program, sampling was conducted to evaluate lake dynamics and to investigate a low concentration zone in the south surface area of the salar (first reported by King, 2018).
- Regular and ongoing lake sampling was conducted during the 2018-21 Program.

Figure 9-2 shows the chronology of the surface brine sampling in 3Q Salar and the three adjacent brine lakes. Sampling methods are described in Section 11. Interpolations of selected surface brine results from 2015-2018 are shown on Figures 7-10 (lithium, potassium, barium, and boron) and 7-11 (chloride, sodium, calcium, and sulfate). The magnesium to lithium (“Mg/Li”) ratio in surface brine is shown on Figure 9-3, where a decreasing trend towards the south is apparent. A bathymetric map of the Lagunas 3Q and Verde is shown on Figure 7-6, and surface and shallow brine hydrochemistry results are discussed in Section 7.9.

9.5 Ongoing Monitoring Programs

A river and lake monitoring program was initiated in 2016, to monitor flow rates and chemistry of streams and rivers that discharge into the salar basin; and to monitor variations in water levels and chemistry of the lakes within the salar (Sections 7.6, 7.7, and 7.9). Water and brine samples, flow measurements, and lake levels are collected monthly at the river and lake monitoring stations shown on Figure 9-2. These samples continue to be collected on an ongoing basis.

Results from the monitoring program were used to help define boundary conditions for numerical modelling (Section 15). Sampling methods are described in Section 11. Results of the monthly flow rate monitoring are shown on Figure 7-5.

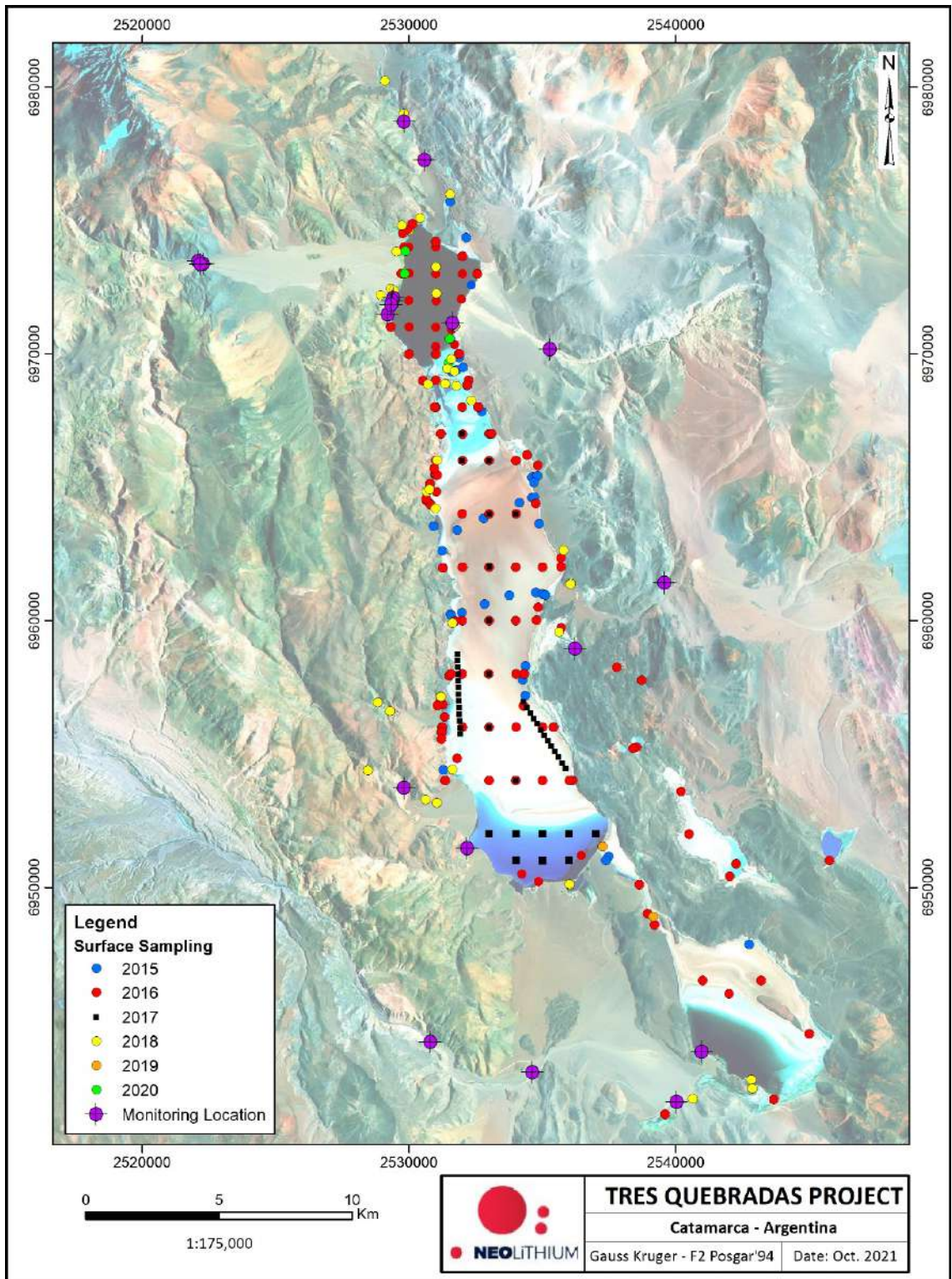


Figure 9-2: Chronology of surface brine sampling and monitoring locations in the 3Q Salar.

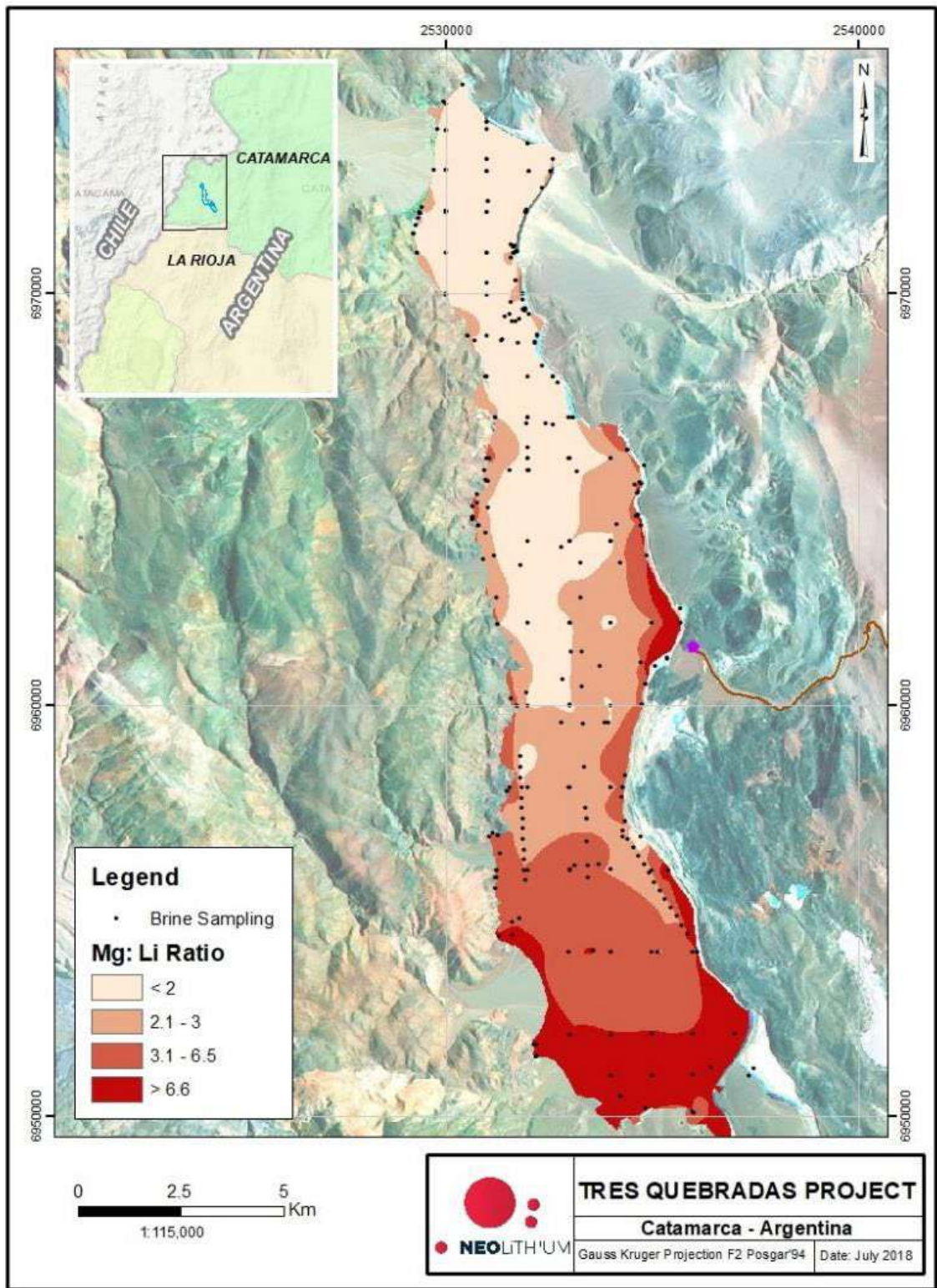


Figure 9-3: Interpolation of the magnesium-lithium ratio in surface brine samples collected in 2015 through 2018.

9.6 Pumping Test Program

9.6.1 Summary of Pumping Test Program Figures

Three rounds of pumping tests have been completed at the 3Q Project, to support Reserve estimation. Pumping tests focused on the shallow units, as the current targets for lithium recovery. Test locations are shown on Figure 9-4, and include:

- 2016/17 Program: Pumping tests were performed on 5 wells and 2 shallow trenches, by Conhidro SRL (“Conhidro”), an Argentinean company. Results were first reported by King (2017).
- 2017/18 Program: Eleven 72-hour pumping tests were conducted. Results were first reported by King (2018).
- 2018-21 Program: One 19-day pumping test was performed at well R-4. Three 72-hour pumping tests were performed at wells R-18, R-23, and R-26. Results for these tests are first reported herein and are summarized in Table 9-3.

All long-term, constant rate pumping tests were re-analyzed as part of the 2018-21 Program. A description of data processing and analysis is provided in Section 9.6.2. Results are summarized in Section 9.6.3 and Table 9-3 below.

9.6.2 Summary of Hydraulic Parameter Analysis and Data Processing

Assessment of hydrogeological parameters was undertaken using small numerical models of the salar, in proximity to each pumping well (in FEFLOW). This approach was used instead of the more traditional approach using pumping test analytical methods, because it can accommodate wells that are screened across more than one unit, and it can provide insight into multi-unit interactions. Brine level responses during pumping tests were simulated in FEFLOW and compared to observed drawdown.

Simplified FEFLOW “box models” were developed for each test, to perform multiple numerical simulations under a range of parameter combinations. Each box model was constructed as follows:

- The model extended horizontally for 2.5 km in each direction from the pumping well, while the thickness was extended from ground surface to 25 m below the bottom of the deepest screened unit intersected by the pumping well. This thickness allowed representation of all screened units as well as a portion of the unit underlying the pumped well. The model thickness was subdivided into 25 uniformly spaced layers.
- Model layers were parameterized with hydraulic conductivity, storage, and porosity values (i.e., for specific yield) consistent with the geologic unit thicknesses intersected at the pumping well platform.
- Lateral boundary conditions were established as natural non-pumped water levels. Pumped brine discharge was simulated at ground surface as a point recharge flux. Lakes and other boundaries were incorporated as reflected in observation data.
- Observation well locations were set at distances based on field measurements.

Simulations were initially parameterized using calibrated values from the PFS modelling (King and Zandonai, 2021) and porosity values from relative brine release capacity (“RBRC”) analysis (Table 10-2). Sensitivity analyses were then performed by sequentially varying the parameter values. Results were graphically analyzed to evaluate best fit values and to understand the degree that pumping test observations constrain the tested parameters. Example simulated drawdowns calculated using best fit parameter values for the pumping test are shown on Figure 9-5.

9.6.3 Summary of Hydraulic Parameter Results

Results of the pumping test analyses provided in Table 9-3 show that hydraulic conductivities are variable throughout the salar. The HPH had the highest conductivity and is expected to dominate brine transport where significant thickness exists. US, LS, and FG were also found to have significant hydraulic conductivity. The PH and MH units had moderate and low hydraulic conductivity values, respectively.

Anisotropy (ratio of horizontal to vertical hydraulic conductivity) values were found to range from a low of 10 to a high of 20,000. A value of 10 is typical of sedimentary sequences, representing fluctuations between higher and lower energy environments throughout depositional history of the unit. Large anisotropy values (100 to 20,000) reflect lumping of finer (e.g., silt) and coarser (e.g., sand) deposits within a geological unit.

Specific storage values were found to be consistent across the salar and are within expected ranges. Pumping test analytical results generally supported porosity values determined through RBRC analyses (Table 10-2).

The hydraulic parameter values determined with the pumping test data, including the hydraulic conductivity (“Kh”), Anisotropy (“Kh/Kv”), and the specific storage coefficient (“Ss”), were used to support the updated numerical Reserve model (Section 15.2).

9.7 Data Processing

Laboratory data and borehole log information were compiled in a Microsoft Access database and processed using Microsoft Excel spreadsheet software. All relevant spatial site information and mapping is compiled in ESRI ArcMap or Manifold System GIS. Google Earth satellite imagery was used to identify topographic and hydrologic features.

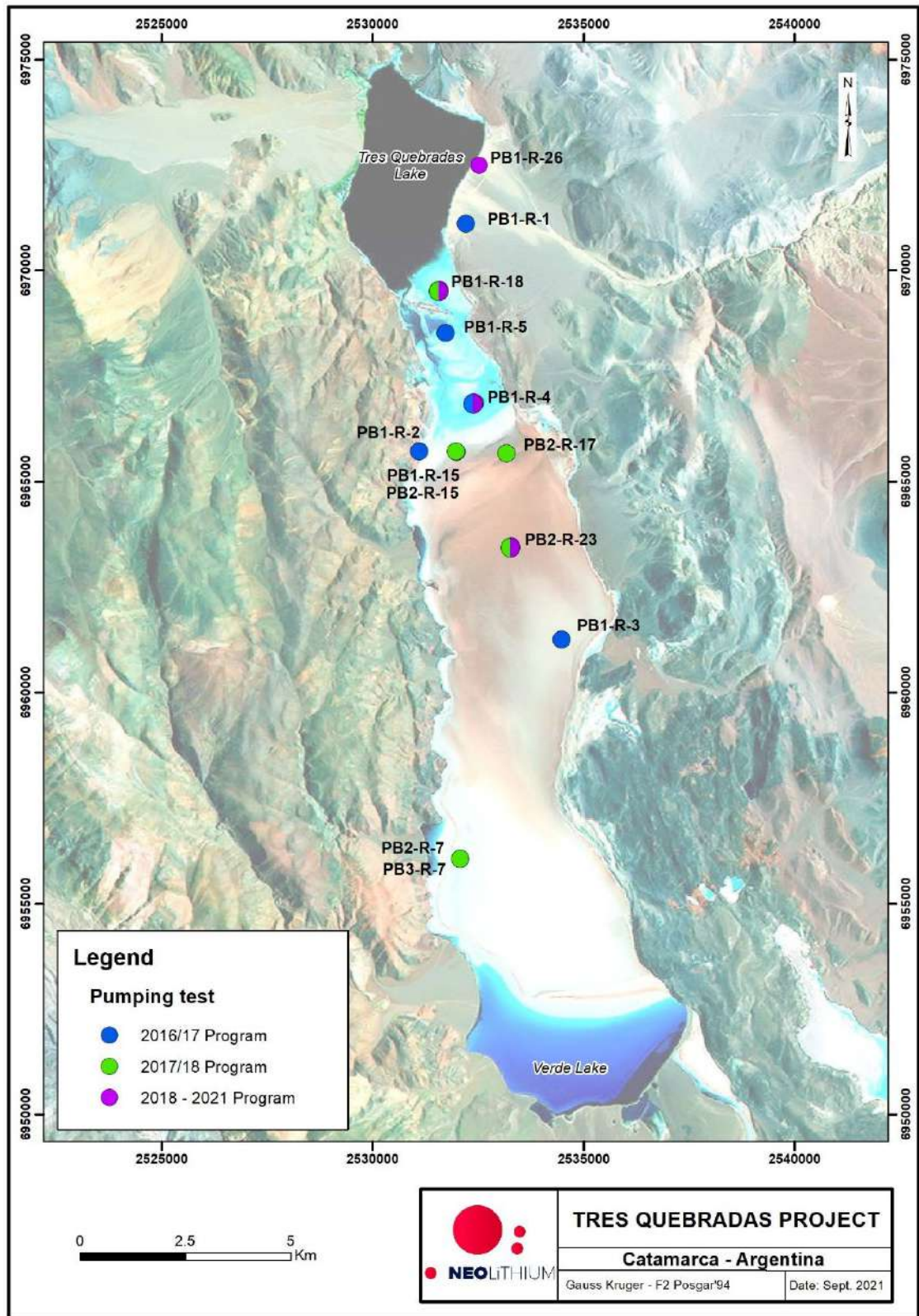


Figure 9-4: Chronology of pumping tests conducted at the 3Q salar.

Table 9-3: Aquifer hydraulic parameters determined from pumping tests, using FEFLOW.

Unit	PB1-R-2	PB1-R-3	PB1-R-4	PB1-R-5	PB2-R-7 PB3-R-7	PB1-R-15 PB2-R-15	PB2-R-17	PB1-R-18	PB2-R-23	PB1-R-26
Hydraulic Conductivity: Kh (m/d)										
Best Fit Kh [Calibrated Range for Kh]										
Hyper-Porous Halite	35 [35-50]	750 [500-750]	290 [200-300]	350 [290-800]	750 [600-800]	100 [80-120]	200 [200]	250 [250-290]	240 [220-250]	-
Upper Sediments	20 [10-20]	20 [2-200]	20 [2-20]	20 [20-200]	0.9 [0.2-1]	5 [3-7]	20 [2-200]	10 [10-20]	-	20 [2-200]
Porous Halite	-	0.05	5	0.05	0.2	5	5	-	0.04	-
Massive Halite	-	0.01	0.01	-	0.01	-	0.01	-	-	-
Lower Sediments	-	-	-	-	-	-	-	-	-	20
Fanglomerate	-	-	-	-	-	-	-	-	-	20
Anisotropy (Kh/Kv)										
Hyper-Porous Halite	100	100	100	100	10	10	10	100	100	-
Upper Sediments	100	100	100	10	20,000	20,000	-	100	-	100
Porous Halite	-	50	100	50	5,000	5,000	5,000	-	10	-
Massive Halite	-	10	10	-	10	-	10	-	-	-
Lower Sediments	-	-	-	-	-	-	-	-	-	100
Fanglomerate	-	-	-	-	-	-	-	-	-	2,000
Specific Storage: Ss (1/m)										
Hyper-Porous Halite	1.0E-04	1.0E-04	1.0E-04	1.0E-04	1.0E-04	1.0E-04	1.0E-04	1.0E-05	1.0E-05	-
Upper Sediments	1.0E-04	1.0E-04	1.0E-04	1.0E-04	5.0E-05	1.0E-04	-	1.0E-04	-	1.0E-04
Porous Halite	-	1.0E-04	1.0E-04	1.0E-04	1.0E-05	1.0E-04	1.0E-04	-	1.0E-04	-
Massive Halite	-	1.0E-04	1.0E-04	-	1.0E-04	-	1.0E-04	-	-	-
Lower Sediments	-	-	-	-	-	-	-	-	-	1.0E-04
Fanglomerate	-	-	-	-	-	-	-	-	-	1.0E-04

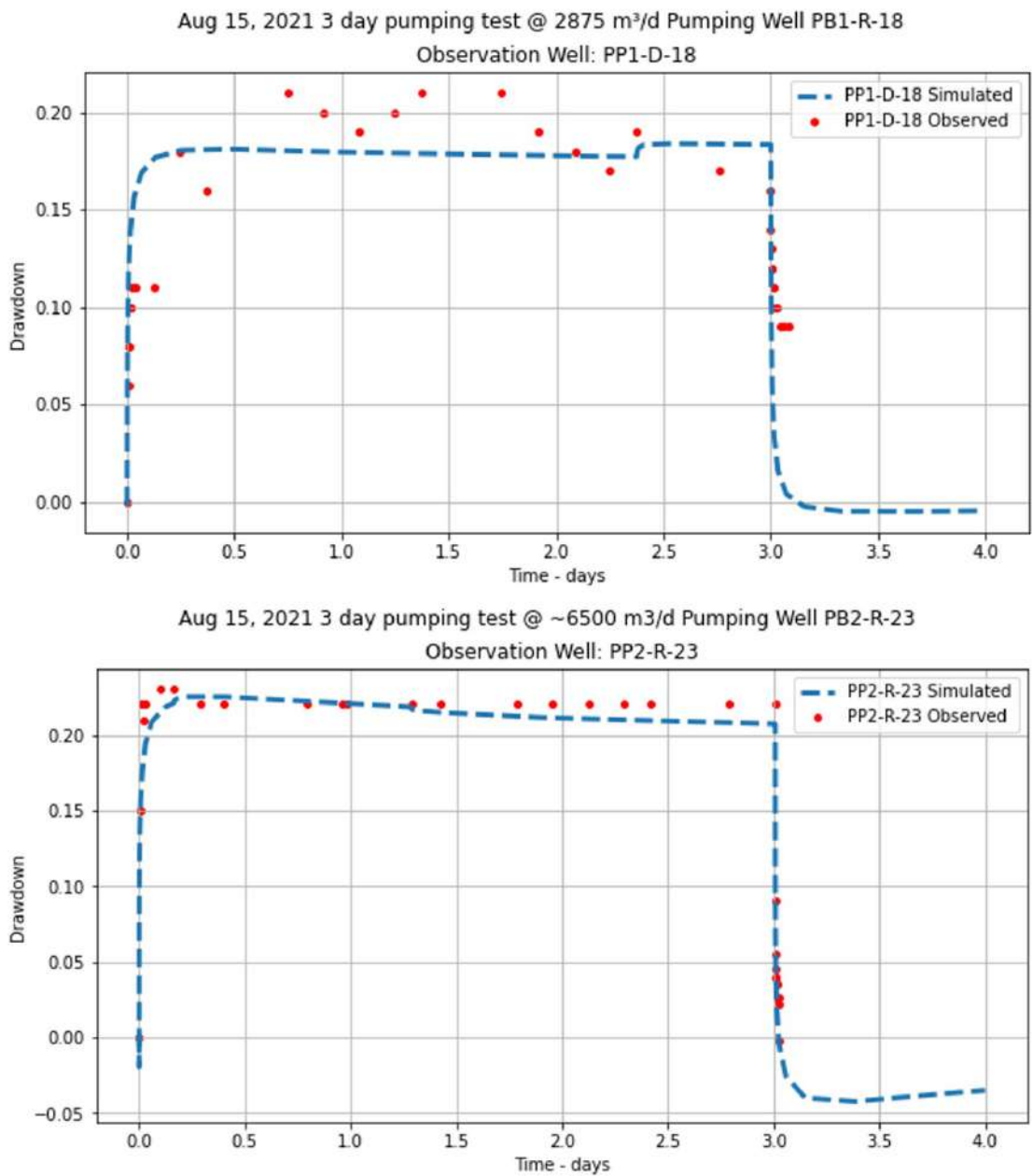


Figure 9-5: Simulated and measured drawdown for 72-hr pumping tests at PB1-R-18 and PB2-R-23.

10. Drilling

10.1 Overview

The location and chronology of boreholes installed to date at the 3Q Project are shown on Figure 10-1. Borehole and well specifications, including packer sampling intervals, are summarized in Appendix E. It is noted that all boreholes are vertical. Three rounds of drilling have been conducted:

- the first round was done during the 2016/17 Field Program, from January to April 2017;
- the second round was done during the 2017/18 Field Program, from October 2017 to April 2018; and
- the third round was done during the 2018-21 Field Program from February to May 2019 and March to June 2021.

The drilling objectives were as follows:

- to obtain samples for characterizing subsurface brine chemistry;
- to characterize salar geology with continuous cores, downhole geophysics, and other drilling information;
- to install pumping and observation wells for hydrogeological characterization; and
- to test for aquifers outside of the previous model domain.

Boreholes were planned and grouped in “platforms” where, if feasible, a diamond borehole was installed first on each platform and used to guide the subsequent installation of rotary boreholes and wells. This approach involved the following planning at a typical platform:

- The diamond borehole was drilled first. The core was logged and downhole geophysics were performed, to obtain a detailed and reliable representation of the subsurface at the platform location.
- Packer samples were collected from the diamond boreholes during drilling, for discrete monitoring of brine at different levels.
- Diamond boreholes were completed as deep observation wells, for use in subsequent pumping tests.
- Based on the diamond core logs, downhole geophysics, and field monitoring of the brine, the remaining wells to be located on the platform were designed. One or more pumping wells were designed and installed by rotary methods to test potentially important brine aquifers.
- If more than one pumping well was installed on the platform (for example, if both a shallow and a deep aquifer were to be tested) then an additional observation well was installed to monitor the test of the second pumping well (the diamond drill well would already be configured to monitor the first pumping well).
- If it was not feasible to drill a diamond borehole on the platform (i.e., due to flowing sands) then the pumping well was designed on the basis of recovered rock chips and downhole geophysics. In that case, the associated observation well was installed by rotary method.
- In some cases, only a diamond borehole was drilled on the platform, with potential to install one or more pumping wells at a later date.

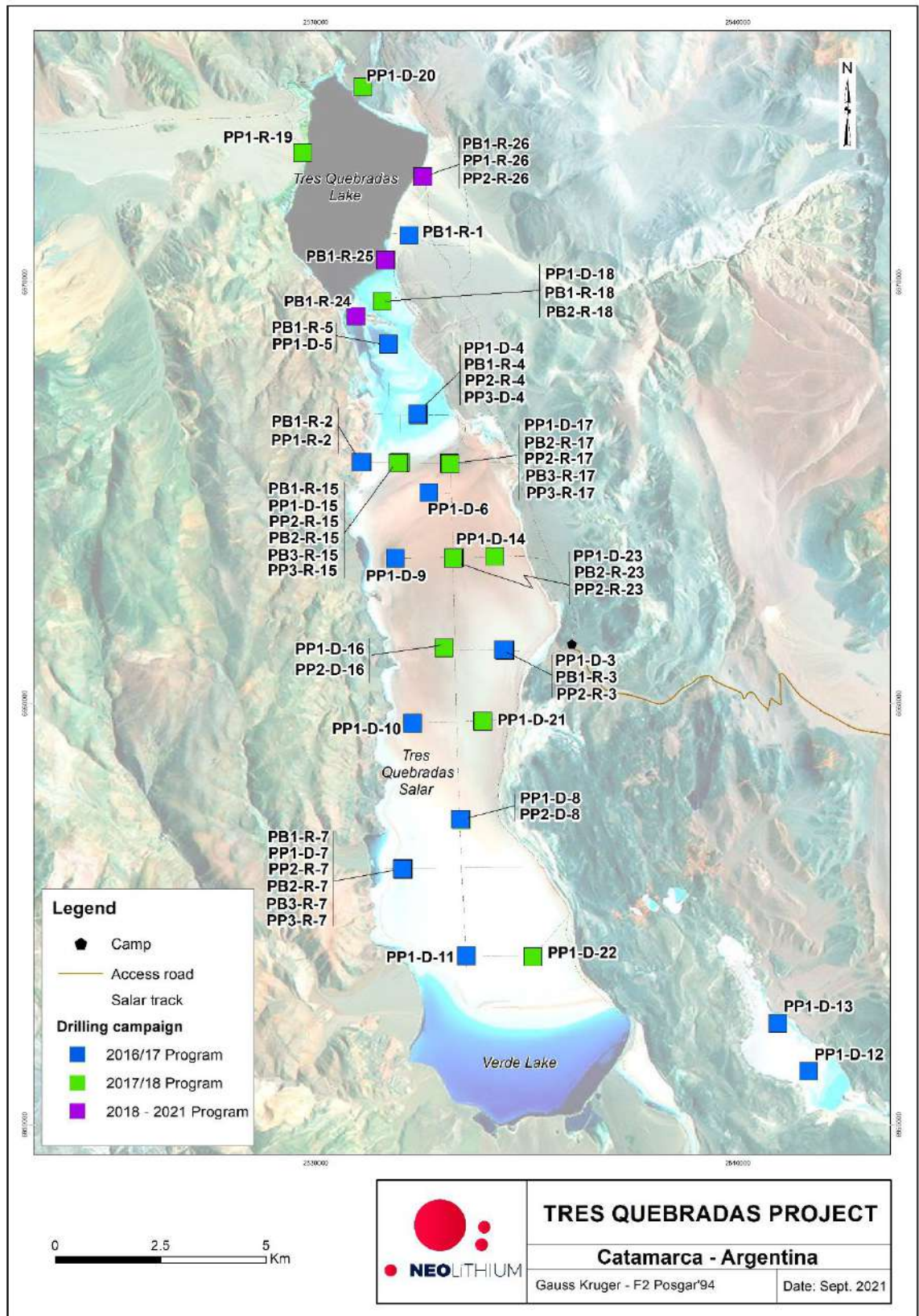


Figure 10-1: Drill platform and borehole locations and chronology – 3Q Project.

10.2 Diamond Drilling

The wells installed with diamond drilling are summarized in Table 10-1. The diamond boreholes were drilled in HQ diameter, to the target depth or to the depth that the equipment was able to

penetrate. If additional penetration was required, the gear was changed to NQ diameter for drilling to the target depth. Core was recovered during drilling and transferred to core boxes. A range of biodegradable additives were used for the drilling, including: Toqueez, Sand Drill, AMC Superlube-Lubricante, AMC Ezee Pac R, AMC CR 650, and Amc Xan Bore.

During the 2016/17 Program, drilling logs were prepared by Conhidro personnel and supervised by Hidroar. An independent review of all cores and logs was conducted by Hidroar. A final review of all cores and logs was conducted by the QP. During the 2017/18 Program, logs were prepared by geologists from NLC. An independent review of all cores and logs was conducted by Santiago Grosso, with an inspection of cores by the QP.

Table 10-1: Summary of diamond drilling contractors and well installation – 3Q Project.

Field Program	Contractor	Wells installed with Diamond Drilling
2016/17	AGV Drilling	PP1-D-3, PP1-D-4, PP1-D-7, and PP1-D-8
	Energold Drilling	PP1-D-5, PP1-D-6, PP1-D-9, PP1-D-10, PP1-D-11, PP1-D-12, and PP1-D-13
2017/18	Energold Drilling	PP1-D-14, PP1-D-15, PP1-D-16, PP2-D-16, PP1-D-18, and PP1-D-20
	Hidrotec	PP1-D-17, PP1-D-19, PP1-D-19, PP1-D-19, PP1-D-21, PP1-D-22, and PP1-D-23

Cores were sampled for analysis of Relative Brine Release Capacity (“RBRC”) during core logging. Samples were collected with the purpose of obtaining an approximate thickness-weighted coverage of the lithological units encountered in the cores. Core samples were placed in 2-inch diameter PVC sleeves, caps were tightly fitted on both ends, and plastic foil was wrapped around the entire sample.

Core samples were shipped to D.B. Stephens and Associates Laboratory in Albuquerque, New Mexico, USA, for RBRC analysis, according to a methodology developed by the laboratory. The RBRC method provides an estimate of the standard hydrogeological property known as Specific Yield (“Sy”), which is the volume of pore solution that will readily drain from a geologic material (see Section 2.4.2).

To conduct the analysis, the undisturbed (or remolded) sample is saturated in the laboratory using a site-specific brine solution. The bottom of the sample is attached to a vacuum pump using tubing and permeable end caps. The top of the sample is fitted with a perforated latex membrane that limits atmospheric air contact with the sample, to avoid evaporation and precipitation of salts. The sample is then subjected to a suction of 0.33 bars for 18 to 24 hours.

The volumetric moisture (brine) content of the sample is calculated based on the density of the brine, the sample mass at saturation, and the sample mass at ‘vacuum dry’. The difference between the volumetric moisture (brine) content of the saturated sample and the volumetric moisture (brine) content of the ‘vacuum dry’ sample is the “relative brine release capacity”. A total of 307 RBRC samples were used from the two rounds of diamond drilling. A summary of results is provided in Table 10-2.

Table 10-2: Summary of RBRC results from the diamond cores.

Lithological Unit	RBRC (%)	Number of Samples
Hyper-Porous Halite	14.74	66
Upper Sediments	9.12	14
Porous Halite	6.33	97
Massive Halite	3.85	84
Lower Sediments	5.18	12
Fanglomerate	11.23	33
Hydrological Basement	1.73	1
TOTAL		307

As the drilling progressed, brine sampling was conducted with double and simple packer systems, depending on the lithological conditions (Section 11.2.2). Observation wells were constructed in the diamond boreholes with 2-inch PVC casing and screen. After construction, the wells were developed and cleaned by air lift methods, evacuating the brine until clear fluid was produced.

Monitoring, logging, and downhole geophysics services (short and long normal resistivity) for the diamond drilling program was provided by Conhidro. A standard diamond drilling setup at the 3Q Project is shown in Photo 10-1, and review of the core is shown in Photo 10-2.



Photo 10-1: Aerial view of diamond drilling platform.



Photo 10-2: Reviewing diamond core, at a storage warehouse in Fiambalá.

10.3 Rotary Drilling

The wells installed with rotary drilling are summarized in Table 10-3. The drilling was traditional, with circulation of bentonite mud, prepared with brine that was obtained at each drilling platform. This method was used for installation of both pumping wells and for any observation wells that were required in addition to those installed by diamond drilling.

Table 10-3: Summary of rotary drilling contractors; monitoring, logging, and downhole geophysical services; and well installation – 3Q Project.

Field Program	Drill Contractor	Drill Monitoring and Core Logging	Wells installed with Rotary Drilling
2016/17	Andina Perforaciones SRL	Conhidro	PB1-R-1, PB1-R-2, PP1-R-2, PB1-R-3, PB2-R-3, PB1-R-4, PP2-R-4, PB1-R-5, PB1-R-7, PP2-R-7, PB2-R-7, PB3-R-7, and PP3-R-7
2017/18	AGV Drilling	Conhidro	PB1-R-15, PP2-R-15, PB2-R-15, PB3-R-15, PP3-R-15, PB2-R-17, PP2-R-17, PB3-R-17, PP3-R-17, PB1-R-18, PP1-R-19, PB2-R-23, and PP2-R-23
2018-21	Hidrotec SRL	NLC	PB2-R-18, PB1-R-24, PB1-R-25, PB1-R-26, PP1-R-26, and PP2-R-26

The pumping wells were drilled with a tri-cone bit, at 8-, 12-, and 15-inch diameter, with installation of 8-inch PVC casing and screen. Gravel was placed around the screen. After installation, wells were cleaned with a 4-inch submersible pump, until clear fluid was produced. Observation wells were drilled at 6 or 8-inch diameter and were installed with 2-inch PVC screen and casing.

Downhole geophysical surveys were conducted by Conhidro during the 2016/17 and 2017/18 drilling campaigns. Surveys included normal resistivity (short and long), single point resistance, and spontaneous potential. During the 2018-21 Program drilling, downhole geophysical surveys were conducted by Hidrotec. In 2019, surveys included normal resistivity (short and long), single point resistance, and spontaneous potential. In 2021, surveys included normal resistivity (short and long), spectral gamma, and spontaneous potential. A rotary drill setup on 3Q Salar is shown in Photo 10-3.



Photo 10-3: Rotary drill setup on 3Q Salar.

11. Sample Preparation, Analyses, and Security

11.1 Overview

All field program oversight (for example, sample collection, drilling, well construction, QA/QC, and secure transport) was performed by Waldo Perez, Ph.D., P. Geo. Based on a review of these components, the QP considers that the 3Q Project dataset and QA/QC procedures are acceptable for evaluation of brine Resources and Reserves, with no significant and systematic bias.

11.2 Sample Collection

11.2.1 Surface Brine and Stream Methods

The chronology of surface brine sampling is shown in Figure 9-2. Surface brine sampling methods have been comparable for all field programs, and were as follows:

- The solar surface crust was excavated with a pick and shovel or with heavy equipment, to a depth of approximately 1 m (Photo 11-1).
- The excavated hole was purged of brine and the brine level was allowed to recover.
- Samples were collected in 500 mL plastic bottles that were rinsed with brine before sample collection.



Photo 11-1: Collecting brine samples from shallow hand-excavated pits.

The methods for collecting lake brine samples have also been comparable for all programs. They were as follows:

- Samples were collected at mid-depth.
- Deeper sectors were sampled from an inflatable boat; shallower sectors with hip waders (Photos 11-2 and 11-3).
- A 2.2 L water collection device was used which could be closed at the desired depth by dropping a weight down the suspension line (Photo 11-3)

- When the sample was retrieved from depth, it was transferred to a 500 mL bottle.
- The depth to the bottom of the lake was measured with a weighted rope.



Photo 11-2: Collecting samples and performing soundings in Laguna 3Q, with hip waders.



Photo 11-3: Collecting samples from Laguna 3Q, from a boat.

Sampling and flow monitoring of surface water streams and rivers was conducted throughout the area that drains to the 3Q Salar. These measurements continue to be collected on an ongoing basis. The methods are as follows:

- Water velocity is measured at several points across a suitable stream reach, using a current meter (Photo 11-4).

- Back in the office, the velocity measurements and the associated cross-sectional areas are used to calculate flow through the reach.
- A streamflow sample is collected in a 500 mL plastic bottle.
- Field parameters are measured (pH, Eh, temperature, and conductivity) (Photo 11-5).



Photo 11-4: Measuring streamflow in 3Q River.



Photo 11-5: Measuring field parameters in streamflow.

11.2.2 Subsurface Brine Sampling

Packers were used to collect brine samples from discrete formation levels in the diamond boreholes (Photo 11-6). Samples were collected primarily with a simple packer apparatus, with

some use of a double packer. The simple packer method for brine sampling from the diamond drill boreholes is as follows:

- When the diamond machine drills to the bottom of the desired sampling interval, the bars are raised to just above the top of the target sampling interval.
- A fluorescein dye solution sufficient to tint the water in the sampling interval is injected through the bars, to tint all the brine in the bottom several metres of the borehole.
- The packer is lowered by wireline to the top of the desired sampling interval. It is then inflated from the surface, which isolates the sampling interval from the remaining (higher) section of the borehole.
- Brine is purged from the packed interval using a compressor-driven airlift apparatus, until at least three packed interval volumes are removed, and the fluorescein tint is no longer evident in the purged brine (Photo 11-7).
- A brine sample is collected into a 500 mL container.

The double packer method is as follows:

- When the diamond machine drills to the target depth of the borehole, the bars are raised to some distance above the top of the desired sampling interval. This distance may depend on any concerns that the driller may have with regard to borehole caving.
- A fluorescein dye solution sufficient to tint the brine inside and outside the sampling interval, is injected through the bars.
- The double packer is lowered so that it straddles the desired sampling interval. It is then inflated from the surface, which isolates the sampling interval from the remaining (higher and lower) sections of the borehole.
- Brine is purged from the packed interval using a compressor-driven airlift apparatus, until at least three packed interval volumes are removed, and the fluorescein tint is no longer evident in the purged brine.
- A brine sample is collected into a 500 mL container.



Photo 11-6: Packer assembly being placed in PP1-D-17.



Photo 11-7: Progressive clearing of the tracer from the packed interval, as purging proceeds.

11.2.3 Pumping Tests

The methodology for pumping tests is as follows:

- A step test is conducted to determine an effective pumping rate for the constant rate test.
- During the tests piezometric levels are measured in the pumping well and in all observation wells and other pumping wells that are available at the given platform, with data loggers and manual measurements.

- Test data were initially interpreted with specialized software (Infinite Extent, full version 4.1.0.1; Stepmaster version 2.1.0.0 (both by Starpoint Software Inc.,) and Well Functions from the program GWW version 1.10; see King (2017)) or by calibration with MODFLOW and PEST (see King, 2018; King and Zandonai, 2021).
- During some pumping tests an attempt was made to determine effective porosity, by injecting a fluorescein tracer into an observation well and recording the time of travel to the pumping well. Initial results indicated that the wells were too distant from each other for tracer capture to occur during the pumping period. Subsequent tests have achieved some limited success in evaluating effective porosity with this method.
- During the 2016/17 Program, trench pumping tests were performed for hydraulic testing of the shallow crust (King, 2017). For the trench tests, pumping was conducted from a “pumping trench”, with drawdown monitoring in two smaller “observation trenches”. A fluorescein tracer was used in one of these tests, to provide an estimate of effective porosity, for comparison with laboratory RBRC measurements.
- During the 2018-21 Program, pumping tests were interpreted, and previous long-term constant rate pumping tests re-interpreted, using a numerical model calibration approach in FEFLOW (see Section 9.6).

The apparatus for a typical pumping test conducted at the site is shown in Photo 11-8.



Photo 11-8: Pumping test setup at well PB2-R-3.

11.3 Sample Preparation

No preparation was required for the brine samples. Samples were delivered by NLC company personnel to Andesmar Transport Company in La Rioja, in the province of Rioja. Andesmar delivered the samples by truck to Alex Stewart Laboratories (“ASL”) in Mendoza, Argentina, for analysis.

11.4 Brine Analysis

ASL is an independent commercial ISO 9001-2008-certified laboratory and was selected for assaying all brine samples from the 3Q Project. ASL used the following analytical methodologies:

- ICP-OES (inductively-coupled plasma—optical (atomic) emission spectrometry) was used to quantify Boron, Barium, Calcium, Lithium, Magnesium, Manganese, and Potassium.
- An argentometric method was used to assay for chloride.
- A gravimetric method was used to analyze for sulfate.
- A volumetric analysis (acid/base titration) was used for evaluation of alkalinity (as CaCO₃).
- Density and total dissolved solids were determined through a gravimetric method.
- A laboratory pH meter was used to measure pH.

11.5 Field QA/QC Program

11.5.1 Summary

Similar QA/QC procedures were used for all 3Q exploration programs and for the ongoing surface water monitoring and sampling program. Results of QA/QC sampling completed during the 2015/16, 2016/17, and 2017/18 programs were first reported in King (2016), King (2017), and King (2018), respectively. The QA/QC results for the 2018-21 Program are first reported herein. Primary components of the field QA/QC program for the 3Q Project included the following:

- During the 2015/16 Program, a reference sample was inserted into the sample stream at a frequency of approximately 1 in 15 samples. The 120 L bulk sample used for this process was collected from the eastern shoreline of Laguna 3Q.
- During subsequent exploration programs, two reference samples were inserted into the sample stream:
 - A mid-range reference sample was inserted into the sample stream at a frequency of approximately 1 in 20 samples. The bulk sample used for this purpose was obtained in March 2016 from the eastern shoreline of Laguna 3Q where mid-range grades were known to occur (through previous sampling). Use of the mid-range sample was discontinued in February 2019 due degradation of the reference sample (Section 11.5.4)
 - A high-range reference sample was inserted into the sample stream at a frequency of approximately 1 in 20 samples. In 2019 the frequency increased to approximately 1 in 15 samples. The bulk sample used for this purpose was obtained in March 2016 from the southeast shoreline of Laguna 3Q where high grades were known to occur (through previous sampling).
- A Round Robin analysis of the high- and mid-range bulk reference samples was conducted by ASL.
- A low-range reference sample (essentially a field blank) was inserted at a frequency of approximately 1 in 15 samples. The bulk sample used for this purpose was obtained from municipal tap water at the Project office in Fiambalá, the nearest town to the site.
- A field duplicate sample was inserted into the sample stream at a frequency of approximately 1 in 15 samples.
- A program of laboratory duplicate sampling was conducted by ASL.
- Sets of independent field duplicate samples were collected by the QP during the 2015/16, 2016/17, and 2017/18 field programs, and during the December 2018 monthly monitoring program (Section 12).

QA/QC results presented in the following subsections summarize all samples collected during the four exploration programs.

11.5.2 Reference Sample Performance in the 2015/16 Sampling Program

Lithium and potassium results for the 2015/16 Program reference samples are shown in Figure 11-1 and 11-2, respectively. The data exhibit a low spread of distribution, which indicates acceptable accuracy (King, 2016). There is no evidence of analytical drift in the 2015/16 Program reference samples.

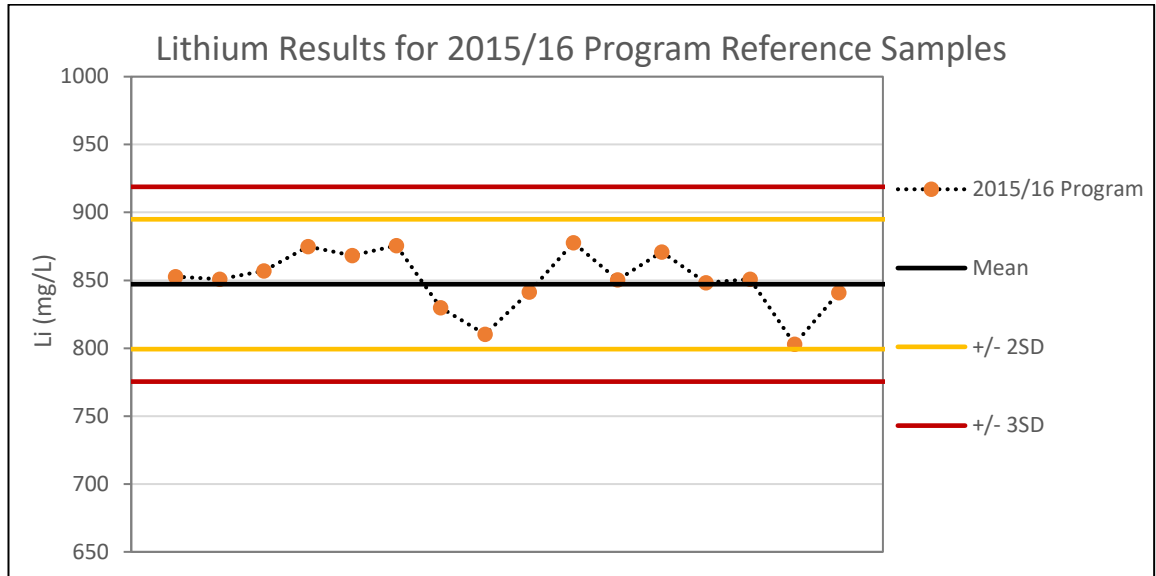


Figure 11-1: Lithium results for the 2015/16 Program reference samples. Statistics calculated from sample results.

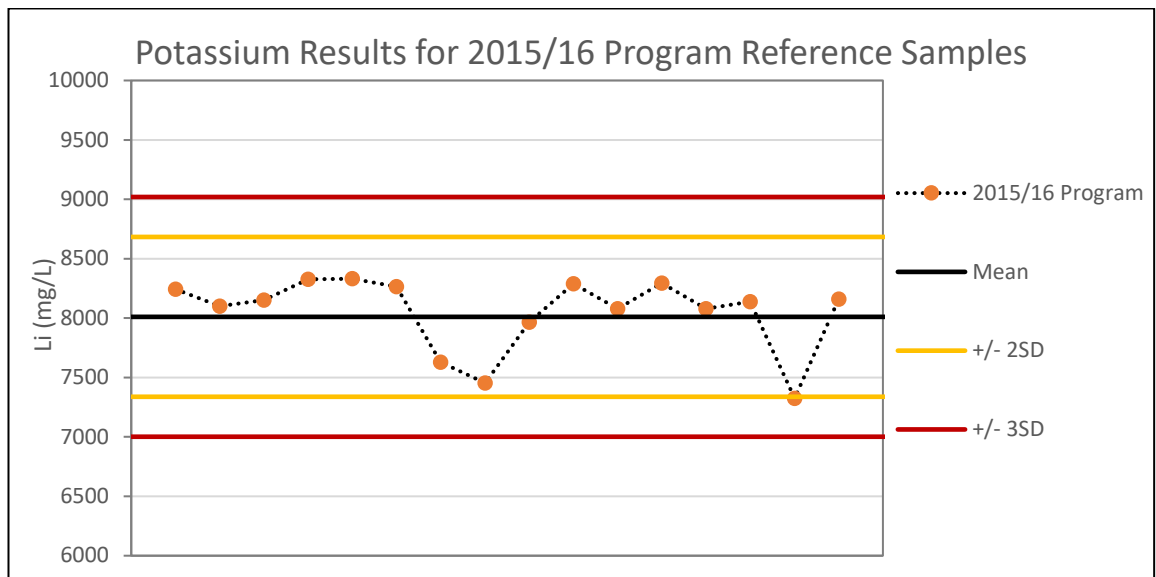


Figure 11-2: Potassium results for the 2015/16 Program reference samples. Statistics calculated from sample results.

11.5.3 Round Robin Analysis of Bulk Reference Samples

The bulk reference samples described above were used as a means of evaluating analytical precision and drift, as the program proceeded. As a first step in using these bulk samples, a Round Robin was conducted by ASL for the mid-range and high-range samples, as part of the 2016/17 Field Program. The purpose was to certify the average content and standard deviation

of lithium, potassium, and calcium using ICP-OES analysis from certified laboratories. The same reference samples were used for the 2017/18 and 2018-21 Programs. Details of the Round Robin analysis of these samples was first reported by King (2017). Full results are provided in Appendix F.

The mid-range reference sample was analyzed by the following laboratories: ASL (Mendoza), ALS (Jujuy), SGS, Segemar, and Induser. The high-range reference sample was analyzed by ASL (Mendoza), ALS (Jujuy), SGS, ACTLABS, Sherrit, Segemar, and Induser.

The results of the Round Robin analysis provide certified mean values and standard deviations (“SD”) for the three tested analytes, in the mid- and high-range reference samples. These statistics are useful for evaluating analytical precision and potential drift as the field program proceeds.

11.5.4 Reference Sample Performance in the 2016/17, 2018/19, and 2018-21 Sampling Programs

As described above, reference samples were used as a benchmark for ongoing evaluation of analytical drift. Mid- and high-range reference sample performance results for lithium are shown in Figures 11-3 and 11-4, respectively. Figures 11-5 and 11-6 show mid- and high-range results (respectively) for potassium.

The mid- and high-range samples for both lithium and potassium display results that are skewed high relative to the certified mean. The skewed results are attributed to inherent brine sample instability, as well as sample storage conditions and leaky storage containers which led to sample degradation caused by evaporation and salt precipitation over time. This issue was first noted by the Company during the 2016/17 Program. At that time, the bulk samples were stored in insufficiently sealed 60 L drums in field tents. The issue was addressed by subdividing the bulk reference samples into smaller ½ L and 20 L containers with better seals. In 2017, the reference samples were moved into the on-sight lab facilities for better environmental control.

The ½ L mid-range reference sample aliquots were used during the 2016/17 Program and the first portion of the 2017/18 Program. Most of these sample results fall within ± two SD of the mean, which is considered the primary control limit for the project. During the 2017/18 Program field staff began using the 20 L mid-range sample aliquot. The 20 L container did not achieve a hermetic seal and the sample suffered additional degradation due to evaporation and salt precipitation. This degradation is reflected by an abrupt increase in lithium results and several failures for lithium (>3 SD from the mean) (Figure 11-3). This reference sample was removed from the QA/QC program in February 2019.

All high-range reference sample aliquots were stored in ½ L containers. As shown in Figure 11-4 and 11-6, the high-range sample data contains nine lithium (15%) and two potassium (3%) failures (>3 SD from the mean). The skewed data and sample failures are attributed to initial deterioration of the bulk reference sample while it was stored in field tents in the larger, 60 L drums. This reference sample was used through the end of the 2018-21 Program.

Results from the field reference sample program do not show evidence of unacceptable analytical drift over time. However, results demonstrate reference sample degradation and instability related to evaporation and salt precipitation. This result is considered acceptable, given the overall strength of the analytical program.

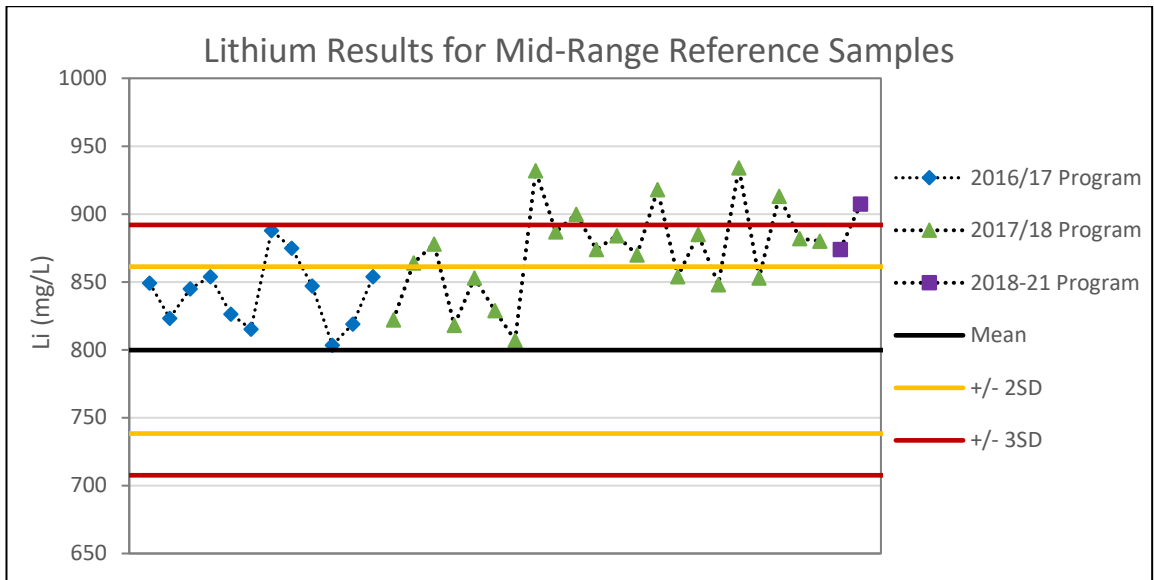


Figure 11-3: Lithium results for mid-range reference samples, compared with Round Robin Mean and Standard Deviation.

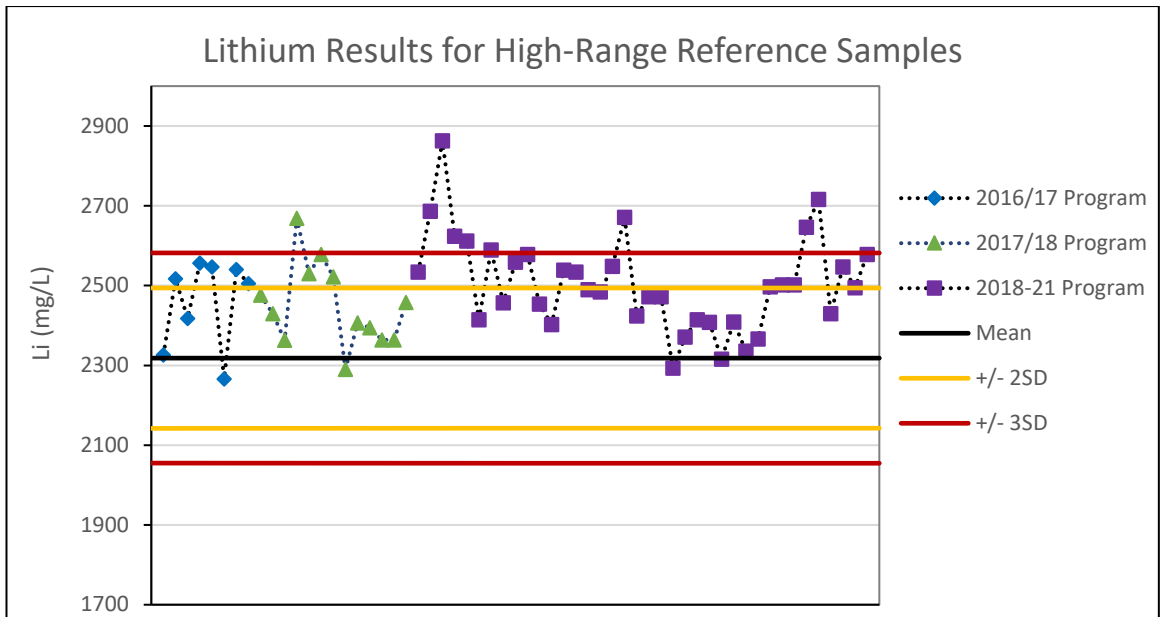


Figure 11-4: Lithium results for high-range reference samples, compared with Round Robin Mean.

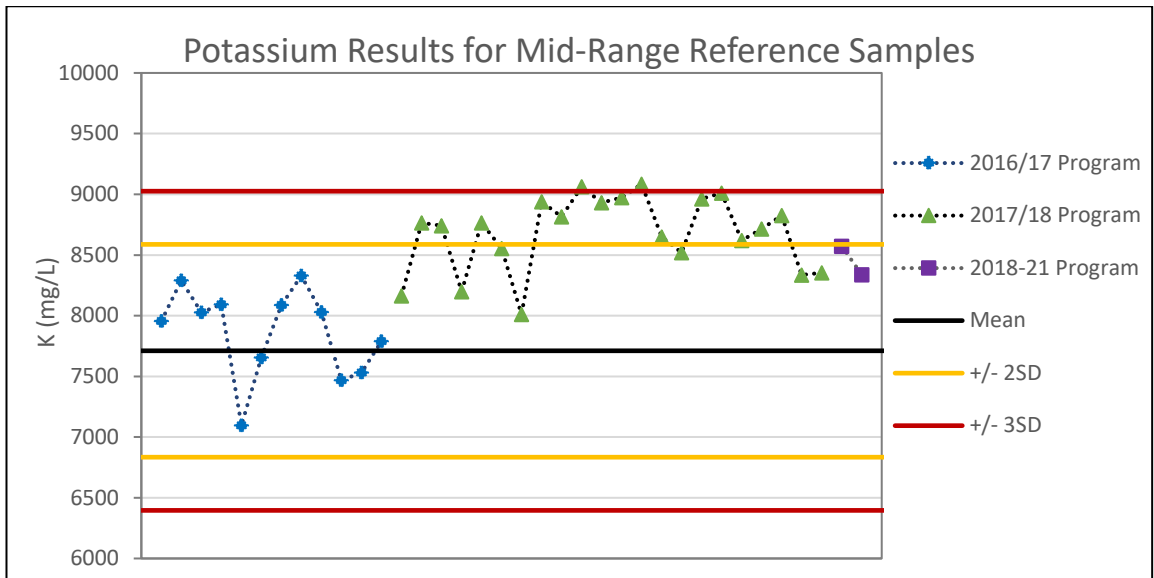


Figure 11-5: Potassium results for mid-range reference samples, compared with Round Robin Mean.

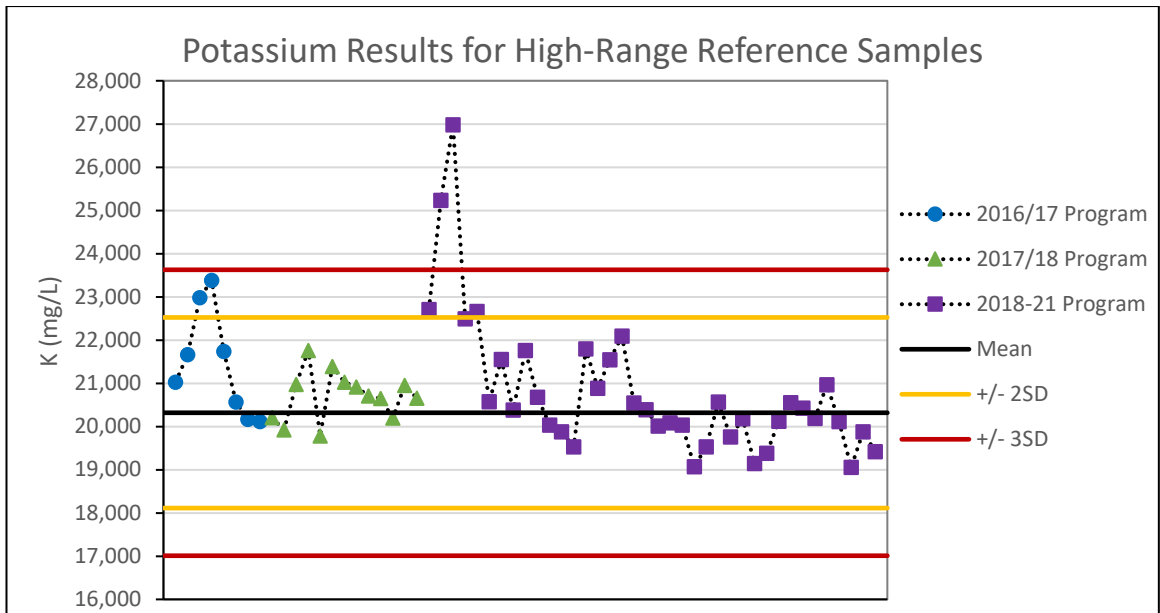


Figure 11-6: Potassium results for high-range reference samples, compared with Round Robin Mean.

11.5.5 Field Duplicate Sample Performance

Lithium, potassium, and magnesium results for 86 field duplicate samples are plotted in Figures 11-7 to 11-9, against their original counterparts.

Most samples plot close to their respective 1:1 lines and fall within the +/-10% lines. However, a single magnesium data point from the 2017/18 Program is an outlier (Figure 11-9). The overall precision of the data is considered acceptable.

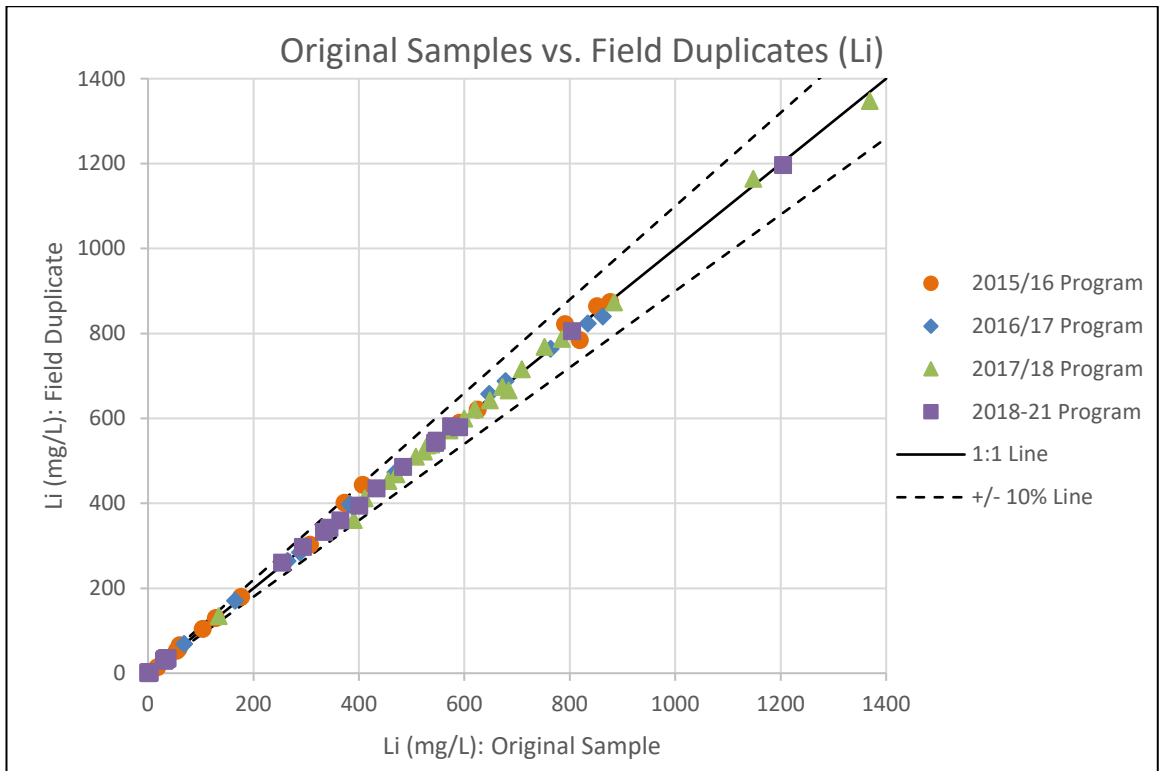


Figure 11-7: Field duplicates versus original sample results for lithium (mg/L).

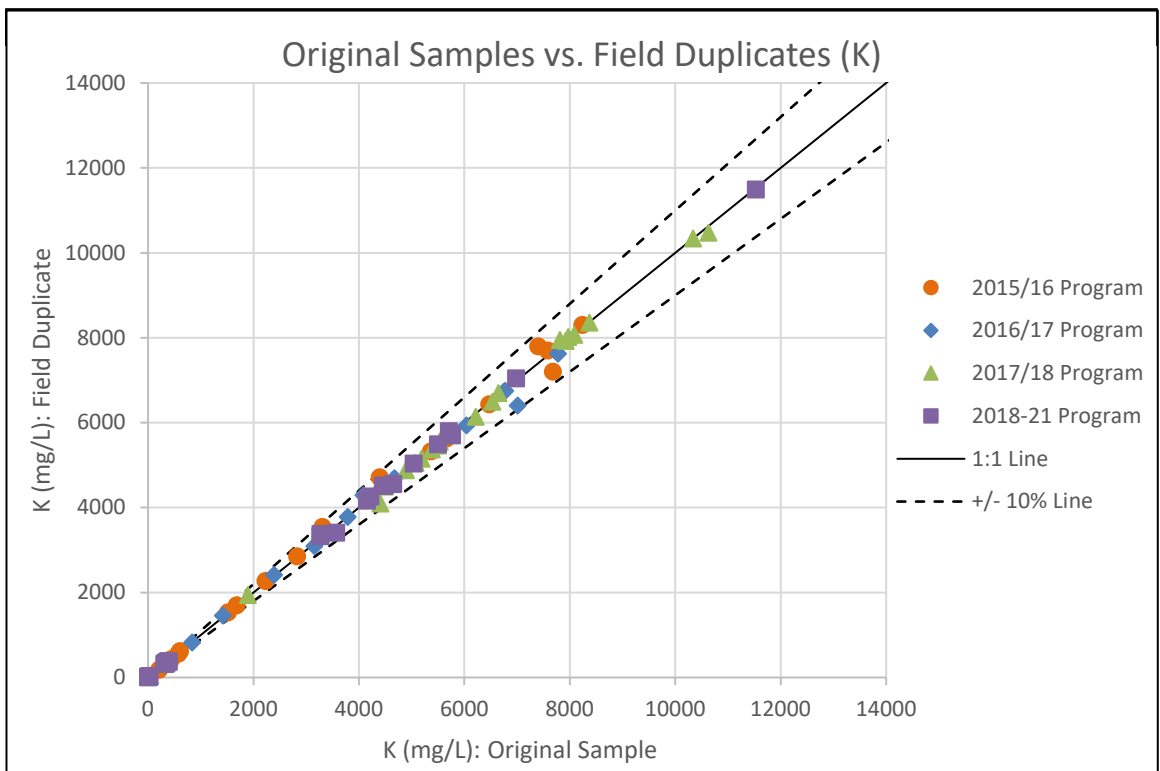


Figure 11-8: Field duplicates versus original sample results for potassium (mg/L).

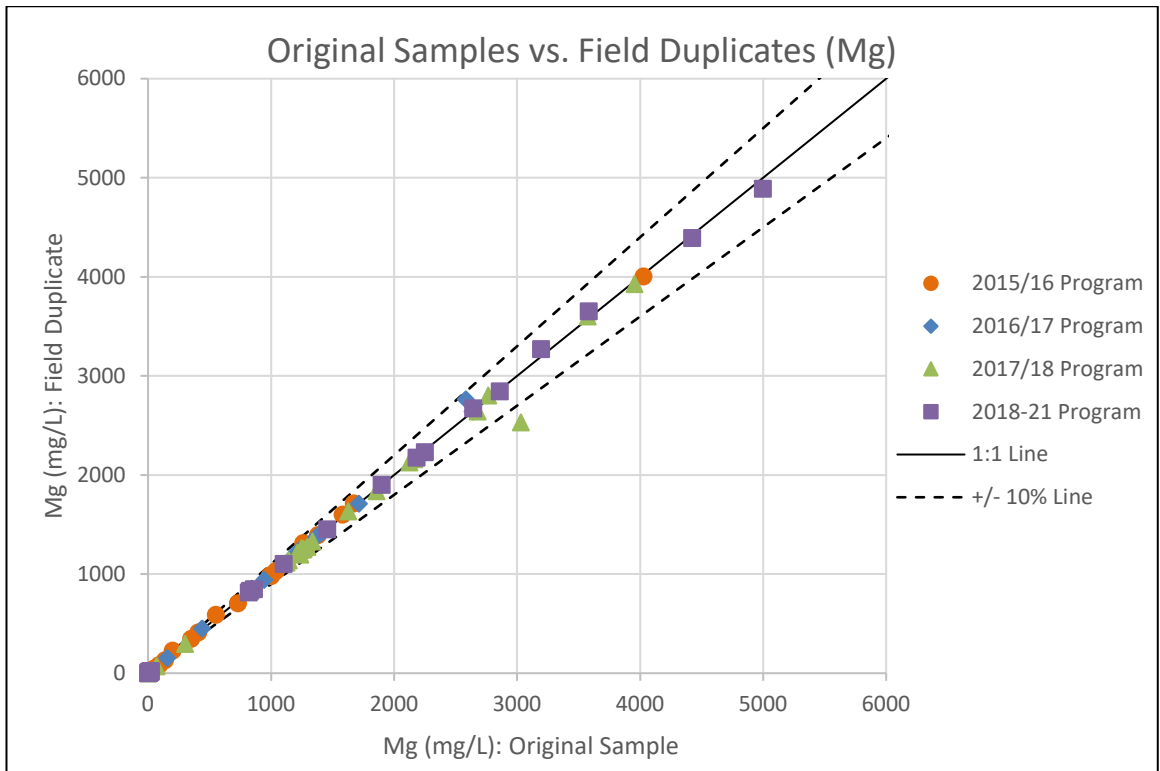


Figure 11-9: Field duplicates versus original sample results for magnesium (mg/L).

11.5.6 Field Blank Performance

Lithium and potassium results for 97 field blank samples (low-range reference samples) are shown in Figures 11-10 and 11-11, respectively. The results assess for cross-contamination in the laboratory and the field (for example, whether the instrumentation was cleaned sufficiently between analysis of samples). Lithium was not detected in any blank sample. Potassium was detected in a single blank sample from the 2018-21 Program; and a 2016/17 sample came close to the detection limit for potassium (Figure 11-11). Overall, field blank performance is considered acceptable.

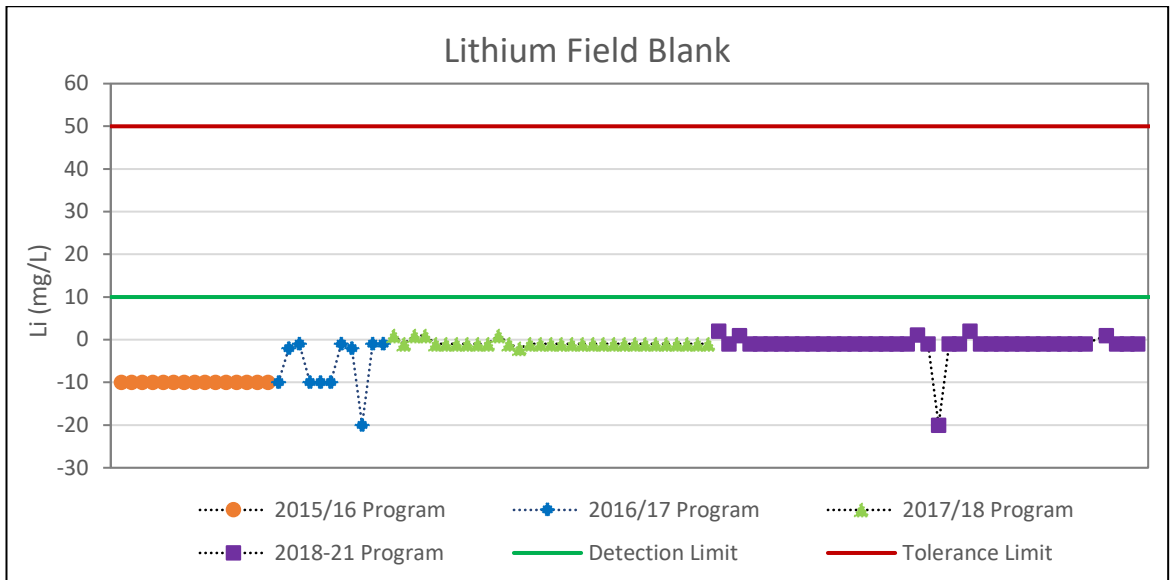


Figure 11-10: Blank sample results for lithium.

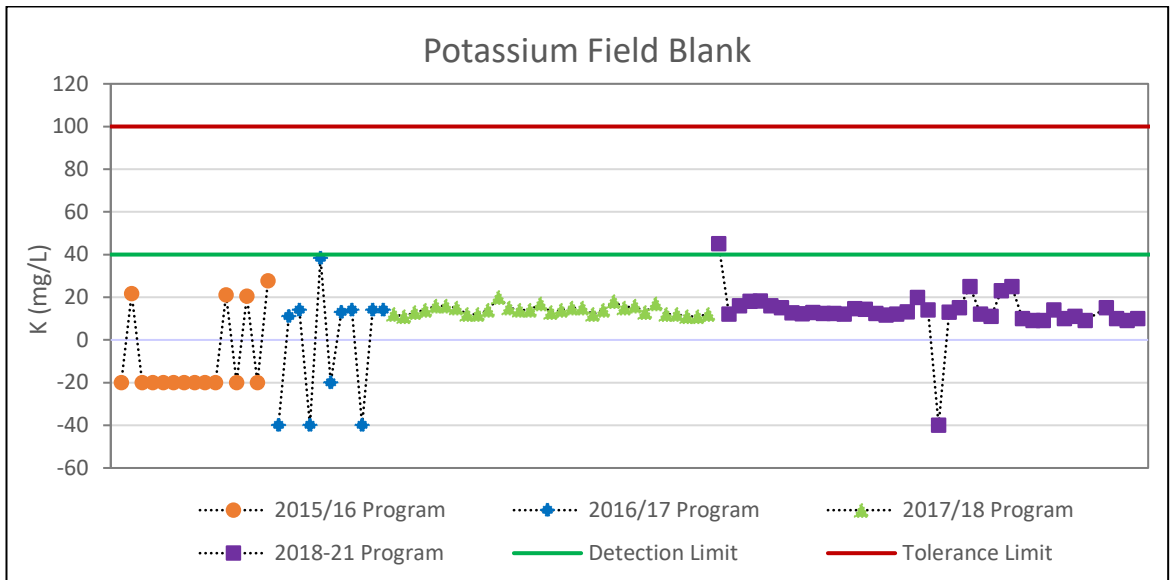


Figure 11-11: Blank sample results for potassium.

11.6 Laboratory Duplicate Analysis

ASL conducts internal laboratory check on overall analytical accuracy for selected primary parameters. Results for lithium, potassium, calcium, and magnesium are shown in Figures 11-12 through 11-15, for all 137 laboratory duplicate analyses performed by ASL during the exploration and ongoing monitoring programs. All laboratory duplicates fall within the $\pm 10\%$ line. The QP is satisfied that these results fall within an acceptable range and are considered acceptable.

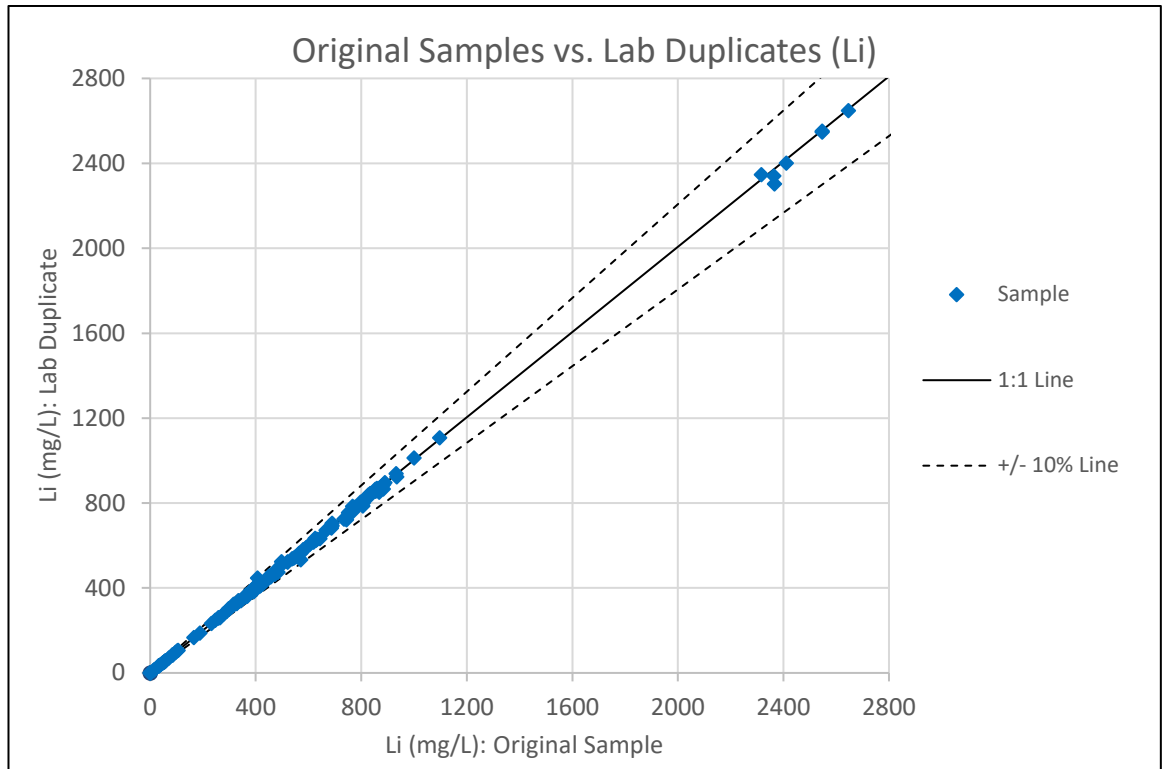


Figure 11-12: ASL internal laboratory duplicate results for lithium.

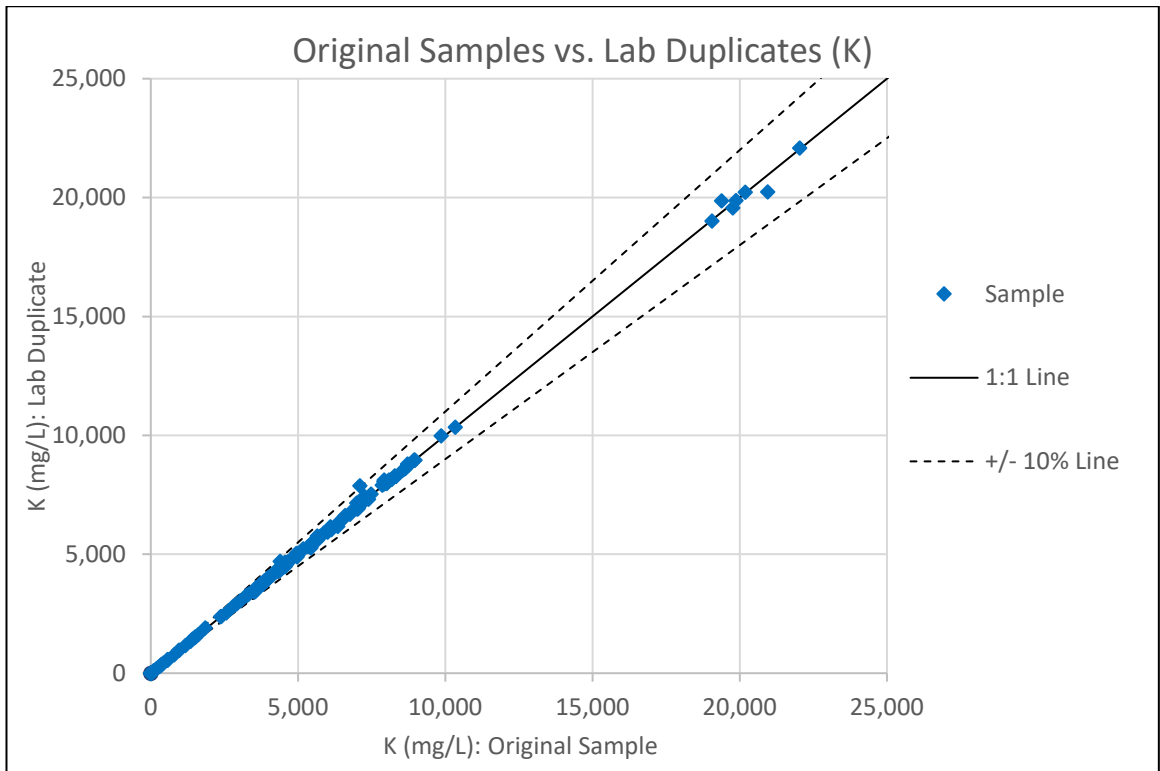


Figure 11-13: ASL internal laboratory duplicate results for potassium.

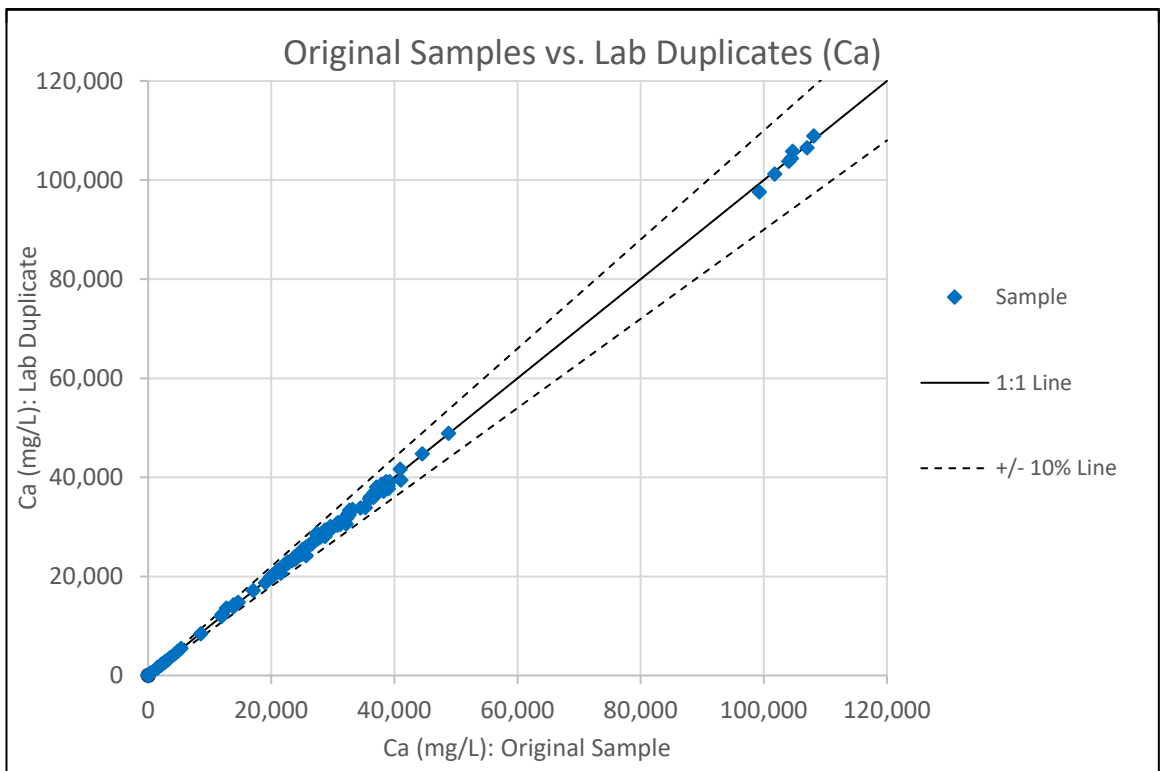


Figure 11-14: ASL internal laboratory duplicate results for calcium.

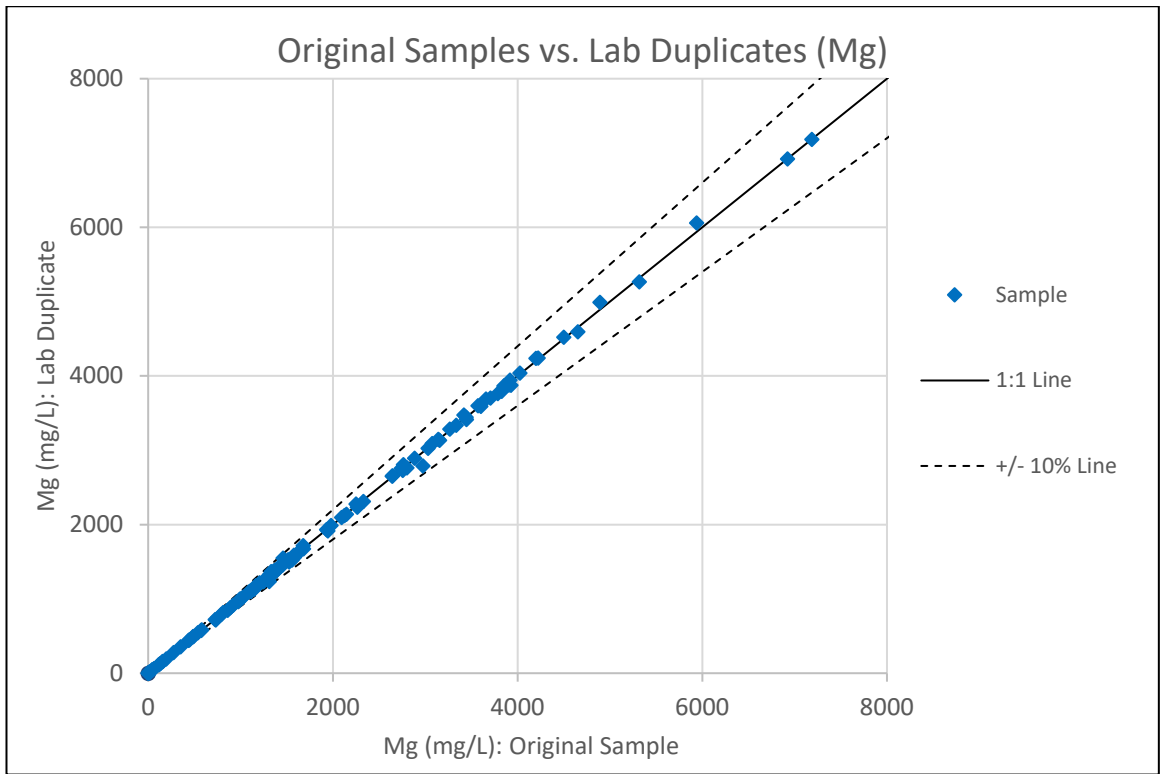


Figure 11-15: ASL internal laboratory duplicate results for magnesium.

11.7 Sample Security

An established chain of custody procedure was used for 3Q Project sampling, storage, and shipping. Samples were periodically driven in Project vehicles to La Rioja, approximately a seven-hour drive from the 3Q Project. In La Rioja, the samples were delivered to Andesmar Transport for immediate truck shipment to ASL in Mendoza, Argentina. Samples were under the control of qualified staff at all times. The QP considers that the sample security measures used for the program are acceptable.

12. Data Verification

12.1 Project Review and Interaction

Dr. Mark King (QP) provided review and input to the design and execution of all rounds of field exploration at the 3Q Project. The QP visited the 3Q Project on five occasions:

- 2015/16 Program: March 2016 for three days to conduct an independent QA/QC program (King, 2016);
- 2016/17 Program: January 2017 for three days during the first drilling campaign (King, 2017);
- 2017/18 Program: October 21-23, 2017 and April 10-14, 2018, during the second drilling campaign (King, 2018); and
- 2018-21 Program: December 12-16, 2018, during the monthly surface water monitoring and sampling program (King and Zandonai, 2021).

During all site visits, sample collection, packaging, and transport as well as field QA/QC procedures and data recording were reviewed. Field methods were observed, including: packer sampling, sample handling and shipping, diamond drilling, pumping tests, core logging and handling, shallow trenching, surface water flow monitoring, and surface water sampling. Previous drilling locations were visited, results available to date were reviewed, and future exploration plans were discussed.

Independent sampling was conducted during these site visits and is summarized in Section 12.2. For all programs, the QP reviewed laboratory results and maintained ongoing technical discourse with Dr. Waldo Perez and other NLC technical staff and contractors.

Project cores and cuttings (and associated logs) were systematically reviewed by the QP on several occasions. The QP also worked out of the Mendoza office of NLC during certain periods of 2017 and 2018, to observe and participate in geological model and brine model development (King, 2017; King, 2018; King and Zandonai, 2021).

The QP did not visit the 3Q Project to observe the third round of drilling (2018-21 Program) due to COVID-19 travel restrictions. No additional independent sampling was conducted after the December 2018 monthly surface water monitoring and sampling program. However, Dr. King was in frequent communication with NLC and the field team to discuss field methods and monitor results related to drilling, brine sampling, pumping tests, and other exploration activities.

The QP also worked closely with Paul Martin, M.Sc., P.Eng., and Martinus Brouwers, M.A.Sc., on development of the FEFLOW geological model and numerical model that support the updated Resource and Reserve Estimates presented in this report (Sections 14 and 15, respectively). Based on these activities, it is the opinion of the QP that an acceptably rigorous set of field and data interpretation methods were used in preparing the updated 3Q Project Mineral Resource and Reserve Estimates.

Claim and permitting information has not been verified by the QP. This information was received in the form of two Title Opinion documents prepared by the legal offices of Martin and Miguens, based in Buenos Aires (Section 4).

12.2 Independent Duplicate Sampling

Independent QA/QC duplicate sampling was conducted by the QP during the following programs:

- 2015/16 Program: independent samples were collected from pre-existing, hand-dug holes across the northern portion of the salar, as well as selected samples sites in Laguna 3Q;
- 2016/17 Program: independent samples were collected from four shallow excavated pits in the northern portion of the salar;
- 2017/18 Program: independent samples were collected from selected wells and field standards; and
- 2018-21 Program: independent samples were collected from established monthly monitoring locations in lakes and rivers during the December 2018 monthly surface water monitoring program.

Results were first reported in King (2016), King (2017), King (2018), and King and Zandonai (2021), respectively. Sampling methodology used by the QP was identical to that used by NLC personnel for the original samples. Samples collected by the QP were submitted with regular monitoring program samples (collected by NLC personnel) with sample numbering and locations that were known only to the QP.

A summary of the results for lithium, potassium, magnesium, and calcium in original and QP duplicate samples are shown on Figure 12-1 through Figure 12-4, relative to a 1:1 line. Overall, the QP duplicate data are in reasonable agreement with the original samples, and results are considered acceptable.

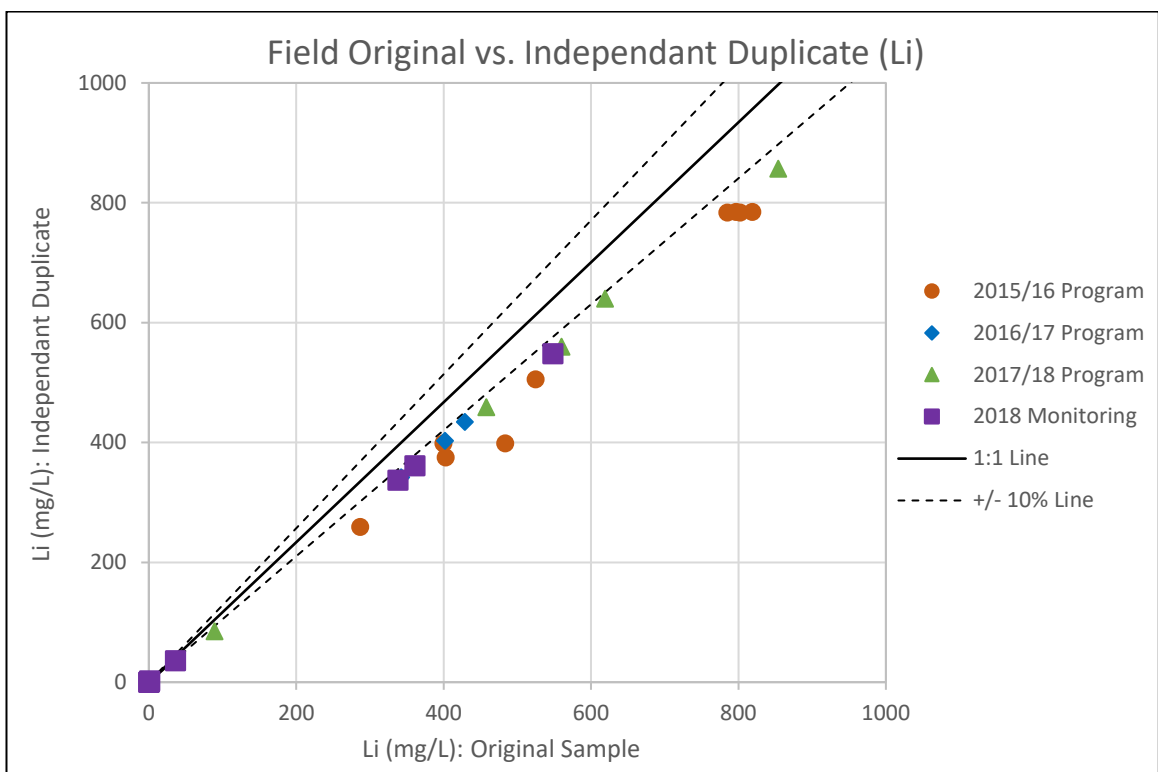


Figure 12-1: Original samples versus QP duplicate lithium samples.

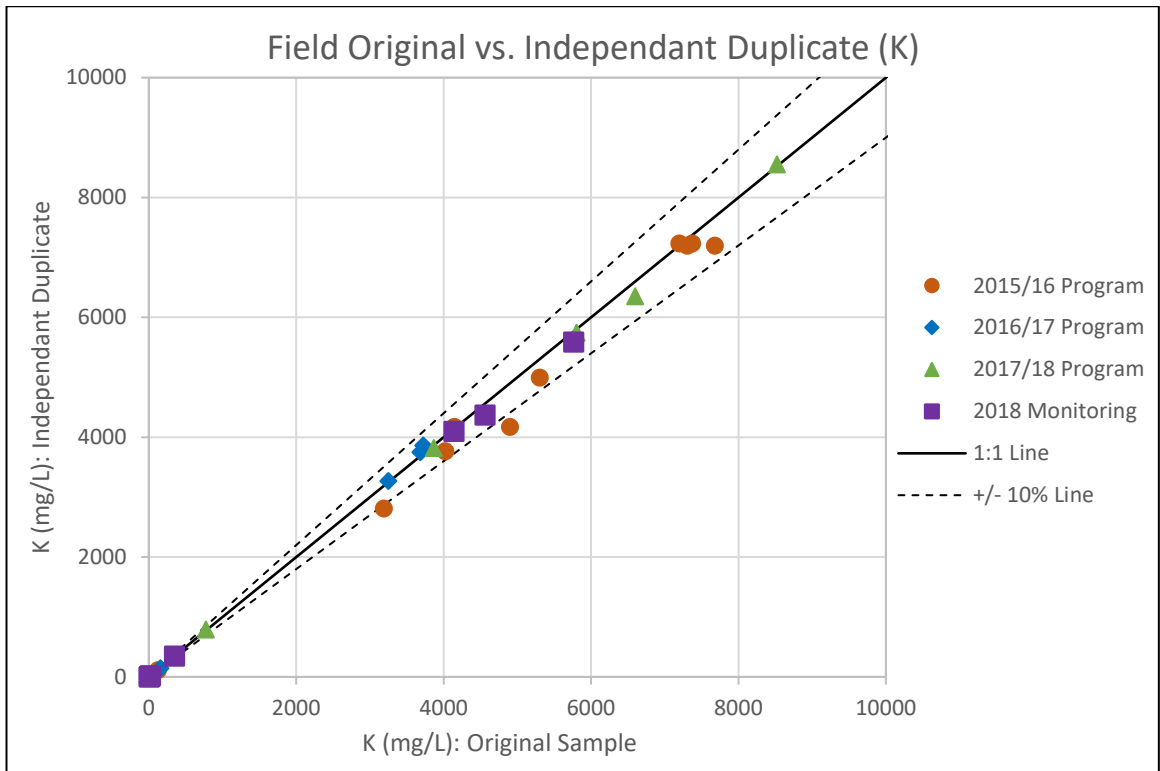


Figure 12-2: Original samples versus QP duplicate potassium samples.

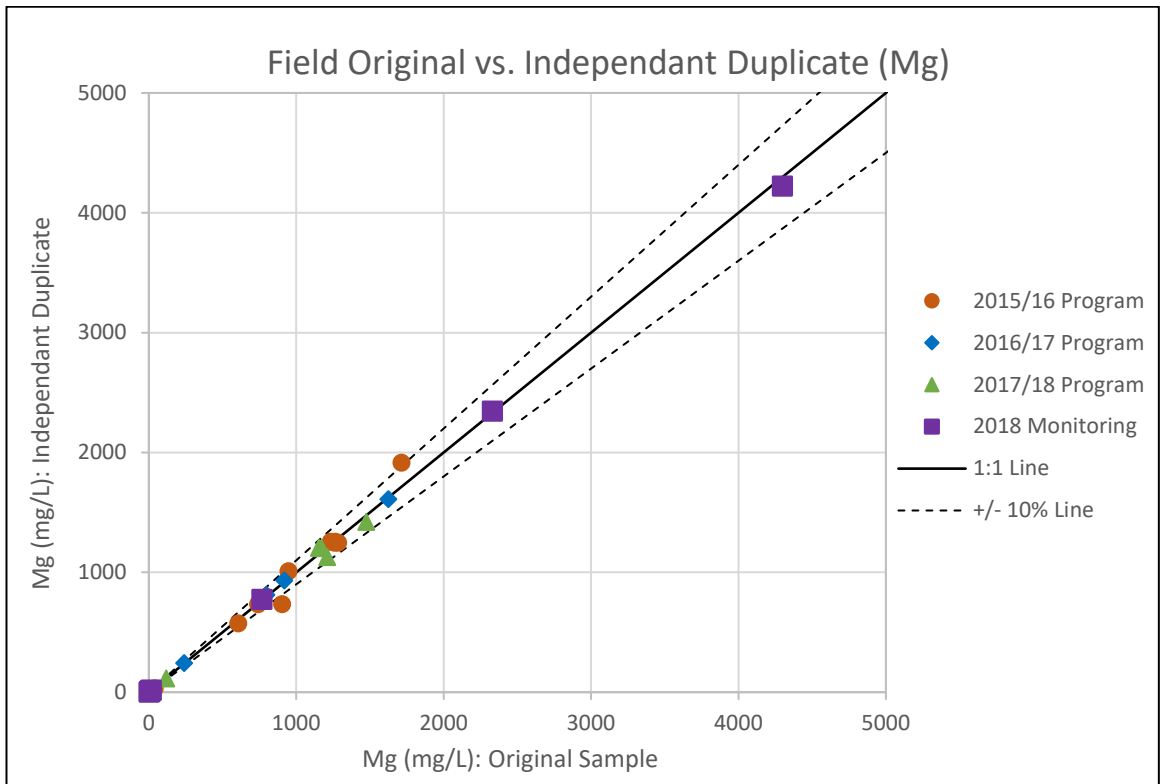


Figure 12-3: Original samples versus QP duplicate magnesium samples.

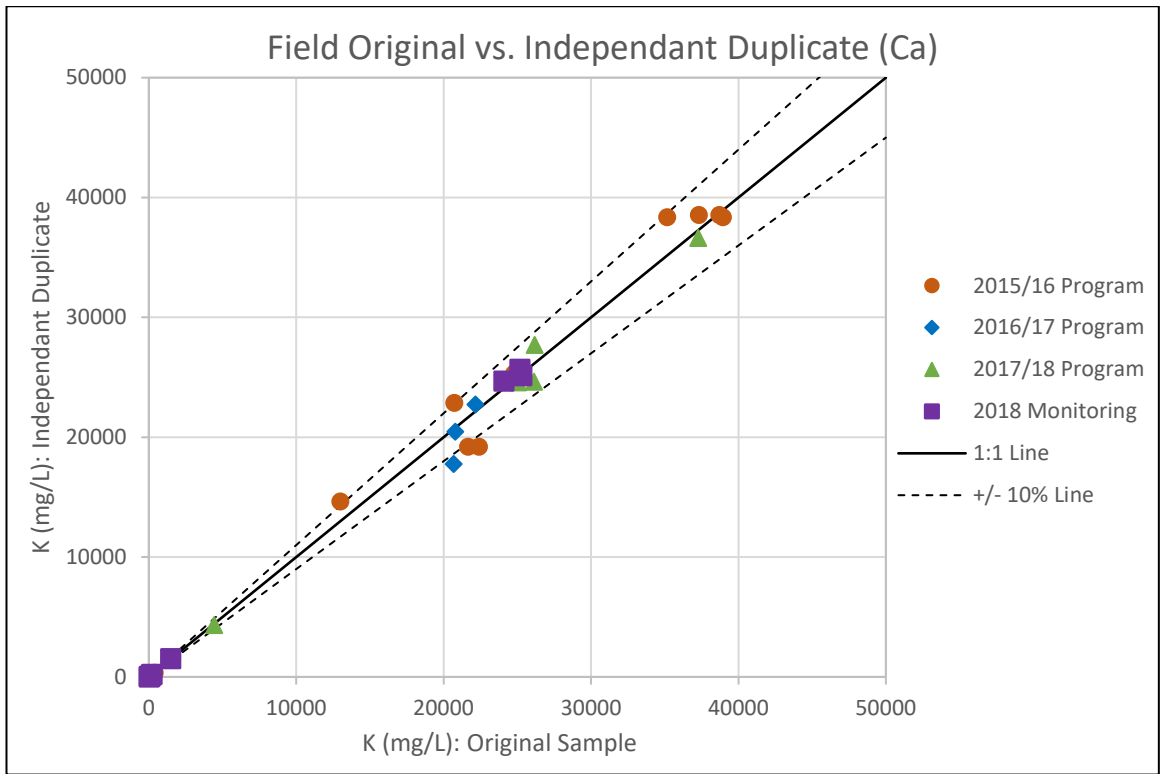


Figure 12-4: Original samples versus QP duplicate calcium samples.

13. Mineral Processing and Metallurgical Testing

13.1 Introduction

NLC has carried out a series of studies, to define the process variables for final design of chemical and physical operations for the 3Q Project. The following sections review the simulation models used in the mass and energy balance calculations and the tests conducted for each stage of the process.

13.2 Modelling of the 3Q Process

NLC developed a simulation tool to define the process baseline. This tool combines salt and brine thermodynamic models, with process equipment models. These simulations were done with gPROMS, a platform developed by SIEMENS PSE.

Aqueous Solutions Aps (Kaj Thomsen) and Hafnium Labs (Bjørn Maribo-Mogensen), both located in Denmark, were engaged to develop a Thermodynamic Property Package (“TPP”) for NLC. The property package calculates ion activity of the liquid phase, solid and liquid enthalpy, liquid density, solid density, slurry density and equilibrium in liquid and solid phase as a function of composition, temperature and pressure. This TPP was customized for the 3Q brine according to the following:

- Species: $\text{CO}_{2(\text{aq})}$, Na^+ , K^+ , Mg^{++} , Ca^{++} , Li^+ , Sr^{++} , H^+ , OH^- , Cl^- , HSO_4^- , H_3BO_3 , BO_2^- , B_2O_7^- , HCO_3^- , CO_3^{--} , and H_2O ;
- Chemical reactions in liquid phase:
 - $\text{H}_2\text{O} \leftrightarrow \text{H}^+ + \text{OH}^-$
 - $\text{H}_3\text{BO}_{3(\text{aq})} \leftrightarrow \text{H}_2\text{O} + \text{H}^+ + \text{BO}_2^-$
 - $\text{H}_2\text{O} + \text{B}_4\text{O}_7^{2-} \leftrightarrow 2\text{H}^+ + 4\text{BO}_2^-$
 - $\text{HSO}_4^- \leftrightarrow \text{H}^+ + \text{SO}_4^{2-}$
 - $\text{CO}_{2(\text{aq})} + \text{OH}^- \leftrightarrow \text{HCO}_3^-$
 - $\text{HCO}_3^- \leftrightarrow \text{H}^+ + \text{CO}_3^{2-}$;
- Salts formed by chemical reaction: Over 30 different Ca, Mg, Li, K, B, and Sr salts were considered;
- Activity coefficients calculation method was UNIQUAC, modified for electrolyte;
- Liquid, solid and slurry density calculations were included; and
- Enthalpy, Gibbs free energy, and chemical equilibrium constants were included.

These models operate in dynamic or steady-state mode. An “ENVIRONMENT” module incorporates the weather variables of 3Q Salar, including:

- maximum, average and minimum daily ambient temperature;
- maximum, average and minimum daily environmental humidity;
- atmospheric pressure;
- wind speed;
- global radiation; and

- dew temperature.

This module allows calculation of the system evaporation rate, considering chemical equilibrium in homogenous-heterogeneous phase, including variables, such as salinity, mass and energy transfer between phases and pond size.

The process library of the model also considers components such as pumps, piping, reactors, pipe splitters, tanks, heat exchangers, physical-chemical analyzers, PLC controls and the chemical conversion module. The latter component constitutes the core of the calculations for mass balance, within reactive systems, in homogenous-heterogeneous phases.

13.3 Modeling of the Solar Evaporation Pond System

Numerous tests and simulations have been carried out, to define the stages of the 3Q Salar Pond System. In previous experimental stages, it became apparent that given the high calcium content in the brine, the Pond System should include two stages: Pre-concentration and Concentration. Experimental work also indicated that a CaCl₂ Crystallization Plant should be included in the process.

The development of conceptual engineering was supported by predictive modelling tools. The models also helped to guide experimental designs for bench scale testing of ponds and chemical pilot plant designs. Two models were developed to define the Pre-Concentration and CaCl₂ system mass balances. They are shown in Figure 13-1 and Figure 13-2, respectively.

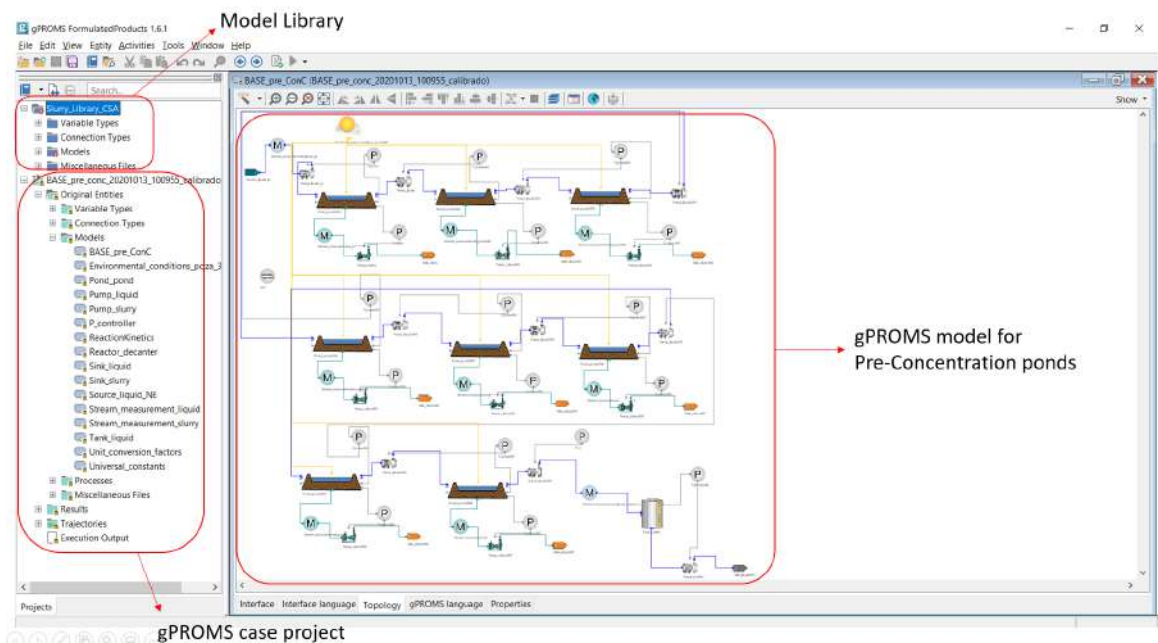


Figure 13-1: Work window for Pre-Concentration Ponds model for the 3Q Project.

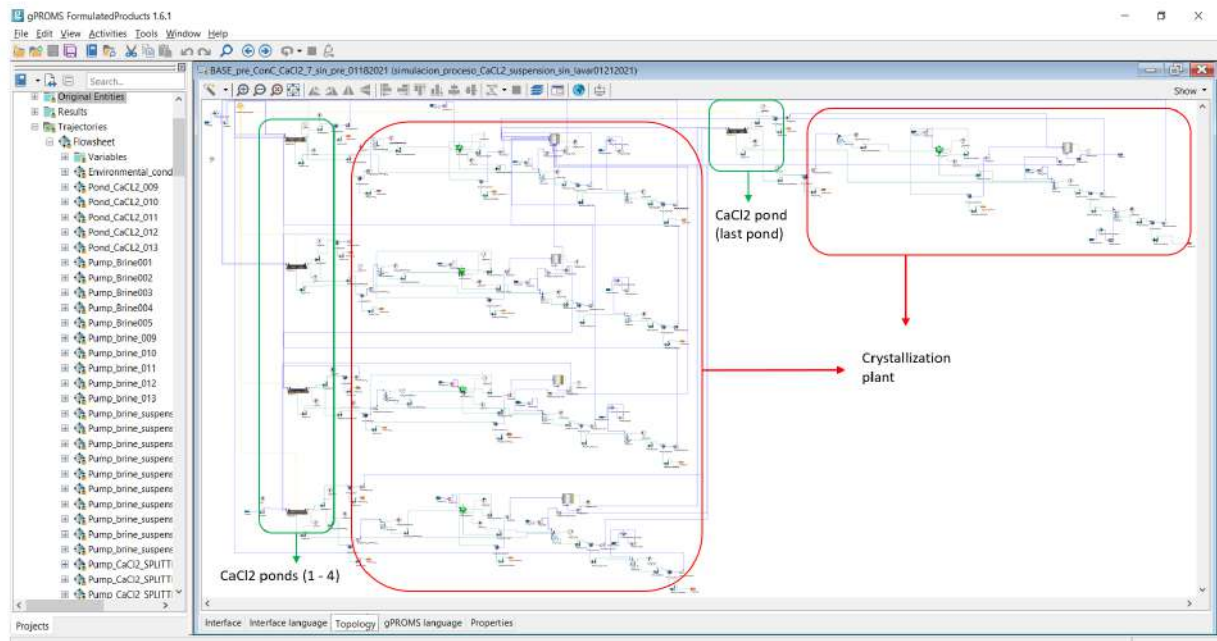


Figure 13-2: Work window for CaCl₂ process model (ponds and CaCl₂ Crystallization Plant) at the 3Q Project.

Both models simulate lithium enrichment from raw brine, through the solar evaporation process, interacting with the CaCl₂ Crystallization Plant. As the brine evaporates, it becomes saturated in salts that precipitate, increasing the lithium concentration in the remaining brine. This occurs because the solubility of lithium chloride is high relative to other potential salts.

The concentration model for the 3Q Project ponds includes two stages:

- **Pre-Concentration Ponds:** The purpose of these ponds is to remove water through evaporation, precipitate sodium chloride (NaCl) and potassium chloride (KCl – KCl•MgCl₂•6H₂O) and to saturate the brine in calcium chloride (CaCl₂•6H₂O).
- **Concentration Ponds System:** This system is designed to remove calcium from the brine, and to increase lithium concentration. Salts precipitated at this stage are calcium chloride (mostly CaCl₂•6H₂O and CaCl₂•4H₂O) and smaller amounts of NaCl, KCl•MgCl₂•6H₂O, and H₃BO₃.

The model combines the operation of the Concentration Ponds and the Crystallization Plant.

13.4 Experimental Work at 3Q Salar

13.4.1 Pre-Concentration Ponds

Experimental work conducted in previous stages for the Pre-Concentration Ponds continues (Photo 13-1). Models and pilot scale tests have confirmed the behavior of the pond brine chemistry. This information supports the detailed engineering phase for the Preconcentration Ponds, and studies continue to be developed to optimize parameters for pond operation and for chemical control of the brine. The variables that have been evaluated include:

- Levels and chemical composition of the brine in the ponds;
- Level control and chemistry of salts in the ponds; and
- Estimation of water inflow contributed by snowfall.



Photo 13-1: Views of Pilot Ponds - 3Q Project.

13.4.2 Concentration Stage

Studies of the concentration stage have continued since 2019, with a focus on maximizing Li recovery from the brine (Photo 13-2). This work includes study of the Concentration Ponds and of CaCl_2 separation, to optimize variables such as:

- CaCl_2 well temperature measurement;
- Salt level control in ponds; and
- Estimation of water flow contributed by snowfall.



Photo 13-2: Work in CaCl_2 Pilot Ponds - 3Q Project.

13.4.3 CaCl₂ Separation

In previous work, antarcticite (CaCl₂•6H₂O) separation was accomplished with crystallizers and thickeners. Follow-up work included the following:

- Tests were carried out with a pilot-size crystallizer which allowed control of crystallization temperature, solid-liquid separation of pulps and temperature.
- Unit operation of solid-liquid separation, after the crystallization process, to ensure maximum recovery of brine impregnated in the crystallized solids.

Results indicated that transport of thickened pulp to the CaCl₂ salt collection area could be hindered by obstruction of the transport duct, due to in situ crystallization caused by cooling of the brine (winter) or redissolution of the solids (summer). In addition, it was observed that:

- All fluid streams related to brine saturated in antarcticite, or near saturation, are extremely sensitive to temperature variation.
- The amount of solid formed from a brine saturated in antarcticite, or near-saturated, depends on the amount of heat extracted from the brine.
- The rate of heat extraction influences the way in which the particles are generated.
- The time spent in a heat transfer process determines the shape and size of the crystals formed.
- Concentrated brine density is strongly affected by the final temperature of the pond. When brine reaches temperatures above 29.9 °C (melting point of the antarcticite), the solid will melt and mix with the concentrated brine, resulting in a sharp increase in density.
- Calcium elimination must be controlled and regulated by heat transfer, to avoid brine loss due to massive solidification.
- Antarcticite does not sequester lithium in its crystalline structure.

Based on these observations, the previous CaCl₂ separation process was changed to an antarcticite crystallization system, with controlled cooling. Further, it was coupled to a solid-liquid separation system, to ensure maximum recovery of lithium.

The following studies were formulated from these results:

- Study of lithium brine crystallization from the Pre-Concentration process;
- Study of the relationship between concentrated brine chemistry and viscosity;
- Study of solid pulps, in particular, liquids from the CaCl₂ process; and
- Characterization of filtered solids from the CaCl₂ stage.

NLC requested a study from the JRI Center for Sustainable Mining Research (CIMS JRI), to identify the appropriate operational conditions to concentrate lithium brine by separating calcium chloride (CaCl₂) crystals through evaporation and cooling (Photo 13-3). Results from these studies support an increase in lithium concentration in the brine through the process stages. They also define characteristics associated with the de-impregnation stage, and support the selection of equipment from specialized vendors.



Photo 13-3: Equipment used in studies by CIMS JRI.

13.5 Lithium Carbonate Process at the Fiambalá Site

13.5.1 Overview

The lithium carbonate production process at the Fiambalá Site previously included the following stages:

- Solvent extraction for boron (SX-B);
- Sulphation for massive calcium abatement;
- Polishing of impurities (Ca, Mg) with mother liquor; and
- Final carbonation for lithium.

Through subsequent optimization studies, the following advances were identified:

- Reduction of external reagents (Na_2SO_4 and CaO) would decrease the impurities in the Li_2CO_3 final product.
- This would have the advantage of reducing discarded solids, with a corresponding reduction in tailings costs.
- The early process stages (0 to 2) do not require heat, thus reducing energy costs.
- Lithium recovery is improved.
- Reagent transport costs are significantly reduced.

For this feasibility stage, the alkaline process considers:

- Boron abatement by solvent extraction, to which an organic washing stage is added;
- Magnesium abatement (at Stage 0) by reacting the brine with lime generated in Stage 1;
- Calcium abatement (at Stage 1) by reacting the brine with NaOH ;
- Residual Calcium Polishing is reduced to a few mg/L by means of a polishing stage, with the addition of Na_2CO_3 ; and
- Lithium carbonate is produced at 70°C .

The work at the Fiambalá Site is supported by a fully-equipped analytical laboratory (Photo 13-4).

13.5.2 Modelling of the Fiambalá Process

The Li_2CO_3 production process in Fiambalá is divided into two parts (Figure 13-3). Initially, the brine that arrives from the salar enters the solvent extraction plant for boron extraction. Subsequently, the boron-free brine passes to the Mg stage (0a) and Ca abatement stage (0b - 2) and the Li carbonation stage (3). Given the complexity of the Fiambalá process, NLC decided to integrate the SX-B process with the downstream chemical process.

The SX-B model incorporates all the liquid-liquid equilibria tested in the laboratory for the extraction, scrubbing and stripping stages. The chemical models used for stages 0 to 3 were those from the thermodynamic package prepared by Aqueous Solutions Aps (Kaj Thomsen) and Hafnium Labs (Bjørn Maribo-Mogensen). The unit process models have been developed and implemented by NLC on the gPROMS platform.

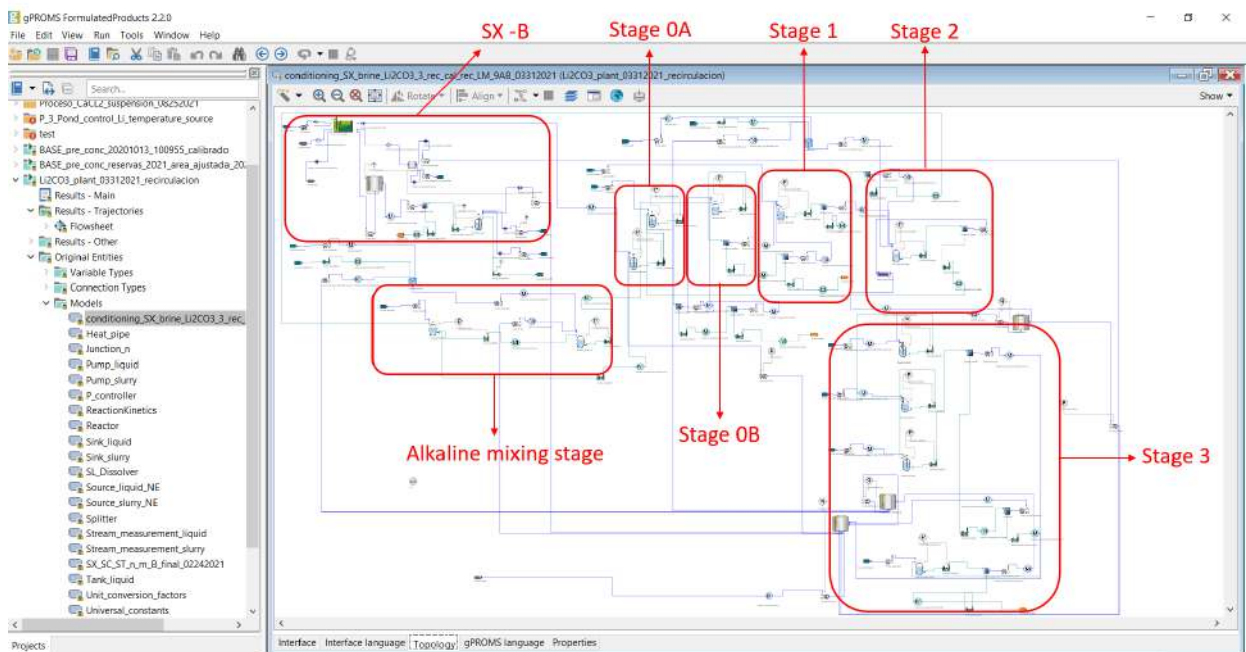


Figure 13-3: Work window for the Fiambalá process model.



Photo 13-4: Analytical laboratory in the Fiambalá Pilot Plant.

13.5.3 Experimental work at Fiambalá

Studies conducted to support the design and operation of the plant include:

- SX studies:
 - Equilibrium Time;
 - Phase separation time;
 - Extraction isotherm at equilibrium time (5% EHD); and
 - Maximum load.
- Scrubbing studies
 - Iron-Zinc and Boron extraction isotherms, at different CaCl_2 concentrations; and
 - RIL treatment by pH change.
- Stripping studies
 - Balance time;
 - Phase breaking time; and
 - Stripping isotherm.

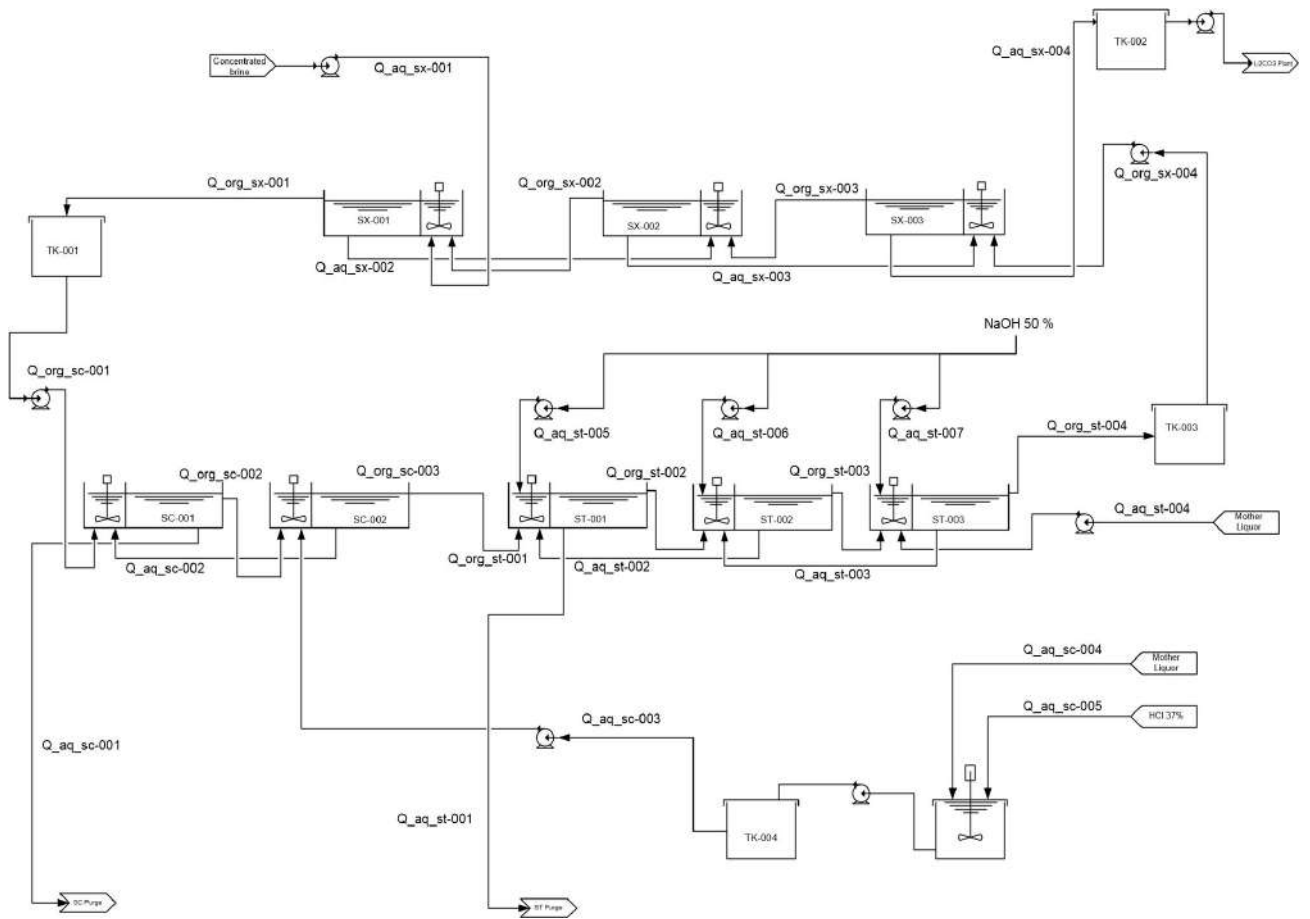


Figure 13-4: SX-B flowsheet.

The SX-B plant configuration is shown in Figure 13-4 and Photo 13-5. The diagram shows a stage labeled "SC", in which the loaded organic from SX is mixed with an acid solution. This stage corresponds to scrubbing the organic to remove Fe and Zn, which are partially co-extracted during the extraction process. These metals interfere in the stripping stage, since they react chemically with the stripping solution, forming solid metal hydroxides that contaminate the organic phase and prevent recovery and recycling.

To avoid the formation of this third phase, it is necessary to add an additional acid washing step with a 0.01 - 0.1 M HCl solution, for complete removal of these metals. Currently, the scrubbing step is in the advanced piloting stage. Generally, this process can remove the remaining 99.9% boron from the Li brine. Lithium losses at this stage are close to zero.



Photo 13-5: SX-scrubbing and stripping tests.

13.5.4 Calcium, magnesium, strontium polishing and production of lithium carbonate.

CaSO_4 precipitation can occur in the equilibrium of calcium with sulfate and also calcium with hydroxyl ion. The latter forms Ca(OH)_2 , which substantially reduces calcium in the liquid and forms an in situ reagent (slaked lime) necessary for elimination of magnesium (previous stage). Characteristics of this process (Photo 13-6) include:

- Less solids mass and volume is produced in the calcium elimination stage. In this case, the reaction product corresponds to Ca(OH)_2 , which is an input for the elimination of magnesium.
- In the alkalization process, magnesium is quantitatively removed.
- In the process of polishing calcium with carbonate, a quantity of CaCO_3 / MgCO_3 / SrCO_3 solids is generated, which are recirculated to the stage where magnesium is eliminated. These solids are re-used in this stage as adsorption media for Mg(OH)_2 , to enable pulp filtering.
- All the alkalization stages occur at room temperature, since under these conditions an acceptable thermodynamic and kinetic stability of acid-base processes is obtained.
- No process water is required for washing, or recovering lithium, from waste solids.
- Wash water is only used in the lithium carbonate wash stage.
- The mother liquor is re-used for reagent preparation, stripping solution B and dilution of concentrated lithium brine.
- The alkaline earth impurities and the lithium carbonate precipitation process can be divided into 4 consecutive stages, numbered 0, 1, 2, and 3, and described further below.



Photo 13-6: Facilities for testing the difference stages of Li_2CO_3 production in the Li_2CO_3 Pilot Plant.

Stage 0

- Studies conducted to investigate this stage sought to reduce calcium and magnesium in the brine, to identify possible losses of Li, and to determine precipitation time (Photo 13-7). This stage is subdivided into 0A and 0B.
- Stage 0A: The objective is to remove magnesium by precipitation, as $\text{Mg}(\text{OH})_2$, and calcium as CaCO_3 . Studies were conducted to determine:
 - Reactions;
 - Equilibrium time;
 - Sedimentation curves;
 - Filtered solids composition; and
 - Percent of solids.
- Stage 0B: The objective is to reduce calcium content. Studies were conducted to determine:
 - Alkaline mixture reaction and equilibrium time;
 - Reactions;
 - Residence time (zero B);
 - Sedimentation curves;
 - Filtered solid composition; and
 - Percent of solids.



Photo 13-7: Pilot settler test and pilot press filter filtration tests.

Stage 1

The objective of this stage is to continue with the elimination of calcium and to verify that there are no Li losses. Studies (Photo 13-8) were conducted to determine:

- Reactions;
- Equilibrium time;
- Sedimentation curves;
- Filtered solids; and
- Percent of solids.



Photo 13-8: Equipment used in stage tests.

Stage 2

The objective of this stage is to verify the polishing stage, to obtain a better distribution of reagents and to obtain a pulp that allows better solid-liquid separation. In this stage, boron- and magnesium-free brine is treated with Na_2CO_3 to eliminate residual concentrations of calcium and strontium that could not be totally eliminated in the previous stages. The pulp obtained in this stage is thickened and sent to Stage 0, for use as a filter medium for $\text{Mg}(\text{OH})_2$. Studies (Photo 13-9) were conducted to determine:

- Reactions;

- Equilibrium time;
- Sedimentation curves;
- Filtered solids; and
- Percent of solids.



Photo 13-9: Equipment used for Stage 2 tests.

Stage 3

The objective of this stage is to test process alternatives. Studies (Photo 13-10) were conducted to determine:

- Reaction, modifying variables (stirring speed, stirrer position, dosages);
- Equilibrium times for each series sub-stage;
- Sedimentation curves;
- Percent of solids; and
- Recovery efficient for lithium carbonate.



Photo 13-10: Equipment used for pilot tests of Stage 3, counter-clockwise from top: carbonation pilot reactors, lithium carbonate filter, and dryer.

13.6 Next Steps

The next steps for mineral processing and metallurgical testing include the following:

- Continuation of pre-concentration and CaCl_2 ponds pilot tests;
- Tests with the crystallizer vendor, and repulping, in conjunction with CIMS-JRI, to establish engineering details of the CaCl_2 process; and
- Continuation of pilot tests with the Li_2CO_3 chemical plant and testing with lithium process equipment vendors.

14. Mineral Resource Estimates

14.1 Method Overview

An updated Mineral Resource Estimate was developed for the 3Q Project using the three-dimensional (“3D”) model FEFLOW (DHI-WASY, 2021). The software was operated by Aqua Insight Inc., specialists in FEFLOW applications. The QP provided technical oversight of the modelling and considers the results to be valid and appropriate for a Measured, Indicated, and Inferred Mineral Resource Estimate, as defined by the CIM and referenced by NI 43-101. The modelling methods are summarized as follows:

1. The existing geological model was brought forward from the 2021 Resource Estimate (King and Zandonai, 2021).
2. New drilling data indicated the need to re-configure the geological model at certain locations.
3. Geological units were re-interpreted along a series of two dimensional (“2D”) sections. This effort was supported by the new drilling and by pre-existing drilling, seismic, and VES results.
4. Interpolation between the 2D sections was conducted within the Project GIS. Final updated surfaces were transferred to FEFLOW to form a fully 3D geological model.
5. Drainable porosity was assigned to each geological unit based on RBRC testing.
6. Measured, Indicated, and Inferred Resource Zones were re-evaluated using a borehole density method supported by variography.
7. Brine sample results were used to interpolate 3D concentration distributions throughout the geological model, for 12 dissolved constituents (Li, Ba, Ca, Fe, K, B, Mg, Mn, Na, Sr, Cl, SO₄). The interpolation was supported by variogram analysis.
8. Brine grade and drainable volume were used to estimate the mass of brine constituents in each geological unit.
9. Measured, Indicated, and Inferred Resources were estimated for two different lithium grade cut-offs.

The QP considers the Resource Estimation methods and results to be reasonable and appropriate. Additional detail on each step is provided in the subsections below.

14.2 Resource Model Development

The surface footprint of the Resource Zone was based on interpreted salar unit boundaries, deposit characteristics, and surface geophysics. The footprint is shown on Figure 14-1, and is described as follows:

- The east and west boundaries were defined as the interpreted outer limits of the salar basin;
- The northern boundary (i.e., in the vicinity of Laguna 3Q) is generally defined by the northern shore of Laguna 3Q, except for the Upper Sediments unit which extends under the lake and into the alluvial fans on the north, east, and west shores of the lake; and
- The Resource Zone extends to the south boundary of Laguna Verde, except for the Upper Sediments and underlying units, which extend some distance south of Laguna Verde.

Geological and hydrogeological information were interpreted to define the distributions of primary geological units under the Resource Zone footprint. Information sources included:

- Visual assessment of relative porosity and permeability in cores;
- Laboratory analytical results for RBRC (indicative of Sy (Section 10.2));

- Borehole logs and downhole geophysics (Section 10); and
- Seismic and VES Surveys (Section 9).

The geology of the Resource Zone was delineated into six primary geological units, as presented in Section 7. Basement rock was excluded from the Resource, based on the assumption that it would not contribute brine that could be recovered as part of the Reserve. The units are briefly described as follows (from upper to lower), with additional detail provided in Section 7.3:

- Hyper-Porous Halite - medium to coarse halite crystals with a high inter-crystalline porosity;
- Upper Sediments - sandstone, gravel, siltstone, and clay; moderate visual porosity;
- Porous Halite - medium to coarse crystals with moderate visual porosity;
- Massive Halite - fine to very coarse white, gray, red, and black cubic crystals, with low visual porosity; some intercalation of reddish clay and possibly organic matter;
- Lower Sediments - sand and siltstones containing minor gypsum laminae; and
- Fanglomerate - clasts of fanglomerates, medium-coarse sandstones, and sedimentary breccias ranging from 2-20 cm in diameter with a red-gray, sandy-shale matrix.

These six geological units were maintained from the previous Mineral Resource Estimate presented in the PFS (King and Zandonai, 2021). To update and re-generate the unit surfaces, a series of 100 sections were developed in the Project GIS (Figure 14-1). Sections were configured to intersect the available borehole data, including the new 2018-2021 Program drilling (Platforms 24, 25, and 26). Unit surfaces were then generated within the Project GIS to define the 3D structure for the updated geological model.

The model was primarily revised in the north, in the vicinity of the 2018-2021 drilling. Some minor changes were also implemented in the southern salar, primarily to simplify and smooth the unit surfaces. The completed surfaces were then combined into a 3D Resource model and imported into FEFLOW. In the geological model, the northern and southern lakes (Lagunas 3Q and Verde) were mapped as independent units, based on measured lake bathymetry (Section 7.6; Figure 7-6).

The change in volume of the updated geological model relative to the PFS is summarized in Table 14-1 and shown graphically on Figure 14-1. Example sections showing modifications in the north and south areas are shown on Figure 14-2. The volume, average thickness, and percent of Resource in each unit is summarized in Table 14-2. Final unit delineations are shown on Figure 14-3.

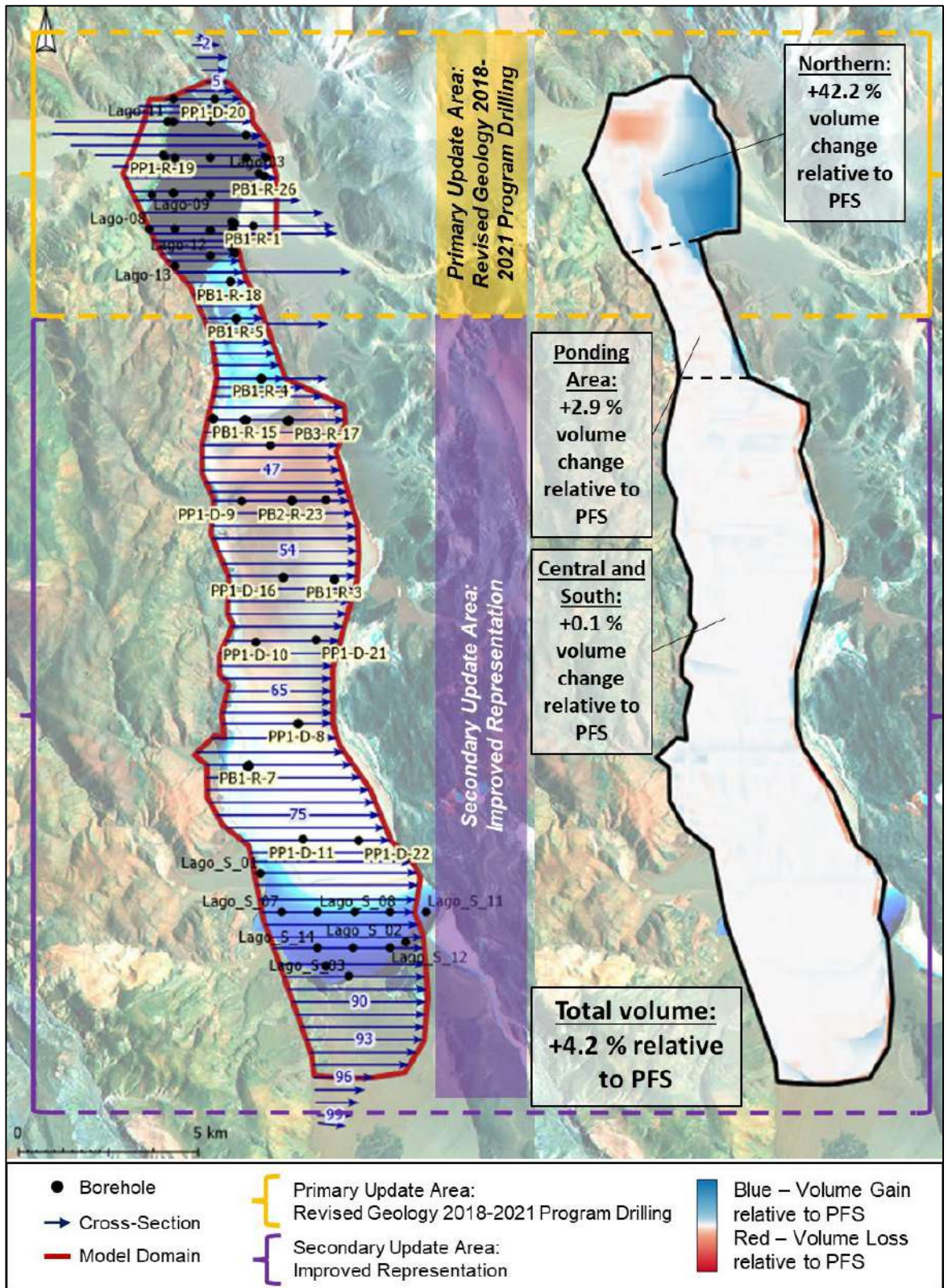


Figure 14-1: Plan of sections used for geological model update (left) and model volume changes relative to the PFS (right).

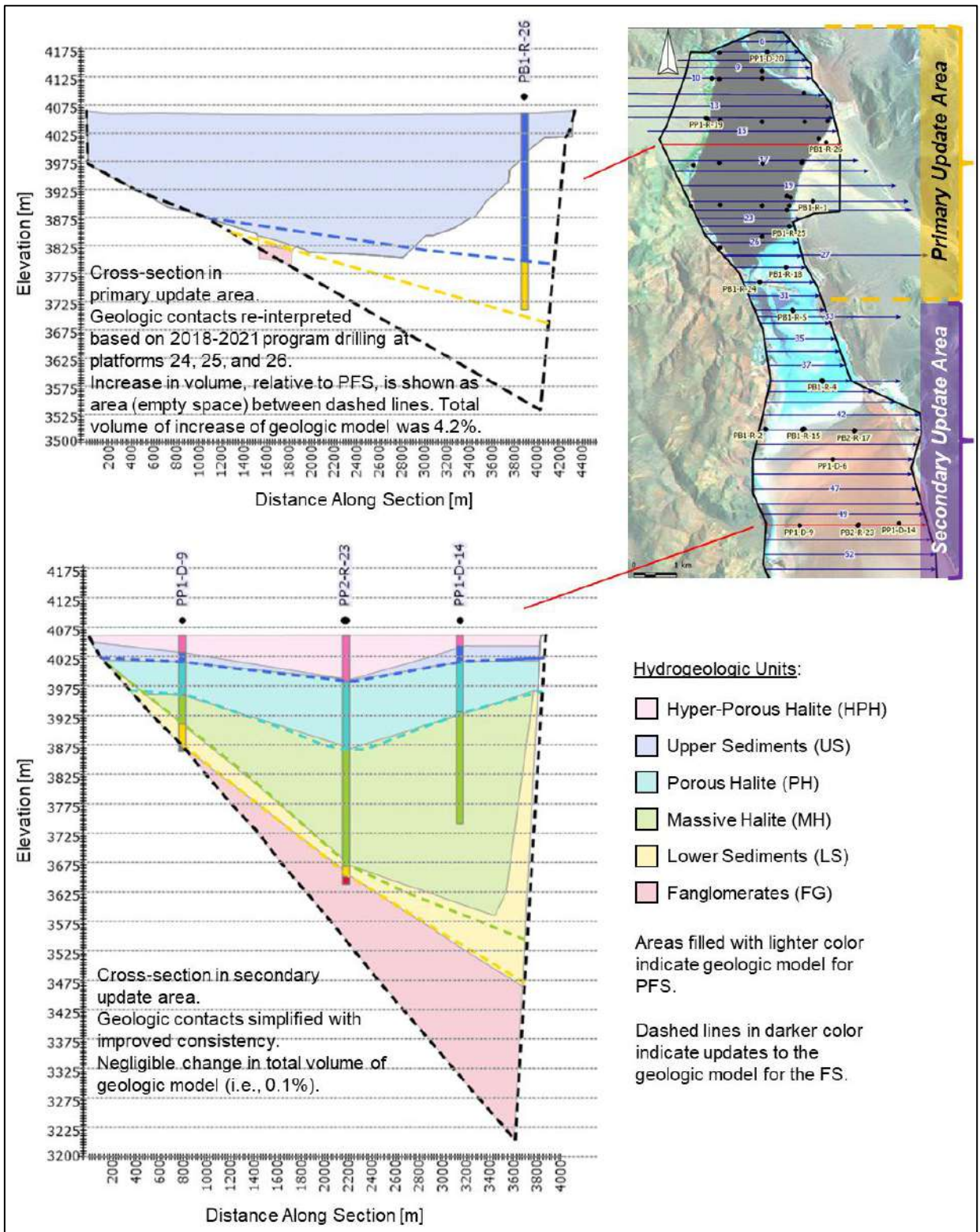


Figure 14-2: Example sections, geological model updates.

Table 14-1: Volume changes in updated geological model relative to the PFS.

Location ¹	Volume (1x10 ⁶ m ³)			Percent Difference
	PFS Geological Model	FS Geological Model	Difference	
Northern	303.86	432.20	+128.30	+42.2%
Ponding Area	184.84	109.13	+5.30	+2.9%
Central and South	2,800.86	2,804.01	+3.10	+0.1%
Total	3,289.66	3,426.34	+136.68	+4.2%

1. Locations are shown on Figure 14-1.

Table 14-2: Summary of primary geological units in the Resource Model.

Primary Geological Unit	Average Thickness [m] ¹	Volume [x10 ⁹ m ³] ¹	Volume [% of Total Model] ¹	Average Specific Yield (%) ²	Resource (%) ³
Hyper-Porous Halite	12.1	1.9	5.8	14.74	10.6
Upper Sediments	47.7	4.3	13.1	9.12	21.3
Porous Halite	59.4	7.0	21.4	6.33	16.4
Massive Halite	105.4	10.3	31.4	3.85	14.9
Lower Sediments	37.6	3.9	11.9	5.18	9.3
Fanglomerate	43.0	5.4	16.3	11.23	25.8
Laguna 3Q	1.0	0.02	<0.1	100	1.1
Laguna Verde	0.5	0.02	<0.1	100	0.6

Notes:

1. Unit thicknesses and volumes are from the Resource model developed in FEFLOW. "Volume" is the bulk volume of the unit, not reflective of porosity.
2. Drainable porosity (specific yield) was estimated as the average of all RBRC results collected from the unit. Additional information on RBRC results is provided in Section 10.
3. Total Resource within 400 mg/L Li cut-off.

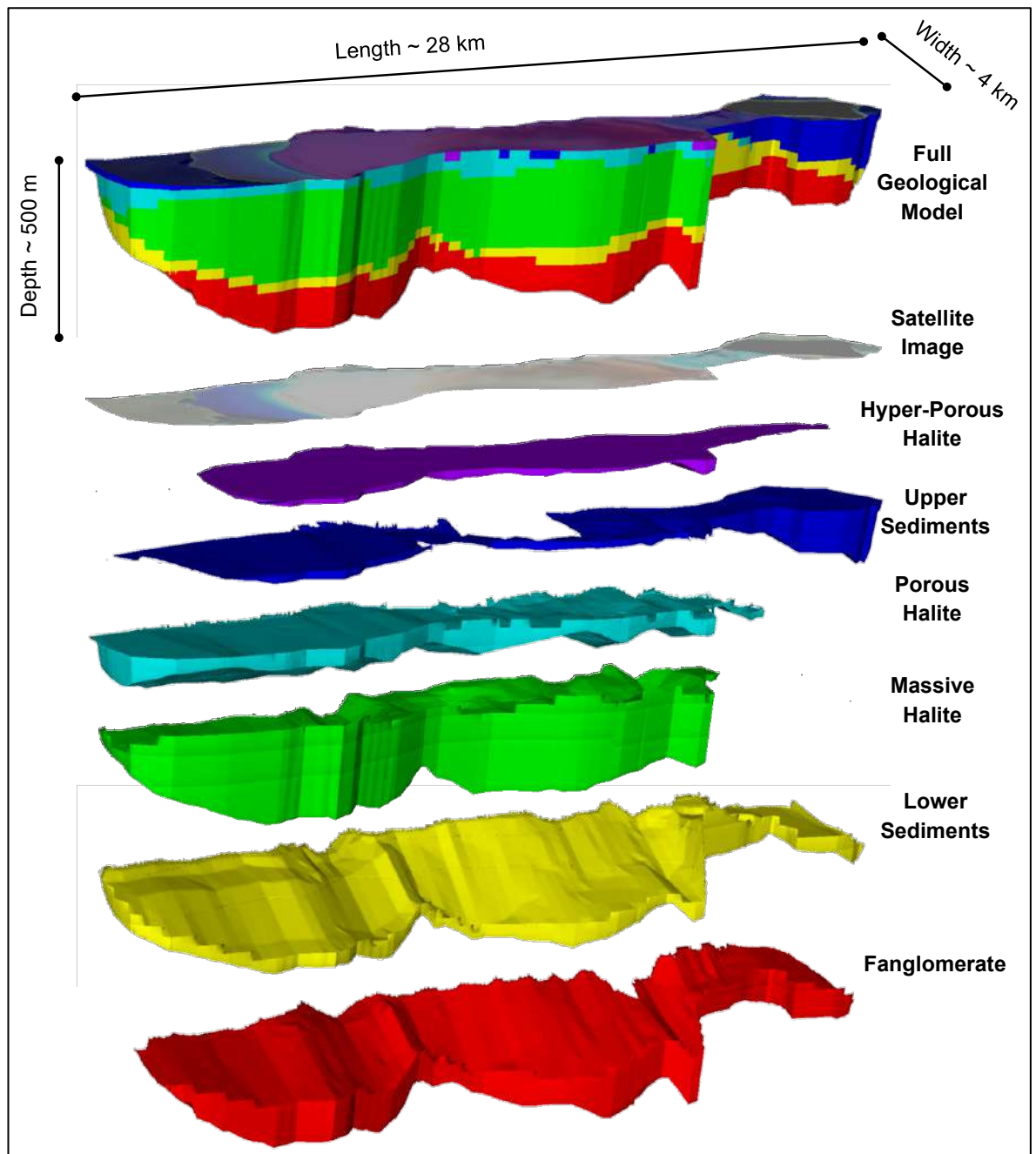


Figure 14-3: 3D configuration of primary geological units in the Resource Model

14.3 Mineral Resource Zones

Measured, Indicated, and Inferred Mineral Resource Zones were classified based on a borehole spacing method, with semi-variogram analysis used to evaluate minimum borehole spacing. In general, the borehole spacing method is a widely used and industry-accepted approach for resource zone classification (for example, Silva and Boisvert, 2014). Resource Zone configurations are summarized in Table 14-3, shown on Figure 14-4, and described as follows:

- Measured Zone – 14 km in length, extending from the north end of the model to the central salar, and to a depth of 150 m.
- Indicated Zone – Underlies the Measured Zone in the north of the model, from 150 to 350 m depth. In the south of the model, the Indicated Zone extends from 0 to 300 m depth.

- Inferred Zone – Underlies the Indicated Zone throughout the model, and extends to the model base.

Table 14-3: Mineral Resource categorization for the 3Q Project, based on borehole spacing and variography. Resource Zones are shown on Figure 14-4.

		Measured	Indicated	Inferred
Depth		Surface to 150 m (3936 m asl)	150 – 350 m	Below 350 m (3736 m asl)
North	Borehole Density (km ² /m)	3.6	14.5	43.5
	Borehole Spacing (km)	1.9	3.8	6.6
Depth			Surface to 300 m	Below 300 m (3786 m asl)
South	Borehole Density (km ² /m)		14.4	28.9
	Borehole Spacing (km)		3.8	5.4

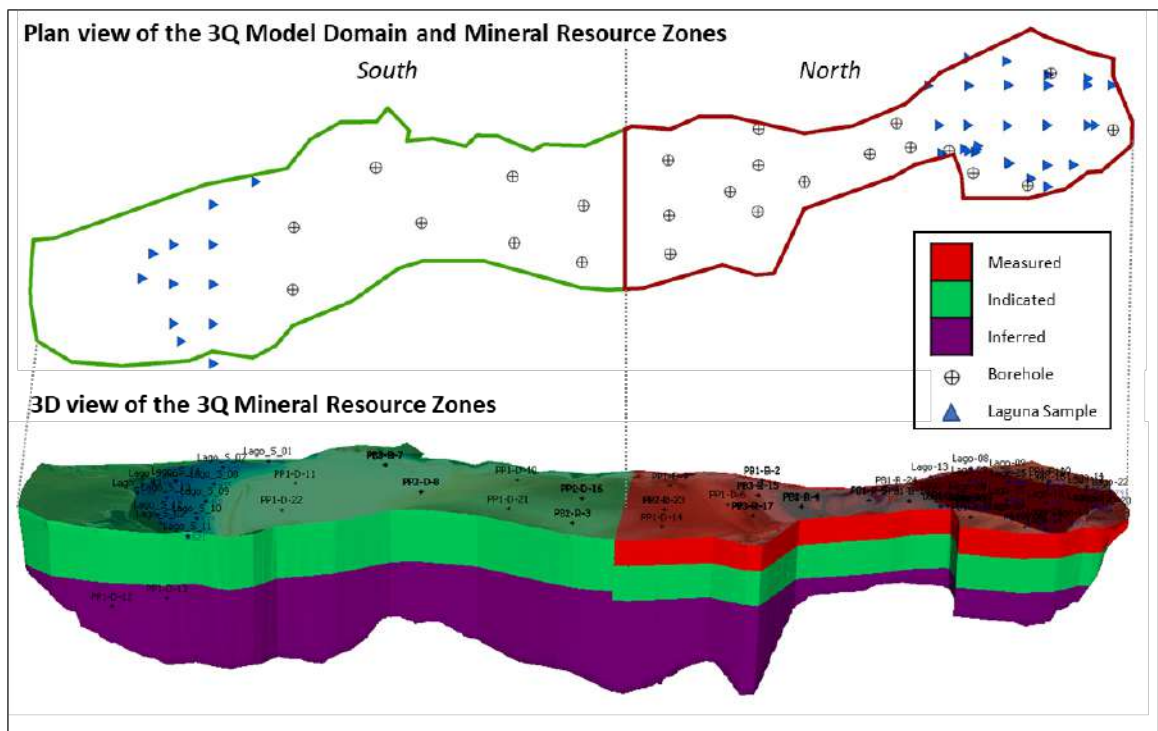


Figure 14-4: Configuration of Resource classification zones defined for the 3Q Project.

14.4 Brine Characterization within the Resource Model

14.4.1 Sample Data

The following selection criteria were used to identify 184 unique sample locations for brine chemistry interpolation:

- Samples used in the brine model were collected from observation wells, pumping wells, discrete level packers (from diamond drill boreholes during drilling), and directly from the two lakes in the Resource Zone (Laguna 3Q and Laguna Verde).

- When multiple sample types were collected from a single borehole, preference was given as follows:
 1. 72-hr and/or longer-term pumping test samples (all samples from a given pumping test were averaged);
 2. Packer samples (a single value was retained for each sample interval);
 3. Sample collected from an installed well using a submersible pump (1 borehole);
 4. Samples collected using airlift methods (1 borehole); and
 5. Step test samples.
- The following sample types were excluded from the interpolation:
 - Samples collected during well cleaning;
 - Samples collected outside of standard exploration activities, including but not limited to isotope samples, grab samples collected using a bailer, and samples collected for other studies; and
 - Samples from surface pit sampling.
- A total of 230 individual brine samples were selected, and sample multiples were averaged to generate 184 depth-discrete brine sample locations that included:
 - 45 lake samples;
 - 17 locations with averaged samples; and
 - 122 single, discrete interval samples.
- Seven samples were excluded from the brine interpolation as they were considered to represent mixing zones at the freshwater / brine interface. These samples (in addition to geophysical surveys) were used to support the interface delineation for subsequent dynamic Reserve modelling.

14.4.2 3D Interpolation of Grade Data

Statistical analysis of the grade samples indicated that the samples had a normal distribution, providing confidence that the grade data are representative of the population. The highest grades were observed within the north-central zone of the salar with grades decreasing toward the north and south. The brine data were interpolated in FEFLOW using the method of Inverse Distance Weighting Squared (“IDW²”). Other methods were evaluated (e.g., IDW, kriging), and all gave similar total mass.

In applying the IDW² method, search ellipses were based on the correlation length (i.e., range) developed through semivariogram analyses. Correlation lengths were tested with and without stationarity, omni-directional vs. directional, and with various lag bin sizes. While correlation lengths of 10,000 m were found to be supported by the data, the semi-variogram range of 6,000 m was found to provide the best fit. As such, search ellipse criteria used in the grade interpolation were:

- Major axis = 6,000 m;
- Semi-major axis = 6,000 m;
- Minor axis = 600 m; and
- Orientation along the axis of the salar (azimuth = 15°), and along the horizontal plane (dip = 0°).

To allow the locally interpolated grades to accurately reflect the grade data closest to each location, yet maintain a smooth, natural transition of grades throughout the salar, the number of samples within search ellipse was limited as follows:

- Measured Zone: max = 10;
- Indicated Zone: max = 20; and
- Inferred Zone: max = 25.

Freshwater wedges located within alluvial fans at the margins of the salar were excluded from the interpolation (and from the Resource model) due to the inherent limitations in interpolating a sharp grade change. The sharp interface was subsequently included, for dynamic Reserve modelling (Section 15)

Quality control checks included comparison of observed and interpolated values, visual inspection of interpolated distribution, evaluation of peak grade areas (e.g., continuity and distribution), and change in predicted mass. While all interpolation methods produced similar total mass, the IDW² method was chosen as it produced the grade distribution most-consistent with the conceptual understanding of resource deposition. Further, IDW² was generally conservative in that it yielded interpolated values in the high-grade zones that were lower than individual peak observations.

Distributions were mapped for brine parameters of primary interest, including: lithium, barium, calcium, iron, potassium, boron, magnesium, manganese, sodium, chloride, strontium, and sulfate. Lithium and potassium results are shown on Figure 14-5 and Figure 14-6, respectively. Lithium grades were highest (i.e., > 1,000 mg/L) immediately south of Laguna 3Q, and decreased to the north and south. Grades were relatively uniform in the vertical dimension. Similar trends were noted for other constituents (e.g. potassium, Figure 14-6).

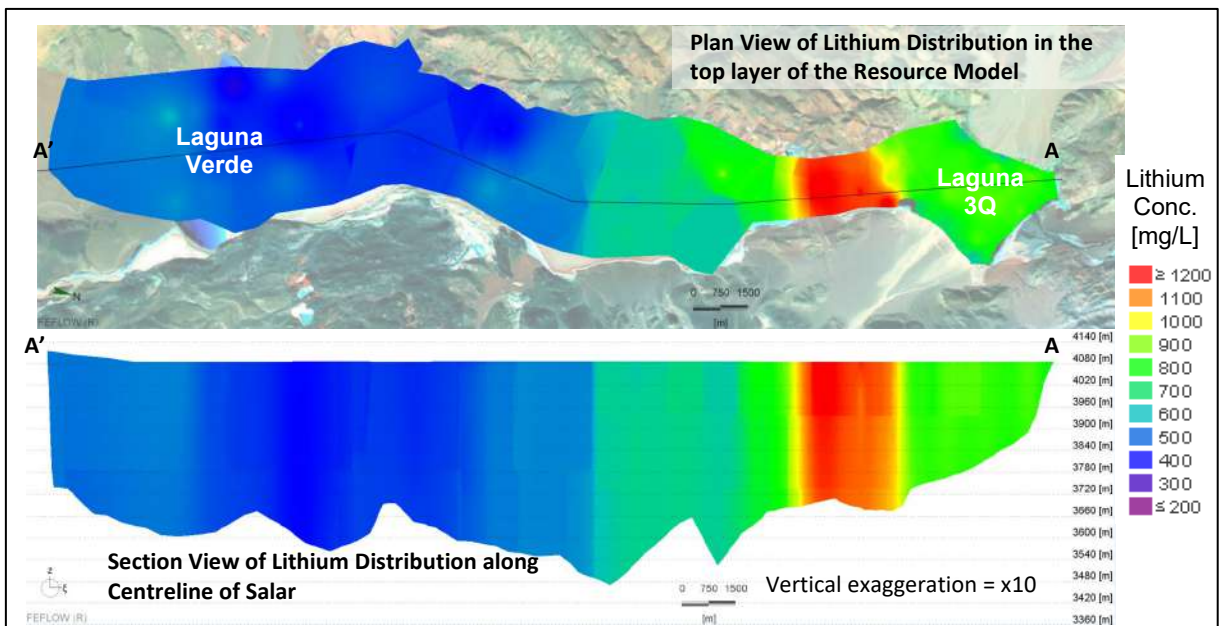


Figure 14-5: Distribution of lithium in the top layer and along the centreline of the Resource Model.

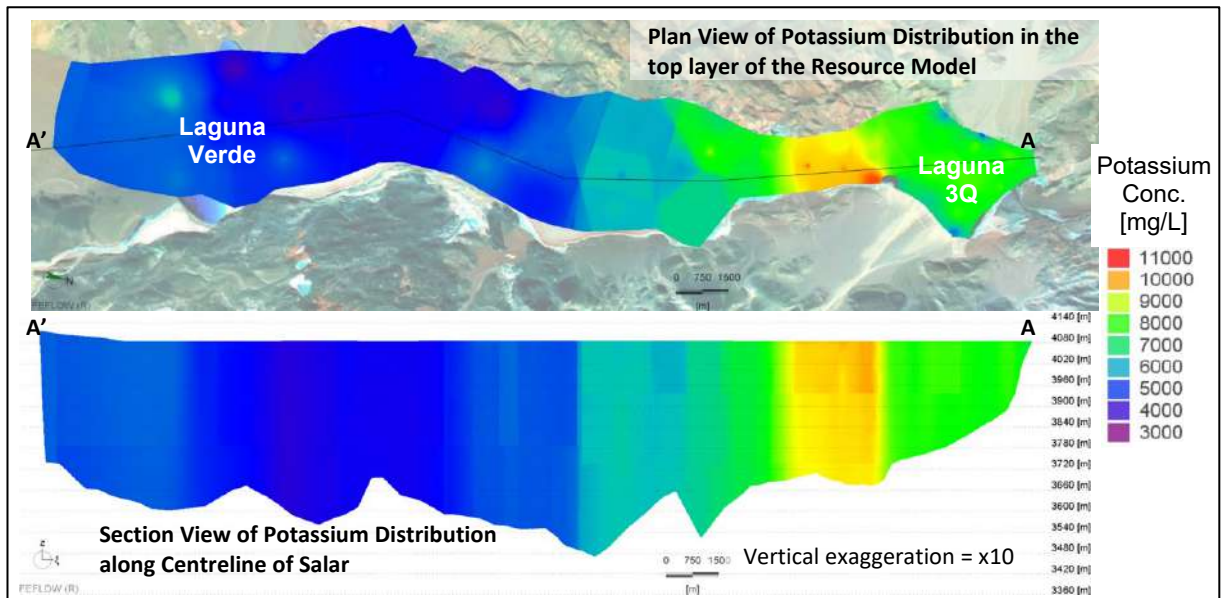


Figure 14-6: Distribution of potassium in the top layer and along the centreline of the Resource Model.

14.4.3 Brine Grade Distribution

The Resource model was evaluated based on lithium cut-off grade and Resource Category. The relationship between lithium cut-off grade, average grade, and mass are shown graphically on Figure 14-7. As indicated by these curves, the quantity of resource below 400 mg/L is negligible. Figure 14-8 illustrates the distribution of lithium within the resource, at cut-off grades of 400, 600, 800, and 1,000 mg/L.

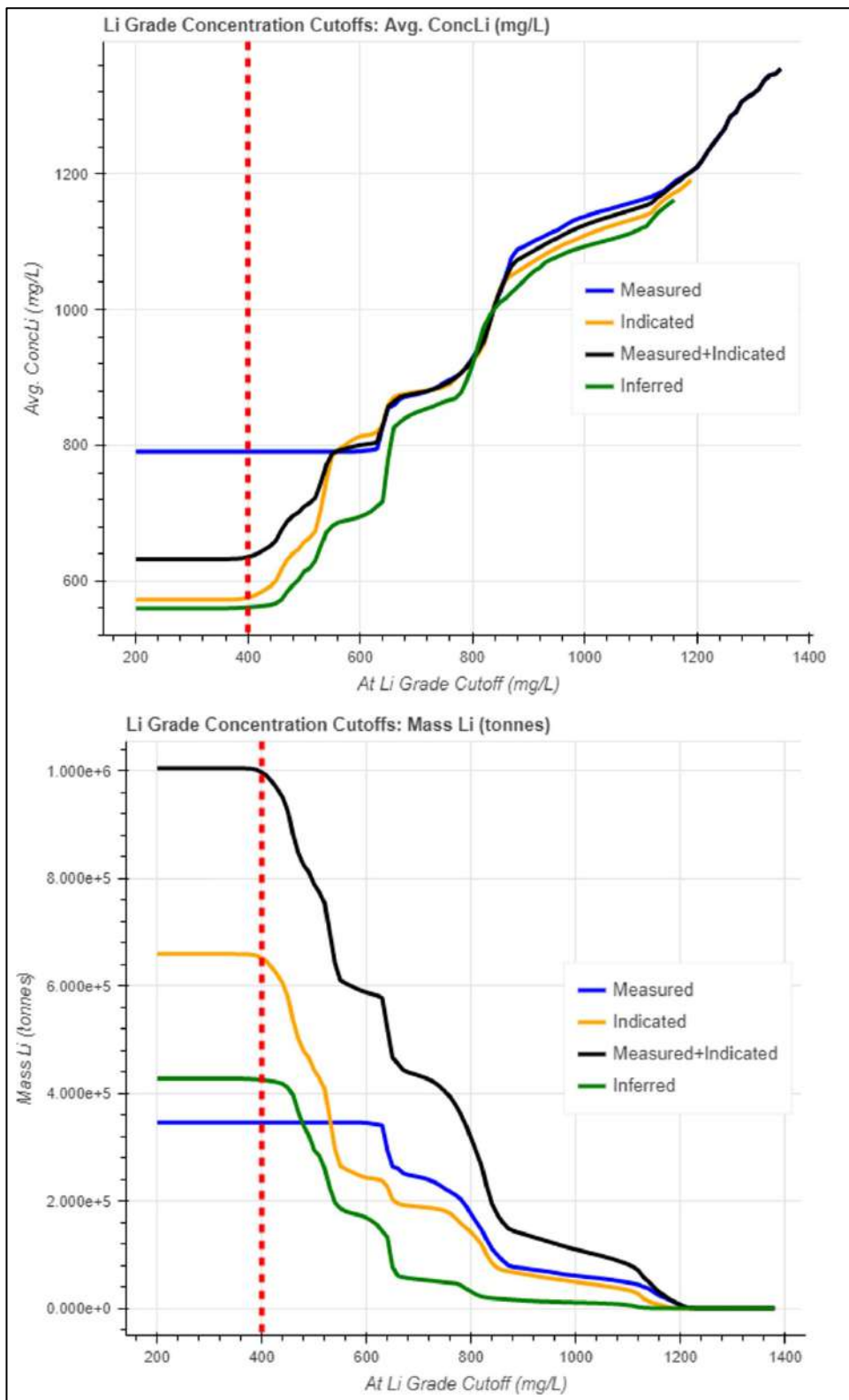


Figure 14-7: Lithium cut-off grade curves for average concentration and mass.

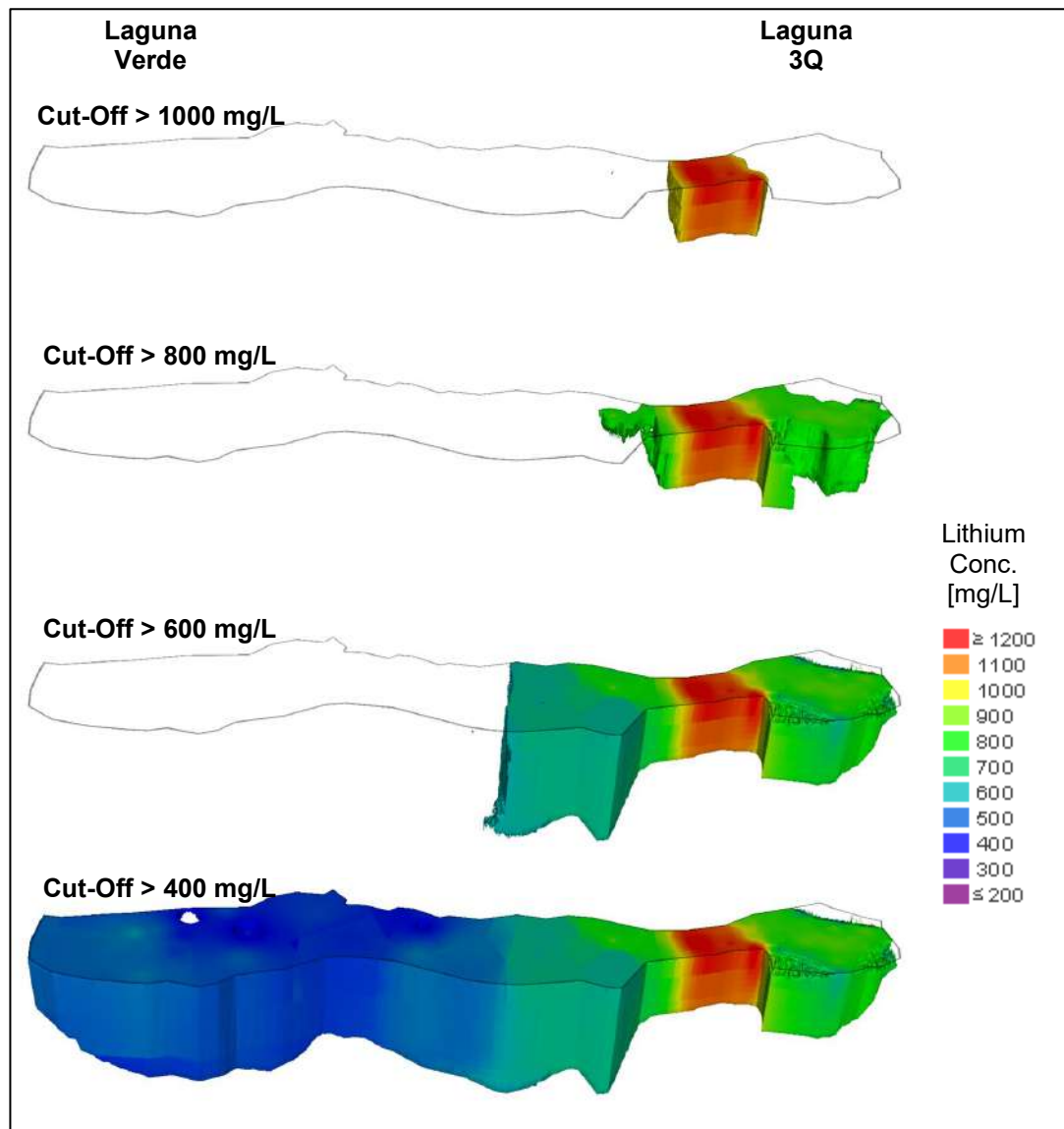


Figure 14-8: Lithium distribution within the Resource, at a range of cut-off grades.

14.4.4 Mineral Resource Model Check

As a check of the Resource calculations, the resource was re-interpolated in Leapfrog software, using the Radial Basis Function. To conduct this check, the geological model was first reconstructed in Leapfrog by exporting the unit surfaces from FEFLOW as point data and then re-interpolating the surfaces within Leapfrog.

Lithium concentrations were also re-interpolated in Leapfrog. A block model with dimensions of 50 m (length and width) x 5 m (depth) was used to sample the lithium concentrations and geological unit volumes, for calculating the mass within each unit. The masses within each unit except the Hyper-Porous Halite were within 1% of those calculated using the FEFLOW model. The mass calculated for the Hyper-Porous Halite was 1.6% lower in Leapfrog than FEFLOW. Total mass in the Leapfrog model was 0.35% less than the mass estimated with FEFLOW.

Overall, these results showed no indication of systematic bias in the Resource Estimate determined using FEFLOW.

14.5 Mineral Resource Estimate

The Mineral Resource Estimate is summarized in Table 14-4, for two cut-off grades: 400 and 800 mg/L. As shown on Figure 14-8, the Mineral Resource defined by the 400 mg/L cut-off extends for the full extent of the Mineral Resource Zone, from Laguna 3Q in the north to Laguna Verde in the south. Meanwhile, the Mineral Resource within the 800 mg/L cut-off is limited to approximately the northern third of the Mineral Resource Zone. The percent of the Resource within each of the primary geological units is shown in Table 14-2.

The presentation of Mineral Resources in this Report conforms with NI 43-101 and CIM Standards. As defined under these standards, Mineral Resources that are not Mineral Reserves do not have demonstrated economic viability. An estimate of Mineral Reserves component of these Resources is described in the next section (Section 15).

Table 14-4: Summary of the Mineral Resource Estimate at lithium grade cut-off values of 800 and 400 mg/L (Effective Date: October 26, 2021).

	Lithium Grade Cut-Off 800 mg/L				Lithium Grade Cut-Off 400 mg/L			
	Measured	Indicated	M&I	Inferred	Measured	Indicated	M&I	Inferred
	Volume [m³]				Volume [m³]			
	2.01E+08	1.55E+08	3.57E+08	3.34E+07	4.50E+08	1.13E+09	1.58E+09	7.57E+08
	Average Concentration [mg/L]				Average Concentration [mg/L]			
Lithium	923	922	923	918	792	576	637	561
Boron	1,352	1,343	1,348	1,308	1,140	787	887	744
Potassium	8,366	8,335	8,353	8,210	7,382	5,616	6,119	5,475
Magnesium	1,532	1,529	1,531	1,535	1,402	2,371	2,095	2,301
Calcium	40,560	40,679	40,611	40,772	35,162	31,026	32,202	30,020
Strontium	730	732	731	735	654	571	595	564
Sodium	78,980	78,405	78,730	77,670	82,702	86,413	85,358	88,494
Sulfate	462	442	453	372	377	308	327	290
	Tonnage¹				Tonnage¹			
Lithium	186,000	143,000	328,000	31,000	356,000	652,000	1,009,000	425,000
Lithium Carbonate	988,000	759,000	1,747,000	163,000	1,897,000	3,472,000	5,369,000	2,261,000
Boron	272,000	208,000	479,000	44,000	513,000	891,000	1,404,000	563,000
Boric Acid	1,555,000	1,187,000	2,741,000	250,000	2,934,000	5,098,000	8,032,000	3,218,000
Potassium	1,682,000	1,288,000	2,970,000	275,000	3,322,000	6,360,000	9,682,000	4,142,000
Potash	3,213,000	2,461,000	5,674,000	525,000	6,346,000	12,147,000	18,492,000	7,911,000
Magnesium	308,000	236,000	544,000	51,000	631,000	2,685,000	3,316,000	1,741,000
Calcium	8,155,500	6,287,000	14,443,000	1,364,000	15,824,000	35,131,000	50,956,000	22,713,000
Calcium Chloride	21,590,000	17,416,000	40,006,000	3,777,000	43,834,000	97,313,000	141,147,000	62,916,000
Sulfate	93,000	68,000	161,000	12,000	170,000	348,000	518,000	219,000
	Ratios				Ratios			
Mg/Li	1.66	1.66	1.66	1.67	1.77	4.12	2.27	4.10
K/Li	9.06	9.04	9.06	8.95	9.32	9.75	6.63	9.75
SO₄/Li	0.50	0.48	0.49	0.41	0.48	0.53	0.35	0.52
Ca/Li	43.94	44.10	44.03	44.42	44.39	53.86	34.91	53.48

Note: ¹ Tonnage values are rounded

15. Mineral Reserve Estimates

15.1 Overview

The Mineral Reserve Estimate for the 3Q Project (effective date October 26, 2021) was supported by a numerical groundwater flow and transport model constructed with the finite-element code FEFLOW (DHI-WASY, 2021). The modelling tools were developed and applied by Paul Martin, M.Sc. and Martinus Brouwers, M.A.Sc. with technical direction of the QP. The model incorporated geological, hydrological, hydrogeological, brine chemistry, and geophysical data from 3Q field programs.

Reserve estimation involved simulating extraction over the planned mine lifespan, to quantify the lithium tonnage produced over that period. This work included testing multiple scenarios of well location, screened interval, and extraction rates to promote effective lithium recovery and to minimize potential laguna drawdown.

The Project Mine Plan specified a processing plant influent flow rate of 260 L/s for the entire 50-year mine life, including an initial two-year pond-filling period. The plan further specified maintenance of a combined lithium grade of between 893 and 960 mg/L in the recovered brine, for as long as possible. These two specifications were designed to provide wellhead recovery and process production of 40,000 and 20,000 tonnes LCE per year, respectively, for as long as possible, assuming approximate processing losses of 50%. Model simulations indicate that the grade specification would be met for the first 20 years of operation, and that grade would decrease thereafter, as lower grade zones are captured.

Reserve Estimate results are summarized as follows:

- Total Reserves (Proven and Probable) are estimated at 1,670,000 tonnes of LCE, over a 50-year life of Project;
- Proven and Probable Reserves for lithium equate to 31% of the Measured and Indicated Resources (5,369,000 tonnes LCE @ 400 mg/L cut-off (Section 14); and
- The average lithium grade predicted for the entire production period is 786 mg/L; it ranges from > 900 mg/L in early years to 585 mg/L at year 50.

Construction, calibration, and application of the numerical modelling tools for reserve estimation are described in the following subsections.

15.2 3D Groundwater Flow Model Construction

15.2.1 Modelling Objectives

The following general objectives were identified for the 3Q Project Reserve Estimate modelling:

- To evaluate feasible brine recovery rates;
- To simulate changes in brine chemistry over time, as the resource is extracted;
- To evaluate potential effects of pumping on surface water body levels; and
- To quantify the recovery of lithium and other brine components.

Consequently, the modelling tools needed to have the capability of generating these types of output.

15.2.2 Conceptual Features

In addition, the modelling tools needed to represent certain hydrologic features considered to be of primary importance to the behavior of brine in the salar and freshwater in salar boundary zones. These features are illustrated in Figure 15-1, and summarized below:

- Precipitation occurs directly to surface of the salar and may evaporate or infiltrate to the shallow brine, through the salar crust.
- Precipitation also occurs in up-slope sub-watershed areas of the salar catchment. Precipitation falling in sub-watersheds may evaporate directly or it may be incorporated into surface and groundwater that flows to the salar boundary zones, primarily as freshwater.
- Under natural conditions, the only outlet of water from the basin is through evaporation. Evaporation is limited to areas where the water table is close to the surface. It is highest in the salt lakes and in salar boundary zones where freshwater occurs near the surface. In terms of rates, freshwater evaporates more rapidly than brine.
- Groundwater reaching the salar boundary from surrounding sub-watersheds tends to flow on top of the denser brine already present in the salar. Consequently, freshwater tends to remain shallow, and salar boundary zones tend to be focal for freshwater evaporation. Evaporation concentrates dissolved minerals within the salar and leads to ongoing additions to the brine resource deposit.
- Evaporation may also occur from the salar crust, when and where the brine level is sufficiently close to the surface. This process produces the rough crust deposits that are present throughout the salar.
- Seasonal brine level fluctuations in the salar are caused by seasonally varying inflows and evaporation. Shorter term fluctuations may occur due to precipitation directly to the salar.
- Under natural conditions, water and brine movement occurs primarily near the ground surface and at the salar margins. Brine movement may be relatively limited at depth in the salar, driven primarily by density gradients.

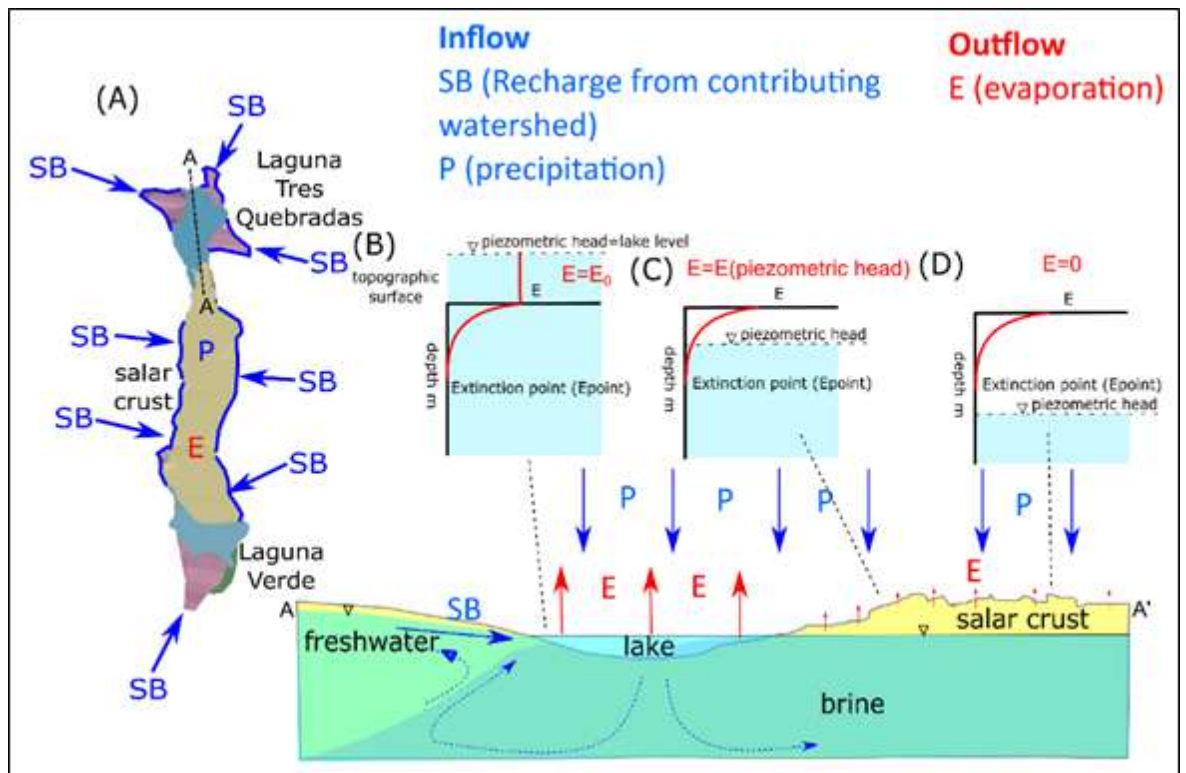


Figure 15-1: Conceptual inflow and outflow features of the 3Q Salar. Lateral inputs from sub-basins and vertical input from precipitation are shown in A (plan and section). B, C, and D show three different scenarios for evaporation outputs.

15.2.3 Modelling Code Selection

FEFLOW (DHI-WASY, 2021) was selected as the software platform for developing the three-dimensional (“3D”) brine Reserve Estimate model, because it has the technical capabilities to represent the primary salar concepts in Section 15.2.2 and to address the objectives in Section 15.2.1. FEFLOW also has a track record for Reserve Estimate applications at salar sites (e.g., Salar Cauchari in Argentina (King et al., 2012) and Salar de Atacama (King et al., 2019)).

The Resource and Reserve models were both generated with FEFLOW, to minimize the potential for approximation errors in transferring geology and brine models between different software packages. The two FEFLOW models are similar, except for mesh size. A finer mesh was used for the Resource model, to enable accurate mass estimates within the irregular surfaces of the geology model. For the Reserve model, a coarser mesh was used, to allow the dynamic model to run within a practical timeframe. Additional mesh details are provided in Section 15.2.4.

FEFLOW was also used to develop two two-dimensional (“2D”) models extending into and under Laguna 3Q from the adjacent alluvial fans. These models used the variable density simulation capabilities of FEFLOW to evaluate freshwater-brine interactions, and illustrated that a uniform density approach to Reserve simulation was reasonable. Simulation details are provided in Section 15.7.4.

15.2.4 Model Domain and Layer Structure

The numerical model domain was designed to encompass the entire geological model of the salar (Section 7). The model footprint includes the surface expression of the salar, and also the near-salar zones of the surrounding alluvial fans (Figure 15-2). In the vertical dimension, the model

extends from the ground surface to the base of salar in-fill geology. The bottom of the model is the basement underlying the salar, assumed to be impermeable (Section 7.1).

Lake bathymetry (Lagunas 3Q and Verde) was incorporated into the model based on previous surveys (Section 7.6.2). The six primary geological units identified at the site were represented with configurations obtained directly from the Resource Model (Section 14.2).

The layer structures of the Resource and Reserve models are shown on Figure 15-3. Relatively small (<1%) differences were noted in brine volume and lithium mass estimates between the Resource and Reserve models, due to the coarser layering and mesh of the latter. The coarser layout of the Reserve model was implemented to achieve practical run times. It is considered to have negligible impact on Reserve estimation results. The discretization details of the Reserve model are as follows:

- The model includes 20 layers, with 14,807 nodes per slice and 28,519 elements per layer.
- There are a total of 247,922 active nodes in the model and 443,251 active elements.
- A finer level of discretization was assigned in the northern zone of the model, where the highest lithium grades and the primary pumping wells are located; this zone also includes the Measured Resource.
- The average length of the triangular elements is 75 m within the northern zone of the model.
- Outside this zone, the average triangular element size is 92 m.
- The model layers were finer in Measured (0-150m) and Indicated (150-350m) resource zones, grading from a thickness of 1.5 m at ground surface to > 50 m below a depth of 350 m.
- Model layers were generally coarser for the Inferred resource zone (> 350m), with variable thickness between 1 m and greater than 100 m.

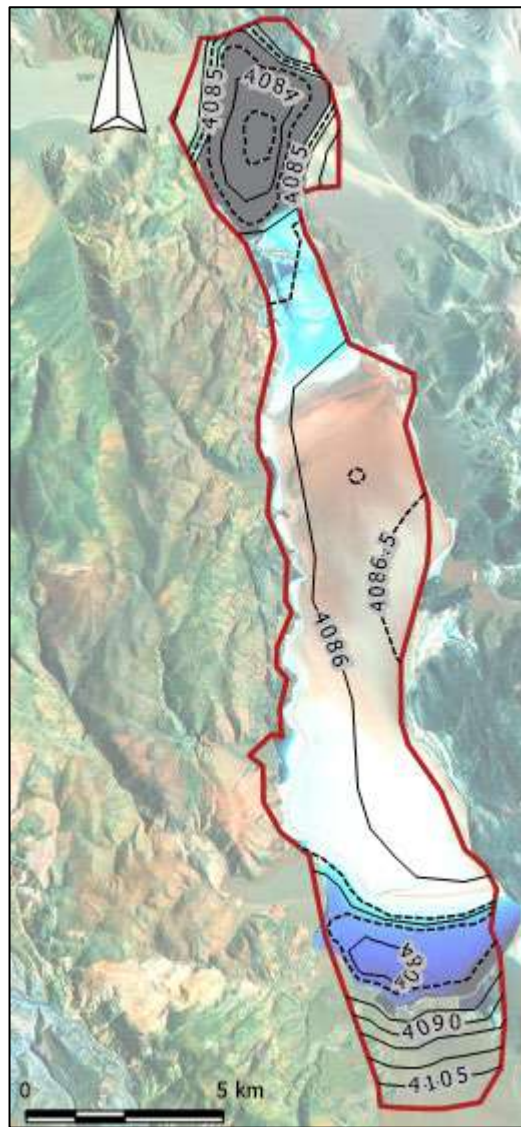


Figure 15-2: Footprint of the Reserve Model and topographic surface elevation.

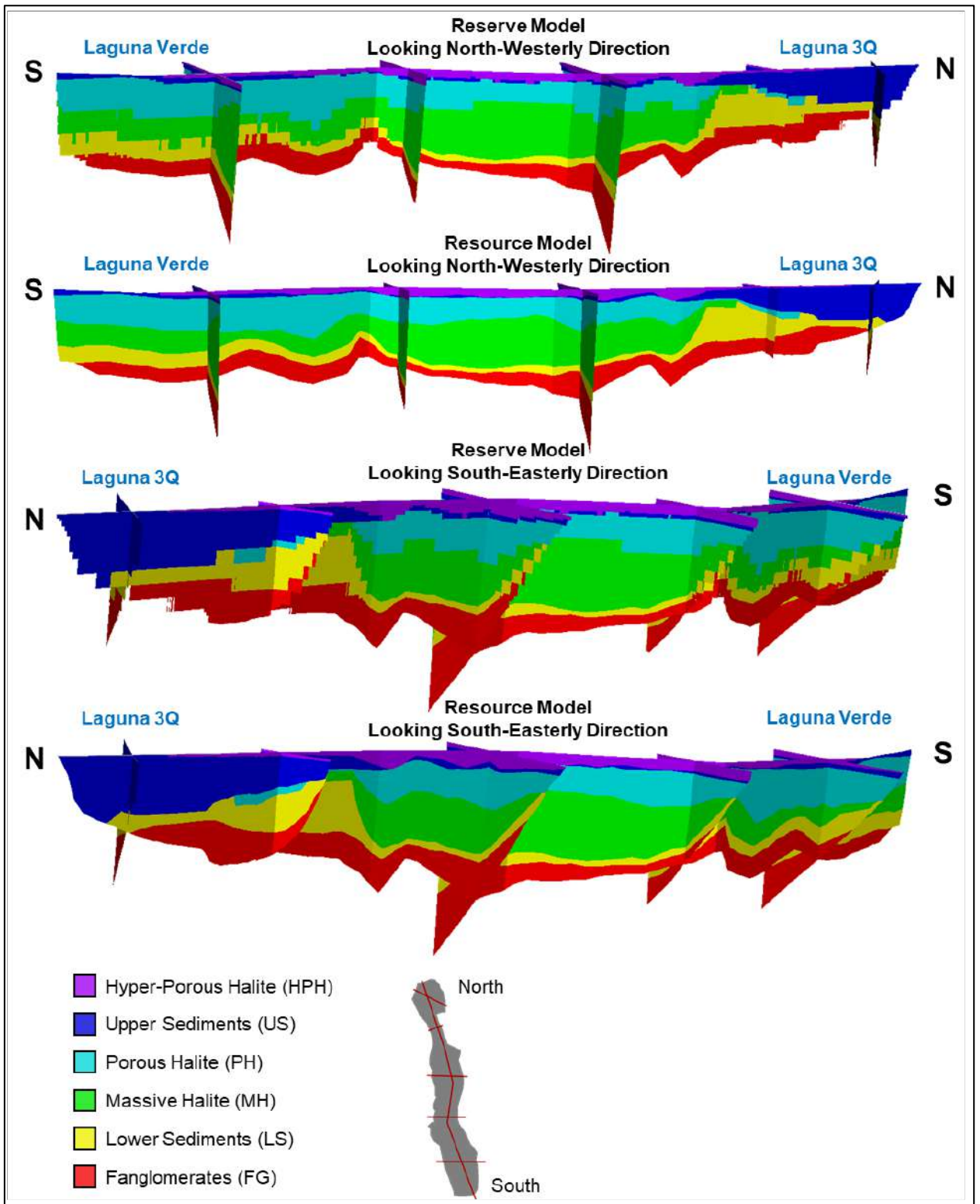


Figure 15-3: 3D fence diagrams showing layering of the Resource and Reserve Models.

15.2.5 Flow Conditions at Numerical Model Boundaries

15.2.5.1 Overview

The flow boundary conditions of the model provide a quantitative description for the movement of water and brine into and out of the model domain. They were designed to represent the conceptual features described in Section 15.2 and illustrated in Figure 15-1. Ongoing measurements at the 3Q Project indicate that annual trends in hydrological and meteorological parameters are relatively consistent from year to year. On that basis, 2017 was identified as representing a typical year, and data from that year was used to represent average future conditions. Uniform density was found to be valid for the 3D model based on the 2D density-dependent modelling completed (Section 15.8), allowing 3D boundary conditions to be applied as brine boundaries.

15.2.5.2 Recharge to the Upper Model Boundary (Precipitation)

Direct precipitation inputs to the model were simulated as a daily variable inflow rate to the top boundary, based on data from the 3Q Project Vaisala weather station. Precipitation data for 2017 through 2020 is summarized in Table 15-1. Average annual precipitation over this four-year period is 80 mm/year. Monthly precipitation is plotted on Figure 15-4. Most of the annual precipitation typically occurs in January and February, and seasonal trends were reasonably consistent from year to year.

Table 15-1: Precipitation statistics for 2017 to 2021.

Statistic	2017	2018	2019	2020	2017-2020 (Average)
Annual Total [mm]	85.4	83.0	97.4	53.4	80
Min Monthly Total [mm]	0.0	0.0	0.0	0.0	0.0
Max Monthly Total [mm]	27.8	67.4	58.6	44.2	67
Average Annual Rate [mm/d]	0.23	0.23	0.27	0.15	0.22

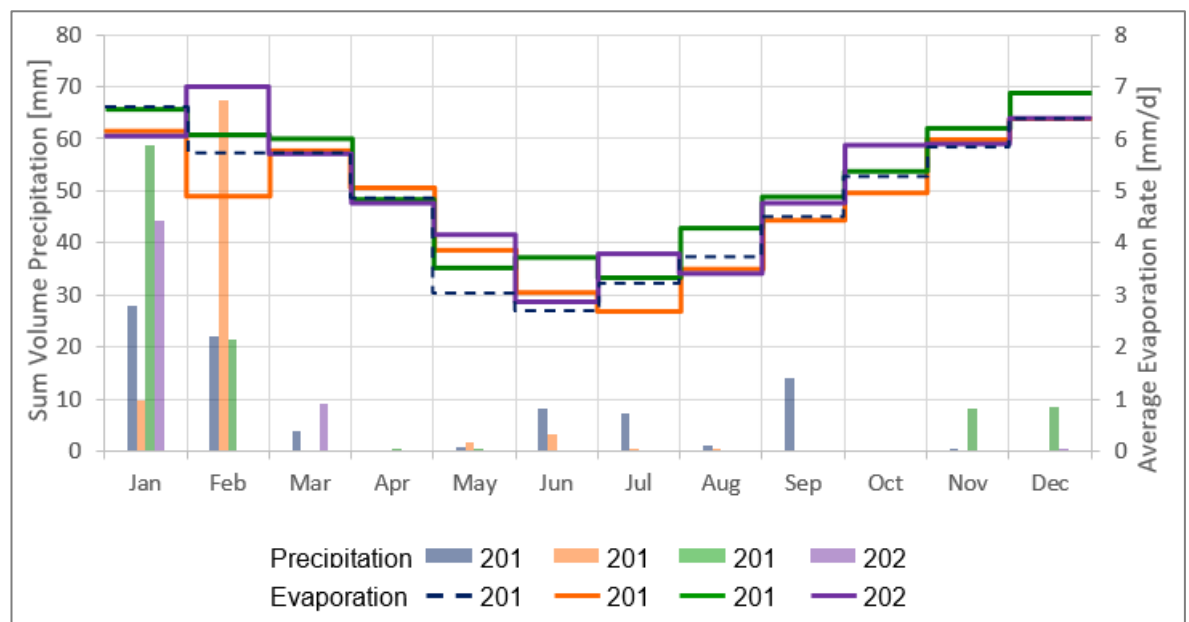


Figure 15-4: Monthly average precipitation and calculated evaporation, from the 3Q Vaisala weather station.

15.2.5.3 Discharge from the Upper Model Boundary (Evaporation)

Evaporation (“E”) was simulated as a seasonally variable rate of outflow from the top of the model domain. The evaporation rate was depth-dependent, according to the equation:

$$E = E_0 \cdot \text{Evaporation Factor} \cdot f_{ev}$$

where E_0 is the free water evaporation rate, *Evaporation Factor* is a correction factor and f_{ev} is the water level Depth-Dependency Factor. These terms are described below.

Free Water Evaporation Rate (E_0)

The E_0 values used in the model were calculated with data from the 3Q Vaisala weather station (relative humidity, air temperature, and wind speed). Results from four years of monitoring (2017-2020) are summarized in Table 15-2. The average E_0 over the four-year period was 4.9 mm/d, and rates were relatively consistent from year to year. A representation of the data as average monthly rates is plotted on Figure 15-4 and, again, a relatively consistent annual trend is indicated.

The E_0 values used in the model were based on 2017, selected as typical of the four-year monitoring period. In the model, values for E_0 were simulated to vary monthly, in a pattern that repeats on an annual basis.

Table 15-2: Summary of free water evaporation rates (E_0), calculated with data from the 3Q Vaisala weather station (2017 to 2020).

Statistic	2017 [mm/d]	2018 [mm/d]	2019 [mm/d]	2020 [mm/d]	2017-2020 [mm/d]
Average Annual Rate [mmd/]	4.8	4.8	5.1	5.1	4.9
Min Monthly Rate [mm/d]	2.7	2.7	3.3	2.9	2.7
Max Monthly Rate [mm/d]	6.6	6.4	6.9	7.0	7.0

Evaporation Factor

Freshwater is known to evaporate more rapidly than brine (e.g., Marazuela et al., 2019). Consequently, zones with elevated Evaporation Factors were defined in the model around freshwater inflows, and lower Factors were defined for the salar crust at large and for the lagunas. The configurations and values for these zones were adjusted through the model calibration process. Calibrated values and spatial distribution of Evaporation Factors are presented in Table 15-3 and Figure 15-5, respectively.

Table 15-3: Calibrated evaporation factors by zone.

Zone	2017 Annual Average E_0 [mm/d]	Calibrated Evaporation Factor	Calibrated Value [mm/d]
Laguna 3Q	4.8	1.15	5.52
Laguna Verde	4.8	1.20	5.76
Sub-basin Inflow	4.8	1.50	7.20
Salar, Zone 1	4.8	0.10	0.48
Salar, Zone 2	4.8	0.25	1.20
Salar, Zone 3	4.8	0.40	1.92
Salar, Zone 4	4.8	1.00	4.80

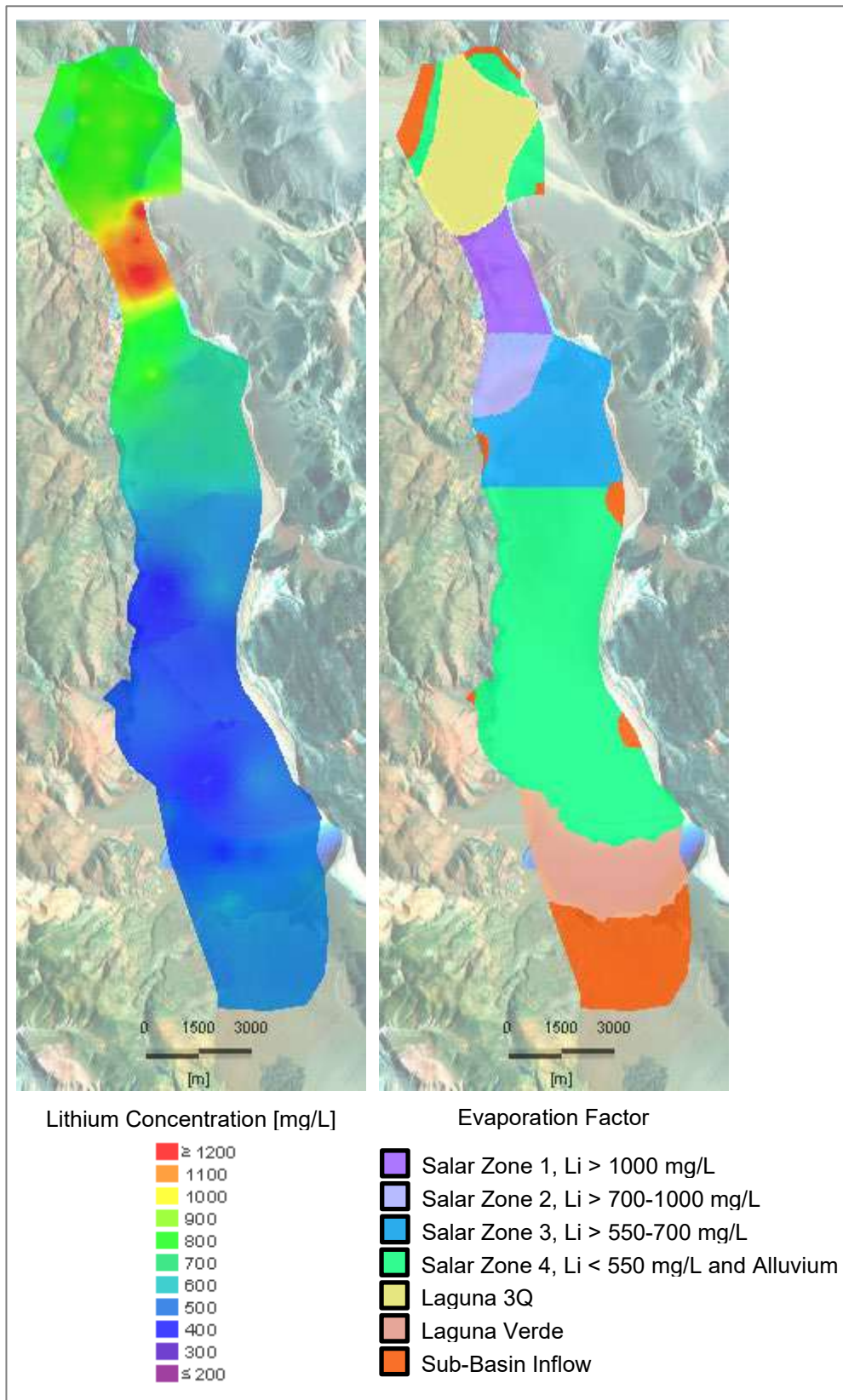


Figure 15-5: Spatial distribution of evaporation factors for salar crust and lakes.

Depth-Dependent Factor (f_{ev})

Evaporation from salar surfaces is known to vary inversely with the depth of the brine/water table below the salar surface (e.g., Johnson et al., 2010). For the salar crust, f_{ev} was used to

dynamically adjust the evaporation rate at each computational node, depending on the underlying water table position (Figure 15-6). When the water table was at or above the ground surface, $f_{ev}=1.0$ and evaporation occurred at E_0 . When it was below ground surface, an exponential relationship was applied to simulate the depth-dependent reduction in evaporation. Extinction depth occurred at the bottom of this range. It was defined as the depth at which evaporation no longer occurs (i.e., $f_{ev}=0$). The calibrated extinction depth was 1.2 m.

The Depth-Dependent Factor (f_{ev}) was used in a different manner for the lakes. Among other factors, total lake evaporation is influenced by lake surface area, which changes with lake level. Meanwhile, the lakes were simulated with constant surface areas. Consequently, a function was introduced to approximate the change in total lake evaporation in response to lake level changes. When the lagunas were at base level, $f_{ev}=1.0$ and evaporation occurred at the calibrated value (Table 15.3). As lake level decreased, the laguna surface area decreased, and f_{ev} was adjusted downward accordingly. The calculated f_{ev} relationships for the lakes (based on surveyed lake bathymetry) and the generalized relationships used in the model are shown on Figure 15-6.

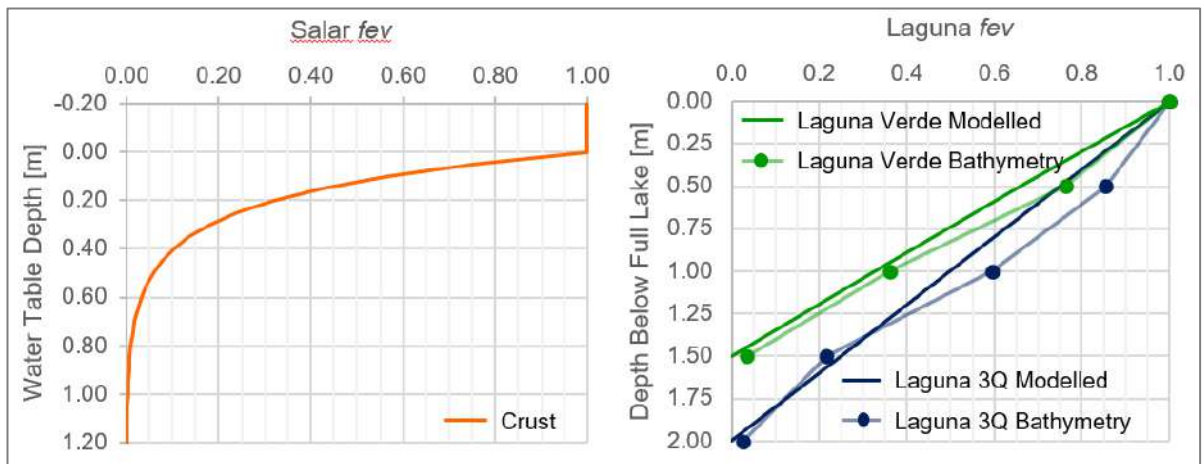


Figure 15-6: Depth-Dependent Factor (f_{ev}), for salar crust and lakes.

15.2.5.4 Inputs from Surrounding Upland Areas (Sub-Basins)

Flow inputs from the sub-basins surrounding the salar were simulated as specified, average inflows. Sub-basin areas and the locations where their flows were input to the model are shown on Figure 15-7. Inflows were applied to model layers 1 and 2, which have depths of 1.5 and 3.0 m bgs, respectively. Sub-basins with smaller inflow rates (i.e., < 250 L/s) were represented with a single point boundary condition. Those with larger rates were represented along a line of boundary points. All other lateral boundaries (for all layers) were simulated as having no flow.

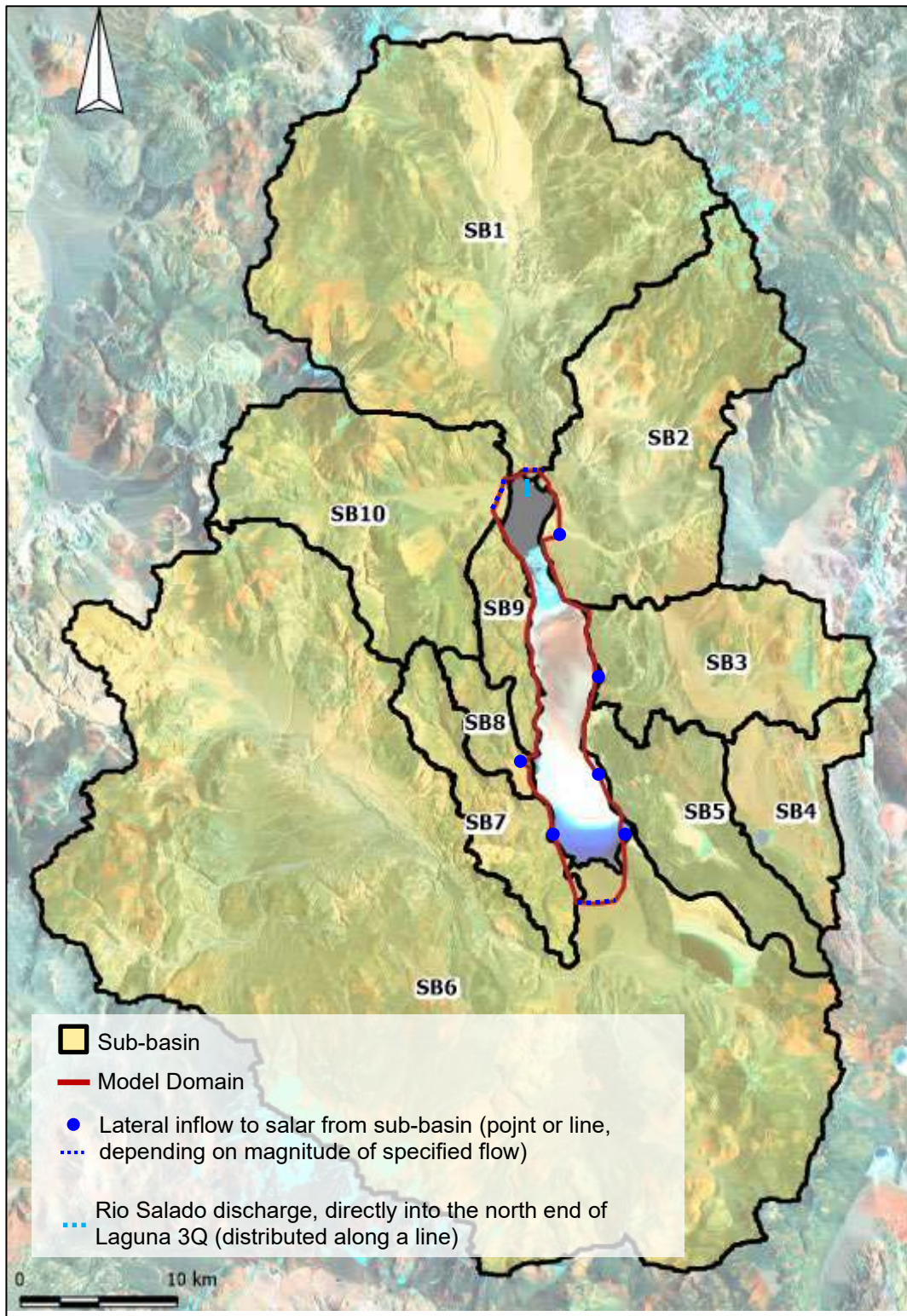


Figure 15-7: Locations of specified lateral inflow into the 3Q Salar and lagunas from surrounding sub-basins.

The average annual outflow from each sub-basin was initially estimated with HEC-HMS (Feldman, 2000), based on 2017 climate data. Precipitation inputs to HEC-HMS were obtained from the 3Q Project Vaisala weather station for the smaller sub-basins and from CHIRPS (2018) for the larger ones. The latter set of sub-basins included areas that were more distal from the salar and at significantly greater elevations. Sub-basin outflow estimates were further adjusted during the calibration process. Initial and calibrated results are summarized in Table 15-4.

Table 15-4: Sub-basin outflows estimated with HEC-HMS, and final calibrated outflows used in the numerical model.

Sub-Basin ID	Area [km ²]	Annual Precipitation [mm/y]	Total Precipitation [L/s]	Estimated Outflow using HEC-HMS [L/s]	Outflow [as % of Total Precipitation]	Sub-Basin Flow Applied to Calibrated Model [L/s]
1 [†]	540	189 ⁽¹⁾	3,234	657	20	644
2	237	190 ⁽¹⁾	1,429	31	2.2	31
3	139	70 ⁽²⁾	308	31	10	28
5	100	70 ⁽²⁾	221	22	10	15
6	1,294	189 ⁽¹⁾	7,525	482	6	332
7	76	134 ⁽¹⁾	325	104	32	104
8	25	70 ⁽²⁾	55	5.5	10	5.5
9	39	70 ⁽²⁾	86	8.6	10	0
10	202	134 ⁽¹⁾	860	384	45	240
TOTAL	2,652		14,042	1,725	12	1,400

[†] HEC-HMS estimated outflow and sub-basin flow applied to calibrated model include average annual flow from Rio Salado.

⁽¹⁾ Precipitation source: Funk et al. (2015).

⁽²⁾ Precipitation source: 3Q Vaisala weather station data for 2017.

Rio Salado flow discharges directly into Laguna 3Q. This river was represented with a line of specified inflow boundary conditions applied to the top of layer 1 within Laguna 3Q (Figure 15-7). Simulated inflow was specified to vary monthly according to measured surface flows from 2017, as shown on Figure 15-8.

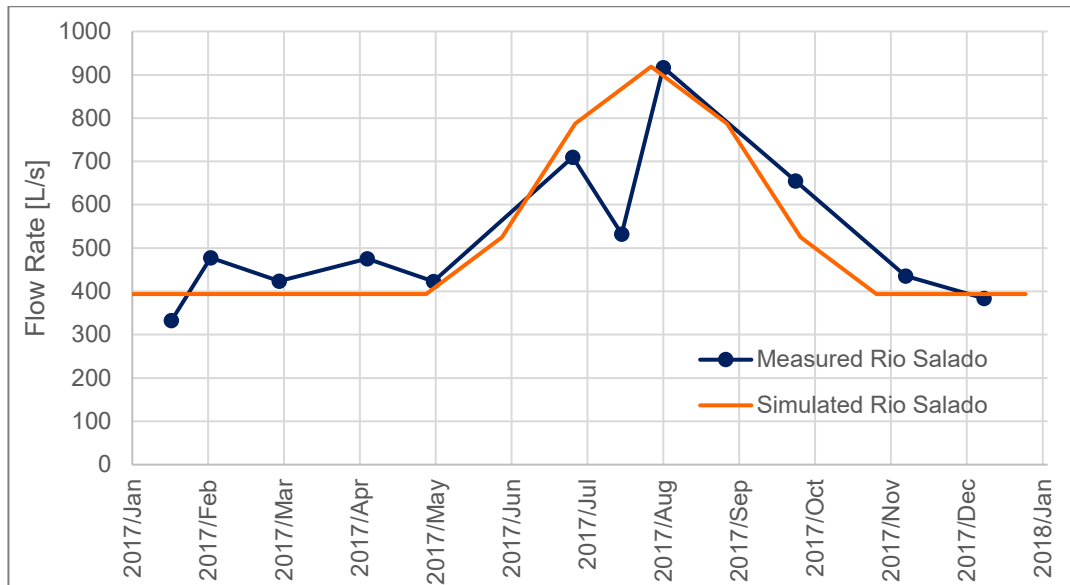


Figure 15-8: Measured and simulated inflow from the Rio Salado, based on 2017 monitoring data.

15.2.6 Model Hydrogeological Properties

Hydrogeological property values used in the model are summarized in Table 15-5 and described below.

Horizontal and Vertical Hydraulic Conductivity (“Kh” and “Kv”, respectively) zones were initially inferred from the results of pumping test analyses (Section 9.6), and some values were further adjusted through the calibration process (Figure 15-9):

- The Hyper-Porous Halite (HPH) is the most permeable unit, with the highest values in the southern crust in the vicinity of Platforms 7 and 3 (Figure 9-4). In the highest-grade area (near Platforms 15 and 18), the HPH was assigned a more moderate hydraulic conductivity.
- The Upper Sediments, Porous Halite, Lower Sediments, and Fanglomerate units were simulated with moderate to low permeability.
- The Massive Halite unit was simulated with a very low hydraulic conductivity value.
- Anisotropy (ratio of Kh to Kv) was typically set at 10, representing the layered nature of the units. Higher anisotropy was assigned to the HPH below 1.5m depth, to represent the more pronounced effect of layering in this highly permeable unit. Vertical hydraulic conductivity was limited to 0.001 m/d.
- The open water of Lagunas 3Q and Verde was represented with a very high hydraulic conductivity (10^6 m/d).

For **Specific Storage Coefficient** (“Ss”), a constant value of 1×10^{-4} 1/m was assigned to all layers. This value was consistent with pumping test results and is within the range of literature values for similar deposits (Freeze and Cherry, 1979).

Specific Yield (“Sy”) values were assigned based on pumping tests (for the near-surface aquifer) and RBRC testing for all units (Section 10.2). An Sy of 1 (i.e., 100% drainable porosity) was applied to Lagunas 3Q and Verde, to represent open water.

Table 15-5: Hydrogeological material properties applied in the Groundwater Flow Model.

Geological Units	Horizontal Hydraulic Conductivity [m/d]	Vertical Hydraulic Conductivity [m/d]		Specific Storage coefficient [1/m]	Specific Yield [%]
		Layer 1	Layer 2-20		
Hyper-Porous Halite (HPH, Zone 1)	290	29	2.9	1x10 ⁻⁴	14.74
Hyper-Porous Halite (HPH, Zone 2)	227	22.7	2.27	1x10 ⁻⁴	14.74
Hyper-Porous Halite (HPH, Zone 3)	975	97.5	9.75	1x10 ⁻⁴	14.74
Hyper-Porous Halite (HPH, Zone 4)	1,000	100	10	1x10 ⁻⁴	14.74
Alluvium Laguna Tres Quebradas	1,000	100	-	1x10 ⁻⁴	9.13
Upper Sediments (US)	20	-	0.2	1x10 ⁻⁴	9.13
Porous Halite (PH, Zone 1)	0.05	-	0.001	1x10 ⁻⁴	6.33
Porous Halite (PH, Zone 2)	4	-	0.04	1x10 ⁻⁴	6.33
Massive Halite (MH)	0.01	-	0.001	1x10 ⁻⁴	3.85
Lower Sediments (LS)	20	-	0.2	1x10 ⁻⁴	5.18
Fanglomerate (FG)	20	-	0.2	1x10 ⁻⁴	11.23
Lakes					
Laguna Tres Quebradas	1,000,000	1,000,000	-	1	100
Laguna Verde	1,000,000	1,000,000	-	1	100

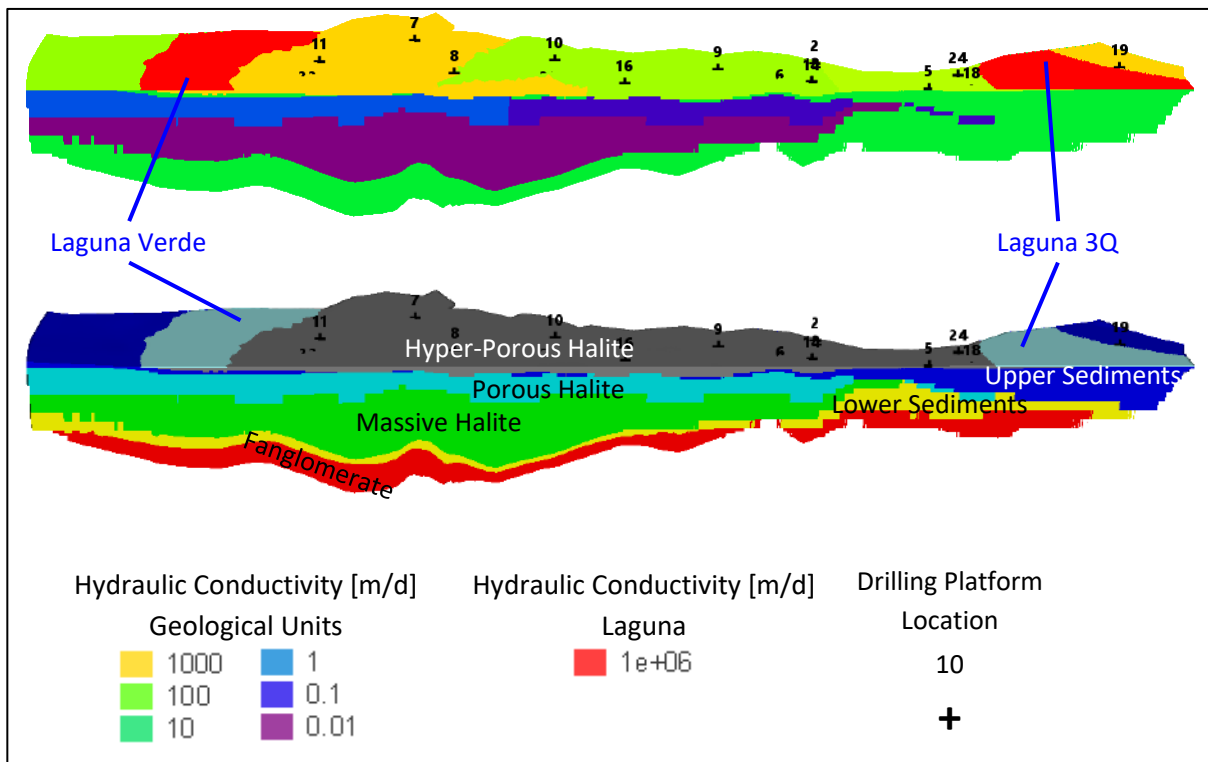


Figure 15-9: 3D view of horizontal hydraulic conductivity (top) and geological units (bottom).

15.3 3D Model Calibration

The 3D numerical flow model was calibrated to observed data, using a two-stage process:

1. **Simulation of long-term average conditions** - The model was run for a period sufficient to stabilize brine levels throughout. Boundary conditions used for this stage included average annual inflow rates from sub-basins and average annual outflow due to evaporation. The model was first run for 100 years with a coarse maximum time step size of 15 days, then run for another 10 years with a finer maximum time step of 5 days. Piezometric levels from the end of this step were used as the initial condition for the next step.
2. **Calibration to 2017 – 2021 brine levels** - This calibration period coincided with available brine level data from salar wells and the lakes. The applied boundary conditions were those described in Section 15.2.5, including: daily precipitation (Section 15.2.5.2), average monthly free water evaporation (Section 15.2.5.3), steady inflow from sub-basins (Section 15.2.5.4), and average monthly Rio Salado inflow (Section 15.2.5.4). The time step was variable through the calibration period, with a maximum of 5 days.

For the calibration process, the following parameters were adjusted: hydraulic conductivity, lateral sub-basin inflow, spatial distribution of the free water evaporation rate (E_0), Evaporation Factor, and evaporation extinction depth beneath the salar crust. These parameters were adjusted to provide a balance between quantitatively fitting to measured brine levels and qualitatively matching the site-wide hydraulic gradients and water budget. Final calibrated values are presented in Section 15.2.

Brine level data used in the calibration is summarized in Table 15-6. The calibration data consisted of measured brine levels from nine observation wells and lake levels from Lagunas 3Q and Verde. Four available observation wells were excluded from the calibration process, due to indications that the measured levels were compromised by salt precipitation. Similarly, later stage data from five wells was excluded from the calibration, due to indication of well plugging.

Table 15-6: Calibration statistics for simulated water level residuals.

Location	Calibration Water Level Period	Residual Statistics ¹			
		Count ²	Mean [m]	Absolute Mean [m]	Root Mean Squared [m]
Residual Statistics by Observation					
PP1-D-2	Partial: Oct.30, 2017 – Jan.25, 2019	452	-0.02	0.07	0.09
PP1-D-3	Full: Oct.30, 2017 – Apr.27, 2021	1274	0.07	0.14	0.17
PP1-D-4	Partial: Oct.30, 2017 – Mar.17, 2018	138	-0.02	0.07	0.09
PP1-D-6	Full: Oct.30, 2017 – Apr.27, 2021	377	0.05	0.14	0.17
PP1-D-8	Full: Oct.30, 2017 – Apr.27, 2021	1274	0.01	0.08	0.09
PP1-D-9	Full: Oct.30, 2017 – Apr.27, 2021	863	-0.17	0.17	0.18
PP1-D-10	Partial: Oct.30, 2017 – Jan.25, 2019	452	0.05	0.06	0.07
PP1-D-11	Partial: Oct.30, 2017 – Jan.25, 2019	268	0.06	0.09	0.10
PP3-R-7	Partial: Oct.30, 2017 – Jan.25, 2019	319	-0.03	0.06	0.07
Laguna 3Q	Full: Oct.30, 2017 – Apr.27, 2021	395	-0.02	0.05	0.06
Laguna Verde	Full: Oct.30, 2017 – Apr.27, 2021	404	0.02	0.04	0.04
Aggregate Residual Statistics for All Observations					
All	Full or Partial	11	0.00	0.09	0.10

¹ Residual calculated as the difference between the observed and simulated values.

² Number of water levels included in calibration period.

The fit of simulated to observed water levels was evaluated with residual statistics, summarized in Table 15-6, defined as the difference between the two. Residual statistics for individual observations were typically 0.1 m or less, indicating good overall agreement. The combined mean residual for the 11 observations points was 0.00 m indicating a balance between simulated and observed conditions, with no systematic bias. Residuals are shown graphically in Figure 15-10.

The calibrated model produced numerically converged simulations with a negligible mass balance residual (i.e., difference between total inflows and outflows was 0.002%).

For both Lagunas, the calibration objective was to obtain a balanced fit between observed water level trends and 2017 evaporation estimates from satellite remote sensing data (IHLLA, 2019). The simulated water levels for Laguna 3Q were an excellent match to observed data and the simulated evaporation rate was 698 L/s compared to an estimate of 677 L/s. At Laguna Verde, simulated water level trends were a good match to observed conditions and the simulated evaporation rate was 444 L/s compared to an estimate of 388 L/s.

The calibration results compare well with large scale hydraulic gradient trends in the salar. The calibrated model indicates a groundwater divide in the central/east area of the salar, mid-way between Lagunas 3Q and Verde, which is consistent with site measurements (Section 7.7). The modelling also re-produced the generally low observed hydraulic gradients in the salar. These low gradients are primarily due to the highly permeable Hyper-Porous Halite, which readily allows flow inputs to disperse.

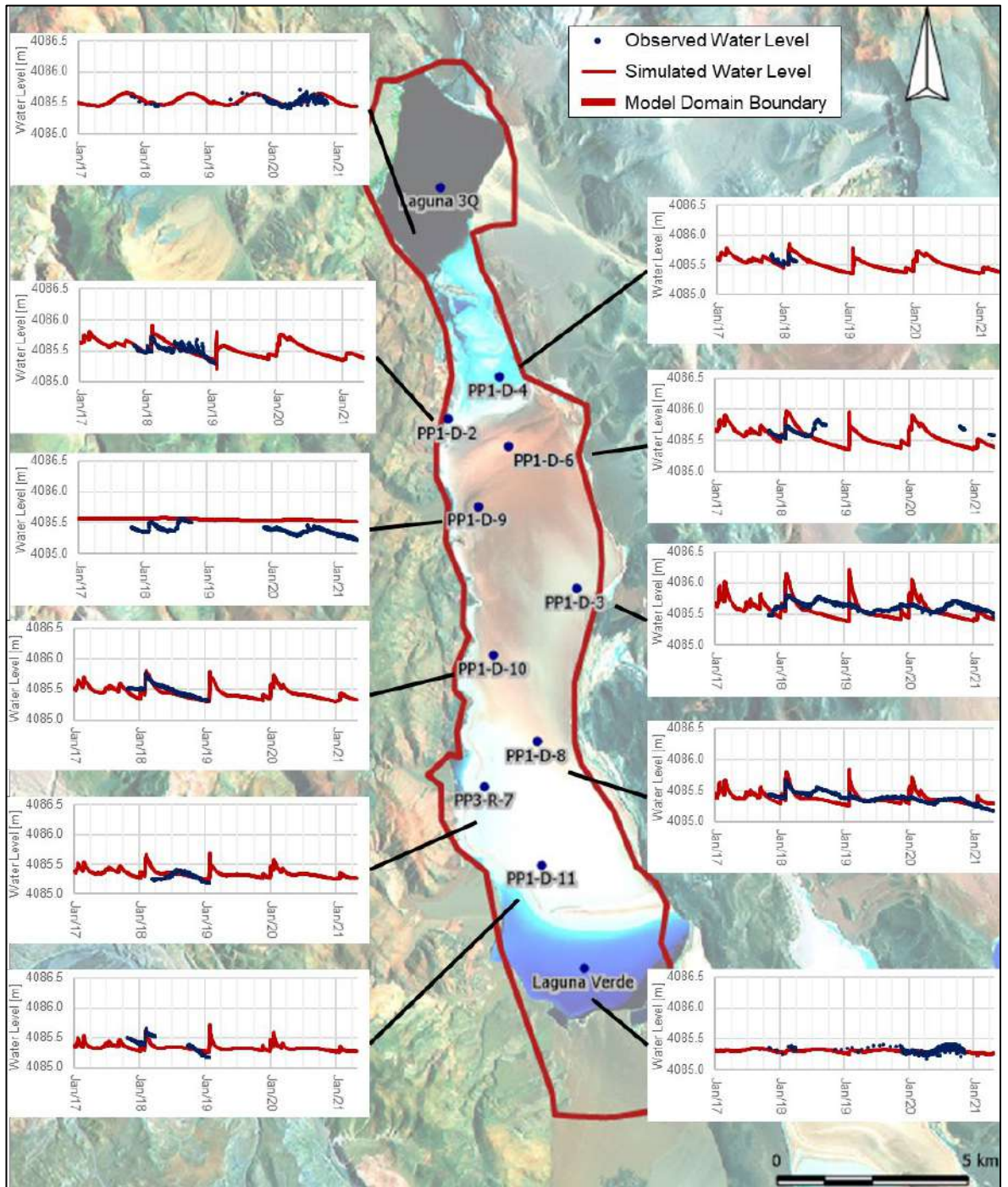


Figure 15-10: Comparison of simulated and measured water levels.

15.4 3D Model Configuration for Evaluating Laguna Drawdown and Water Balance Changes

A limited re-configuration was implemented on the calibrated model, to enable evaluation of the potential laguna drawdown due to long-term production, as well as changes to the salar water balance under pumping conditions. The effects of primary interest from pumping are related to changes in the lake levels due to pumping. Consequently, these model runs were based solely on flow evaluation, and not the movement and recovery of lithium and other solutes. Results are provided in Section 15.7.

The re-configuration of the calibrated model included:

- Pumping well locations and a rate schedule for the 50-year lifespan of the Reserve Estimate was specified.
- Precipitation was represented using average monthly 2017 precipitation rates.
- Evaporation pond infrastructure was represented as intercepting precipitation and evaporation, thus preventing both these processes from occurring relative to the underlying salar. Consequently, precipitation and evaporation were omitted from the planned pond infrastructure footprint.

The production pumping scenario used for this purpose was identical to the one used for the Reserve Estimate. It was developed through an iterative process and was based on engineering constraints provided by NLC. A description of the constraints and the final pumping scenario is provided in Section 15.6.

15.5 3D Model Configuration for Evaluating Reserves

15.5.1 Overview

The calibrated flow model was configured to simulate the behaviour of dissolved solutes including lithium and other brine components (K, B, Mg, Ca, Sr, Na, and SO₄). Part of this configuration involved simplifying flow boundaries to ensure that the Reserve simulation was conservative (i.e., recovered mass was limited to the Resource as defined in Section 14). The changes and additions were related to the following:

- Boundary conditions for flow;
- Solute boundary conditions;
- Solute and geological unit properties related to transport;
- Initial solute distributions throughout the model; and
- Simulation controls (equation, tolerance, and time steps).

These are further described below.

15.5.2 Flow Boundary Changes

The following changes were made to flow boundary conditions:

- The approach for simulating discharge and recharge relative to the salar crust was updated so that only the net exchange was simulated. This approach avoided accumulation or addition of solute at the top model boundary.
- Laguna levels were assigned as specified head boundaries. This simplification allows the net exchange with the underlying brine to be determined by the model while providing additional model stability and efficiency for mass transport simulation.

15.5.3 Solute Boundary Conditions

Solute boundary conditions applied to the model for Reserve estimate simulations included the following:

- A solute boundary condition was added to Laguna 3Q to simulate inflow concentrations consistent with those observed in Rio Salado (i.e., at 35 mg/L lithium).
- All freshwater inflows from sub-basins were assigned a mass concentration of 15 mg/L lithium. This concentration was based on samples from Rio Vega del Pissis.
- Pumping wells were assigned to recover Resource mass. Well boundary conditions consist of a specified volumetric rate, and a screen length over which volume and mass are removed.

15.5.4 Transport Properties for Solutes and Geological Units

Transport properties were assigned as follows:

- **Porosity:** set to be consistent with Sy characterization (Table 15-5);
- **Longitudinal Dispersivity:** 30 m for all units, 1,000 m for Lagunas 3Q and Verde;
- **Transverse Dispersivity:** 10 m for all units, 1,000 m for Lagunas 3Q and Verde; and
- **Diffusion:** global value of 1×10^{-9} m²/s.

The latter three parameter values are consistent with literature values (Schwartz and Zhang, 2003) and the first is an approximation based on site-specific sampling.

15.5.5 Initial Brine Distribution

The initial concentration distributions of lithium and the other solutes (K, B, Mg, Ca, Sr, Na, and SO₄) were based on the brine chemistry interpolations in the Resource Model, as described in Section 14. Three dimensional and plan views of lithium grades in Reserve model are shown in Figure 15-11.

15.5.6 Mass Transport Simulation Controls

Reserve estimation was simulated with the convective form of the advection-dispersion equation rather than the divergence form, as the latter can result in mass accumulation errors at outflow boundaries (Diersch, 2014).

Time steps were assigned to promote model stability and reasonable run times. The initial time step was 0.001 days with a growth factor between time steps of 1.5. Time stepping was allowed to vary adaptively, and the maximum time step was approximately 260 days. Total simulation time was 50 years, consistent with the Project life span.

An error tolerance of 1e-4 was specified (more stringent than the default of 1e-3) to promote an accurate mass balance during the simulation. The standard Galerkin-FEM approach was applied, to avoid smearing of concentration gradients.

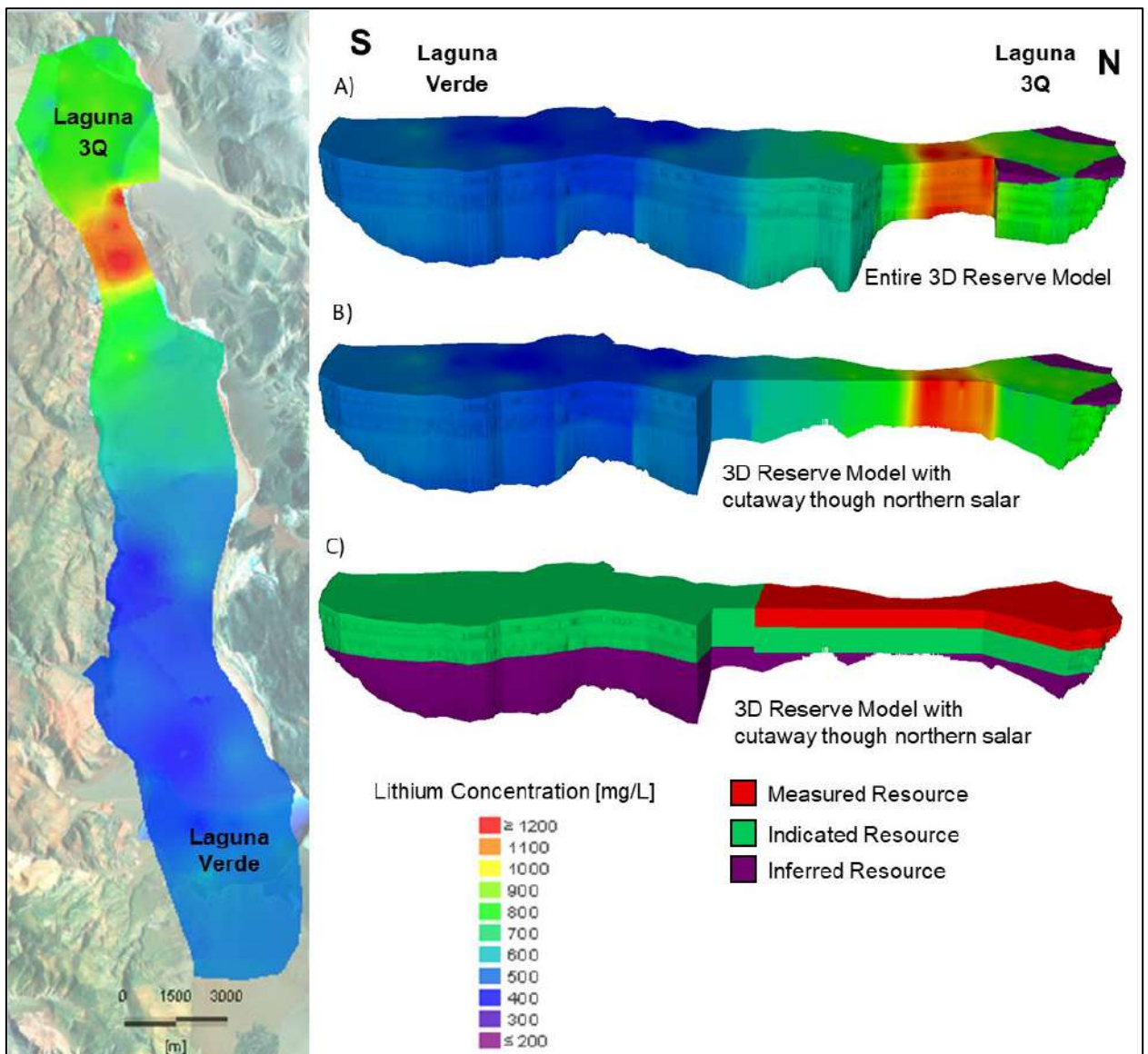


Figure 15-11: Initial lithium grade distribution in plan view (A) and three-dimensional full and cut-away views (B). Resource zones (C).

15.6 Constraints for the Reserve Estimation Pumping Scenario

15.6.1 Overview

Through discussions with NLC, a series of brine production constraints were identified, related to target grades, flows, and duration. The model was run iteratively to define a pumping scenario (i.e., well numbers, well configurations, and pumping rates) that could effectively meet these constraints for the defined duration, or for as long as possible. The constraints and the final pumping scenario are described below.

15.6.2 Wellfield Constraints and Final Configuration

A primary constraint for the production wells was that drawdown should remain above the screened section of the wells. If excessive drawdown was predicted, then additional wells would be added to the simulation at appropriate spacing. In terms of general well locations, the grade constraints described in Section 15.6.3 required that the wellfield is located in the higher-grade northern area of the Resource Zone. This northern area also addressed the constraint for

Reserves categorization which specified that recovery should focus on Measured and Indicated Resources.

Production wellfield scenarios were adjusted iteratively in the model to identify configurations that could effectively meet all constraints. The final selected scenario included a total of 15 production wells, as shown in Figure 15-12. Additional wellfield details are provided in Section 16. The wells were grouped into the following three series:

- **A-series wells** – Selected to meet grade constraints. This series consisted of 9 wells (3 existing and 6 new) that targeted the highest-grade lithium Resource (>1,000 mg/L).
- **B-series wells** – Selected to meet early pond-filling requirements, and to blend with A-series wells to meet the lithium grade target of 940 mg/L. This series consisted of four wells, all existing, within the mid-grade lithium Resource (>650 mg/L) in the northern salar.
- **C-series wells** – Selected to enhance LCE recovery after the 20 years of production. This series consisted of 2 wells, 1 existing and 1 new, located east of Laguna 3Q. They target the highest-grade lithium Resource simulated to be available after 20 years of production (~ 800 mg/L).

Simulated production wells are screened within the Measured and Indicated Resource zones. Production well depth and screen placement were designed to minimize mixing between brine layers and the capture of any shallow freshwater that may be introduced to the system (i.e., through direct precipitation or lateral recharge). With the specified screen placement depth, there is minimal brine recovery from the Inferred Resource zone, which intersects the three deepest geological units (Massive Halite, Lower Sediments, and Fanglomerate).

The QP considers that the simulated wellfield is appropriate for Reserve estimation.

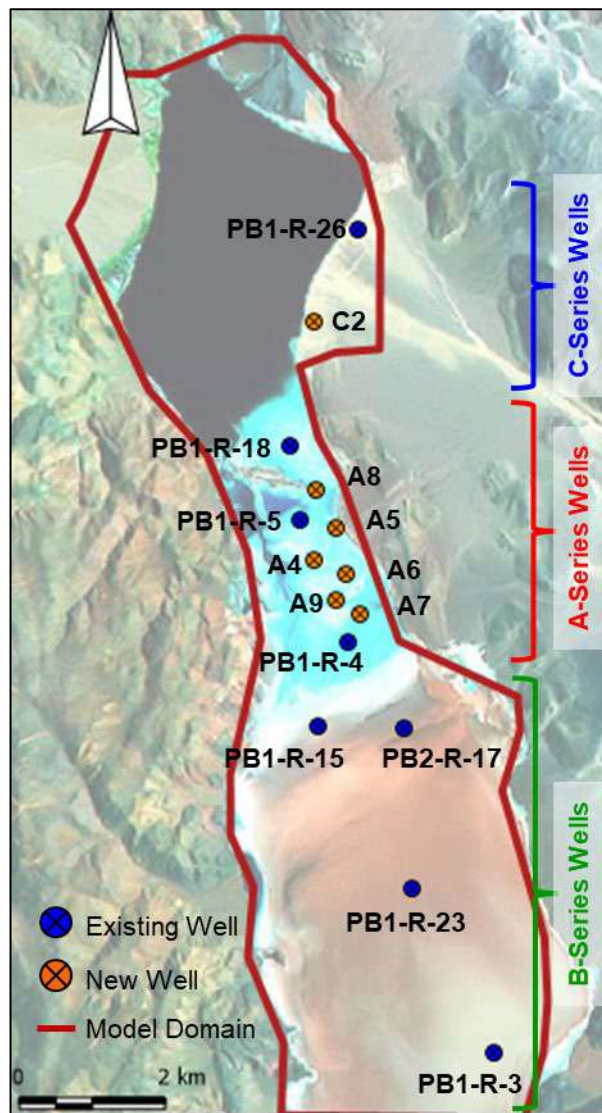


Figure 15-12: Locations of the existing and future production wells.

15.6.3 Grade, Flow and Timing Constraints for Wellhead Recovery

The following constraints were specified as targets for brine recovery:

- The target duration of production is 50 years.
- Production will commence with an initial pond-filling period consisting of:
 - nine months of pumping at 196 L/s at a target blended lithium grade of 647 mg/L;
 - followed by eight months of pumping at 305 L/s at a target blended lithium grade of 647 mg/L;
 - followed by four months of pumping at 305 L/s at a target blended lithium grade of 940 mg/L.
- After initial pond-filling, the target for pumping is to maintain an average rate of 260 L/s.
- After initial pond-filling, the target wellhead production rate is approximately 40,000 tonnes/year of lithium carbonate equivalent (“LCE”). This is achieved with the target pumping rate (260 L/s) and a target blended lithium grade of 940 mg/L, with a tolerance of between 893 and 960 mg/L. The blended grade of recovered brine should be maintained in this range for as long as possible.

- Existing wells should be used to the maximum extent possible with new wells added as required, to meet LCE targets.

15.6.4 Constraint for Reserves Categorization

As discussed in Section 2, Proven Reserves must be drawn from Measured Resources and Probable Reserves from Indicated Resources (in accordance with NI 43-101). The possible methods to achieve this categorization are different than those used for solid rock deposits, due to the fluid nature of brine.

To honour this constraint, the change in lithium mass within each Resource Zone (Measured, Indicated, and Inferred) was tracked as the production simulation proceeded, independently of the brine pumped from production wells. This allowed for Proven and Probable Reserves to be estimated based on the ongoing mass changes in each Resource zone. It also provided a quality check on the total amount of lithium recovery simulated from the production wells.

15.7 Reserve Estimate Results

15.7.1 Overview

To estimate Reserves, the model was setup and run with the final wellfield scenario and the Reserve constraints discussed in Section 15.6. Model results include the following predictions for the 50-year simulated Project life span:

- Lithium Reserve Estimate (grade and quantity of lithium recovered from production wells);
- Volume of brine recovered;
- The concentration of other selected constituents (K, B, Mg, Ca, Sr, Na, and SO₄) in the recovered brine; and
- Drawdown at the simulated production wells and in Lagunas 3Q and Verde.

Results are presented in the following subsections.

15.7.2 Lithium Reserve Estimate

The lithium Reserve Estimate is summarized and illustrated in the following for the 50-year Project life:

- Table 15-7 summarizes lithium grade and brine quantity pumped (at well heads), and the Proven and Probable lithium recovered (expressed as Lithium metal and LCE).
- Figure 15-13 shows wellhead LCE production rate for each series of wells and in total. It also shows the cumulative wellhead LCE production for each series of wells and in total.
- Figure 15-14 shows cumulative wellhead LCE production from Measured, Indicated, and Inferred Zones and the Total Reserve Recovered (Proven + Probable).
- Figure 15-15 shows the predicted evolution of average lithium grade recovered from each series of wells and in total.

As shown in Table 15-7, the Total Reserve Estimate (50-year mine life) is approximately 1,671,900 tonnes LCE, which includes Proven Reserves of approximately 1,084,300 tonnes LCE and Probable Reserves of approximately 587,600 tonnes LCE. The total Reserve represents approximately 32% of the Measured and Indicated Resources (400 mg/L cut-off).

As indicated in Section 2, the Mineral Reserves are comprised of the Measured and Indicated Mineral Resources which are simulated to be recovered at pumping wells. Mineral Reserves are not in addition to Mineral Resources.

Table 15-7: Summary of the lithium Reserve Estimate – 3Q Project.

Year	Brine Volume ¹ [Mm ³]	Average Lithium Grade ¹ [mg/L]	Lithium Metal [tonnes]		LCE [=5.32xLi] [tonnes]		Resource Recovered ² [%]
			Proven	Probable	Proven	Probable	
1	4.7	655	1,689	1,377	8,993	7,331	0.3
2	9.6	747	3,977	3,181	21,171	16,931	0.7
3-10	65.6	942	38,549	22,111	205,187	117,694	6.0
11-20	82.0	922	48,853	24,850	260,034	132,273	7.3
21-30	82.0	775	41,647	20,454	221,677	108,873	6.2
31-40	82.0	708	37,415	19,535	199,150	103,979	5.6
41-50	82.0	626	31,570	18,695	168,040	99,507	5.0
20 Years	161.9	912	93,068	51,520	495,384	274,229	14.3
Total 50 Years (Reserve Estimate)³	408	786	203,700	110,200	1,084,300	587,600	31

1. Brine produced from outside the Measured + Indicated Resource is included here but excluded from Reserves.
 2. Based on Measured + Indicated Resources of 5,369,000 tonnes LCE (400 mg/L cut-off) as presented in Section 14.
 3. Reserve Estimate numbers have been rounded.

The predicted progression of Reserve recovery is shown in Figure 15-13. Production ramps up in years 1 and 2, during pond-filling which primarily involves the mid-grade B-series wells. Thereafter, wellhead production is relatively constant at approximately 40,000 tonnes/year until year 20. During this period, LCE is primarily recovered from the A-series wells. At year 20, recovery shifts to the C-series wells, with some continuing support from the A-series. This shift is due to predicted grade decreases in the A-Series wells. From year 20 to year 50, the wellhead recovery rate is predicted to gradually decrease from approximately 35 to 25 tonnes/year LCE.

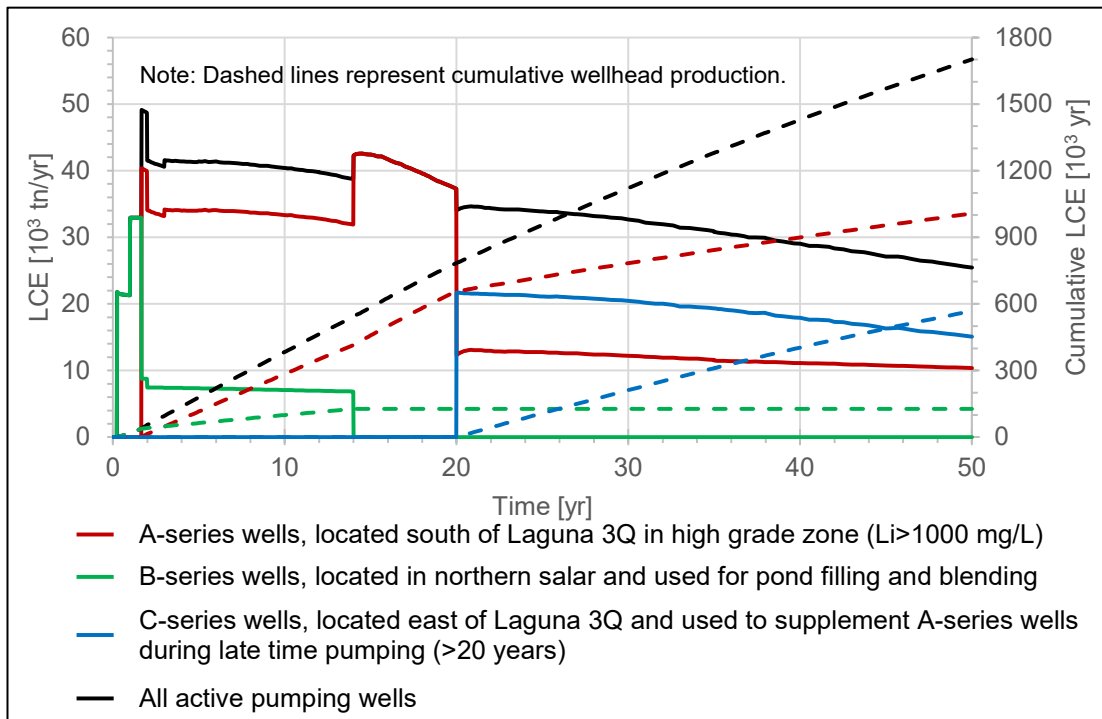


Figure 15-13: Simulated wellhead LEC production over the 50-year Project life.

As shown in Figure 15-14, the majority of the recovered LCE is from Measured and Indicated Resources. The uniform rate of LCE recovery is due to consistent pumping and relatively steady (although slightly decreasing) grades over the 50-year period.

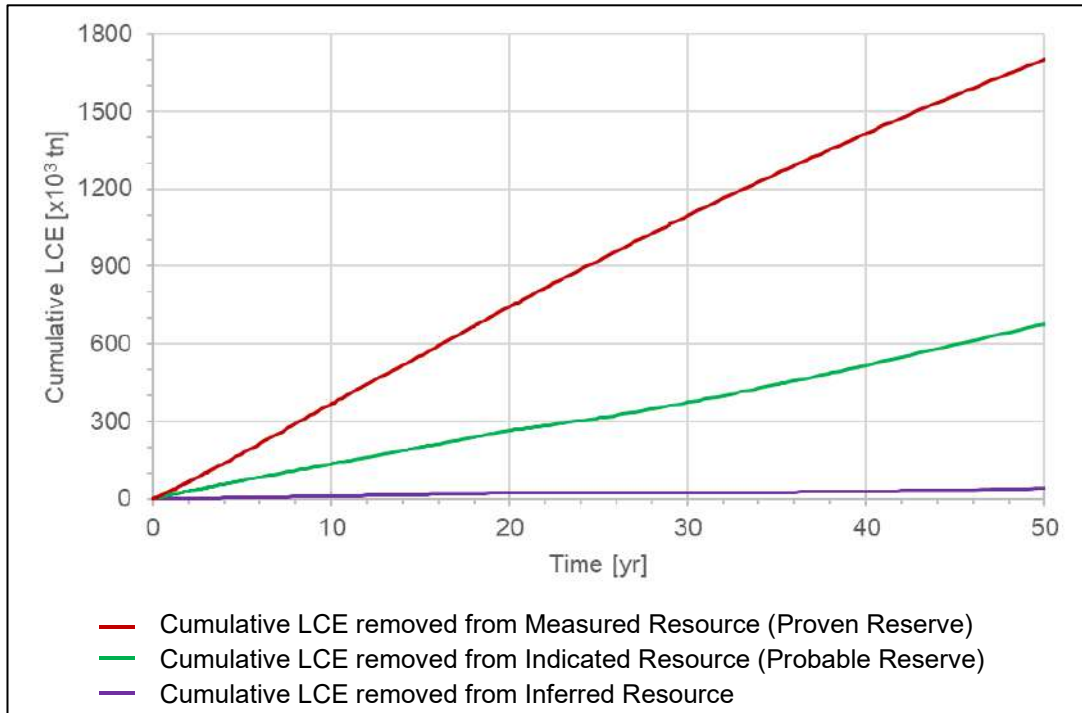


Figure 15-14: Simulated Reserves over the 50-year Project life.

Figure 15-15 illustrates the relatively consistent grades that are simulated to be recovered by the designed set of pumping wells. Grade declines reflect the recovery of the highest-grade zones.

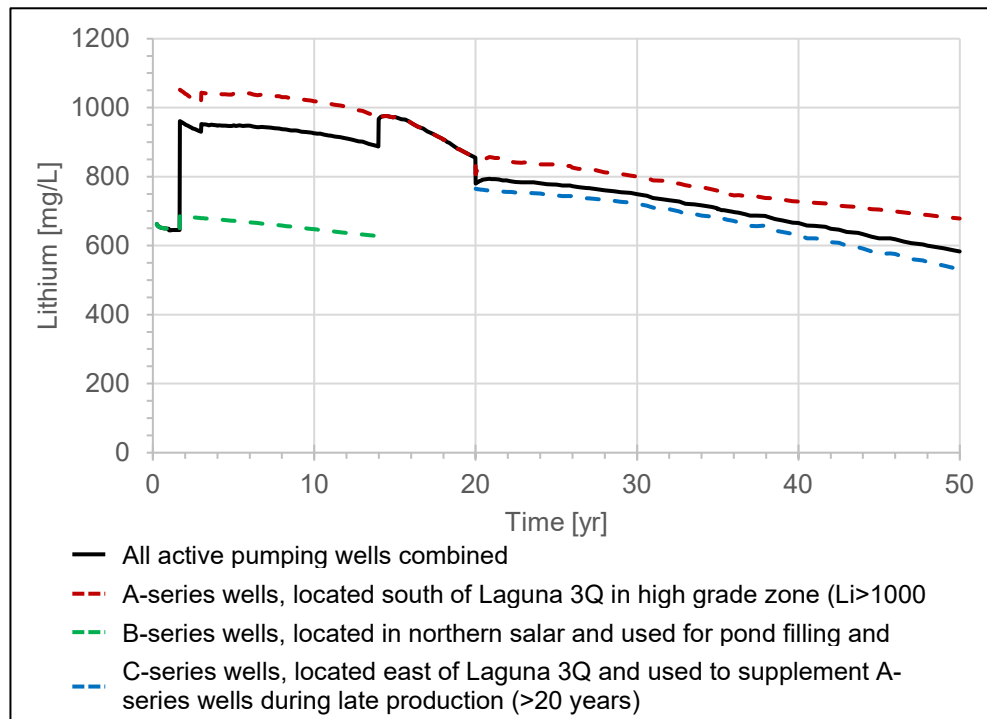


Figure 15-15: Simulated average lithium grade trends in pumped brine over the 50-year Project life.

Results for Other Brine Components

Estimated concentrations for potassium, boron, calcium, magnesium, sodium, strontium, and sulfate were required for brine processing considerations. These are presented in Table 15-8.

Table 15-8: Concentration trends for additional components in the recovered brine over the 50-year Project life.

	Production Interval (years)							
	1	2	3-10	11-20	21-30	31-40	40-50	1-50
Brine Volume (Mm³)	4.7	9.6	65.6	82.0	82.0	82.0	82.0	407.9
Lithium (mg/L)	655	747	942	922	775	708	626	786
Potassium (mg/L)	6,403	7,020	8,249	8,140	7,074	6,577	5,834	7,119
Boron (mg/L)	920	1,007	1,221	1,235	1,131	1,049	932	1,105
Calcium (mg/L)	29,444	33,296	41,476	40,116	34,690	31,595	27,806	34,773
Magnesium (mg/L)	1,407	1,475	1,703	1,628	1,306	1,193	1,062	1,368
Sodium (mg/L)	90,170	85,998	76,632	74,995	77,677	72,327	64,986	73,683
Strontium (mg/L)	587	641	756	731	644	586	515	641
Sulfate (mg/L)	252	257	262	267	371	376	347	325

15.7.3 Drawdown in Production Wells and Lakes

The predicted progression of drawdown in the simulated production wells is shown in Figure 15-16, and well locations are shown on Figure 15-11. Maximum drawdown for the A-, B- and C-series wells was approximately eight, three, and four metres, respectively. The capture of brine by the production wells is shown in a series of figures in Appendix G. Drawdown predictions using both the laguna drawdown model (Section 15.4) and the Reserve model (Section 15.5) are consistent.

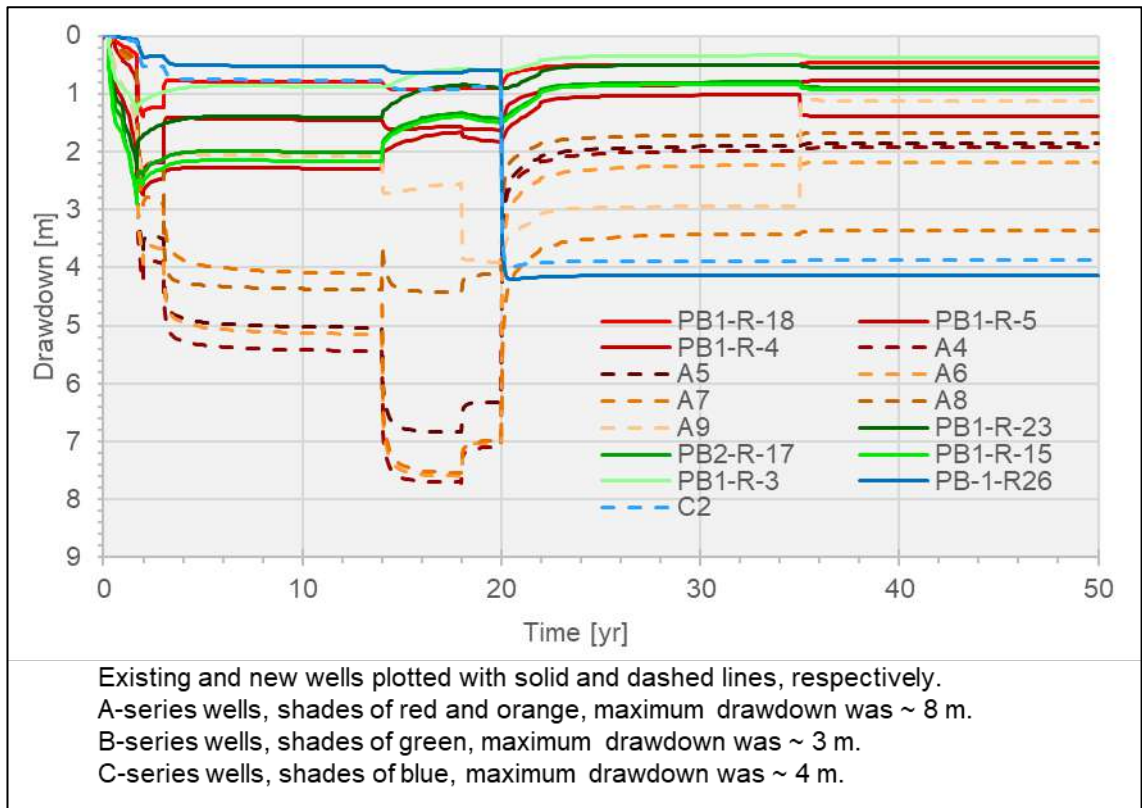


Figure 15-16: Temporal evolution of simulated drawdown in the production wells.

Predicted average annual drawdown in Lagunas Tres Quebradas and Verde over the 50-year pumping period, as predicted using the laguna drawdown model (Section 15.4), are shown on Figure 15-7. The maximum simulated drawdown in Laguna Tres Quebradas was predicted to be 0.11 m and it occurred at approximately 25 years of pumping. Maximum simulated drawdown in Laguna Verde was 0.02 m, at approximately 14 years of pumping.

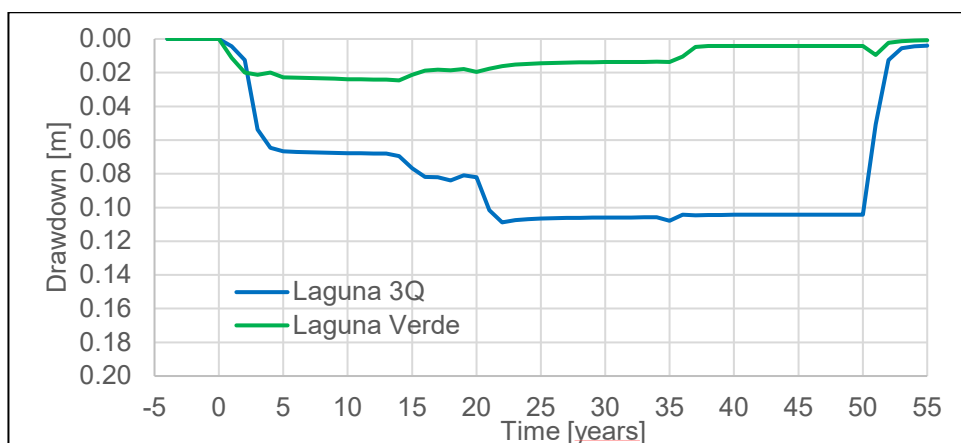


Figure 15-17: Temporal progression of simulated average annual drawdown in Lagunas 3Q and Verde.

The predicted drawdown in the lagunas and in the salar is presented on Figure 15-18. Predicted drawdown is shown as snapshots at 0, 10, 20, and 50 years.

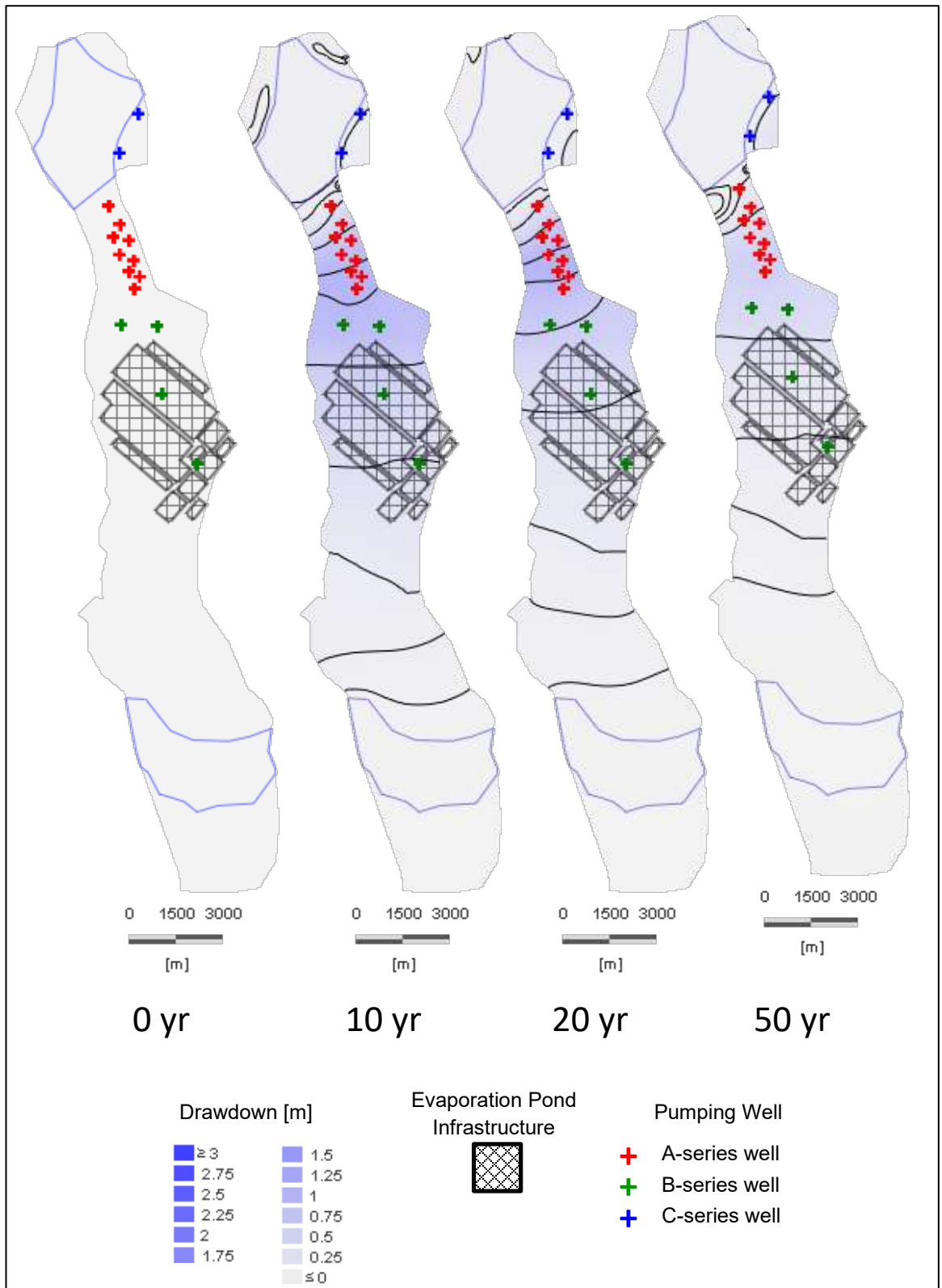


Figure 15-18: Temporal progression of simulated drawdown at ground surface.

The simulated water budget for the 50-year Project life, and five years before and after, is presented in Figure 15-19. The figure shows water budget components on an average annual basis, as predicted using the laguna drawdown model (Section 15.4). The time-period is subdivided into segments A, B, C, and D: segments A and D represent the time before and after

operations, while periods B and C represent two differing pumping periods during operation. Key observations from this figure include:

- Groundwater and surface water inflow (lateral sub-basin and Rio Salado inflow) was constant (i.e., is not affected by pumping).
- Production pumping starts with pond-filling (year 0, segment B) and then decreases for the remainder of the production period (segment C).
- In general, the increased output from pumping is counter-balanced by decreased output from evaporation.
- Evaporation from the salar crust and alluvium decreases as pumping starts. This response is caused by a combination of: 1) a decrease in the potential crust evaporation area due to evaporation pond construction; and 2) drawdown of the brine table due to pumping.
- Evaporation from the lagunas decreases as pumping starts. This response is due to the small decrease in laguna levels (drawdown in Figure 15-17).
- As pumping shifts from the B-series to C-series wells (i.e., at year 20), some of the decrease in evaporation shifts from the salar crust to Laguna 3Q.
- Evaporation becomes similar to pre-production levels within a few years after cessation of pumping. Evaporation from the salar crust is slightly less during the post-production period due to the simulated ongoing presence of the evaporation ponds.

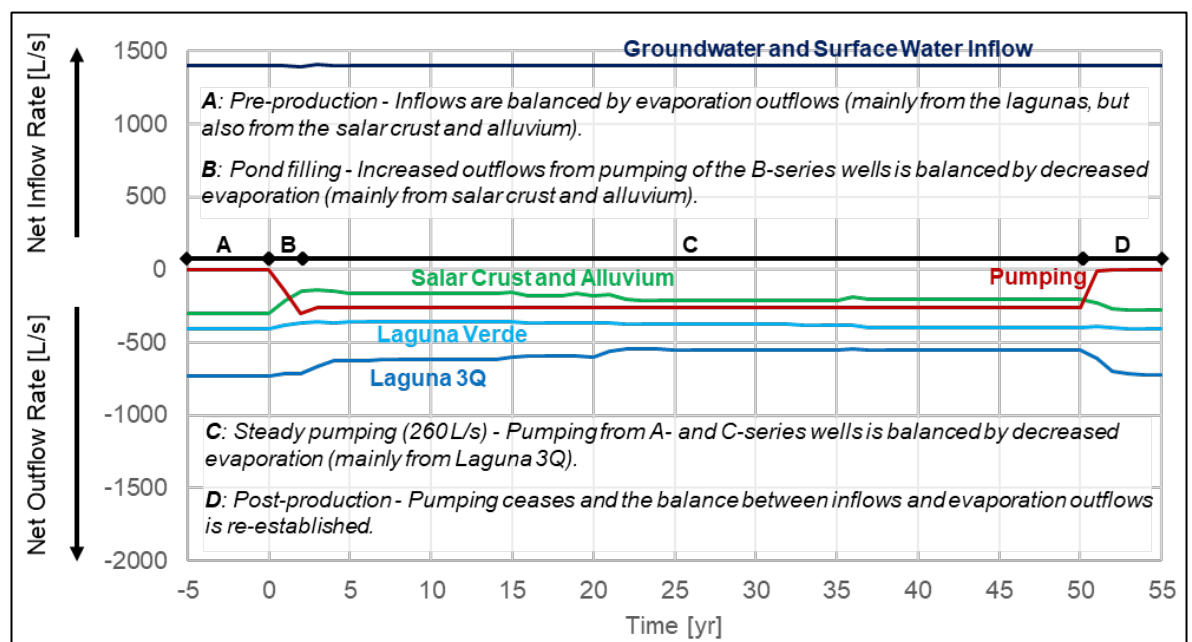


Figure 15-19: Progression of the simulated water budget.

15.7.4 Uncertainty Analysis

An analysis was conducted to assess the potential effects of model parameter uncertainty on the two model outputs of primary interest: the Reserve Estimate and drawdown estimates. The two model parameters identified as having the greatest potential for significant levels of uncertainty in this regard were hydraulic conductivity and specific storage.

Uncertainty analysis results for these two parameters are presented in Table 15-9. The range of tested parameter values were consistent with material observations and pumping test evaluations. Testing over these ranges produced nearly equivalent Reserves (i.e., within 3% of

base) while maintaining well drawdown levels considered to be reasonable and practical for production. Results also indicated that the effects on laguna levels would be minor, over the tested ranges.

Table 15-9: Sensitivity of Reserve Estimation and drawdown to hydrogeological characterization.

Case	Description of Hydrogeological Parameters	Prediction Sensitivity		
		Reserve Estimate [tonnes]	Maximum Drawdown at Pumping Wells [m] [†]	Maximum Laguna Changes
Base (Reserve Estimate model)	Applied parameters (K and Ss) of the calibrated model	Proven = 1,084,300 Probable = 586,600	A-series = 8 B-series = 3 C-series = 4	<u>Laguna 3Q</u> : 0.11 m drawdown <u>Laguna Verde</u> : 0.02m drawdown
Higher Anisotropy	Applied vertical hydraulic conductivity of PFS; Kv=0.001 m/d for all geological units	Within 3% of Base	A-series = 17 B-series = 4 C-series = 16 1.5X to 4X Base	Moderately reduced effect on lakes
Lower Lateral Hydraulic Conductivity for Shallow Units	<u>HPH</u> : Max K _h =500 m/d compared to 1,000 m/d for Base <u>US</u> : Max K _h =10 m/d compared to 20 m/d for Base	Within 1% of Base	A-series = 8 B-series = 2 C-series = 6 Similar to Base	Moderately reduced effect on lakes
Lower Specific Storage	Applied S _s =1x10 ⁻⁵ 1/m compared to 1x10 ⁻⁴ 1/m for Base	Within 1% of Base	A-series = 8 B-series = 3 C-series = 4 Same as Base	Effects similar to Base
Higher Specific Storage	Applied S _s =5x10 ⁻⁴ 1/m compared to 1x10 ⁻⁴ 1/m for Base	Within 1% of Base	A-series = 8 B-series = 3 C-series = 4 Same as Base	Effects similar to Base

[†] Available drawdown ranged from 32 to > 200 m.

In addition, certain aspects of the Reserve Estimate model were identified as qualitatively conservative (i.e., providing a degree of mass under-estimation) including the following:

- Water inputs from sub-basins and direct precipitation were simulated as non-reactive with salar solids. However, any water entering the salar would tend to mobilize salts and lithium from the solids, and would not persist as freshwater within the salar.
- The re-generation of brines due to ongoing evaporation of inflowing water is not represented in the Reserve Estimate model. However, evaporation will tend to limit the movement of freshwater into the salar, and this process will be accentuated by density contrasts, which will tend to keep incoming freshwater on top of the brine that is already present in the salar.

15.8 2D Model of Freshwater / Brine Interaction

15.8.1 Overview

Two 2D variable-density, cross-section models were generated to evaluate the effects of pumping on the freshwater / brine interface around Laguna 3Q. The models were situated to evaluate the highest sub-basin inflow areas, namely from the Rio Salado and Rio 3Q basins (Figure 15-20). The models are approximately 2 km long and they extend to depths of 266 m and 350 m, for Rio 3Q and Rio Salado, respectively.

The 2D models were derived from the 3D model, with the geological units, hydraulic properties, and boundary conditions extracted directly from the 3D model. Drawdown predicted with the 3D model was used as a time-varying head condition along the southern 2D model boundaries (i.e., beneath Laguna 3Q). Other boundary conditions for the 2D models included:

- Inflow from the upgradient watershed applied as a constant flux;
- Equivalent freshwater heads applied beneath the laguna;
- Evaporation from both the laguna margins (as indicated by salt crust and vegetation on Figure 15-20) as well as from the laguna itself;
- Freshwater inflow concentration of 30 mg/L TDS; and
- Initial conditions to reflect the observed salar brine density of 1.21.



Figure 15-20: Location of 2D density dependent flow and transport models.

15.8.2 Freshwater / Brine Interface Under Pre-Development Conditions

The freshwater / brine interface was calibrated to the vertical concentration differences observed in PP1-D-20. The simulated interaction between the freshwater and brine zones under natural (i.e., pre-development, non-pumping) conditions is shown in Figure 15-21. The results represent the inferred freshwater wedge, and they indicate that the extent of the wedge is limited due to:

- Evaporation of freshwater at the salar margin;
- Mixing with the existing salar brine; and

- Buoyancy forces created by density differences which force freshwater upward to the ground surface.

The density differences and discharges due to evaporation at the laguna margin cause deep brine convection currents to form, circulating from deep under the laguna and then upward, toward the laguna margin. This simulation is consistent with the relatively uniform brine concentrations observed with depth throughout the salar. Further, it provides physics-based support for observations of stratified freshwater/brine zones, and the limited extent of freshwater at salar margins.

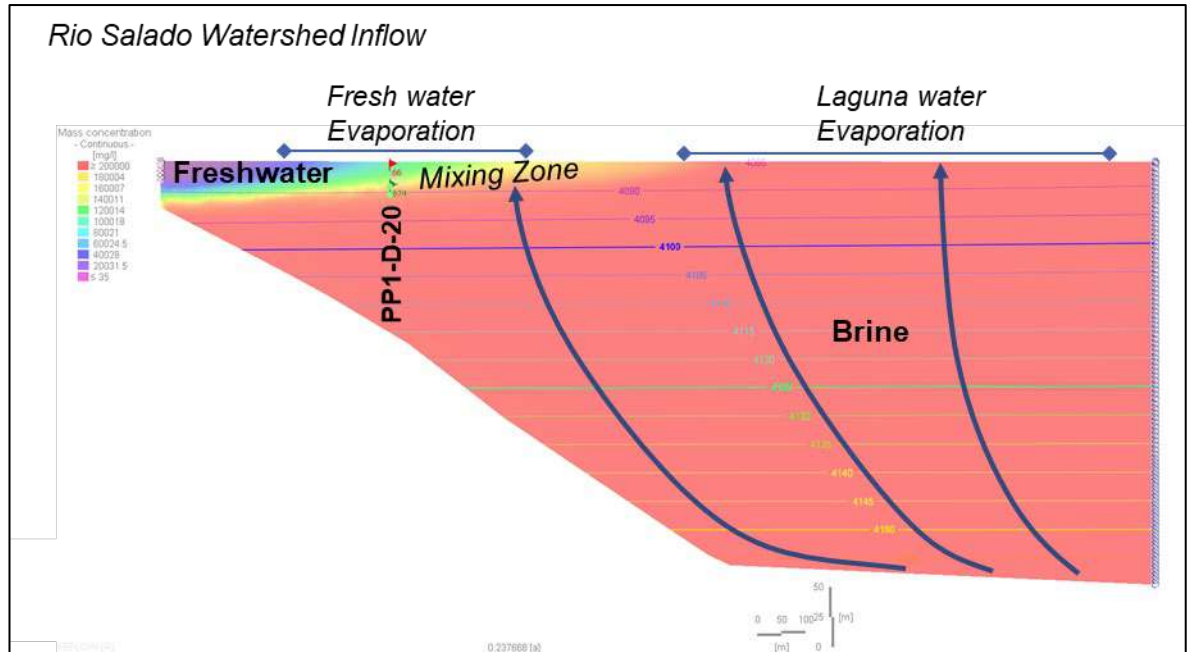


Figure 15-21: Freshwater and mixing zones at the margins of the 3Q Salar, as simulated in the 2D variable density model under natural conditions.

15.8.3 Freshwater / Brine Interface Under Brine Pumping Conditions

To simulate the effect of planned resource extraction, drawdown due to pumping (as simulated with the 3D model) was applied as a southern boundary condition for the calibrated 2D models. For this purpose, time-varying, depth-dependent drawdown was extracted from the 3D model at a series of points corresponding to the southern 2D model boundaries (Figure 15-22). The point drawdown values were used to modify the equivalent freshwater head boundary condition over the pumping period (i.e., 50-years of planned pumping).

Density-dependent simulations were conducted for the 50-year pumping period to evaluate for potential changes in the freshwater/brine interface. Drawdown at the southern boundaries of the 2D models (i.e., beneath Laguna 3Q) was predicted to peak at 1.3 m (Rio 3Q model) and at 1.78 m (Rio Salado model, shown in Figure 15-22). The predicted freshwater/brine interfaces are shown in Figure 15-23, for the Rio Salado model. The figure shows that the location and character of the interface is predicted to remain unchanged over the pumping period.

The basis for the static interface was further evaluated by comparing the gradients generated by the density differences in the system (0.2 m/m) and those due to pumping (0.00065), across the model domain. This comparison indicates that the density effects are substantially greater than the effects of drawdown caused by pumping. Consequently, the natural density gradients tend to maintain the freshwater/brine interface at a stable position as pumping proceeds.

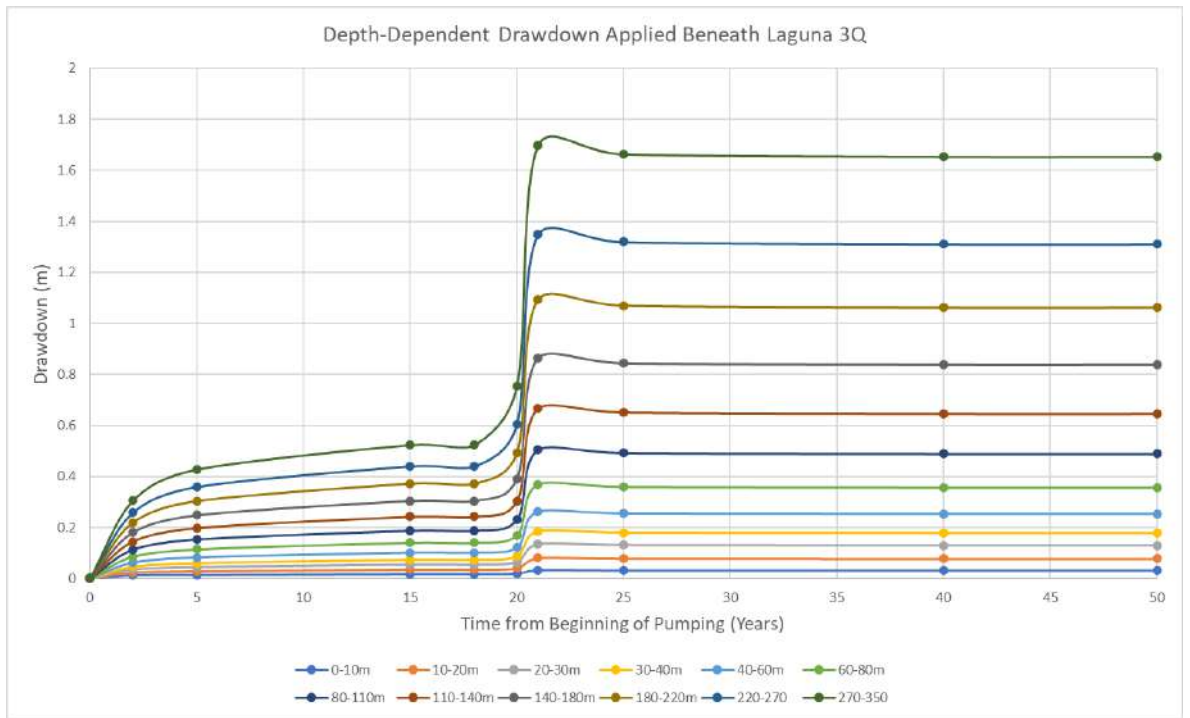


Figure 15-22: Depth-dependent drawdown applied beneath Laguna 3Q for the Rio Salado 2D model.

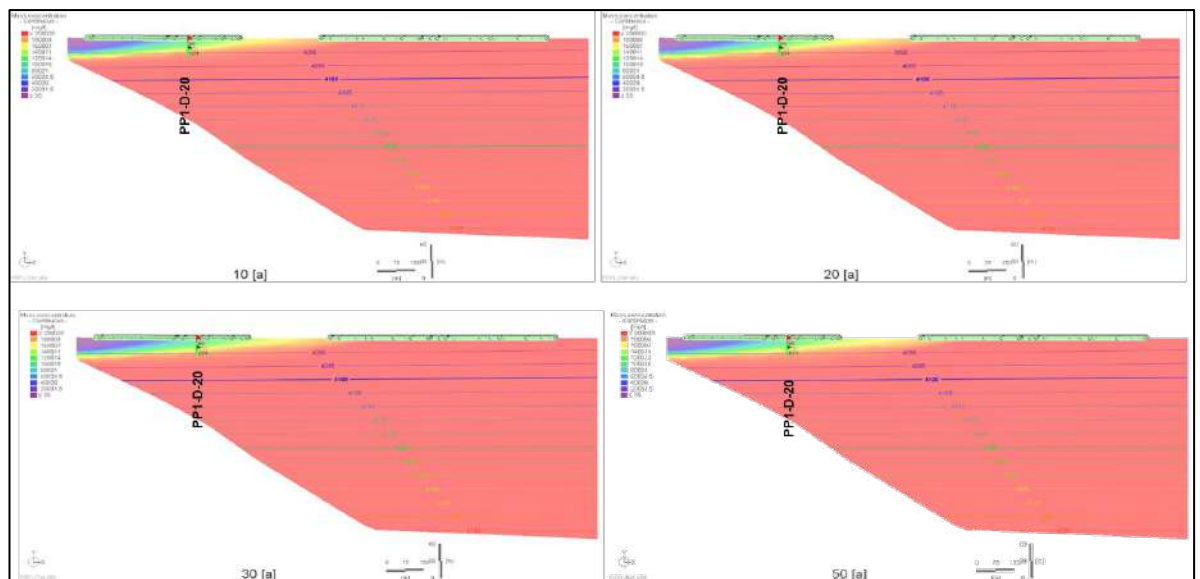


Figure 15-23: Simulated change in the freshwater / brine interface due to pumping – 2D Rio Salado model.

15.9 Closing

Salar flow systems are naturally complex, to a degree that cannot be fully replicated in a numerical model. Consequently, the development of a numerical model to simulate such a complex natural system is a process of identifying and implementing reasonable and acceptable approximations of the system. The validity of predictions from such models depends on the quantity and quality of system data, the methods by which those data are used in the model, and the modelling objective(s).

The QP is of the opinion that the salar modelling described in this Section was conducted in a manner that meets or exceeds the level of care and skill normally exercised by engineering and science professionals that are qualified to conduct this type of work. The QP is of the further opinion that the numerical model described herein and developed to simulate the complex 3Q Salar flow system is reasonable and acceptable for the objective of Reserve Estimation.

16. Mining Methods - Wellfield

The design constraints for the brine production wellfield are described in Section 15. The final configuration of well locations, screen depths, and pumping rates was the result of an iterative process to identify a system that could effectively meet the constraints. The final configuration is summarized in the following:

- Production well construction specifications are provided in Table 16-1.
- The pumping rate schedule is provided in Table 16-2.
- Well locations are shown on Figure 16-1, with an annotated plot of pumping rates.

Table 16-1: Construction specifications for the production wells, as simulated for the Reserve Estimate.

Series Name	Well Name	Existing Well	First Year Required	Easting	Northing	Screen Depth [m]	Maximum Drawdown [†] [m]
A1	PB1-R-18	Yes	2	2531562	6969530	0.5 – 100	1.38
A2	PB1-R-5	Yes	2	2531727	6968515	0 – 43	2.43
A3	PB1-R-4	Yes	2	2532428	6966863	0 – 70	2.30
A4	A4	No	2	2531930	6967946	200 – 250	7.71
A5	A5	No	2	2532229	6968406	200 – 300	6.84
A6	A6	No	4	2532385	6967761	200 – 300	7.60
A7	A7	No	14	2532563	6967230	200 – 300	7.55
A8	A8	No	2	2531952	6968928	200 – 300	4.43
A9	A9	No	14	2532228	6967414	20 – 55	3.92
B1	PB1-R-23	Yes	1	2533264	6963430	0.5 – 99.9	2.82
B2	PB2-R-17	Yes	1	2533172	6965664	3 – 105.6	2.85
B3	PB1-R-15	Yes	1	2531992	6965711	4 – 30.3	2.87
B4	PB1-R-3	Yes	1	2534476	6961260	0 – 43	1.36
C1	PB1-R-26	Yes	20	2532521	6972483	259 – 362	4.21
C2	C2	No	20	2531921	6971217	250 – 363	3.99

[†] Maximum simulated drawdown over 50-year Project life.

Table 16-2: Pumping rate schedule for the production wells, as simulated for the Reserve Estimate.

Year	Pumping Rates from Simulated Production Wells [L/s]															
	PB1-R-18 A1	PB1-R-5 A2	PB1-R-4 A3	A4	A5	A6	A7	A8	A9	PB1-R-23 B1	PB2-R-17 B2	PB1-R-15 B3	PB1-R-3 B4	PB1-R-26 C1	C2	Total
1										37.2	37.2	37.1	37.1			148.5
2	12.5	12.5	12.5	12.5	12.5	12.5				74.8	74.8	44.1	35.8			304.5
3	32.5	32.5	32.5	32.5	32.5	32.5				21.7	21.7	21.7				260
4			26	42.2	42.2	42.2		42.2		21.7	21.7	21.7				260
5			26	42.2	42.2	42.2		42.2		21.7	21.7	21.7				260
6			26	42.2	42.2	42.2		42.2		21.7	21.7	21.7				260
7			26	42.2	42.2	42.2		42.2		21.7	21.7	21.7				260
8			26	42.2	42.2	42.2		42.2		21.7	21.7	21.7				260
9			26	42.2	42.2	42.2		42.2		21.7	21.7	21.7				260
10			26	42.2	42.2	42.2		42.2		21.7	21.7	21.7				260
11			26	42.2	42.2	42.2		42.2		21.7	21.7	21.7				260
12			26	42.2	42.2	42.2		42.2		21.7	21.7	21.7				260
13			26	42.2	42.2	42.2		42.2		21.7	21.7	21.7				260
14			26	42.2	42.2	42.2		42.2		21.7	21.7	21.7				260
15				61.8	61.8	61.8	61.8		13							260
16				61.8	61.8	61.8	61.8		13							260
17				61.8	61.8	61.8	61.8		13							260
18				61.8	61.8	61.8	61.8		13							260
19				55.3	55.3	55.3	55.3		39							260
20				55.3	55.3	55.3	55.3		39							260
21								52	39					84.5	84.5	260
22								52	39					84.5	84.5	260
23								52	39					84.5	84.5	260
24								52	39					84.5	84.5	260
25								52	39					84.5	84.5	260
26								52	39					84.5	84.5	260

Year	Pumping Rates from Simulated Production Wells [L/s]															
	<i>PB1-R-18</i> A1	<i>PB1-R-5</i> A2	<i>PB1-R-4</i> A3	A4	A5	A6	A7	A8	A9	<i>PB1-R-23</i> B1	<i>PB2-R-17</i> B2	<i>PB1-R-15</i> B3	<i>PB1-R-3</i> B4	<i>PB1-R-26</i> C1	C2	Total
27							52		39					84.5	84.5	260
28							52		39					84.5	84.5	260
29							52		39					84.5	84.5	260
30							52		39					84.5	84.5	260
31							52		39					84.5	84.5	260
32							52		39					84.5	84.5	260
33							52		39					84.5	84.5	260
34							52		39					84.5	84.5	260
35							52		39					84.5	84.5	260
36			39				52							84.5	84.5	260
37			39				52							84.5	84.5	260
38			39				52							84.5	84.5	260
39			39				52							84.5	84.5	260
40			39				52							84.5	84.5	260
41			39				52							84.5	84.5	260
42			39				52							84.5	84.5	260
43			39				52							84.5	84.5	260
44			39				52							84.5	84.5	260
45			39				52							84.5	84.5	260
46			39				52							84.5	84.5	260
47			39				52							84.5	84.5	260
48			39				52							84.5	84.5	260
49			39				52							84.5	84.5	260
50			39				52							84.5	84.5	260

Note: Well name in *italic* font denotes existing well.

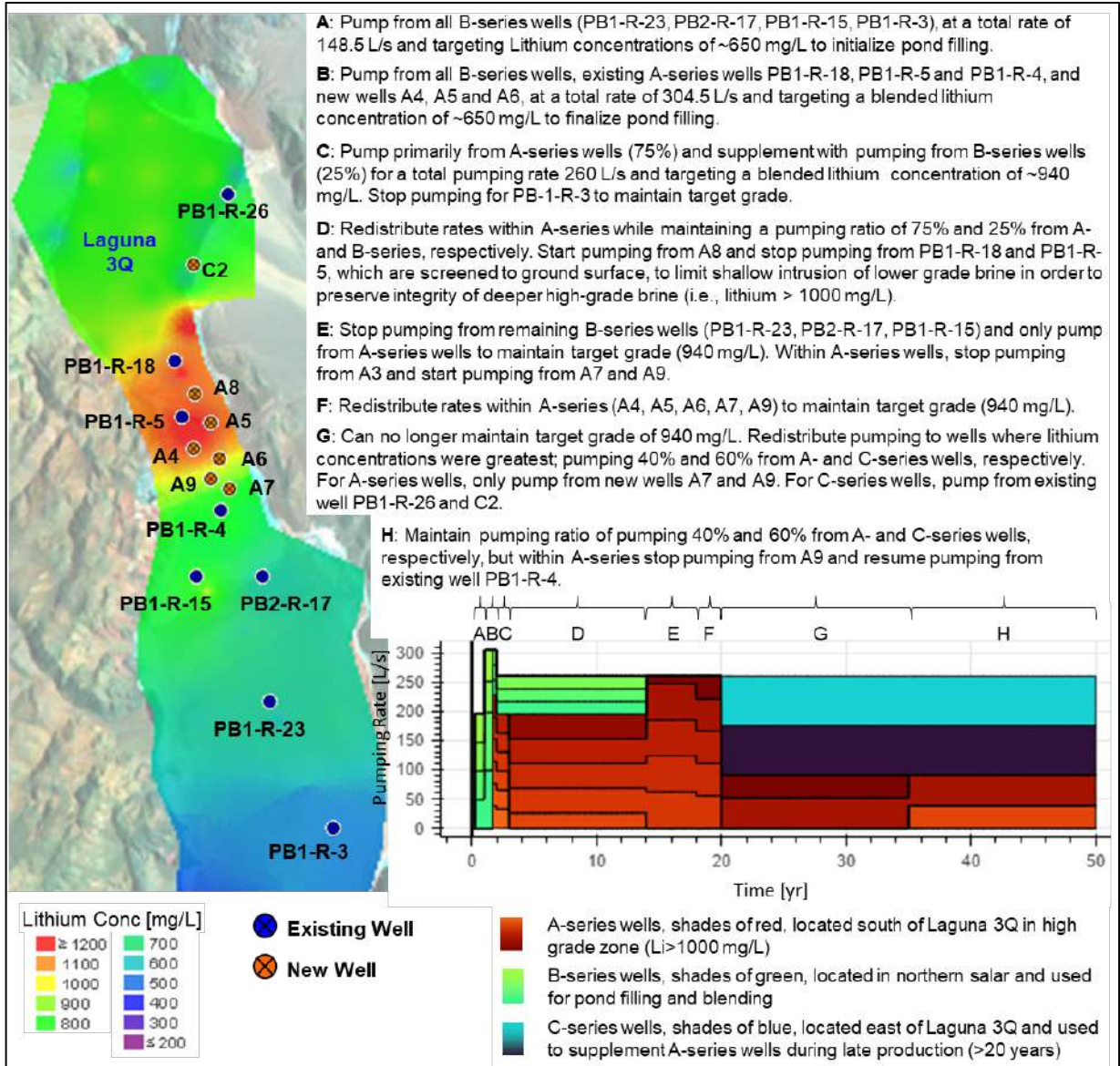


Figure 16-1: Wellfield and distribution of pumping rates, as simulated for the Reserve Estimate.

17. Recovery Methods

17.1 Overview

As indicated before, the 3Q Project production installations are split between two sites, the first one being located on the Tres Quebradas Salar, and the second one is in the vicinity of the Fiambalá town. Road distance between these places is approximately 160 km. The Salar Site is the location of the Brine Wells, the Evaporation Ponds, as well as the CaCl_2 Crystallization Plant, while the Fiambalá Site will be the location of the Lithium Carbonate Plant. Concentrated brine will be trucked from the salar site to the Fiambalá site¹. NLC has determined that there are CAPEX and OPEX savings associated with reducing the project's imprint on the salar, in addition to lower environmental impact, as well as better personnel welfare. This, considering that the salar site is at an average altitude of 4,100 metres above sea level (m asl), and accordingly, it has a harsh mountain climate, and it is not inhabited, while the Fiambalá site is at an altitude of 1,500 m asl, thus it enjoys a moderate climate, and some personnel conveniences.

The 3Q Project considers the design of production wells, evaporation ponds, a crystallization plant and a lithium carbonate plant, in order to obtain 20,000 TPY of battery grade Lithium Carbonate (Li_2CO_3). As a general description of the operations to be carried out on the salar site, we mention that the process considers extracting brine from wells located on the salar underground, within the Project's properties. Brine extracted from the wells, will be sent, initially, to pre concentration ponds and later to concentration ponds. On both types of ponds, a high proportion of the water contained within the brine will evaporate, through the action of radiation, as well as wind and other environmental conditions. This will also generate the precipitation of the majority of the salts contained in the brine. Since the 3Q salar brine has a high calcium content, elimination of this contaminant requires additional removal in a CaCl_2 Crystallization Plant. More details of the operations of this unit are presented in section 17.1.2 When the brine reaches a suitable lithium concentration, it will be fed to the dispatch ponds, located near the CaCl_2 Crystallization Plant. Then, it will be transferred to the Fiambalá Site, using dedicated tanker trucks. A summary of this process is presented on General Block Diagram in Figure 17-1.

The Fiambalá Li_2CO_3 Plant includes, as its first stage, the removal of the boron contained in the brine through a solvent extraction (SX) process. There on, the boron free brine will be pumped to precipitation Stage 0, where calcium (Ca) and magnesium (Mg) will be removed through the addition of reagents, followed by solid-liquid separation. Given the high Ca content of the concentrated brine, after Stage 0, another stage is considered, in order to precipitate more of the Ca contained in the brine and re-use it within the process. This is carried out in Stage 1, through the addition of sodium hydroxide (NaOH), followed by solid-liquid separation. While the solids from Stage 1 are re-used in Stage 0, Ca reduced brine is pumped to the next stage (Stage 2), to remove all remaining Ca present in the brine. This is done through the addition of a soda ash solution, followed by solid-liquid separation. Finally, when all the contaminants are removed, the brine will feed a lithium carbonate precipitation stage, where Li_2CO_3 solids will precipitate through the addition of a soda ash solution (Na_2CO_3). Precipitated solid lithium carbonate will then be fed solid-liquid separation equipment, to

¹ It is worthwhile to mention that both SQM and Albemarle, both long time established lithium producers in Chile, operate in this manner.

remove excess liquids, as well as for washing the final product. Dewatered solids will feed the Li_2CO_3 drying stage.

After the drying stage, solid battery grade lithium carbonate will be packed and stored in the final product warehouse, to be finally transported to its final destination.

Overall lithium recovery of nearly 51% is expected, considering processes at the evaporation ponds and the lithium carbonate plant.

A more detailed description of the processes at both the solar installations, and the lithium carbonate plant will be presented in the following sub-sections.

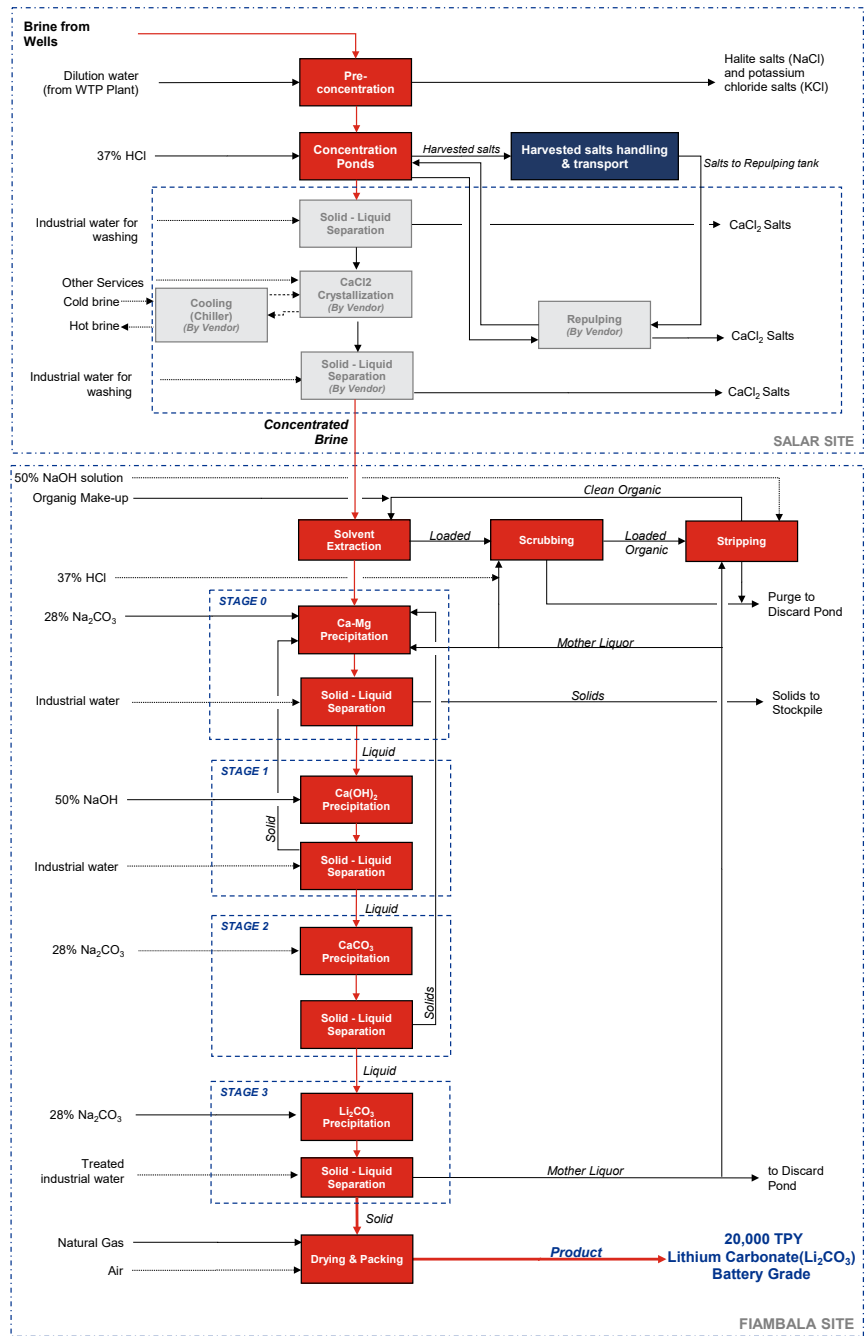


Figure 17-1: Block diagram of the process.

17.2 Salar Site

The Salar Site, as previously mentioned, is located on and next to the 3Q Salar. This site includes the brine extraction wells, the evaporation ponds and the CaCl₂ Crystallization Plant (from now on Crystallization Plant).

17.2.1 Brine Extraction Wells

Brine will be pumped from each of the wells, according to the extraction rate defined by hydrogeological considerations, and the mass balance requirements of the project. Generally, a higher extraction rate will be carried out during the summer season, due to a higher water evaporation rate, and a lower extraction rate is defined for the winter, since in this season, a lower evaporation rate takes place in the Salar. Brine from each extraction well will be pumped, through individual pipelines, to the first two pre-mixing ponds. These will operate in parallel and will allow brine mixing from all the different wells, generating a homogeneous brine that will feed the first evaporation ponds. Brine residence time at the pre-mixing ponds will be short. The pre-mixing ponds will feed the first pond of each the pre-concentration string, through a gravitational channel, avoiding the use of pumps in this specific brine transfer point.

Brine extraction wells will be located according to the hydrogeological characteristics of the salar.

17.2.2 Evaporation Ponds and CaCl₂ Crystallization Plant for Brine Concentration

All the evaporation ponds in this project are designed as units with a low height and a high base area, this favors the evaporation of the water present in the brine. Water evaporation will saturate the brine, changing the equilibrium point of all ions present in it, thus allowing precipitation of salts inside the ponds, due to the change in the interaction between the ions. Precipitated salts in the ponds will be harvested (removed) periodically, by mechanical means.

The 3Q Project considers two types of ponds, as follows:

a) Pre-concentration ponds

In these ponds the first stage of the evaporation pond process takes place. Brine from extraction wells is pumped directly to two pre-mixing ponds, where the brine coming from all the wells will be mixed. As a result, a homogeneous brine will be fed to the first pre-concentration pond of each string.

In this project, the pre-concentration ponds consist of two strings that operate in parallel, where each string will be divided in two evaporation ponds with a larger base area, named PC ponds and K ponds. The main salts that will precipitate are halite (NaCl) and mixture of halite/potassium chloride (NaCl/KCl) respectively. Brine will be pumped, controllably, from the PC to the K pond, in each string.

Salts will be periodically harvested from all ponds using harvesting equipment (front loaders, solid transfer trucks, among others), and will be transported to designated areas for stockpiling.

To promote a more efficient evaporation of the water contained in the brine, both the PC ponds and the K ponds will be subdivided into 4 ponds with a smaller base area, which, in turn will be divided into different sectors, through baffles. Brine will flow freely through the open channel between the baffle and the pond berm. Brine flow in the open channel will be controlled, if necessary, through the addition of salt bags. A total of 16 pre-concentration ponds are considered in this process, 8 ponds per string.

When brine from the last K pond of each string, reaches an appropriate lithium concentration level, its chemical composition will be sampled and analyzed. When the brine reaches the defined lithium concentration, the saturation point for calcium chloride (CaCl₂) is also reached, so that

the brine is ready to be pumped as pre-concentrated brine to the next stage of the process, the concentration ponds.

Dilution water is also considered for all brine transfer pumps, to reduce salt scaling within the pumps, that is normally occurs in brine transfer equipment, in lithium projects. This dilution water also allows reduction in maintenance periodicity required for this type of equipment. In this project, reject water from the reverse osmosis plant will be considered as dilution water, to reduce the consumption of industrial water in the process.

No reagents are required in the pre-concentration ponds.

A general scheme for the brine extraction wells pre-mixing ponds and pre-concentration ponds is presented in Figure 17-2.

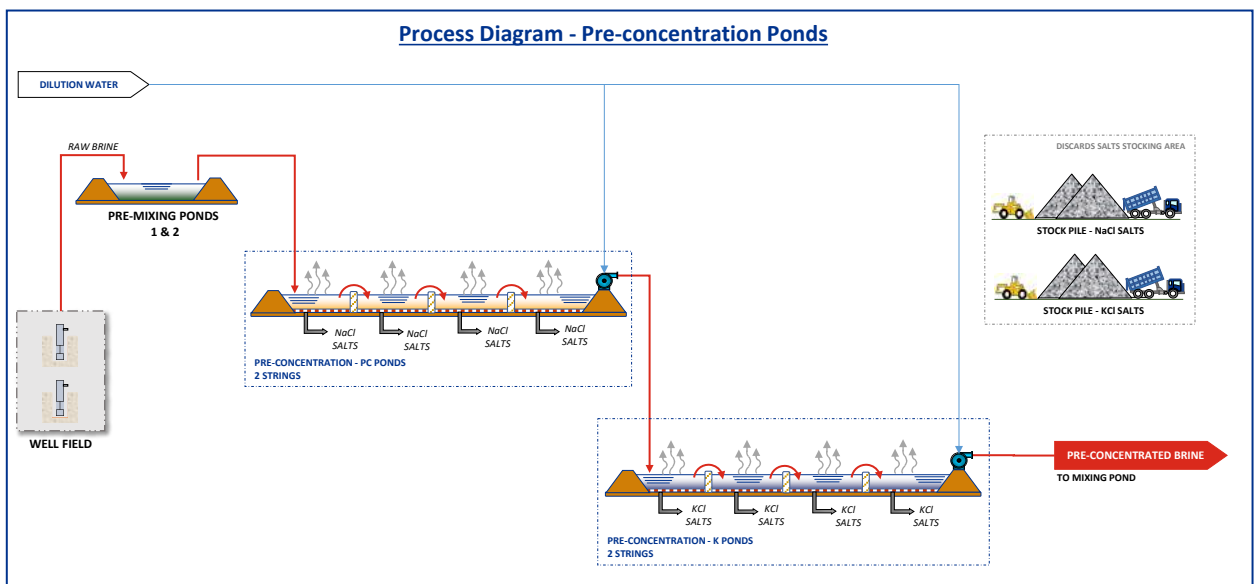


Figure 17-2: Brine extraction well and pre-concentration ponds.

b) Concentration Ponds and CaCl_2 Crystallization Plant

To continue with the evaporation process and salt precipitation, further concentration ponds are considered down the evaporation process: These are fed with brine from the last pre-concentration pond of each string and have a lithium concentration of 0.29%.

Given that inlet brine for this project has a high calcium (Ca) content, the process requires that the concentration ponds evaporate water from the brine allowing the removal of calcium through the precipitation of calcium chloride ($\text{CaCl}_2 \cdot 6\text{H}_2\text{O}$). Brine from both strings of the pre-concentration ponds is firstly fed to two mixing ponds, which operate in parallel, and have a low residence time. These mixing ponds are mainly used for blending the brine from both pre-concentration strings, allowing a homogeneous brine to be fed to the concentration ponds.

From the mixing ponds, the brine flows, through transfer channels, to the first pond from each string of the concentration ponds.

The concentration ponds consist of 5 stages, where the first and second stages include 3 strings operating in parallel, while the third, fourth and fifth stages include only two ponds operating in parallel.

The main goal of this process step is to concentrate lithium through the massive elimination of Ca by precipitation of $\text{CaCl}_2 \cdot 6\text{H}_2\text{O}$ (Antarcticite). However, the solubility of this salt is sensitive to changes in temperature in the range between 7 to 28 ° C, so in summer its behavior tends to dissolve this salt formed during the day and to recrystallize at night. On the other hand, in the winter period, the salt will accumulate in ponds without major variation in solubility due to day-night thermal oscillation. Therefore, this process has been designed with two modes of operation, to ensure the formation of salt in cold (Winter) and hot (Summer) periods. In winter, when the average environmental temperature is below 7°C, the Li concentration and calcium elimination process occurs mainly in ponds. On the other hand, in summer when the temperature is higher than 7°C an auxiliary cooling system is used in crystallizers to stabilize the Antarcticite, remove it and separate it from the lithium-enriched brine. Both modes of operation are explained in more detail in the following paragraphs:

Winter Operation Mode (Figure 17-3 Green line): The brine is concentrated in lithium and removes Ca as $\text{CaCl}_2 \cdot 6\text{H}_2\text{O}$ (leaving this salt in the respective pond for later dry harvest) from concentration pond 1 to concentration pond 5 without going through the cooled crystallizers since the average ambient temperature is low enough to allow the precipitation and stabilization of $\text{CaCl}_2 \cdot 6\text{H}_2\text{O}$ in pools (Figure 17-3, green lines). The salts harvested from each of the concentration ponds have a significant amount of brine concentrated in lithium impregnated which must be recovered in mechanized plant operation.

The recovery of impregnated brine and therefore of the lithium contained in this brine, consists of taking the harvest salts to a temporary storage place, to then be sent to the stage of Harvest Salt Treatment where in reactors a solid-liquid pulp is formed with brine from concentration pond 1 (which is the pond with the lowest lithium concentration and is also saturated in $\text{CaCl}_2 \cdot 6\text{H}_2\text{O}$) in order to “leach” lithium impregnated in harvest salts and finally subject the pulp to intensive filtration with equipment machined to minimize lithium losses at this stage. The lithium-enriched “Mother Liquor” from the harvest salts is returned to concentration pond 1 and concentration pond 2 to continue the process from pond to pond downstream until the required concentration of Li is reached.

Summer Operation Mode (Figure 17-3 Orange line): The brine is concentrated in lithium and removes Ca as $\text{CaCl}_2 \cdot 6\text{H}_2\text{O}$ (leaving this salt in the respective pool for later dry harvest) from concentration pond 1 to concentration pond 5 passing in the interleaved way by the cooled crystallizers (Figure 17-3, orange lines) since at this time of year the ambient temperatures are higher than in Winter, less calcium precipitates, which slows down the lithium concentration and makes it necessary to cool the brine externally to force crystallization of calcium that does not precipitate in ponds due to higher temperatures of the summer. As in winter mode, the salts harvested from each of the concentration ponds have a significant amount of brine concentrated in lithium impregnated which must be recovered in a mechanized plant operation (“Harvest Salt Treatment”).

The brine that enters the crystallizers is cooled from 15°C to 7°C with a cooling system. As the brine cools, it becomes supersaturated in $\text{CaCl}_2 \cdot 6\text{H}_2\text{O}$ and crystallizes within the crystallizers. The pulp

formed is centrifuged and the brine is recovered to be sent to the next solar evaporation pond. This process is repeated from stage 1 to 5, to finally achieve a brine of around 3.2-3.3% in Li.

The only reagent that will be required in the concentration ponds will be hydrochloric acid (HCl). This acid will be used for brine pH control, in the fourth pond of each string. pH control is required since, in this stage, brine presents a high boron (B), level at which it could generate unwanted co-reactions with brine lithium. The addition of HCl promotes the generation of boric acid (H_3BO_3), preventing these unwanted reactions, thus avoiding lithium losses due to its co-precipitation in the concentration ponds.

Since the concentration ponds for each stage will always feed a stage of the Crystallization Plant, pumps will be required at the outlet of each pond. For the concentration ponds, no continuous dilution water will be required. Only washing with industrial water will be considered for the pumps and pipelines, operation to be carried out periodically. This is possible based on the calcium salts generated in these ponds being easily diluted in water, so continuous dilution is not required.

As mentioned in the general description, the Crystallization Plant will consist of two main areas, which are:

- **5 stages of specific unit operations:** these stages will allow the removal of calcium salts from the brine. All five stages will operate similarly, but consider progressively smaller equipment, as the stages advance, since the brine that feeds each stage further down the line will have less calcium content to be removed.

Each stage will consist of the following unit operations:

- a) **Polishing filter:** brine from the concentration ponds will first feed a polishing filter, to remove any solids present in the brine. Solids will be transported to a final stockpile and the liquid will feed the crystallizer.
 - b) **Crystallizer:** the filtered brine will then feed a crystallizer, in which, through the reduction in brine temperature, $CaCl_2$ crystals will precipitate, removing the calcium present in the brine as salts.
 - c) **Centrifuge:** the outlet brine from the crystallizers, which contains precipitated $CaCl_2$ salt, will feed a centrifuge for solid-liquid separation. Solids generated from the centrifuge will feed a transport belt and be carried directly to a final discard stockpile. The liquids generated from the centrifuge, which is a calcium reduced brine, will feed the next unit operation (polishing filter).
 - d) **Polishing filter:** brine from the centrifuge will feed a final polishing filter, to separate any solids that still remain in the brine. Solids will be transported to a defined discard stockpile. The brine from the polishing filter will feed the concentration pond of the next stage.
- **One repulping stage:** all harvested salt from the concentration ponds will have entrained brine, which must be recovered to increase total lithium recovery. This will be carried out through a salt repulping stage.
 - Harvested salts from the concentration ponds will be carried to a temporary stockpile, where they will be loaded to a lump breaker, which will then feed a transport belt. The salts will then be fed to 3 decanters that operate in parallel, where, with the addition of low lithium

brine (from the first stage), the solids will be washed, and lithium entrained in the solids will be released from the solids to the brine.

- The outlet pulp from the decanters will then feed 3 centrifuges, that operate in parallel. Outlet solids from the centrifuge will be dumped directly to a transport belt, for transfer to a final discard stockpile. The outlet brine, or mother liquor, will be fed back to the first and second stage concentration ponds.

From the fifth crystallization stage, the lithium concentrated brine will feed two dispatch ponds. These will be covered with a plastic membrane, to avoid any further water evaporation from the brine. The dispatch ponds will also act as a buffer for any flow variations from the Crystallization Plant. From these ponds, brine tanker trucks will be loaded to carry the brine directly to the Fiambalá Site.

A general scheme for the different stages of the concentration ponds and the Crystallization Plant are presented in Figure 17-3.

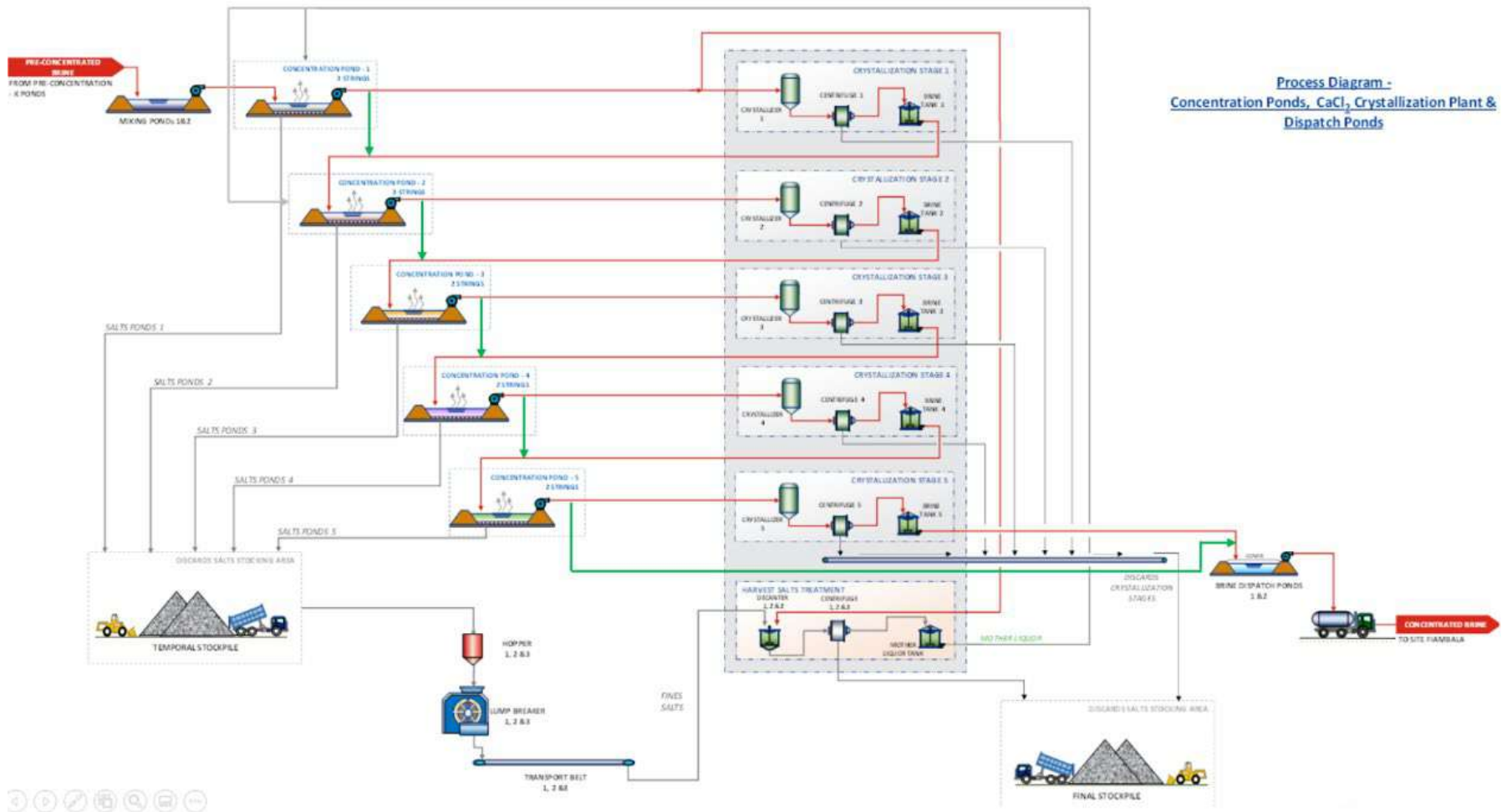


Figure 17-3: Concentration Ponds and Crystallization Plant.

Table 17-1 presents the main process mass balance results to be considered for the pre-concentration and concentration ponds.

Table 17-1: Main Mass Balance Results for the Pre-concentration and Concentration ponds

Compound/type	Units	Initial values
Total base area for pre-concentration ponds	ha	449.1
Total base area for concentration ponds	ha	94.1
Estimated treated brine from brine wells (average) (Estimated density = 1.23 t/m ³)	TPY	9,961,844
Harvested salts from pre-concentration ponds	TPY	1,763,443
CaCl ₂ process to final disposal	TPY	2,071,453

17.3 Fiambalá Site

The brine from the Salar Site will be transported by tanker truck to the Fiambalá site, which is located in the vicinity of the town of the same name. This site comprises the complete Lithium Carbonate Plant, including all services necessary for the production plant. The following sections will describe all the process installations within this site.

17.3.1 Lithium Carbonate Plant

The Lithium Carbonate Plant is a chemical facility that receives concentrated brine from the Salar Site, and, through a series of chemical processes and unit operations, generates battery grade lithium carbonate. The first stages of the process are designed to remove the impurities still present in the brine. The purpose of the final stages of the plant is to precipitate the lithium carbonate and the remove all moisture contained in it, ending with packing and storage of the final product. More details of each stage of the process are presented below.

17.3.1.1 Reception Ponds and Solvent Extraction

Brine transported from the Salar Site will be received in the Fiambalá Site and unloaded from the tanker trucks to two reception ponds. As is the case with the dispatch ponds in the salar, these ponds are also covered with a plastic membrane, to avoid further water evaporation from the brine. The main brine stock for the process corresponds to the reception ponds, rather than in the salar dispatch ponds, to guarantee brine feed to the Li₂CO₃ Plant, in case of problems in the roads due to weather, or any other unexpected issues.

From the reception pond, the brine will be fed to the first stage of the Li₂CO₃ Plant, which is the Solvent Extraction Stage (SX), designed to complete removal of boron (B), still present in the brine. For this objective, the SX Stage is subdivided in 3 substages:

- Extraction: In this substage brine high in B is mixed with an organic liquid compound specially designed for this process, where, due to different solubilities, both become immiscible, allowing later separation of both liquids in the settler. To achieve mixing and separation of both liquids,

this operation is carried out inside mixer settler equipment, which operates in series. Due to mixing of these two liquids, the organic compound extracts the B from the brine, generating boron free brine, which is pumped to the next stage of the process (Stage 0). The boron loaded organic is pumped to a scrubbing substage.

- Scrubbing: The purpose of this substage is the removal of inorganic species at a trace level that could be co-extracted by the organic from the concentrated brine, avoiding any problems in the Stripping substage. For its operation, an acid pH is required, for which concentrated HCl (37%) will be added together with mother liquor from the lithium carbonation stage as scrubbing solution. This substage generates both a discard solution, which is pumped to a purge tank (from there it will be sent to final discard ponds), and a loaded organic conditions to be treated in the stripping substage.
- Stripping: This substage is designed to unload the boron element from the loaded organic, generating a clean organic to be recirculated within the process. For this to occur, the loaded organic must be contacted with an aqueous solution that has a basic pH (10-11). This is mother liquor, which is recirculated from the Stage 3 (described in Section 13.5.4), and mixed with sodium hydroxide (NaOH), at a concentration of 50%. This substage generates both a boron-rich aqueous solution, which is pumped to the purge tank, and a clean organic which is recirculated to the extraction substage.

A general scheme for this stage is presented in Figure 17-4.

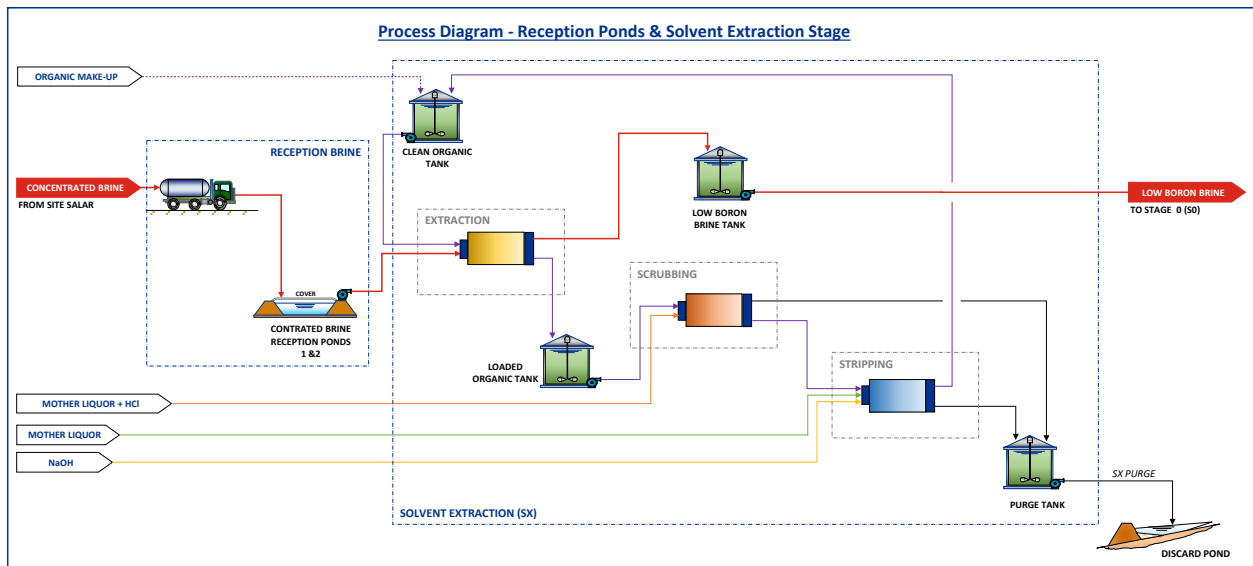


Figure 17-4: Reception Ponds and SX.

17.3.1.2 Stage 0 – Ca and Mg Removal

The boron free brine, from the SX stage, will then be fed to the calcium (Ca) and magnesium (Mg) precipitation stage, also known as Stage 0. Precipitation of all remaining magnesium within the brine, as magnesium hydroxide ($Mg(OH)_2$), will be obtained through the addition of chemical reagents, based on an increase in pH of the solution. Additionally, calcium carbonate ($CaCO_3$) is added as a concentrate pulp from Stage 2 since is required to absorb the $Mg(OH)_2$ formed in this process,

facilitating the subsequent filtration stage. To achieve the precipitation of these elements, Stage 0 is subdivided into substages A and B.

Substage A is fed with boron free brine, together with lime milk ($\text{Ca}(\text{OH})_2$) recirculated from Stage 1 solids, calcium carbonate (CaCO_3) recirculated from Stage 2 solids and recirculated mother liquor from Stage 3. Mixing of all these streams, in special purpose reactors, results in precipitation of $\text{Mg}(\text{OH})_2$ which is adsorbed on the CaCO_3 surface, being then separated from the brine in thickeners and filters. While the filtered solids are sent to a final disposal stockpile, the solids and the Mg reduced brine are pumped to substage B. Substage A occurs at ambient temperature.

In substage B, filtered brine, a solution of soda ash (Na_2CO_3 at a concentration of 28%), mother liquor from Stage 3 and milk of lime from Stage 1, will all be fed an agitated reactor. This mixture allows precipitation of the Mg and Ca still present in the brine. The pulp which contains precipitated solids continues to a thickener and filters, allowing the removal of $\text{Mg}(\text{OH})_2$ and CaCO_3 as filtered solids, which are also sent to a final disposal stockpile.

The Mg free brine is sent to the next area of the Plant, Stage 1. A general scheme of Stage 0 is presented in Figure 17-5.

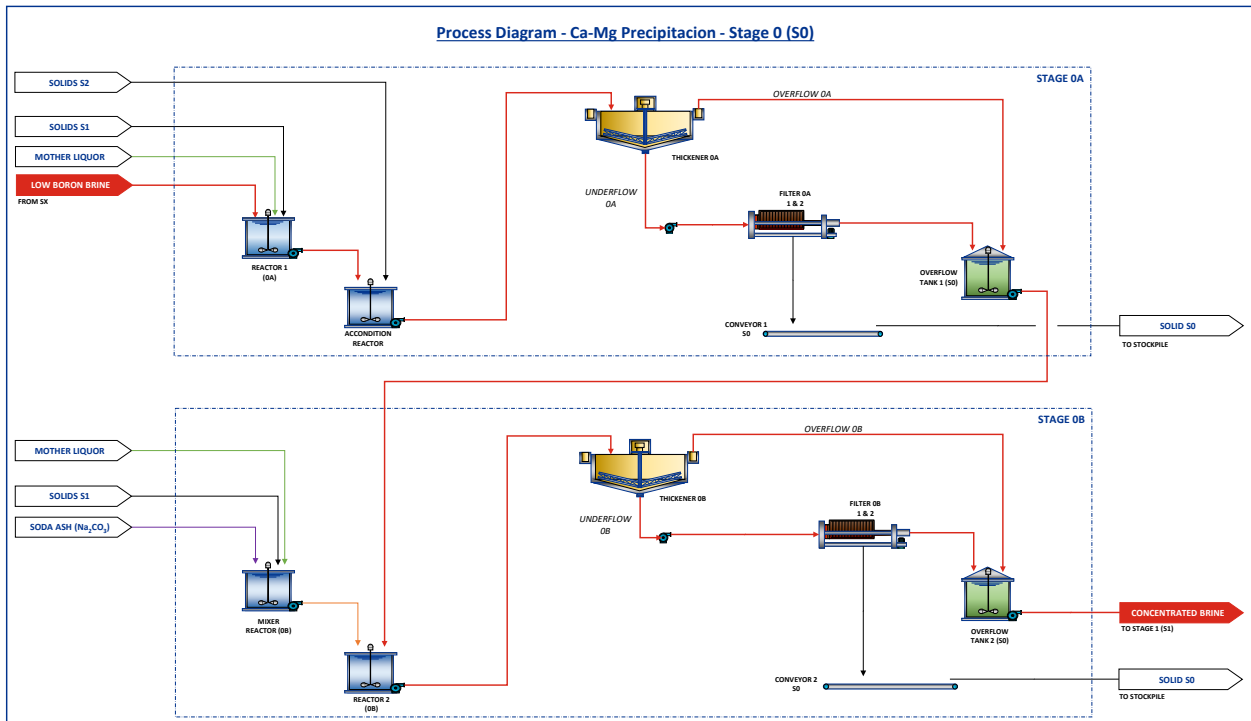


Figure 17-5: Stage 0 – Ca and Mg Removal.

17.3.1.3 Stage 1 – $\text{Ca}(\text{OH})_2$ Precipitation

Brine with a lower Ca content will feed the next stage of the process, known as the $\text{Ca}(\text{OH})_2$ precipitation stage, or Stage 1. In this stage, the Ca content within the brine, is reduced due to precipitation of calcium hydroxide ($\text{Ca}(\text{OH})_2$). The solids precipitated in this stage will be recirculated to Stage 0, to provide an alkaline environment for Mg precipitation.

For precipitation of $\text{Ca}(\text{OH})_2$, Mg free brine will be fed to an agitated reactor, together with caustic soda (NaOH), which has a concentration of 50%, allowing precipitation of the required solids, at

ambient temperature. This brine will then be fed to a thickener and filters. While the solids generated in this stage are recirculated within the process (to Stage 0), the liquid produced in this stage is Ca reduced brine.

The Ca reduced brine will then be sent to the next area of the Plant, Stage 2. A general scheme of Stage 1 is presented in Figure 17-6.

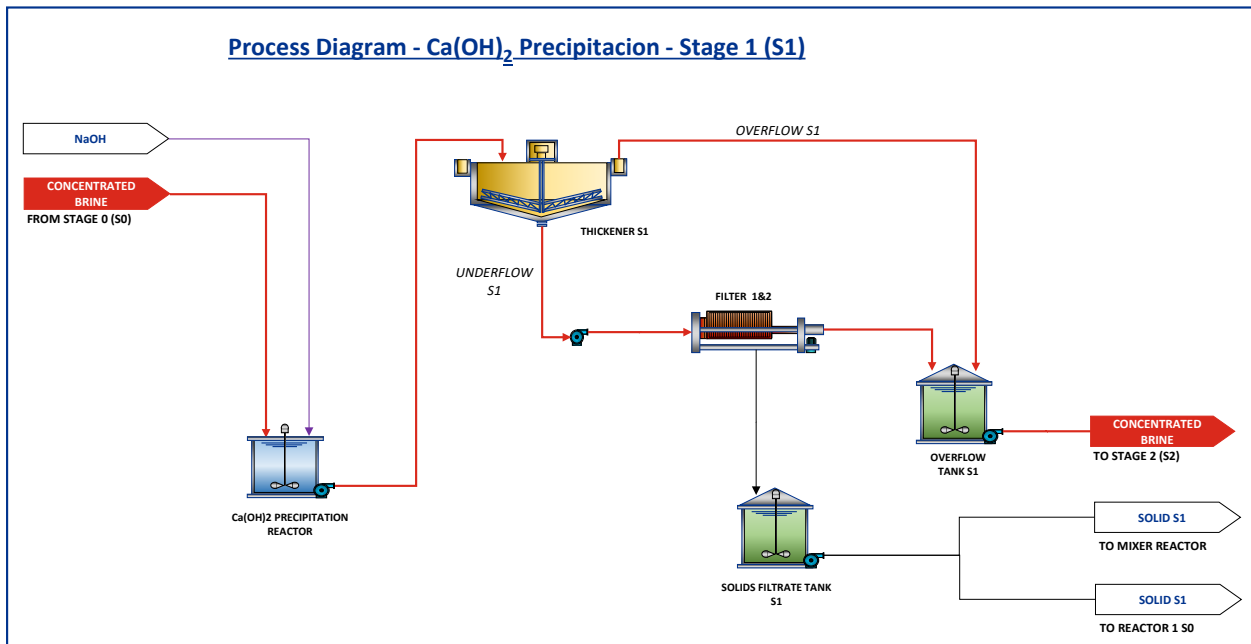


Figure 17-6: Stage 1 – Ca(OH)₂ Precipitation.

17.3.1.4 Stage 2 – CaCO₃ Precipitation

To remove any remaining contaminants within the brine, a final polishing stage is carried out in Stage 2. This step is also known as the calcium carbonate (CaCO₃) precipitation stage. In this stage, brine from Stage 1 will be fed to an agitated reactor. A Na₂CO₃ solution prepared at a 28% is added. The elevated preparation temperature is required to prevent precipitation problems for this reagent. In this reactor, brine from the previous stage, and a soda ash solution will be mixed, precipitating CaCO₃ solids. This stage is carried out at ambient temperature.

Brine with precipitated solids will then be pumped to a thickener, where the overflow (Ca free brine) will be sent directly to the next stage of the Plant. The underflow will be recirculated to Stage 0, substage A, to act as a filtering aid in the process, and to be finally eliminated from the process through the filtration equipment in that stage.

The Ca free brine will be sent to the next area of the Plant, Stage 3. A general scheme of Stage 2 is presented in Figure 17-7.

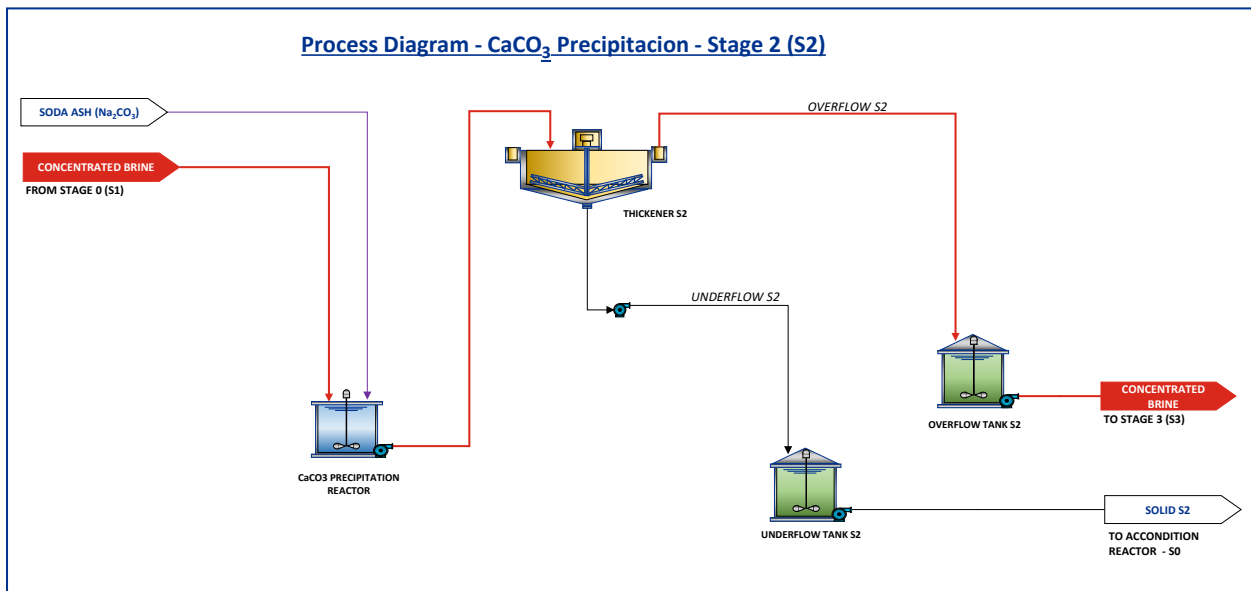


Figure 17-7: Stage 2 – CaCO₃ Precipitation.

17.3.1.5 Stage 3 – Li₂CO₃ Precipitation

Purified concentrated lithium brine from Stage 2 will then be fed to Stage 3, also known as the lithium carbonate (Li₂CO₃) precipitation stage. In this stage, the process must occur at 70°C, to facilitate lithium carbonate precipitation. For this process, inlet brine temperature must firstly be increased to 70°C, through heat exchangers, which will use hot water as the heating agent.

Heated brine, at 70°C, then feeds a circuit of mixing reactors, which operate in series, to allow accurate residence time of the brine, in each reactor, thus allowing proper formation of Li₂CO₃ precipitated solids. A heated soda ash solution, also at 70°C, and with a concentration of 28%, will also be fed to each chemical reactor, where the dissolved Li in the brine reacts with the soda ash solution and precipitates lithium carbonate.

Brine with precipitated Li₂CO₃ will then be fed to a hydro cyclone battery, reducing the water content of the precipitate slurry. Then the hydro cyclone underflow will be fed to peeler centrifuges, which allow both washing of the solids, as well as reduction of their moisture content, generating lithium carbonate with a 15% moisture. These solids will then be fed to the final stage of the Plant, the Drying and Packing area.

Liquids removed from the lithium carbonate in this stage, are defined as mother liquor, and are mainly reused within the process due to their high carbonate content. If there is any excess mother liquor that cannot be reused, it is discarded and pumped directly to specific mother liquor discard ponds.

A general scheme of Stage 3 is presented in Figure 17-8.

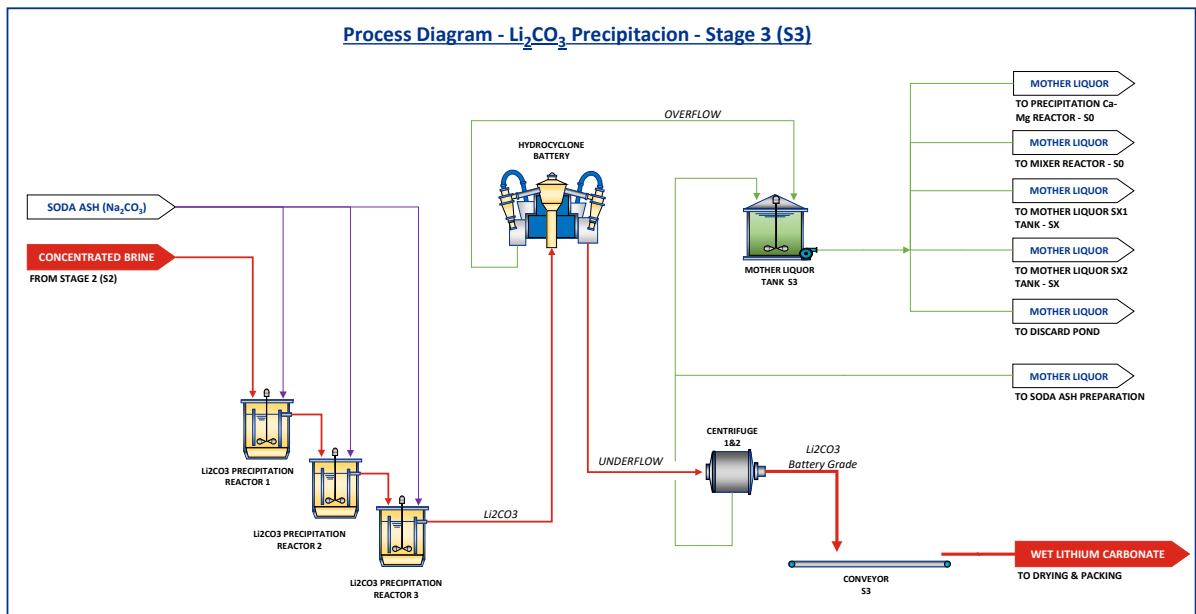


Figure 17-8: Stage 3 – Li₂CO₃ Precipitation.

17.3.1.6 Drying and Packing

The final stage of the lithium carbonate plant considers a direct-fired rotary dryer, a rotary tube cooler and a maxi bag filler. Lithium carbonate with a 15% moisture content feeds the rotary dryer, obtaining a final product with a 0.3% moisture content. Outlet temperature of the final product from the rotary dryer is 140°C. This temperature must be reduced to 40°C, to avoid damaging the maxi bag material, hence a rotary tube cooler is included. Final product transport, in this area, will be carried out through pneumatic transport. An automatic maxi bag filler is required for packing all the lithium carbonate. All filled maxi bags will then be sealed, and transported to the final product warehouse, for subsequent transportation to the market. A general scheme of the drying and packing stage is presented in Figure 17-9.

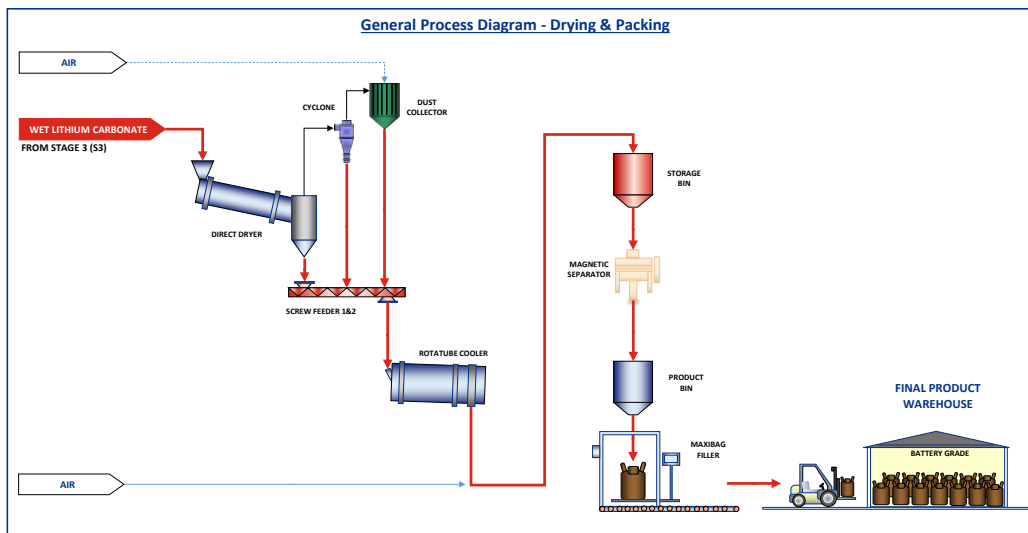


Figure 17-9 Drying and Packing.

17.3.2 Reagents for the Process

As described above, the process requires a series of reagents to obtain the final product, namely battery grade Li_2CO_3 . The main reagents used in the process are sodium carbonate (Na_2CO_3) and sodium hydroxide (NaOH), with a consumption of approximately 54,000 tonnes/year and 30,000 tonnes/year respectively.

17.3.3 Water for the Process

Water will be required in the process for different tasks, such as reagent preparation, final product washing, among others. The Plant design considers using the following types of water:

- **Industrial water:** This resource will be obtained directly from the water well. Industrial water is mainly used to feed the Water Treatment Plant, as well as other smaller uses, such as filtering equipment washing.
- **Treated industrial water:** This input will be generated at a Water Treatment Plant, and will be used mainly for reagent preparation, final product washing, among others. This water will be obtained, mostly, through reverse osmosis.
- **Process water:** This feed is water generated in the process and is reused within different stages of the Plant. Some examples of process water are: RO plant reject, which will be used mainly used as dilution water for the evaporation ponds; mother liquor generated can be used for soda ash preparation; and other smaller water recirculation.

Industrial water consumption for the Fiambalá Site will be from a water well, which is estimated at 10.07 L/s. For the Salar Site, industrial water will come from water catchments located by Rio Zeta and Escombrera, and the estimated consumption will be 3.79 L/s

17.3.4 General Equipment Cleaning

Brine is the main raw material used in this process, both at the Salar Site and the Fiambalá Site. Due to the high ion content within the brine, and its saturation point, it is necessary to include cleaning and/or washing equipment, in different stages of the process. Each area will require different types of cleaning/washing, described as follows:

- 1) **Evaporation ponds:** scaling is generated both in evaporation ponds transfer pumps and pipelines. This is due to the brine being saturated with different salts, which tend to adhere to different surfaces.
In the pre-concentration ponds, scaling (from NaCl and KCl salts) will be controlled and reduced through the use of continuous dilution water for each transfer pump. at a rate of 1.0% of the flow that is being transferred by the pump. This will produce a small dilution of the brine but will result in reduced scaling and incrustation within pumps and pipelines.
In the concentration ponds, scaling will also occur in pumps and pipelines, but since the precipitated salt is mainly CaCl_2 , it can easily be removed with periodic washes, with industrial water. All pumps from this area will have specific piping connections, to allow washing campaigns.
- 2) **Lithium carbonate Plant:** brine can also generate scaling inside the equipment and pipelines of the Li_2CO_3 Plant; hence they must be periodically cleaned through acid washing. This acid washing will be carried out with a sulphuric acid solution, at a concentration of 18%, and washing campaigns will be defined according to the operational area requirements, and analysis of scaling growth,

inside each item of equipment. The used solution, generated after equipment cleaning, will be sent directly to the discard ponds.

17.3.5 Solid Discard Management

The types of solid discards generated from the process are as follows:

- Salar Site:
 - Harvested salts from the pre-concentration ponds: These that consist mainly of NaCl and KCl. Salts discards will be harvested periodically, according to a harvesting schedule defined by the operational area. Then, they will be trucked to a stockpile, to be stored in areas specifically defined for each of these salts.
 - CaCl₂ salts from the Crystallization Plant: These will be generated from the polishing filters and centrifuges from the plant. These salts will be dumped, from each centrifuge, to a transport belt, and then will also be trucked to their final stockpile.
- Fiambalá Site:
 - Solid discards from the Lithium Carbonate Plant are mainly impurities removed from Stage 0 of the process and contain a mixture of Mg(OH)₂/NaCl/CaCO₃ and Ca(OH)₂/CaCO₃. These solids will be transported by truck and stockpiled accordingly.

All solid discards are to be disposed of according to all environmental requirements

18. Project Infrastructure

18.1 Area and Facilities

18.1.1 General Overview

The 3Q Project includes development of 3 main areas: the 3Q Salar Site, the Access Road and the Property available in the Industrial Park of Fiambalá. The following sections present a more detailed description of all project installations, located both on the Salar and the Fiambalá sites.

18.1.2 Salar site – Wellfield, Evaporation Ponds, and Industrial Facilities

As mentioned before, the brine extraction wells, the evaporation ponds and the crystallization plant will be located on the Salar site. Main physical areas and installations specified for the project are presented in Figure 18-1. These can be described as follows:

- A Brine Wellfield area will be set on the north side of the Evaporation Ponds. Each well will be located according to the hydrogeological studies carried out for Project 3Q.
- Some of the brine extraction wells will be located on the berms of the evaporation ponds.
- Industrial water catchment areas are to be located alongside the Rio Escombrera and Rio Zeta.
- All pre-concentration evaporation ponds will be located on top of the 3Q Salar. These ponds are designed and sized for the final production of 20 kTPY of lithium carbonate, battery grade.
- All concentration evaporation ponds, to be located south-east of the pre-concentration ponds, on top of the 3Q Salar, designed for the same requirements.
- A Crystallization Plant, to be located south-east of the concentration ponds, beside the 3Q Salar and within the Project's tenements.
- Salt and process solid discards areas, which will be located according to environmental requirements.

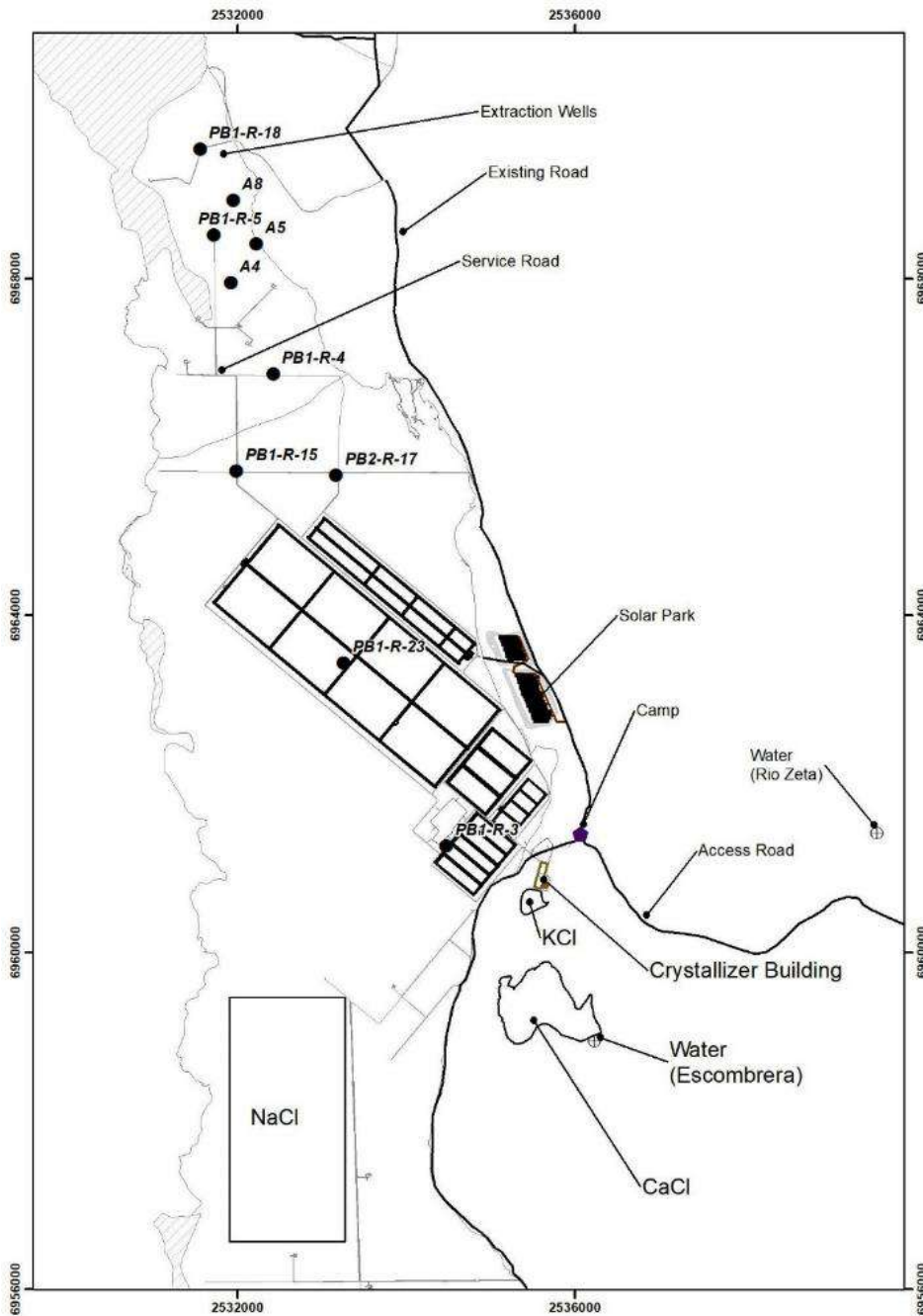


Figure 18-1: Main installations for the salar site.

18.1.2.1 Brine Wellfield

Brine wells will normally operate continuously at their average capacity, but, depending on brine processing requirement variation, due to seasonal changes, some wells may be taken off operations. It is expected that, in the summer season, all brine wells will be operating at their average capacity, while in the winter season, fewer wells will be needed to meet brine process requirements.

All brine extraction wells will be equipped submersible pumps with variable speed drives. They will be electrically fed from an electrical network that originates at a thermal electrical generation plant and at a photovoltaic generation plant, both described in more detail in section 18.2.2.6 of

this document. Flow from each well will be measured and controlled through in place instrumentation. Brine will be pumped from each brine extraction well through independent pipelines to both pre-mixing ponds, to then feed each string of the pre-concentration ponds.

18.1.2.2 Pre-concentration Evaporation Ponds

Pre-concentration (PC) evaporation ponds will be fed from two pre-mixing ponds that are fed from the brine extraction wells. Production of 20 kTPY of lithium carbonate requires a PC pond area of approximately 449.1 ha.

As a summary of description of evaporation ponds in Chapter 17, there will be two types of PC ponds, as is described below:

- PC ponds: in these, the main salt that precipitates is NaCl. These ponds are fed from two pre-mixing ponds through open channels, so pumping will not be required at this point. The PC ponds have a larger area and consider two strings operating in parallel. Each string considers a larger pond, divided by baffles into four smaller ponds, so brine will flow freely between the smaller ponds, at a controlled rate. At the end of the fourth pond of each string, brine will be pumped to the next type of ponds, defined as K ponds.
- K ponds: In these ponds the main salts that precipitates are for NaCl/KCl. K ponds have a smaller area than the PC ponds and are built with the same considerations as the PC ponds. They consider two strings operating in parallel, and each string considers a larger pond, divided by baffles into four smaller ponds. At the end of the fourth pond of each string, brine will be pumped to the mixing ponds, that are the start of the concentration stage ponds.

Design of all ponds considers surface leveling. Pond berms will be built with material from the area. Waterproofing of the base and sides of the ponds is required to prevent brine infiltration, thus, a liner layer, with a geomembrane and a geotextile material, is included in pond design.

As mentioned in section 17 of this document, it is required that salts that precipitate at the bottom of the pre-concentration ponds be harvested periodically, according to a schedule determined by salt precipitation rate, as well as pond depth. Harvested salts will then be transported to a salt stockpile area.

18.1.2.3 Concentration Ponds

As described in section 17 of this document, the next stage of the process includes both the concentration ponds and the Crystallization Plant, since the process requires five stages that operate in series between the concentration ponds and the plant.

Brine from the pre-concentration ponds is firstly fed to the mixing ponds, which consist of two ponds that operate alternately, to homogenize the brine from both pre-concentration strings, allowing a uniform brine to be fed to the first stage of the concentration ponds. These ponds will be located contiguous to the last K pond. From the mixing ponds, brine will be pumped to the first pond of each string of the concentration ponds.

The concentration ponds will be located southeast of the PC ponds. These ponds will operate by stage and operate alternately with each stage of the Crystallization Plant (for more details, refer to section 17 of this document).

Both the first stage, and the second stage of the concentration ponds, consider three ponds that operate in parallel, one pond always being in harvesting stage and the other two ponds in operational (evaporation) duty. The third, fourth and fifth stages of the concentration ponds consider two ponds each. These operate in parallel and will be harvested according to the schedule for this process.

The fourth stage of concentration ponds requires the addition of hydrochloric acid (HCl) for its process. HCl will be brought from the Fiambalá Site. This reagent will be stored in tanks located next to the fourth stage concentration ponds, to shorten reagent pipelines. HCl tanks will consider all safety measures required for this reagent.

Since each concentration pond stage will operate alternately with the Crystallization plant, pumping is needed at the outlet of each concentration pond. All pumps will be fed from the same electrical network as the pre-concentration ponds.

18.1.2.4 Crystallization plant

The Crystallization Plant will be located south-east of the concentration ponds. According to the description of this area in section 17 of this document, this plant will be fed with brine from each stage of concentration ponds, to remove the Ca present in the brine as CaCl_2 . This plant will consist of five stages, all of them being housed in the same building.

18.1.2.5 Dispatch Ponds

Concentrated brine, produced at the fifth stage of the Crystallization Plant, will be pumped to the dispatch ponds, for final storage. The Project considers the use of two dispatch ponds, located next to the Crystallization Plant. These ponds are smaller in area than the concentration ponds and will be covered with a liner to avoid additional water evaporation from the brine. Concentrated brine from these ponds will be pumped onto special purpose trucks for transportation to the Fiambalá site. Truck loading installations will be located next to the dispatch ponds. These ponds can also act as a buffer, for expected process seasonal flow changes from the evaporation ponds.

18.1.2.6 Electrical sources for the Salar Site

Electrical power for pre-concentration ponds, concentration ponds, crystallization plant, dispatch ponds and all ancillary installations will be distributed through a network to be fed from both a thermal electrical generation plant, and a photovoltaic (solar) generation plant to be built in the Salar.

Installed photovoltaic generating power will be 4 MWh. Thermal generation (LNG fueled) will provide the electrical energy required during night or when solar energy is not sufficient.

18.1.2.7 Salar Site Internal Roads

Project design includes internal roads for this complete area. These roads will connect the pre-concentration ponds, concentration ponds, the crystallization plant, as well as the salt stockpiles and all other ancillary installations in this site. In the evaporation ponds sector, internal roads will be used as operational and maintenance vehicular roads, and for truck circulation, during pond harvesting activities. The rest of the internal roads within the Salar site, will be used by operational vehicles, reagent, and concentrated brine truck circulation, among other uses. Roads will also consider pedestrians circulation where required, for monitoring and maintenance activities. Roads will also be connected to the access control and workers camp area.

18.1.2.8 Industrial Facilities for the Salar Site

Main permanent facilities to be built at the Salar site are as follows:

- Process installations:
 - Pre-concentration ponds
 - Concentration ponds

- Crystallization plant (which include all defined equipment: crystallizers, polishing filters, centrifuges, chiller)
- Dispatch ponds and truck loading area
- Process Ancillary Services:
 - Compressed air generation, storage and distribution
 - Industrial water treatment plant for production of soft treated water
 - Hydrochloric acid storage and distribution
 - Electrical generation and distribution (thermal and solar)
- General Ancillary Services
 - Truck and lightweight vehicles workshop
 - Access control station
 - Truck scales
 - Truck parking area
 - Wastewater treatment plant
 - Workers camp installations
 - Canteen/kitchens
 - Laundry rooms
 - Dining rooms
 - Common rooms (recreational activities)
 - Emergency fire stations, plant fire system
 - Polyclinic (first aid area)
 - Fuel storage and distribution stations
 - Non-hazardous and domestic industrial waste management areas
 - Hazardous waste area
- Temporary installations
 - Contractors camp installations

All permanent facilities, as well as temporary facilities, are presented in Figure 18-2. Additionally, Figure 18-3 shows more details on the workers camp installations (capacity 354 persons), and Figure 18-4 shows the contractors camp installations (capacity 214 persons) people. Both the contractors and the workers camps will be built in stages, based on the construction and production schedule for the Project.

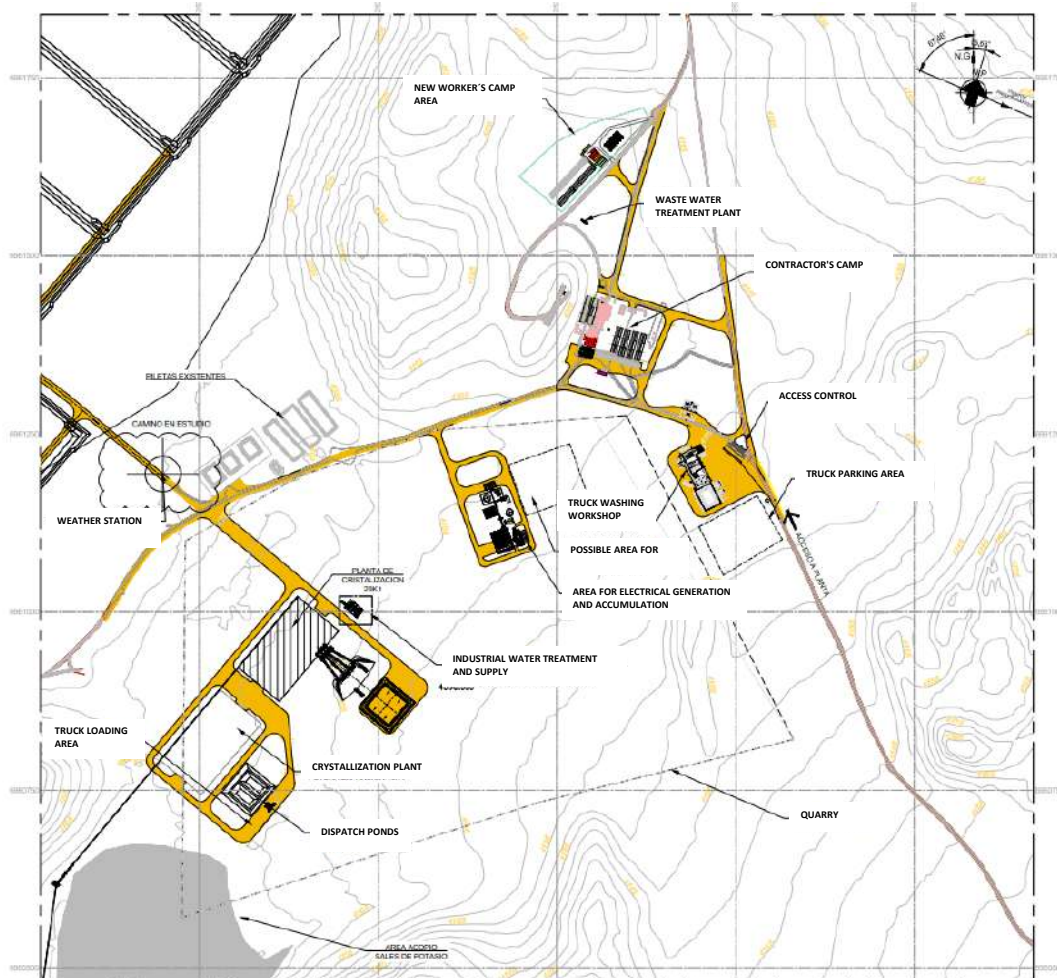


Figure 18-2: Salar site – main installations.

18.1.2.9 Permanent Industrial Facilities for the Salar Site

Workers Camp (Construction Camp and Operations Camp)

Main facilities that will be considered for both the workers camp and the constructor camp which include installations such as dormitories, dining room, recreational areas, among others.

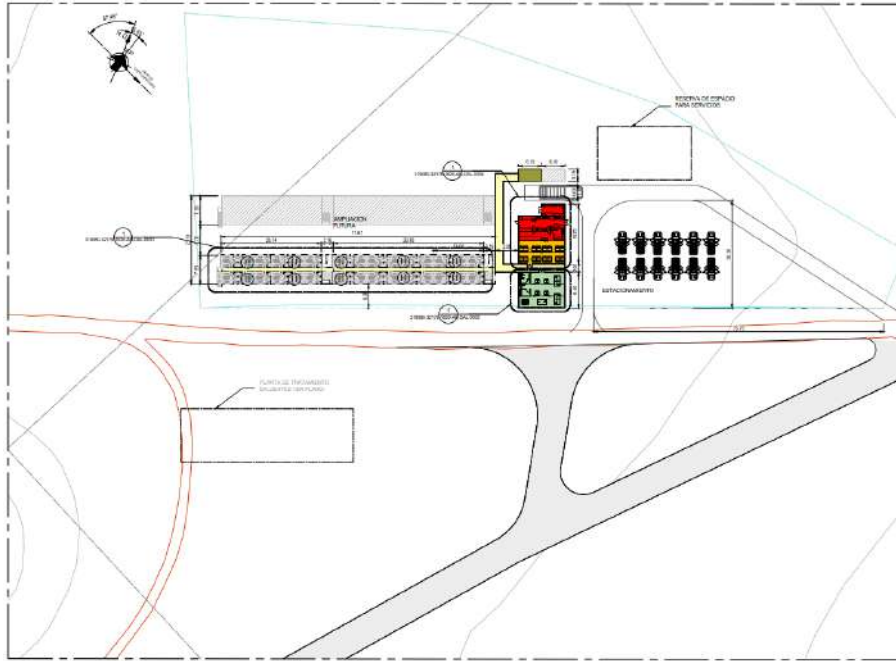


Figure 18-3: Salar site – workers camp.

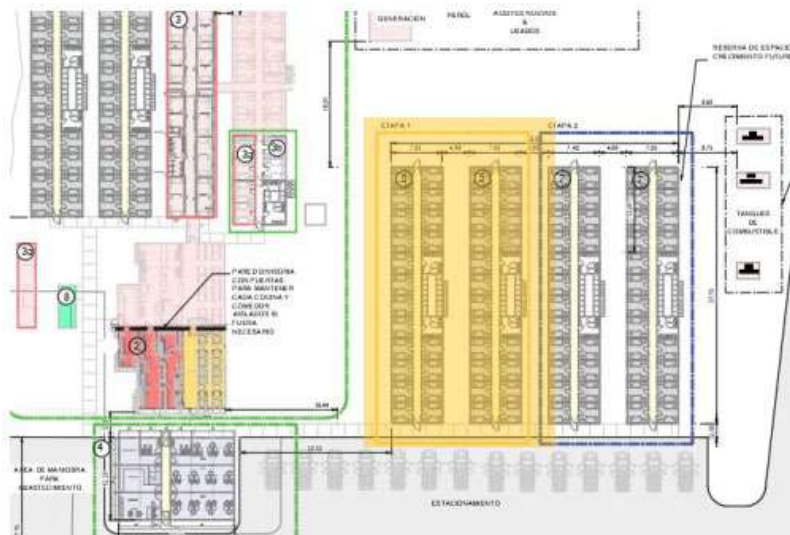


Figure 18-4: Salar site – contractor's camp.

HCl Storage and Distribution

The only reagent required by the process at the Salar site is HCl, which is received in liquid state at the plant, and must be stored in tanks complying with this reagent's requirements. Parapets are considered around the storage tanks to contain any spillages. This reagent will be used in the process in the same concentration as it is received from the supplier, thus only distribution pumps are considered for this purpose.

Compressed Air Storage and Distribution

The Crystallization plant requires dry compressed air for its process and instrumentation. A complete compression and distribution system is considered for the Site, and an independent system is considered for the Truck workshop.

Industrial Water Treatment Plant

As mentioned before, industrial water required by the Salar site process will be obtained from the Zeta and Escombrera rivers. This water will be directed to two industrial water tanks, and there on pumped to all required areas. It is estimated that the industrial water consumption in the Salar site will be 3,79 L/s.

The following types of water will be used on the Salar Site:

- Industrial water: Obtained as indicated above. This water will be used in processes where there are no special requirements of water quality. Some applications for this type of water are:
 - Pump washing water
 - Evaporation ponds pump dilution water (if required).
 - Water treatment plant feed.
- Treated Industrial Water: also known as soft water produced by the treatment plant. This type of water is required by specific processes of the crystallization plant, as well as for sanitary uses.
- Clean potable water to be used in the Salar site sanitary system, including changing rooms, dormitories, offices, camps, among others. Clean, or sanitary water will not be potable.
- Water used for drinking purposes will be obtained from authorized companies, who will transport this water to the plant periodically and feed the potable water tanks.

Electrical Substation and Generator Plant

As previously mentioned, electrical energy for the Salar Site will be provided by thermal and photovoltaic generation. Power will be distributed to the different areas of the Site through an aerial network. If there are major restrictions for aerial, underground distribution will be used. It is estimated that the electrical power required for the Project on the Salar Site will be approximately 4 MWh.

Control Rooms

Control rooms are considered for the crystallization plant. They will be housed in the interior of the industrial buildings, including accommodation for the operators during working hours (heating, restrooms, potable water, etc.).

Ancillary Services

Ancillary facilities are required for the Salar Site of the Project, as follows:

- Access control area, which includes the main entrance to the plant, control office, luggage control room, restrooms and vehicle parking area.
- Truck scale for all cargo vehicles that enter or leave the site.
- Truck workshop to provide maintenance services to all the site vehicles, including salt removal equipment. This facility will include all workshop standard areas, such as storage places, mechanical and electrical workshops for vehicle maintenance, waste yards, and a sludge degreasing treatment for all wastewater generated within the shop.
- Wastewater treatment plant (WWTP) for processing wastewater generated at restrooms, bathrooms, camp kitchens, among others.

- Fire protection system, including an industrial water storage tank and pumps system (electrical and diesel) that feed the plant's wet network, all in compliance with NFPA's standards.
- Diesel fuel storage and distribution stations to feed all site's vehicles (lightweight vehicles, harvesting trucks, operational trucks, vans, buses, and heavy equipment required by the project during construction and operation). Diesel fuel will arrive at the site via tanker trucks, and it will be stored in a tank battery. The tanks will then feed the diesel distribution station, to provide fuel to all vehicles. All safety measures required regarding design and operation of the fuel storage facility will be considered.
- Polyclinic, or first aid medical centre, is required to provide first aid to the site's personnel. Design of this area will be in accordance with health/medical regulations. A qualified health professional will be responsible for this area.

Temporary Installations

Temporary installations are required for the construction of the Project. These will be sized based on the Project's construction phase requirements.

Contractor's Installations

These are the facilities required for the workers that will construct the plant and the Salar installations. They will be located in the area presented in Figure 18-2, and will include, at least, the following:

- Contractors Offices
- Warehouses
- Workshops
- Storerooms
- Worker's camp
 - Dining rooms
 - Dressing rooms
 - Sanitary facilities
- Concrete plant
- Non-hazardous and domestic industrial waste management areas
- Hazardous waste area
- Other facilities

18.1.3 Fiambalá Site – Industrial Facilities

Concentrated brine will arrive on dedicated tanker trucks to the Fiambalá Site. All installations at this site will be permanent since no workers or contractors camp will be required due to the proximity of this installation to the town.

Main installations for this site are as follows:

- Lithium Carbonate Plant, which includes all operations and processes to obtain battery grade lithium carbonate.
- Discard stockpile

- Mother liquor and SX discard ponds
- Ancillary installations that support the Lithium Carbonate Plant.

These installations will be described in detail in the sections below. A general overview of them is presented in Figure 18-5.

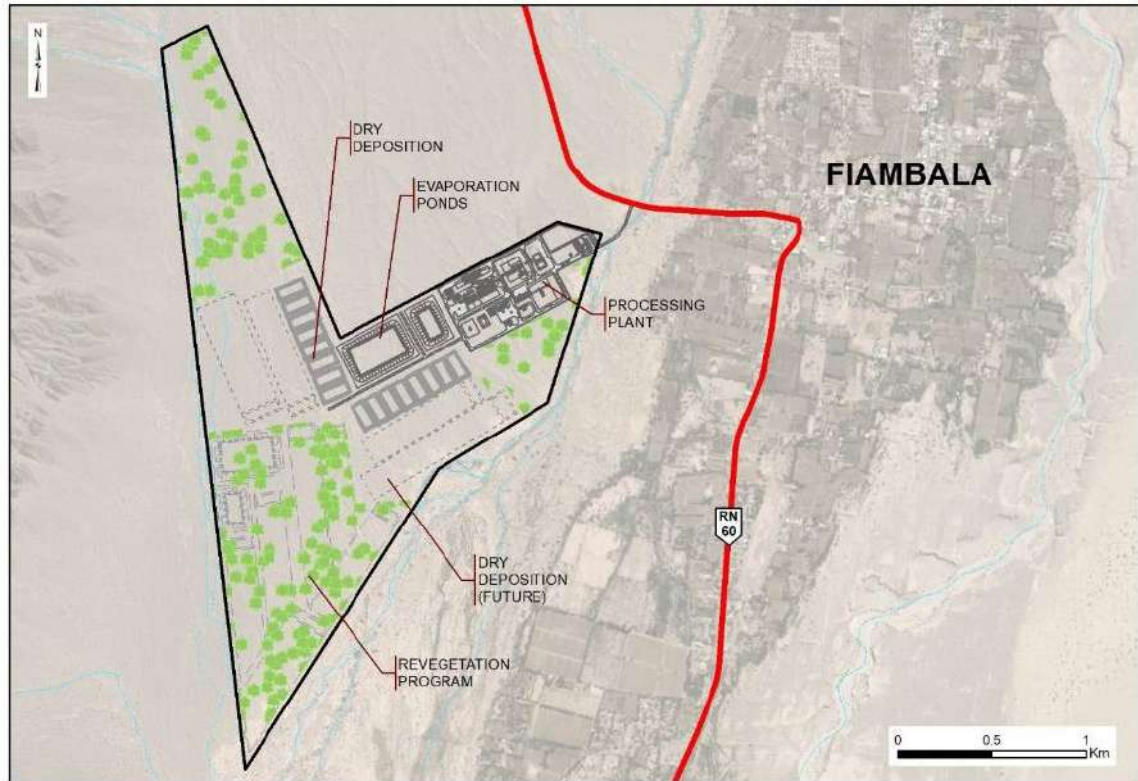


Figure 18-5: Fiambalá site – general installations.

Trucks with concentrated brine will arrive to the site through route 60, from the north, and after passing the access control, will reach the reception ponds to unload the brine feeding the plant.

A more detailed view of the Fiambalá site is presented in Figure 18-6 below, which will be described in detail in Section 18.1.4). The plant also contains all ancillary services that will support the production of lithium carbonate.

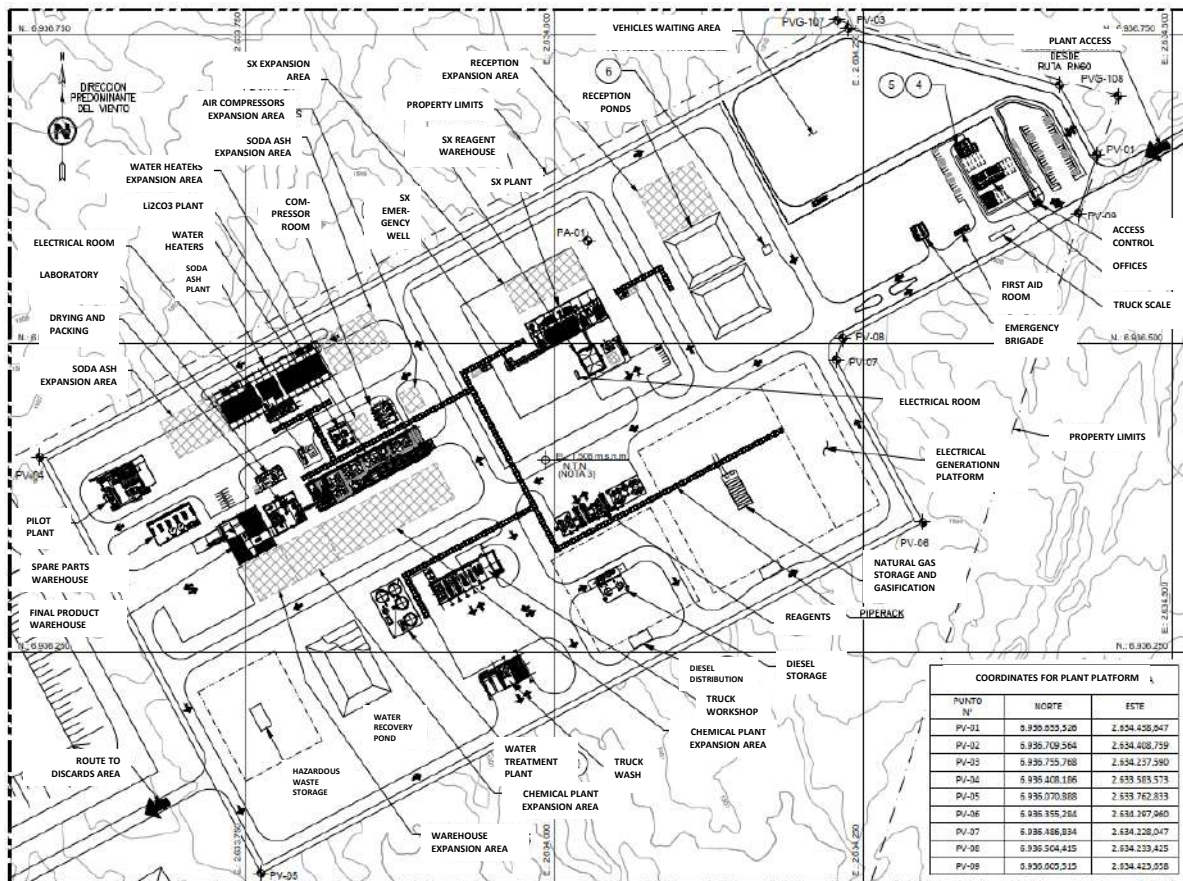


Figure 18-6: Fiambalá site – plant installations.

As described in section 17 of this document, the Lithium Carbonate Plant consists of a series of production stages, designed to obtain battery grade lithium carbonate at the end of these processes. The main stages or sub-areas considered within the lithium carbonate plant are:

- Solvent extraction (SX)
- Chemical Plant, including the following areas:
 - Calcium-magnesium removal
 - Calcium hydroxide removal
 - Calcium carbonate removal
 - Lithium carbonate precipitation
- Drying and packaging and final product warehouse: At these installations, lithium carbonate will be dried, packaged and stored

18.1.4 Permanent Facilities in the Fiambalá Site

The following installations are considered in the Project's industrial area:

- Main process installations: all installations that are directly related to the production of lithium carbonate, such as:
 - Reception Ponds
 - Lithium Carbonate Plant (including control rooms)

- Process Ancillary Services: all installations that support or feed the main process directly, as follows:
 - Reagent storage and preparation
 - Soda ash (Na_2CO_3)
 - Caustic soda (NaOH)
 - Hydrochloric acid (HCl)
 - Sulphuric acid (H_2SO_4)
 - SX reagents
 - Compressed Air generation, storage and distribution.
 - Industrial water treatment plant for production of soft treated water
 - Water recovery pond
 - Water heaters area
 - Electrical generation through generators (only for emergencies, the main electrical source will be the electrical network from Tinogasta town, through a dedicated supply line).
 - Natural gas storage and gasification area
 - Connection to electrical network

- General Ancillary Services: all installations that are required within the plant for its operation, but do not feed/support the process directly, which are:
 - Truck and lightweight vehicles workshop (including washing area)
 - Access control station
 - Administration building (offices)
 - Truck scales
 - Truck parking area
 - Laboratory
 - Wastewater Treatment Plant
 - Warehouses (final product, hazardous waste, spare parts, others according to plant requirements)
 - Emergency fire stations, fire system plant
 - Polyclinic (first aid area)
 - Fuel storage and distribution stations (for trucks and lightweight vehicles)
 - Non-hazardous and domestic industrial waste management areas
 - Hazardous waste area

All installations will be located on the plant platform and may be seen in detail in Figure 18-6. More details of the installations are presented below.

18.1.4.1 Reagent Storage Preparation

The reagents that are required by the process are received in solid or liquid state and, accordingly, must be stored in warehouses or tanks. Each reagent will be prepared, if required, in individual plants that include all operations to generate a reagent with the characteristics that are required by the process.

Tanks for all liquid reagents will include parapets to contain spillages. All reagents that are stored as solids inside warehouses will consider the required distance between them, as well as containment pits, to control potential spillages. Reagents will be stored in areas according to their chemical properties

18.1.4.2 Compressed Air Storage and Distribution

To comply with the requirement of process and instrumentation of dry compressed air, a complete compressor and distribution system is considered for the Project. Additionally, an independent compression system is considered for the Truck workshop.

18.1.4.3 Industrial Water Treatment Plant

Industrial water required by the process, at the site, will be extracted from industrial water wells located near the plant in Fiambalá. From the well, two industrial water tanks will be fed, then from these tanks, water will be pumped to all required areas. It is estimated that the industrial water consumption for the complete process in Fiambalá) will be 10.07 L/s.

The following types of water will be used for the Project:

- Industrial water: To be obtained directly from the water wells. This water will be used in processes where there are no specific requirements for water quality. Some applications of this type of water are in:
 - Equipment washing, especially filters considered inside the lithium carbonate plant and for reagent preparation.
 - Sulphuric acid dilution. The resulting solution will be used for plant equipment washing. This process is carried out periodically, when equipment scaling must be removed.
 - Feed for the Water Treatment Plant, to generate treated industrial water (soft water).
- Treated Industrial Water: Soft water obtained from the Water Treatment Plant, and which is required by specific processes of the Lithium Carbonate Plant. Some applications for this type of water are:
 - Reagent preparation
 - Final product washing
 - Water heater make-up
 - Clean water production
- Clean Water to be used in the complete sanitary system of the Fiambalá Site (changing rooms, dormitories, administrative building, offices), and will not be potable. Potable water will be obtained from authorized companies, who will transport this water to the plant periodically and feed the potable water tanks.

18.1.4.4 Electrical Substation and Generator Plant

Electrical energy for the Site will be provided by a connection to the area network, through a substation located within the plant. This source will be backed up by local gas engine driven

generation, to support critical process equipment in an eventual electrical supply interruption. From the substation, electrical energy will be distributed to the different areas of the Site through an aerial network. If there are major restrictions for aerial, underground distribution will be used. It is estimated that the electrical power required for the Project on this site will be 2.68 MWh.

18.1.4.5 Hot Water Generation and Distribution

Hot water heaters are considered for the Project, to provide this element for the heat exchangers, as well as for final product washing. Two hot water heaters that operate in parallel will be installed inside a specific area (see Figure 18-6 for location).

18.1.4.6 Control Rooms

Control rooms are considered for the installation, with the main such room being located at the Lithium Carbonate Plant. All control rooms are included in the interior of the industrial buildings and consider accommodations for the operators during working hours (heating, restrooms, potable water, among others). Figure 18-7 presents the control room defined for the Lithium Carbonate Plant.

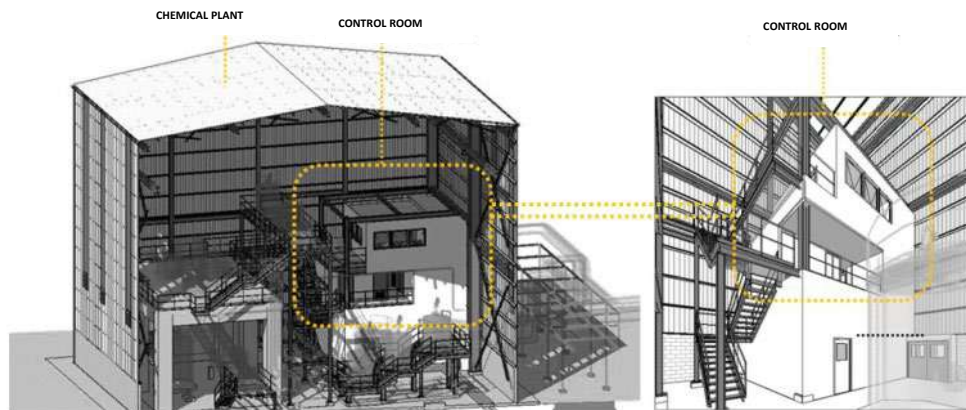


Figure 18-7: Fiambalá site – control room for the Lithium Carbonate Plant.

18.1.4.7 General Ancillary Services

Additional ancillary facilities are required for the Project, as follows:

- Access control area, similar to the Salar site, and including the main entrance to the plant, a control office, a luggage control room, restrooms and a vehicle parking area. Figure 18-8 presents a general 3D projection of the access and control area.



Figure 18-8: Fiambalá site – plant access.

- Offices required for the plant’s administrative personnel, including a cafeteria for the personnel and a parking area. Figure 18-9 presents an illustrative 3D projection of how the outside of the plant.



Figure 18-9: Fiambalá site – offices.

- Laboratory for process quality control. It will include all equipment required for chemical analysis of brine and solid samples, particle size analysis, moisture analysis, among other services. Measures of these variables provide information for proper operation of the process, as well as ensuring the final quality of the product. Figure 18-10 presents a general 3D projection of the laboratory building.



Figure 18-10: Fiambalá site – laboratory building.

- Truck scale for all cargo vehicles that enter or leave the site.
- Truck Workshop to provide maintenance services to all vehicles of the plant. This facility will include all standard areas for a workshop, such as storage areas, mechanical and electrical workshops for vehicle maintenance, waste yards and a sludge degreasing treatment for all wastewater generated within it.
- Wastewater treatment plant (“WWTP”) for the treatment of all wastewater generated at the workshop.
- Fire protection system, including an industrial water storage tank and pumps system (electrical and diesel), that feed the plant’s wet network, all in compliance with NFPA’s standards.
- Diesel fuel storage and distribution stations, to feed plant construction and operational vehicles. Diesel fuel will arrive on tanker trucks and will be transferred to the storage tanks. The fuel tanks will then feed the distribution station serving all vehicles. This installation will be built accordingly to required safety measures.
- First aid centre, designed to provide primary help to the personnel with regards to emergencies or accidents that may occur in the site. Only a small centre is required in this Site, since the town’s hospital centre is nearby. The internal distribution of this centre will be according to health/medical regulations, and a qualified health professional will oversee this area.

19. Market Studies and Contracts

19.1 Benchmark Mineral Intelligence Market Study

In August 2021 the Company engaged Benchmark Mineral Intelligence (“BMI”) to complete a comprehensive analysis of the lithium market including current and future demand, current and future supply, and related lithium pricing forecasts. In September 2021 BMI provided an updated report reflecting changing markets for lithium carbonate. This report is summarized below and located in its entirety in Appendix H.

19.1.1 Lithium Demand

Lithium-ion batteries have become the dominant battery technology for use in Electric Vehicles (EVs), as well as consumer electronics and stationary grid storage. This dominance is likely to continue given the level of investment in lithium-ion battery cell capacity being undertaken at present versus other battery technologies. The primary reason for this is the high-energy density of the technology—crucial where space and weight are a factor—its low maintenance requirements, and the fact it is relatively economic compared to other battery technologies at present.

The majority of lithium bearing minerals are sold into the chemicals sector to produce lithium carbonate or hydroxide. This market is widely forecast to see sustained growth over coming decades as the electric vehicle market increasingly displaces internal combustion engine (ICE) vehicles.

There is an ongoing need for capacity investments in lithium raw material extraction, chemical processing, and cathode manufacturing throughout the life of our forecast to 2040. Given the direction of travel and level of investment in the downstream of the electric vehicle supply chain, at an auto-manufacture and battery cell level, there is an impending shortfall in the midstream supply chain which needs to be addressed.

The level of financing needed to bridge this gap is relatively small compared to the investment being made in vehicle and battery cell manufacturing, so we feel it is highly likely that actors in these areas of the supply chain will take steps to ensure supply availability.

19.1.2 Lithium Supply

Global lithium supply is currently consolidated among a small number of producers. This is forecast to change in coming years, however, as a raft of new brine and hard-rock deposits progress from development stage through to production.

Lithium raw material projects in jurisdictions close to or in areas of future high demand, namely Europe and North America, are at a distinct advantage in terms of potential for development. This arises from an imbalance in the geography of supply towards Latin America and Asia, including Australia. Battery cell manufacturers are planning capacity investments closer to where their key customers—automotive manufacturers—are located.

These consumers will wish to source at least part of their supply from local sources. This will cut down on lead times—an increasingly important factor given the larger market share of lithium hydroxide, which has a limited shelf life—reduce freight costs, and minimize default risks. There is also likely to be decreased jurisdictional risk by having less concentrated supply, and localised raw material supply will aid optimal and cost-efficient procurement practices within the value chain.

The resulting supply demand balance for mined lithium indicates a significant short to medium term deficit of lithium supply in the market.

19.1.3 Lithium Costs

Lithium is sourced from either brine operations or those generically described as hard rock, with the balance of supply moving towards brine over time. Most of the world's brine capacity is in Latin America, with some production from China. Hard-rock supply is more widely spread geographically, with Australia a major supplier.

Total cash costs for lithium carbonate and hydroxide production range from around USD 4,500/t LCE (lithium carbonate equivalent) to >USD 9,000/t LCE over the forecast period, with hard-rock resources generally dominating the higher-cost portion of the curves. Most of the new capacity coming online in the forecast period is expected to have production costs of >USD 6,000/t LCE, which broadly puts it in the upper half of the cost curves.

For the most part, this will also be hard-rock capacity. The more expensive suppliers of this type are forecast to have production costs ranging from around USD 6,000–9,000/t LCE in 2025. By that time, brine producers should see further improvement in their cost position versus new, hard-rock market entrants. Brine producers' costs are expected to be solidly anchored within the middle of the global lithium carbonate cost curve by 2025, and by 2030 to constitute the bulk of the curve's second quartile.

19.1.4 Lithium Pricing

Benchmark's price forecast methodology considers three temporal horizons: short-term, medium-term, and long-term.

- Short-term methodology: The short-term outlook on price developments is guided by primary price research conducted by Benchmark's analysts to ascertain the current direction of market pricing.
- Medium-term methodology: Medium- and long-term pricing in commodity markets is often determined by the level at which the highest-cost producer needed to supply the market can continue to operate; for lithium this would be at a cash cost level of around USD 9,000/t LCE (2020 real terms) in 2025. This point informs the medium-term price forecast, but due to the ongoing need to incentivise new projects, market prices are likely to be well above this level. The outlook for 2022–2030 has lithium demand growth forecast to significantly outpace increases in supply. The market weakness in 2020 is projected to have added to the probability of delays in the development of projects in the possible and probable categories. Lithium prices will rise due to market deficits and the need to stimulate investment successively each year. Prices are likely to rise well above marginal production costs.
- Long-term methodology (2030–2040): There will be an ongoing requirement for new greenfield capacity over the course of the forecast period. As the lower-cost new supply comes online there will be a need for the development of higher capital cost projects over time. The outlook for 2030–2040 assumes that new capacity projects, both planned and coming online, are reduced. Based on the pipeline of announced projects, higher prices are expected to encourage as-yet-unannounced projects. This pipeline of new projects will begin to come through over the coming decade to meet rising demand. Ultimately prices will settle close to a long-term average of USD 12,110/t for lithium carbonate and USD 12,910/t for lithium hydroxide (both in real 2021 terms). At these price levels IRRs provide sufficient incentive for investment over the forecast period.

Price forecasts for lithium carbonate are presented in Figure 19-1, and are detailed in Table 19-1.

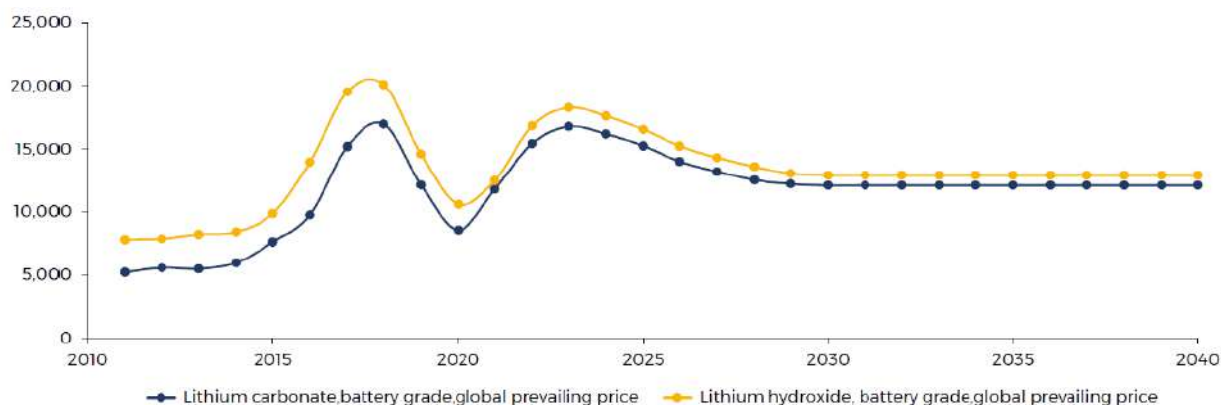


Figure 19-1: Price forecast for battery-grade lithium carbonate and lithium hydroxide, 2020 real terms (USD/MT).

Table 19-1: Price forecast for battery grade lithium chemicals, 2020 real terms (USD/MT).

	2015	2016	2017	2018	2019	2020	2021	2022	2023	2024	2025	2026	2027	2028	2029	2030
Lithium Carbonate, Battery Grade, Global																
Prevailing Price																
Real																
2021	7,633	9,752	15,198	16,979	12,147	8,553	11,800	15,445	16,790	16,200	15,250	14,015	13,209	12,538	12,229	12,110
Nominal							11,800	15,725	17,393	17,065	16,325	15,208	14,520	13,953	13,771	13,792
Lithium Hydroxide, Battery Grade, Global																
Prevailing Price																
Real																
2021	9,878	13,963	19,540	20,121	14,602	10,614	12,500	16,850	18,295	17,620	16,564	15,239	14,324	13,608	13,064	12,910
Nominal							12,500	17,156	18,952	18,560	17,731	16,535	15,746	15,144	14,711	14,703
Spodumene 6%, Australia FOB, Battery Market																
Material																
Real																
2021	647	697	783	932	620	407	649	719	720	690	669	636	616	599	588	577
Nominal							649	732	746	727	716	690	677	667	662	657
Premium Lithium Carbonate - Lithium Hydroxide																
							700	1,405	1,505	1,420	1,314	1,224	1,115	1,070	835	800

19.2 Pricing For Economic Analysis

The Economic Analysis for the 3Q Project (Section 22) utilized the Battery Grade Lithium Carbonate pricing scenario up to 2030 and extended the base price of USD 12,110 to the end of the mine life.

19.3 Contracts

As of the date of this study, the Company had not signed any sales contracts for its future production of lithium carbonate.

20. Environmental Studies, Permitting, and Social or Community Impact

20.1 Sustainability Program

The NLC sustainability program emphasizes three main pillars: Environmental, Social, and Governance (“ESG”). Following the international commitments of United Nations on Climate Change, NLC has embraced Sustainability Development Goals (“SDGs”) as a guide, seeking to create a high standard sustainable industry.

For this purpose, NLC worked with worldwide recognized specialists in Social Responsibility, international companies and local universities and chambers, Environmental consulting companies and local authorities of the province of Catamarca.

20.2 Environmental

20.2.1 Introduction

NLC hired two consulting companies to conduct environmental studies: GT Ingeniería SA (“GT”) and Servicios Integrales Mineros Catamarca SRL (“Seimcat”). GT developed the following documents:

- The Environmental Baseline Study, completed in 2018;
- The Environmental Impact Report (“EIR”) for the exploration stage, completed in 2019; and
- The first version of the Environmental Impact Assessment (“EIA”) for the exploitation stage of the 3Q Project, completed in 2019.

Seimcat completed the following documents:

- Updated Environmental Impact Report (“EIR”) for the exploration stage in 2021; and
- The updated Environmental Impact Assessment (“EIA”) for the exploitation stage, completed in 2021.

These activities are complete, and the authorities have reviewed the updated EIA and provided feedback that was incorporated is the last update of the EIA. The report is now ready to be presented in a public audience to be held on December 17, 2021, according to the Ministry of Mining, State of Catamarca, Provincial Directorate of Environmental Management Mining “DIPGAM”.

20.2.2 Permits and Authorities

Argentina has a federal system of organization, and each province owns the natural resources within its boundaries. Therefore, each province administers laws of mining procedures according to the administrative or judicial structure of the concession authority. In the case of Catamarca, all social and environmental permits for mining projects are granted by the Province of Catamarca Ministry of Mining, currently under the responsibility of Dr. Maria Fernanda Avila. The Provincial Director of Mining Environmental Management (DIPGAM), headed by mining engineer Antonella Velazco, is responsible for environmental regulations.

The following permitting activities are completed or are in process, in association with the 3Q Project:

- The initial environmental permit concerning the properties was obtained by the submission of NLC's Affidavit of non-invasive prospecting activities required by the Catamarca SEM resolution # 450/11. This affidavit indicated required initial activities in the areas under exploration. The affidavit was delivered to the SEM of Catamarca Province on April 14, 2016.
- On September 9, 2016, by resolution # 738/2016 the SEM issued its Environmental Impact Statement ("EIS"), whereby the EIR submitted by NLC for the 3Q Project was approved. This EIS permits all exploration and pre-production activities at the 3Q Project up to and including the construction of pilot evaporation ponds and pilot production plant.
- The environmental baseline study ("EBS") was presented to the environmental authorities (DIPGAM) in October 2018.
- Permits for generation of hazardous waste, management of solid urban waste, and collection of water for current tasks were renewed at the end of 2018.
- The updated exploration EIR and the response to Notification 031/18 was delivered to the SEM in July 2018. Observations and questions highlighted by the SEM were answered in December 2018 and the SEM issued its EIS in January 2019.
- An Addendum of the EIR was presented in January 2019 to authorities, for the installation of a pilot plant in the city of Fiambalá.
- The first bi-annual update of the EIR (exploration stage) was sent to SEM authorities and approved in February 2019.
- The EIA for the exploitation stage of the Project was presented to the SEM of Catamarca Province in April 2019.
- The EIA has been evaluated. LIEX responded to comments through technical meetings with the Authority.
- The next step is the Public Hearing and technical talks on the Citizen Participation process, to be held on December 17, 2021.
- The EIR for the exploration stage of the Magdalena Exploration Claim was submitted to the SEM in August 2019. The EIR is currently under review.

20.3 Environmental Baseline Studies

Overview

Environmental baseline studies ("EBS") for the Project and access road began in October 2016 and were submitted to the environmental authorities in October 2018. Both the EBS and the EIR are critical for the evaluation of environmental liabilities. These reports provide early indications of potential impacts associated with production, so that effective mitigation can be achieved through appropriate pro-active management techniques.

GT coordinated the field campaigns and basic studies for the 3Q Project EBS, including various reports of accredited professionals. GT members who took part in the EBS review and in the environmental studies include Mario Cuello (Geologist), Bernardo Parizek (Biologist), Valeria Angela (Chemical Engineer), and Pedro Alcaraz (Agronomist). Brief findings of each study are summarized in the sections below.

Climate

Climate studies based on the 3Q Vaisala weather station data, regional data, and satellite remote sensing data (IHLLA 2018a, b; Zotelo, 2018).

Air Quality (IL & A Ingeniería, 2018)

Environmental air quality was measured at the Project and the Fiambalá locations. Air quality measurements include particulates less than 10 microns, sulfur dioxide, carbon monoxide, nitrogen dioxide, ozone, hydrogen sulfide, and lead. The ambient noise was also measured at the 3Q Salar and camp area. All measured parameters are within the allowed limits.

Water Quality (Induser Laboratory, 2018)

As part of the EBS and subsequent monitoring, NLC sampled and analyzed surface water in November 2018. Samples were taken for bacteriological analysis at four sites: Río Zeta, Río Laguna Verde, Río Tres Quebradas, and the project Camp (kitchen).

The samples were submitted for analysis to Dres. Laboratory Lejtman, with duplicate sample sent to the Ministry of Health of the Province of Catamarca. The values obtained from the bacteriological analysis categorize the water as suitable for human consumption according to the standards established by Article 982 of the Argentine Food Code (Res. 68/2007 and 196/2007 Amendment).

Geomorphology (Baez and Grosso, 2018)

The Project area is surrounded by mountain ranges and is characterized by the following low-lying intermontane geofoms: pedemontanas accumulation plains, alluvial fans, salt flats, vegas associated with permanent flow and peri-salar runoff, and lagoons. The accumulation plains and salt flats dominate the study area.

Soils (Izquierdo et al., 2018)

The soils of the Puna Region are classified as Entisoles, which lack soil horizon development. The soils have variable granulometry, with grain sizes ranging from silt to gravel. The soils present in the study area include the El Cuerno soils (964.5 ha), Laguna Verde soils (1,294.5 ha), Tres Quebradas soils (227 ha), Pissis and Los Patos soils (747 ha), Pissis volcanic soils (1,475.5 ha), Cerro Nacimiento soils, (914.5 ha), and lithosols and outcrops (38,783.5 ha).

Due to strong soil and climatic limitations, the study area is not suitable for cultivation. The value of the area is linked to the preservation of wildlife and use as a recreational area.

Flora (Salinas, 2018, 2017a, b)

The Project area lies within an eco-region that is analogous to the Altoandina phytogeographic province in Argentina. It is characterized by high-altitude deserts, thin grassy steppes, wetlands, and coastal grasslands. Nine units of vegetation have been differentiated within the area of influence of the Project. These units include the salar edge, Adino desert, Pasto Vicuña steppe, wetlands, coast grass, grassland island, rocky area and slopes of the Salado River, Roquedal de Tolilla steppe, and high arid desert.

The salar edge and Adino Desert units are completely devoid of vegetation; whereas the wetlands vegetation unit hosts the highest number of plant species. Fifteen species of vascular plants are recognized in the entire area of influence, mostly associated with Laguna 3Q wetlands. The most common flora identified in the monitoring programs include Pasto vicuña (*Stipa frígida*), *Patosia clandestina*, *Oxychloe andina*, *Ranunculus uniflorus* and *Puccinellia frígida*.

Fauna (Barrionuevo, 2018a, b, c; Burgos, 2017)

42 species were identified through fauna surveys of the Project area, including 1 reptile, 5 mammals, and 36 birds. *Liolaemus poecilochromus* were the only reptile species recorded. Mammal species identified are *Vicugna vicugna*, *Puma concolor*, *Pseudalopex culpaeus*, *Lepus europaeus*, and *Rodentia* sp.

Most of the birds identified are waterfowl and shorebirds that frequent Laguna 3Q, the mouth and lagoon of the Salado River and the vega environments. The bird species recorded include *Anas flavirostris oxyptera*, *Andean Becasina*, *Calidris bairdii*, *Calidris fuscicollis*, *Charadrius alticola*, *Fulica cornuta*, *Leucophaeus pipixcan*, *Lophonetta specularioides*, *Oressochen melanopterus*, *Phalaropus tricolor*, *Phoenicoparrus andinus*, *Phoenicoparrus jamesi*, *Phoenicopterus chilensis*, and *Tringa melanoleuca*. Those linked to the vega environments are *Attagis gayi*, *Lessonia oreas*, *Thinocorus orbignyianus*, and *Thinocorus rumicivorus*. It is notable that the three species of *Phoenicopteridae* (*Phoenicoparrus andinus*, *Phoenicoparrus jamesi*, and *Phoenicopterus chilensis*) counted during summer 2019 represent more than 68.5% of the total number of birds surveyed. Within and around the Project area, birds are most abundant in the two wetlands. In 2019, birds were only observed to mate in Laguna Los Aparejos.

Landscape and Glaciology (Izquierdo et al., 2018)

The study area was divided into four landscape zones based on topographical characteristics (altitude and slope), which largely determine the functional structure of the landscape. These units include the volcanos, high altitude ridges and peaks, Tres Quebradas salar and wetlands, Tres Quebradas salar plain.

Although the Project is situated in the Abaucán and Laguna Verde basin, which hosts the highest concentration of glaciers in Catamarca province, there are no glaciers or perennial snow patches in the study area. Permafrost is present and many periglacial geofoms have been identified. These geofoms indicate that processes associated with freezing cycles and permafrost play a key role in the landscape of the area.

Hydrology and Hydrogeology (Tálamo, 2018)

Hydrology and hydrogeology of the 3Q Project are described in Section 7.

Palaeontology (Gravriloff and Maruaga, 2018)

No fossils or traces of fossils have been found in the Project area to date. The Paleogene – Miocene aged sediments of the Laguna Verde strata are the only outcropping rocks in the area with fossil potential. These strata may represent a source of future fossil discoveries.

Limnology and Microbiology (Farias, 2018)

Planktonic and benthic communities were analyzed at seven sites in the Project area. Two microbial ecosystems of interest were detected around Laguna 3Q: the sulfur field and the “microbialitos” zone. A summary of the limnology of the main bodies of water of the Project is presented in Table 20-1.

Oncolites are distributed over an area of approximately 14,000 m², which extends longitudinally in the N-S direction and occupies the southeastern portion of Rio Salado, approximately 550 m from the mouth of the river.

Table 20-1: Taxa of cyanophytes, diatoms, chlorophytes, and indicator invertebrates in sites nearby the 3Q salar.

	Taxa	Site*	Season**
CYANOPHYTES	<i>Croococcaceae sp.1</i>	1	Sp-F-Su
	<i>Oscillatoriaceae sp. 1</i>	2	F-W-Su
	<i>Oscillatoria sp. y</i>	3	F-W-Su
	<i>Oscillatoriaceae sp. 1</i>		Su
	<i>Pseudanabaena sp.</i>	4	Sp-F-W-Su
	<i>Oscillatoria sp</i>		Sp-F-W-Su
	<i>Oscillatoriaceae sp. 1</i>	5	W-Su
	<i>Oscillatoria sp.</i>	6	Sp
	<i>Oscillatoriaceae sp. 1</i>	7	W-Su
INVERTEBRATES	<i>Copépodos harpacticoideos</i>	1	F-Su
	<i>Mononchoides sp.</i>		F-Su
	<i>Amphipoda</i>	2	Sp
	<i>Acari</i>	3	Su
	<i>Tardigrada</i>		
	<i>Harpacticoidea</i>	4	Sp-F-W-Su
	<i>Rotíferos</i>		F-Su
	<i>Tripylidae</i>	5	F-W
	<i>Tripylidae</i>	6	F
	<i>Ostracoda</i>	7	Su

	Taxa	Site*	Season**
DIATOMS	<i>Achnanthes thermalis</i>	1	Sp-F-Su
	<i>Navicula sp1</i>		Sp-F
	<i>Nitzschia sp1</i>		Sp-F
	<i>Achnanthes thermalis</i>	2	Sp-F-W-Su
	<i>Achnanthes brevipes</i>		Su
	<i>Nitzschia sp. 6</i>		F-W-Su
	<i>Achnanthes thermalis</i>	3	Sp-F-W-Su
	<i>Navicula sp1</i>		Sp-F-W-Su
	<i>Nitzschia sp3</i>		Sp-F-W-Su
	<i>Achnanthes sp1</i>	4	Sp-F-W-Su
	<i>Achnanthes thermalis</i>		F-W-Su
	<i>Halamphora atacamana</i>		Sp-F
	<i>Halamphora coffeaeformis</i>		Sp-W-Su
	<i>Navicula sp1</i>	5	Sp-F-Su
	<i>Nitzschia sp1</i>		Sp-F
	<i>Achnanthes thermalis</i>		Sp-F-W-Su
	<i>Navicula sp1</i>		Sp-F
	<i>Nitzschia sp3</i>	6	Sp-F-W
	<i>Achnanthes sp1</i>		Sp-F
	<i>Achnanthes thermalis</i>		Sp-F
	<i>Halamphora atacamae</i>		Sp-F
	<i>Navicula sp1</i>	7	Sp-F
	<i>Nitzschia sp1</i>		Sp-F
	<i>Achnanthes brevipes</i>		W-Su
	<i>Achnanthes thermalis</i>		W-Su
	<i>Denticula sp3</i>	7	W-Su
	<i>Nitzschia sp10</i>		W-Su
	<i>Nitzschia sp3</i>		W-Su

* Sites: 1. Azufre camp, 2. Rio Salado, 3. Vega, 4. microbiology station, 5. salar's edge, 6. brine, 7. Vega Grande
**Seasons: Sp. Spring, Su. Summer, F. Fall, W. Winter

Social Studies (Cunto, 2018)

The area of direct influence covers the urban centres of Tinogasta (25,000 inhabitants) and Fiambalá (5,000 inhabitants). Among the primary activities in the region, agriculture is the most important.

In Tinogasta, industry is considered the second most important economic activity, and is dominated by wineries and olive and raisin production. Industries are predominantly family-type enterprises, and less often cooperatives between producing families.

A large part of the local economy depends on public employment (provincial, municipal, and state subsidies) and trade. The commercial structure of Fiambalá is limited with little diversity. Nevertheless, it forms the supply centre of the municipality and communities located in the north acquire their goods and services in Fiambalá. This allows a certain extent of autonomy and independence. Tinogasta is an alternative shopping centre for the region.

Archaeology (Ratto, 2016 and 2017)

Field surveys uncovered four archaeological sites in the Project area:

- TQ-1 consists of a set of three parapets, possibly for hunting purposes, with numerous lithic nodules and obsidian debris.
- TQ-2 is an apacheta built on the path that connects the project area with Cerro Tres Cruces. TQ-1 and 2 are located north of Laguna 3Q.

- TQ-3 and TQ-4 are logistical sites related to camelid hunting activities. The sites are considered multi-period because the artifacts found at the sites extend from pre-Inca to modern materials. Artifacts recovered at these sites include modern metal stakes, nineteenth century lilac glass, an Inca projectile point (age assumed based on design of the point), and co-existing circular and quadrangular enclosures indicative of pre-Incan cultural activity. TQ-3 and 4 are located in the southern area, west of the Laguna Negra.

Legal (Vila Melo, 2018)

All work for the 3Q Project was carried out in compliance with the requirements of the Environmental Protection Law for Mining Activity No. 24,585 and complementary regulations.

The National Mining Code was also considered, whose basic purpose is to establish regulatory norms for the granting of concessions for the exploration and exploitation of minerals.

Vehicular Transit (Valdivia 2018)

Ruta Nacional 60 ("RN60") is the only road that connects with the access road to the 3Q Project. RN60 is currently used by local traffic accessing the northern portion of Argentina, and by tourist vehicles in the Tinogasta department. The road has become an important tourist corridor that includes La Ruta of Adobe, Fiambalá, the Quebrada de Las Angosturas and Los Seismiles among other tourist attractions. According to 2016 census data obtained from the National Highway Administration, the Chaschuil-Limite section of RN60 has a daily average of 40 vehicles / day. 76.2% of traffic is considered light vehicles.

The Project access road is approximately 90 km long and meets the RN60 at the beginning of the road to Cerro Pissis. This road is used in summer by recreational visitors to the area.

20.3.1 Exploitation Environmental Impact Report

A complete assessment of the impact of the 3Q project over the environment was started by GT Engineering and completed by Seimcat. The main impacts have been identified, based on the current engineering plans and previous environmental baseline studies.

Environmental impacts for the 3Q Salar and its access will be moderate during the construction and operation stages and can be reverted or mitigated in the short, medium, and long term. The following potential impacts, both positive and negative, were identified for the 3Q Project and its access:

- Changes in the landscape due to occupation of the physical space in the area of the 3Q Project, on the Project access road, and in the area that will be established for the construction and operation of the evaporation ponds and camp;
- Changes in the topography and soils, due to the permanent construction of evaporation ponds;
- Noise level increases caused by the use of equipment, machinery, and vehicles in the 3Q Project, on the road connecting the 3Q Project site, and especially in the area of the evaporation ponds and salt piles;
- Deterioration of air quality, due to the emission of particles and combustion gas from the operations carried out in the salt flat and in the evaporation ponds, salt removal, construction of landfills and the use of equipment, machinery, and vehicles in the salar;
- Alteration, limited to a specific area, of flora processes and dynamics due to the emission of dust and air contaminants resulting from the Project operations;

- Alteration to fauna habitats due to partial reduction of vegetation cover (access road), emission of noise and vibrations, and the site camp;
- Diversification of land use and change in the productive matrix of Tinogasta and La Paz department;
- Increase in productive activity, training of personnel, employment, and development of local suppliers;
- Greater control in the remote area and improved accessibility to the tourist zones of Pissis and surrounding areas; and
- Increasing knowledge and protection of high Andean wetlands (Puna and Alto-Andino ecosystem).

20.4 Social Responsibility Plan

NLC has developed a Social Responsibility Plan (“SRP”), designed as a tool for managing community affairs and strengthening the relationship between the Company and the communities in Tinogasta department. The purpose of the SRP is to facilitate communication with the local population, and to strengthen the communication and connection with institutions and public agencies of Fiambalá and Tinogasta municipalities, which are present in the area of influence of the Project. This SRP is led by the community relations team located in Fiambalá and directed by Lic. Matias Berardini.

The SRP programs developed by NLC are as follows:

- Communication with the community;
- Visits to the project organized for schools, community leaders, and people interested in the project sponsored by the company;
- Community training programs (over 1,000 people attended so far) of non-mining activities including cooking, electricity, driving, sexual education, and pottery, among others;
- Generation of local employment opportunities;
- Local contract and purchase of goods and services;
- Development of production and training projects;
- Support to sport, cultural, and educational activities;
- Coordination of community actions and standardization of collaboration processes;
- Implementation of the procedure and registration of claims and concerns (according to international standard);
- Standardization of community policies and programs;
- Support for local purchasing and work in trade training;
- Transmission of knowledge and technology to promote sustainability; and
- Community visits to the 3Q Project.

In 2021, NLC will continue to develop and implement the SRP, as in previous years.

20.5 Governance

NLC's sustainability policy establishes the following values: quality, safety, health, environment, and community. In addition to strict compliance with current legal obligations, the company also considers socio-environmental responsibilities required to provide a satisfactory response to the expectations of the stakeholders regarding the Project. The Company is committed to developing and implementing strategies to promote sustainable development and to protect the environment and the welfare of the people who may be affected by the operations of the Project.

These strategies include the following:

- In 2018 and 2019, NLC reviewed and updated the Company's management system to align with the principles of e3 Plus (as developed by the Prospectors & Developers Association of Canada) and to incorporate the e3 Plus sociological model.
- In November 2018, work began to certify the SRP under international standards on corporate social responsibility ("CSR") for the mining sector. This is an unprecedented case in Argentina for the mining exploration stage. Certification of the SRP will facilitate professionalization of employees in the community relationship office and other areas of the company in topics such as dialogue, sustainability, community commitment, efficiency, and internal administrative technical coordination.
- Dr. Jan Boon and Mr. Pablo Lumerman were hired in 2018 to facilitate certification by developing and implementing an auditable set of procedures and protocols that address all dimensions of the CSR. Both individuals are specialists in Transformational Dialogue processes and have in depth knowledge of mining activities in Latin America.
- The proposal set forth by Dr. Boon and Mr. Lumerman adopts and adapts the e3 Plus protocols by incorporating the sociological model proposed in Dr. Boon's doctoral thesis, along with select guidelines of the HMS protocols (towards a sustainable mining program supported by the Argentine Mining Chamber). The proposal was developed to fulfill the requirements of an exploitation stage. Implementation of the protocols and procedures began in December 2018 with training of NLC personnel. Training continued in February 2019 and an initial evaluation will be carried out at the end of July 2019 to corroborate the progress of the project.














Subject material in the trainings include the following:

- Introduction to an open dialog;
 - Guiding principles and human rights;
 - Evaluation of social impact in the value chain;
 - Conflict transformation;
 - Preparation of internal company baseline;
 - Training in CSR program, e3 Plus;
 - Models and protocols for e3 Plus implementation;
 - HMS principles (TSM – towards a sustainable mining program supported by the Argentine Mining Chamber)
- In February 2021, NLC reorganized the Executive Committee ("EC") and determined the new members. Now EC is formed by the leaders of all areas and the President of the company.

Work on the CSR Program is based on the needs of the company in relation to the community, the environment, and good practices.

- In March 2021, NLC contracted Golder, an international company and leader in ESG, to conduct an external Due Diligence of the social responsibility program of the company. Golder was asked to evaluate the social management and performance of the Project against implementation and compliance with International Finance Corporation (“IFC”) Sustainability Policy and Performance Standards, including aspects related to the overall governance of the company and management of the Project. The overall purpose of the evaluation is to provide information to investors on material risks that could affect the financial or operating performance of the Project and Company. The ESG evaluation is focused primarily on the social environment and therefore concentrated on assessing Project preparedness and current performance related to labour issues, human rights risks, corruption by company staff, and the relationship between Neo Lithium and nearby communities, including addressing and managing community expectations. While the Project may not seek out IFC financing, the IFC Performance Standards currently define international best practice and have been adopted by and referenced in the Equator Principles (“EPs”), a financial industry benchmark for determining, assessing, and managing environmental and social risks in projects. At present 123 Financial Institutions in 37 countries have signed on to the EPs. The EPs require applicants to adhere to applicable IFC Performance Standards and place specific emphasis on environmental and social impact assessment, development of an environmental and social management system, stakeholder engagement, grievance management and independent monitoring and reporting.
- In April 2021, NLC, through its Argentinian subsidiary LIEX, signed a commitment with the Argentine Chamber of Mining Entrepreneurs to adopt the protocols of the HMS program. Universidad Nacional de San Martin (“UNSAM”) was hired to guide the process of the development of the Sustainability program.
- In May 2021 UNSAM and the company started to work on the protocols of the program HMS, that will be used by the company. The first three protocols have been adopted and the company has commitment is to adopt the rest during 2021 and 2022. The first three are:
 - Protocol for interaction with the community;
 - Water Management Protocol; and
 - Crisis and Communications Protocol.
- In August 2021 UNSAM did a community perception study that yielded information on the way the community perceived the Project and the company.
- In August 2021 the Executive Committee started a four-week training program with the LIQUEN team, led by Pablo Lumerman and accompanied by specialist from the UNSAM.
- In September 2021, Golder presented the final Due Diligence report, that shows the advances of NLC social responsibility, environmental, and governance program.
- The company is committed to the UN Sustainable Developments Goals (“SDGs”), which can be viewed at <https://sdgs.un.org/goals>. Actions taken by NLC to support the UN SDGs are summarized in Table 20-2.

Table 20-2: Actions by NLC which support the UN Sustainable Development Goals.

Action	SDG
Provided a new water well to the community of Fiambalá.	
Targeting to maximise use of renewable energy, the majority of the power to be used at the Salar and processing plants will come from Photovoltaic plants.	
Lithium production can also be clean, minimizing CO ₂ emissions at every instance possible.	
Natural Area Protection Proposal, extensive hydrological and hydrogeological studies in the region.	
Natural Area Protection Proposal to preserve local flora and fauna.	
Local development and local employment, also providing support to artisanal industries (leather, agricultural, construction industries).	
Supporting Local communities with Dengue and COVID emergencies.	
Community and Employee development programs in place. Support to cultural and sporting community activities.	
HHRR policies in place to ensure equal employment, conditions, and opportunities.	
Supporting local communities with local procurement and local sourcing. Improved life balance avoiding living in camps.	
Long term employment, long life project. Lithium is a new industry with huge growth potential.	
NLC operates its piloting plant locally in Fiambalá, to promote local development, training, and community engagement.	
NLC creates opportunities for people with disabilities.	

21. Capital and Operating Costs

21.1 Capital Cost Estimate

21.1.1 Capital Expenditures – CAPEX

Capital expenditures are based on a sustained operating capacity of 20,000 tonnes of lithium carbonate per year. Capital equipment costs have been obtained from solicited budget price information and Worley’s in-house recent historical data.

These estimates are dated in the third quarter of 2021. No provision has been included to offset future cost escalation, since expenses, as well as revenue are expressed in constant dollars of the above-mentioned period. Accuracy of the estimate is expected to be within a +/-15% range.

The capital costs include direct and indirect costs for:

- Brine production wellfields and pipeline delivery system,
- Evaporation ponds,
- Crystallization plant,
- Lithium carbonate plant, and
- Infrastructure.

Capital investment for NLC’s 3Q Project, including equipment, materials, indirect costs, and contingencies during the construction period is estimated to be USD 370.5 million. Possible capitalized interest expenses incurred during the construction period are excluded. Out of the above total, Direct Project Costs represent USD 286.9 million, Indirect Project Costs represent USD 43.9 million, and the provision for Contingencies is USD 39.7 million. The former represents 15.3% of direct project costs, while the latter is 12.0% of direct + indirect project costs.

Working capital requirements are estimated to be USD 15.9 million; in addition, sustaining capital expenditures add up to USD 126.5 million over the 50-year evaluation period of the project.

Total capital expenditures are summarized in Table 21-1, which follows:

Table 21-1: Total capital expenditures for the 3Q Project.

Area	Description	Projected Budget USD 000
	Direct Costs	
1000	Brine Extraction Wells	19,875
2000	Evaporation Ponds	100,451
5000	Crystallization Plant	36,584
6000	Lithium Carbonate Plant	65,212
8000	General Services	19,450
9000	Infrastructure	45,358
	Total Direct Costs	286,928
	Indirect Cost	43,920
	Direct + Indirect Costs	330,849
	Contingencies	39,702
	TOTAL CAPEX	370,551

21.1.2 Brine Production Wellfield and Pipeline Delivery System

A fifteen wells brine production field will be drilled and constructed in the Salar. The brine production field will have an average delivery capacity of approximately 750 m³/h. Brine discharge from each wellhead is conveyed through a feeder pipeline system into the two premixing ponds.

The capital cost estimate for the brine production wellfield and pipeline delivery system is as detailed in Table 21-2.

Table 21-2: Brine production wellfields and pipeline delivery system cost estimate.

Area	Description	Projected Budget USD 000
1000	Brine Extraction Wells	19,875

21.1.3 Evaporation Ponds

The solar evaporation ponds system includes two strings of four, large, PC pre concentration ponds, which will feed six K (Potassium Chloride) pre concentration ponds, also arranged in two strings. The two final K ponds feed the two mixing ponds. In turn, these feed the five stages concentration ponds, which feed and interact with the five stages of the crystallization plant.

Brine transfer from one pond to the next, will be done mainly by means of gravity overflow, but pumping will be required at each of the concentration ponds. All the ponds have a waterproofing system, which includes an HDPE membrane and a geotextile, for resistance to impacts and punctures. A cost estimate for the evaporation ponds system is provided in Table 21-3.

Table 21-3: Evaporation ponds cost estimate.

Area	Description	Projected Budget USD 000
2000	Evaporation Ponds	
	Pre concentration Ponds	52,872
	Concentration Ponds	39,989
	Harvesting Equipment	7,590
	Total	100,451

21.1.4 Crystallization Plant

As indicated in previous sections, at the end of the evaporation and concentration ponds sits a CaCl₂ crystallization plant, whose objective is to remove this compound from the brine and salts that feed it. This installation will be provided by KBR Inc. of Houston, Texas. Investment in this plant is shown in Table 21-4.

Table 21-4: Crystallization plant cost estimate.

Area	Description	Projected Budget USD 000
5000	Crystallization Plant	36,584

21.1.5 Lithium Carbonate Plant

The two main components of the lithium carbonate plant are:

- Chemical Plant, including the following areas:
 - Calcium-magnesium removal,
 - Calcium hydroxide removal,
 - Calcium carbonate removal, and
 - Lithium carbonate precipitation.
- Reactant's preparation area.

All these areas will be located inside the same building, organized, and distributed to optimize plant lay out. A cost estimate for the lithium carbonate plant is provided in Table 21-5.

Table 21-5: Lithium carbonate plant cost estimate.

Area	Description	Projected Budget USD 000
6000	Lithium Carbonate Plant	
	Chemical Plant	51,688
	Reactants Preparation	13,524
	Total	65,212

21.1.6 General Services

The main auxiliary services required by the Salar and Fiambalá installation are: water supply storage and distribution, fuel storage and distribution, thermal power units, electrical generation and distribution, fire control systems, washing system and automation, and communications (Table 21-6).

Table 21-6: General services cost estimate.

Area	Description	Projected Budget USD 000
7000	General Services	
	Industrial Water Supply	6,475
	Plant utilities	5,739
	Power generation and distribution	7,235
	Total	19,450

21.1.7 Infrastructure

Infrastructure cost estimates are summarized in Table 21-7. Main facilities included in the infrastructure item are:

- Truck and harvest machinery workshop,
- Salar access road improvements,
- Fiambalá plant power line,
- Plant buildings: Administration office, laboratories, control rooms, warehouses, etc.,
- Access control area,
- Camps: Workers, polyclinic, dining room, other,
- Truck scale,
- Access and internal roads, and
- Sanitary installations.

Table 21-7: Infrastructure cost estimate.

Area	Description	Projected Budget USD 000
8000	Infrastructure	
	Truck & harvest equipment, maintenance shop	6,244
	Salar road improvements	11,476
	Workers' camp and other infrastructure	19,942
	Tinogasta - Fiambalá electrical line	5,400
	Other auxiliary buildings	2,296
	Total	45,358

21.1.8 Exclusions

The following items were not included in this estimate:

- Sunk and legal costs,
- Special government incentives and allowances,
- Owner's costs beyond direct project administration and execution, such as permitting and construction insurance,
- Escalation,
- Interest and financing costs,
- Start-up costs beyond those specifically included, and
- Additional exploration expenses.

21.1.9 Currency

All values are expressed in third quarter 2021 US dollars (“USD”). The average official exchange rate between the Argentinian peso and the US dollar during this period was Arg. \$99.4 / USD, however, since as stated above, all costs have been expressed in USA dollars, thus variations in the above rate have no impact on project costs. In addition, no provision for escalation has been included since both revenues and expenses are expressed in constant value dollars.

21.2 Operating Cost Estimate

On the following section we show the principal components of the estimated operating expenses for NLC’s 3Q Project.

The operating cost estimate was prepared on the basis of a yearly production of 20,000 tonnes of Li₂CO₃. This estimate is based upon process definition, laboratory work, reagents consumption rates, and other information developed by NLC, or its advisors.

Informative vendor quotations have been used for reagents costs. Expenses estimates, as well as manpower levels are based on information provided by NLC. Energy prices, such as trucked LNG, Diesel fuel and electricity, and reagents prices, correspond to expected costs for products delivered at either or both project locations.

21.2.1 Operating Expenses Summary – OPEX

Operating expenses are summarized in Table 21-8. Chemical reagents are the major operating cost of the project, followed by salt removal, transportation, and energy costs. The other significant expense item is manpower.

Table 21-8: Total operational expenditures for the 3Q Project.

Operation Costs	USD / tonne Li ₂ CO ₃	Total USD / Year
Direct Costs		
Chemical Reagents	1,580	31,599,353
Salt Removal and Transport	372	7,434,633
Energy	315	6,295,434
Manpower	264	5,271,845
Reagents & Other Items Transport	329	6,576,850
Direct Costs Subtotal	2,859	57,178,115
Indirect Costs		
Catering & Camp Services	63	1,255,600
General & Administration - Local	32	633,789
Indirect Costs Subtotal	95	1,889,389
TOTAL PRODUCTION COSTS	2,953	59,067,504

21.2.2 Ponds and Plants Reagents Costs

Reagent costs for the ponds and plants are summarized in Table 21-9. Over 95% of the chemical costs correspond to Soda Ash and Sodium Hydroxide costs, of which 4.65 tonnes (combined) are required to produce a single tonne of Li_2CO_3 .

Table 21-9: Ponds and plants reagents costs.

Description	Formula	Tonnes or m^3 / year	USD / Tonne or m^3	USD / year	Tonne or m^3 / Tonne Li_2CO_3	USD / Tonne Li_2CO_3
SALAR						
Hydrochloric Acid (37%)	HCl	8,028	156	1,252,368	0.40	63
LITHIUM CARBONATE PLANT						
Soda Ash	Na_2CO_3	53,280	339	18,077,904	2.66	904
Sodium Hydroxide (50%)	NaOH	30,228	395	11,940,060	1.51	597
Hydrochloric Acid (37%)	HCl	1,558	156	242,986	0.08	12
Other Reagents				86,035	-	4.3
CHEMICAL CONSUMPTION TOTAL		93,094		31,513,318	4.65	1,580

21.2.3 Salt Harvest and Transport

This item corresponds to the costs incurred in harvesting the pre concentration and concentration ponds and transporting discarded salts to their established dumping place, within NLC's surface property and according to its EIA (Environmental Impact Assessment), which is in preparation. Salts to be transported also include those produced at the crystallization plant.

Total material to be transported is approximately 5.6 million tonnes/year. Costs shown in Table 21-10 correspond to direct costs of the operation, excluding salaries, which are accounted for in Personnel cost item.

Table 21-10: Salt harvesting and transportation costs.

Harvested Salts	Tonnes / year	USD / year	USD / Tonne	USD / Tonne Li_2CO_3
Harvested salts from pre-concentration ponds	1,763,525	3,303,467	1.9	165
Harvested salts from pre-concentration ponds	1,974,057	2,256,027	1.1	113
Discard salts from the crystallization plant	1,864,326	1,875,139	1.0	94
Total	5,601,908	7,434,633	4.0	372

21.2.4 Energy Cost

Major energy items at the Salar site are the electrical energy required by the wells, the ponds, and the crystallization plant. Electrical energy is produced on site, with both solar energy and gas-powered motor-generator units. At the Fiambalá site, heat is required for process water and lithium carbonate drying. In addition, electrical power for the plant is drawn from the grid. Details are shown in Table 21-11.

Table 21-11: Energy costs.

Energy consumption	Daily consumption m ³ /d	USD / m ³	USD / year	USD / Tonne Li ₂ CO ₃
SALAR				
Electrical energy (LNG)	35.0	247.5	3,162,333	158
LITHIUM CARBONATE PLANT				
Process water heating (LNG)	8.7	220.3	699,626	35
Lithium carbonate drying (LNG)	15.5	220.3	1,246,460	62
Electricity	MW / day	USD / MW		
Grid power	43.2	75.3	1,187,015	59
Total Energy Cost			6,295,434	315

21.2.5 Manpower, Catering and Camp Services Cost

Headcount for the plant was estimated on the basis of experience in similar facilities. Personnel salaries and benefits were projected from data for mining operations in Argentina, provided by NLC (Table 21-12).

Costs relating to plant administrative personnel and the Head Office are included in the General & Administrative item, shown in Table 21-15.

Table 21-12: Manpower costs.

Personnel Costs	Staff	USD / year	USD / Tonne Li ₂ CO ₃
SALAR	172	2,530,487	127
Hydrogeology and ponds	34	489,321	24
Crystallization plant	56	729,321	36
Laboratory	22	375,145	19
Engineering & maintenance	20	412,428	21
Mobile equipment operators	18	230,680	12
Administration	22	293,592	15
FIAMBALÁ	188	2,741,358	137
Lithium Carbonate Plant	61	840,001	42
Engineering & maintenance	64	946,018	47
Administration	63	955,339	48
Totals	360	5,271,845	264

21.2.6 Catering and Camp Services Cost

Catering and camp services are estimated in Table 21-13.

Table 21-13: Catering and camp services costs.

Catering Costs	Staff	USD / day	USD / year	USD / Tonne Li ₂ CO ₃
SALAR				
Personnel	86	40	1,255,600	63
Total	86	40	1,255,600	63

21.2.7 Maintenance Cost

As this is considered a remote operation there is a large team that will handle in-house maintenance. The cost of that personnel is under Manpower Costs (Table 21-12).

Maintenance costs for mobile equipment have been included in the items of Brine Transport, Reagents Transport and Harvesting. Cost to repair physical facilities (ponds, buildings, etc.) are included under Sustain Capex of those facilities.

21.2.8 Transportation Costs

Transportation costs include brine conveyance from the Salar to the Fiambalá plant, as well as haulage of the different reagents, from their origin, to either of the project locations (Table 21-14).

Table 21-14: Product transportation costs.

Transportation Costs	m ³ or Tonne / year	USD / m ³	USD / year	USD / Tonne Li ₂ CO ₃
Brine transport (m3)	125,004	21.4	2,673,806	134
Reagents Transport (Tonne)	94,374	41.4	3,903,044	195
Totals	219,378	62.7	6,576,849.9	329

21.2.9 Indirect Costs

Indirect costs include management compensation and other expenses, 25 people which brings the total number of staff required to run the operation to 385 (Table 21-15). Costs exclude Board of Directors compensation and expenses, and any other expenses above those corresponding to the company's local General Manager.

Table 21-15: Indirect costs.

Head Office Costs	USD / year	USD / Tonne Li ₂ CO ₃
General & administration	633,789	32
Totals	633,789	32

22. Economic Analysis

22.1 Overview

This section analyzes the economic feasibility of NLC's 3Q Project. To carry out the project's economic evaluation, we utilized a cash flow model that allows before and after tax analysis. Capital and operating costs estimates presented in the previous sections, as well as an assumed production program and the pricing forecast included in Section 19 are the main inputs for this model.

Model results include the project's NPV at different rates, IRR and payback period. These metrics were calculated for different scenarios; in addition, a sensitivity analysis on the most important revenue/cost variables was performed.

22.2 Evaluation Criteria

Main evaluation criteria applied in the Project's evaluation are as follows:

- Long term price projections for lithium carbonate have been obtained from BMI's 3Q Feasibility Study of August 2021, and updated in September 2021, to reflect the latest changes in lithium prices. This study covers the 2021 – 2040 period. Since LOM considerations allow the Project to operate until 2073, prices for the 2041 – 2073 period were assumed constant, at the 2040 level.
- The analysis considers an average production rate of 20,000 TPY of battery grade lithium carbonate (BGLC). This production rate is achieved in the second year of operations.
- Production ramp up starts in 2024, under a very tight construction schedule. 12,635 Tonnes of TG lithium carbonate are produced in this year, of which half is considered to be technical grade lithium carbonate, and the other half is assumed to meet BG standards. Full production rate of slightly over 20,000 Tonnes of BGLC is obtained in 2025. Production stays at an average of 20,365 Tonnes of BGLC for the initial 20 years, declining gradually to 8,423 Tonnes at the end of the 50 year LOM. Average production for the whole period is 16,951 Tonnes.
- Project duration: Time allowed for engineering, permits and construction is 2 and a half years, with production starting at the end of this period.
- Mineral resources defined in Section 14 allow for a projected operating period of 50 years, at the stated production rates.
- CAPEX and OPEX presented in Section 21 correspond to the process described on Section 17.
- Equity basis: For economic evaluation purposes, it has been assumed that 100 % of capital expenditures, including pre-production expenses and working capital are financed solely with owner's equity.

22.3 Income Tax and Royalties

The following tax assumptions and criteria have been considered in the project's evaluation:

22.3.1 Income Taxes

- Argentinian tax information² indicates that Argentinian federal income tax rate applicable to NLC, given its stability tax agreement with the Argentinian government, is 30%. In addition, it has been assumed that, given there is an existing double tax avoidance treaty between Argentina and Canada³, the 13% Argentinian withholding tax dividends is a credit towards the Canadian income tax of the project's shareholders⁴. Thus, a total tax rate of 30% has been applied in the cash flow model.
- There is no additional income tax applied at the Provincial level.
- Mining legislation includes a provision for rapidly accelerated depreciation of capital goods. This provision results in losses for tax purposes in the early operating phase of the project, losses which can be carried forward indefinitely.
- The existing NLC exploration and other capitalized project expenditures, at the date of its stability tax agreement, amount to approximately USD 12 million. The economic model assumes that these expenditures can also be used as amortization once the project starts operations⁵.

22.3.2 Value Added Tax

Value added tax in Argentina has different rates, the general case being 21%, while the rate on capital goods is 10.5 % and that applied to public services such as electricity or gas is 27%. In the case of long lead projects, such as this, VAT law allows for direct recovery from the government of VAT paid during the construction period. Additionally, in the case of companies that export all or nearly all of their production, they can recover directly from the government VAT paid on all supplies. Considering that this draw back system is complex and time consuming, the model considers that CAPEX VAT payments are recovered two years after payment. The delay in recovering OPEX VAT has been estimated as one year.

22.3.3 Royalties

22.3.3.1 Governmental Royalties

In Argentina, underground resources belong to the Federal Provinces, which grant mining concessions to explorers and producers. Most of the Argentinian Provinces, including Catamarca, where 3Q Salar is located, have signed an agreement (Acuerdo Federal Minero, or AFM) with the Federal Government to limit these royalties to a rate of 3% of extracted mineral value. Cost assumptions indicate that this translates into an approximate 2.4% actual royalty rate on revenues.

However, Argentinian tax reports indicate that this agreement has not yet passed the Argentinian Congress, thus its rules may yet change, but currently Catamarca and most other Argentinian Provinces charge a 3% royalty rate, as assumed here. It is to be noted though that the AFM allows the Provinces to collect an additional 1.5 % royalty rate for specific uses. The AFM also increases the base of the royalty to full revenues, disallowing deduction of operating costs, as presently done. This

²Impuesto a las Ganancias Beneficiarios Del Exterior, Regimen de Retencion con Carácter de Pago Único y Definitivo. Oscar A. Fernandez, Contador Público (UBA), Especialista en Derecho Tributario, 31 de Julio, 2020.

³Convention Between Canada and the Argentine Republic for the Avoidance of Double Taxation and the Prevention of Fiscal Evasion with Respect to Taxes on Income and on Capital. April 1993.

⁴This assumption has not been ratified by outside legal/tax experts.

⁵Ibid.

economic evaluation has not considered these proposed changes in royalty payments, since their approval is uncertain, and has been pending in the Argentinian Congress for several years.

22.3.3.2 Other Royalties

NLC indicates it has an agreement to pay a 1.5 % gross royalty to the “Project’s “Founders”, on revenues from exploitation of the 3Q mineral properties. This royalty is included on the costs considered in the cash flow model.

22.4 Capital Expenditures

Capital expenditures for the NLC’s 3Q Project, including equipment, materials, indirect costs and contingencies during the construction period, are estimated to add up to USD 371 million, as shown in Table 21-1. In the same section, we indicate that working capital requirements are projected to be USD 16 million; sustaining capital expenditures are estimated to amount to USD 127 million over the horizon of the project. The estimated CAPEX schedule for the 3Q Project is shown in Table 22-1

Table 22-1: Capex schedule for the 3Q Project.

Area	Description	Capex Schedule			
		2022	2023	2024	Total
1000	Brine Extraction Wells	16,171			16,171
2000	Evaporation Ponds	37,352	80,930	6,225	124,508
5000	Brine Treatment Plant		18,292	18,292	36,584
4000	Lithium Carbonate Plant		42,600	42,600	85,200
5000	General Services				-
6000	Infrastructure	14,680	9,786		24,466
	Subtotal	68,203	151,608	67,117	286,928
	Indirect Cost	10,440	23,207	10,274	43,920
	Contingencies	4,719	10,489	24,494	39,702
	TOTAL	83,362	185,304	101,885	370,551

22.5 Production Ramp Up and Schedule

As mentioned in Section 22.1, production ramp up starts in 2024 when 6,317 tonnes of TGLC and an equal amount of BGLC is produced. Full production rate of slightly over 20,000 tonnes of BG lithium carbonate is obtained in 2025. Average production rate of 20,365 TPY of BGLC is achieved from production year 2 to year 20. Following Table 22-2 below, shows a summary of the project’s ramp up schedule and the long term production program used for the economic analysis.

Table 22-2: Production ramp up and schedule.

Year	2024	2025	2033	2043	2053	2063	2073
	1	2	10	20	30	40	50
Li ₂ CO ₃ Production Tonnes (Battery grade)	6,317	20,506	20,114	17,194	16,279	14,426	8,423
Li ₂ CO ₃ Production Tonnes (Technical grade)	6,317	-	-	-	-	-	-
Li₂CO₃ Production Tonnes (Total grades)	12,635	20,506	20,114	17,194	16,279	14,426	8,423

22.6 Operating Costs

As indicated on section 21.2.1, Table 21-8, direct operating costs per tonne of lithium carbonate are estimated to be USD 2,858. Indirect unit operating costs are estimated to be 95 USD/tonne. As a result, total estimated operating costs are 2,953 USD/tonne.

22.7 Lithium Carbonate Prices

BMI prepared a custom study for NLC on the Lithium Carbonate market and projected future production capacity, product demand and prices. This study is presented in an abridged form, in Section 19 of this report. Since, on the one hand, BMI’s report covers the 2021 – 2040 period, and on the other hand, LOM considerations allow the Project to operate until 2073, prices for the 2040 – 2073 period were assumed constant, at the 2040 level. These prices are shown on Figure 22-1 and in Table 22-3.

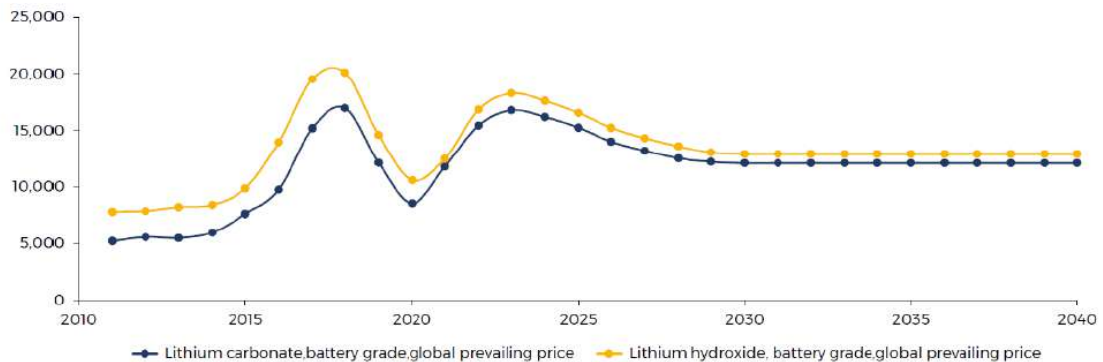


Figure 22-1: Projected lithium carbonate prices⁶.

22.8 Production Revenues

Production revenues result from projected production quantities shown in Table 22-2 and product prices, shown in Table 22-3. Resulting revenues for selected years are shown in Table 22-4.

⁶ Figure taken from BMI’s report mentioned in the main text.

22.9 Investment and Depreciation

Investment takes place between the years 2022 and 2024, and values are as per Table 22-1. Depreciation is in accordance with the accelerated rates permissible under Argentinian tax and mining laws. These regulations allow a depreciation rate of 60% of the net asset values in the first year of operations, and a rate of 20% in the following two years. The application of the previously mentioned rates, results in tax losses in the first years, which can be carried forward until extinguished.

Sustaining Capital has been estimated as USD 2,869,000 per year, but this rate is reached gradually in the seventh year of operations. This rate is maintained over the life of the project, except in its last year of operations. The investment and depreciation schedule is summarized in Table 22-5.

Table 22-3: Projected lithium carbonate prices.

Battery Grade Lithium Carbonate Prices - Constant (2020) USD / Tonne							
Year	USD / Tonne	Year	USD / Tonne	Year	USD / Tonne	Year	USD / Tonne
2022	15,445	2035	12,110	2048	12,110	2061	12,110
2023	16,790	2036	12,110	2049	12,110	2062	12,110
2024	16,200	2037	12,110	2050	12,110	2063	12,110
2025	15,250	2038	12,110	2051	12,110	2064	12,110
2026	14,015	2039	12,110	2052	12,110	2065	12,110
2027	13,209	2040	12,110	2053	12,110	2066	12,110
2028	12,538	2041	12,110	2054	12,110	2067	12,110
2029	12,229	2042	12,110	2055	12,110	2068	12,110
2030	12,110	2043	12,110	2056	12,110	2069	12,110
2031	12,110	2044	12,110	2057	12,110	2070	12,110
2032	12,110	2045	12,110	2058	12,110	2071	12,110
2033	12,110	2046	12,110	2059	12,110	2072	12,110
2034	12,110	2047	12,110	2060	12,110	2073	12,110

Table 22-4: Production revenues, constant 2020, USD 000.

Revenues per Project Year	2024	2025	2033	2043	2053	2063	2073	Total
	1	2	10	20	30	40	50	
BGLC Revenue	102,342	312,722	243,582	208,219	197,135	174,703	102,003	10,332,962
TGLC Revenue	92,108	-	-	-	-	-	-	92,108
Total Revenues	194,450	312,722	243,582	208,219	197,135	174,703	102,003	10,425,070

22.10 Cash Flow Projection

Capital expenditures, operating expenses, revenue, income taxes, royalties, amortization, depreciation, working capital, etc., determined on the previous sections, constitute the inputs for the cash flow model. The result is presented in Table 22-5.

Table 22-5: Investment and depreciation schedule - USD 000.

Item / Year	2022	2023	2024	2025	2026	2027	2028	2029	2030	2073	Totals
			1	2	3	4	5	6	7	50	
Plant Investment	83,362	185,304	101,885	-	-	-	-	-	-	-	370,551
Cumulative Plant Investment	83,362	268,666	370,551	370,551	370,551	370,551	370,551	370,551	370,551	370,551	
Amortization of Exploration Exp.		-	(2,400)	(2,400)	(2,400)	(2,400)	(2,400)				(12,000)
Yearly Depreciation	-	-	(222,330)	(74,110)	(74,110)	-	-	-	-	-	(370,551)
Cumulative Depreciation	-	-	(222,330)	(296,441)	(370,551)	(370,551)	(370,551)	(370,551)	(370,551)	(370,551)	
Net Asset Values	83,362	268,666	148,220	74,110	-	-	-	-	-	-	-
Sustaining Capital	-	-	-	574	1,435	2,008	2,295	2,582	2,869		126,535
Cumulative Sustaining Investment	-	-	-	574	2,008	4,017	6,312	8,895	11,764	126,535	
Yearly Depreciation			-	(191)	(669)	(1,339)	(1,913)	(2,295)	(2,582)	-	(126,535)
Cumulative Depreciation			-	(191)	(861)	(2,200)	(4,112)	(6,408)	(8,990)	(126,535)	
TOTAL YEARLY DEPRECIATION			(222,330)	(74,301)	(74,780)	(1,339)	(1,913)	(2,295)	(2,582)	-	-

Capitalized Exploration Expenses
USD
12,000,000

Table 22-6: Project summary cash flow projection - USD 000.

NLC 3Q PROJECTED CASH FLOW SCHEDULE														
Year	2022	2023	2024	2025	2026	2027	2028	2029	2033	2043	2053	2063	2073	Total
Period			1	2	3	4	5	6	10	20	30	40	50	
Revenues	-	-	194,450	312,722	290,146	272,596	259,021	251,838	243,582	208,219	197,135	197,135	197,135	10,425,070
Li2CO3 Battery grade	-	-	102,342	312,722	290,146	272,596	259,021	251,838	243,582	208,219	197,135	174,703	102,003	10,332,962
Li2CO3 Technical grade	-	-	92,108	-	-	-	-	-	-	-	-	-	-	92,108
Cash Expenditures	-	-	(50,007)	(75,568)	(70,014)	(63,942)	(67,109)	(70,326)	(68,595)	(58,728)	(55,636)	(50,386)	(56,454)	(2,935,060)
OPEX Li2CO3	-	-	(42,517)	(63,382)	(58,703)	(53,258)	(57,153)	(60,802)	(59,401)	(50,869)	(48,195)	(42,783)	(22,112)	(2,484,742)
Provincial Royalty	-	-	(4,558)	(7,480)	(6,943)	(6,580)	(6,056)	(5,731)	(5,525)	(4,720)	(4,468)	(4,631)	(5,251)	(257,444)
Founder's Royalty	-	-	(2,917)	(4,691)	(4,352)	(4,089)	(3,885)	(3,778)	(3,654)	(3,123)	(2,957)	(2,957)	(2,957)	(165,993)
Mining Licenses	-	-	(15)	(15)	(15)	(15)	(15)	(15)	(15)	(15)	(15)	(15)	(15)	(762)
Remediation	-	-	-	-	-	-	-	-	-	-	-	-	-	(26,119)
Operating Cash Flow	-	-	144,442	237,154	220,132	208,654	191,912	181,513	174,987	149,491	141,500	146,749	140,681	8,131,156
Operating Margin %	-	-	74%	76%	76%	77%	74%	72%	72%	72%	72%	74%	71%	-
Non Cash Expenditures	-	-	(226,856)	(79,870)	(80,115)	(6,402)	(7,170)	(5,336)	(2,869)	(2,869)	(2,869)	(2,869)	-	(535,205)
Depreciation	-	-	(222,330)	(74,301)	(74,780)	(1,339)	(1,913)	(2,295)	(2,869)	(2,869)	(2,869)	(2,869)	-	(497,086)
Amortization	-	-	(2,400)	(2,400)	(2,400)	(2,400)	(2,400)	-	-	-	-	-	-	(12,000)
Remediation Allowance	-	-	(2,126)	(3,169)	(2,935)	(2,663)	(2,858)	(3,040)	-	-	-	-	-	(26,119)
Profit Before Taxes	-	-	(82,414)	157,283	140,017	202,252	184,741	176,177	172,117	146,621	138,630	143,880	140,681	7,595,951
Income Taxes	-	-	-	(22,461)	(42,005)	(60,676)	(55,422)	(52,853)	(51,635)	(43,986)	(41,589)	(43,164)	(42,204)	(2,278,785)
Profit After Taxes	-	-	(82,414)	134,823	98,012	141,576	129,319	123,324	120,482	102,635	97,041	100,716	98,477	5,317,166
Depreciation, Amortization & Allowance	-	-	226,856	79,870	80,115	6,402	7,170	5,336	2,869	2,869	2,869	2,869	-	535,205
Operating After Tax Cash Flow	-	-	144,442	214,693	178,127	147,978	136,490	128,660	123,351	105,504	99,910	103,585	98,477	5,852,371
Non Operating Cash Flow	(92,115)	(204,761)	(103,830)	1,387	11,349	419	(4,086)	(4,263)	(2,670)	(533)	(2,670)	(2,641)	11,427	(472,485)
Total Investment	(83,362)	(185,304)	(101,885)	-	-	-	-	-	-	-	-	-	-	(370,551)
VAT on CAPEX	(8,753)	(19,457)	(10,698)	-	-	-	-	-	-	-	-	-	-	(38,908)
Refund VAT on CAPEX	-	-	8,753	19,457	10,698	-	-	-	-	-	-	-	-	38,908
Sustaining Capital	-	-	-	(574)	(1,435)	(2,008)	(2,295)	(2,582)	(2,869)	(2,869)	(2,869)	(2,869)	-	(126,535)
A - Working Capital	-	-	(10,629)	-	-	-	-	-	-	-	-	-	-	(10,629)
Working Capital Δ	-	-	-	(5,216)	1,170	1,361	(974)	(912)	111	1,305	111	127	9,214	10,629
VAT on OPEX	-	-	-	(12,280)	(11,364)	(10,298)	(11,116)	(11,884)	(11,608)	(9,922)	(9,394)	(8,325)	(4,203)	(475,727)
Refund VAT on OPEX	-	-	-	-	12,280	11,364	10,298	11,116	11,696	10,954	9,482	8,426	6,416	471,524
Cash Flow Before Interest and Tax	(92,115)	(204,761)	40,612	238,541	231,480	209,073	187,825	177,250	172,317	148,958	138,830	144,108	152,108	7,630,548
Accumulated Cash Flow (Before Interest and Tax)	(92,115)	(296,876)	(256,263)	(17,723)	213,758	422,830	610,656	787,905	1,484,041	3,180,965	4,603,990	6,082,100	7,630,548	
Income Taxes (30%)	-	-	-	(22,461)	(42,005)	(60,676)	(55,422)	(52,853)	(51,635)	(43,986)	(41,589)	(43,164)	(42,204)	(1,422,228)
After Tax Cash Flow	(92,115)	(204,761)	40,612	216,080	189,475	148,397	132,403	124,396	120,682	104,972	97,241	100,944	109,904	5,351,762
Accumulated After Tax Cash Flow	(92,115)	(296,876)	(256,263)	(40,183)	149,292	297,689	430,092	554,488	1,044,655	2,233,389	3,226,882	4,262,285	5,351,762	
Cumulative Profit Before Taxes	-	-	(82,414)	74,869	214,886	417,138	601,879	778,057	1,464,620	3,158,585	4,590,362	6,066,049	7,595,951	
Cumulative Profit After Taxes	-	-	(82,414)	52,408	150,420	291,997	421,316	544,640	1,025,234	2,211,010	3,213,253	4,246,235	5,317,166	

22.11 Economic Evaluation Results

The cash flow projection presented in Table 22-6 produces the project economic results presented in Table 22-7.

Table 22-7: Before and after taxes, economic results.

ECONOMIC RESULTS		BEFORE TAXES	AFTER TAXES
NPV 6%	MMUSD	2,195	1,529
NPV 8%	MMUSD	1,630	1,129
NPV 10%	MMUSD	1,255	864
	IRR	46.7%	39.5%
PAYOUT (from initial investment)		2 Y & 1 M	2 Y & 3 M

22.11.1 Sensitivity Analysis

In order to explore the sensitivity of the project results to changes on assumed values of relevant variables, such as lithium carbonate prices, production level, Project CAPEX and OPEX, a sensitivity analysis with respect to these variables was carried out. All results shown in this section correspond to after tax basis.

22.11.1.1 Project Sensitivity

Table 22-8 and Figure 22-2 indicate that the project's economic results are relatively sensitive to both LC price and plant production. Thus a 25% change in LC price produces a 41% change in project Net Present Value ("NPV") (8%). In the same manner, a similar change in LC production produces a 31% change in project NPV (8%). On the contrary, the project's economic results are relatively insensitive to changes in both CAPEX and OPEX. Corresponding changes in the project's economic results, in the face of a 25% change in the latter variables, produce only a 6% change in NPV(8%) for CAPEX, and a 9% change in NPV(8%) for OPEX. The result for CAPEX is positively remarkable, because it is a variable that often is underestimated, yet in this case, a 25% increase in CAPEX would produce only a 6% reduction in NPV(8%).

Table 22-8: Project After Taxes, NPV (8%) sensitivity.

Driver Variable	Base Case Values		Project NPV 8% (MMUSD)				
			75%	90%	100%	110%	125%
CAPEX	MMUSD	371	1,195	1,155	1,129	1,103	1,064
Price	USD/tonne	12,326	668	945	1,129	1,314	1,590
Production	Tonnes/year	20,000	776	988	1,129	1,270	1,482
OPEX	USD/tonne	2,937	1,236	1,172	1,129	1,087	1,023

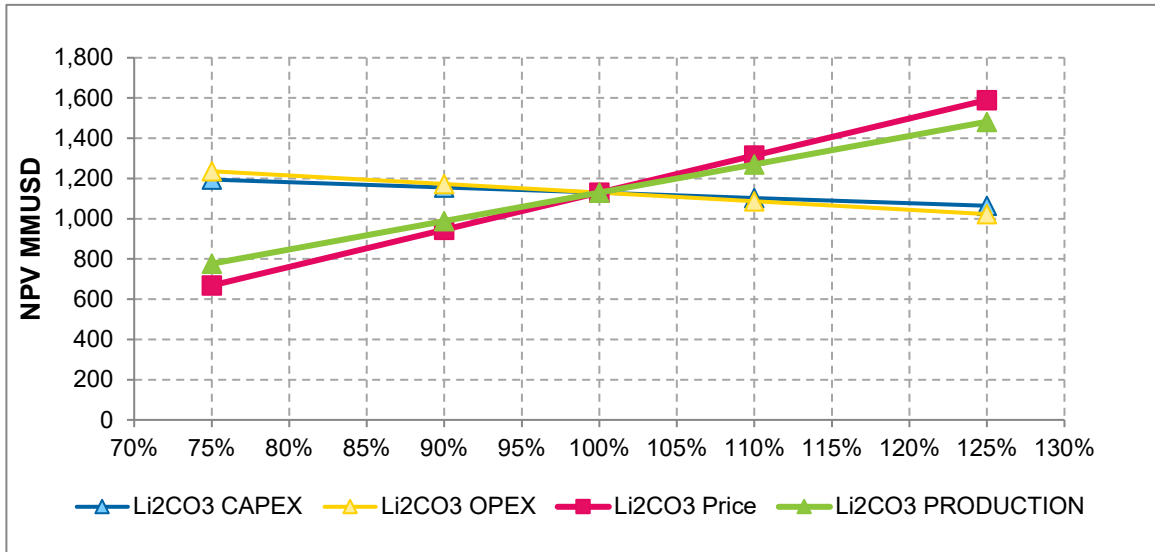


Figure 22-2: Project after taxes, NPV (8%) sensitivity.

The project’s Internal Rate of Return (“IRR”) sensitivity is in general similar to NPV sensitivity, except that in this case, CAPEX sensitivity is somewhat higher, since a 25% change in this variable produces either an 11% increase in IRR or a 7% decrease (Table 22-9, Figure 22-3).

In summary, it can be said that the project is robust, since changes in the main variables do not severely impact its economic results.

Table 22-9: Project After IRR Taxes sensitivity.

Driver Variable	Base Case Values		IRR				
			75%	90%	100%	110%	125%
CAPEX	MMUSD	371	50.6%	43.3%	39.5%	36.3%	32.4%
Price	USD/tonne	12,326	27.6%	34.9%	39.5%	43.9%	50.4%
Production	Tonnes/year	20,000	30.5%	36.0%	39.5%	42.9%	48.0%
OPEX	USD/tonne	2,937	41.9%	40.5%	39.5%	38.5%	37.0%

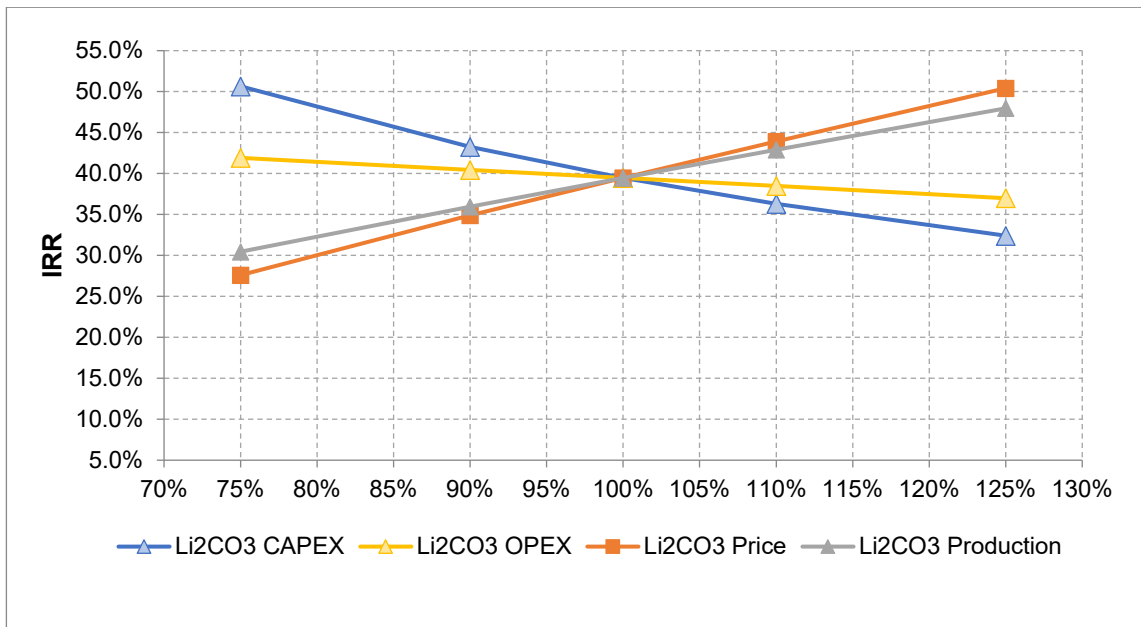


Figure 22-3: Project After Taxes IRR sensitivity.

23. Adjacent Properties

There are no known properties adjacent to the 3Q Project where lithium prospecting has been conducted. The only known previous exploration campaigns were for gold and copper, and include the following:

- Work was conducted in 1995 to 1998 by El Dorado Gold Corporation, in the western area of the catchment (vicinity of Valle Ancho River) where they drilled, trenched, and conducted a large geophysical and exploration campaign in an area that is spanned both Catamarca and La Rioja Provinces. The access road to the 3Q Project area was constructed at that time.
- Rio Tinto PLC conducted exploration, trenching, and drilling in the vicinity of Valle Ancho River from 2004 to 2005.
- East of the salar basin the company Newcrest conducted drilling, trenching and mineral exploration in a porphyry, in 1995 and 1996. Rugby Minerals conducted additional exploration in the same area, in 2011.
- In 2019 through 2021, NGEx Minerals conducted sampling, geophysics, and geological mapping at the Valle Ancho copper-gold project. The project area covers approximately 1,000 km² in the western area of the catchment and encompasses the area previously explored by El Dorado Gold Corp, Newcrest, and Rio Tinto.

The nearest lithium brine prospects, projects, and mines are:

- The Fenix Lithium Mine, located 250 km NNE of the 3Q Project in the Hombre Muerto Salar in the same Province in which the 3Q Project is located (Catamarca), in operation since 1998 and owned today by Livent corp.
- Sal de Vida Project located in Hombre Muertos salar and operated by Galaxy Corp. Galaxy completed an updated feasibility study in 2021. Since the company is listed in the Australian Stock exchange the feasibility study is not publicly available.
- Sal de Oro Project located in Hombre Muerto salar and operated by Posco Corp. No information is publicly available on this project.
- The Laguna Verde Project is located 200 km NNE, in Chile. Hinner (2009) prepared a NI 43-101 report for Etna Resources Inc., documenting an evaluation of this lithium prospect. Exploration is ongoing by Ultra Resources.
- The Blanco Project, Maricunga Salar, is located 340 km NNW, also in Chile. A NI 43-101 Definitive Feasibility Study Report was prepared on behalf of Minera Salar Blanco (Worley Parsons and Flo Solutions, 2019) which documented a Reserve Estimate for Maricunga. An updated Resource for the Blanco Project was recently prepared on behalf of Minera Salar Blanco (Reidel, 2021).

It is noted that information on any property other than the 3Q Project is not indicative of the mineralization on the 3Q Project.

24. Other Relevant Data and Information

There is no other data or information relevant to this report.

25. Interpretation and Conclusions

25.1 Brine Resources and Reserves

Preparation of the updated Mineral Resource and Reserve Estimates documented in this report, with an effective date of October 26, 2021, was prepared by Mark King, Ph.D., P.Geo., F.G.C.. The mineral deposits that are the focus of these estimates are related to lithium in brine contained within salar deposits and two brine lakes in the 3Q Salar.

The Mineral Resource and Reserve Estimates conform with National Instrument 43-101 (NI 43-101) and the Canadian Institute of Mining, Metallurgy, and Petroleum Definition Standards for Resources and Reserves (CIM Standards). The following interpretations and conclusions are supported by the 3Q Project data collected to date:

- Conditions in the 3Q Salar have led to the accumulation of brine with economic grades of lithium.
- The data indicate that the highest grades occur in the north end of the Resource zone, just south of Laguna 3Q. An evaluation of evaporation pathways indicates that the lithium accumulation is due to evaporation of the inflowing rivers and geothermal springs, especially Rio Salado.
- A numerical flow and transport model was developed to support the updated Reserve Estimate for the Project. The model was developed with FEFLOW software, and it is considered to provide a reasonable representation of site conditions. The model allows prediction of brine recovery trends for the Reserve Estimate.
- Within the wellfield simulated in the model, brine recovery is focused on Measured and Indicated Resources, primarily in the upper three geological units (Hyper-Porous Halite, Upper Sediments, and Porous Halite). The lowest two salar units (Lower Sediments, and Fanglomerate) are known to have reasonable permeability and good lithium grades. However, they are not currently targeted for brine recovery, because they are almost entirely classified as Inferred Resources.
- The northern area of elevated grade is a particularly useful location to conduct deeper sampling and hydraulic testing, aimed at converting Inferred Resources to Indicated or Measured.
- Numerical modelling results indicate that the 50-year production scenario would have minimal drawdown effects on the Laguna 3Q and Laguna Verde.
- The thickness of the deep Fanglomerate unit remains mostly unconfirmed. It was intercepted by six boreholes but only two reached the bottom of the unit.
- A trend of decreasing magnesium to lithium ratio is indicated towards the north of the Resource zone.

25.2 Infrastructure and Process Design

Infrastructure

- Salar Site:
 - The Pre-Concentration Ponds and Concentration ponds will be constructed in the centre of the salar with aggregate sourced nearby. The walls of the ponds and general orientation of the ponds are designed to allow harvesting, and to maximize evaporation.
 - The NaCl salts removed from the Pre-Concentration Ponds will be stockpiled in the south sector of the Salar and will be used as a platform to support future ponds. Potassium salts will be disposed of in a separate stockpile, outside the Salar, for possible future use.
 - For salts removed from the Calcium Removal Ponds System a Salt Storage Facility (SSF) will be built on the southeast side of the Salar. The SSF will include two storage areas with capacities of 8 Mm³ and 42 Mm³ ensuring capacity to the end of life of mine.
 - Power generation is projected to be produced by means of a Photovoltaic - Gas Hybrid System, which reduces power costs. This system can use Gas (LNG) to supply additional energy when loads are high or to minimize fuel consumption when loads are low.
 - The industrial water requirements in the Salar will be supplied from regionally available and permitted water wells and from water recovered from the Calcium Chloride Deposit Area.
 - The existing access road to the site will be enhanced to allow the safe transit of trucks and lorries.
- Fiambalá:
 - The Processing Plant will be built in the Industrial Park of Fiambalá. This Plant will have a Boron Extraction System, Calcium and Magnesium removal circuits, Lithium Carbonate precipitation, Drying, Packaging, and Storage areas preparing for the export of Lithium Carbonate.
 - The liquid waste from the Solvent Extraction stage and solid waste from the Alkali Process will be disposed of in storage ponds that include all the necessary infrastructure required by National Regulations.
 - Electricity provided to Fiambalá town comes from Tinogasta Transformer Station via a 33 kV Medium Voltage Line. At present, electricity transport capacity is saturated by Fiambalá local demand. Consequently, it is expected that a second 33 kV Medium Voltage Line capable of transporting the 8 MW required by the plant will be constructed.
 - A Water Treatment Plant will be installed to supply drinking water and high purity water required for the process. The industrial water sources are permitted water wells located in the area within the industrial facilities.
 - Maintenance facilities are also included in the design within the Fiambalá facilities.

Process and Design

- The 3Q brine Pre-Concentration process can be carried out in a conventional manner (classic dry-harvest operation) through solar evaporation ponds.

- The lithium concentration process for the pre-concentrated brine can be carried out with crystallizers to remove $\text{CaCl}_2 \cdot 6\text{H}_2\text{O}$ from the brine.
- The sequence of evaporation, saturation, supersaturation, and precipitation can be achieved by combining ponds (evaporation) and crystallizer plant (solids handling and solid-liquid separation).
- Boron at the salar is removed by adding a controlled amount of concentrated HCl to promote the formation of H_3BO_3 .
- SX-B process in Fiambalá is able to quantitatively remove boron without lithium co-extraction.
- The Alkaline Process developed by our technicians can produce battery grade lithium carbonate at a very competitive cost economizing as well as reducing freshwater consumption.
- The Pilot Lithium Carbonate Plant in Fiambalá has validated the process design by producing the desired quality of lithium carbonate within the requested parameters of a potential customer.

25.3 Economic Analysis

The economics of the 3Q Project are robust and consider all the previous analysis and proper inputs defined by NLC for 50 years of production. The items considered include:

- CAPEX: the capital investment to build the 20,000 TPY lithium carbonate 3Q Project is USD 370.5 million with an accuracy of +/- 15%. This cost covers ponds, facilities, equipment, infrastructure, direct and indirect costs and includes USD 39.7 million in contingency allowance.
- OPEX: the operating cost of the project has been estimated at USD 2,953 with an accuracy of (+/- 15%) for the 20,000 TPY lithium carbonate production. This cost puts the 3Q project in the lowest quartile cost of production of all lithium projects.
- CAPEX and OPEX estimates for the Project yield approximately USD 1,129 million of NPV, 39.5% of IRR and a Payback period of approximately 2 years and 3 months after taxes, evaluated in real terms for year 2021. Further, the timing for the Project is favorable, given the forecasted demand for lithium over the next 50 years.
- Sensitivity Analysis: shows the project is very resilient under economic pressure. Its low cost structure makes it an attractive investment even under low price scenarios that are typical in the mining industry. Lithium carbonate price has the highest impact on NPV and IRR; while CAPEX and OPEX have a lesser effects on the total results.

25.4 Project Risks

The project has identified the following risks to be noted:

- All conceptual models (like the hydrogeological model) have a degree of risk and uncertainty that should be considered when evaluating the project.
- DFS does not include a detailed design of all facilities. This means problems or discrepancies may arise during later stages that could affect reagent consumptions, production yields or production costs in general.
- Quality of reagents could have a significant impact on production quality, yield, or costs.
- Political instability could affect mining policies which could negatively affect the project.

- Process: equipment selected may not perform as per expectations. There are a number of factors (like altitude, weather, materials of construction) that could impact production equipment performance which the manufacturers may not be aware of.
- It is possible that COVID related control measurements, may not have been considered in the cost and or schedule of the project.

25.5 Conclusions

NLC has de-risked the 3Q Project technically and financially. A systematic low-cost approach and innovative search was applied to overcome the complexity of the brine and site logistics. The recovery process shows a significantly positive NPV for the Project.

Technical work conducted to date is favorable for the economic outlook of the 3Q Project, including the following results.

- 3Q Project exploration has supported the estimation of Mineral Resources and Reserves. The project contains sufficient mineral Reserves to support the feasibility of a 20,000 TPY Lithium Carbonate production facility with a 50-year mine life.
- Pumping tests and numerical modelling have confirmed the capacity of the aquifers at the site to produce the brine required by the mine plan.
- The economics of the 3Q Project are robust and consider all the previous analysis and proper inputs defined by NLC for 50 years of production.
- The market conditions look optimal due to a very high demand scenario that will continue to grow for the foreseeable future.
- In total, the project is attractive for investment and development.

26. Recommendations

26.1 Brine Resources and Reserves

The following exploration and analysis activities are proposed to potentially increase Mineral Resources and Reserves:

Mineral Resources

- It is recommended to drill at least 3 wells down to at least 400 m below salar surface elevation (> 3686 m asl) in the northern high-grade zone to potentially deepen the Measured and Indicated Resources to 250 and 400 m depth, respectively.
- The lower permeable units (Lower Sediments and Fanglomerate) contain about 30% of the Resource, all in the Inferred category. It is recommended to drill six more deep boreholes (target depth 800 m) in the central and northern salar, to potentially deepen the Measured and Indicated Resource zones.
- It is also recommended to drill at least 3 boreholes down to 400 m below ground surface in the Blue Sky zone to the east and south of Laguna 3Q. This area is also east of the current Resource model, and the objective of this drilling is to potentially expand the model towards the east.

Mineral Reserves

- Five additional long term pumping tests should be conducted in association with the Resource drilling recommended above. The tests would target the Lower Sediments and Fanglomerate at depth under the high-grade northern zone, and the Blue Sky zone to the east of the current Resource model. The objective of the tests is to characterize the hydraulic properties of the drilled units.
- Monitoring should continue for the rivers (flow and chemistry), salar brine levels, lake levels and meteorology.
- Results from all the investigations recommended above (drilling, sampling, pumping tests) should be used to define additional Measured and Indicated Resources, as appropriate. The numerical FEFLOW model should then be revised and re-run, to update Reserves.
- The FEFLOW numerical model should be updated on an ongoing basis, as additional exploration, early production, and environmental monitoring data become available.

26.2 Engineering

This DFS Report indicates favorable economics for the 3Q Project. It is recommended that NLC move forward to complete Detailed Design and commence Construction of critical infrastructure (Roads and Camps), subject to financing.

Recommendations for the 3Q Project

- Continuing immediately with the Detailed Engineering of the Calcium Chloride crystallizer plant.
- Pilot Plant: It is recommended that the pilot plant is changed to operate on continuous basis to simulate potential problems, and to start training future operators.
- It is recommended that subproducts are studied and developed as part of the strategy to minimize waste and further utilize potential project resources.

- A cost - benefit analysis should be conducted to evaluate truck fleet ownership versus truck fleet contracting. This study should be preceded by a more detailed transportation evaluation to minimize distances and operational costs.
- Engineering Optimization should be conducted for plant layouts to minimize construction costs and to further define equipment selection criteria (cost, quality, reliability, etc.).

27. List of Abbreviations

%	:	percentage
°C	:	temperature in degrees Celsius
2D	:	two dimensional
3D	:	three dimensional
3Q	:	Tres Quebradas (Project)
asl	:	above sea level
ASL	:	Alex Stewart Laboratories
B	:	boron
Ba	:	barium
BG	:	battery grade
bgs	:	below ground surface
BMI	:	Benchmark Mineral Intelligence
Ca	:	calcium
Ca/Li	:	calcium to lithium ratio
CaCl ₂ •6H ₂ O	:	antarcticite
CaCO ₃	:	calcium carbonate
Ca(OH) ₂	:	calcium hydroxide
CaSO ₄ •2H ₂ O	:	gypsum
CAPEX	:	Capital Cost Estimates
\$CDN	:	Canadian Dollars
Cl	:	chlorine
cm	:	centimetre
CSR	:	corporate social responsibility
DIPGAM	:	Ministry of Mining, State of Catamarca; Provincial Directorate of Environmental Management Mining
<i>E</i>	:	evaporation
<i>E_o</i>	:	free water evaporation rate
EBS	:	environmental baseline studies
EC	:	Executive Committee
Eh	:	electrical potential (redox state)
EIR	:	Environmental Impact Report
EIS	:	Environmental Impact Statement
EPs	:	Equator Principles
ESG	:	Environmental, Social, and Governance
<i>f_{ev}</i>	:	Depth-Dependent Factor
Fe	:	iron

FG	:	Fanglomerate (geological unit)
FS	:	Feasibility Study
g/ml	:	grams per milliliter
GIS	:	geographic information system
GPS	:	global positioning system
GT	:	GT Ingeniería SA
GWI	:	Groundwater Insight Inc.
ha	:	hectare
H ₃ BO ₃	:	boric acid
HCl	:	hydrochloric acid
HPH	:	Hyper-Porous Halite (geological unit)
hr	:	hour
H ₂ SO ₄	:	sulphuric acid
ICP-OES	:	inductively coupled plasma – optical emission spectrometry
IDW	:	Inverse Distance Weighting
IDW ²	:	Inverse Distance Weighting Squared
IFC	:	International Finance Corporation
IRR	:	Internal Rate of Return
K	:	potassium
K/Li	:	potassium to lithium ratio
KCl	:	potassium chloride
Kh	:	horizontal conductivity
Kh/Kv	:	anisotropy in hydraulic conductivity
km	:	kilometre
km ²	:	square kilometre
km/h	:	kilometres per hour
kTPY	:	kilotonne per year
Kv	:	vertical hydraulic conductivity
L	:	litre
L/s	:	litres per second
LC	:	lithium carbonate
LCE	:	lithium carbonate equivalent
Li	:	lithium
Li ₂ CO ₃	:	lithium carbonate
LIEX	:	LIEX S.A. (wholly owned, Argentinean subsidiary of NLC)
LNG	:	liquified natural gas
LS	:	Lower Sediments (geological unit)
m	:	metre
m ³	:	cubic metres

m/d	:	metres per day
mg	:	milligram
Mg	:	magnesium
mg/L	:	milligrams per litre
Mg/Li	:	magnesium to lithium ratio
Mg(OH) ₂	:	magnesium hydroxide
MH	:	Massive Halite (geological unit)
mL	:	millilitre
mm	:	millimetre
mm/d	:	millimetres per day
mm/y	:	millimetres per year
Mm ³	:	million cubic metres
MMUSD	:	million United States dollars
MW	:	megawatt
MWh	:	megawatt hour
Na	:	sodium
NaCl	:	halite
Na ₂ CO ₃	:	sodium carbonate
NaOH	:	sodium hydroxide
NFPA	:	National Fire Protection Association
NI	:	National Instrument
NLC	:	Neo Lithium Corporation
NPV	:	Net Present Value
OPEX	:	Operating Cost Estimates
P	:	total porosity
PC	:	pre-concentration ponds
PCA	:	principal component analysis
PFS	:	Pre-Feasibility Study
pH	:	measure of acidity or alkalinity
PH	:	Porous Halite (geological unit)
QA/QC	:	quality assurance/quality control
QP	:	Qualified Person
RBRC	:	relative brine release capacity
RC	:	reverse circulation
RO	:	reverse osmosis
SD	:	standard deviations
SDGs	:	UN Sustainable Developments Goals
SEM	:	Catamarca Mining State Secretary
Semicat	:	Servicios Integrales Mineros Catamarca SRL

SO ₄ ²⁻	:	sulfate
SO ₄ /K	:	sulfate to potassium ratio
SO ₄ /Li	:	sulfate to lithium ratio
SO ₄ /Mg	:	sulfate to magnesium ratio
SO ₄ ²⁻	:	sulfate
Sr	:	strontium
SRP	:	Social Responsibility Plan
Ss	:	specific storage
SX	:	solvent extraction
Sy	:	specific yield
t	:	tonnes
t/y	:	tonnes per year
TDS	:	total dissolved solids
TG	:	technical grade
TPY	:	tonnes per year
TSX	:	Toronto Stock Exchange
UNSAM	:	Universidad Nacional de San Martin
US	:	Upper Sediments (geological unit)
USD	:	United States dollar
VES	:	Vertical Electrical Sounding geophysical survey
WOR	:	Worley
W/m ²	:	Watts per square metre
WWTP	:	wastewater treatment plant
y	:	year
Zn	:	zinc

28. Date, Signature, and Certificate

CERTIFICATE OF QUALIFIED PERSON

I, Mark W.G. King, served as supervising QP for certain items of the “Feasibility Study Technical Report on the Tres Quebradas Lithium Project, Catamarca Province, Argentina” (specific Sections noted in point 5., below). This report (the “Report”) was prepared for Neo Lithium Corp. and has an effective date of October 26, 2021. In my role as QP, I do hereby certify that:

1. I am employed as President and Senior Hydrogeologist with Groundwater Insight Inc., 3 Melvin Road, Halifax, Nova Scotia, B3P 2H5, telephone 902 223 6743, email king@gwinsight.com.
2. I have the following academic and professional qualifications and experience:
 - a. Academic
 - i. B.Sc. (Geology), Dalhousie University, Halifax, Nova Scotia, 1982
 - ii. M.A.Sc. (Civil Eng.), Technical University of Nova Scotia, 1987
 - iii. Ph.D. (Earth Science), University of Waterloo, Waterloo, Ontario, 1997
 - b. Professional
 - i. Registered Professional Geoscientist of Nova Scotia (membership #84); Serving on Admissions Board of the Association
 - ii. Member of Association of Groundwater Scientists and Engineers (membership #3002241)
 - iii. Member and a previous Director for the International Association of Hydrogeologists
 - c. Experience and Areas of Specialization Relevant to this Report
 - i. Technical involvement in lithium brine projects, in various levels of detail, on more than 20 salars in Chile, Argentina and Nevada
 - ii. Numerical modelling of groundwater flow and solutes in groundwater
 - iii. Field delineation and monitoring of solutes in groundwater
 - iv. Organic and inorganic groundwater geochemistry
 - v. 33 years of experience in groundwater quality and quantity projects.
3. I am a qualified person (“QP”) for the purposes of National Instrument 43-101 – Standards of Disclosure for Mineral Projects (the “Instrument”).
4. While working on the current previous Technical Reports for the 3Q Project, I visited the Project six times. During the current report, I was prevented from visiting the Project, due to COVID restrictions. Visits to the project include:
 - a. March 2016 for three days
 - b. January 2017 for three days

- c. October 2017 for three days
 - d. April 2018 for five days
 - e. December 2018 for five days
5. I am responsible for technical review and supervising the preparation of the following Items of this Report: Sections 4 to 12, 14 to 16, 20, and 23, as well as associated information in Sections 1, 2, 3, 25, and 26).
 6. I am independent of Neo Lithium Corp. as described in Section 1.5 of the Instrument.
 7. The scope of my previous involvement with the Tres Quebradas Salar was in connection with the preparation of four previous Technical Reports on the Project, dated June 6, 2016; May 23, 2017; August 15, 2018; and April 1, 2021.
 8. I have read the Instrument and this Report has been prepared in compliance with the Instrument.
 9. As of the effective date of this Report, and to the best of my knowledge, information and belief, this Report contains all scientific and technical information that is required to be disclosed to make this Report not misleading.

Effective Date: October 26, 2021

Date of Signing: November 25, 2021

"Mark King"

"sealed"

Original signed and stamped by Mark

W.G. King, Ph.D., P. Geo., F.G.C

CERTIFICATE OF QUALIFIED PERSON

I, Marek Dworzanowski, served as supervising QP for certain items of the “Feasibility Study Technical Report on the Tres Quebradas Lithium Project, Catamarca Province, Argentina” (specific Sections noted in point 5., below). This report (the “Report”) was prepared for Neo Lithium Corp. and has an effective date of October 26, 2021. In my role as QP, I do hereby certify that:

1. I am employed as an Independent Consulting Metallurgical Engineer, Les Chenes, Lieu dit Langlade, 82110 Trejols, France, telephone +33 563392126, email marek.dworzanowski@gmail.com
2. I have the following academic and professional qualifications and experience:
 - d. Academic
 - iv. B.Sc. (Honours), in Mineral Processing, University of Leeds, 1980
 - v. Adjunct Professor of Metallurgical Engineering, School of Chemical & Metallurgical Engineering, University of the Witwatersrand, South Africa, 2016 to 2022
 - e. Professional
 - i. Registered Chartered Engineer with the Engineering Council of the United Kingdom, membership number 485805
 - ii. Honorary Fellow of the Southern African Institute of Mining and Metallurgy (FSAIMM), membership number 19594
 - iii. Fellow of the Institute of Materials, Minerals and Mining (FIMMM), membership number 485805
 - f. Experience and Areas of Specialization Relevant to this Report
 - vi. Technical involvement in lithium brine projects, in various levels of detail, on 6 salars in Chile and Argentina
 - vii. Experience in the design and operation of all the unit processes that make up the production of lithium carbonate from brine
 - viii. 41 years of experience in the global mining industry
3. I am a qualified person (“QP”) for the purposes of National Instrument 43-101 – Standards of Disclosure for Mineral Projects (the “Instrument”).
4. I visited the 3Q Project during 11-13 February 2021, inspecting all the facilities at the salar and in Fiambalá.
5. I am responsible for technical review and supervising the preparation of the following Items of this Report: Sections 13, 17, 18, 19, 21, 22, and 24 as well as associated information in Sections 1, 2, 3, 25, and 26).
6. I am independent of Neo Lithium Corp. as described in Section 1.5 of the Instrument.
7. I have read the Instrument and this Report has been prepared in compliance with the Instrument.

8. As of the effective date of this Report, and to the best of my knowledge, information and belief, this Report contains all scientific and technical information that is required to be disclosed to make this Report not misleading.

Effective Date: October 26, 2021

Date of Signing: November 25, 2021

"Marek Dworzanowski"

Original signed by

Marek Dworzanowski CEng, BSc(Hons), Hon FSAIMM, FIMMM

29. References

- Baez, G. and Grosso, S., 2018.** Geología – Geomorfología Proyecto Tres Quebradas. Report prepared for Neo Lithium Corp.
- Barrionuevo, C., 2018a.** Línea Base Ambiental, Fauna de Vertebrados Terrestres. Report prepared for Neo Lithium Corp.
- Barrionuevo, C., 2018b.** Fauna de Vertebrados Terrestres Tramo: Fiambalá - Ingreso al Puesto La Coipa (RN 60). Primavera de 2017. Report prepared for Neo Lithium Corp.
- Barrionuevo, C., 2018c.** Fauna de Vertebrados Terrestres a través de un gradiente altitudinal. Recorrido: Ingreso al Puesto La Coipa (RN 60) – Ingreso al Campamento Minero. Primavera de 2017. Report prepared for Neo Lithium Corp.
- Burgos, F., 2017.** Fauna, Proyecto Tres Quebradas, Departamento Tinogasta Provincia de Catamarca. Report prepared for Neo Lithium Corp.
- Burga, E., Burga, D., Weber, D., Sanford, A., and Dworzanowski, M., 2020.** *Updated Feasibility Study and Mineral Reserve Estimation to Support 40,000 tpa Lithium Carbonate Production at the Cauchari-Olaroz Salara, Jujuy Province, Argentina.* Report prepared for Lithium Americas. NI 43-101 technical report filed on the Canadian Securities Administrators System for Electronic Document Analysis and Retrieval (SEDAR).
- Canadian Securities Administrators, 2005.** National Instrument 43-101, Standards of Disclosure for Mineral Projects. 13p.
- CIM Standing Committee on Resource and Reserve Definitions, 2014.** CIM Definition Standards-For Mineral Resources and Mineral Reserves. https://mrmr.cim.org/media/1128/cim-definition-standards_2014.pdf
- Climate Hazards Group InfraRed Precipitation with Station data (CHIRPS), 2018.** CHIRPS: Rainfall Estimates from Rain Gauge and Satellite Observations. <https://www.chc.ucsb.edu/data/chirps>.
- Cunto, V., 2018.** Estudio de Línea de base Socioeconómica, Micro región Tinogasta, Provincia de Catamarca, República Argentina, Marzo 2018. Report prepared for Neo Lithium Corp.
- Diersch H-J.G., 2014.** FEFLOW Finite Element Modeling of Flow, Mass and Heat Transport in Porous and Fractured Media. Springer. Berlin. 996 pp. 2014.
- DHI WASY, 2021.** FEFLOW (Version 7.4). Software.
- Farias, M. E., 2018.** Línea de base Limnología Proyecto Tres Quebradas. Report prepared for Neo Lithium Corp.
- Feldman, A.D. 2000.** Hydrologic modelling system HEC-HMS: technical reference manual. US Army Corps of Engineers, Hydrologic Engineering Center.
- Fetter, C.W., 1994.** Applied Hydrogeology. Prentice Hall Inc., Upper Saddle River, New Jersey.
- Freeze, R.A., and Cherry, J.A., 1979.** Groundwater. Prentice Hall Inc., Englewood Cliffs, New Jersey.
- Funk, C., Peterson, P., Landsfeld, M., Pedreros, D., Verdín, J., Shukla, S., Husak, G., Rowland, J., Harrison, L., Hoell, A., and Michaelsen, J., 2015.** The climate hazards infrared precipitation with stations- a new environmental record for monitoring extremes. Scientific Data 2, 150066. doi:10.1038/sdata.2015.66.

Gravriloff, I. and Muruaga, C., 2018. Estudio de Línea de Base Paleontológico, Proyecto 3Q- Tres Quebradas. Report prepared for Neo Lithium Corp.

Hains, D.H., 2012. CIM Best Practice Guidelines for Resource and Reserve Estimation for Lithium Brines. CIM Estimation Best Practice Committee. <https://mrmr.cim.org/media/1041/best-practice-guidelines-for-reporting-of-lithium-brine-resources-and-reserves.pdf>.

Hinner, J. E., 2009. Technical Report on the Laguna Verde Salar Project and other Salar Properties held by South American Lithium Company S.A. Cerrada Third Region, Copiapo, Chile.

Houston, J., and Gunn, M., 2011. *Technical report on the Salar de Olaroz lithium-potash project, Jujuy Province, Argentina.* Prepared for Orocobre Ltd. NI 43-101 Technical Report filed on the Canadian Securities Administrators System for Electronic Document Analysis and Retrieval (SEDAR).

IHLLA, 2018a. Flow numerical modeling and simulation of exploitation scenarios in salar de Tres Quebradas, Fiambalá, Catamarca, Argentina. Unpublished report prepared for Neo Lithium Corp.

IHLLA, 2018b. Hidroquímica del salar de Tres Quebradas. Unpublished report prepared for Neo Lithium Corp.

IHLLA, 2019. Estimación de la evaporación en el Salar 3Q. Unpublished report prepared for Neo Lithium Corp.

IL & A, Ingeniería laboral y Ambiental S.A.; Enero, 2018. Estudio línea de base de calidad de aire proyecto Tres Quebradas, departamento Tinogasta- Catamarca. Report prepared for Neo Lithium Corp.

Induser Laboratory, 2018. Calidad de Agua. Report prepared for Neo Lithium Corp.

Izquierdo, A., Vaieretti, M.V., Harguindeguy, N.P., Foguet, N., Chiappero, F. and Navarro, C., 2018. Paisaje y Suelo, Informe final Línea de base Proyecto Tres Quebradas, Marzo 2018. Report prepared for Neo Lithium Corp.

Johnson, E., Yáñez, J., Ortiz, C. & Muñoz, J., 2010. Evaporation from shallow groundwater in closed basins in the Chilean Altiplano. *Hydrol. Sci. J.* 55(4), 624–635.

King, M., 2016. *Technical Report on the Tres Quebradas Lithium Project, Catamarca Province, Argentina.* Prepared for POCML 3 INC. and Neo Lithium Corp. by Groundwater Insight Inc. NI 43-101 technical report filed on the Canadian Securities Administrators System for Electronic Document Analysis and Retrieval (SEDAR).

King, M., 2017. *Mineral Resource Estimate Technical Report on the Tres Quebradas Lithium Project Catamarca Province, Argentina.* Prepared for Neo Lithium Corp. by Groundwater Insight Inc. NI 43-101 technical report filed on the Canadian Securities Administrators System for Electronic Document Analysis and Retrieval (SEDAR).

King, M., 2018. *Updated Mineral Resource Estimate Technical Report on the Tres Quebradas Lithium Project Catamarca Province, Argentina.* Prepared for Neo Lithium Corp. by Groundwater Insight Inc. NI 43-101 technical report filed on the Canadian Securities Administrators System for Electronic Document Analysis and Retrieval (SEDAR).

King, M. and Zandonai, G. 2021. *Amended Preliminary Feasibility Study (PFS) – 3Q Project, Catamarca, Argentina.* Prepared for Neo Lithium Corp. by Groundwater Insight Inc. and GHD. NI 43-101 technical report filed on the Canadian Securities Administrators Systems for Electronic Document Analysis and Retrieval (SEDAR).

King, M., Kelley, R., and Abbey, D., 2012. *Reserve Estimation and Lithium Carbonate and Potash Production at the Cauchari-Olaroz Salars, Jujuy Province, Argentina.* NI 43-101 Feasibility Report prepared

for Lithium Americas Corporation. Report filed on the Canadian Securities Administrators System for Electronic Document Analysis and Retrieval (SEDAR).

King, M., García, J., Calderón, C., Figueroa, F., Mehech, I., 2019. *Informe Técnico de Recursos y Reservas de Lito en la concesión minera de Albemarle en el Salar de Atacama, Chile*. NI 43-101 compliant Technical Report Prepared for Albemarle Corporation. Report submitted to the Chilean Nuclear Energy Commission (CCHEN).

Martin and Miguens, 2021a. Oficina Abogados. LIEX Title Opinion, Buenos Aires. February 9, 2021.

Martin and Miguens, 2021b. Oficina Abogados. LIEX Title Opinion, Buenos Aires. October 1, 2021.

Marazuela, M.A., Vázquez-Suñé, E., Ayora, C., García-Gil, A., Palma, T., 2019. The effect of brine pumping on the natural hydrodynamics of the Salar de Atacama: The damping capacity of salt flats. *Science of The Total Environment*, vol. 654, p. 1118-1131.

National Instrument 41-101, 2016. NI 43-101 Standards of Disclosure for Mineral Projects.

Pavlovic, P. and Fowler, J., 2004. Evaluations of the potential of Salar Del Rincon brine deposit as a source of lithium, potash, boron, and other mineral resources. Technical report.

Pitts, R., 2017. *Preliminary Economic Assessment (PEA) 3Q Project*. NI 43-101 technical report prepared for Neo Lithium Corp. by GHD. Report filed on the Canadian Securities Administrators System for Electronic Document Analysis and Retrieval (SEDAR).

Ratto, N., 2016. Caracterización arqueológica del área del proyecto Tres Quebradas, Minas Lodomar I a la XI, departamento Tinogasta, Catamarca. Report prepared for Neo Lithium Corp.

Ratto, N., 2017. Estudio de Línea de impacto arqueológico del proyecto Tres Quebradas, Fiambalá Departamento Tinogasta, Catamarca, Noviembre 2017. Report prepared for Neo Lithium Corp.

Reidel, F., 2017. *Resource Estimate for Lithium & Potassium Sal de los Angeles Project*. Report prepared for LithiumX. NI 43-101 technical report filed on the Canadian Securities Administrators System for Electronic Document Analysis and Retrieval (SEDAR).

Reidel, F., 2021. Lithium Resources Update, Minera Salar Blanco, Stage 1 (Old Code Concessions) III Region, Chile. NI 43-101 technical report prepared for Minera Salar Blanco by Atacama Water Consultants. Report filed on the Canadian Securities Administrators System for Electronic Document Analysis and Retrieval (SEDAR).

Roskill, 2009. Roskill: Lithium Market Reports, 2009: <https://roskill.com/>.

Rosko, M., A, Sandford, J. Riordan, B. Talbot. 2021. *Sal de Vida Project, Salar del Hombre Muerto, Catamarca Argentina*. Prepared for Galaxy Resources Ltd. By Montgomery and Associates. NI 43-101 Technical Report filed on the Canadian Securities Administrators System for Electronic Document Analysis and Retrieval (SEDAR).

Salinas, R., 2017a. Flora y Vegetación, Tramo Fiambalá - La Ciopa, dpto. Tinogasta, Catamarca, Argentina. Report prepared for Neo Lithium Corp.

Salinas, R., 2017b. Flora y Vegetación, Tramo La Ciop- Campamento Tres Quebradas, dpto. Tinogasta, Catamarca, Argentina. Report prepared for Neo Lithium Corp.

Salinas, R., 2018. Flora- Vegetación, Proyecto Tres Quebradas, Minas: LODOMAR I a X, Departamento Tinogasta, Provincia Catamarca, Argentina. Marzo 2018. Report prepared for Neo Lithium Corp.

Schwartz F.W. and Zhang, H., 2003. *Fundamentals of Groundwater*. Second Edition. John Wiley & Sons. 583 pp. 2003.

Silva, D.S.F. and Boisvert, J.B., 2014. Mineral resource classification: a comparison of new and existing techniques. *Journal of the Southern African Institute of Mining and Metallurgy [online]*. Vol. 114, n. 3, pp. 256-273.

SQM, 2009. US SEC Report Form 2-F.

Tálamo, E., 2018. Caracterización Hidroquímica –Extracto para Equipo de Ingeniería de 3Q – LIEX S.A. Report prepared for Neolithium Corp.

Valdivia, O., 2018. Estudio de Línea de Base Tránsito Vehicular, Proyecto 3 Quebradas, departamento Tinogasta, Provincia de Catamarca, Enero 2018. Report prepared for Neo Lithium Corp.

Vila Melo, 2018. Compendio legal del proyecto 3 Q y área de influencia.

Worley Parsons and Flo Solutions, 2019. *Definitive Feasibility Study of MSB Blanco Lithium Carbonate Project*. Prepared for Minera Salar Blanco by Worley Parsons and Flo Solutions, NI 43-101 technical report filed on the Canadian Securities Administrators System for Electronic Document Analysis and Retrieval (SEDAR).

Zotelo, C.H., 2018. Informe Meteorológico y climatológico para informe Impacto ambiental (IIA) Tres Quebradas – Fiambalá, provincia Catamarca, Argentina. Report prepared for Neo Lithium Corp.

Appendices

Appendix A – SELLEY LOG - LOG AND CORRELATION LINE LOCATIONS



Figure A-1: Selley log locations and correlation line.

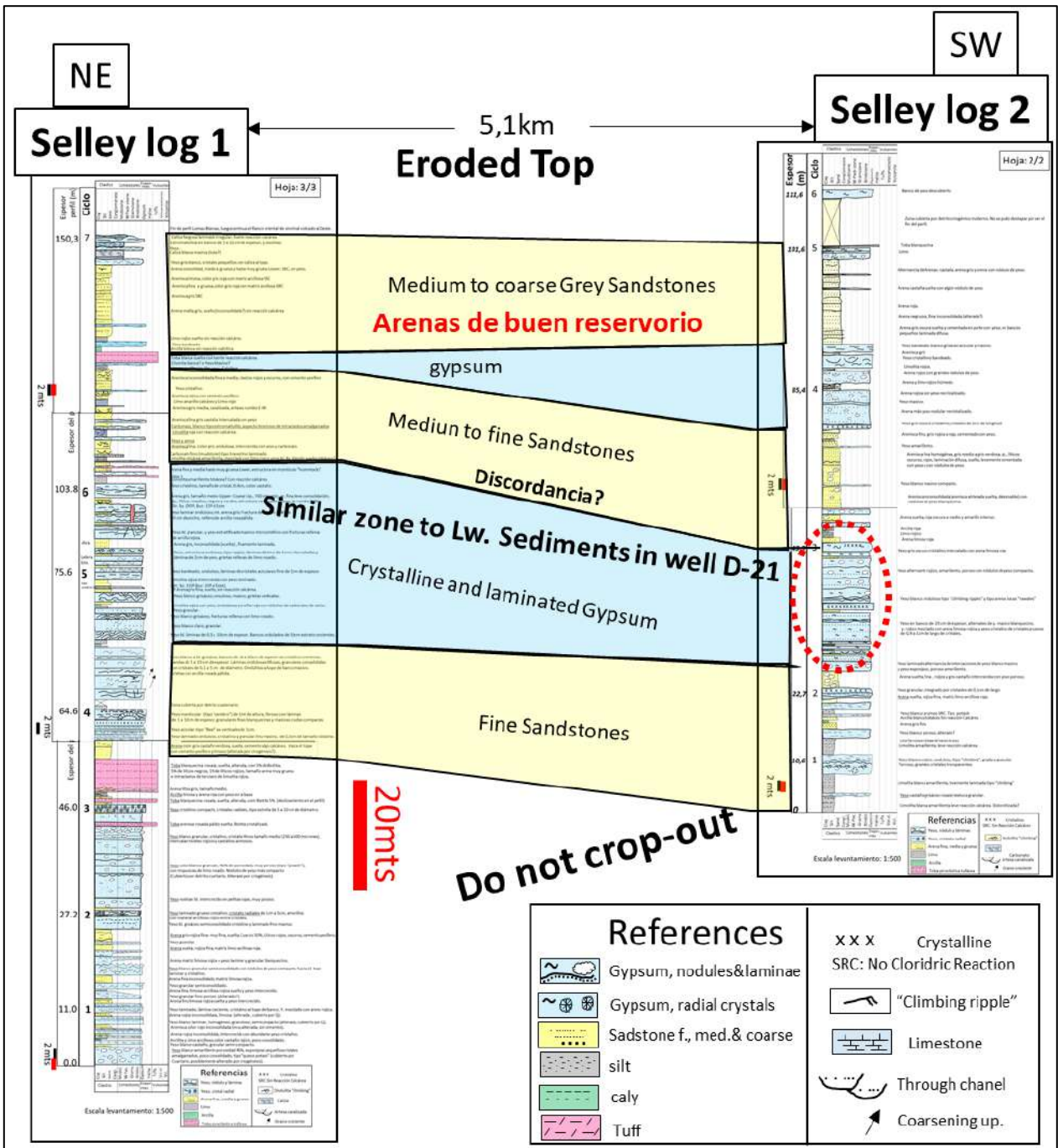


Figure A-2 Correlation of two outcrop Selley Logs, on the eastern margin of 3Q Salar.

Appendix B – ISOPACH MAPS FOR THE SIX SALAR UNITS

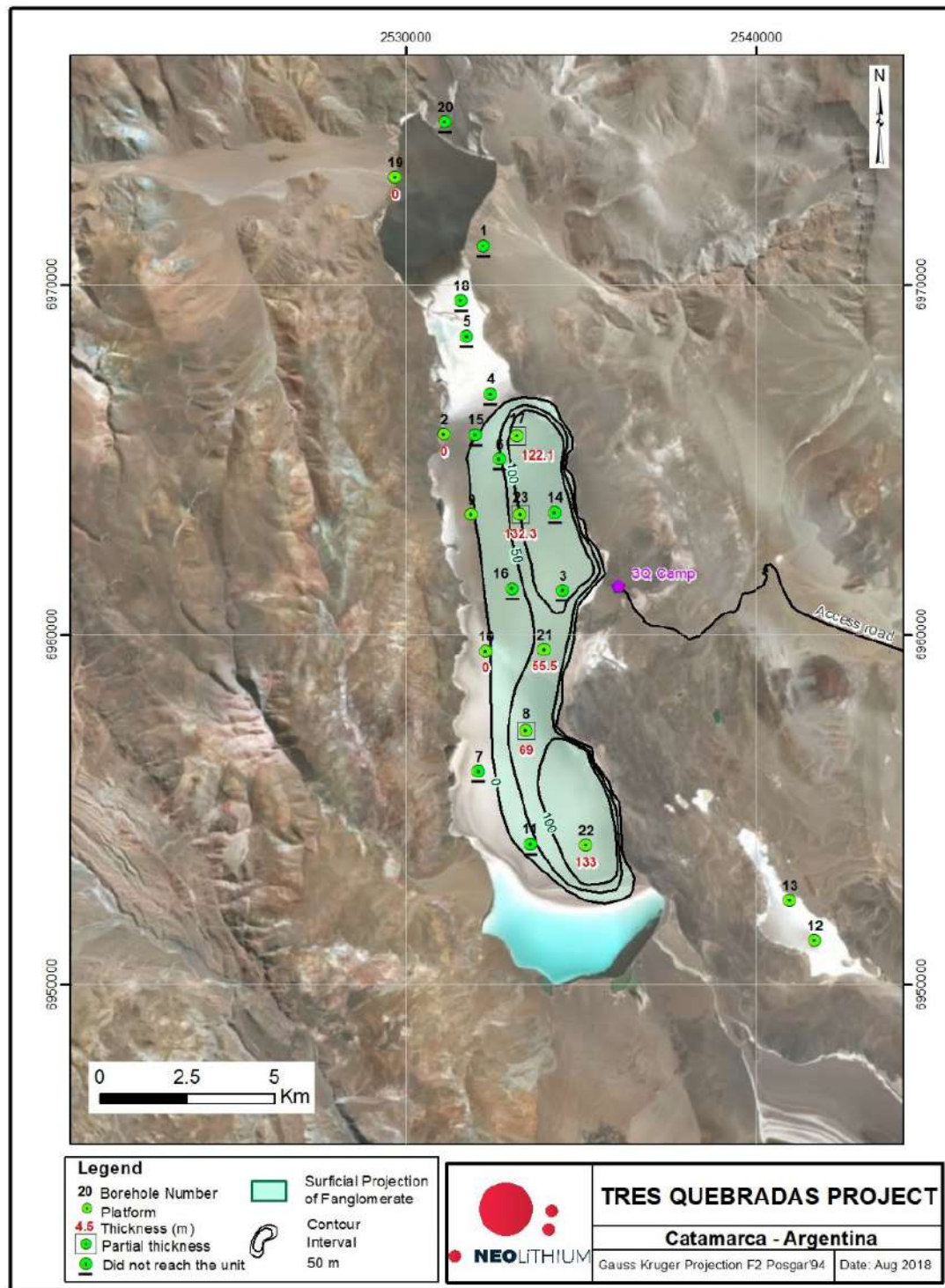


Figure B-1: Isopach map for the Fanglomerate unit.

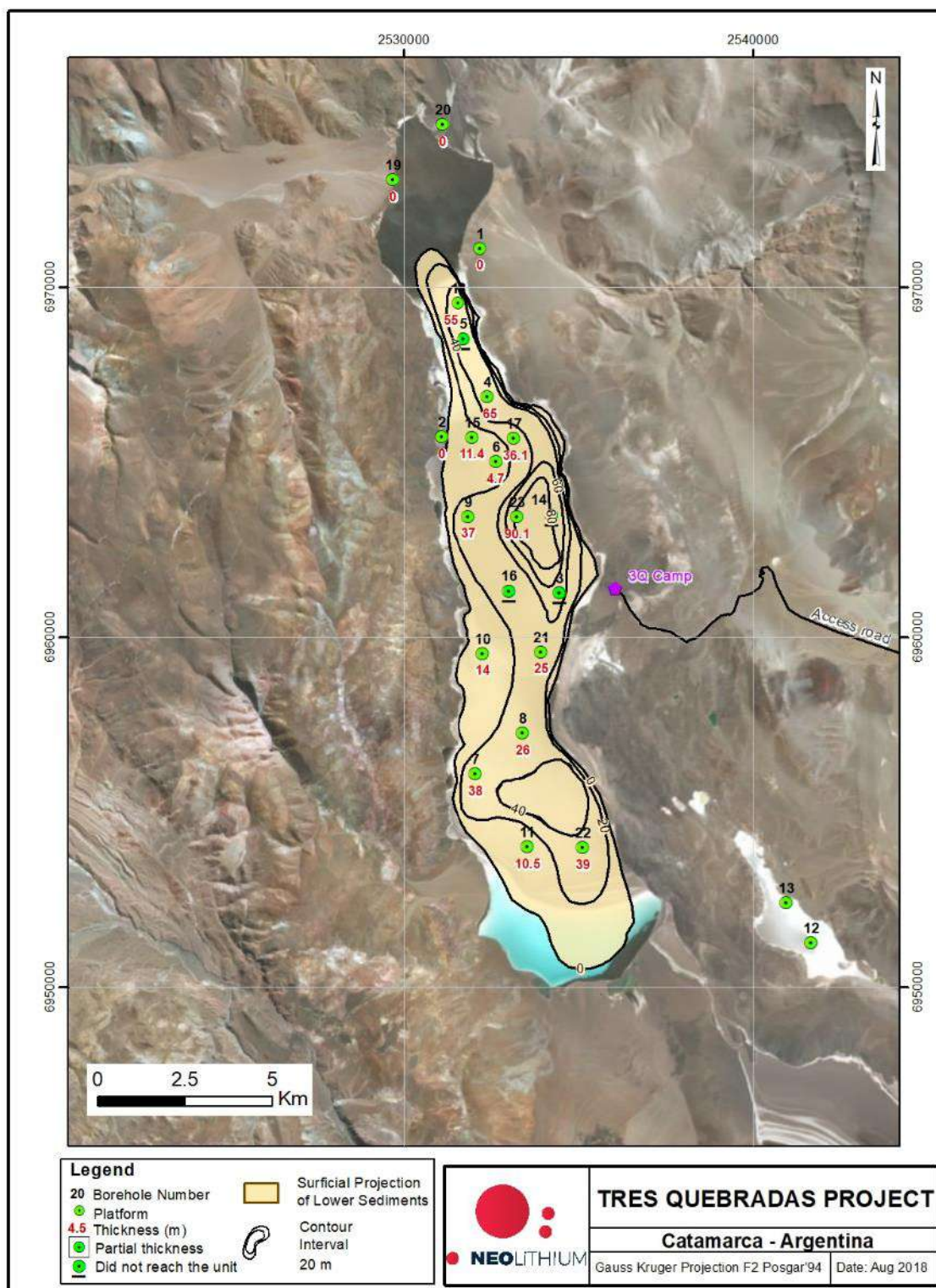


Figure B-2: Isopach map for the Lower Sediments unit.

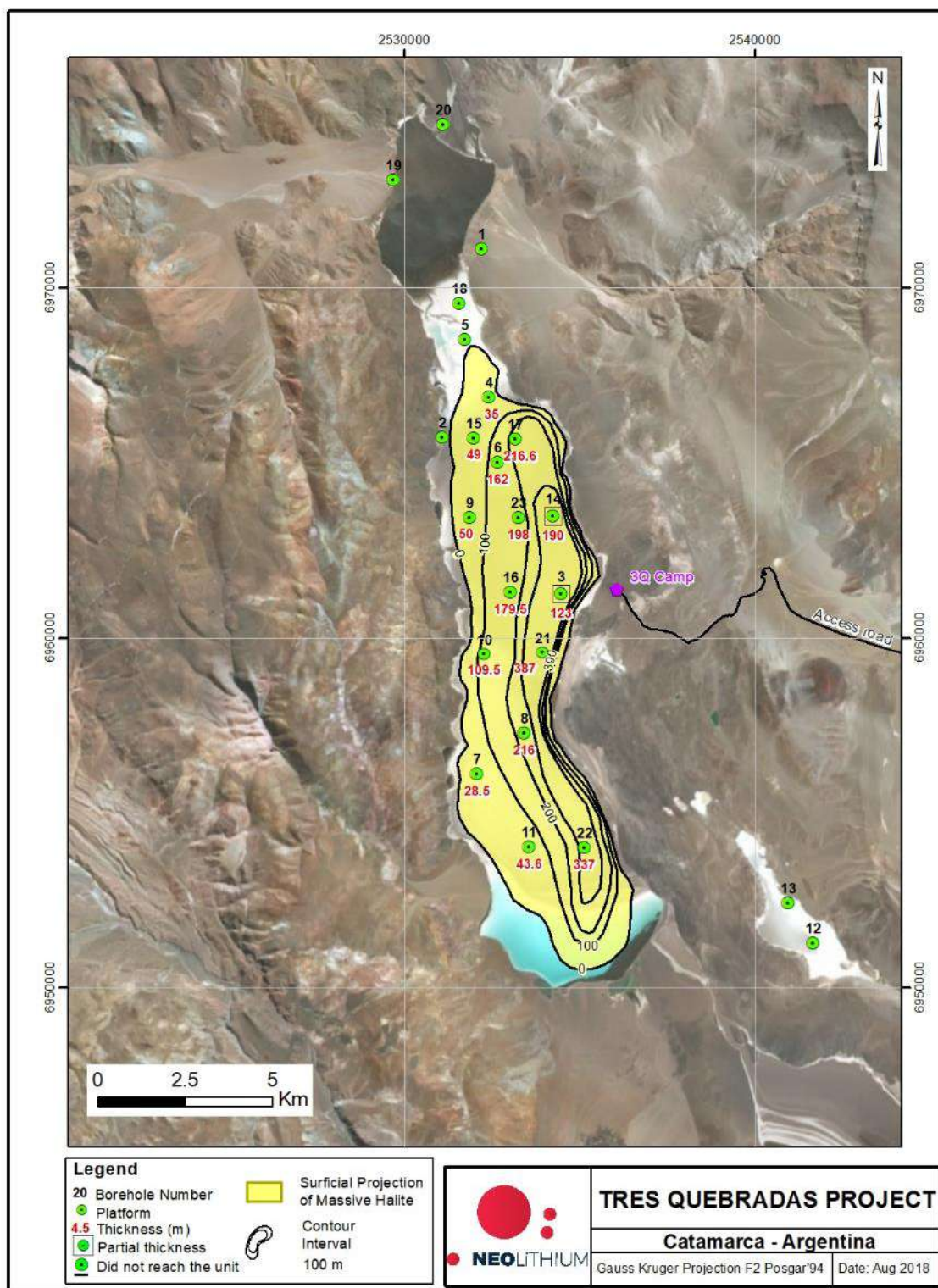


Figure B-3: Isopach map for the Massive Halite unit.

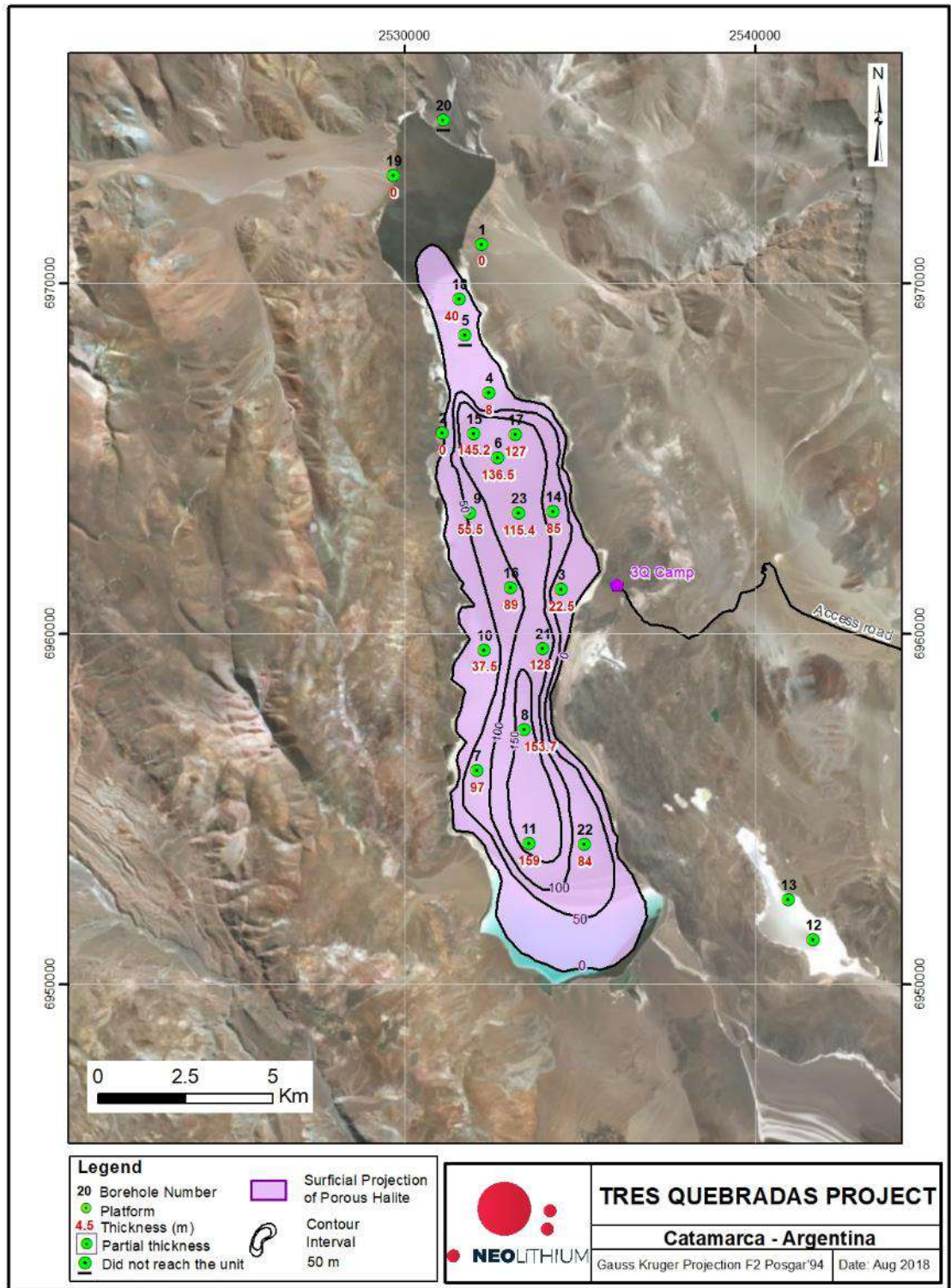


Figure B-4: Isopach map for the Porous Halite unit.

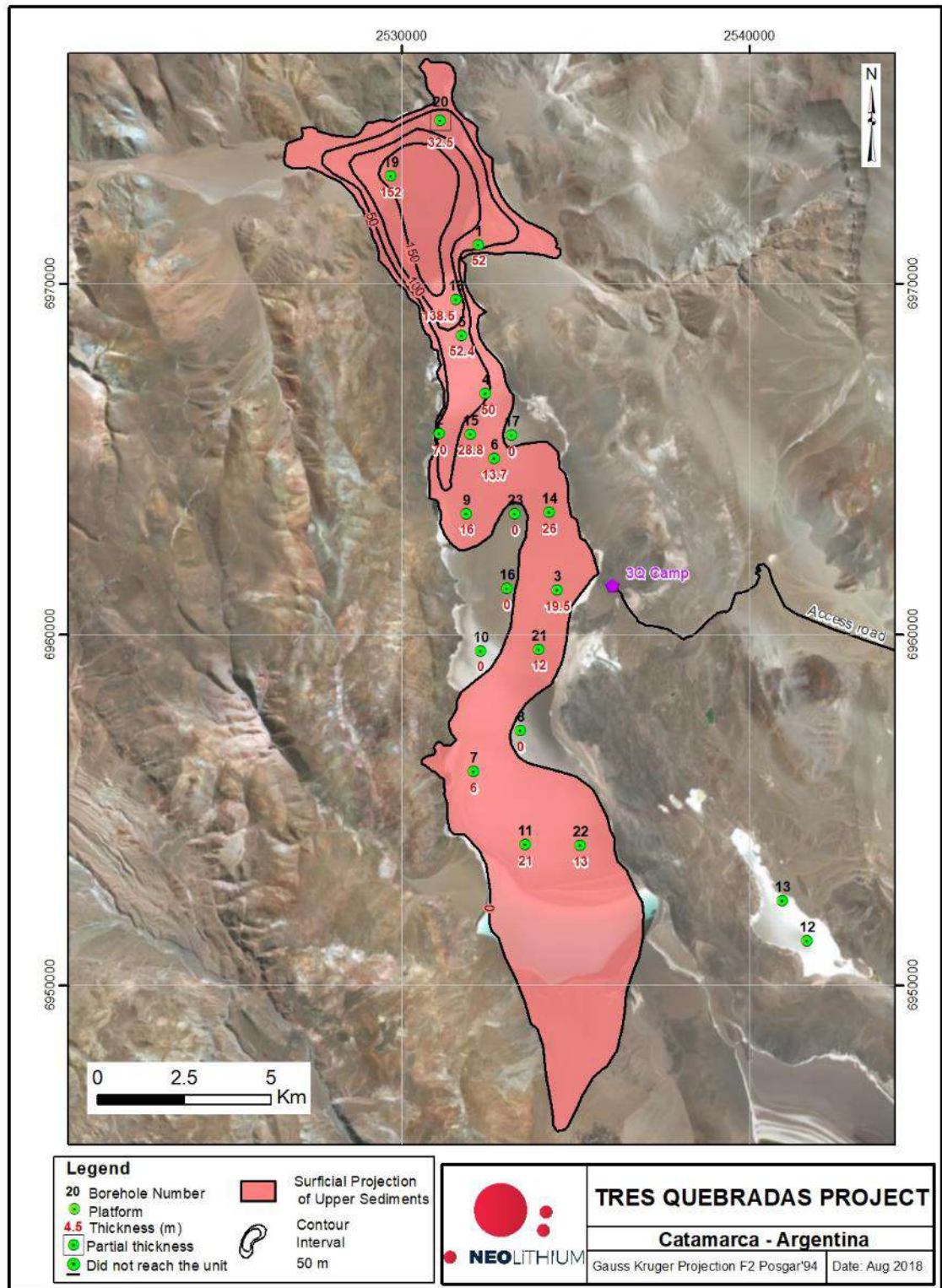


Figure B-5: Isopach map for the Upper Sediments unit.

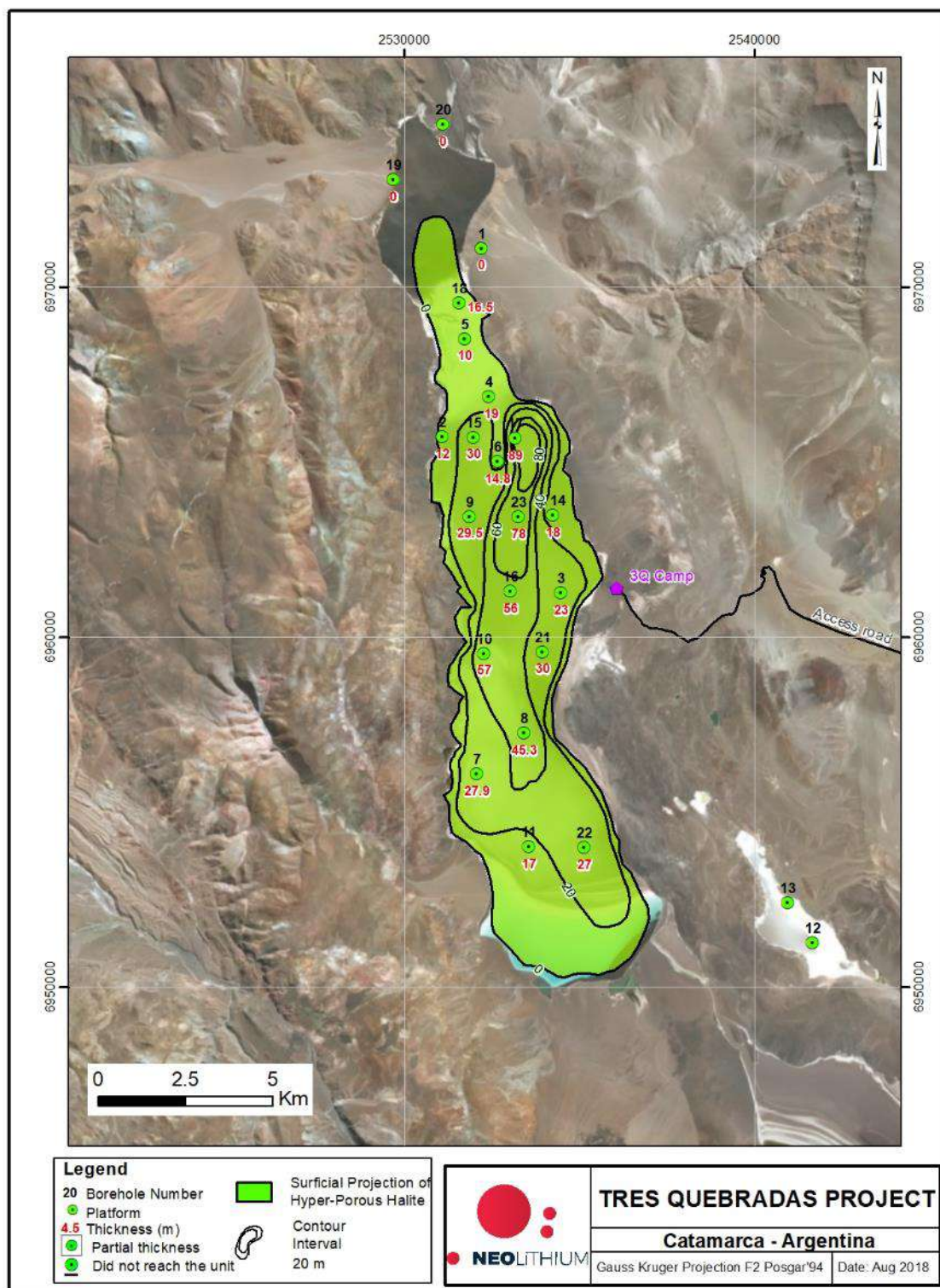


Figure B-6: Isopach map for the Hyper-Porous Halite unit.

Appendix C – VES SECTIONS FROM THE 2017/18 PROGRAM

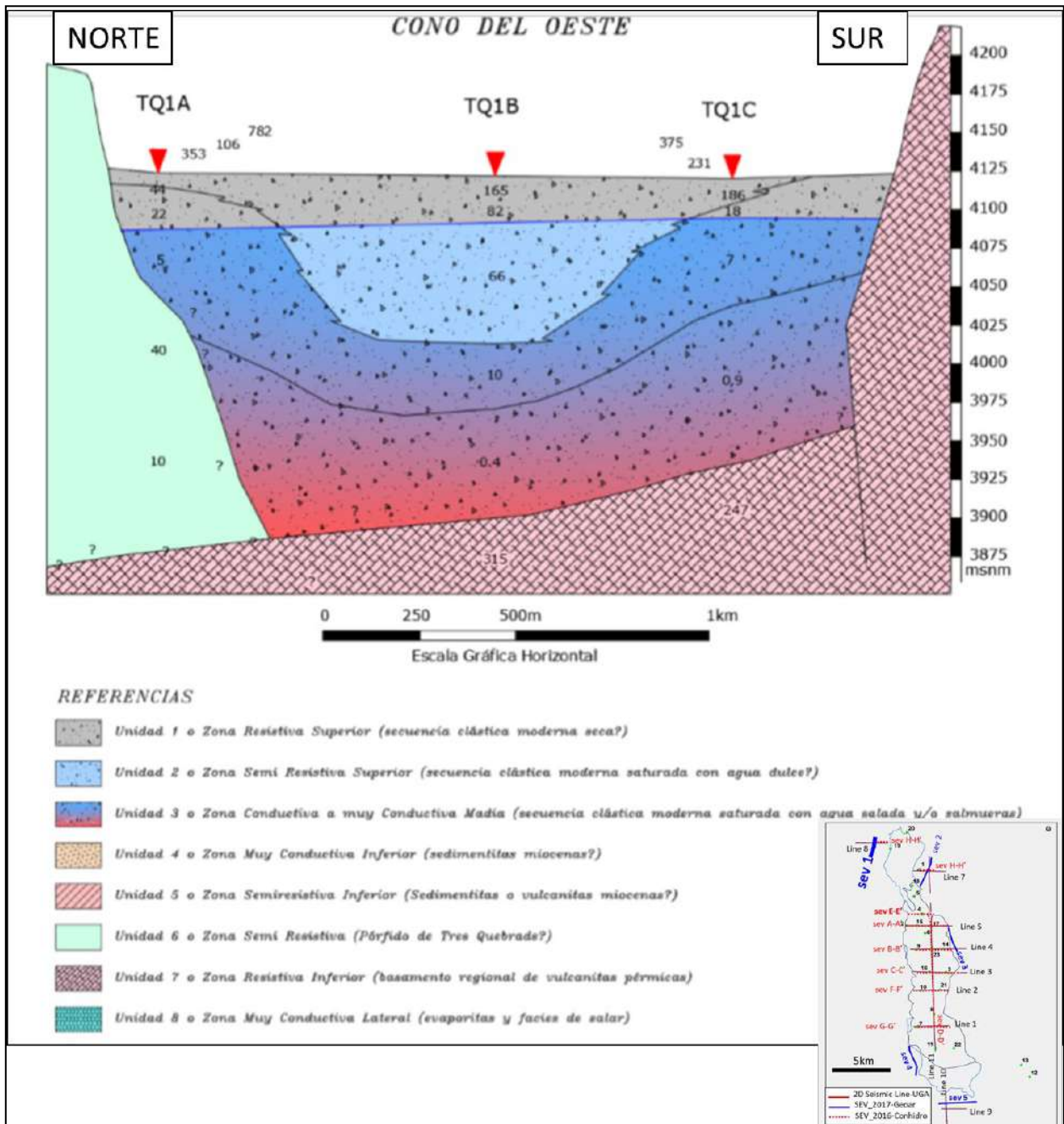


Figure C-1: Isopach map for the Hyper-Porous Halite unit.

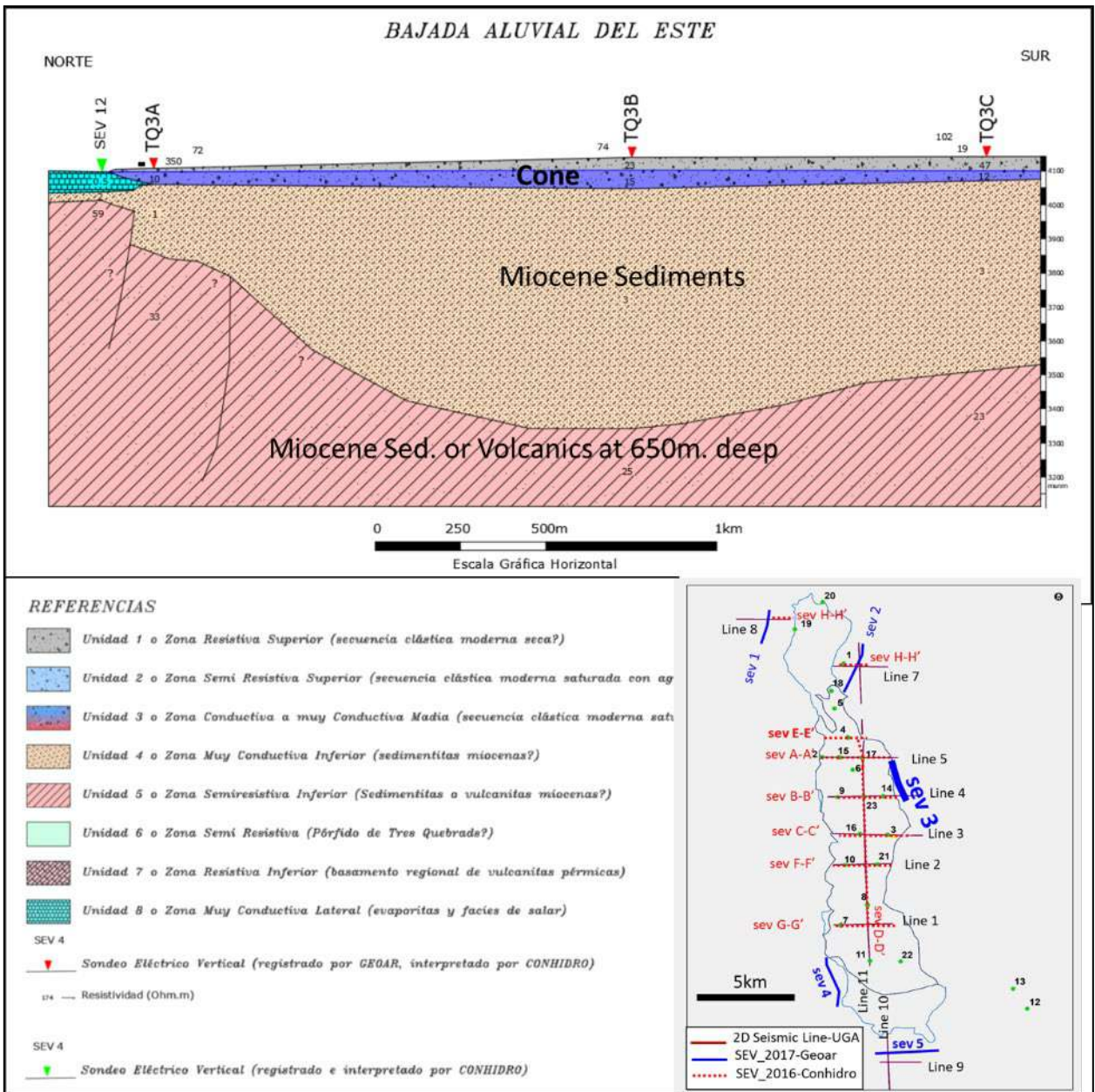


Figure C-2: VES section 3.

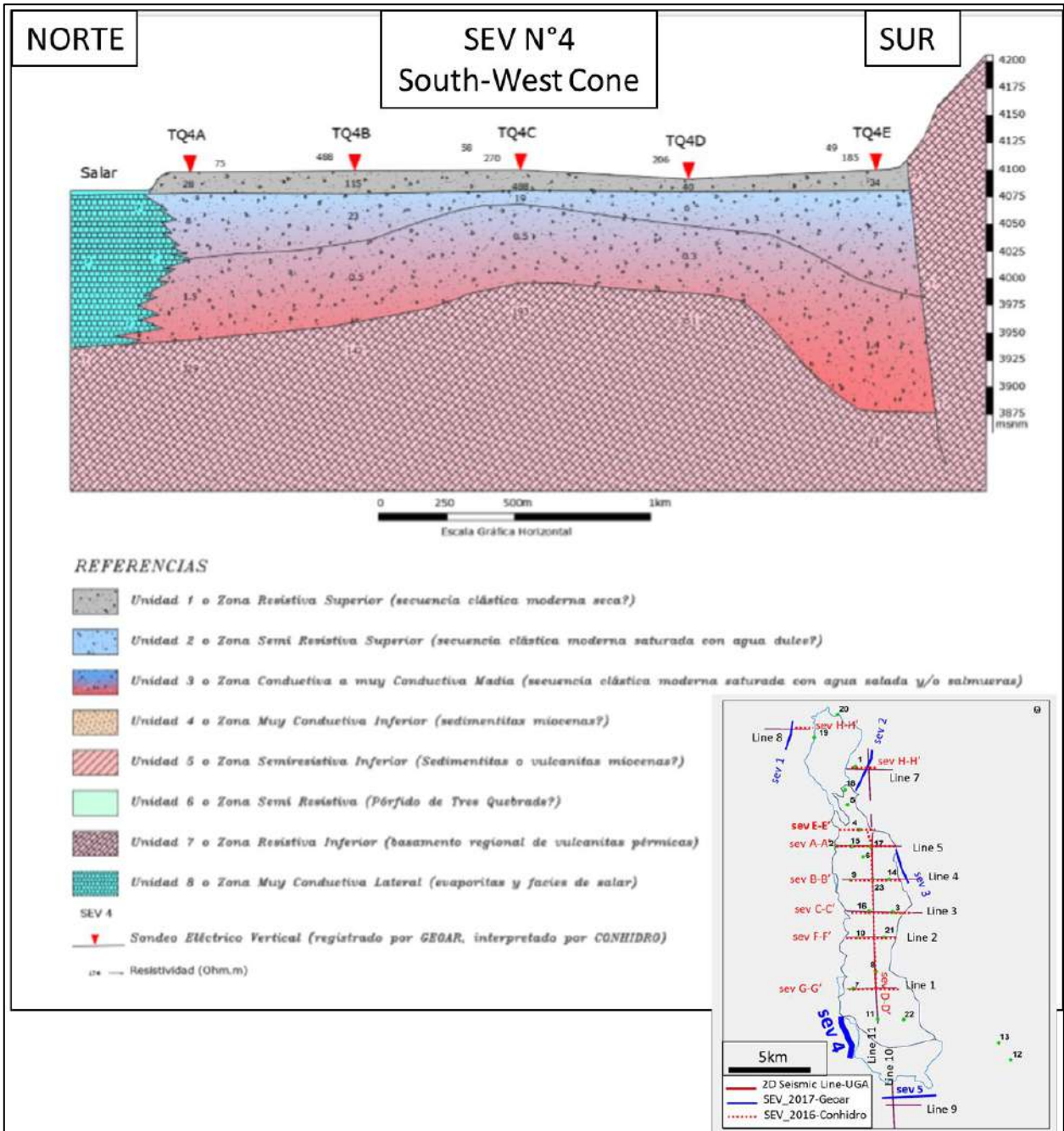


Figure C-3: VES section 4.

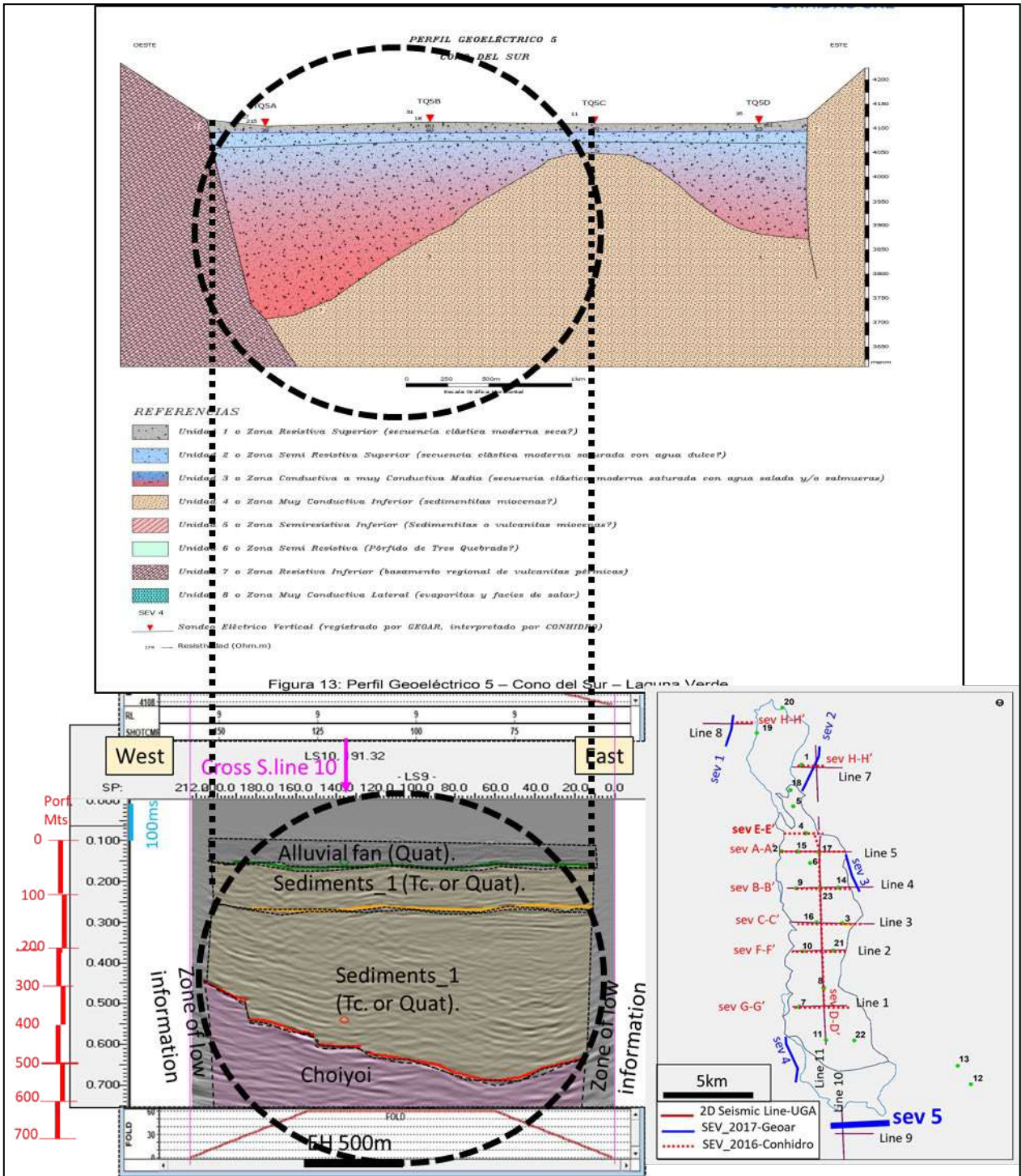


Figure C-4: VES section 5.

Appendix D – INTERPRETED SEISMIC SECTIONS

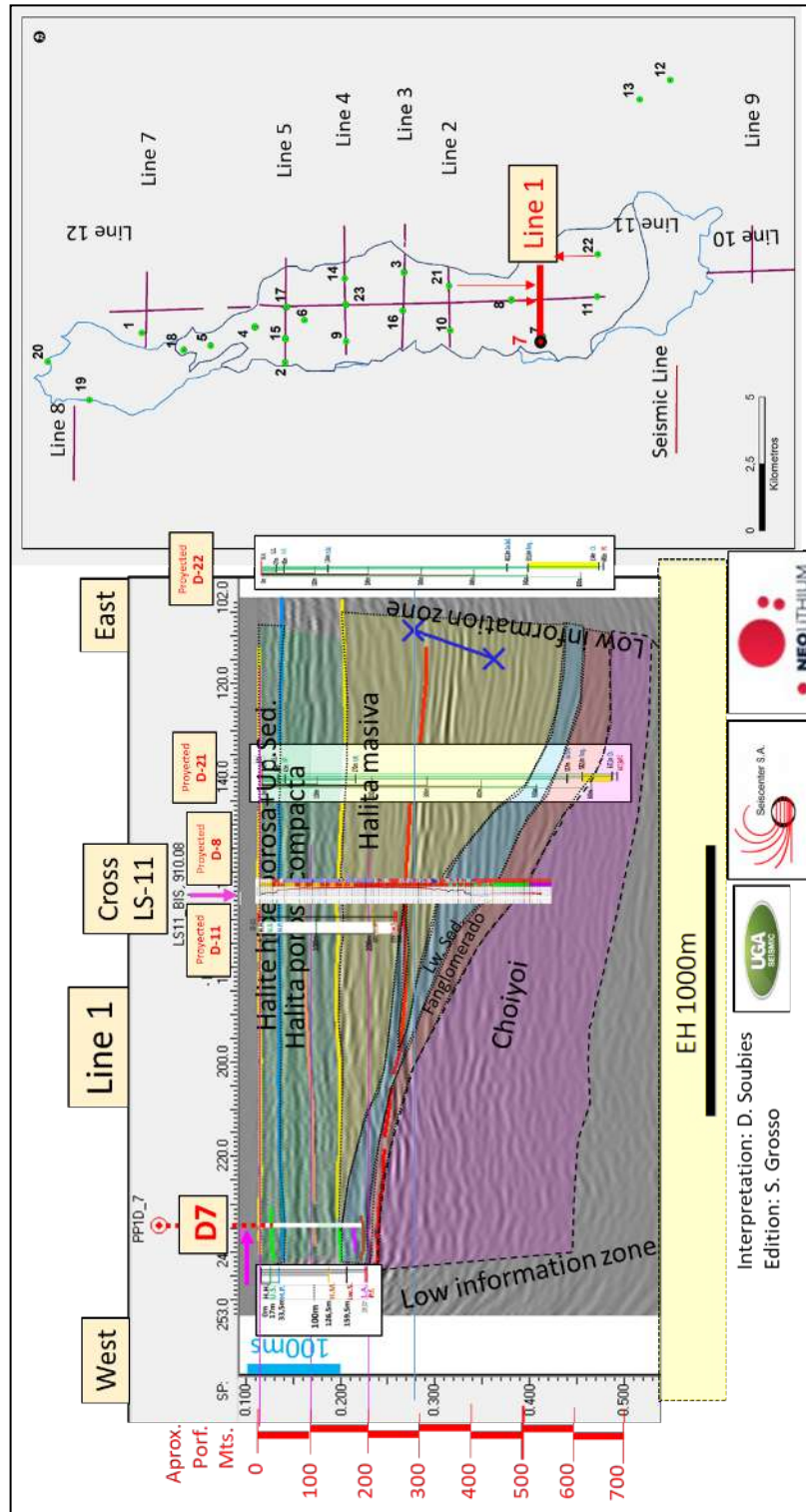


Figure D-1: Section interpretation of seismic line 1.

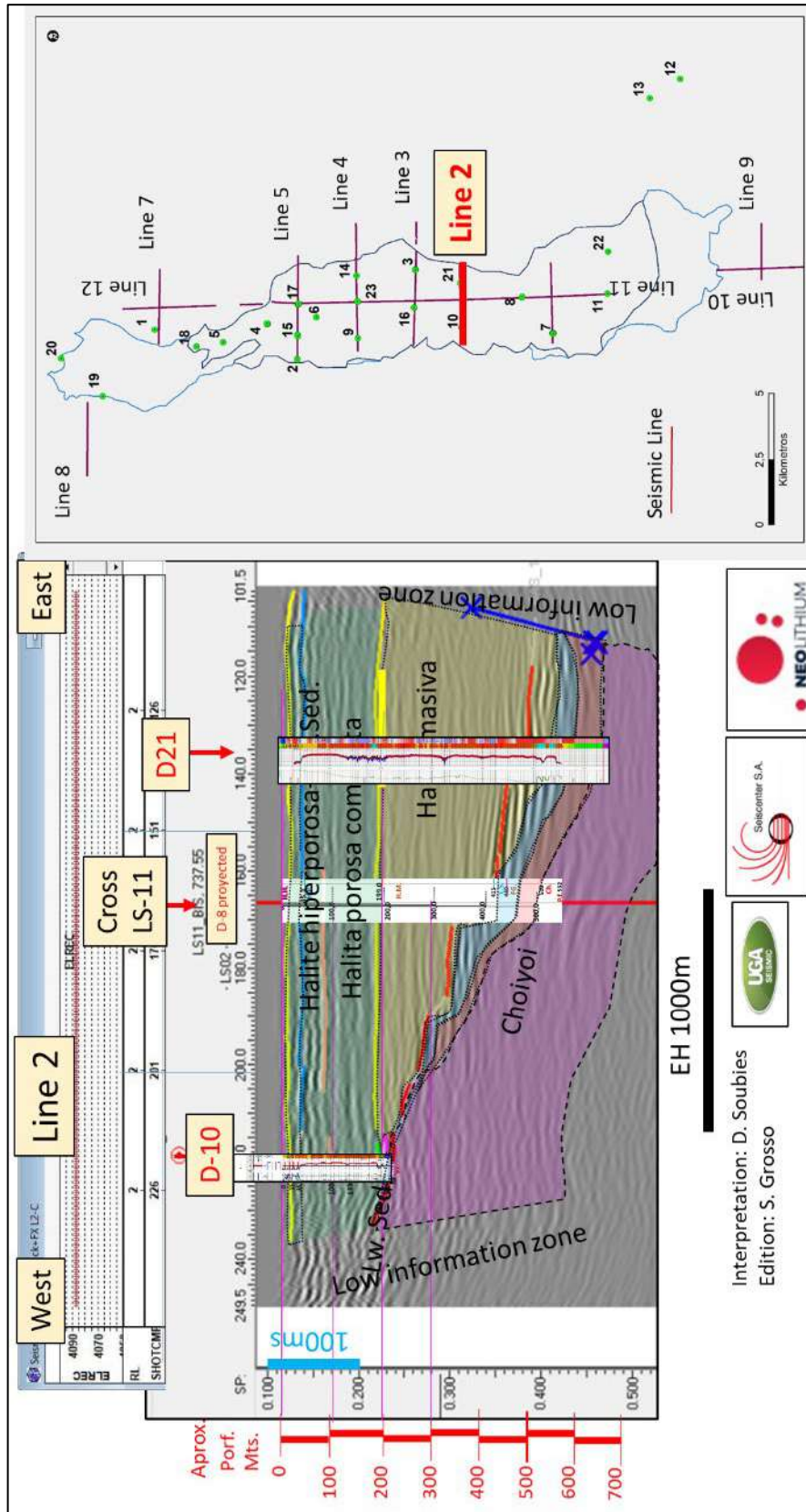


Figure D-2: Section interpretation of seismic line 2.

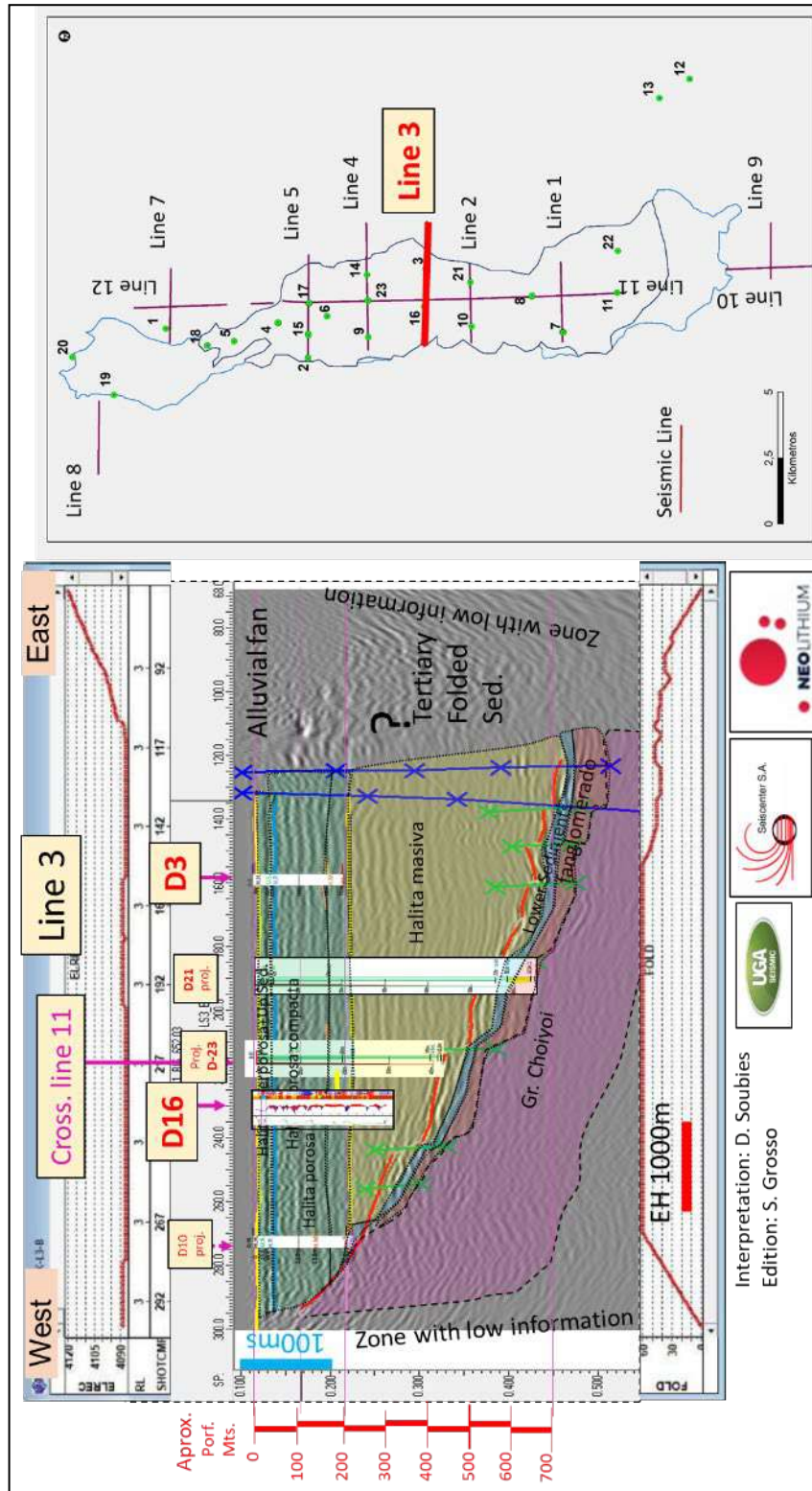


Figure D-3: Section interpretation of seismic line 3.

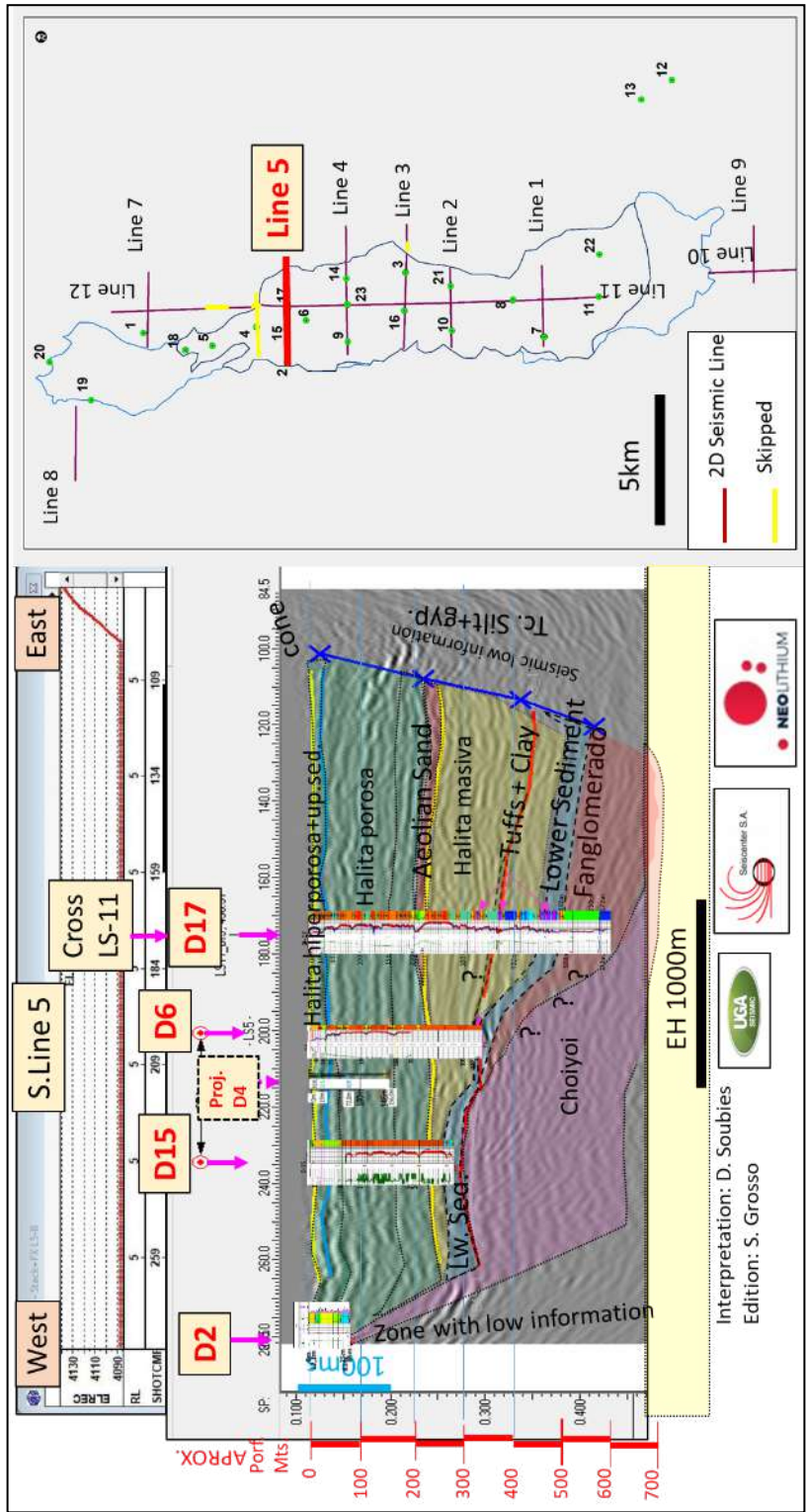


Figure D-4: Section interpretation of seismic line 5.

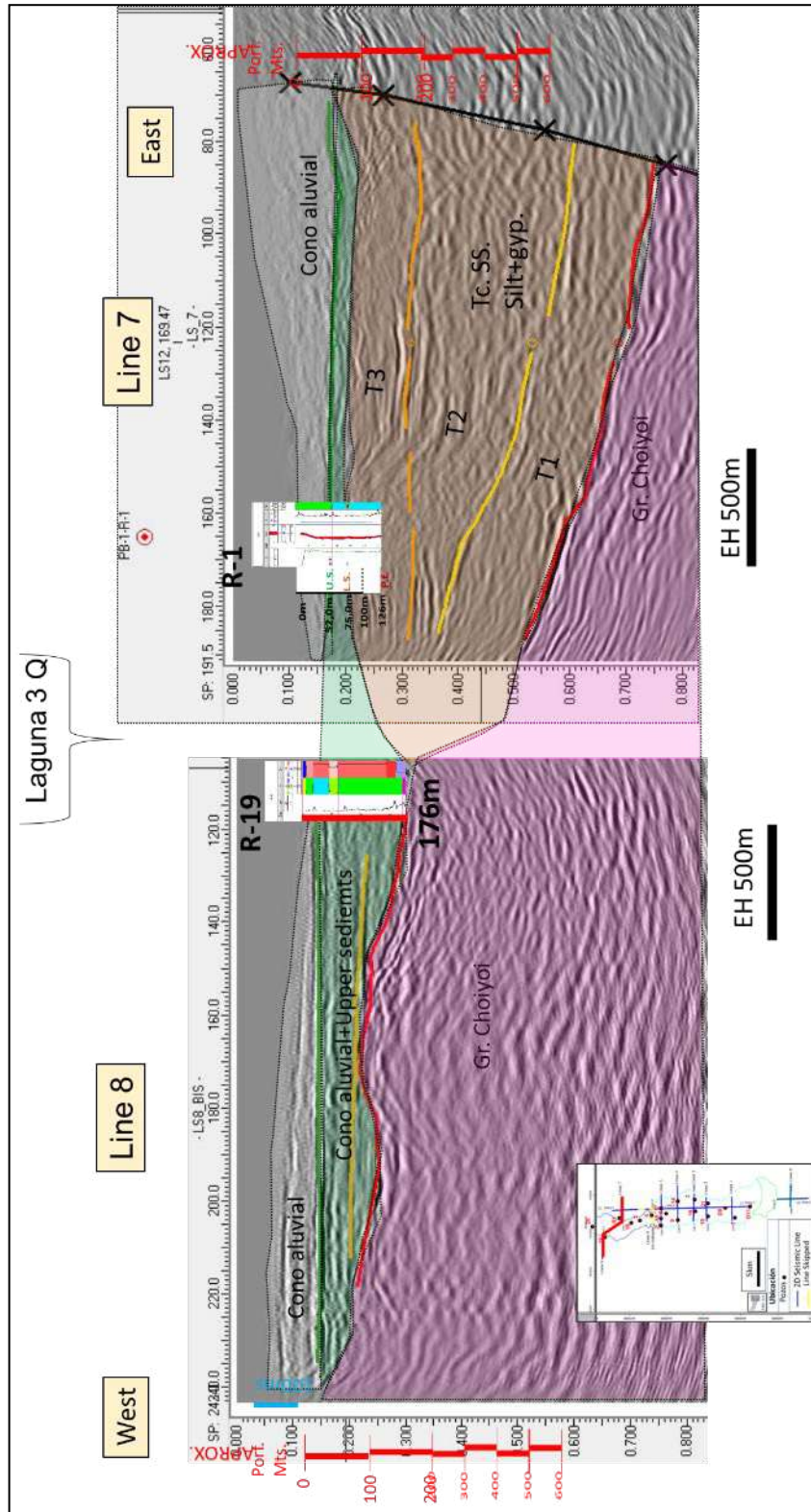


Figure D-5: Section interpretation of seismic line 7.

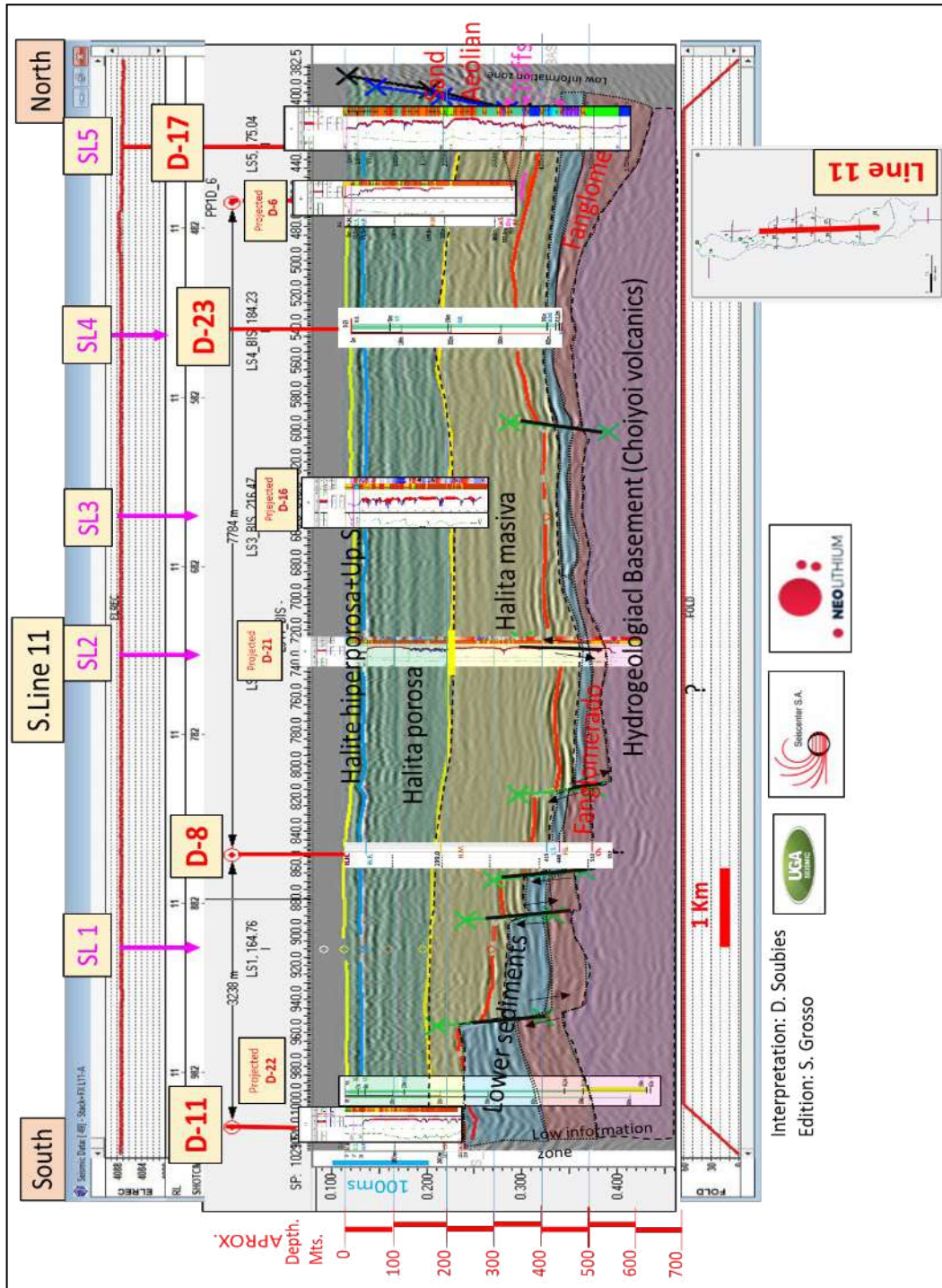


Figure D-7: Section interpretation of seismic line 11.

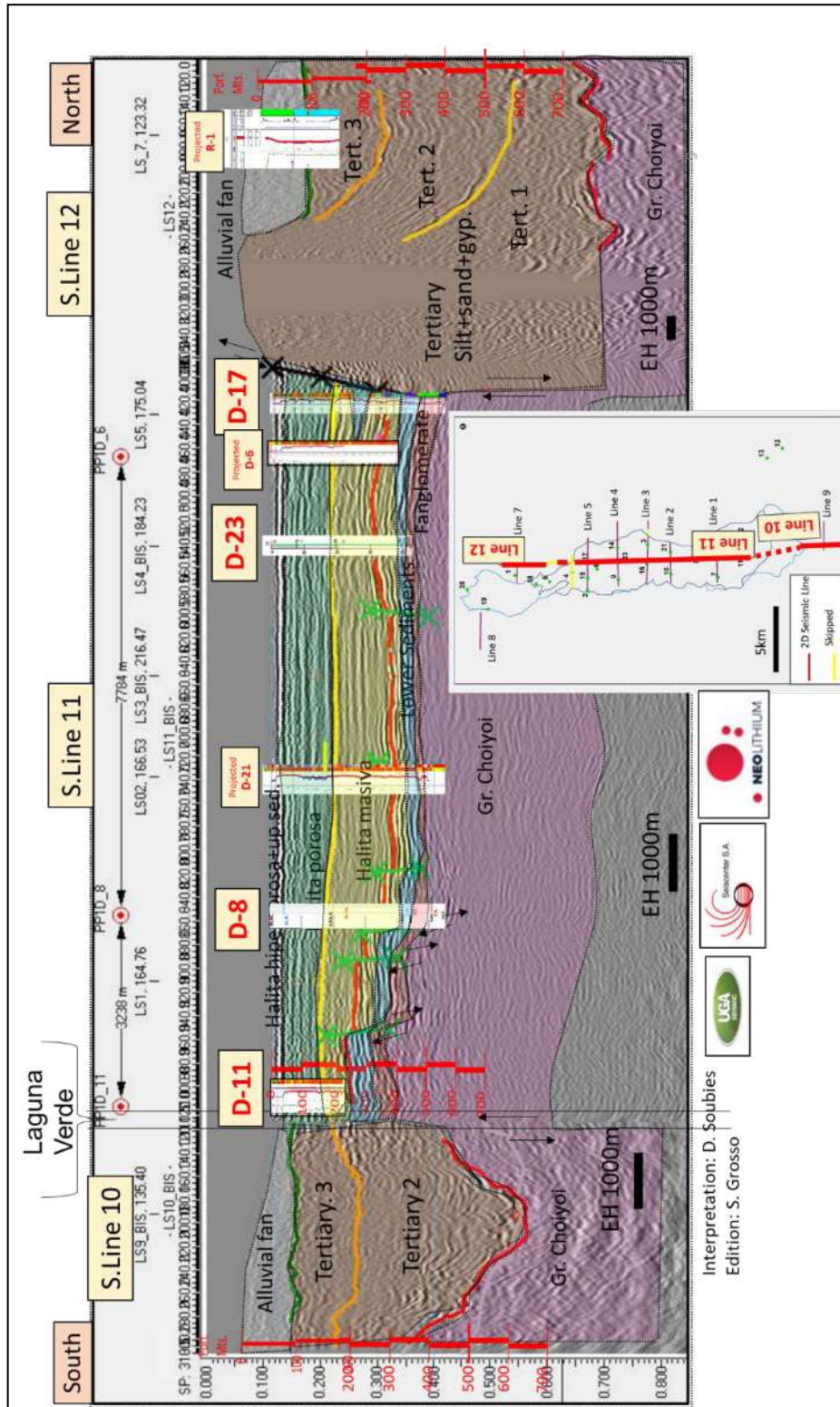


Figure D-8: Section interpretation of a composite of seismic lines 10, 11, and 12.

Appendix E – SUMMARY OF ALL DRILLING SPECIFICATIONS

Table E-1: Summary of drilling specifications – diamond and rotary methods (vertical holes).

Platform	Borehole ID	Depth (m)	Drilling Method	Well Construction		Type of Well	Packer Sampling Interval	
				Screen/Gravel Pack Interval			From (upper; m)	To (lower; m)
				From (upper; m)	To (lower; m)			
1	PB1-R-1	126.00	Rotary	31.00	52.00	Pumping Well	—	—
2	PP1-R-2	75.00	Rotary	5.49	70.28	Obs Well	—	—
	PB1-R-2	85.00	Rotary	1.00	82.00	Pumping Well	—	—
3	PP1-D-3	192.50	Diamond	0.00	195.00	Obs Well	16.00	17.00
							28.00	29.00
							40.00	41.00
							50.00	51.00
							90.00	91.00
PB1-R-3	43.00	Rotary	0.00	43.00	Pumping Well	—	—	
						PP2-R-3	42.00	Rotary
4	PP1-D-4	69.50	Diamond	0.00	69.50	Obs Well	43.00	49.70
	PB1-R-4	156.00	Rotary	0.00	70.38	Pumping Well	—	—
	PP2-R-4	72.00	Rotary	0.00	72.00	Obs Well	—	—
	PP3-D-4	187.80	Diamond	77.00	186.20	Obs Well	77.00	112.80
5	PP1-D-5	62.90	Diamond	0.00	62.90	Obs Well	13.60	20.20
							31.85	55.25
PB1-R-5	42.00	Rotary	0.00	42.00	Pumping Well	—	—	
6	PP1-D-6	338.30	Diamond	0.00	29.90	Obs Well	10.00	28.00
							32.00	62.45
							65.00	100.00
							110.00	165.00
							165.00	200.00
206.00	251.40							
7	PP1-D-7	197.50	Diamond	155.00	197.50	Obs Well	10.00	44.00
							45.00	68.00
							72.00	100.00
							110.00	160.00
	156.00	197.00						
	PB1-R-7	204.00	Rotary	145.00	204.00	Pumping Well	—	—
	PB2-R-7	132.00	Rotary	28.00	125.60	Pumping Well	—	—
PP2-R-7	130.00	Rotary	40.00	126.67	Obs Well	—	—	
PB3-R-7	36.00	Rotary	1.00	36.00	Pumping Well	—	—	
PP3-R-7	37.00	Rotary	1.00	35.05	Obs Well	—	—	
8	PP1-D-8	357.50	Diamond	0.00	46.37	Obs Well	10.00	30.50
							50.00	95.00
							105.00	128.00
							135.00	175.00
							200.00	242.00
							245.00	287.00
	290.00	329.00						
	PP2-D-8	552.00	Diamond	444.00	552.00	Obs Well	10.50	30.00
							40.00	84.00
							93.00	150.00
							150.00	195.00
							240.00	300.00
							312.00	372.00
							402.00	432.00
441.00							470.50	
480.00	510.00							
510.00	536.00							
536.00	551.00							

Platform	Borehole ID	Depth (m)	Drilling Method	Well Construction		Type of Well	Packer Sampling Interval	
				Screen/Sand Pack Interval			From (upper; m)	To (lower; m)
				From (upper; m)	To (lower; m)			
9	PP1-D-9	197.75	Diamond	145.00	189.73	Obs Well	10.50	45.00
							45.00	85.00
							85.00	120.00
							130.00	177.25
							170.00	197.75
10	PP1-D-10	219.00	Diamond	0.00	36.50	Obs Well	10.00	39.65
							44.75	83.85
							95.00	135.00
							145.00	181.45
							185.00	219.00
11	PP1-D-11	251.25	Diamond	0.00	41.00	Obs Well	10.25	30.10
							40.00	80.45
							85.00	120.10
							125.00	161.25
							165.00	194.80
195.00	236.00							
12	PP1-D-12	89.95	Diamond	0.00	5.89	Obs Well	—	—
13	PP1-D-13	13.40	Diamond	0.00	11.78	Obs Well	—	—
14	PP1-D-14	320.60	Diamond	238.00	310.00	Obs Well	16.15	19.15
							56.85	61.85
							117.75	122.75
							172.45	177.45
							252.40	257.40
271.00	320.00							
15	PP1-D-15	270.45	Diamond	6.00	30.00	Obs Well	16.30	21.30
							64.00	67.80
							76.30	87.30
							140.00	151.80
							179.30	189.80
	232.00	238.80						
	PP2-R-15	67.00	Rotary	22.50	60.00	Obs Well	—	—
PP3-R-15	218.60	Rotary	62.00	216.10	Obs Well	—	—	
PB1-R-15	32.00	Rotary	4.00	30.30	Pumping Well	—	—	
PB2-R-15	67.00	Rotary	25.80	59.40	Pumping Well	—	—	
PB3-R-15	221.00	Rotary	63.00	217.44	Pumping Well	—	—	
16	PP1-D-16	324.55	Diamond	Not enabled		Obs Well	16.00	22.35
							33.90	41.90
							67.50	75.60
							86.00	102.85
							106.00	132.85
							162.30	175.75
							227.30	238.25
	247.25	272.75						
290.00	324.55							
PP2-D-16	72.30	Diamond	0.00	34.10	Obs Well	30.00	72.00	

Platform	Borehole ID	Depth (m)	Drilling Method	Well Construction		Type of Well	Packer Sampling Interval	
				Screen/Sand Pack Interval			From (upper; m)	To (lower; m)
				From (upper; m)	To (lower; m)			
17	PP1-D-17	592.00	Diamond	479.00	587.10	Obs Well	18.00	20.00
							33.00	35.00
							48.00	50.00
							72.00	74.00
							87.00	89.00
							132.00	134.00
							144.00	169.00
							186.00	200.00
							201.00	220.00
							223.00	241.00
							479.00	484.00
							486.00	505.00
							491.50	530.00
	PP2-R-17	108.00	Rotary	1.20	104.10	Obs Well	—	—
	PP3-R-17	260.00	Rotary	109.50	258.00	Obs Well	—	—
	PB2-R-17	107.60	Rotary	3.00	105.60	Pumping Well	—	—
	PB3-R-17	260.00	Rotary	108.00	258.80	Pumping Well	—	—
18	PP1-D-18	84.00	Diamond	3.00	71.20	Obs Well	28.50	30.80
							61.00	67.00
							76.00	84.00
	PB1-R-18	216.00	Rotary	0.50	99.84	Pumping Well	—	—
	PB2-R-18	208.00	Rotary	Not enabled			—	—
19	PP1-R-19	177.00	Rotary	60.00	84.10	Obs Well	—	—
20	PP1-D-20	38.50	Diamond	Not enabled		Obs Well	7.00	13.00
							19.00	20.50
							26.00	29.00
21	PP1-D-21	647.50	Diamond	577.40	625.10	Obs Well	22.00	28.00
							36.00	60.00
							288.00	309.00
							328.00	357.00
							393.00	453.00
							556.00	580.00
							588.00	606.00
							601.00	631.00
601.00	647.50							
22	PP1-D-22	643.00	Diamond	460.00	625.10	Obs Well	16.00	28.50
							58.00	87.00
							149.00	204.00
							455.00	468.00
							501.00	542.50
							533.00	623.00
616.00	643.00							
23	PP1-D-23	423.50	Diamond	5.00	100.10	Obs Well	14.00	26.00
							32.00	71.00
							75.00	116.00
							125.00	170.00
							175.00	206.00
							230.00	302.00
							311.00	386.00
							407.00	421.50
	PP2-R-23	100.10	Rotary	0.50	100.00	Obs Well	—	—
	PB2-R-23	100.00	Rotary	0.50	99.90	Pumping Well	—	—
24	PB1-R-24	156.00	Rotary	16.00	156.00	Pumping Well	—	—
25	PB1-R-25	270.00	Rotary	87.00	252.00	Pumping Well	—	—
26	PB1-R-26	362.00	Rotary	259.00	362.00	Pumping Well	—	—
							—	—
							—	—
	PP1-R-26	282.00	Rotary	260.00	282.00	Obs Well	—	—
	PP2-R-26	18.00	Rotary	0.00	18.00	Obs Well	—	—

Appendix F – ROUND ROBIN REPORTS FOR MID-RANGE AND HIGH-RANGE REFERENCE SAMPLES



**Alex Stewart
Argentina S.A.**
Official ASIC Member

Rodríguez Peña 1140
(M5516BBX) Luzuriaga, Maipú, Mendoza:
T: +54 261 4932253
F: +54 261 4931603
E: atencion.cliente.mza@alexstewart.com.ar
W: www.alexstewart.com.ar

CERTIFICADO DE ANALISIS

MATERIAL DE REFERENCIA (MR)

Standard <i>MR Salmuera Líquida</i>	Código de Análisis M179782
---	---

Elemento	Valor Certificado [mg/l]	Incertidumbre Expandida [mg/l]
Litio (Li)	2318	± 237
Potasio (K)	20318	± 2.246
Calcio (Ca)	103508	± 10.519

Método de Análisis Inductively Coupled Plasma (ICP) (Li, K, Ca)
--

Compañía: LIEX S.A.
Solicitante: Waldo Perez

Información adicional

El valor certificado fue obtenido a partir de los resultados de un programa de ensayos de interlaboratorios.
La incertidumbre expandida fue calculada para un nivel de confianza de 95% con un factor de cobertura K=2.

Total de muestras analizadas por determinación: 17 (Homogeneidad: 10)
Muestras analizadas por laboratorio: 1 (10 para ASA para el estudio de Homogeneidad)
Laboratorios participantes: 8 (ASA NOA*, Induser, Sherritt, ACTLAB, Segemar, ALS, SGS y ASA*)
*nombres simplificados

Origen del material: salmuera líquida
Destino del MR: salmuera líquida para ser utilizado para interlaboratorio

Homogeneidad: se efectuó sobre 5 botellas seleccionados aleatoriamente y por duplicado

Almacenamiento: mantener en envase bien cerrado a temperatura ambiente y libre de humedad.
Forma de empleo: se recomienda homogeneizar el material con agitación antes de usar.
Nota de seguridad: tomar las precauciones normales de trabajo para este tipo de material

El presente material fue evaluado bajo los lineamientos de la norma ISO GUIDE 35:2006E.

Brom. Lorena Llanos
Supervisora de Calidad

Lic. Rubén Walter Cairo
Gerente del Departamento Calidad

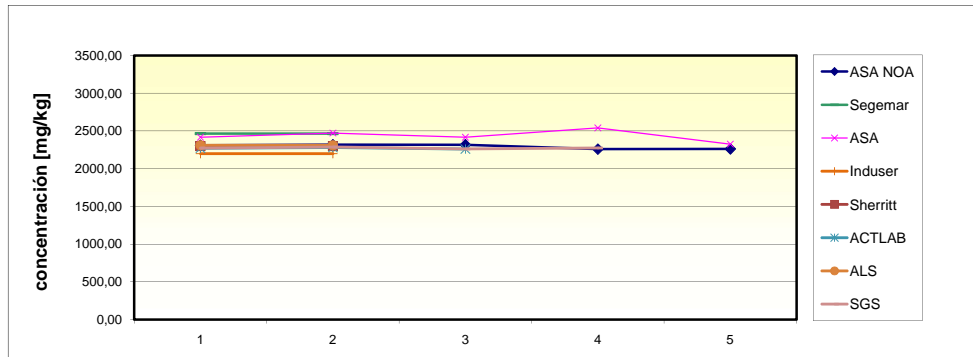
29 de mayo de 2017
Fecha de emisión

Para cualquier otra información comunicarse con: atencion.cliente.mza@alexstewart.com.ar

Litio (Li)

LABORATORIOS:	ASA NOA	Segemar	ASA	Induser	Sherritt	ACTLAB	ALS	SGS	OBSERVACIONES	
MÉTODO:	ICP OES	ICP OES	ICP OES	ICP OES	Spectroscopy	ICP OES	ICP OES	ICP OES		Sólo se envía una muestra a cada laboratorio. Los valores detallados son repeticiones de una misma muestra.
Concentración (mg/l)	2311,00	2464,00	2417,28	2200,00	2300,00	2270,00	2310,00	2273,00		
	2318,00	2464,00	2471,89	2200,00	2300,00	2280,00	2310,00	2287,00		
	2317,00		2417,28			2260,00		2261,00		
	2259,00		2539,71					2274,00		
	2262,00		2325,65							
Media	2293	2464	2434	2200	2300	2270	2310	2274		
Desviación Standard	30,2	0,0	78,9	0,0	0,0	10,0	0,0	10,6		
Varianza	910,3	0,0	6227,5	0,0	0,0	100,0	0,0	112,9		

GRÁFICO:



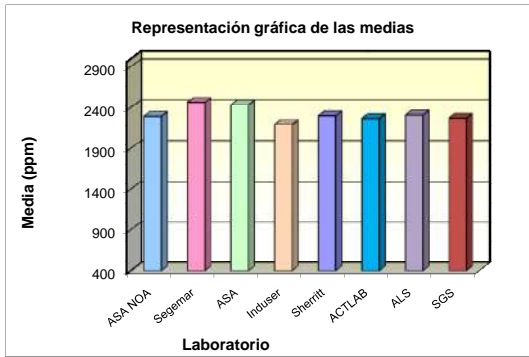
1. Cálculo del valor medio y la desviación standard correspondiente a cada parámetro y cada laboratorio.
 En el presente estudio se asume normalidad para cada secuencia de análisis por laboratorio, suponiendo que los métodos empleados están validados.

Laboratorio	Media	Desv std de cada laboratorio	RSD%
ASA NOA	2293	30,2	1,32
Segemar	2464	0,0	0,00
ASA	2434	78,9	3,24
Induser	2200	0,0	0,00
Sherritt	2300	0,0	0,00
ACTLAB	2270	10,0	0,44
ALS	2310	0,0	0,00
SGS	2274	10,6	0,47

Estadística Descriptiva (nivel de confianza 95%)	
Promedio de la Media	2318,19
Media	2318,19
Mínimo	2200,00
Máximo	2464,00
Rango	264,00
Suma	18545,51
Mediana	2296,70
Moda	#N/A
Cuenta	8
Coficiente de Asimetría	0,79
Curtosis	-0,07
S de la Media	87,86
RSD%	3,79
Varianza de la muestra	7719,26
Error Estándar	31,06

Total de muestras analizadas:	8
Muestras analizadas por laboratorio:	1
Laboratorios participantes:	8

2. Representación gráfica de la media y de la desviación standard por laboratorio :



3. Estudio de Homogeneidad - Cálculo de la Incertidumbre

Datos provenientes de ANOVA del análisis de varios paquetes o "botellas" de muestras de los cuales se sacan muestras y se analizan

LABORATORIO:					
NUMERO DE BOTELLA	1	2	3	4	5
Concentracion (mg/l)	2417,28	2539,71	2325,65	2266,11	2556,38
	2504,69	2546,57	2471,89	2417,28	2517,46
Media	2461	2543	2399	2342	2537
Desviación Standard	62	5	103	107	28
Varianza	3820	24	10694	11426	757

Los valores se presentan por orden de análisis acorde a lo suministrado por cada laboratorio para una mejor apreciación de su comportamiento real.

Análisis de varianza de un factor

RESUMEN

Grupos	Cuenta	Suma	Promedio	Varianza
Columna 1	2	4922,0	2461,0	3820,3
Columna 2	2	5086,3	2543,1	23,5
Columna 3	2	4797,5	2398,8	10694,2
Columna 4	2	4683,4	2341,7	11426,3
Columna 5	2	5073,8	2536,9	757,5

ANÁLISIS DE VARIANZA

Origen de las variaciones	suma de cuadrados	Grados de libertad	Medio de los cuadrados	F	Probabilidad	valor crítico para F
Entre grupos	61017,0	4	15254,3	2,9	0,1	5,2
Dentro de los grupos	26721,7	5	5344,3			
Total	87738,7	9				

$$s_L^2 = \frac{CM_{entre} - CM_{dentro}}{n_0}$$

CM _{entre}	61017,0
CM _{dentro}	26721,7
n=n° repeticiones	2
n° botellas	5,00

Promedio de los cuadrados

Desviación Standard entre laboratorios $s_L =$

Desviación Standard del proceso o repetibilidad $s_r =$

Incetidumbre combinada entre botellas $u_{bb} = \sqrt{\frac{CM_{dentro}}{n} \cdot \frac{2}{v_{CMdentro}}}$ $v = \text{grado de libertad} = n^\circ \text{ de análisis totales} - 1$

Incetidumbre combinada entre botellas (u_{bb} o u) $u(x) =$ mg/l Este es el módulo correspondiente a la homogenización.

4. Cálculo de la Incertidumbre Expandida

$$U_{MR} = k \cdot \sqrt{u_{char}^2 + u_{bb}^2 + u_{lts}^2 + u_{sts}^2}$$

Incetidumbre expandida (factor de cobertura k=2) $U_{MR} =$ mg/l Suponiendo $u_{sts} = 0$
 %

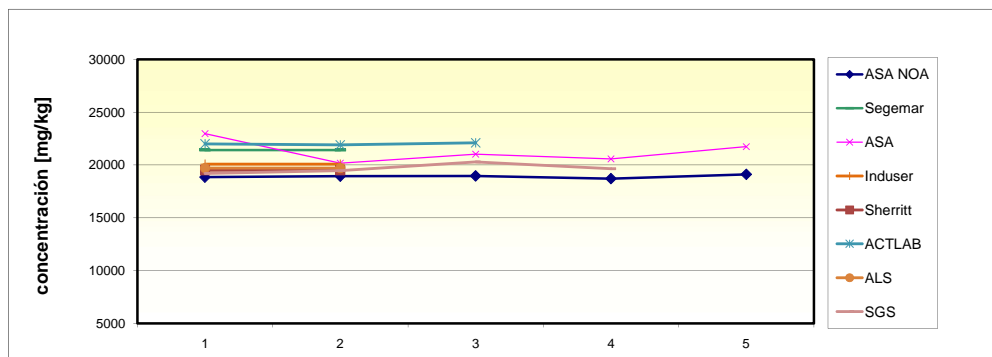
Conclusion Final:

El valor certificado es mg/l rango de concentración

Potasio (K)

LABORATORIOS:	ASA NOA	Segemar	ASA	Induser	Sherritt	ACTLAB	ALS	SGS	OBSERVACIONES
MÉTODO:	ICP OES	ICP OES	ICP OES	ICP OES	ICP OES	ICP OES	ICP OES	ICP OES	
Concentración (mg/l)	18845	21414	22965	20080	19500	22000,00	19700,00	19190,00	
	18936	21414	20164	20080	19500	21900,00	19700,00	19469,00	
	18962		21024			22100,00		20285,00	
	18706		20570					19648,00	
	19111		21734						
Media	18912	21414	21291	20080	19500	22000	19700	19648	
Desviación Standard	149,7	0,0	1102,1	0,0	0,0	100,0	0,0	464,6	
Varianza	22400,5	0,0	1214579,5	0,0	0,0	10000,0	0,0	215858,0	

GRÁFICO:



1. Cálculo del valor medio y la desviación standard correspondiente a cada parámetro y cada laboratorio.
En el presente estudio se asume normalidad para cada secuencia de análisis por laboratorio, suponiendo que los métodos empleados están validados.

Laboratorio	Media	Desv std de cada laboratorio	RSD%
ASA NOA	18912	149,7	0,79
Segemar	21414	0,0	0,00
ASA	21291	1102,1	5,18
Induser	20080	0,0	0,00
Sherritt	19500	0,0	0,00
ACTLAB	22000	100,0	0,45
ALS	19700	0,0	0,00
SGS	19648	464,6	2,36

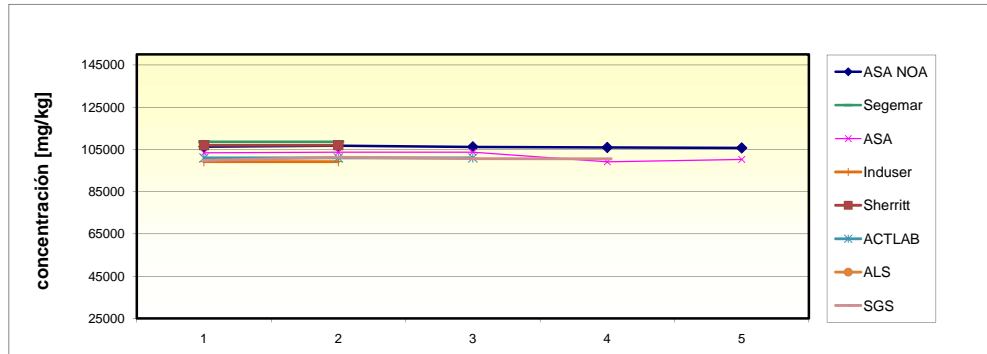
Estadística Descriptiva (nivel de confianza 95%)	
Promedio de la Media	20318,2
Media	20318,2
Mínimo	18912,0
Máximo	22000,0
Rango	3088,0
Suma	162545,4
Mediana	19890,0
Moda	#N/A
Cuenta	8
Coficiente de Asimetría	0,44
Curtosis	-1,41
S de la Media	1102,68
RSD%	5,43
Varianza de la muestra	1215895
Error Estándar	389,85

Total de muestras analizadas:	8
Muestras analizadas por laboratorio:	1
Laboratorios participantes:	8

Calcio (Ca)

LABORATORIOS:	ASA NOA	Segemar	ASA	Induser	Sherritt	ACTLAB	ALS	SGS	OBSERVACIONES
MÉTODO:	ICP OES	ICP OES	ICP OES	ICP OES	ICP OES	ICP OES	ICP OES	ICP OES	
Concentración (mg/l)	106314	108623	103349	99200	107000	101000,00		99813,00	Sólo se envía una muestra a cada laboratorio. Los valores detallados son repeticiones de una misma muestra. ALS: reporta >10000
	106749	108623	103658	99200	107000	101000,00		101268,00	
	106186		103722			101000,00		100589,00	
	105893		99091					100557,00	
	105693		100236						
Media	106167	108623	102011	99200	107000	101000	#DIV/0!	100557	
Desviación Standard	406,3	0,0	2185,7	0,0	0,0	0,0	#DIV/0!	594,4	
Varianza	165112	0,0	4777166	0,0	0,0	0,0	#DIV/0!	353360,3	

GRÁFICO:



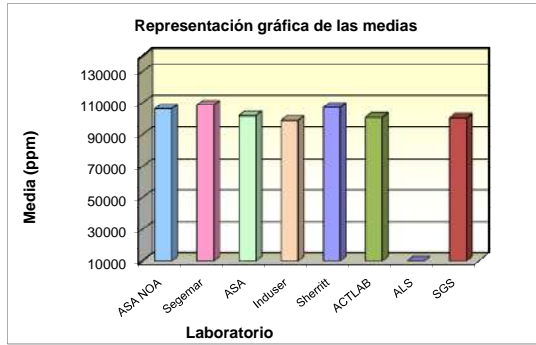
1. Cálculo del valor medio y la desviación standard correspondiente a cada parámetro y cada laboratorio.
En el presente estudio se asume normalidad para cada secuencia de análisis por laboratorio, suponiendo que los métodos empleados están validados.

Laboratorio	Media	Desv std de cada laboratorio	RSD%
ASA NOA	106167	406,3	0,38
Segemar	108623	0,0	0,00
ASA	102011	2185,7	2,14
Induser	99200	0,0	0,00
Sherritt	107000	0,0	0,00
ACTLAB	101000	0,0	0,00
ALS			
SGS	100557	594,4	0,59

Estadística Descriptiva (nivel de confianza 95%)	
Promedio de la Media	103508
Media	103508
Mínimo	99200
Máximo	108623
Rango	9423
Suma	724558
Mediana	102011
Moda	#N/A
Cuenta	7
Coficiente de Asimetría	0,33
Curtosis	-1,97
S de la Media	3679,38
RSD%	3,55
Varianza de la muestra	13537800
Error Estándar	1390,67

Total de muestras analizadas:	8
Muestras analizadas por laboratorio:	1
Laboratorios participantes:	8

2. Representación gráfica de la media y de la desviación standard por laboratorio :



3. Estudio de Homogeneidad - Cálculo de la Incertidumbre

Datos provenientes de ANOVA del análisis de varios paquetes o "botellas" de muestras de los cuales se sacan muestras y se analizan

LABORATORIO:					
NUMERO DE BOTELLA	1	2	3	4	5
Concentracion (mg/l)	103658	102622	90261	103722	99091
	100236	99565	99082	103349	103658
Media	101947	101093	94671	103536	101375
Desviación Standard	2420	2162	6237	264	3229
Varianza	5856305	4673236	38903256	69565	10429516

Los valores se presentan por orden de análisis acorde a lo suministrado por cada laboratorio para una mejor apreciación de su comportamiento real.

Análisis de varianza de un factor

RESUMEN	Grupos	Cuenta	Suma	Promedio	Varianza
Columna 1		2	203894	101947	5856305
Columna 2		2	202187	101093	4673236
Columna 3		2	189342	94671	38903256
Columna 4		2	207071	103536	69565
Columna 5		2	202749	101375	10429516

ANÁLISIS DE VARIANZA

Origen de las variaciones	suma de cuadrados	Grados de libertad	Medio de los cuadrados	F	Probabilidad	valor crítico para F
Entre grupos	92793989	4	23198497	2	0	5
Dentro de los grupos	59931877	5	11986375			
Total	152725866	9				

$$s_L^2 = \frac{CM_{entre} - CM_{dentro}}{n_0}$$

CM _{entre}	92793989
CM _{dentro}	59931877
n=n° repeticiones	2
n° botellas	5,00

Promedio de los cuadrados

Desviación Standard entre laboratorios $s_L =$

Desviación Standard del proceso o repetibilidad $s_r =$

Incertidumbre combinada entre botellas $u_{bb} = \sqrt{\frac{CM_{dentro}}{n} \cdot \frac{2}{v_{CMdentro}}}$ $v =$ grado de libertad = n° de análisis totales - 1

Incertidumbre combinada entre botellas (u_{bb} o u_L) $u(x) =$ mg/l Este es el módulo correspondiente a la homogenización.

4. Cálculo de la Incertidumbre Expandida

$$U_{MR} = k \cdot \sqrt{u_{char}^2 + u_{bb}^2 + u_{lts}^2 + u_{sts}^2}$$

Incertidumbre expandida (factor de cobertura k=2) $U_{MR} =$ mg/l Suponiendo $u_{sts} = 0$
 %

Conclusion Final:

El valor certificado es mg/l rango de concentración -



**Alex Stewart
Argentina S.A.**
Official ASIC Member

Rodríguez Peña 1140
(M5516BBX) Luzuriaga, Maipú, Mendoza:
T: +54 261 4932253
F: +54 261 4931603
E: atencion.cliente.mza@alexstewart.com.ar
W: www.alexstewart.com.ar

CERTIFICADO DE ANALISIS

MATERIAL DE REFERENCIA (MR)

Standard <i>MR Salmuera Líquida</i>	Código de Análisis M167800
---	---

Elemento	Valor Certificado [mg/l]	Incertidumbre Expandida [mg/l]
Litio (Li)	799.8	± 63
Potasio (K)	7711	± 880
Calcio (Ca)	37956	± 1.489

Método de Análisis Inductively Coupled Plasma (ICP) (Li, K, Ca)
--

Compañía: LIEX S.A.
Solicitante: Waldo Perez

Información adicional

El valor certificado fue obtenido a partir de los resultados de un programa de ensayos de interlaboratorios. La incertidumbre expandida fue calculada para un nivel de confianza de 95% con un factor de cobertura K=2.

Total de muestras analizadas por determinación: 15 (Homogeneidad: 10)
Muestras analizadas por laboratorio: 5 (10 para ASA para el estudio de Homogeneidad)
Laboratorios participantes: 5 (ASA NOA*, Induser, SGS, Segemar y ASA MAZA*)
*nombres simplificados

Origen del material: salmuera líquida
Destino del MR: salmuera líquida para ser utilizado para interlaboratorio

Homogeneidad: se efectuó sobre 5 botellas seleccionados aleatoriamente y por duplicado

Almacenamiento: mantener en envase bien cerrado a temperatura ambiente y libre de humedad.
Forma de empleo: se recomienda homogeneizar el material con agitación antes de usar.
Nota de seguridad: tomar las precauciones normales de trabajo para este tipo de material

El presente material fue evaluado bajo los lineamientos de la norma ISO GUIDE 35:2006E.


Brom. Lorena Llanos
Supervisora de Calidad


Lic. Rubén Walter Cairo
Gerente del Departamento Calidad

23 de setiembre de 2016
Fecha de emisión

Para cualquier otra información comunicarse con: atencion.cliente.mza@alexstewart.com.ar

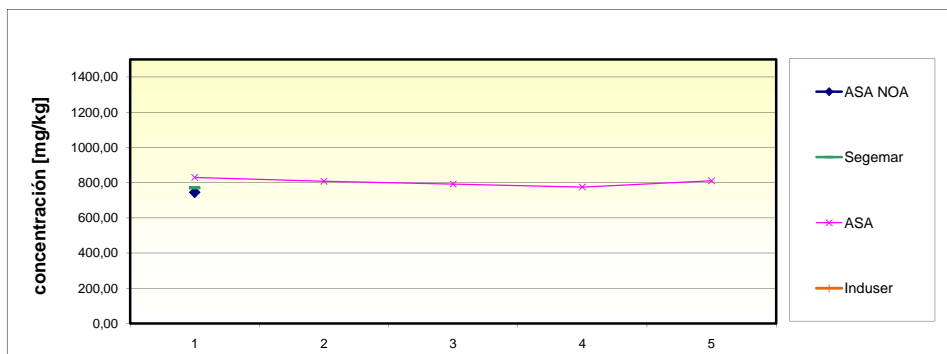


Litio (Li)

LABORATORIOS:	ASA NOA	Segemar	ASA	Induser	SGS
MÉTODO:	ICP OES	ICP OES	ICP OES	ICP OES	ICP OES
Concentración (mg/l)	745.00	770.00	829.73		829.00
			808.00		839.00
			792.00		
			775.00		
			810.21		
Media	770	770	803		834
Desviación Standard			20.6		7.1
Varianza			424.2		50.0

OBSERVACIONES
ASA NOA, Segemar e Induser: se envió una muestra.
SGS: Se envió dos muestras.
Induser: se elimina el valor de la muestra, 652, por ser muy bajo con respecto al promedio de los demás

GRÁFICO:



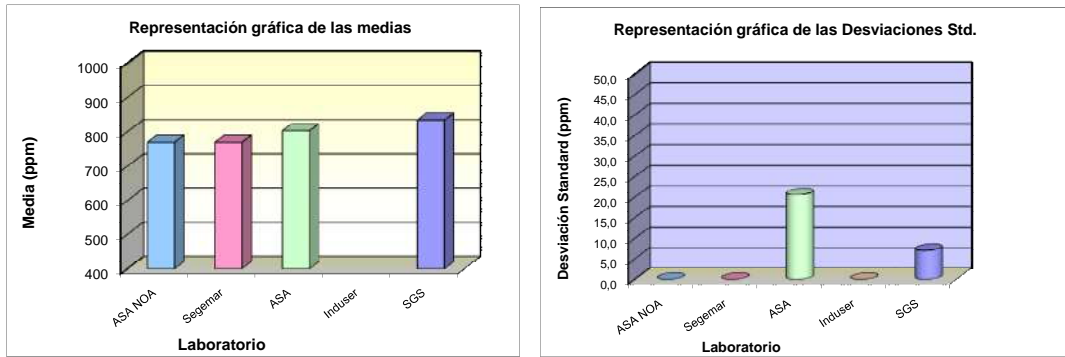
1. Cálculo del valor medio y la desviación standard correspondiente a cada parámetro y cada laboratorio.
 En el presente estudio se asume normalidad para cada secuencia de análisis por laboratorio, suponiendo que los métodos empleados están validados.

Laboratorio	Media	Desv std de cada laboratorio	RSD%
ASA NOA	770		
Segemar	770		
ASA	803	20.6	2.56
Induser			
SGS	834	7.1	0.85

Estadística Descriptiva (nivel de confianza 95%)	
Promedio de la Media	794.25
Media	794.25
Mínimo	770.00
Máximo	834.00
Rango	64.00
Suma	3176.99
Mediana	786.49
Moda	770.00
Cuenta	4
Coefficiente de Asimetría	0.80
Curtosis	-1.56
S de la Media	30.73
RSD%	3.87
Varianza de la muestra	944.18
Error Estándar	15.36

Total de muestras analizadas:	9
Muestras analizadas por laboratorio:	1
Laboratorios participantes:	4

2. Representación gráfica de la media y de la desviación standard por laboratorio :



3. Estudio de Homogeneidad - Cálculo de la Incertidumbre

Datos provenientes de ANOVA del análisis de varios paquetes o "botellas" de muestras de los cuales se sacan muestras y se analizan

LABORATORIO:					
NUMERO DE BOTELLA	1	2	3	4	5
Concentración (mg/l)	829.73	808.00	792.00	775.00	810.21
	802.93	822.77	810.43	798.84	820.33
Media	816.33	815.39	801.21	786.92	815.27
Desviación Standard	18.95	10.44	13.03	16.86	7.16
Varianza	359.1	109.1	169.8	284.1	51.3

Los valores se presentan por orden de análisis acorde a lo suministrado por cada laboratorio para una mejor apreciación de su comportamiento real.

Análisis de varianza de un factor

RESUMEN

Grupos	Cuenta	Suma	Promedio	Varianza
Columna 1	2	1632.667679	816.3338395	359.1397519
Columna 2	2	1630.770895	815.3854476	109.0896734
Columna 3	2	1602.428397	801.2141983	169.8028988
Columna 4	2	1573.838496	786.919248	284.1369458
Columna 5	2	1630.542322	815.2711612	51.28313202

ANÁLISIS DE VARIANZA

Origen de las variaciones	suma de cuadrados de libertad de los cuas	F	Probabilidad	valor crítico para F		
Entre grupos	1325.114864	4	331.278716	1.701566072	0.284940539	5.192167773
Dentro de los grupos	973.4524018	5	194.6904804			
Total	2298.567266	9				

$$s_L^2 = \frac{CM_{entre} - CM_{dentro}}{n_0}$$

CM _{entre}	331.3
CM _{dentro}	194.7
n=n° repeticiones	2
n° botellas	5.00

Promedio de los cuadrados

Desviación Standard entre laboratorios $s_L = 12.87$

Desviación Standard del proceso o repetibilidad $s_r = 13.95$

Incertidumbre combinada entre botellas $u_{bb} = \sqrt{\frac{CM_{dentro}}{n} + \frac{2}{v} CM_{dentro}}$ $v = \text{grado de libertad} = n^{\circ} \text{ de análisis totales} - 1 = 9.00$

Incertidumbre combinada entre botellas (u_{bb} o $u(x) = 6.774$ mg/l Este es el módulo correspondiente a la homogeneización.

4. Cálculo de la Incertidumbre Expandida

$$U_{MR} = k \cdot \sqrt{u_{char}^2 + u_{bb}^2 + u_{lts}^2 + u_{sts}^2}$$

Incertidumbre expandida (factor de cobertura k=): $U_{MR} = 62.93$ mg/l Suponiendo $u_{sts} = 0$
 7.92 %

Conclusion Final:

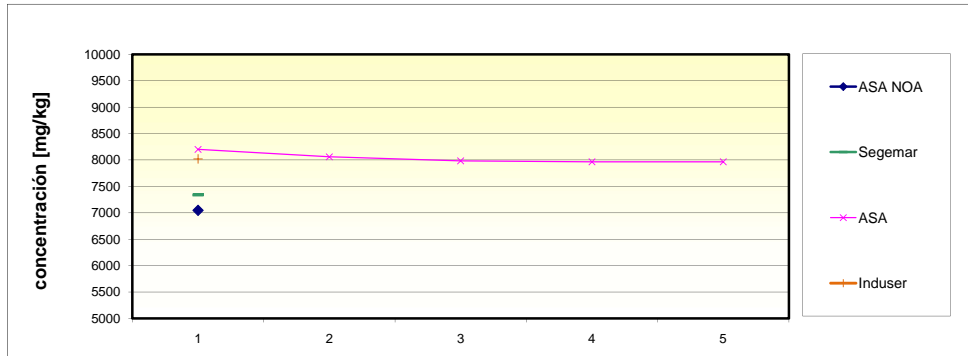
El valor certificado es 794.2 ± 62.9 mg/l rango de concentración $731.32 - 857.18$

Potasio (K)

LABORATORIOS:	ASA NOA	Segemar	ASA	Induser	SGS
MÉTODO:	ICP OES	ICP OES	ICP OES	ICP OES	ICP OES
Concentración (mg/l)	7047	7338	8200	8020	7470
			8060		7370
			7984		
			7966		
			7965		
Media	7047	7338	8035	8020	7420
Desviación Standard			100.2		70.7
Varianza			10041.2		5000.0

OBSERVACIONES
ASA NOA, Segemar e Induser: se envió una muestra.
SGS: Se envió dos muestras.

GRÁFICO:



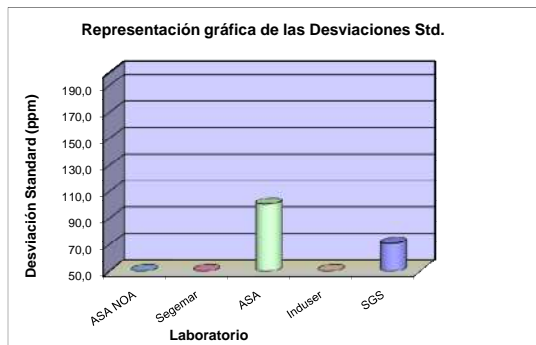
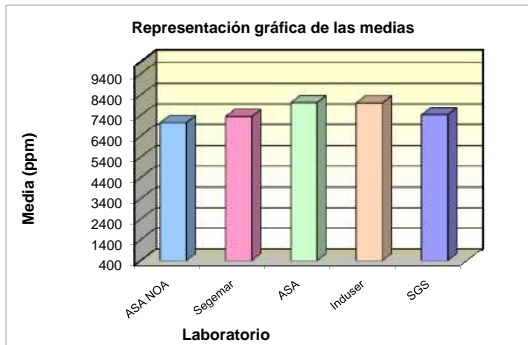
1. Cálculo del valor medio y la desviación standard correspondiente a cada parámetro y cada laboratorio.
En el presente estudio se asume normalidad para cada secuencia de análisis por laboratorio, suponiendo que los métodos empleados están validados.

Laboratorio	Media	Desv std de cada laboratorio	RSD%
ASA NOA	7047		
Segemar	7338		
ASA	8035	100.2	1.25
Induser	8020		
SGS	7420	70.7	0.95

Estadística Descriptiva (nivel de confianza 95%)	
Promedio de la Media	7572.0
Media	7572.0
Mínimo	7047.0
Máximo	8034.8
Rango	987.8
Suma	37859.8
Mediana	7420.0
Moda	#N/A
Cuenta	5
Coficiente de Asimetría	0.14
Curtosis	-2.39
S de la Media	438.29
RSD%	5.79
Varianza de la muestra	192095
Error Estándar	196.01

Total de muestras analizadas:	10
Muestras analizadas por laboratorio:	1
Laboratorios participantes:	5

2. Representación gráfica de la media y de la desviación standard por laboratorio :



3. Estudio de Homogeneidad - Cálculo de la Incertidumbre

Datos provenientes de ANOVA del análisis de varios paquetes o "botellas" de muestras de los cuales se sacan muestras y se analizan

LABORATORIO:					
NUMERO DE BOTELLA	1	2	3	4	5
Concentracion (mg/l)	8200.01	8059.61	7983.74	7965.77	7964.91
	8100.03	8150.38	8078.75	8078.98	8138.06
Media	8150.02	8104.99	8031.24	8022.37	8051.49
Desviación Standard	70.70	64.18	67.18	80.05	122.43
Varianza	4997.9	4119.4	4513.6	6408.4	14989.6

Los valores se presentan por orden de análisis acorde a lo suministrado por cada laboratorio para una mejor apreciación de su comportamiento real.

Análisis de varianza de un factor

RESUMEN

Grupos	Cuenta	Suma	Promedio	Varianza
Columna 1	2	16300.03128	8150.015638	4997.90172
Columna 2	2	16209.98432	8104.99216	4119.409466
Columna 3	2	16062.48755	8031.243777	4513.561687
Columna 4	2	16044.74756	8022.373778	6408.385072
Columna 5	2	16102.97392	8051.486958	14989.56348

ANÁLISIS DE VARIANZA

Origen de las variaciones	suma de cuadrados	Grados de libertad	Medio de los cuadrados	F	Probabilidad	valor crítico para F
Entre grupos	23439.07268	4	5859.768169	0.836420971	0.55626526	5.192167773
Dentro de los grupos	35028.82143	5	7005.764285			
Total	58467.8941	9				

$$S_L^2 = \frac{CM_{entre} - CM_{dentro}}{n_0}$$

CM _{entre}	5860
CM _{dentro}	7006
n=n° repeticiones	2
n° botellas	5.00

Promedio de los cuadrados

Desviación Standard entre laboratorios $S_L =$

Desviación Standard del proceso o repetibilidad $s_r =$

Incertidumbre combinada entre botellas $u_{bb} = \sqrt{\frac{CM_{dentro}}{n} + 4 \frac{2}{V_{CM_{dentro}}}}$ $v =$ grado de libertad = n° de análisis totales - 1

Incertidumbre combinada entre botellas (u_{bb} o $u(x) =$ mg/l Este es el módulo correspondiente a la homogenización.

4. Cálculo de la Incertidumbre Expandida

$$U_{MR} = k \cdot \text{raiz}(u_{char}^2 + u_{bb}^2 + u_{lts}^2 + u_{sts}^2)$$

Incertidumbre expandida (factor de cobertura $k =$ $U_{MR} =$ mg/l Suponiendo $U_{sts} = 0$
 %

Conclusion Final:

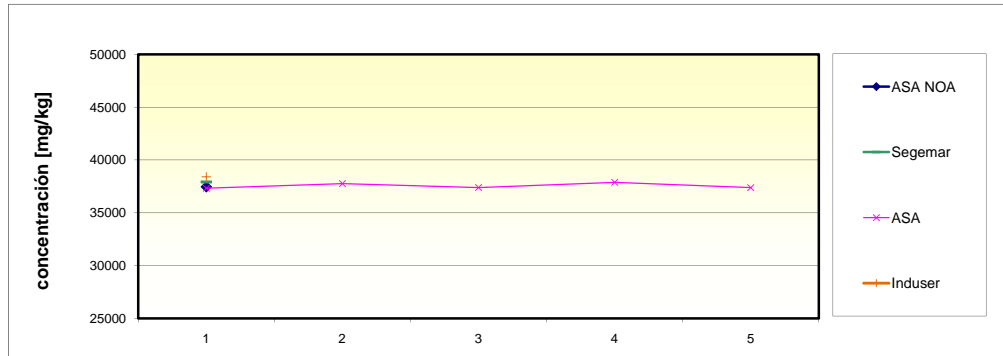
El valor certificado es mg/l rango de concentración

Calcio (Ca)

LABORATORIOS:	ASA NOA	Segemar	ASA	Induser	SGS
MÉTODO:	ICP OES	ICP OES	ICP OES	ICP OES	ICP OES
Concentración (mg/l)	37462	37915	37321	38400	39100
			37764		39400
			37386		
			37880		
			37380		
Media	37915	37915	37546	38400	39250
Desviación Standard			256.3		212.1
Varianza			65715.2		45000.0

OBSERVACIONES
ASA NOA, Segemar e Induser: se envió una muestra.
SGS: Se envió dos muestras.

GRÁFICO:



1. Cálculo del valor medio y la desviación standard correspondiente a cada parámetro y cada laboratorio.
 En el presente estudio se asume normalidad para cada secuencia de análisis por laboratorio, suponiendo que los métodos empleados están validados.

Laboratorio	Media	Desv std de cada laboratorio	RSD%
ASA NOA	37915		
Segemar	37915		
ASA	37546	256.3	0.68
Induser	38400		
SGS	39250	212.1	0.54

Estadística Descriptiva (nivel de confianza 95%)	
Promedio de la Media	38205
Media	38205.24
Mínimo	37546.20
Máximo	39250.00
Rango	1703.80
Suma	191026.20
Mediana	37915.00
Moda	37915.00
Cuenta	5
Coficiente de Asimetría	1.19
Curtosis	1.30
S de la Media	658.08
RSD%	1.72
Varianza de la muestra	433066.79
Error Estándar	294.30

Total de muestras analizadas:	10
Muestras analizadas por laboratorio:	1
Laboratorios participantes:	5

Appendix G – PARTICLE TRACKS FROM FEFLOW, SHOWING PRODUCTION WELL CAPTURE ZONES

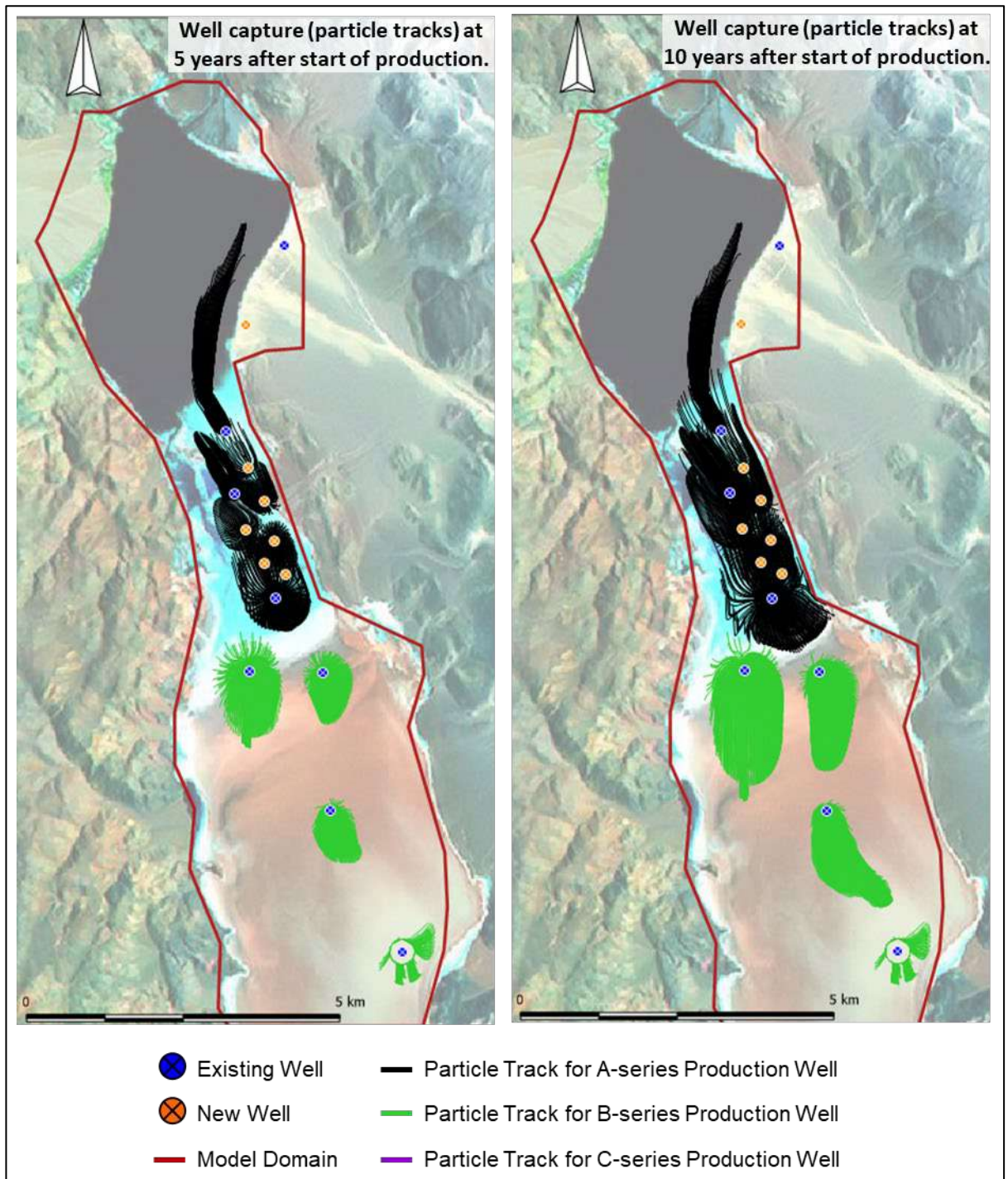


Figure G-1: Well capture (particle tracks) at five and 10 years after start of production. The 3D particle tracks are projected onto the 2D surface image.

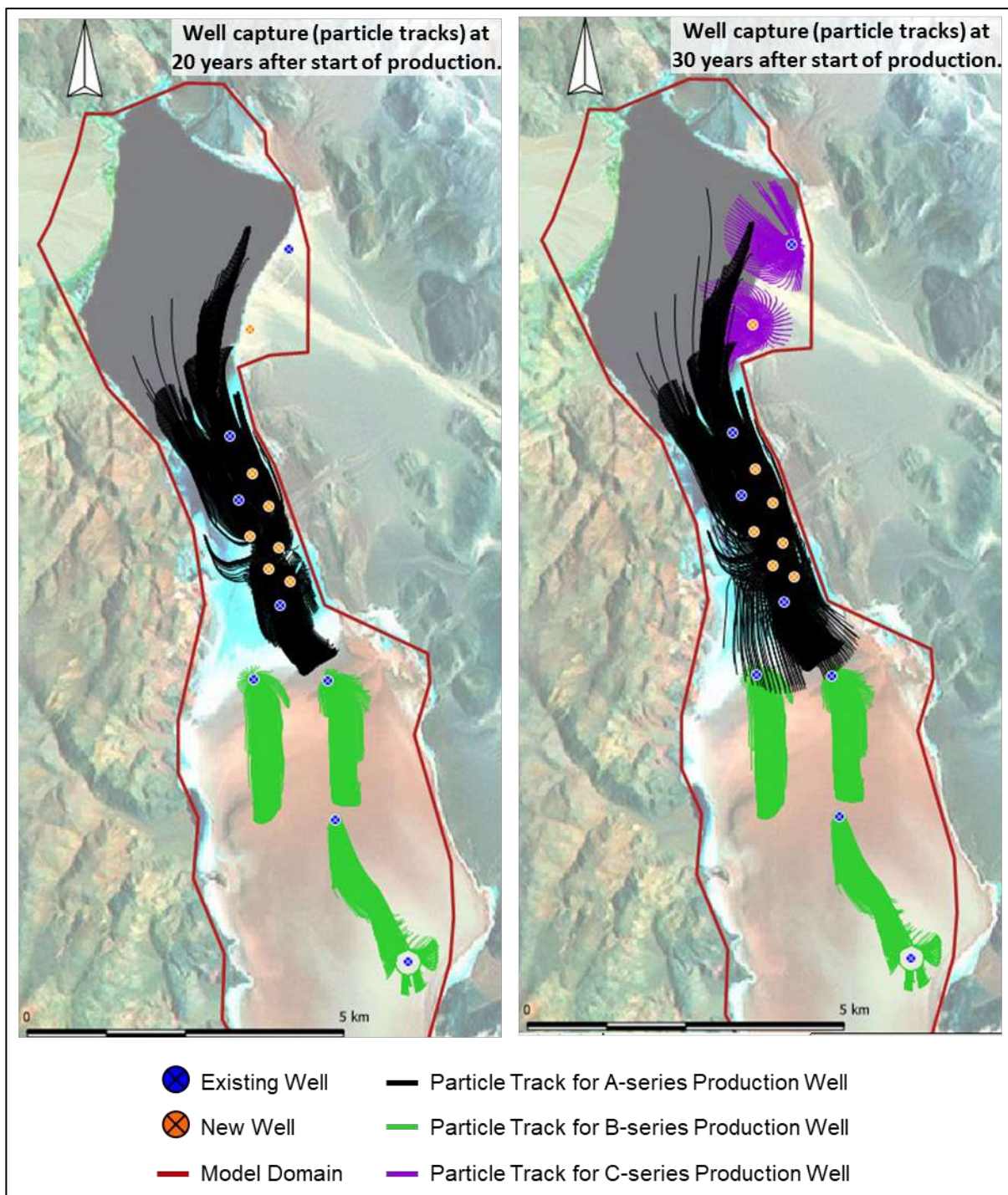


Figure G-2: Well capture (particle tracks) at 20 and 30 years after start of production. The 3D particle tracks are projected onto the 2D surface image.

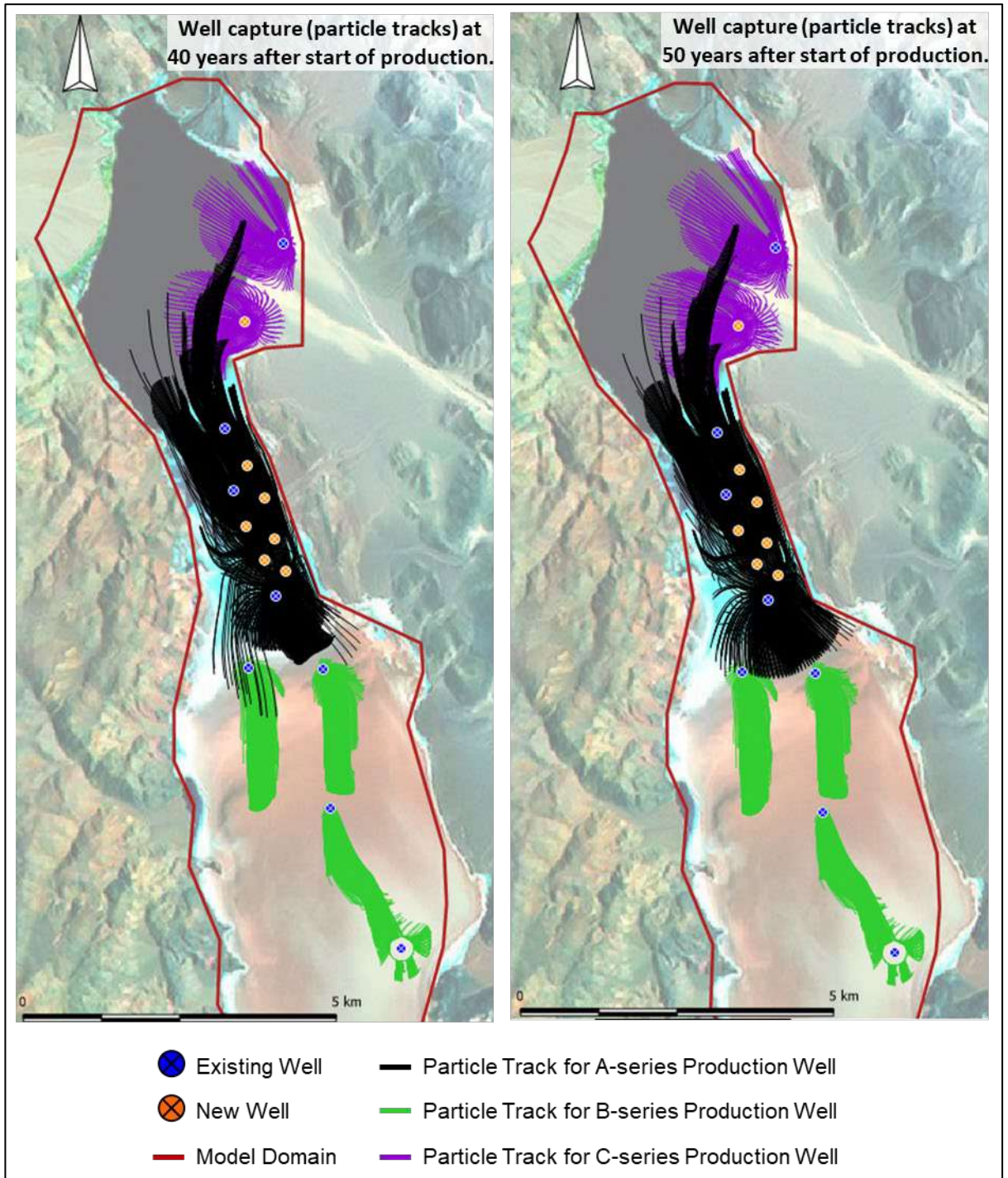


Figure G-3: Well capture (particle tracks) at 40 and 50 years after start of production. The 3D particle tracks are projected onto the 2D surface image.

Appendix H – LITHIUM MARKET REPORT FOR NLC



Report for: Neo Lithium

3Q Feasibility Study

October 2021

Contents

Executive Summary	2
Lithium and Lithium-ion Batteries: Introduction	4
The Role of Lithium in Lithium Battery Cell Technology	7
Figure Six: Main components of a Li-ion battery	8
Cathode Technology	10
Competitive threats: the role of Solid State	14
Lithium Demand	16
Megafactory Capacity	19
Lithium-ion Cathode Plant Capacity	19
Lithium Supply	21
Lithium Chemical Supply	26
Lithium Production Costs	29
Lithium Industry Cost Methodology	30
Lithium Pricing	32
Lithium Price Forecast Methodology and Pricing Outlook	33

Executive Summary

This report has been prepared on behalf of Neo Lithium. Neo Lithium has commenced a Feasibility Study (FS) to evaluate the development of the 3Q lithium project in Argentina. Neo Lithium is developing the 3Q asset into production as one of the world's largest lithium brine producers

Based on the findings of research for this report, we make the following key observations on the lithium market and the prospects for Neo Lithium as a supplier of battery-grade Lithium.

- Lithium-ion batteries have become the dominant battery technology for use in Electric Vehicles (EVs), as well as consumer electronics and stationary grid storage. This dominance is likely to continue given the level of investment in lithium-ion battery cell capacity being undertaken at present versus other battery technologies. The primary reason for this is the high-energy density of the technology—crucial where space and weight are a factor—its low maintenance requirements and the fact it is relatively economic compared to other battery technologies at present.

Global Lithium Demand

- The majority of lithium bearing minerals are sold into the chemicals sector to produce lithium carbonate or hydroxide. This market is widely forecast to see sustained growth over coming decades as the electric vehicle market increasingly displaces internal combustion (ICE).
- There is an ongoing need for capacity investments in lithium raw material extraction, chemical processing and cathode manufacturing throughout the life of our forecast to 2040. Given the direction of travel and level of investment in the downstream of the electric vehicle supply chain, at an auto-manufacture and battery cell level, there is an impending shortfall in the midstream supply chain which needs to be addressed.
- The level of financing needed to bridge this gap is relatively small compared to the investment being made in vehicle and battery cell manufacturing, so we feel it is highly likely that actors in these areas of the supply chain will take steps to ensure supply availability.
- The outlook for the battery cathode chemistry mix indicates a move towards high-nickel NCM technologies, which favours the use of lithium hydroxide in the production of cathodes.

Lithium Price Outlook

- As a result—and despite the weakness in lithium pricing in 2020—we expect prices will recover (as shown by recent indicators in 2021) in order to incentivise investment in both raw material and chemical processing capacity. For lithium carbonate and hydroxide we forecast long-term pricing to settle in the region of USD13,000 per tonne. This is based

on an incentive price analysis for a 'typical' greenfield lithium project with capex of USD500 million, and opex of USD 4,000 per LCE tonne, generating an IRR of 35%.

Global Lithium Supply

- Lithium raw material projects in jurisdictions close to or in areas of future high demand, namely Europe and North America, are at a distinct advantage in terms of potential for development. This arises from an imbalance in the geography of supply towards Latin America and Asia, including Australia. Battery cell manufacturers are planning capacity investments closer to where their key customers—automotive manufacturers—are located. These consumers will wish to source at least part of their supply from local sources. This will cut down on lead times—an increasingly important factor given the larger market share of lithium hydroxide, which has a limited shelf life—reduce freight costs and minimize default risks. There is also likely to be decreased jurisdictional risk by having less concentrated supply, and localised raw material supply will aid optimal and cost-efficient procurement practices within the value chain.

Competitive threats

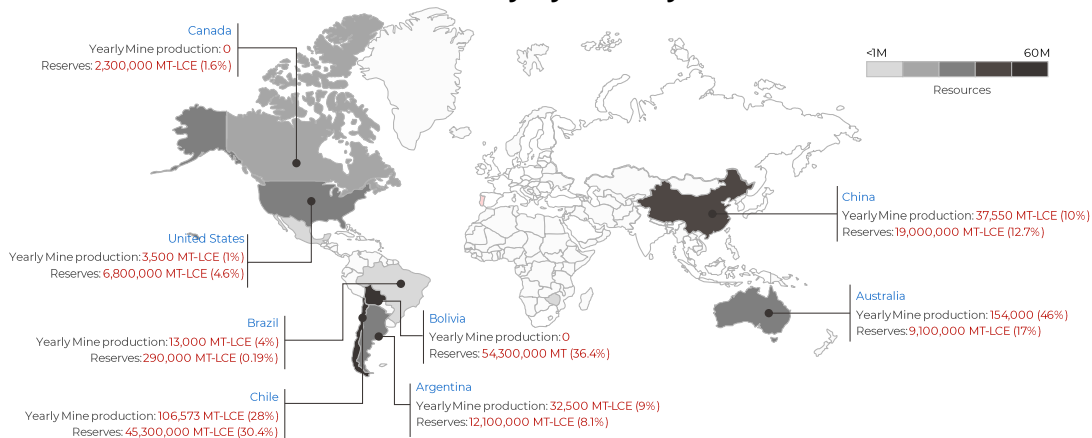
- Solid-state lithium metal batteries—the alternative to lithium-ion batteries that is currently closest to commercial viability in the EV space—would have little impact on lithium chemical demand. The risk of substitution in solid-state lithium metal batteries applies to the anode (graphite potentially displaced by lithium metal) rather the cathode, which remains largely unchanged.

Lithium and Lithium-ion Batteries: Introduction

Lithium, the lightest of all metals, is used in batteries, ceramics, glass, metallurgy, pharmaceuticals, air treatment and polymers. It is largely produced in one of two ways: by extraction from lithium-bearing brines drawn from sedimentary basins or from the processing of granitic pegmatite ores (hard rock), the most significant of which is spodumene.

Broadly speaking, brine production is dominated by South American sources of supply, while Australia is the main source of hard-rock supply (see: **Figure One**). Other sources of lithium exist—such as clays and geothermal brines—but these are yet to be proven on a commercial scale.

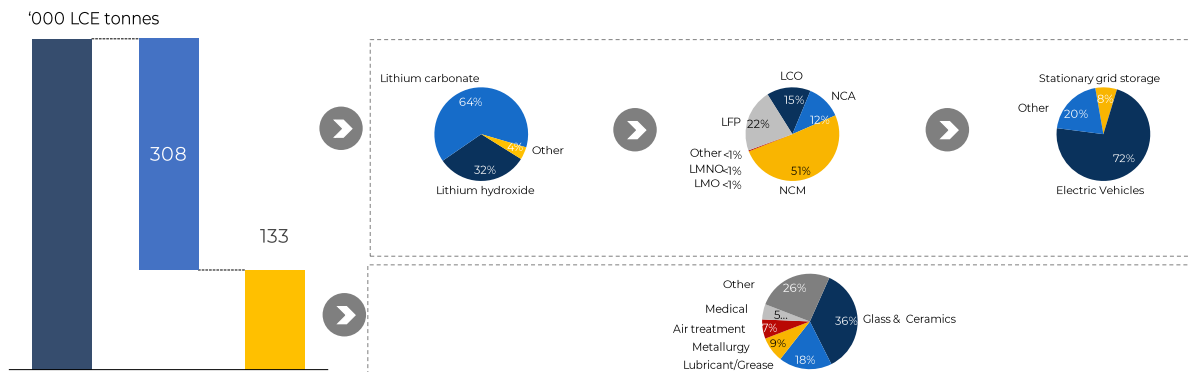
Figure One: Lithium resource availability by country



Source: Benchmark Mineral Intelligence

Brine and hard-rock sources of lithium are commonly converted into lithium chemicals—either lithium carbonate or lithium hydroxide. These are used directly in various applications—lithium-ion batteries, for example—or submitted to additional processing for niche uses. As the precise content of lithium chemicals differ, supply and demand are denominated in terms of lithium carbonate equivalent (LCE). For example, lithium hydroxide contains less lithium than lithium carbonate.

Until recently, the bulk of global lithium supply was consumed in industrial applications unrelated to the lithium-ion battery (LiB) sector. In 2015 more than two-thirds of lithium demand came from an assorted group of end uses, including glass production, ceramics manufacture and lubricants. However, since at least 2015 the LiB sector has emerged as the dominant driver for lithium demand. In 2021 almost 70% of estimated lithium consumption—approximately 308Kt LCE out of a global market of 442Kt LCE—is attributable to the battery sector (**Figure Two**).

Figure Two: Lithium Demand Breakdown by End-Use


Source: Benchmark Mineral Intelligence

The emergence of electric vehicles (EVs) as a competitive option to fossil fuel consuming internal combustion engine (ICE) vehicles has been the primary cause of the transformation in lithium demand. In the same vein, the likely replacement of ICEs by EVs will define the evolution of lithium demand in years to come.

There are three main factors driving the adoption of EVs to varying degrees across different national markets:

- Emissions legislation:** in all major vehicle markets there has been an ongoing tightening of limits for vehicle emissions for OEMs to meet with regards to fuel economy and CO₂, as well as air quality issues around nitrogen oxides (NOx) and particulate matter. The European Union has generally led the world in formulating these standards, which have been subsequently adopted by legislators in other countries in various forms. For instance, major Chinese cities have chosen to transition to China 6 standards for light-duty vehicles (Euro 6 equivalent) in 2020, despite being given the option of a delay until early 2021. From 2021, however, only vehicles that meet China/Euro 6 emissions standards can be sold in or imported to China. The issue for OEMs has been that their two traditional technologies—diesel and gasoline engines—perform well on either fuel economy or emissions metrics, but not both simultaneously. Diesel technology performs well against fuel economy and CO₂ standards, but poorly on NOx and particulate matter, necessitating significant technological intervention in the form of selective catalytic reduction that increases the cost of the vehicle.
- OEMs adopt electric vehicle models:** The second factor, therefore, is that in the face of tightening standards for air quality, it is now very difficult for OEMs to meet fuel economy and CO₂ standards without adopting some form of electrification in their model line ups. As a result, OEMs have developed and made significant investments in electrification strategies to meet existing and future challenges. It is important to point out, however, that not all OEMs are pursuing this strategy at the same pace, and many have an intermediate strategy of adoption of hybrid technology before moving to full electric later. Tesla, which was founded in 2003 and marketed its first electric vehicle in 2008, is currently at the forefront of the sector's development, at least in Western markets. It has made substantial investments in cell and EV making capacity. The company also has ambitions to invest in the battery raw material supply chain and to

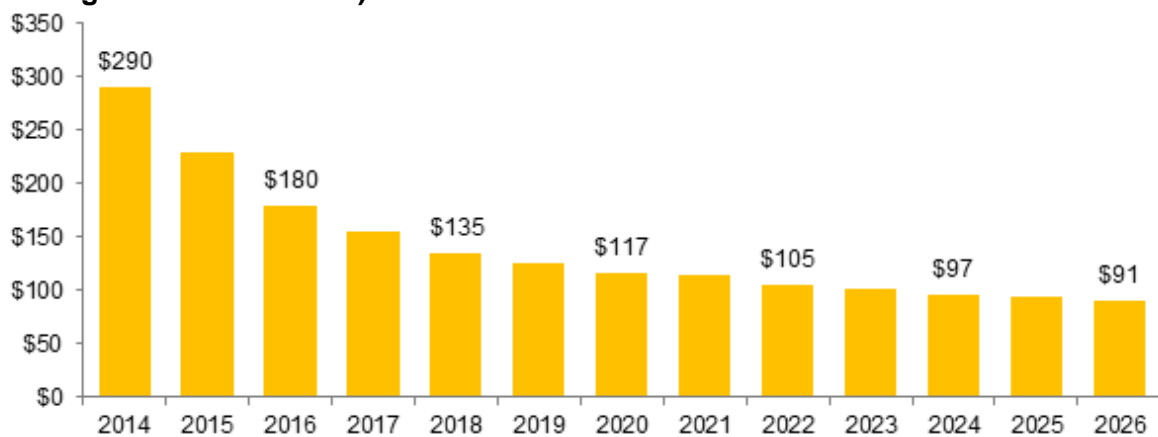
rationalize downstream manufacturing processes. Tesla has to date stolen a march on western major western automakers. But many, including Volkswagen, the world’s largest OEM, are rapidly shifting their focus to developing the EV supply chain. Meanwhile in China, several EV producers have responded to supportive policy signals from central government by both investing in cell capacity and in projects aimed at securing long-term supply of battery raw materials.

- **Governments promoting electrification efforts via incentives and subsidies for EV purchases and production:** To date China has had one of the most generous subsidy programs worldwide. This program was to be wound down and replaced by a VAT reduction scheme and other financial incentives for new energy vehicles. However, the emergence of the COVID pandemic led to an extension of the Chinese subsidy program, with both high energy density and low-priced EV models retaining support.

Elsewhere, governments in major vehicle market have some form of either direct subsidy or fiscal advantage to support incentives. Moreover, measures that specifically favor EV adoption have been included in numerous national governments’ fiscal policy response to the COVID pandemic. The German government’s actions have been particularly noteworthy, for example. Despite the importance of ICE vehicle manufacturing to the German economy, the country’s government increased its subsidies on EVs, made no comparable concession for ICEs, and instead restated its commitment to effectively increase taxes on ICE vehicles in 2021.

Owing to the scheduled investment in vehicle electrification and as the market builds scale, OEMs and battery makers will be able to significantly reduce the cost of EVs at a cell, battery pack and vehicle platform level. As a result, the price for EVs is forecast to approach parity with ICE vehicles by the middle of this decade (**Figure Three**).

Figure Three: Lithium-ion battery cell cost forecast \$/kWh* (average NCM cell cost including cathode evolution)



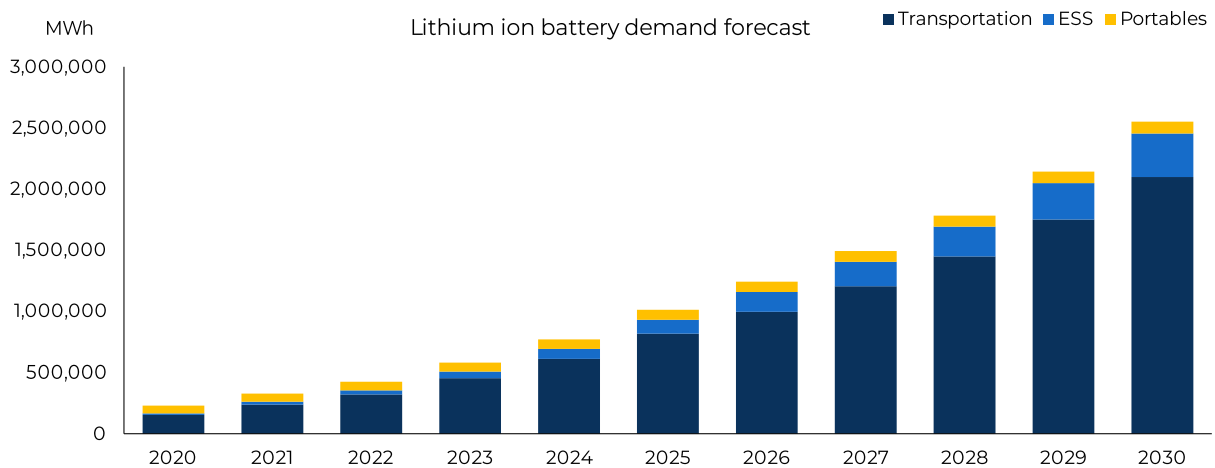
*Assuming flat future raw material prices, excludes margin, module and pack costs, figures account for top 80% of producers by scale only.

Source: Benchmark Mineral Intelligence

A further important point is that these investments, which we estimate at USD300 billion for vehicle and battery pack production, and a further USD160 billion in battery cell capacity investment by 2030, will need to be amortised over the next decade at least. This provides a strong barrier to entry for rival battery and other zero-emissions technologies over the same period.

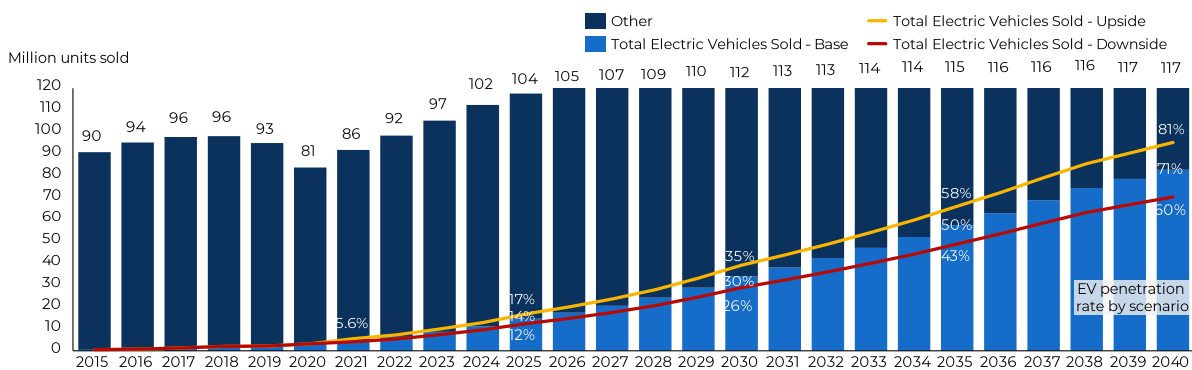
Even if the future adoption of EVs is slower than our base-case assumption, lithium demand from EV batteries is still estimated to grow at a CAGR of more than 41% between 2020-25 and by roughly 22% between 2025-30.

Figure Four: Li-ion battery demand forecast by sector, GWh, 2015-40



Source: Benchmark Mineral Intelligence

Figure Five: EV sales as share of total cars, million units sold, 2015-40

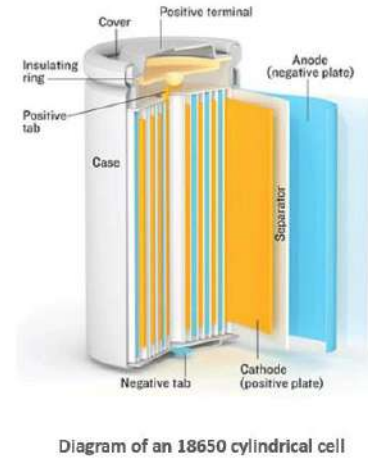
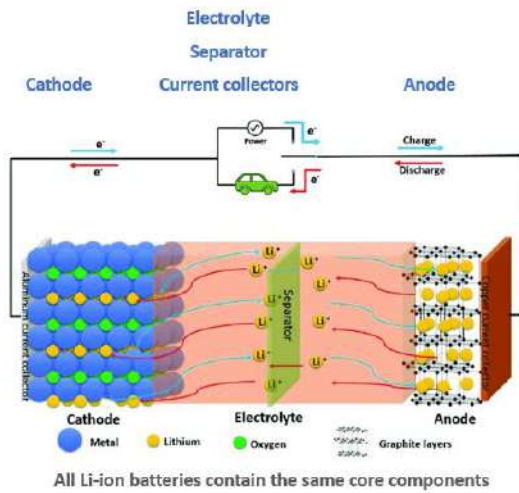


Source: Benchmark Mineral Intelligence, Rho Motion

The Role of Lithium in Lithium Battery Cell Technology

All LiBs can be broken down into a single battery cell. Each LiB contains the key components of a cathode, an anode, electrolyte, a separator, and current collectors. However, LiBs can vary greatly based on material choice and intended application. **Figure Six** shows the composition and structure of the batteries, indicating where and how each of the raw materials required is used.

Figure Six: Main components of a Li-ion battery



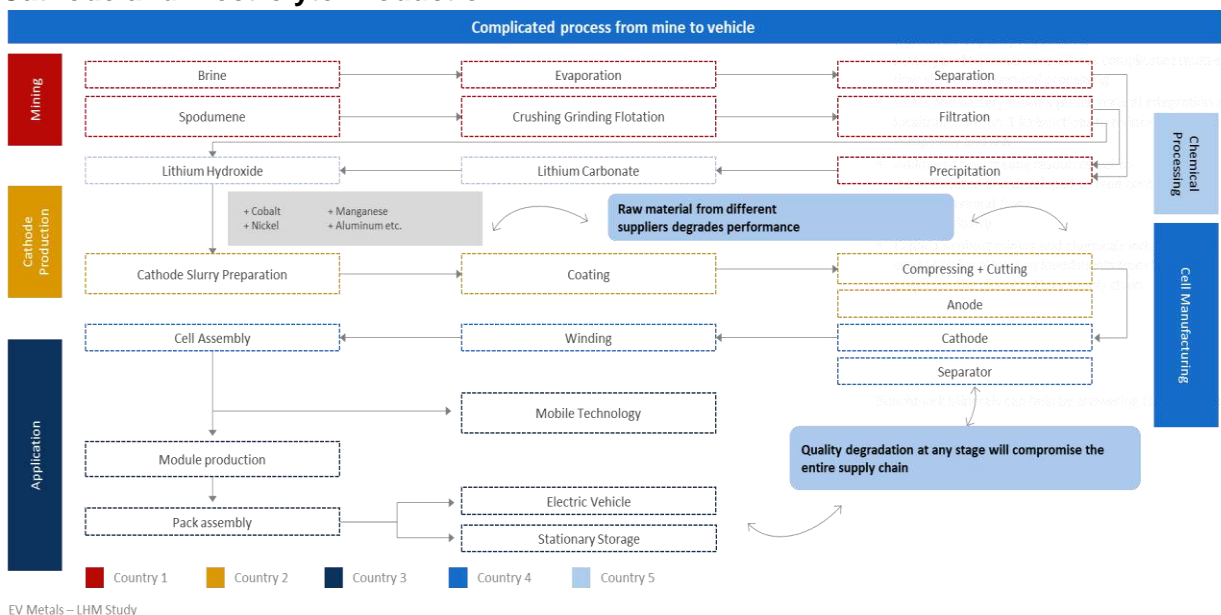
Source: Benchmark Mineral Intelligence

Lithium is a key component across the structure of the battery: it is present both in the cathode and the electrolyte, allowing charge to flow between the anode and cathode.

The full supply chain for lithium, from upstream production of brine and hard-rock concentrate, through to downstream application in LiB cells in EVs and stationary storage units, is complex and often disaggregated.

The high purity levels required for battery performance necessitates complicated multi-step flow sheets for chemical processing (**Figure Seven**). Western OEMs and battery makers are starting to show a preference for vertical integration and localization in secure jurisdictions to reduce supply chain complexity and risk.




Figure Seven: Battery Industry Demand for High-Quality Lithium Chemicals for Cathode and Electrolyte Production



Source: Benchmark Mineral Intelligence

There are three main LiB cell formats: **cylindrical**, **prismatic** and **pouch**. Each format offers various performance characteristics. An overview of each cell type is provided in **Table Two**.

Table Two: Overview: Lithium-ion Battery Types

Battery Type	Image	Description
Cylindrical		This is Tesla’s cell of choice. Offers good cycling ability, longevity and is economical to produce. For EV use, two sizes are now available, 18650 (18 mm in diameter and 65 mm tall) and 2170 (21 mm in diameter and 70 mm tall). As the number of cells in an EV are in the thousands, individual cell failure does not unduly impede vehicle performance. The cell is heavy, leading to lower gravimetric energy density than other cell formats. The cell has a lower packaging density due to space cavities. Common applications include power tools, laptops, e-bikes and EVs
Prismatic		Prismatic cells are encased in aluminium or steel for stability. Due to its rectangular shape, the cell provides a good use of space within an EV battery module, allowing for multiple model configurations within a battery pack. The design allows for some selling during performance. Prismatic cells can be relatively expensive to manufacture, are less efficient in thermal management, and potentially have a shorter cycle life than the cylindrical type. Key applications of prismatic cells are for EVs and energy storage systems.
Pouch		Pouch cells use a laminated architecture in a bag. The cells are space efficient, achieving 90–95% packaging efficiency. They are also relatively light weight compared to cylindrical and prismatic cells. The cell needs allowance to expand in the battery compartment. Pouch cells are commonly used in portable electronics and EVs.

Source: Benchmark Mineral Intelligence

Table Three outlines the main performance, chemical and cost characteristics of LiB technologies.

Table Three: Performance, Chemical and Cost Characteristics of Lithium-ion Battery Technologies

Battery Chemistry	Chemical Symbol	Raw Materials	Specific Energy (Wh/kg)	Cycle Life	Voltage (v)	Cell Cost (US\$ per kWh)
LFP	LiFePO ₄	Cathode: lithium–iron–phosphate Anode: graphite	120	2000+	3.30	160
NCM111	LiNiMnCoO ₂	Cathode: lithium–nickel–cobalt–manganese Anode: graphite	180	1,000–2,000	3.70	170
NCM523	LiNiMnCoO ₂	Cathode: lithium–nickel–cobalt–manganese Anode: graphite	220	1,000–2,000	3.70	130
NCM622	LiNiMnCoO ₂	Cathode: lithium–nickel–cobalt–manganese Anode: graphite	240	1,000–2,000	3.70	130

Battery Chemistry	Chemical Symbol	Raw Materials	Specific Energy (Wh/kg)	Cycle Life	Voltage (v)	Cell Cost (US\$ per kWh)
NCM811	LiNiMnCoO ₂	Cathode: lithium–nickel–cobalt–manganese Anode: graphite	280	1,000–2,000	3.70	120
NCA	LiNiCoAlO ₂	Cathode: lithium–nickel–cobalt–aluminium oxide Anode: graphite	240	500–1,000	3.60	120
LTO	Li ₄ Ti ₅ O ₁₂	Cathode: LMO or NCM Anode: titanate	50–80	3,000–7,000	2.40	>1000
LMO	LiMn ₂ O ₄	Cathode: lithium–manganese oxide Anode: graphite	100–150	300–700	3.70	>300
LMNO/LMCO	LiNiMnCoO ₂	Cathode: lithium–nickel–manganese–cobalt oxide Anode: graphite	100–150	300–700	3.70	>300
LCO	LiCoO ₂	Cathode: lithium–cobalt oxide Anode: graphite	260	500–1,000	3.60	230

Source: Benchmark Mineral Intelligence

There is often a trade-off between specific energy, cycling ability (battery life) and cost. For EVs, high specific energy, coupled with strong cycling ability, is crucial as it allows the vehicle to achieve a functional driving range with a battery size and cost that is technically and economically viable for a mass-market vehicle.

EV manufacturers are trying to simultaneously reduce the vehicle costs and increase range and capacity. At the LiB cell level, this has placed a priority on increasing cells' specific energy (Wh/kg) and energy density (Wh/L), while also reducing raw material costs where permitted by the requirements of safety.

Cathode Technology

The pursuit of these goals has led to innovations in cathode technology.

Tesla adopted a nickel–cobalt–aluminium (NCA) cathode chemistry approximately 10 years ago as a solution to the range and performance problems that had hampered EV uptake until that point. However, in subsequent years, Western OEMs generally settled on nickel–cobalt–manganese (NCM) cathode technologies as a more stable means of achieving competitive specific energy levels at an acceptable cost. Variations of NCM chemistry have emerged, the general pattern being that they offer superior energy density by increasing nickel content at the expense of cobalt. This provided the dual benefit of lowering costs (cobalt is comparatively expensive) and reducing the OEMs' exposure to the cobalt supply chain, which commonly can be traced back to the Democratic Republic of Congo (DRC), one of world's least-stable states.

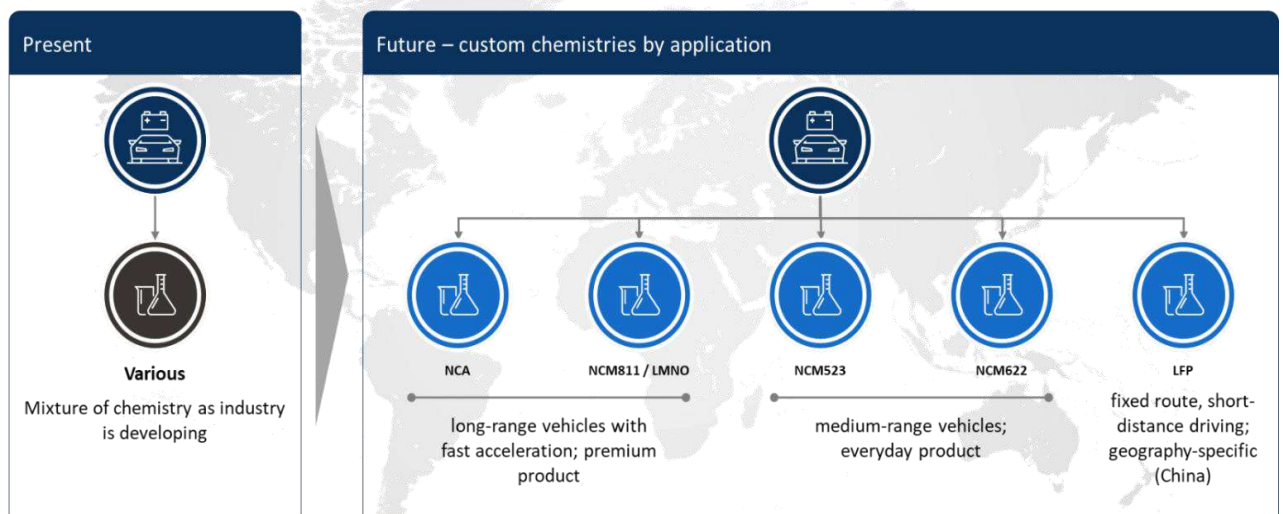
OEMs are currently overcoming the inherent complications of producing NCM811 (higher nickel content entails less stability and requires more stringent control of operating conditions during manufacture; it also requires the use of lithium hydroxide). Benchmark

forecasts that this will take time. **The OEMs’ investment schedules imply that NCM811 will become the dominant LiB cathode chemistry type post-2025.**

This view remains unaffected by the renewed interest shown in lithium–iron–phosphorus (LFP) chemistry. LFP chemistry benefits from comparatively low-cost raw materials, notably, lithium carbonate is used, which represents a cost saving versus high-nickel NCM chemistries that require more costly lithium hydroxide. However, LFP cells provide lower energy density and poorer range capacity than NCM variants. Recent improvements in the performance of LFP technology mean it will likely make up a larger proportion of EV battery capacity in markets, in China and India, for example, where the limitation in vehicle range is perceived as less of a flaw than in the view in western Europe and North America. The potential for more widespread adoption of LFP cathode chemistry across all EV markets is considered to be limited.

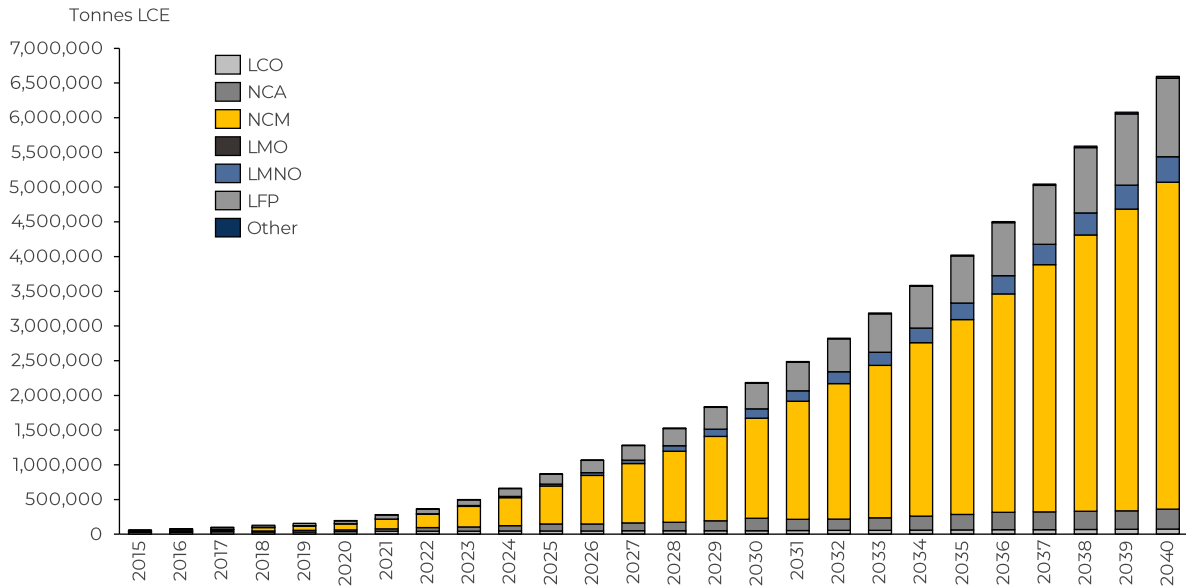
Figure Eight summarizes the cathode chemistries and characteristics from the perspective of the EV market. **Figure Nine** provides an overview of the lithium demand by cathode type. **Figure Ten** shows the NCM battery technology forecast for the period 2015–2030.

Figure Eight: Cathode Chemistries and Characteristics in the EV Market



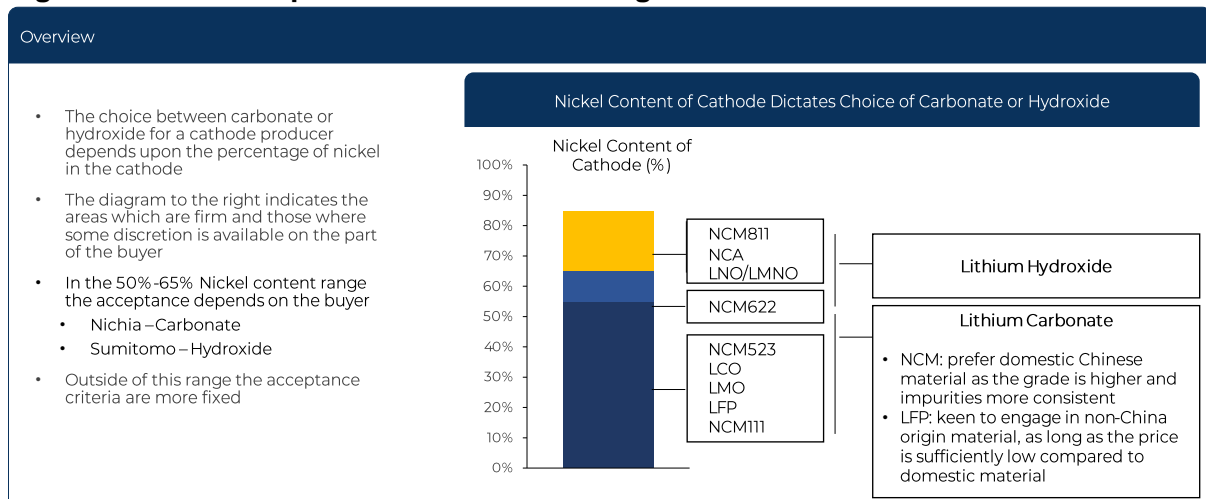
Source: Benchmark Mineral Intelligence

Figure Nine: Lithium Demand by Cathode Type

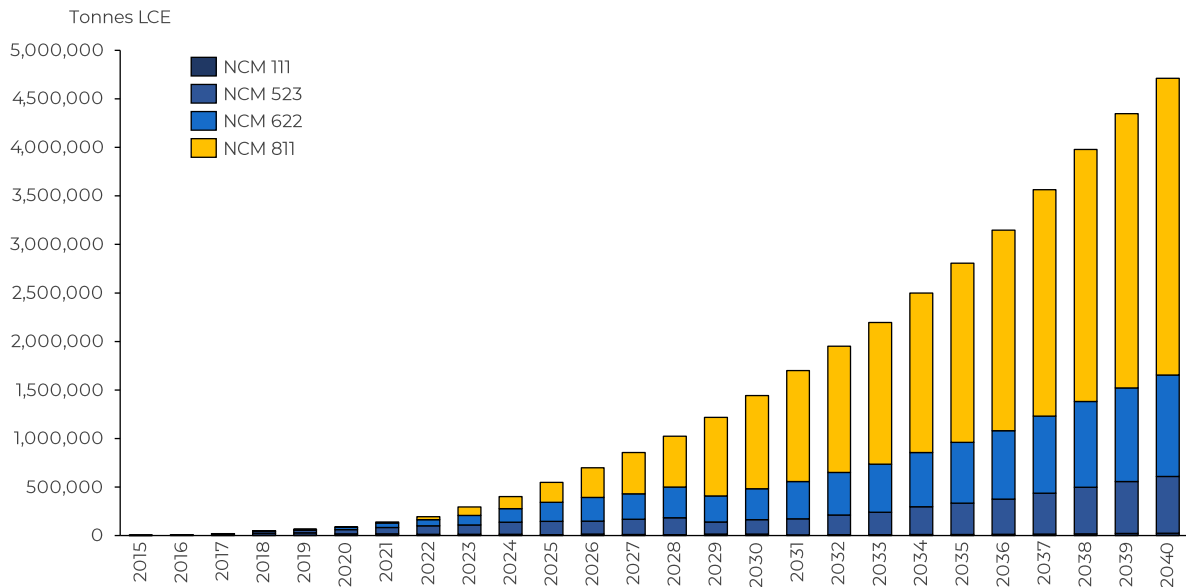


Source: Benchmark Mineral Intelligence

Figure Ten: Lithium product demand resulting from NCM cathode



Source: Benchmark Mineral Intelligence

Figure Eleven: NCM Cathode demand forecast, GWh, 2015-40


Source: Benchmark Mineral Intelligence

The lithium intensity of competing LiB cathode chemistries is relatively similar. **Table Four** shows that 1 kWh of LiB capacity made from various cathode types requires between around 0.8–0.9 kg of LCE.

Table Four: Lithium Intensity of Lithium-ion Battery Cathode Chemistries

LiB Cathode Type	2020 (kg LCE/kWh)
LCO	0.8
NCA	0.85
NCM	0.874
LMO	0.84
LMNO	0.8
LFP	0.854

Source: Benchmark Mineral Intelligence

Consequently, **efforts by the OEMs to reduce cell production costs are currently not overly preoccupied with lithium.** In the immediate future, potential reductions in LiB cathode costs will likely come from a reduction in the use of cobalt, and greater efficiencies and scales in the manufacturing process.

While immediate cost concerns may not be primarily focused on lithium, **there is disquiet about the availability of lithium in the medium- and long-term, particularly the lithium hydroxide required by high-nickel NCM cells.** This obviously has implications for lithium prices and, in turn, cell costs.

Beyond improvements to the cathode, greater effort will be made to improve LiB cell energy density and lower input costs via changes to anode technology. Graphite, whether synthetic or natural, is the material of choice for LiB anode technology. That will remain the case for the foreseeable future, although anode producers are increasingly seeking to add silicon to graphite to boost the material's specific energy capacity. This development will do little to change the amount of lithium used per LiB cell.

Competitive threats: the role of Solid State

Competition to lithium-ion batteries could come from several sources, the main examples of which are outlined in **Table Five**. However, each of these candidates currently have drawbacks to their application, in some cases highly serious ones. Moreover, solid-state lithium metal batteries—the alternative to lithium-ion batteries that is currently closest to commercial viability in the EV space—would have little impact on lithium chemical demand. The risk of substitution in solid-state lithium metal batteries applies to the anode (graphite potentially displaced by lithium metal) rather the cathode, which remains largely unchanged.

In contrast, displacement of lithium-ion batteries by sodium-ion technology in the EV space would entail changes in lithium consumption. However, this is an extremely immature technology that we believe has little chance of widespread commercialisation within the next 15 years. Laboratory projects have yet to prove that sodium-ion batteries can last long enough to be applicable to EVs. Sodium is also a heavier element than lithium, so it will be difficult for sodium-ion batteries to reach the levels of energy density achievable with lithium-ion batteries. Finally, there is also no guarantee that the existing lithium-ion battery infrastructure could be adapted to produce sodium-ion batteries. Given the vast amount of investment currently flowing into the development of the lithium-ion battery supply chain, this constitutes an obstacle which the latter technology will struggle to overcome for some time.

Vanadium flow batteries may have potential application in the energy storage field in future. But once again the potential lead time for this development will be long and, more importantly, will have no impact on lithium demand from the EV sector, by far the most dynamic end-use market over our forecast period.

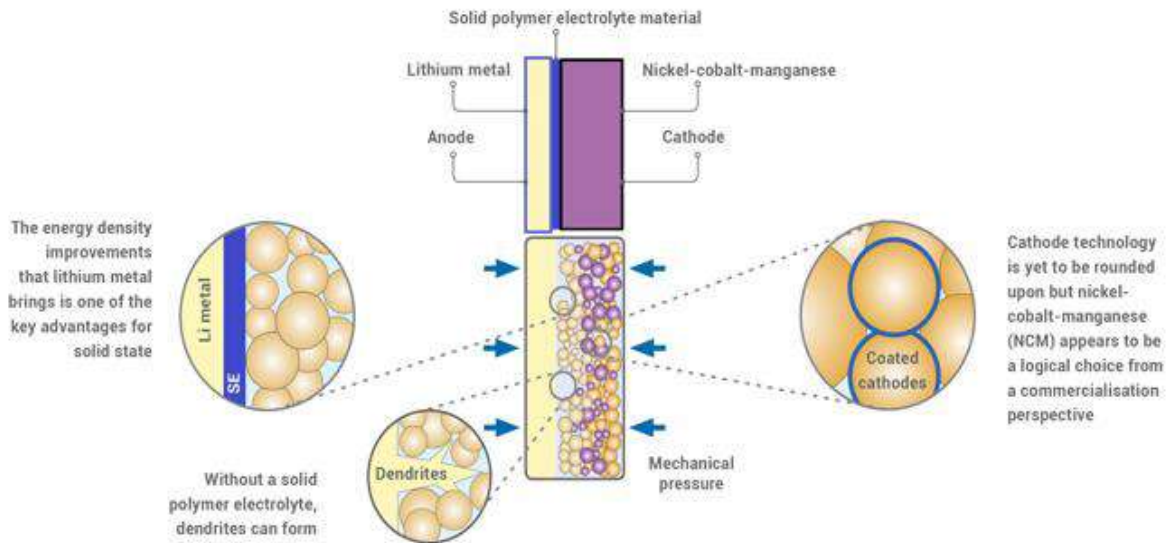
Table Five: Battery Technology and characteristics

Battery Technology	Application	Stage of Development	Specific Energy Wh/kg
Lithium Ion	EV	Widespread commercial adoption	100-300
Lithium Metal (solid state)	EV	R&D	400-500
Sodium ion	EV	Concept/ Innovation	90-115
Vanadium Flow	Stationary Storage	R&D	10-20

Source: Benchmark Mineral Intelligence

Significant attention has been placed on solid-state battery cells and this merits attention. In these cells the graphite/silicon anode would be replaced by a lithium-metal anode, and conventional liquid electrolyte would be replaced by either a solid inorganic or polymer electrolyte.

Figure Twelve: Components of a Solid-State Battery



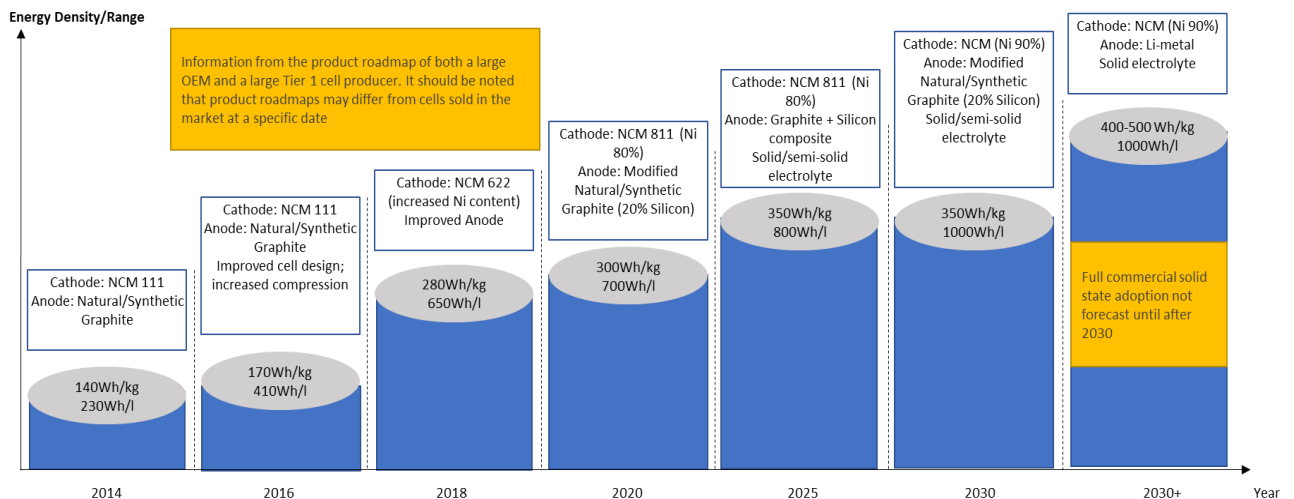
Source: Benchmark Mineral Intelligence

Solid-state cell technology could be commercialised within the next five years; however, it is likely to take longer (post-2030) for the technical challenges of solid-state cell technology to be overcome and the transition to commercial production to be made.

It is not yet clear whether solid-state cells can operate efficiently at low temperatures and avoid the risk of short-circuiting due to the formation of lithium-metal dendrites. Fundamental questions about the exact form of lithium needed for solid-state cells also remain to be answered.

The technology is unlikely to quickly be able to compete with existing technologies based on cost, and so will likely be constrained to niche applications for some time. **However, given that solid-state battery technology is likely to be more lithium-intensive than competing alternatives, its slow development will certainly do nothing to undermine growth in future lithium demand (Figure Thirteen).**

Figure Thirteen: Lithium-ion Battery Development



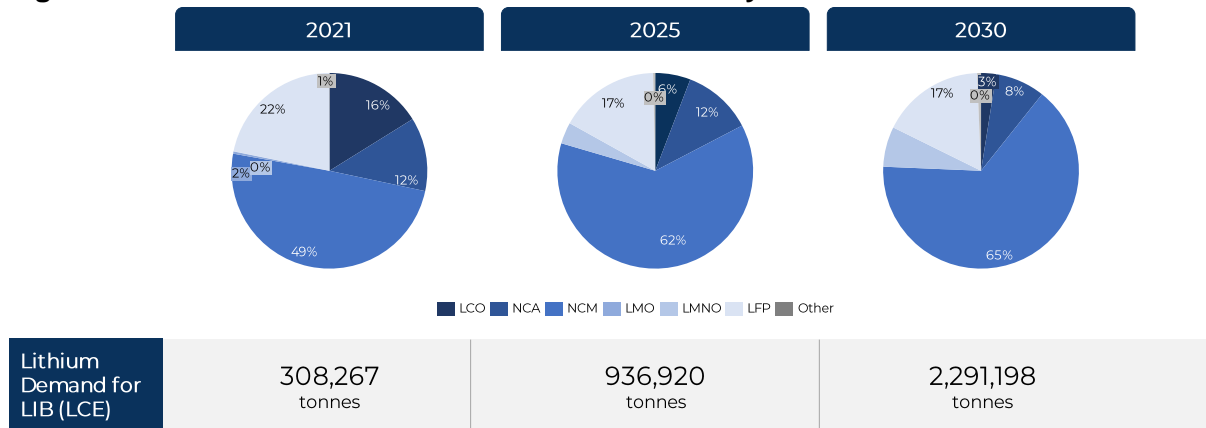
Source: Benchmark Mineral Intelligence

Lithium Demand

As previously mentioned, of the 442,000 t of LCE consumed globally in 2020, 308,000 t LCE went to the battery sector, and 133,000 t to other industrial uses. Battery demand for lithium is dominated by the EV sector, which accounted for almost 70% of battery demand for the year (2021). Non-battery, or ‘Other demand’, for lithium will for the most part comprise of end uses that consume various lithium chemicals, predominantly, but not exclusively, lithium hydroxide and carbonate.

However, some of the lithium consumed by the glass and ceramics sector will be in the form of a mineral concentrate (spodumene or lepidolite). Material specification will tend to differ between application. For example, spodumene concentrate used to manufacture ceramics is unlikely to be optimal for processing into battery-grade lithium hydroxide. The importance of battery sector demand for lithium is set to grow significantly over time. By 2030, the global lithium market is expected to have grown to just under 2.4 Mt LCE, of which just under 2.2 Mt LCE will be for use in batteries, with 80% of those batteries deployed in EVs (**Figure Fourteen**).

Figure Fourteen: 2030 Lithium Demand Breakdown by End-Use



Source: Benchmark Mineral Intelligence

By 2040, global lithium demand is forecast to reach around 6.8 Mt, with roughly 6.6 Mt devoted to battery applications.

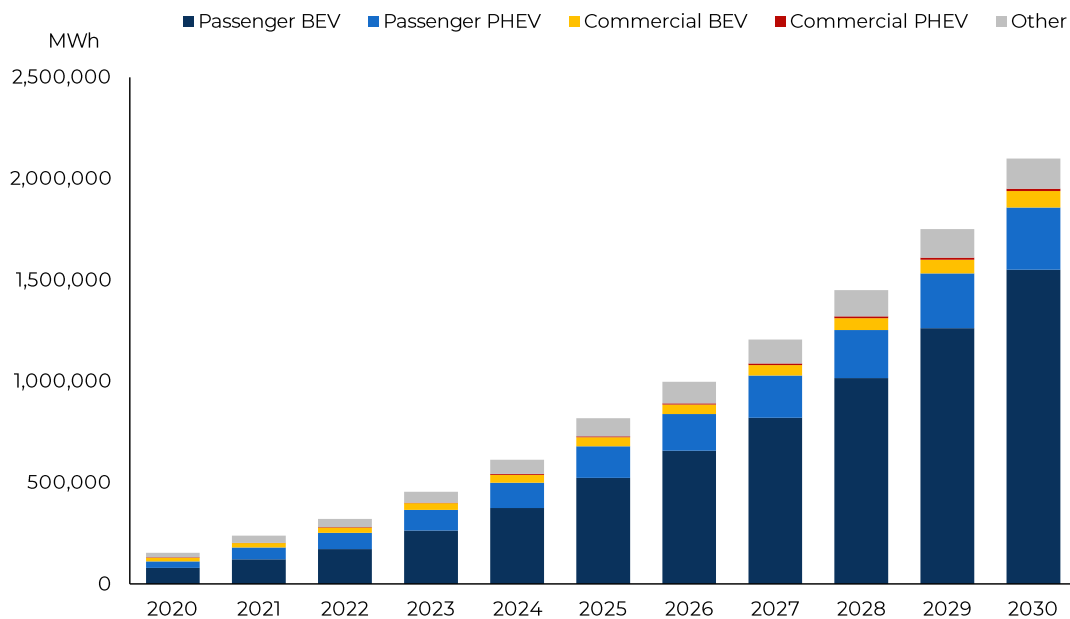
These high-level changes are underpinned by an expected growth in dominance of NCM cathode chemistry. By 2030, NCM cells are forecast to consume almost 80% of lithium used in the battery sector, up from about 43% in 2020.

The rise in NCM cells is also expected to be accompanied by a shift in the form of lithium chemical consumption. Lithium hydroxide will account for half of the lithium consumed in batteries in 2030, an increase from about one quarter in 2020. By 2040, when global lithium demand is forecast to hit 6.8 Mt, around 60% of lithium consumption in LiBs will occur in the form of lithium hydroxide.

The specifics of lithium demand growth in the various battery application sectors over the next 10 years include:

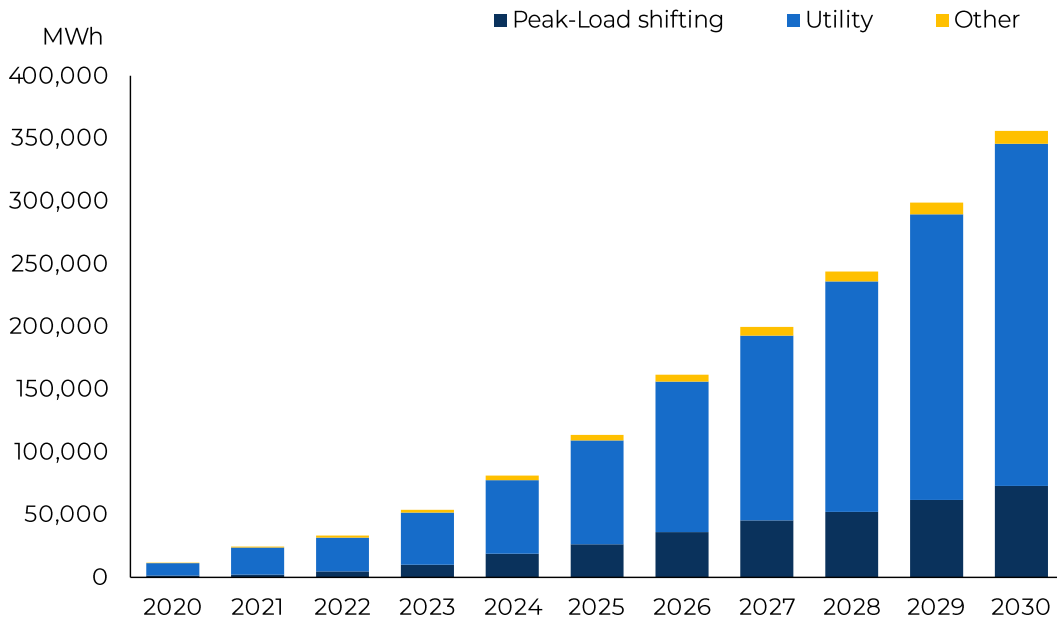
- Transportation:** EV adoption rates will have the largest impact on LiB demand over the forecast period. EV sales are expected to reach 11.8 M units by as early as 2025 (up from an estimate of around 1.9 M units in 2020) which would equate to a 11.2% penetration rate. The demand model includes upside/downside cases to this base assumption, but the base case forecasts EV demand to increase at a CAGR of 30% over the coming 10 years. The EV forecast is based on a range of factors, ranging from the legislative to the technical. Another layer of assumptions relating to battery chemistry and cell pack sizes is applied to arrive at overall cell and raw material demand projections. Forecasts are benchmarked against plans announced by OEMs to invest in EVs.

Figure Fifteen: EV Driven Lithium Ion Battery Demand



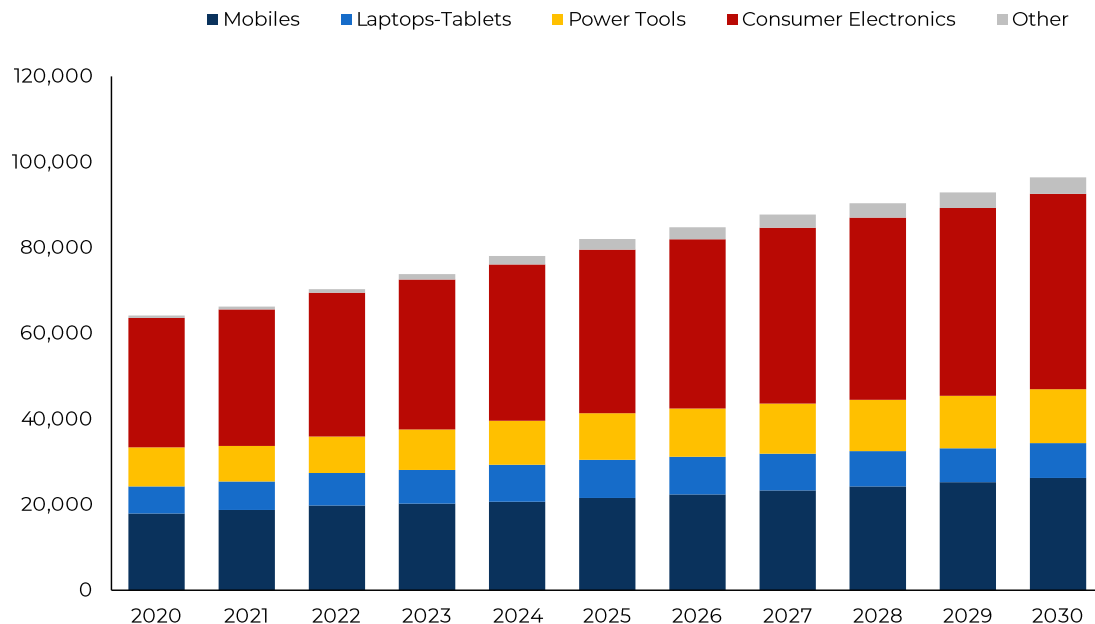
- Stationary storage:** Growth of LiB demand from stationary storage applications is expected to accelerate through to the mid-2020s before subsequently slowing as markets become more mature. The cost and quality improvements in battery chemistry for EV applications will facilitate high penetration levels in a range of residential and commercial markets, despite LiB not necessarily being the most efficient technology to use in these areas. Stationary storage demand is forecast to grow at a CAGR of 41%, over the next 10 years, overtaking portable electronic demand by 2025.

Figure Sixteen: ESS Driven Lithium Ion Battery Demand



- **Portable electronics:** Demand growth rates from portable electronics have gradually slowed since the mid-2000s. While growth will continue from these markets, the rate is expected to be limited due to the maturity of key application markets. The stability, density, and availability of the LCO cathode means this will remain the primary chemistry choice in these markets, although some high-nickel chemistries are being deployed in power tools and powerpack applications.

Figure Sixteen: Portables Driven Lithium Ion Battery Demand



Megafactory Capacity

To meet the forecasted increase in global LiB demand, significant investments were made and are scheduled to be made in battery cell manufacturing capacity. The rate of investment in cell manufacturing has increased rapidly in recent years. From less than 750 GWh of capacity in 2020, over 2.34 terawatt hours of battery cell manufacturing capacity is expected to have been built by the end of 2025, across more than 186 operating plants. In terms of the geographical split of this capacity, nearly 70% will be in China in 2025, with Europe potentially the second-largest producer of battery cells by region.

Lithium-ion Cathode Plant Capacity

Battery cathode plants, where lithium chemicals are converted into cathode active material before that in turn is used in cell making, have to date been built in only three countries: China, Japan, and South Korea.

Approximately two-thirds of the lithium carbonate and lithium hydroxide used in global battery production during 2020 was consumed in Chinese cathode plants. Most of the remainder was split almost equally between Japan and South Korea, with comparatively small shares used in Taiwan, North America, and Europe.

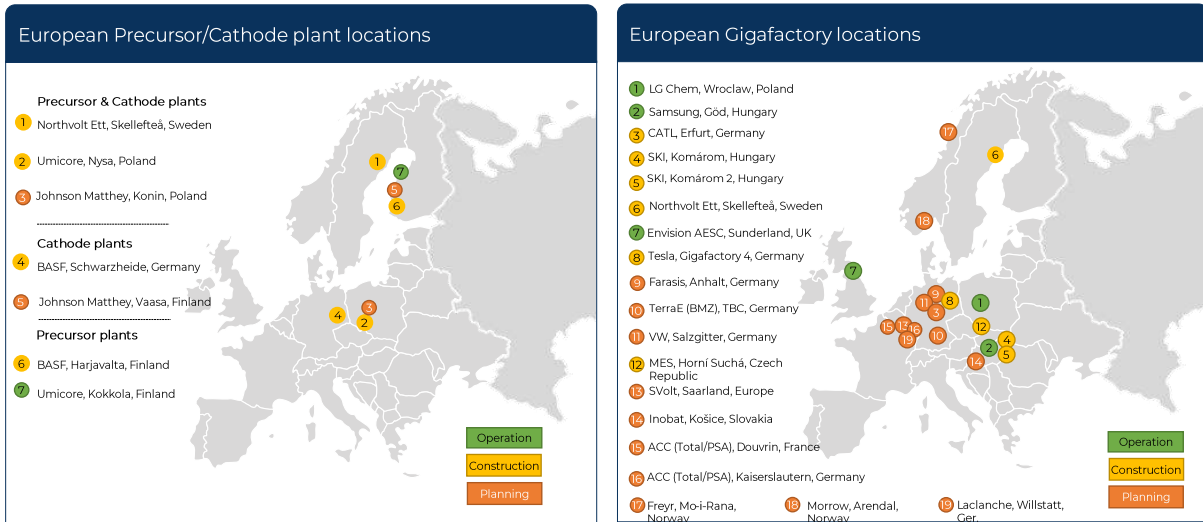
China is forecast to remain the largest national producer of cathode material over the next decade. Slightly less than 40% of the cathode capacity currently under construction or in planning in China is scheduled to be either NCM 811 or NCA, which will require the use of lithium hydroxide rather than lithium carbonate. An additional 18% or so this capacity under construction or in planning is forecast to be NCM 622, which can use either lithium hydroxide or carbonate.

Cathode capacity additions are planned in Japan, South Korea, and Europe, which will be, for the most part, NCM 811 or NCA capacity. Firm details of cathode capacity being either built or planned in North America have yet to be made public, although Tesla recently expressed its intention of building cathode capacity. Overall, the plans to build cathode capacity outside of China are currently comprehensively overshadowed by Chinese plans.

Both the European Union (EU) and the United States of America (USA) currently appear to be structurally 'short' of local cathode capacity through to until at least 2030.

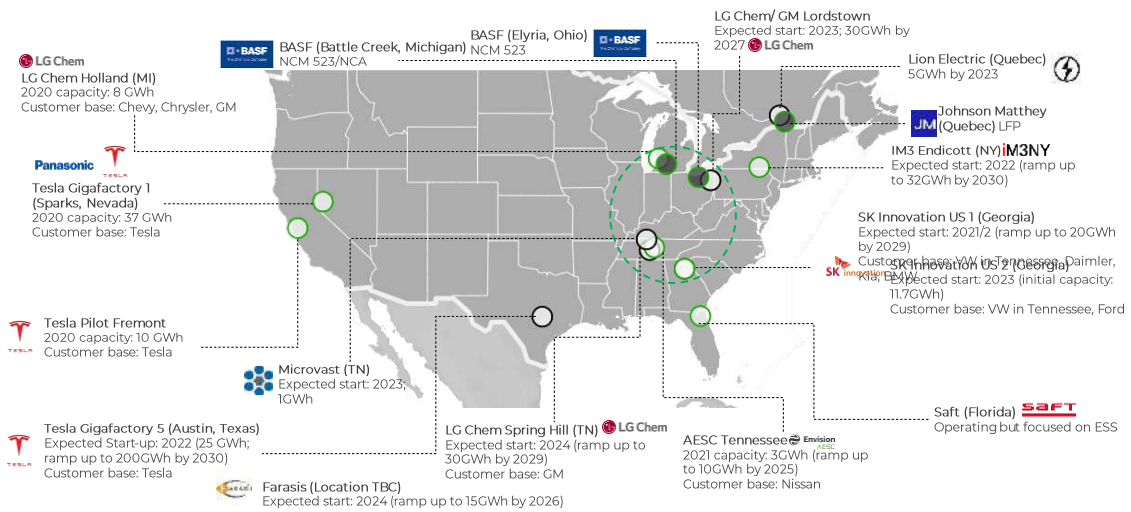
In Benchmark's view, there is a strong probability that additional cathode projects will emerge in the EU and the USA, however. Western OEMs are advocating for elements of the EV supply chain to be brought closer to their home operational hubs, as this both reduces working capital requirements and mitigates excessive reliance on Chinese-based supply. Lithium chemical consumption in the EU and USA would increase at the expense of consumption in China and other Asian markets.

Figure Seventeen: Development of the European supply chain



Source: Benchmark Mineral Intelligence

Figure Eighteen: Development of the North American supply chain

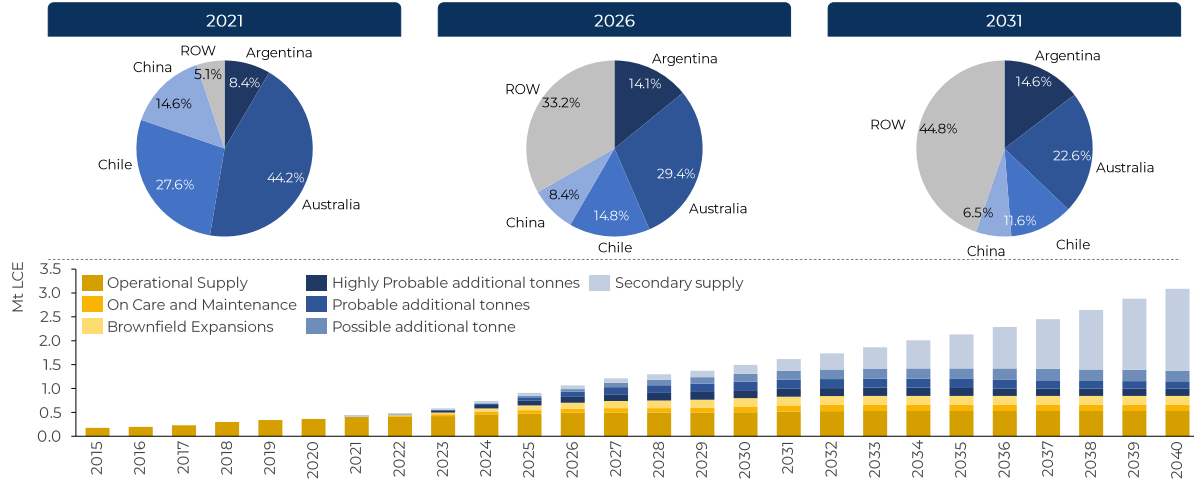


Source: Benchmark Mineral Intelligence

Lithium Supply

Global lithium supply is currently consolidated among a small number of producers. This is forecast to change in coming years, however, as a raft of new brine and hard-rock deposits progress from development stage through to production (**Figure Eighteen**).

Figure Eighteen: Lithium raw material supply: 2021, 2025, and 2030



Source: Benchmark Mineral Intelligence

There are four main regions which supply the majority of the mined lithium to the market – these are outlined below

Argentina

Incumbents: Livent, Orocobre

- There are currently two lithium producers in Argentina; Livent and Orocobre. These producers operate from the Salar del Hombre Muerto and Salar de Olaroz respectively. Livent is expected to produce 17.5kt LCE, while Orocobre is expected to produce 14kt LCE of lithium carbonate in 2021. Both will be at capacity in 2021, and both have expansion plans which Benchmark expects to be operational by 2023

Next Generation: Neo Lithium, Lithium Americas, POSCO, Millennial Lithium, Galaxy

- Argentina hosts some of the industry’s most developed new projects, most notably the Lithium Americas Cauchari/Olaroz project, which Chinese converter Ganfeng took a 51% stake in in January 2020. This project is likely to be next lithium greenfield project to come online in Argentina. Benchmark’s latest model remains unchanged expecting 6kt LCE in 2022.



- Argosy Minerals’ Salar del Rincon is targeting commercial production that same year, but unlikely to produce meaningful volumes until 2023.
- POSCO’s Hombre Muerto, Millennial Lithium’s Pastos Grandes, and Galaxy Resources’ Sal de Vida projects are all likely to begin production by 2023.
- Rincon Lithium, Eramet, Neo Lithium, and Lake Resources all have projects which Benchmark has made provision for in 2024. Portofino Resources, Pepininni Lithium Lito Minera (Ganfeng) and Albemarle also have projects in the region; insufficient information is available to make an assessment on when these projects will enter the market.

Chile

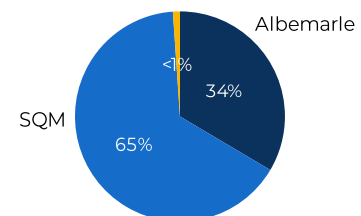
Incumbents: SQM, Albemarle

- **SQM** is expected to produce 78kt LCE of lithium carbonate at Salar del Carmen and convert 10kt LCE of this to lithium hydroxide. SQM’s ambitious expansion plans present some upside potential. While there is some potential for output to be higher, Benchmark has applied a conservative approach in line with past reliability on expansion announcements
- **Albemarle** is expected to produce 36.5kt LCE of lithium carbonate in 2021. Albemarle’s La Negra III / IV (+40 kT LCE expansion) continues to be on track for construction in 2021.



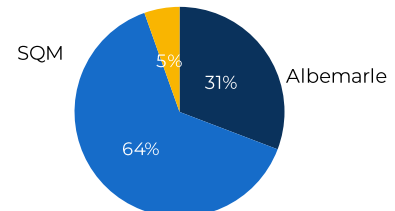
2025

Minera Salar Blanco (MSB)*



2030

Minera Salar Blanco (MSB)*



Next Generation: Minera Salar Blanco (MSB), Lithium Chile, Wealth Minerals

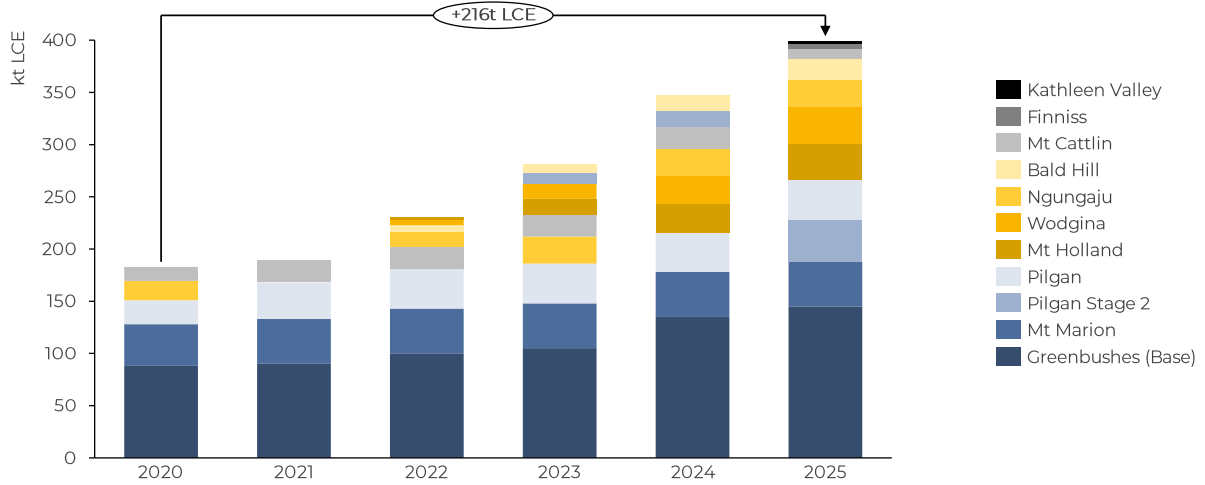
- **MSB** is targeting an initial capacity of 15kt LCE for its Maracunga project. The company recently entered into a non-binding MoU with Mistui for potential off-take and funding rights for the Stage One of the Project.
- **Lithium Chile** owns fourteen projects and is collaborating with Summit Nanotech to demonstrate the viability of its DLE process.
- **Wealth Minerals** holds concessions in close proximity to SQM’s production sites, but no recent development updates have been given.

Australia

There were five spodumene producers operating in 2020, although this was consolidated to four by early 2021. Pilgangoora (AJM), recently acquired by Pilbara Minerals, will remain in care and maintenance for the foreseeable future. Alita Resources’ Bald Hill project is currently in care and maintenance but may be brought back online by 2022.

In terms of new projects, Albemarle/Mineral Resources' Wodgina & SQM/Wesfarmers' Mt Holland are most likely near-term entrants, while Core Lithium's Finniss project is slated to begin production in 2023.

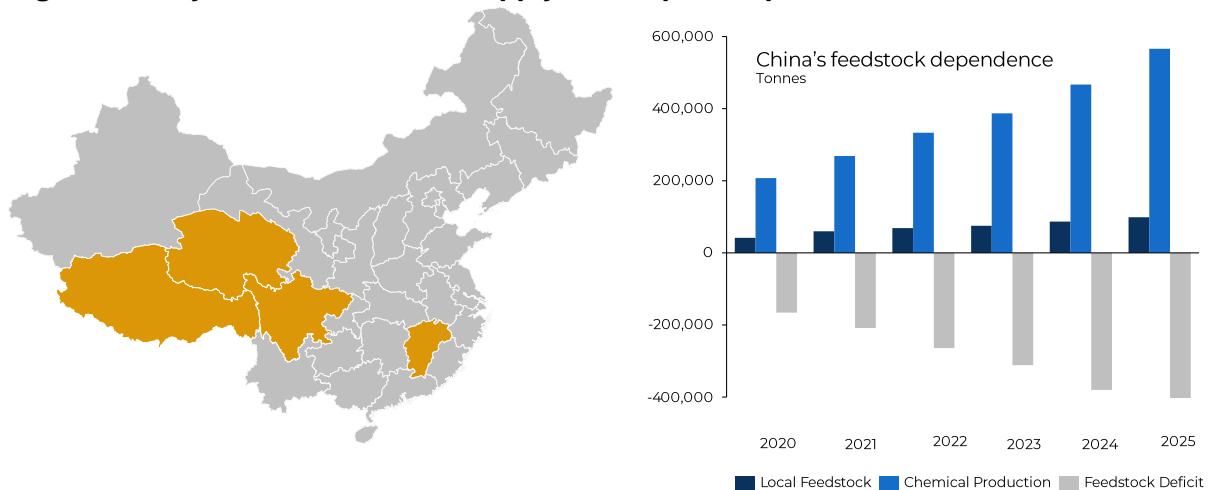
Figure Nineteen: Australian Lithium Supply Forecast



China

China is expected to produce ~270kt LCE of lithium chemicals in 2021. Despite this, just under 60kt LCE of lithium will be mined domestically. The balance will be made up by imports, predominantly spodumene from Australia. In 2020, Australia exported around 170kt LCE of spodumene concentrates. Exports will increase this year, with 66kt LCE so far exported. China also imports some lithium from South America, with SQM's share of imports to the country increasing. In 2020, SQM exported around 30kt LCE to China, exceeding that arriving from Livent, Albemarle and Orocobre combined.

Figure Twenty: Chinese Lithium Supply and Import Dependence



Rest of World

There are various projects across the rest of the world, most commonly spodumene focused, but with some brine and geothermal projects included. The map and chart below show the scale of this and the global supply forecast from projects

Figure Twenty-one: Global Lithium Project Map

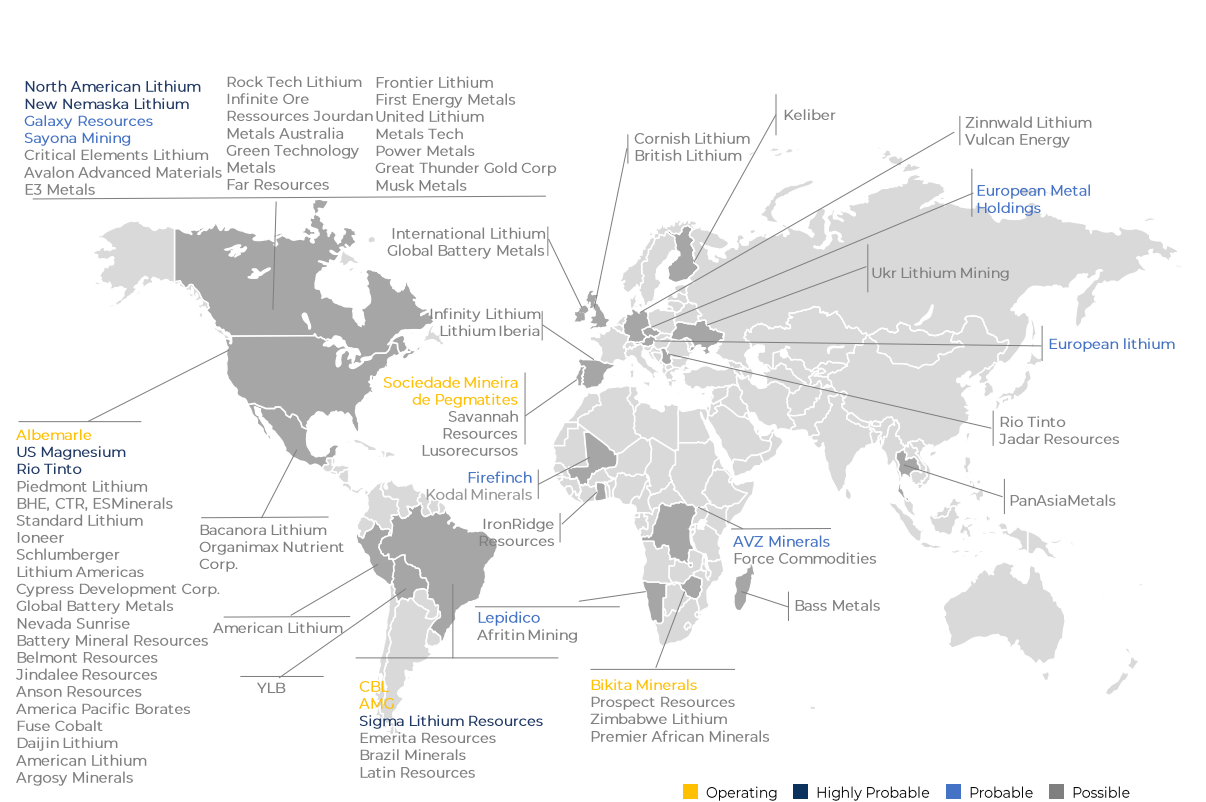
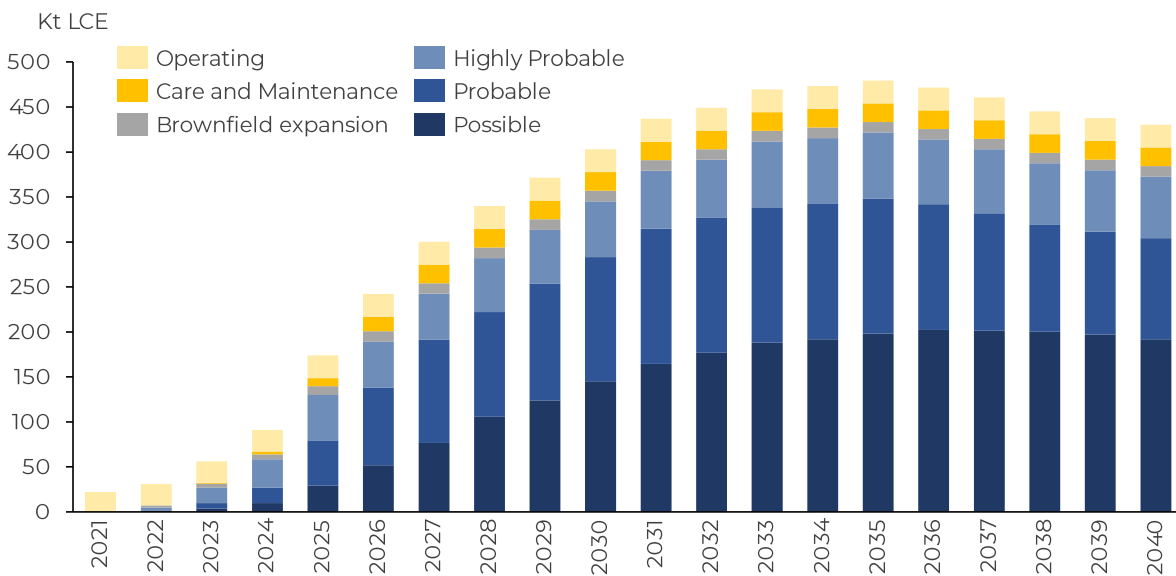
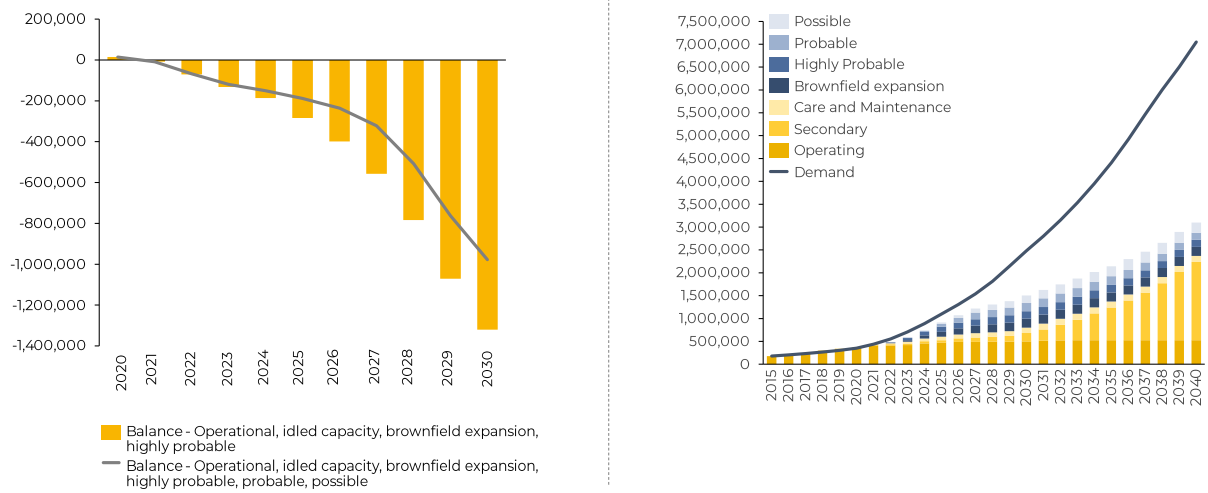


Figure Twenty-two: High level lithium supply forecast



The resulting supply demand balance for mined lithium is shown in the following chart and indicates a significant short to medium term deficit in the market

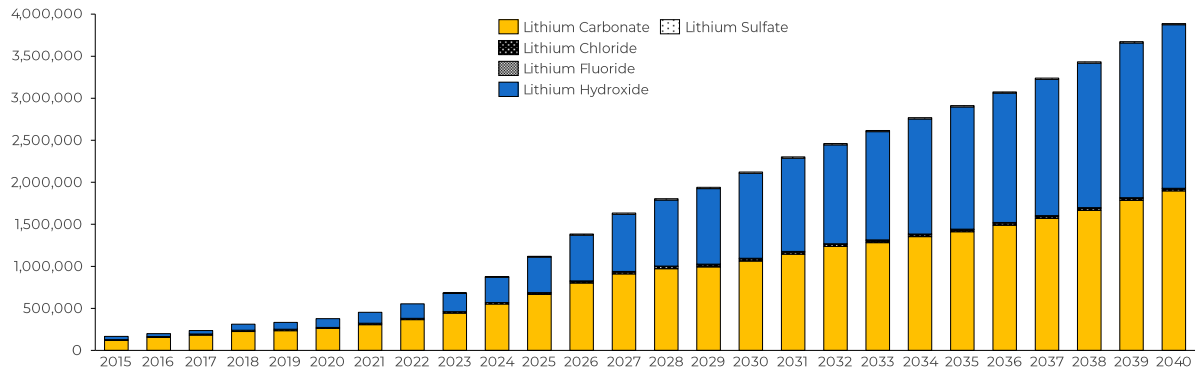
Figure Twenty-Three: Lithium supply demand balance



Lithium Chemical Supply

Most future demand growth will be for batteries for EVs. As the market for EVs expands and the balance of chemistry shifts towards high-nickel cathodes, **cathode manufacturers are expected to increasingly move towards the use of lithium hydroxide (Figure Twenty-three)**. This preference for lithium hydroxide for the manufacture of nickel-rich cathodes results from the faster degradation of hydroxide versus carbonate in the cathode manufacturing process, which requires less energy and is therefore more cost efficient.

Figure Twenty-Four: Cathode lithium requirements

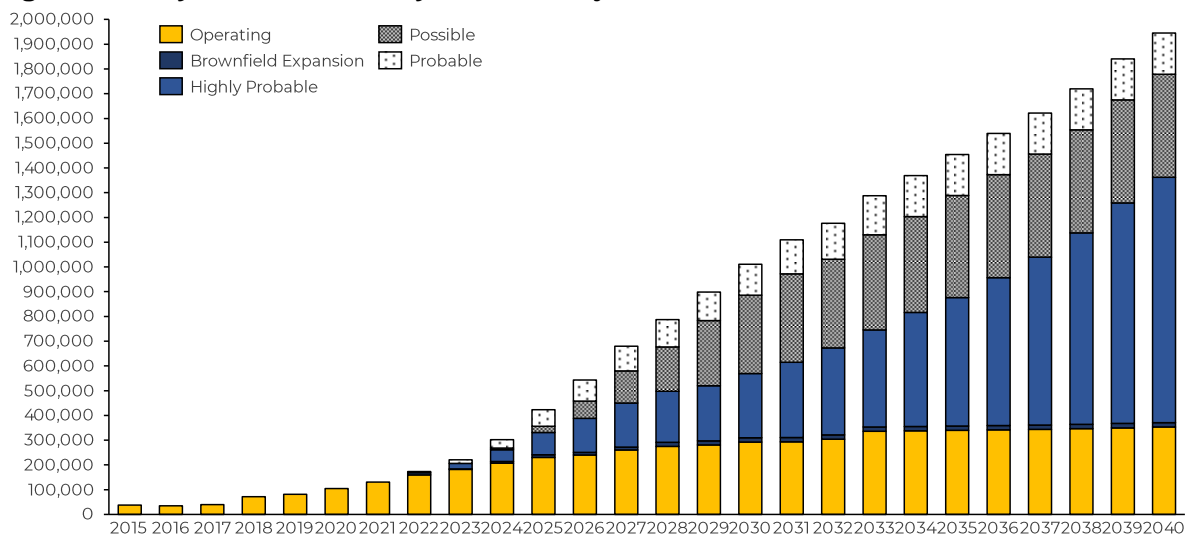


Source: Benchmark Mineral Intelligence

Lithium hydroxide also allows for improved material crystallinity, greater structural purity and less mixing of lithium and nickel in the lithium layer relative to lithium carbonate. When using lithium hydroxide, lithium content is fully incorporated within the structure of the NCM hydroxide. By contrast, use of lithium carbonate can result in excess free lithium, leading to an increase in material pH that can cause gelling of the cathode slurry and swelling of the cell upon cycling.

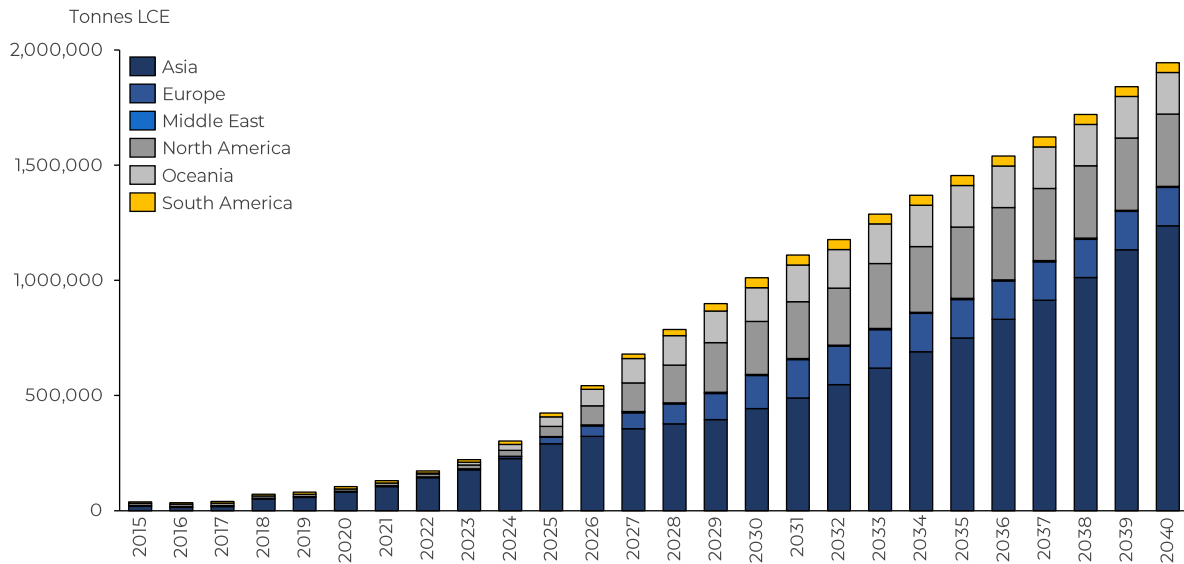
This, will see lithium hydroxide capacity increase significantly in future with many projects planned as can be seen in the following chart

Figure Twenty-Five: Lithium Hydroxide Project Forecast



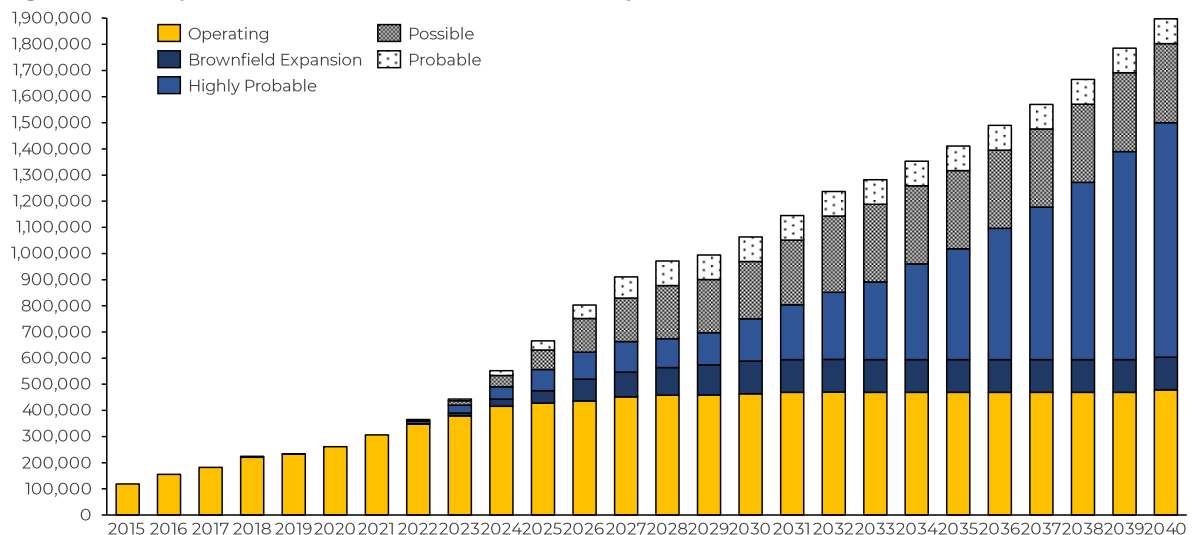
China is the key supplier of lithium hydroxide to the global market and will continue in this position for the foreseeable future. Chile is also a large supplier and will continue, albeit at a lower percentage of the global total. Australia will see the largest growth in supply largely as a result of new spodumene projects and the refining capacity constructed by firms such as Albemarle and Tianqi to process this material.

Figure Twenty-Six: Lithium Hydroxide Geographic Forecast



This is not to say that lithium carbonate will not also see huge growth over the period as can be seen in the chart below showing lithium carbonate projects

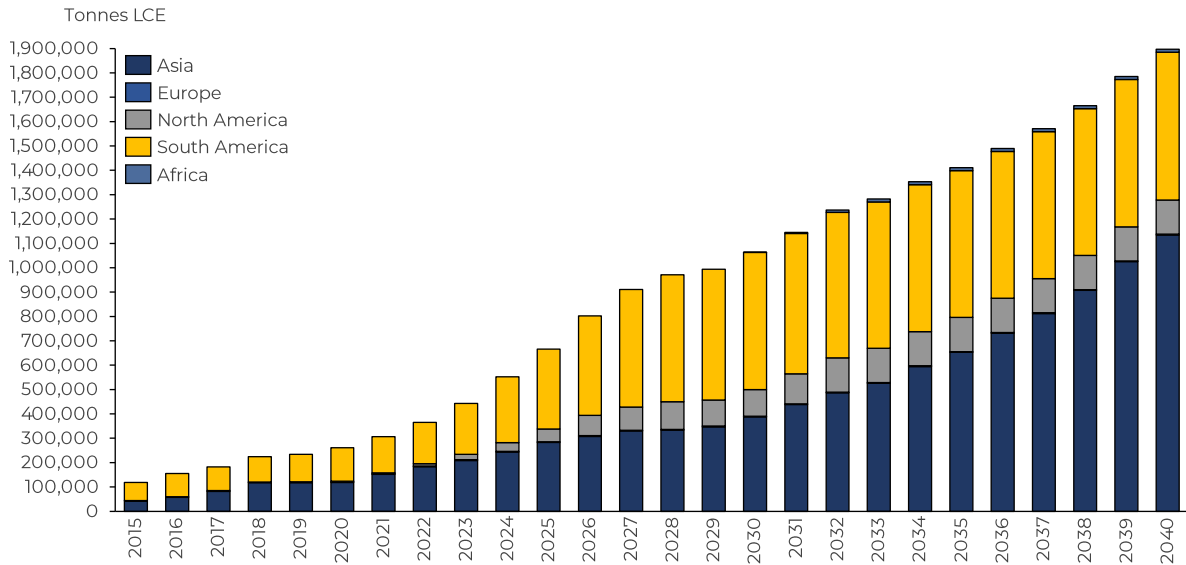
Figure Twenty-Seven: Lithium Carbonate Project forecast



Source: Benchmark Mineral Intelligence

Lithium carbonate is predominantly sourced from Asia and Latin America and this is expected to remain in future as new projects come on stream and existing producers continue to expand.

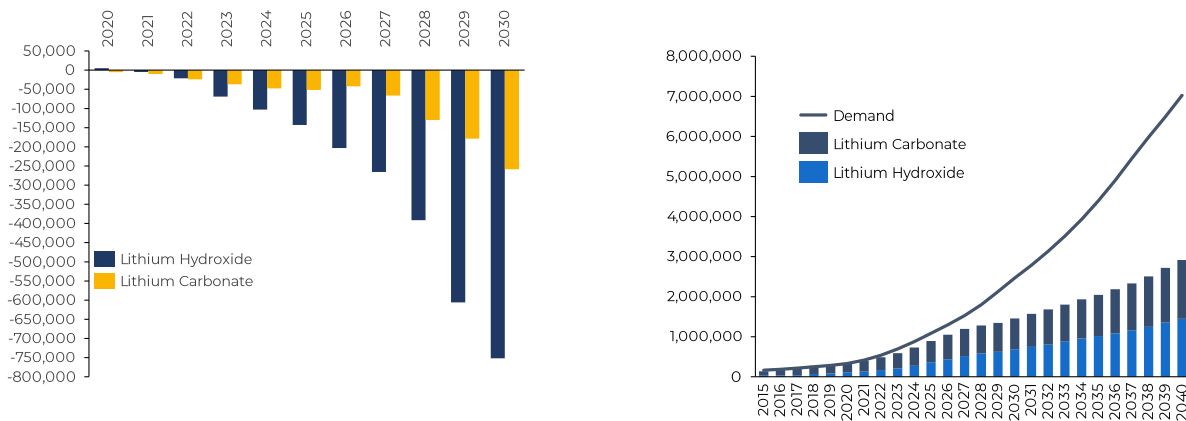
Figure Twenty-Eight: Lithium carbonate refined supply by region: 2015 – 2040



Source: Benchmark Mineral Intelligence

The resulting supply demand balance for lithium chemicals shows that both carbonate and hydroxide are forecast to be in a significant deficit in future.

Figure Twenty-Nine: Lithium chemical supply demand balance



Source: Benchmark Mineral Intelligence

Lithium Production Costs

As described earlier, lithium is sourced from either brine operations or those generically described as hard rock, with the balance of supply moving towards the latter over time. Most of the world's brine capacity is in Latin America, with some production from China. Hard-rock supply is more widely spread geographically, with Australia a major supplier.

Total cash costs for lithium carbonate and hydroxide production range from around US\$4,500/t LCE to >US\$9,000/t LCE over the forecast period, with hard-rock resources generally dominating the lowest-cost portion of the curves. Most of the new capacity coming online in the forecast period is expected to have production costs of >US\$6,000/t LCE, which broadly puts it in the upper half of the cost curves.

For the most part, this will also be hard-rock capacity. The more expensive suppliers of this type are forecast to have production costs ranging from around US\$6,000–9,000/t LCE in 2025. By that time, brine productions should see a relative improvement in their cost position versus new, hard-rock market entrants. Brine producers' costs are expected to be solidly anchored within the middle of the global carbonate cost curve by 2025, and by 2030 to constitute the bulk of the curve's second quartile.

Towards the latter part of the forecast period there is a marked requirement for additional lithium capacity to come onstream to meet rising demand. Where this capacity will be commissioned is not certain.

Lithium prices are forecast to remain in a range needed to stimulate this new investment, given that geological constraints are not an issue. To cover the difference in the demand and supply forecasts a 'potential' supply category was added to the data; costs for this supply are not included in the cost curves in this sub-section, however.

For reference, cost levels are assumed to be the same as current outlooks for new brownfield capacity. Necessary unplanned greenfield supply for lithium is assumed to come on at a mid-operating cost level, based on the proposed operating expenditure of projects that have already been announced and projections of development over time.

Lithium Industry Cost Methodology

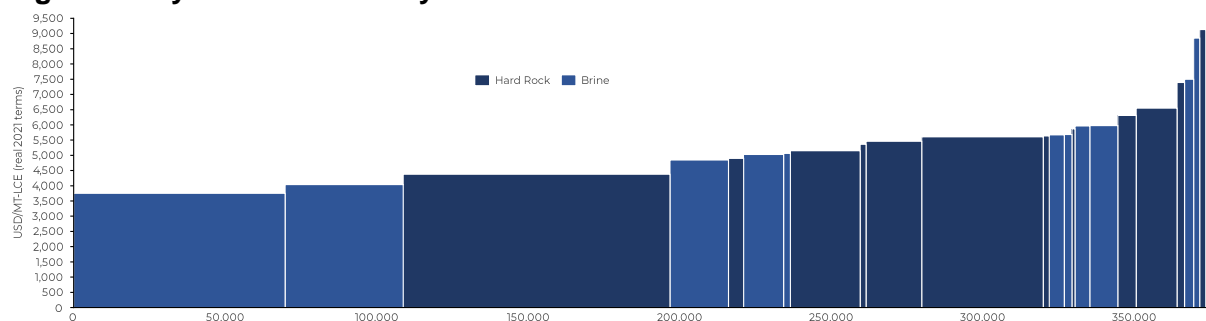
Benchmark uses a bottom-up cost modelling analysis to reach industry costs for lithium, and cross-references these with top-down information sources, including company financial reports and primary research using our network of industry contacts, including mining and chemical processing engineers.

The following factors are used to arrive at a representative ‘total cost’ figure for each operation under review:

- **Cash/operating costs:** This includes mine site, general and administration, sustaining capex, energy, labour, shipping costs to point of processing and reagent costs.
- **Capital charge:** Benchmark uses an annuity calculation for unit capital costs over a mine life of 25–30 years. Interest is charged at each operation, using a weighted average cost of capital (WACC) approach, plus application of a risk premium depending on the asset jurisdiction and profile.
- **Tax and royalty charges:** Returns for investors are net of taxes. A consideration is made for each operation’s marginal corporate tax rate in the jurisdiction as well as specific royalty charges for each resource.

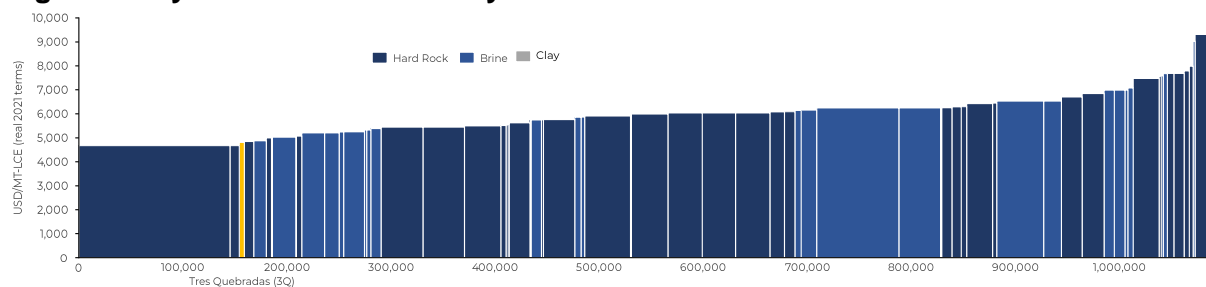
Figure Thirty to Thirty-Three provide the forecast lithium total cost curves for the period 2020–2035.

Figure Thirty: Lithium industry total cost curve - 2020



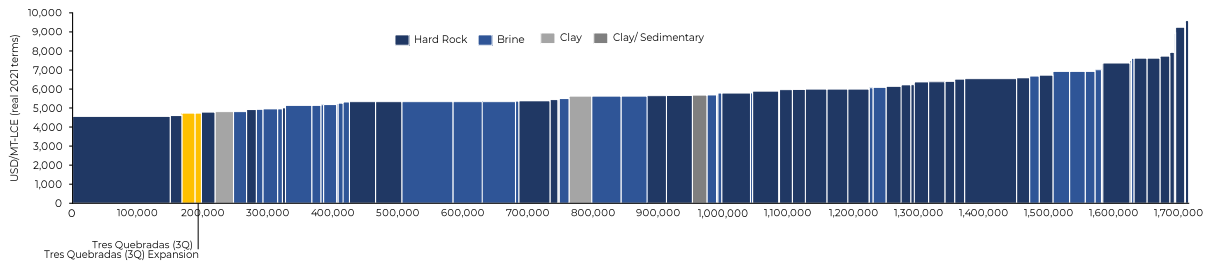
Source: Benchmark Mineral Intelligence

Figure Thirty-One: Lithium industry total cost curve – 2025



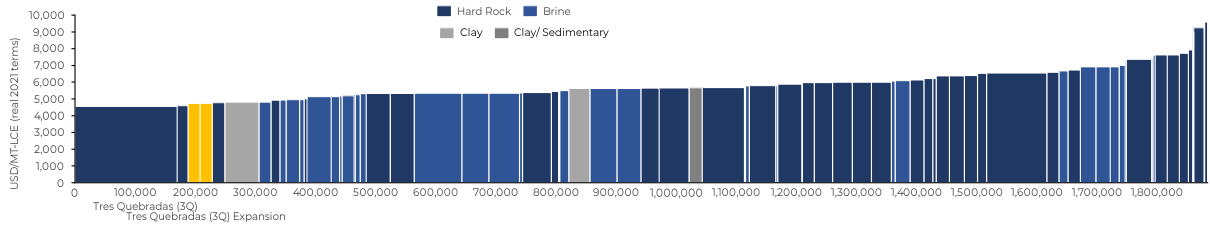
Source: Benchmark Mineral Intelligence

Figure Thirty-Two: Lithium industry total cost curve – 2030



Source: Benchmark Mineral Intelligence

Figure Thirty-Three: Lithium industry total cost curve – 2035



Source: Benchmark Mineral Intelligence

Lithium Pricing

Lithium is not quoted on a major exchange, so there is no readily available benchmark information on pricing. There is no terminal market for the metal, although the London Metals Exchange (LME) is working to launch a futures contract. In the absence of an industry-wide pricing benchmark, lithium has tended to be sold based on negotiations between buyer and seller. Historically, this has encompassed annual or multi-year supply contracts, with prices fixed for the duration of the agreement.

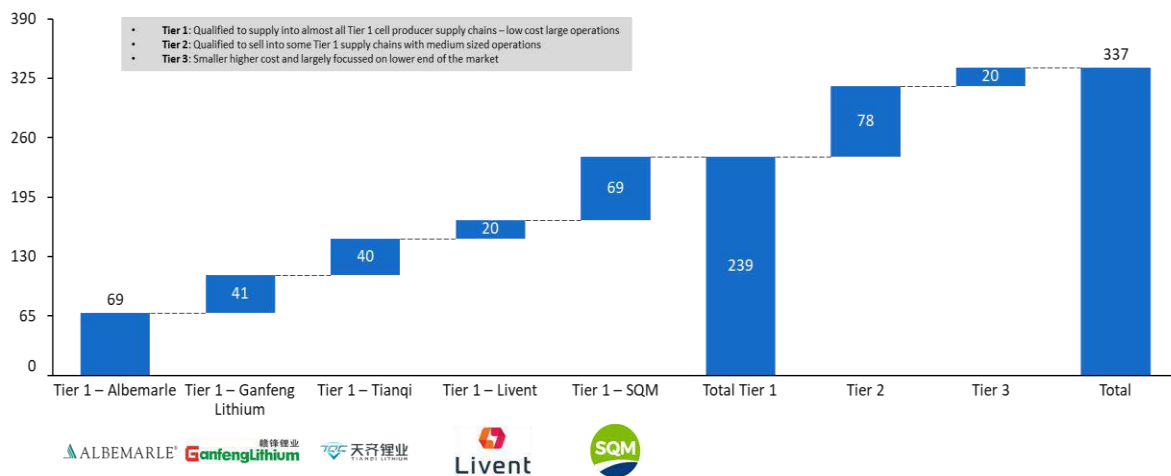
More recently, however, long-term supply contracts are increasingly being structured to allow for quarterly pricing breaks; the intention being that these will better reflect changing market fundamentals. These contracts in some cases reference price assessments currently available from several information providers, or else are simply negotiated each quarter by the parties involved.

Spot market liquidity for lithium chemicals tends to be most prevalent in China. There is reluctance among suppliers of specialist lithium chemicals, such as battery grade lithium hydroxide, to extrapolate Chinese spot market trends more widely. These suppliers argue that Chinese spot market prices do not reflect the kind of premiums that should be attached to guarantees of consistent supply and quality.

This view has recently been undermined due to the global oversupply of lithium. Some lithium chemical producers, particularly new incumbents looking to cement their place in the supply chain, are understood to have offered beneficial terms to cell-making OEMs to lock in volume offtakes. Benchmark does not believe this approach is sustainable. **Benchmark's opinion is that lithium prices, whether contract or spot, will have to settle at a level that incentivises sustained supply increases through the 2020s and beyond.**

In the recent past battery producers tended to source raw materials and simply pass on those costs, which could be volatile, to the OEMs that bought their battery cells. However, the ramp-up in battery capacity and EV vehicle production has encouraged some OEMs and battery makers to negotiate directly with raw material producers to secure supply. This approach ensures security of the raw material supply and the OEMs and battery makers benefit from any price discounts negotiated with lithium chemical producers.

Figure Thirty-Four: Tier 1 suppliers account for ~70% of current lithium chemicals supply ('000s)



Source: Benchmark Mineral Intelligence

Lithium Price Forecast Methodology and Pricing Outlook

Benchmark's price forecast methodology considers three temporal horizons: short-term, medium-term, and long-term.

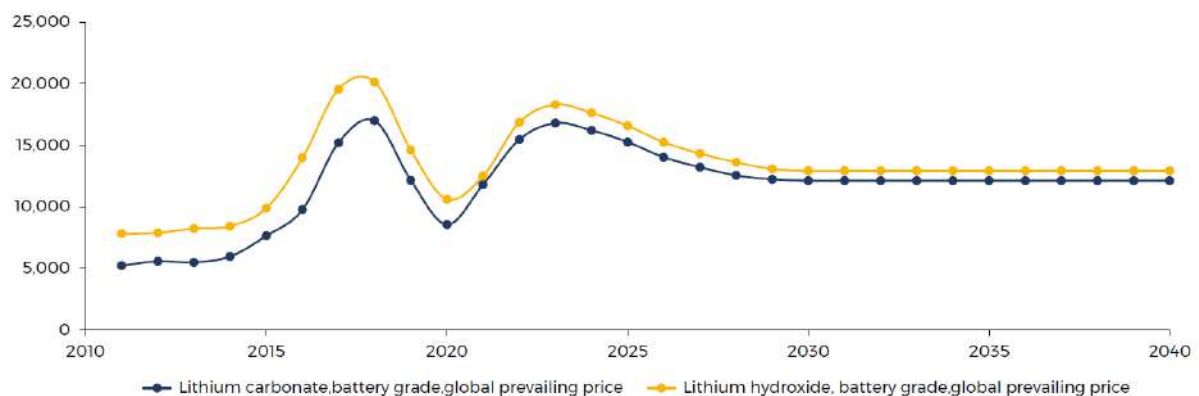
- Short-term methodology:** The short-term outlook on price developments is guided by primary price research conducted by Benchmark's analysts to ascertain the current direction of market pricing.
- Medium-term methodology:** Medium- and long-term pricing in commodity markets is often determined by the level at which the highest-cost producer needed to supply the market can continue to operate; for lithium this would be at a cash cost level of around US\$9,000/t LCE (2020 real terms) in 2025. This point informs medium-term price forecast, but due to the ongoing need to incentivise new projects market prices are likely to be well above this level. The outlook for 2022–2030 has lithium demand growth forecast to significantly outpace increases in supply. The market weakness in 2020 is projected to have added to the probability of delays in the development of projects in the possible and probable categories. Lithium prices will rise due to market deficits and the need to stimulate investment successively each year. Prices are likely to rise well above marginal production costs.
- Long-term methodology (2030–2040):** There will be an ongoing requirement for new greenfield capacity over the course of the forecast period. As the lower-cost new supply comes online there will be a need for the development of higher capital cost projects over time. The outlook for 2030–2040 assumes that new capacity projects, both planned and coming online, are reduced. Based on the pipeline of announced projects higher prices as expected to encourage as-yet-unannounced projects. This pipeline of new projects will begin to come through over the coming decade to meet rising demand. Ultimately prices will settle close to a long-term average of US\$12,110/t for lithium

carbonate and US\$12,910/t for lithium hydroxide (both in real 2021 terms). At these price levels IRRs provide sufficient incentive for investment over the forecast period.

The result of this analysis upon the price forecast is discussed in the points below:

- **Short term:**
 - Lithium prices increased in Q1 and into early Q2 as a result of strong EV demand.
 - Carbonate prices have tailed off as the market holds off buying further inventory at elevated prices and added supply from Qinghai brine projects in China has begun to filter through to the market.
 - Overall, supply tightness is now being eased by additional carbonate supply, whereas the same is not happening for hydroxide. Hydroxide prices have therefor regained their premium over carbonate.
- **Medium term:**
 - Chinese conversion facilities are able to produce hydroxide directly from spodumene and are often able to move flexibly between hydroxide and carbonate production. This means that the price range between carbonate and hydroxide is unlikely to widen dramatically in the medium term
 - While the higher price environment has started to incentivise supply investments, there is still a long way to go to meet the looming deficit in both carbonate and hydroxide.
- **Long term:**
 - Prices are expected to increase but likely to be unsustainable at US\$16-18,000/t. Even in the case where supply cannot meet demand, prices will likely stay high but fall back to a sustainably higher price which is able to incentivise new supply. While the chemicals industry in China seems to have little barrier to ramping up, supply bottlenecks at the mine-site level exist and will need to be solved.
- **Long-term price incentives:**
 - Benchmark believes that the long-term incentive price for lithium carbonate of US\$ 12,110/tonne will be required to sustain new project development post-2030

Figure Thirty-Five: Lithium Chemicals Battery-Grade Price Forecast, Real 2020 (US\$/MT)



Source: Benchmark Mineral Intelligence

It should be noted that the lithium price is a global price and as such an FOB price would be considered the same as the benchmark. It is likely that the material from 3Q would be sold into Europe or North America, as such it would be expected that the same price would be paid CFR China as CFR Europe or North America

	2015	2016	2017	2018	2019	2020	2021	2022	2023	2024	2025	2026	2027	2028	2029	2030
Lithium Carbonate, Battery Grade, Global																
Prevailing Price																
Real																
2021	7,633	9,752	15,198	16,979	12,147	8,553	11,800	15,445	16,790	16,200	15,250	14,015	13,209	12,538	12,229	12,110
Nominal																
							11,800	15,725	17,393	17,065	16,325	15,208	14,520	13,953	13,771	13,792
Lithium Hydroxide, Battery Grade, Global																
Prevailing Price																
Real																
2021	9,878	13,963	19,540	20,121	14,602	10,614	12,500	16,850	18,295	17,620	16,564	15,239	14,324	13,608	13,064	12,910
Nominal																
							12,500	17,156	18,952	18,560	17,731	16,535	15,746	15,144	14,711	14,703
Spodumene 6%, Australia FOB, Battery Market																
Material																
Real																
2021	647	697	783	932	620	407	649	719	720	690	669	636	616	599	588	577
Nominal																
							649	732	746	727	716	690	677	667	662	657
Premium Lithium Carbonate - Lithium Hydroxide																
				3,141	2,455	2,061	700	1,405	1,505	1,420	1,314	1,224	1,115	1,070	835	800

